

T-2540

PERMEABILITY OF UNSATURATED, FRACTURED
METAMORPHIC ROCKS NEAR AN
UNDERGROUND OPENING

by

Parviz Montazer


8410110374 840906
PDR WASTE
WM-11 PDR

A thesis submitted to the Faculty and the Board of Trustees of the Colorado School of Mines in partial fulfillment of the requirements for the degree of Doctor of Philosophy (Geological Engineering).

Golden, Colorado

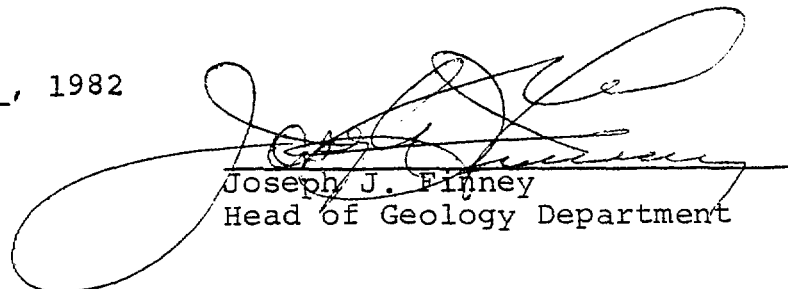
Date Nov 22, 1982

Signed: 
Parviz Montazer

Approved: 
A.K. Turner
Thesis Advisor

Golden, Colorado

Date Nov. 23, 1982


Joseph J. Finney
Head of Geology Department

ABSTRACT

The measurement and analysis of the rock-mass permeability of unsaturated fractured hard-rock masses have been hindered by the:

- a) lack of appropriate experimental data,
- b) weakness in existing data reduction procedures, and
- c) unavailability of suitable testing equipment.

Knowledge of such permeabilities has become vital in such applications as high level radioactive waste disposal siting and in other similar large underground engineering works.

This study was undertaken to answer these permeability measurements and analysis problems. An opening 100 meters below the surface and located in Precambrian migmatite-biotite gneisses of the Idaho Springs Formation of the Colorado Front Range of the Rocky Mountains, was used as a test location. The room is 30m by 5m by 3m high and is in the hydrogeologic zone of vertical gradient where unsaturated conditions occur. Forty-two NX-boreholes were drilled in radial directions from the room, and three NX-boreholes were drilled in longitudinal direction and in a horizontal plane one meter above the floor.

Multichamber packer injection testing equipment was developed to characterize the in-situ permeability of the fractured rock around the room. Using steady state tests

with less than 0.2 MPa of overpressure, the equipment is capable of detecting zones with permeabilities as low as 10^{-17} cm² (one nanodarcy). Employing transient tests, the lower limit is determined by the leakage around the packers. The equipment can detect leakage around the packers. Fracture continuity can be delineated with cross-hole tests.

This equipment was tested inside an NX-borehole drilled along the center line of a concrete column 4m long and 0.6m in diameter. Permeability to nitrogen of a 5cm core from the column agrees with that obtained from packer testing of the column (1.3×10^{-13} cm²). Permeability to water of the incompletely saturated column and permeability to carbon dioxide of the air dried core are in the order of 10^{-15} cm².

Detailed fracture mapping of the walls of the room, logging of the oriented core, and visual examination of the borehole walls with a borescope and a T.V. camera revealed two persistent, nearly vertical fracture sets: one with N50-60E strike, which is parallel to the foliation and is almost perpendicular to the axis of the room, and the second set with N40-50W strike. Shallow-dipping fractures are scarce. Radial boreholes are blind to the foliation fractures. Longitudinal boreholes sample both vertical sets, but are biased in favor of the foliation fractures.

An analytical method was developed to prepare a data

base from all the various sampling methods used. This data base contains information about fracture geometry, position with respect to the global coordinate system, and characteristics. Information about fractures can be generated along any arbitrary scanline using the data base.

Nitrogen was used as the injection fluid most often because it was found to be more suitable for testing unsaturated fractured rock with very low water potential. Carbon dioxide and water were also used as injection fluids to determine the response of the test media to the injection fluid.

All boreholes were systematically tested using a sequentially overlapping interval method of sampling. Steady state, pressure fall-off, and pulse tests were used. Individual fractures were selected and were cross-hole tested with all three fluids and employing a variety of testing methods. One of the longitudinal boreholes was tested using variable interval method to determine the scale effects.

Analysis of the data reveals that absolute values of permeabilities cannot be determined by single tests.

A non-linear relationship is observed in many cases for pressure-nitrogen permeability (P-P) relationships. It is postulated that positive slopes for P-P curves are due to unsaturated state of the rock and P-P curves with negative

slopes are because of combination effects of Klinkenberg, lubrication, complexity of the fracture network, and boundary conditions. In high conductivity, clean fractures these effects are insignificant. Injection of water into the fractured rock creates uncertain boundary conditions that may hinder analysis of the results.

Analysis of the existing theories suggests that an approach combining D'Arcies law and the Klinkenberg effect may prove useful in solving the difficulties of analyzing permeabilities of unsaturated fractures. By following this process a suitable data reduction technique was developed.

A number of nitrogen injection tests with a wide range of test pressures is required to estimate the intrinsic permeability. In a low permeability medium with low negative water potential (NWP), nitrogen provides better results than water or carbon dioxide. When such a medium is nearly saturated (high NWP), alternate injections of nitrogen and water may provide characteristic capillary pressure-relative permeability relationships. Pressure-permeability relationships can be employed to compare qualitatively variation of effective permeabilities along and between boreholes.

Using P-P curves, saturated permeabilities were estimated from steady state nitrogen injection tests. Permeabilities transverse to the room axis range from 10^{-14} to 10^{-9} cm²,

an overall value of 10^{-11} cm². Parallel to the room, permeabilities range from 3×10^{-13} to 10^{-6} cm². Overall permeability in the longitudinal borehole 1.2m from the room is one order of magnitude smaller than the longitudinal borehole 4 m (12 ft.) from the room. Permeability of the shear zone crossing these boreholes is two orders of magnitude smaller near the room than 4m away. Geometric mean of the permeability in the first 0.5m of the radial boreholes is one order of magnitude larger than the geometric mean of the permeability of all the radial boreholes.

Water testing of the longitudinal borehole farthest from the room both during and after excavation showed a slight decrease in the permeability of the rock mass (15m or 45 ft. long test zone) after blasting of one of the faces of the room.

Spatial and temporal permeability trends may be attributed to the modification of the rock mass caused by excavation of the room. Blasting modification seems to be most significant for the natural fractures oriented parallel to the axis of the room, but this effect is limited to the first half meter. The permeability of this thin envelope is significantly higher than the rest of the rock mass. In this envelope, the matrix permeabilities are in the same order of magnitude as in the rest of the five meter thick envelope. Furthermore, the

stress modification is suggested to be the cause of lower near-field radial permeabilities in a horizontal plane passing through the axis of the room and may also have caused an increase in longitudinal permeability. These modifications are limited to the first 1.5m from the surface of the opening.

It is concluded that in unsaturated fractured rocks, testing with nitrogen exaggerates permeability of the high conductivity fractures and facilitates their detection. The skin damage caused by stress redistribution and blasting is favorable for underground disposal of the radioactive water and other engineering projects where low radial permeability is an important design factor.

TABLE OF CONTENTS

	<u>Page</u>
VOLUME 1	
ABSTRACT	iii
LIST OF FIGURES	xv
LIST OF TABLES	xxi
LIST OF PLATES	xxi
NOMENCLATURE	xxii
ACKNOWLEDGEMENTS	xv
1. INTRODUCTION	1
1.1 Description of the Problem	1
1.2 Scope of the Research	4
1.3 Purpose and Objectives	7
2. SURVEY OF PREVIOUS WORK	8
2.1 Introduction	8
2.2 Flow of Fluids Through Fractures	10
2.3 Effect of Stress and Pore Pressure	13
2.4 Significance of the Scale of Study	15
2.5 Methods of Fracture Parameter Measurements	16
2.6 Methods of <u>In-Situ</u> Permeability Measurements	17
2.7 Overview	18

	<u>Page</u>
3. THEORETICAL CONSIDERATION	20
3.1 What is a Fractured Medium?	20
3.2 Flow Through Parallel Plates	22
3.2.1 Single Phase Flow	22
3.2.2 Two Phase Flow	28
3.3 Summary	39
4. GEOLOGIC ENVIRONMENT OF THE EDGAR MINE	41
4.1 Introduction	41
4.2 Geologic Setting of the Edgar Mine	44
4.3 Geology of the CSM/ONWI Room	47
4.4 Hydrogeologic Characteristics of the Mine	59
4.5 State of the Stress	70
4.5.1 Stresses Around the CSM Experi- mental Mine	70
4.5.2 The State of Stress Around the CSM/ONWI Room	71
4.6 Summary	74
5. FRACTURE CHARACTERIZATION	77
5.1 A Requirement for Permeability Characterization	77
5.2 Field and Laboratory Methods	79
5.2.1 Drilling and Core Recovery Operations	79
5.2.2 Core Logging Methods	82
5.2.3 Fracture Mapping	86
5.2.4 Visual Examination of the Borehole Walls	89
5.2.5 Quality Control	93
5.3 Data Analysis	94

	<u>Page</u>
5.3.1 Data Treatment	94
5.3.2 Surveying Data	95
5.3.3 Preparation of a Data Base	95
5.3.4 Generating Data Along a Scanline	101
5.3.5 Analysis of the Orientations	102
5.3.6 Determination of True Spacing, Frequency and RQD	103
5.3.7 Analysis of Borescope and T.V. Camera Data	105
5.4 Results	111
5.4.1 Overall Fracture Distribution	111
5.4.2 Fracture Orientation	112
5.4.2.1 Television and Borescope Surveys	112
5.4.2.2 Line Mapping	120
5.4.2.3 Core Logging	125
5.4.3 Fracture Frequency, RQD and Spacing.	129
5.5 Summary	138
6. DESIGN, FABRICATION, AND CALIBRATION OF THE PERMEABILITY TESTING EQUIPMENT	140
6.1 Design Criteria	140
6.2 Instrumentation	142
6.2.1 Packer System	142
6.2.2 Flowmetering System	149
6.2.3 Data Acquisition System	152
6.2.4 Calibration	155
6.3 Summary	156
7. TESTING OF PACKER EQUIPMENT IN A CONCRETE COLUMN MODEL	159
7.1 Preparation of the Model	159
7.2 Testing of the Model Using the Main Probe	161
7.3 Testing of the Sample of Concrete	162
7.4 Data Analysis	169

	<u>Page</u>
7.4.1 Concrete Core Sample	169
7.4.1.1 Steady State Gas Injection.	169
7.4.1.2 Analysis of Decay and Pulse Tests	171
7.4.2 The Concrete Column	183
7.5 Results	183
7.6 Summary	189
8. FRACTURE PERMEABILITY CHARACTERIZATION	190
8.1 Rationale	190
8.2 General Testing Procedures	191
8.2.1 Steady State	192
8.2.2 Decay After Steady State Test	194
8.2.3 Pulse Test	195
8.3 Systematic Injection Testing with Nitrogen	196
8.3.1 Longitudinal Boreholes	196
8.3.2 Radial Boreholes	198
8.3.3 Data Analysis	199
8.3.3.1 Steady State Radial Flow	199
8.3.3.2 Analysis of Pressure Pulse Tests	205
8.3.3.3 The Computer Code	209
8.3.4 Results of Systematic Nitrogen Injection	211
8.3.4.1 Longitudinal Boreholes	211
8.3.4.2 Radial Boreholes	221
8.4 Variable Interval Testing	223
8.4.1 Scale Effects	224
8.5 Cross-Hole Testing	230
8.5.1 Testing Procedures	232
8.5.2 Analysis of the Data	234
8.5.3 Results	234
8.5.3.1 Pressure Profile Along the Shear Zone	234

	<u>Page</u>
8.5.3.2 Cross-Hole Testing of Boreholes RHE-1 and RHE-2	238
8.6 Evaluation of the Preliminary Water Testing	250
8.6.1 Original Instrumentation	
8.6.2 Data Analysis.	251
8.6.3 Results	256
8.6 Summary	261
9. DISCUSSION AND ANALYSIS OF THE RESULTS	263
9.1 Analysis of the Pressure-Permeability Trends from Systematic Nitrogen Injection Tests	264
9.1.1 Causes for the Inverse Pressure- Permeability Relation	265
9.1.2 Causes for the Trends of the Second Kind	267
9.1.2.1 Increase in Permeability with time	267
9.1.2.2 Increase in Permeability with Pressure: A Concep- tual Model	269
9.1.3 Rationale for Comparison of Permeabilities	272
9.2 Variation of Permeability Along Fractures .	273
9.3 Variation of Permeability Along Radial Boreholes	276
9.4 Explanation for the Observed Spatial Trends	279
9.4.1 Effects of Blasting	279
9.4.2 Effects of Stress Modification . . .	286
9.4.3 Prediction of the Fracture Deformation	288
9.5 Anisotropy	293
9.6 Summary	295

	<u>Page</u>
10. ENGINEERING IMPLICATIONS	297
10.1 Fracture Sampling	297
10.2 Testing Design	299
10.2.1 Saturated Rocks	299
10.2.2 Unsaturated Rocks	301
10.3 Design of Underground Excavations	302
11. CONCLUSIONS	305
12. RECOMMENDATIONS	310

VOLUME 2

BIBLIOGRAPHY OF FRACTURE HYDROLOGY	312
--	-----

VOLUME 3

APPENDIX I: Plastic Dough Core Orienter	389
APPENDIX II: Analysis of Surveying Data	402
APPENDIX III: BSCOPE, A Computer Code for Reducing Data From Borehole Surveys with T.V. Camera and Other Visual Instruments	409
APPENDIX IV: Fracture Frequency and RQD	421
APPENDIX V: Computer Code PERMEA	523
APPENDIX VI: Permeability-Pressure Plots for the Longitudinal Boreholes	582
APPENDIX VII: Permeability Plots Along the Radial Borehole	609

LIST OF FIGURES

<u>Figure</u>		<u>Page</u>
3.1	Schematic diagram showing flow through parallel plates and a natural fracture.....	26
3.2	Capillary rise in a parallel plate model...	30
4.1	Site of experimental room.....	42
4.2	Plan view of the CSM/ONWI Room, with key to borehole names.....	43
4.3	A portion of the west wall of the CSM/ONWI Room.....	48
4.4 to 4.10	Explanation for Figures 4.4 to 4.10.....	49
4.4	Horizontal geologic section through the ONWI Room.....	50
4.5	Geologic cross-section through the first round.....	51
4.6	Geologic cross-section through the second round.....	52
4.7	Geologic cross-section through the third round.....	53
4.8	Geologic cross-section through the fourth round.....	54
4.9	Geologic cross-section through the fifth round.....	55
4.10	Geologic cross-section through the sixth round.....	56
4.11	Schematic cross-section through the Miami Tunnel, showing the hydrogeological zonation of the fractured rocks.....	60
4.12	View of the Miami portal showing water outflow during spring 1980.....	62

<u>Figure</u>	<u>Page</u>
4.13 Monthly precipitation for the Squaw Mountain station.....	64
4.14 View 30m inside Miami tunnel showing water flowing from an usually dry fracture.	65
4.15 Miami tunnel (to the left) and D-left drift (to the right) intersection showing water seepage.....	68
4.16 Simplified geologic map of the CSM/ONWI room showing stress elipsoids near the shear zone.....	72
4.17 Stereographic projections of the principal axes of stresses in the west wall, a = 30 cm, and b = 4m from the wall.....	73
4.18 Variation of axial stress near the opening.	76
5.1 Facsimile of preliminary core log at the site.....	80
5.2 Core immediately after removal from borehole.....	81
5.3 Oriented core with the top line marked.....	81
5.4 Matched pieces of core being logged for fractures.....	84
5.5 Facsimile of data for longitudinal boreholes.....	85
5.6 Facsimile of data from radial boreholes...	87
5.7 Line mapping of the walls.....	88
5.8a,b Borehole T.V. camera and accessories used to map the borehole walls.....	91
5.9 Relationship between strike, dip and normal vectors defining a planar feature..	96
5.10 Vectors involved in defining a planar feature by sampling along a scanline.....	99

<u>Figure</u>		<u>Page</u>
5.11	Borehole orientation in a) global system, b) local coordinate system.....	107
5.12	Relationship between the T.V. camera in the borehole with the CRT screen.....	110
5.13 a-f	Fracture orientation patterns from radial borehole logs.....	114
5.14	Contour diagram on lower hemisphere Schmidt equal-area net of 710 fracture orientations from the mapping of mining faces.....	119
5.15 a-e	Patterns of fracture orientation from mapping of the walls.....	121
5.16 a-c	Fracture orientation patterns from longitudinal borehole logs.....	126
5.17 a-e	Fracture frequency and RQD along longitudinal boreholes.....	132
6.1	Schematic diagram for the instrumentation of injection testing.....	144
6.2a	The middle chamber of the main probe being tested for leaks.....	145
6.2b	The pulse tester which is housed along with a transducer in the middle chamber....	146
6.2c	The outer pressure port of the main probe..	147
6.3	The monitoring probe.....	148
6.4	The flow tank system.....	150
6.5	The tracer line system.....	151
6.6	The rotameter array, connected in series to provide a full range of 0.01 cc/min of water (1cc/min of air) to 25 lit/min of water (70 lit/min of air).....	153
6.7	The data acquisition system.....	154

<u>Figure</u>		<u>Page</u>
6.8	The main probe is inserted into a long piece of steel pipe for calibration..	157
7.1	The concrete column being tested with nitrogen with the main probe set in the center hole.....	160
7.2	Drilling of a 15 cm (5.9") core from the concrete column.....	163
7.3	The 15 cm (5.9") diameter core.....	164
7.4	Five cm (2 in.) diameter cores were obtained in the laboratory from the 15 cm core. The wax in the pores (white spots) are applied to protect the sleeve of the triaxial cell and prevent leakage.....	165
7.5	A standard triaxial cell was modified to test the 5 cm cores.....	166
7.6	Schematic diagram showing the modified triaxial cell.....	167
7.7	Schematic diagram showing the variables used for deriving flow equations.....	172
7.8	Type curve for pressure decay test of cylindrical core sample. Downstream pressure is constant.....	179
7.9	Sample 1 decay test no. 4 (carbon dioxide) downstream pressure + 1.51 psi...	180
7.10	Results of testing the concrete column and samples with nitrogen.....	184
7.11	Results of testing the concrete column and samples with CO ₂ and water.....	186
8.1	Theoretical flow pattern through a fracture at right angle to the borehole..	201
8.2	Pulse test analysis for borehole no. RDD-4, interval 9-11.5 feet.....	210

<u>Figure</u>		<u>Page</u>
8.3	Flow chart showing the data handling and analysis by the computer code PERMEA..	212
8.4	Pressure-flow history for BH. No. PA-2, Int. 47-54, X = Flow, O = Pressure	213
8.5	Permeability along the longitudinal boreholes.....	215
8.6	Variation of permeability with pressure, fracture F1.....	216
8.7	Variation of permeability with pressure, fracture F5.....	216
8.8	Variation of permeability with pressure, fracture F3.....	217
8.9	Variation of permeability with pressure, fracture FS4.....	217
8.10	Variation of permeability with pressure, fracture F12.....	218
8.11	Pressure-permeability plots for the variable intervals in borehole PA-2...	225
8.12	Permeabilities (solid lines) at infinite pressure for various intervals in borehole PA-2. Dashed lines show the fracture frequency (from detailed core logging) for the same intervals.....	227
8.13	Permeabilities for various intervals predicted by the SOI method from systematic nitrogen testing.....	229
8.14	Pressure history during cross-hole testing of the shear zone.....	235
8.15	Normalized pressure profiles at the steady state points (see Figure 8.14) in the plane of the shear zone.....	237
8.16	T.V. camera view of the fracture selected for cross-hole testing in RHE-1.....	239

<u>Figure</u>	<u>Page</u>
8.17 The simplified fracture map of the room showing a near vertical fracture crossing boreholes RHE-1 and RHE-2.....	240
8.18 Pressure-flow history: Nitrogen Test No. 1, Boreholes RHE-1 and RHE-2.....	241
8.19 Pressure-flow history: carbon dioxide test no. 2.....	243
8.20 Pressure-flow history: water displacing carbon dioxide.....	244
8.21 Pressure-flow history: water test no. 2. Boreholes RHE-1 and RHE-2.....	246
8.22 Pressure-flow history: nitrogen displacing water. Boreholes RHE-1 and RHE-2.....	248
8.23 Pressure-permeability of the fracture shown in Figure 8.16 and 8.17.....	249
8.24 Schematic diagram showing the flow domain during injection into a vertical parallel plate model saturated with air.....	252
8.25 Graph of A versus P_0/γ for the two conditions of radial flow and that shown in Figure 8.24.....	252
8.26 Plan view of the CSM/ONWI room during its construction. The interval shown was tested before and after the hatchured area was blasted.....	257
8.27 Pressure-permeability plot for water tests conducted before and after blasting of one of the faces.....	258
8.28 Comparison between injection testing with water and nitrogen for borehole PA-1..	259
9.1 Hypothetical unsaturated fracture a,b during injection testing with a gas.....	270
9.2 Distribution of the means of the logarithms of permeabilities and fractures indices along four groups of boreholes.....	278

<u>Figure</u>		<u>Page</u>
9.3	Looking into one of the radial horizontal boreholes. Note the offset along the fracture intersected by the borehole.....	281
9.4	Schematic diagram showing the outline of the opening just before detonation of the peripheral blast holes.....	285
9.5	Stress deformation graph for a fracture induced in a sample from Idaho Springs formation.....	290
9.6	Variation of hydraulic conductivity in a fracture with increasing stress for three different-size rock samples.....	292

LIST OF TABLES

Table 5.1	Summary of significant fracture orientations.....	130
Table 9.1	Comparison between the predicted and calculated values of fractures deformation.....	294

LIST OF PLATES

Plate 1	Fracture distribution map of CSM/ONWI room, Colorado School of Mines Experimental Mine, Idaho Springs, Colorado....	back pocket of Vol. 1
---------	---	--------------------------------

NOMENCLATURE

A_s	=	cross-sectional area of the core
B	=	Klinkenberg constant
C	=	continuity parameter
D	=	dip vector
d_1, d_2, d_3	=	components of dip vector
d	=	distance
E_1, E_2	=	vectors in plane of the fracture
e	=	equivalent parallel plate aperture (width)
g	=	acceleration due to gravity
h_c	=	height of capillary rise
k_l	=	permeability to liquid
k_g	=	permeability to gas
K_{pp}	=	coefficient of parallel plate permeability
k_{pp}	=	permeability of the parallel plate
K	=	coefficient of permeability
L	=	length of the test zone
L_s	=	length of the sample
L_{sc}	=	scanline length
m	=	molecular weight of the gas
M_w	=	mass flow rate in the test zone
N_b	=	normal to fracture in borehole coordinates
N_p	=	unit normal vector to fracture plane
n_1, n_2, n_3	=	components of N_p

N_m	=	mean normal vector
$n'_{i,j}$	=	direction cosine matrix
N_{gi}	=	unit normal vector in global coordinates
P_c	=	capillary pressure
P, p	=	pressure
\hat{Q}	=	mass flow rate
Q	=	volume flow rate
q	=	flow rate per unit width
R	=	gas constant
R_c, R_b, R_p	=	position vectors
R_{sc}	=	scanline vector
r_w, r_b	=	radius of the borehole
r_3	=	radial distance to the boundary
r', r''	=	radius of curvature
S	=	strike vector
s_1, s_2, s_3	=	components of S
s	=	spacing
s_m	=	mean spacing
T	=	absolute temperature
T_o	=	absolute temperature at reference
t	=	time
V	=	volume
\hat{V}	=	specific mass flux
\vec{V}	=	velocity vector

V_1, V_2, V_3	=	components of \vec{V}
W_{sn}	=	screen width
X	=	body forces
x_i	=	cartesian coordinate axes
z	=	elevation head
α_i	=	angles in the cylindrical coordinate system
β	=	half the field of view angle
γ	=	inclination
ϕ	=	azimuth
λ	=	fracture frequency per meter
μ	=	dynamic viscosity
ρ	=	density
σ	=	stress
σ_{ij}	=	interfacial tension between two substances
ϕ	=	porosity
Φ	=	potentiometric head
ω	=	equivalent fracture aperture

ACKNOWLEDGEMENTS

This investigation was conducted under the auspices of the Office of Nuclear Waste Isolation of Battelle Memorial Institute, Columbus, Ohio.

I wish to express my gratitude toward Dr. A. Keith Turner, who has kindly and patiently advised me since 1975. His careful and critical review of the several drafts of this thesis has made its completion possible. I am also gratefully indebted to Dr. W.M. Hustrulid for his guidance, advice and support throughout all phases of this investigation. The support of Mr. William Ubbes of the ONWI is greatly appreciated.

My thanks to Drs. T.L.T. Grose, C.A. Kohlhass, and Keenan Lee, the committee members, for their help, encouragement and useful discussions. I am especially thankful to Dr. Lee for his continuous support throughout my education at Colorado School of Mines. Dr. D.M. Bass of the Petroleum Department is greatly appreciated for his critical review of the thesis. I am also grateful to Dr. R.M. King of the Mining Department for his interest in this project. Dr. Ove Stephansson of the University of Lulea, Sweden, is appreciated for helpful discussions.

Special thanks to Dr. John Gale of the University of Waterloo and Craig Forster for their technical advice on the instrumentation. I would also like to express my appreciation to Wayne Wall and Jack Cox of the CSM Computing Center for their advice and help in selection, set-up, and repair of the data acquisition system. I am also indebted to Don Szilagyi for his help on several instances of equipment breakdowns.

I also appreciate the enthusiastic cooperation and help of Leslie Sour, Fal Thamir, Lise Brinton, Carlos Paiz, David Reimers and Mike Winter, who spent long hours logging the core, mapping the walls and monitoring the tests. I am especially thankful to Leslie Sour for drafting many of the figures and spending tedious hours of office and mine work. The computer code for plotting the outlines of the room was written by Manouch Bahavar. I am very grateful to Sharon Nicastro, Rebecca Marsh, and Louise Wildeman for their great skill in typing the thesis. Gideon Chitombo, Wadood Elrabaa, and Paul Rosasco provided critical data.

Unfortunately there is not a strong enough word in the dictionary to enable me to express my appreciation to my wife, Parvin, who helped prepare the final draft of the thesis and without whose support and encouragement completion of this work would not have been possible.

1. INTRODUCTION

1.1 Description of the Problem.

The permeability of a fractured rock mass and its potential modification by construction of large surface or underground structures or by exploitation of its natural resources are extremely important for site selection, construction designs, and production techniques in many engineering projects. Examples of such projects include: disposal of high-level radioactive waste (HLRW) in geologic formations; underground storage of petroleum products; underground powerhouse construction; large dams and related structures; oil shale exploitation, extraction and control of methane in coal seams; mine drainage control; and exploitation of naturally fractured reservoirs. The majority of the rock types encountered within such projects have very low matrix permeability, but are fractured to great depths. Therefore, the main concern in these rocks is the extent to which the fractures may contribute to the permeability of the rock mass and to what degree this permeability may be altered by the construction of an underground opening or a surface structure.

The concern about the hazards associated with the disposal of high level radioactive waste has led

investigators to consider various possible alternative disposal methods. One of the most promising methods is storage of HLRW in carefully excavated underground caverns. Several geologic environments are currently under investigation as possible sites. They include four major rock groups: salt and related deposits, argillaceous rocks, volcanic rocks, and plutonic and high-grade metamorphic rocks (Asher, 1978). The crystalline group, including both igneous and metamorphic rocks, has been given more consideration recently because of potential difficulties foreseen for many sites in the other groups. This has opened a new era in the field of flow through fractured media as tremendous amounts of badly needed data are being collected.

Crystalline rocks are always fractured to some degree. The fractures may be closed or open at greater depths due to the existence of an overall high stress field. Numerous laboratory and field studies have indicated that fracture conductivity is extremely sensitive to the state of the stress and pore pressure in these rocks, but experiments and research concerning the effect of underground openings on the permeability of fractured rock are limited.

Fisekci and Barron (1975), using straddle packer techniques, showed that permeability of coal reduces to a background level at a distance of ten meters from the ribs. Barron (1978) modified this technique to investigate

the integrity of coal pillars and concluded that the permeability decreased sharply in the center of the pillar. Rodionov, et al. (1981) found an increase in permeability due to blasting in a homogeneous rock mass. Gale, et al. (1977) emphasized the effect of stress relaxation on permeability around underground repositories in crystalline rocks. Gale, et al. (1981) conducted a series of permeability tests in the crystalline rocks of Stripa, Sweden, to investigate this concept.

However, none of these experiments considered a concurrent in-situ stress evaluation, and in all cases there was no attempt to conduct tests parallel to the long axis of the opening. Neither has there been an attempt to study the effect of smooth-wall blasting on permeability. Furthermore, these previous investigations have led to the general conclusion that excavation of underground openings induces an increase in permeability of the fractured host rocks.

Blasting methods commonly used to excavate underground storage rooms changes the properties of the host rock. Blasting damage can be minimized with careful, efficient blasting techniques (Holmberg, 1981). However, removal of the rock modifies the state of the stress in the immediate vicinity of the excavation. Such changes could modify the ground water flow field, a significant factor in radionuclide transport around an underground

repository. This effect can be used advantageously if the behavior of the fracture system around the opening is known.

The analysis of fracture permeability is also essential in proper planning for borehole plugging and repository sealing programs. Understanding the unsaturated flow through fractures is also significant in estimating water inflow during the active life of a repository and during resaturation after decommissioning. Therefore, it is necessary to apply instrumentation, measurement methods, and data analysis techniques to understand the behavior of the fracture system around proposed repository sites.

1.2 Scope of the Research

The present investigation has focused on fracture permeability characterization techniques needed to study the suitability of a site for HLRW storage. The aspects considered are the relationships among geological, mechanical, and hydrological properties of the fractured rock. The research consisted of four parts, as follows:

- 1) A test site was selected within the Colorado School of Mines experimental mine. A new room, excavated below ground surface and 200m into the mine as part

of a research program for the Office of Nuclear Waste Isolation (ONWI) of the Battelle-Columbus Laboratories under contract with the U.S. Department of Energy, was selected for study. The test site, designated the CSM/ONWI room, was the subject of detailed fracture mapping. Cores obtained from exploratory and test boreholes were logged in detail with respect to fractures.

- 2) The research included the design, assembly, and testing of appropriate equipment to measure the low permeabilities encountered in crystalline rocks at depth. The equipment was modified and additional data collected as necessary to achieve this goal. Economy and feasibility, as well as precision, were of prime concern in equipment design.
- 3) Tests of the permeability of the metamorphic rocks were run, using this equipment. Systematic nitrogen injection testing at short intervals was used for deterministic permeability sampling of the boreholes. Cross-hole testing with water, nitrogen and carbon dioxide was employed for determination of permeability trends and investigation of the effect of the state of saturation on permeability results.

- 4) Evaluation of the results from these tasks was carried out to obtain an understanding of the behavior of the fractures and the fluid-fracture interactions near the CSM/ONWI room.

1.3 Purpose and Objectives

The purpose of this research has been to investigate permeability characteristics of the crystalline rocks surrounding the CSM/ONWI room through observation and experiments conducted in the CSM Experimental Mine.

The specific objectives of the research are:

- 1) To prepare a descriptive conceptual model for the test site with emphasis on the hydrological and geological characteristics that may affect the interpretation of the permeability test results.
- 2) To employ some of the current techniques and to develop new methods for fracture characterization needed to evaluate permeability traits near an underground opening.
- 3) To improve current instrumentation for injection testing of very low permeability, unsaturated,

fractured crystalline rock.

- 4) To evaluate validity of the steady state, packer injection test results under controlled conditions.
- 5) To study the spatial distribution of the permeability; in the five meter thick envelope around the CSM/ONWI room, in order to delineate trends that might be attributed to the creation of the opening.
- 6) To use the equipment to evaluate the nature and extent of damage to the rock surrounding an underground excavation by employing packer injection techniques.
- 7) To understand the physical laws controlling the behavior observed during these experiments.

2. SURVEY OF PREVIOUS WORK

2.1 Introduction.

A tremendous volume of literature exists concerning the occurrence and movement of fluids in porous media, but comparatively little research has been done with respect to flow through fractured media. Nonetheless, in the last two decades the amount of literature dealing with the occurrence and flow of fluids in fractured media has increased exponentially.

Some of the earliest works to be mentioned in the United States are those of Ellis (1906 and 1909), who studied the occurrence of groundwater in crystalline rocks of Connecticut and probably was the first to mention closure of joints with depth as affecting the groundwater supply.

Recent developments of the theoretical and applied aspects of fracture hydrology have been due to the realization of the significant differences between the characteristics of fractured and porous media with respect to fluid flow. Such characteristics have been studied by Brace (1976), Brace and Martin (1968), Brace and Orange (1968), Brace et al. (1966), Brace et al. (1968), Brace et al. (1965), and Gale (1975).

As "hard rock" is encountered with increasing frequency

in engineering projects, the need for a more complete understanding of fractured media has become apparent. Examples of increased benefits and better results gained through differentiation between porous and fractured media are numerous.

In the field of petroleum engineering, effective secondary recovery of oil from fractured reservoirs cannot be accomplished without a thorough understanding of the behavior of such reservoirs (Warren and Root, 1963; Kazemi, 1969; Kazemi and Seth, 1969; Nelson and Handin, 1977; Parsons, 1966 and 1972; Barfield, et al., 1959; Raush and Beaver, 1964; etc.).

The foundation engineer can no longer afford to base his computations on the assumption that fractured rocks behave as porous media.

Experience with drainage of underground excavations and slope cuts in fractured rock has led the civil engineer to pay more attention to the behavior of fluids in fractured rock (see for example, the Proceedings of International Symposium on Percolation Through Fissured Rock, 1972). Recently, the need for underground storage of commercial fluids, underground repositories for nuclear waste, subsurface disposal of industrial waste, extraction of geothermal energy, more complete understanding of seismic phenomena,

and so forth, has initiated a large number of investigations in the field of fracture hydrology (see for example: the Proceedings of the First International Symposium on Storage in Excavated Rock Caverns, 1978; Witherspoon and Gale, 1977; the Second U.S. Symposium on the Development and Uses of Geothermal Resources, 1975; Subsurface Space, 1980).

2.2 Flow of Fluid Through Fractures

In early attempts to model fluid flow in fractures, the fractures were assumed to act as planar conduits. With this assumption and using the Navier-Stokes equation researchers have derived an equation of flow through parallel plates analogous to the Poiseuille equation for flow through tubes (Lamb, 1932; Romm, 1966; Gale, 1975; etc.)

The parallel plate analogy has been used to study problems of flow through fractured media (for example Lomize 1951; Romm and Pozinenko, 1963; Snow, 1965; Parsons, 1966; Wittke and Louis, 1966; Kiraly, 1969; Wilson and Witherspoon, 1970; Castillo, 1972; Bear, 1972; Gale, 1975; etc.). Snow (1965) used this analogy in a general three-dimensional form to show the applicability of Darcy's Law to fractured media. Chernyshev (1972), Baker (1955) and others also have arrived at the conclusion that D'Arcy's law may be extended to a

fractured medium. All such derivations suffer from the fact that, in nature, fractures are not planar conduits, and have variable apertures and non-parallel faces and are finite in extent. Two-dimensional numerical modeling by Long, et al. (1982) showed that this is true only for media intersected by fractures infinite in extent or by a large number of interconnected, finite fractures.

Lomiz (1951) and later Louis (1969) and Iwai (1976) studied the effects of aperture variation and fracture roughness on the hydraulic properties of fractures. The applicability of their results to real field conditions has not, however, been shown.

It should be mentioned that some investigators (for example Sharp, 1970) have questioned the applicability of the plane, Poiseuille equation to fractures; however, Witherspoon and Gale (1977) have questioned the accuracy of Sharp's measurements and rejected his arguments. Gale (1982) concluded from laboratory data that at high normal stresses across the fracture, the Poiseuille's equation is no longer valid. This is explained by the present author to be due to the higher roughness coefficient (mean height of the asperities/mean fracture aperture) at higher normal stresses. In fact Gale, by his recent data, has confirmed the validity of Sharp's experiments.

A significant fracture parameter, in parallel plate modeling, is the aperture. Permeability of fractures is very sensitive to this parameter. Snow (1965, 1966, and 1968) has shown that from fracture geometry and aperture the permeability can be computed and the principal axis of directional permeability determined. Snow (1966) has also suggested a method of determining in situ anisotropy by injection tests in three orthogonal holes. This would require predetermination of the principal axis of anisotropy. He suggests the use of statistical methods (developed by him in 1965) to determine the principal axis. This would be a good method if techniques to measure aperture were well developed. Rocha et al. (1977), using a similar mathematical approach, developed a field method for determination of anisotropy.

Some investigators have searched for methods of aperture determination (Bianchi, 1968; Bianchi and Snow, 1969; Harper and Hinds, 1978). However, attempts to correlate the computed permeability with the measured permeability have failed (Snow, 1972a), due partly to methods of data collection and, more significantly, to the assumption that fractures behave as parallel plates.

2.3 Effect of Stress and Pore Pressure

Aperture deformation is an important characteristic of fractured media. It controls permeability, and has been the subject of study by many investigators (Shehata, 1971; Snow, 1972c; Goodman, 1974; Gale, 1975 ; Iwai, 1976; unpublished results reported by Witherspoon and Gale, 1977; Gale, et al., 1979a; Gale, 1980). Many discrepancies in the results of injection tests have been attributed by Snow (1972a) to this phenomenon rather than to other effects such as turbulence. The results obtained by Banks (1972) and Maini, et al. (1972) show a nonlinear relationship between flow rate and hydraulic gradient even at low pressures. Snow (1972a) states that "...there is no way to evaluate the deduction that little deformation takes place upon injection." The fracture stiffness, which controls aperture deformation, was an unknown property in those experiments. Aperture closure is a function of the state of stress in the rock and the fluid pressure in the fracture (Shehata, 1971; Snow, 1972c; Gale, 1975 and 1982).

The velocity with which a given fluid flows between parallel plates is directly related to the square of the aperture (see following section) and the flowrate itself varies with the cube of the aperture. Thus, it can be seen that the flowrate is extremely sensitive to aperture

deformation. Unless filled with a mineral stronger than the rock matrix, fractures are more deformable than the rock. Stresses applied to the rock are transferred across the fracture through the asperities. The contact area across a fracture is much smaller than that of the grain to grain contact within the rock matrix; therefore, the stress concentration is much greater in the asperities than in the rock matrix. This results in larger deformation in the fracture aperture than in the matrix.

Pore pressure in the fracture tends to separate the two walls by reducing the effective stress; i.e., an increase in fluid pressure tends to oppose fracture closure caused by applied stress.

Gale (1975), Gale, et al. (1979a and 1979b), and Pratt, et al. (1977) measured aperture deformation both in the laboratory and in the field. Bernaix (1967) and Jouanna (1972) have demonstrated the dependency of the fracture aperture on the state of the effective stress. These authors have shown that aperture deformation is dependent in a nonlinear fashion on the applied stress. However, no universal relationship between fracture strain and stress similar to that known for rock deformation has been discovered.

2.4 Significance of the Scale of the Study

In studying fractured media the sample size is an important factor determining the method of approach to problems of fluid flow. On a regional scale, fractured rock may be assumed to behave as an anisotropic, heterogeneous, porous medium. However, on smaller scales, such as those dealt with in mine drainage problems, underground storage of fuel, etc., the assumption may no longer be valid. Thus, in order to interpret correctly the nature of flow, the characteristics of the fractured medium (fracture geometry, interconnectivity, continuity, aperture distribution, etc.) should be known. Currently there is no well-defined size limit above which fractured media can be treated as porous media. In cases where the matrix has noticeable permeability and porosity the problem of sampling size limit becomes more complicated (Price, 1976 Warren and Root, 1963; Parsons, 1966 and 1972; Long, et al., 1982).

Fractures exist in almost any rock type, varying in form from microcracks to joints and faults. Joints, faults, and even microcracks generally occur in preferred orientations depending on the stress history of the rock. A dense rock with microcracks in its crystal structure may exhibit extremely low permeability. Such a medium on a macroscopic scale can be dealt with as an anisotropic

porous rock. On the other hand, a fault zone filled with gouge may be considered as a porous medium on the scale of a sample of the gouge itself. These examples emphasize the fact that the distinction between porous and fractured media depends on the size of the sample, as well as other intrinsic characteristics of the rock.

2.5 Methods of Fracture Parameter Measurement

Efficient techniques of statistical sampling of fracture orientation are highly developed in the field of rock mechanics. Systematic sampling and the detail-line method of sampling, on exposed surfaces of the rock, both underground and on the surface, are well-known methods which involve measurement of all joints, their spacing and continuity along a line of specified length (Priest and Hudson, 1976 and 1981). Oriented core logging, cameras, dip-meters (resistivity type), and more recently impression packers (Harper and Hinds, 1978; and Fairhurst, et al., 1979) and acoustic logging (Koerperich, 1978) have been used with varying degrees of success for fracture detection and for fracture orientation determination in boreholes.

Borehole photography, fluorescent dye, and impression packers have been used to measure fracture aperture. Borehole

photography does not give accurate measurements of aperture because the fracture aperture as exposed in the borehole has been distorted by drilling (Snow, 1972a). The use of fluorescent dye (Bianchi, 1968) has also failed because of the capillary spread of the dye at the intersection of the aperture with the rock face. The results of the impression packer method with respect to permeability calculation have not been published as of this date. However, all these methods suffer from the fact that they measure only the aperture at the exposed surface, where it has been distorted by the drilling operation and the resultant stress modified around the borehole. A method is needed to measure apertures in an undisturbed environment.

2.6 Methods of In-Situ Permeability Measurements

Steady state injection testing of packed-off borehole intervals has been the most widely accepted method of measuring the permeability of fractured rock (Zeigler, 1976; Louis, 1974; Gale, 1975; Maini, 1971). Other methods, such as pumping tests and aquifer injection tests, are used to determine the overall transmissivity of fractured aquifers (Gringarten and Witherspoon, 1972; Maini, et al., 1972; Matthews and Russell, 1967; Earlougher, 1977; Papadopolous,

1967). Packer testing gives data from which the hydraulic conductivity of a few fractures isolated in the sealed off section of a borehole can be calculated. These tests provide information only for the behavior of fractures in the immediate vicinity of the borehole. Recently, methods have been developed to acquire information at greater distances from the borehole (Gale, 1975; Wang, et al., 1977). Pumping tests, on the other hand, affect a much larger area of the aquifer, but do not indicate accurately the characteristics of single fractures unless the producing (or injecting) zone consists of a single fracture, a rare occurrence.

Conventional packer testing as used in damsite investigations and similar projects is usually not properly instrumented and as a result, details of fracture behavior cannot be readily determined.

2.7 Overview

The technology for fracture characterization for the purpose of studying the flow through saturated fractured rocks is more or less established. Fracture properties can only be statistically represented because of the inconsistencies in nature of the fractures. Fracture aperture

is the parameter that cannot be measured accurately by direct methods. Indirect methods, such as packer testing of fractures isolated in boreholes, are costly and slow for detailed fracture mapping. In addition, complexity of the fracture networks reduces the reliability of the aperture measurements. Geophysical methods are needed to estimate fracture aperture over a relatively large area around boreholes.

A number of simple models have been developed that can incorporate the statistical or deterministic characteristic of a fractured rock to study its hydrological properties. However, the methods by which field data should be collected to best represent the rock properties have not been established. Whether or not an equivalent porous medium can be found for naturally fractured rocks is still debatable.

The problem of flow through unsaturated fractures has been only recently addressed, and it seems that a great deal of research is required before this problem can be at least partially solved. A great deal can be learned from works done in petroleum and geothermal reservoir engineering.

3. THEORETICAL CONSIDERATION.

3.1 What is a Fractured Medium?

Although generally well understood, fractured media are difficult to define since in nature all gradations from purely fractured to purely porous media can be found. In contrast to porous media, which are assumed to consist of tubular openings, fractured media are assumed to consist of blocks with low permeability and irregular shape (the matrix) separated by planar conduits with conductivities several orders of magnitude greater than the matrix, but with much smaller storage capacities.

A fractured medium may be generally defined as a space occupied by solid or porous blocks of material (matrix blocks) separated by planar conduits (or tabular voids), provided that the overall properties of the medium are significantly different from a continuum formed by the same matrix blocks. Almost all solids fall into this category at various scales. A single crystal with good cleavage, any non-porous crystalline rock at the hand specimen scale, and almost all hardrocks at medium-sized construction scales fall into this category. It is evident that this definition implicitly requires a scale or a "sample size". An aggregate of the single grains in a sandstone is considered as a porous medium at hand specimen scale. The same sandstone as an aquifer (or reservoir) in a fractured formation

is a double porosity medium. It is common to refer to the matrix porosity as primary porosity and to the fracture porosity as secondary porosity. An extensive review of various fractured media is given by Snow (1965) and will not be repeated here.

In studying fractured media certain simplifying assumptions may allow replacing them with equivalent porous media. This is done to take advantage of the vast amount of theoretical background that has been established in dealing with porous media. Nevertheless, there are no circumstances in nature that would allow such substitutions without significant errors introduced into one or more aspects of the flow phenomena. Some of these problems will be discussed in the following sections.

Natural fractures are not planar, rather they form very irregular and uneven surfaces, separation of which is both spatially and temporally variable. Yet, the theory of flow through fractured media was initiated by simulation of the single fractures with parallel plates. Following is a brief review of the developments of the theory of the flow through parallel plates with an emphasis on the behavior of the fluid in such a system.

3.2 Flow Through Parallel Plates.

3.2.1 SINGLE PHASE FLOW.

The Navier-Stokes equation of motion of viscous compressible fluid with constant viscosity may be written as (Pai, 1956):

$$\rho \frac{DV_1}{Dt} = X_1 - \frac{\partial p}{\partial x_1} + \mu \left[\frac{\partial^2 V_1}{\partial x_1^2} + \nabla^2 V_1 - \frac{2}{3} \frac{\partial}{\partial x_1} \nabla \cdot \vec{V} + \frac{\partial^2 V_2}{\partial x_1 \partial x_2} + \frac{\partial^2 V_3}{\partial x_1 \partial x_3} \right] \quad (3.2.1)$$

and similar expressions for V_2 and V_3 , where:

ρ = fluid density

$\frac{D}{Dt}$ = total derivative = $\frac{\partial}{\partial t} + V_1 \frac{\partial}{\partial x} + V_2 \frac{\partial}{\partial y} + V_3 \frac{\partial}{\partial z}$

X_i = component of the body forces in the i th direction
($i=1,2,3$)

p = pressure

V_i = component of velocity in the i th direction

\vec{V} = the velocity vector with components V_i

μ = viscosity

x_i = cartesian coordinate axes.

For steady one dimensional flow between parallel plates this equation reduces to (neglecting body forces):

$$\frac{\partial p}{\partial x_1} = \mu \left[\frac{4}{3} \frac{\partial^2 v_1}{\partial x_1^2} + \frac{\partial^2 v_1}{\partial x_3^2} \right] \quad (3.2.2)$$

The continuity equation is:

$$\frac{\partial(\rho v_1)}{\partial x_1} = 0 \quad (3.2.3)$$

For an ideal gas, the equation of the state is:

$$p = \rho \frac{RT}{M} \quad (3.2.4)$$

Where:

M = molecular weight of the gas

R = the gas constant

T = absolute temperature

p = absolute pressure.

Substitution of equations 3.2.3 and 3.2.4, into equation 3.2.2 yields equation 3.2.5 which is 2nd order, non-linear partial differential equation:

$$\frac{1}{V_1} \frac{\partial T}{\partial x_1} - \frac{T}{V_1^2} \frac{\partial V_1}{\partial x_1} = \frac{\mu M}{\rho_0 V_0 R} \left[\frac{4}{3} \frac{\partial^2 V_1}{\partial x_1^2} + \frac{\partial^2 V_1}{\partial x_3^2} \right] \quad (3.2.5)$$

Where ρ_0 and T_0 are density and temperature at some reference point respectively.

For incompressible flow $\partial \rho / \partial x = 0$, and the continuity equation becomes:

$$\frac{\partial V_1}{\partial x_1} = 0 \quad (3.2.6)$$

and equation 3.2.2 reduces to:

$$\frac{\partial p}{\partial x_1} = \frac{\partial^2 V_1}{\partial x_3^2} \quad (3.2.7)$$

To evaluate compressible flow, equation 3.2.5 should be solved. Illingsworth (1950) and Pai (1956) could not find a closed form solution for a plane Poiseuille flow of a compressible fluid which is of interest here. Numerical solution of equation (3.2.5) will not be useful because at this stage an expression for the elemental volume, that can be later integrated in space and time is needed.

However, it is a common practice (e.g. Rose, 1960; Klinkenberg, 1941) to assume that equation 3.2.6 is also valid for compressible flow. This assumption is considered valid here.

Equation 3.2.7 can be easily integrated as pressure is independent of the x_3 -axis. For flow through parallel plates (Figure 3.1) with no slip ($v_1=0$ at $x_1=0$ and $x_1=e$) integration results in:

$$v_1 = \frac{1}{2\mu} x_3 (e-x_3) \frac{dp}{dx_1} \quad (3.2.8)$$

where e is the width. The mean velocity can be found by:

$$\bar{v}_1 = \frac{1}{e} \int_0^e v_1 dx_3 = \frac{-e^2}{12\mu} \frac{dp}{dx} \quad (3.2.9)$$

This is the familiar parallel plate flow equation that has been derived by numerous investigators.

In the case of flow of gases equation 3.2.9 is valid for general orientation of the parallel plates because the effect of gravity can be neglected. On the other hand for liquid flow, gravity is an important body force and cannot be neglected. It can be shown (Gale, 1975) that by including gravity, 3.2.9 becomes:

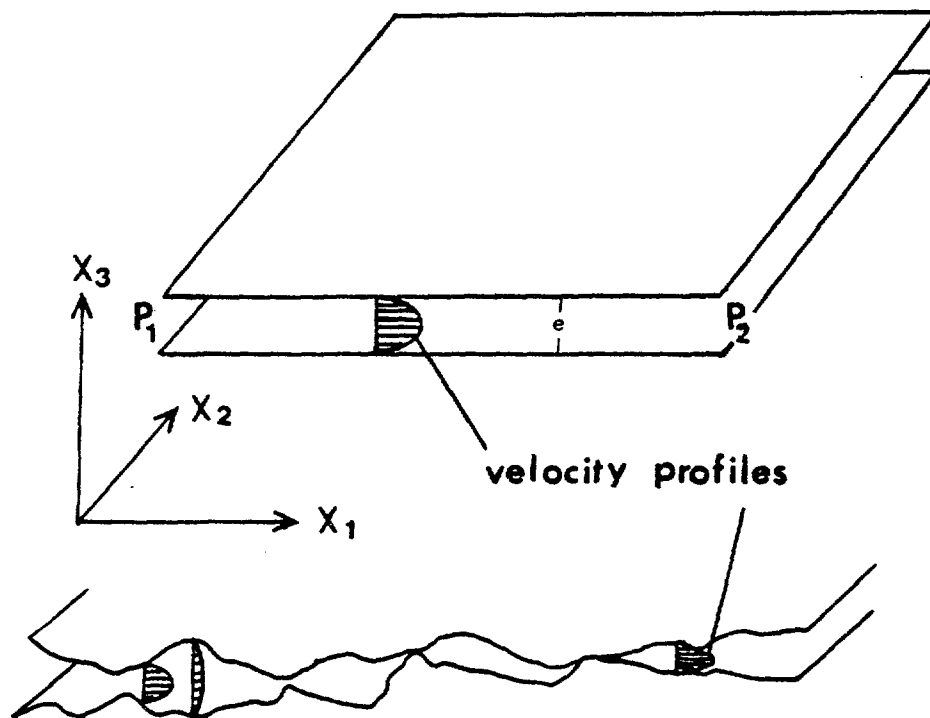


FIGURE 3.1. Schematic diagram showing flow through parallel plates and a natural fracture.

$$\bar{V}_1 = \frac{-e^2 \rho g}{12\mu} \frac{\partial \phi}{\partial x_1} \quad (3.2.10)$$

where

$$\phi = \frac{p}{\rho g} + Z \text{ is the piezeometric head.}$$

Equation 3.2.10 may be considered as the general equation of flow through parallel plates, however, throughout this paper wherever the flow of an ideal gas is concerned, equation 3.2.9 will be used.

Integration of equation 3.2.7 between the boundaries gives the flow rate per unit width (q_1):

$$q_1 = -\frac{\rho g e^3}{12\mu} \frac{\partial \phi}{\partial x_1} \quad (3.2.11)$$

This equation is of fundamental importance, as it is analogous to D'Arcy's equations of flow through porous media and capillary tubes.

By comparison to D'Arcy's equation:

$$q_i = -KA \frac{\partial \phi}{\partial x_i} \quad (3.2.12)$$

the coefficient of permeability (K_{pp}) of the parallel plate model can be written as:

$$K_{pp} = \frac{\rho g e^2}{12\mu} \quad (3.2.13)$$

from which the intrinsic permeability becomes

$$k_{pp} = \frac{e^2}{12} \quad (3.2.14)$$

These equations are the basis for the development of the concept of "the equivalent porous media" for fractured media which was reviewed in the foregoing sections.

3.2.2 TWO PHASE FLOW.

The purpose of this section is to review some basic concepts of unsaturated flow through fractures. A sound theoretical model simulating two phase flow through fractured rock does not exist at this writing and development of such a theory will not be attempted because lack of experimental data would render any such development speculative. However it was deemed essential to consider certain aspects of the theory of the two phase flow in fractured rocks in order to be able to interpret the results obtained in this investigation. The phases considered here are a gas (air, nitrogen or carbon dioxide) and a liquid (water).

Consider a pair of flat glass plates put together to simulate a fracture. Where one edge of this plate is submerged in water, (as shown in Figure 3.2) water will rise to a height h_c above the free water surface. From force equilibrium, this height is given by:

$$h_c = 2\sigma_{gl} \frac{\cos\theta}{e\rho g} \quad (3.2.15)$$

where $\cos \theta = (\sigma_{sg} - \sigma_{sl})/\sigma_{gl}$ from Young's equation, and:

σ_{ij} = interfacial tension between substances i and j with subscripts s, l and g referring to solid, liquid and gas (here glass, water and air) respectively.

θ = angle between σ_{gl} and solid surface measured in the liquid.

ρ = density of liquid (gas density is ignored here)

g = acceleration due to gravity.

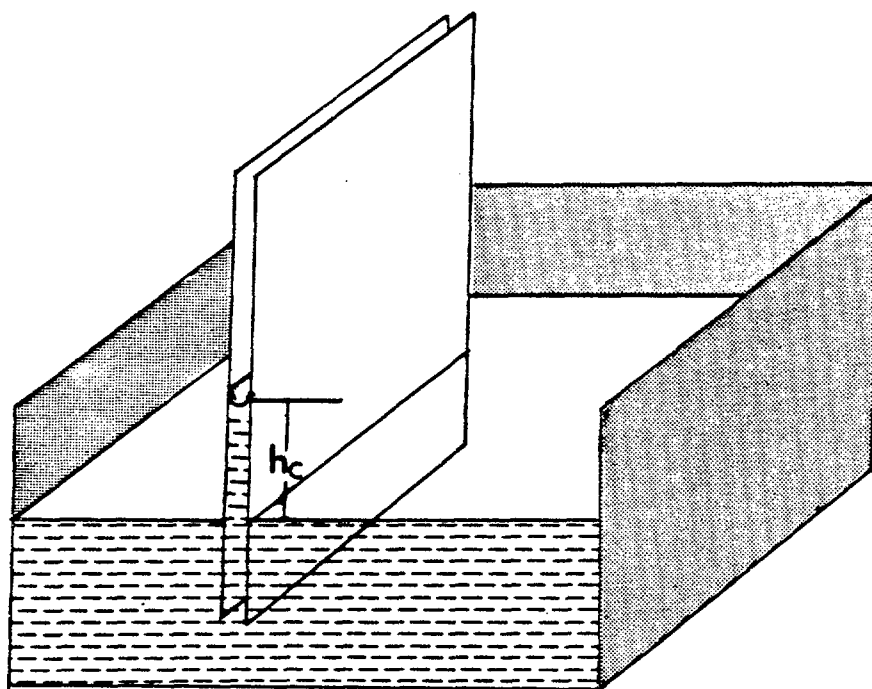


FIGURE 3.2. Capillary rise in a parallel plate model.

Equation 3.2.15 may be written in terms of pressure:

$$p_c = \frac{\sigma_{gl} \cos\theta}{\frac{1}{2} e} \quad (3.2.16)$$

where p_c is the capillary pressure between air and water. Comparing this with the general equation for capillary pressure between two fluids (Bear, 1972; and Morel-Syvetoux, 1969)

$$p_c = \sigma_{12} \cdot (1/r' + 1/r'') = 2\sigma_{12}/r^* \quad (3.2.17)$$

where r' and r'' are radii of curvature in two orthogonal directions, it can be seen that in fractures, r^* is equivalent to $(e/2)\cos\theta$. This is obtained by setting r'' equal to infinity in eq. 3.2.17.

If the plate is removed from the water, but its verticality is maintained, the water level will fall to a distance h_c from the edge. This is because at the edge both r' and r'' are infinite and there is zero capillary pressure at the edge. This is of significance in narrow fractures which intersect wider fractures in an unsaturated fractured medium. That is to say in vertical unsaturated fractures, if assumed as parallel plates, water continues to flow downwards until it either reaches the saturated zone or another fracture with larger aperture.

However, fractures are not planar-parallel plate conduits. The contacts between asperities act as grain contacts in a sand and form restricted passages. In the unsaturated stage, water is held against gravity by these restricted passages. This is one case where the parallel plate analogy loses its value as a modelling tool. It is important to note that even a discrete model consisting of varying aperture-parallel plates cannot model such a system; because the latter system is incapable of holding water against gravity. Nevertheless, the former system is extremely similar to a two dimensional elongate porous medium, and for this reason it is believed that some of the concepts of two dimensional flow through porous media would apply to that of a fractured medium which has solid matrix blocks. However, as will be discussed later, there are few similarities between a porous medium and a double porosity medium.

Some terms can be borrowed from porous media literature (see e.g. Bear, 1972) to facilitate discussion as well as preventing redundancy and confusion.

In the two phase flow through geologic formations, one of the phases is normally a wetting phase. In case of water and air system, water is normally the wetting fluid. A fluid is said to be wetting when $\theta < 90^\circ$ (measured in the fluid in consideration). In this dissertation only the water-air system is considered and it is always assumed that

the system is preferentially water wet.

At low water saturations (S_w) (above hygroscopic), a film of water is formed on each of the faces of the fracture which are in contact; only at the tip of the touching asperities where they form pendular rings. These are referred to as pellicular sheets (to be distinct from pellicular water). In case of a double porosity medium, the pendular rings around the grains (or crystals) of the matrix are joined together to form pendular nets. This is an important state of saturation for the present study, as it is believed that a majority of the fractures are in this state. In this state, water does not move through the fracture but the pendular nets form routes for any excess water to flow through by sheet flows. In such a double porosity medium water may be moving through the matrix while the fractures are still in the pellicular stage.

When water saturation is increased in the fracture, an equilibrium stage is reached at which a vertical fracture is incapable of holding any more water and flow will initiate. This is referred to as the critical saturation. In a vertical fracture, unless some potential pressure gradient is established, this saturation cannot be increased. On the other hand, a nearly horizontal fracture can be completely filled with water without the existence of any pressure gradient. This is another significant

difference between fractured and porous media. Above the critical water saturation, the state of saturation of water is referred to as funicular.

As is the case with porous media in normal conditions, it is almost impossible to completely saturate a fracture that is initially filled with air and is bound by solid matrices. Part of the gas phase is always trapped in small pockets (largest available openings). The gas is then said to be in insular state and the saturation is referred to as the irreducible gas saturation (S_{g0}). The opposite is also true, the same medium saturated with water cannot be completely saturated with gas as pendular water cannot be removed (irreducible water saturation) unless extremely high pressure gradients are imposed on the system.

As was mentioned earlier, in nature all fractures are bound by porous matrices. In crystalline rocks the porosity of the matrix is formed by extremely small cracks and crystal faces. At a depth below evaporation influence, the matrix may be completely saturated through ages of contact with water, yet at great distances above the ground water table. The reason is that the pellicular water is sufficient to completely fill all the microcracks and capillary forces are great enough to overcome gravitational effects.

In such a system, as far as the fractures are concerned, there is no such thing as irreducible water

saturation. By increasing the air pressure around the pendular rings (at low saturations), water will begin to flow into the matrix until an equilibrium is reached. At this point the pressure around the pendular rings becomes equal to the increased capillary pressure (Figure 9.1). However as soon as the pressure is removed, water will flow back from the matrix to enlarge the pendular rings around the asperities.

This transient behavior is one of the difficulties encountered when testing an unsaturated fracture with a gas. For example, in an attempt to establish a steady state condition, the pressure in the injection zone generally increases as the test is continued. As the pressure increases the water saturation decreases and causes an increase in effective permeability to the gas. In porous media similar effects also occur except that in this case, the effective permeability to the non-wetting fluid increases slightly as the flow rate increases and the residual saturation of the wetting phase is independent of the pressure.

In studying the unsaturated flow through a single natural fracture, there are two situations that are of significance when flow of a gas at low water saturations is considered. One is the "lubrication effect" which was studied by Rose (1960). The other effect is referred to

as "slip phenomena" and was extensively investigated by Klinkenberg (1941) and many others (see Scheidegger, 1960 for references).

Rose (1960) used a parallel plate model with and without eddy pockets to show that at low saturations of a wetting fluid, with higher viscosity than the non-wetting fluid, the volumetric flux of the latter could be higher than when the media are completely saturated with the non-wetting fluid. He refers to this as "lubrication effect," that is, the resistance to flow is smaller with the presence of the wetting fluid. In such a case the relative permeability (effective permeability/absolute permeability) to the non-wetting fluid of the media may be greater than unity.

This is the case when the velocity at the conduit walls is not zero. Here the conduit wall includes the contact between the two fluids.

The case of the slip phenomena is another case where the velocity at the walls of the conduit is not zero even in the case of single phase flow. This phenomenon was explained by Klinkenberg (1941) to be because the average velocity of the gas molecules bouncing back and forth from the walls of the conduit is not zero. He studied the flow of several gases through various porous media and found

the relationship between the permeabilities to a liquid (k_ℓ) and to a gas (k_g) is:

$$k_\ell = k_g \left(1 + \frac{B}{p}\right) \quad (3.2.18)$$

where p is the pressure and B is a constant which depends on the properties of the medium.

This equation indicates that at low pressures the permeability of the porous medium to a gas may be much greater than that of the same to a liquid. Although no experimental results are available for fractures or parallel plate conduits, it is believed that similar effect exists in a fracture.

When a gas is flowing at low pressures through a fracture which has low water saturation, the lubrication and slip have additive effects. Therefore, considerable deviation from D'Arcian flow may occur. Such deviations are significant when testing a medium for its permeability.

Another factor that has not been considered to this point is the mass flow continuity. Gases have a tendency to be adsorbed on the surfaces of the rock. This is referred to as surface adsorption. The larger the specific surface area of the medium, the greater number of molecules would be adsorbed per unit volume of the rock. Therefore, in a complex fracture network and in fractures that are filled with fine argillaceous material, a considerable amount of

the gas may be adsorbed by the medium. The effect is that the medium is acting as a sink by itself and the right side of the equation (3.2.3) is no longer zero. The amount of gas adsorbed is very small compared to the mass that is injected for permeability testing, except at low gas concentrations (low pressures). Nevertheless, when a porous or fractured rock is being injection tested it is advisable to use a gas that already occupies the media. For example, nitrogen would be a suitable gas for an air-filled medium.

The foregoing discussion reveals some of the problems that are involved with interpretation of a gas injection test conducted in an unsaturated fractured rock. When a high conductivity, unsaturated fracture is injected with nitrogen, the effective permeability at low pressures may be higher than the permeability to a liquid. At higher pressures, the effective permeability may become lower than the permeability to a liquid. This pressure is near the threshold pressure, that is, the pressure required to displace a considerable amount of the wetting phase. As the steady state pressure is increased above the threshold pressure, the effective conductivity increases and approaches the conductivity to a liquid. Therefore, if the pressure-permeability trend, obtained from a range of steady state injection tests, is extrapolated to the infinite pressure,

the permeability to a liquid can be reliably approximated.

In case of a low conductivity fracture, the initial areal saturation of the fracture is high. Therefore, the effective permeability is very low and the Klinkenberg effect cannot cause it to exceed or even approach the liquid permeability. The effective permeability to the gas increases with increase in pressure, but is always smaller than the liquid permeability. An extremely high pressure is required to reduce the saturation of the wetting phase to zero. Such pressure is not desirable as it would cause fracture deformation. Nevertheless, the pressure-permeability trend may be extrapolated to the infinite pressure to estimate the liquid permeability.

3.3 Summary

The parallel plate analogy of fractures is invalid for both one phase and two phase flow. An "equivalent" parallel plate may, however, be used to model single phase flow through a fracture. For two phase flow it is suggested that an equivalent two dimensional (tabular) porous medium be used. Gas flow through an unsaturated fracture is affected by the slip phenomenon and lubrication effect. These effects may cause enhancement of the conductivity of the fracture.

Theoretically, when an ideal gas is injected into an unsaturated fracture, with increase in pressure the effective conductivity may:

- a) increase due to increase in gas saturation;
- b) become equal to the saturated conductivity;
- c) exceed the saturated conductivity due to lubrication and Klinkenberg effects, and
- d) decrease to the saturated conductivity.

Some of these steps may be absent, depending upon the nature of the fracture.

4. GEOLOGIC ENVIRONMENT OF THE EDGAR MINE

4.1 Introduction.

The Edgar Mine, the experimental mine of the Colorado School of Mines, is located northwest of the town of Idaho Springs, about 65 km (40 miles) west of Denver, Colorado. Figure 4.1 shows the plan view of the mine at the 2400 m (7880 ft.) level. The CSM/ONWI room, located as shown, was excavated during the summer of 1979 for installation of a thermomechanical test facility. Careful smooth-wall blasting techniques were used to create the opening (Holmberg, 1981; Hustrulid, et al., 1980). This room is approximately 100 m (300 ft.) below the ground surface and is 30 m (100 ft.) long, 3 m (10 ft.) high, and 5 m (15 ft.) wide as shown in Figure 4.2. Forty-five NX boreholes were diamond drilled in and around the room shortly after its excavation. Forty-two of these were drilled from inside the room in six radial sets. The seven holes of each set are arranged as shown in Figure 4.2b. The west side of the room is paralleled by three longitudinal boreholes drilled from A-left that extend the entire length of the room.

For convenience of reference, boreholes are designated according to their position. PA-1 through PA-3 are longitudinal boreholes drilled parallel to the central axis of

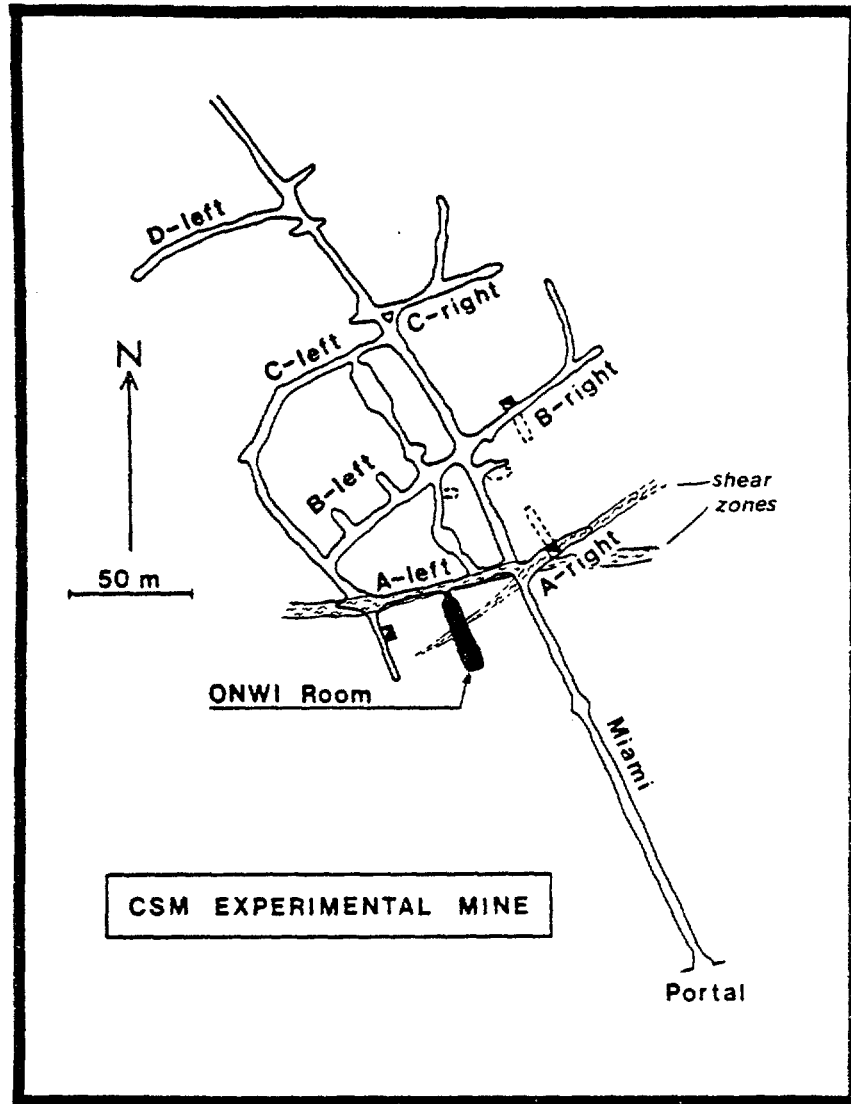


FIGURE 4.1. Site of Experimental Room. (Source of base map: Van Huffel, 1975).

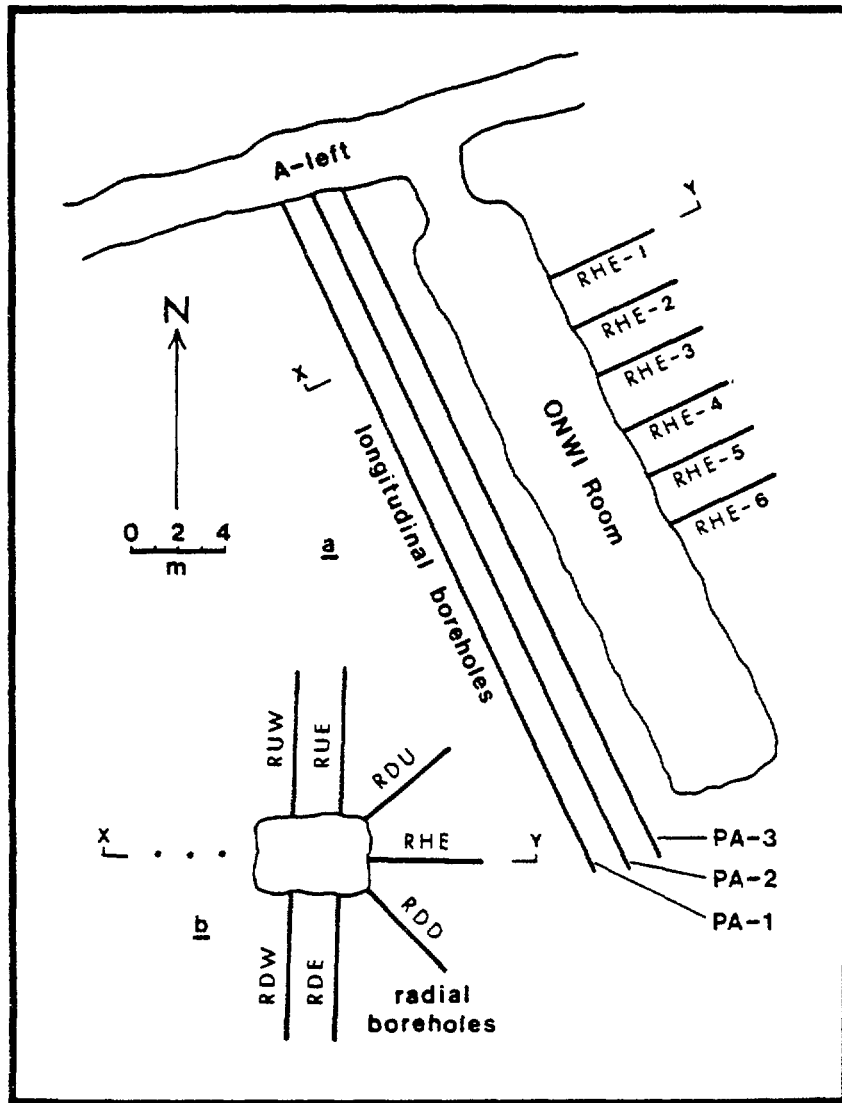


FIGURE 4.2. Plan view of the CSM/ONWI Room, with key to borehole names.

the room (Figure 4.2a). The labels of the radial boreholes start with letter R and the second letter indicates whether they are uphole (U), downhole (D) or horizontal (H). Diagonal upholes are designated as RDU and diagonal downholes are referred to as RDD. The last letter shows in which side of the room they are drilled (E - east and W - west). The rings are numbered from 1 to 6 starting at the entrance of the room.

4.2 Geologic Setting of the Edgar Mine.

Idaho Springs is located in the east-central portion of the Front Range in the Southern Rocky Mountain physiographic province and on the southeastern edge of the Colorado Mineral Belt (Lovering and Goddard, 1950). The eastern flank of the Front Range in this area consists mainly of Precambrian granitic rocks, paragneisses and paraschists, and associated metaigneous formations (Boos, 1954). The rocks have undergone great deformations and intense alterations.

During the Precambrian, the region was subjected to a long period of regional metamorphism involving two stages of plastic deformation (Sheridan and Marsh, 1976). This was followed by three periods of igneous activity during which the Boulder Creek, Silver Plume, and Pikes Peak granites, and their associated rocks, were intruded.

These events were followed by late Precambrian to late Cretaceous epeirogenic movements which were interrupted by a taphrogenic event in late Paleozoic time (Grose, 1972) which resulted in the formation of the Ancestral Rocky Mountains.

The Laramide Orogeny, which caused the formation of the majority of the obvious structures in the Rocky Mountain region, lasted from Late Cretaceous through Eocene. Late Cenozoic epeirogenic movements followed this orogeny which was interrupted locally by taphrogenic block faulting.

The local geology of the Idaho Springs and Central City areas has been extensively studied by numerous investigators, (Lovering and Goddard, 1950; Boos, 1954; Sims, et al., 1958; Harrison and Wells, 1959; Harrison and Moench, 1961; Moench et al. 1962; Moench, 1964; and Sheridan and Marsh, 1976). An excellent review of the works pertinent to the experimental site has been prepared by Hutchinson (1981).

The experimental mine is structurally located to the northwest of the Idaho Springs anticline, which is asymmetric with its axis trending approximately N55E, and to the northeast of the Idaho Springs Fault which trends approximately N60W. The main rock types are Precambrian granite gneiss and pegmatites, quartz gneiss, biotite gneiss, amphibolite, and Tertiary porphyry dikes. Three nearly vertical joint sets were reported by Harrison and Moench

(1961) for this area:

- a) striking N15W and dipping 85SW, which will be referred to as "regional cross joints";
- b) striking N55E and dipping 80NW, which will be designated as the "regional diagonal joints"; and
- c) striking N75E and dipping 80NW, which coincides with the general trend of the foliation and will be referred to as "foliation joints".

The large fractures (faults and shear zones), however, form a vertical conjugate system with strikes of about N60W and N55E. The major principal stress responsible for this system should have been horizontal and trending east-west with the intermediate principal stress being vertical. The origin of this tectonic stress system is attributed to the Laramide Orogeny (Harrison and Moench, 1961). Knowing that this orogeny was followed by a different tectonic stress system (post-Laramide epeirogeny with a vertical major principal stress according to Grose, 1972), it is not expected that any of the residual stresses attributable to Laramide orogeny can be detected. However, the persistence of a fracture system that can be related to a specific geologic

event is of paramount importance in studying the trends of regional migration of contaminants in hydrogeological domains of crystalline rocks.

4.3 Geology of the CSM/ONWI Room.

Many small, tight folds associated with migmatization can be seen on the walls of the room (Figure 4.3). The rock around the room is strongly foliated with the foliation striking N70E and dipping 70NW. The main rock type is a medium to coarse-grained (quartz monzonite migmatite)* and occasionally fine-grained migmatite biotite gneiss. Figure 4.4 is a horizontal geologic section through the room at one meter above the floor, in the plane containing the three longitudinal boreholes. Figures 4.5 to 4.10 are a series of vertical geologic sections drawn through the planes of rings 1 to 6 of the radial boreholes (Figure 4.2).

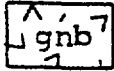
A pegmatite body of irregular shape occurs in the south end of the room (Figure 4.4). This feature can be consistently observed at the end of each longitudinal borehole, with its vertical northern contact striking N25E. The extent of this pegmatite body to the south and west is

*All petrographic identifications were made by examination of hand specimens.

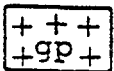
FIGURE 4.3. A portion of the west wall of the CSM/ONWI Room. Note the pygmatic folding in the migmatite biotite gneiss (photo about two meters across).

EXPLANATION

(For Figures 4.4 to 4.10)



Black to white, banded, fine to medium and occasionally coarse-grained, migmatite biotite gneiss (biotite quartz monzonite migmatite). Percentage of quartz and feldspar varies considerably. Ptygmatic folding is abundant in this unit.



Light grey to white, medium to very coarse-grained, granite pegmatite. Quartz content varies considerably and may be as much as 90% in an irregular body in the roof rock (round 3).



Greenish black, very fine to fine-grained chloritized hornblende biotite-gneiss. Foliation is very inconspicuous to slightly schistose.



Alteration zones (hatchures overlay the original rock type) - mostly chloritization with minor sericitization.

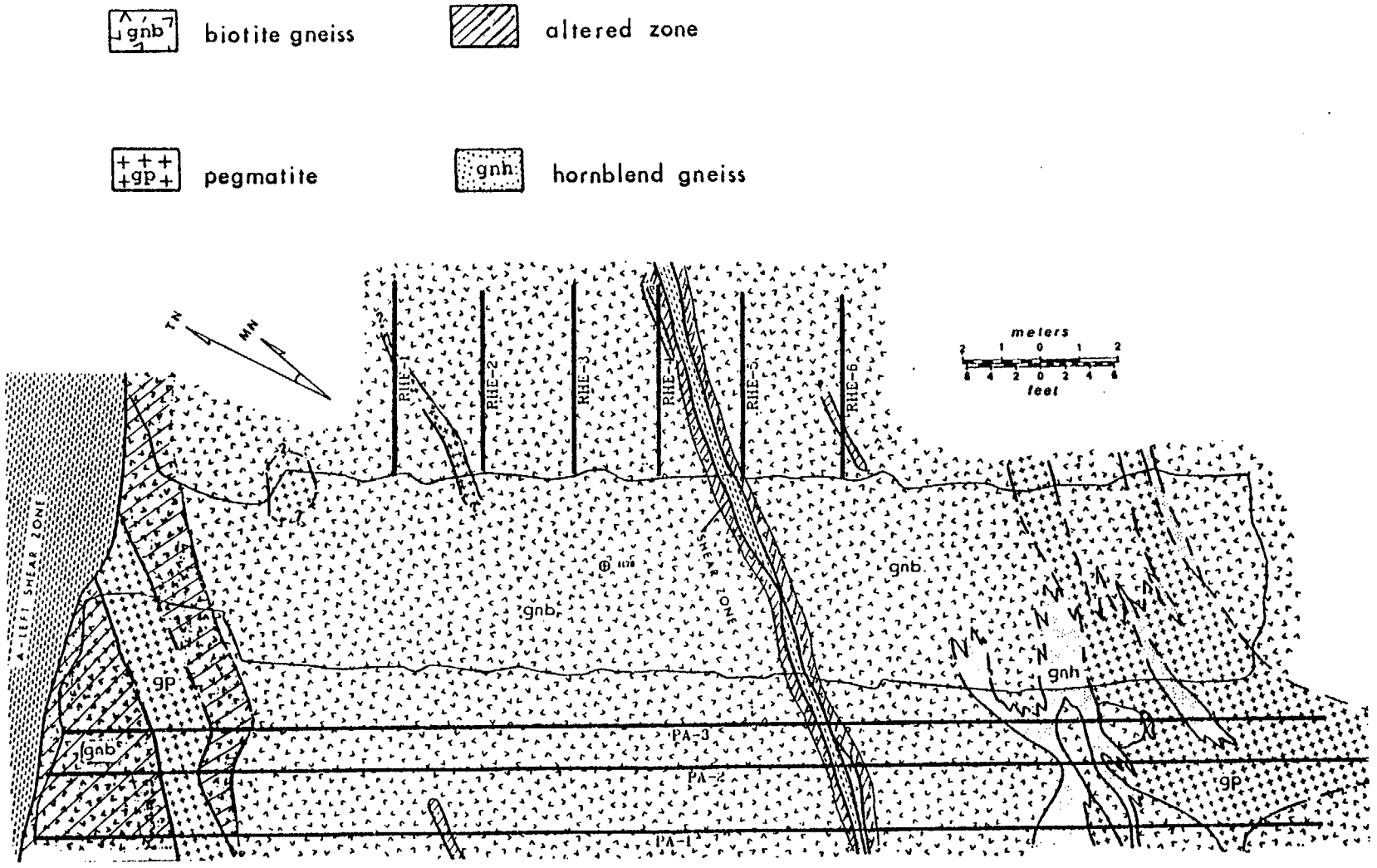


FIGURE 4.4. Horizontal geologic section through the ONWI Room.

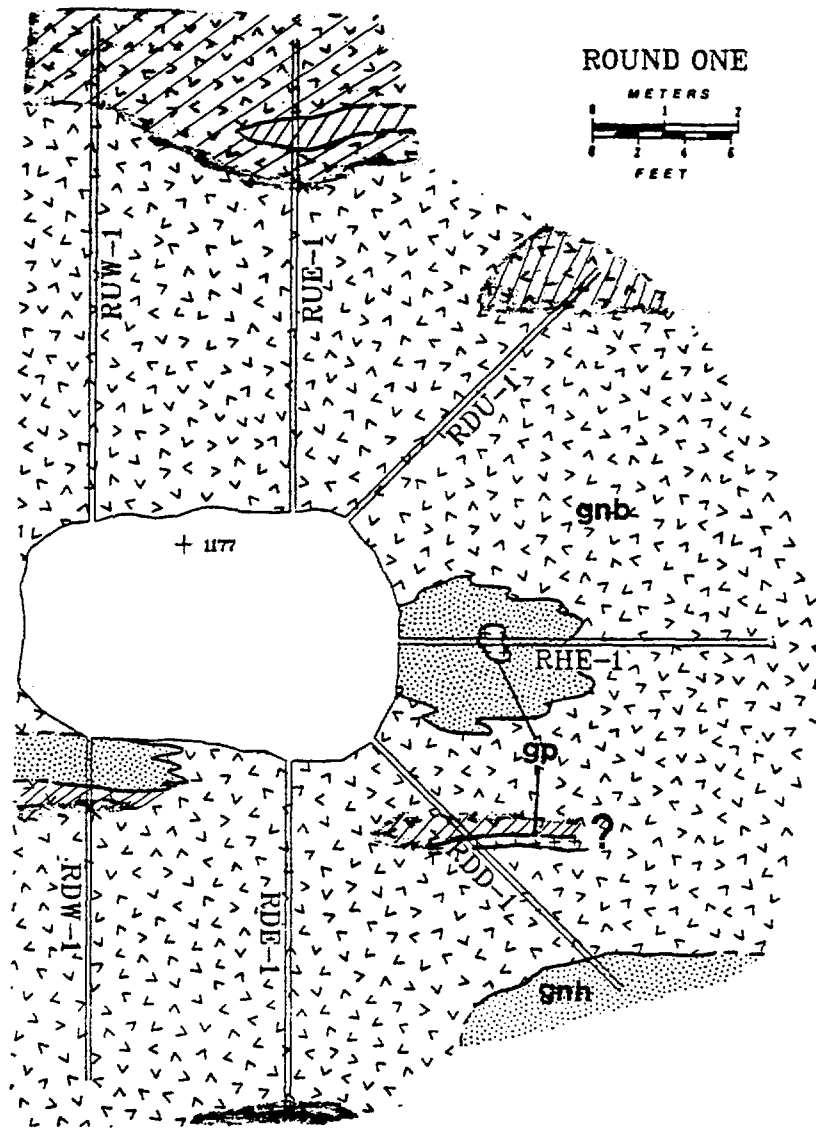


FIGURE 4.5. Geologic cross-section through the first round.

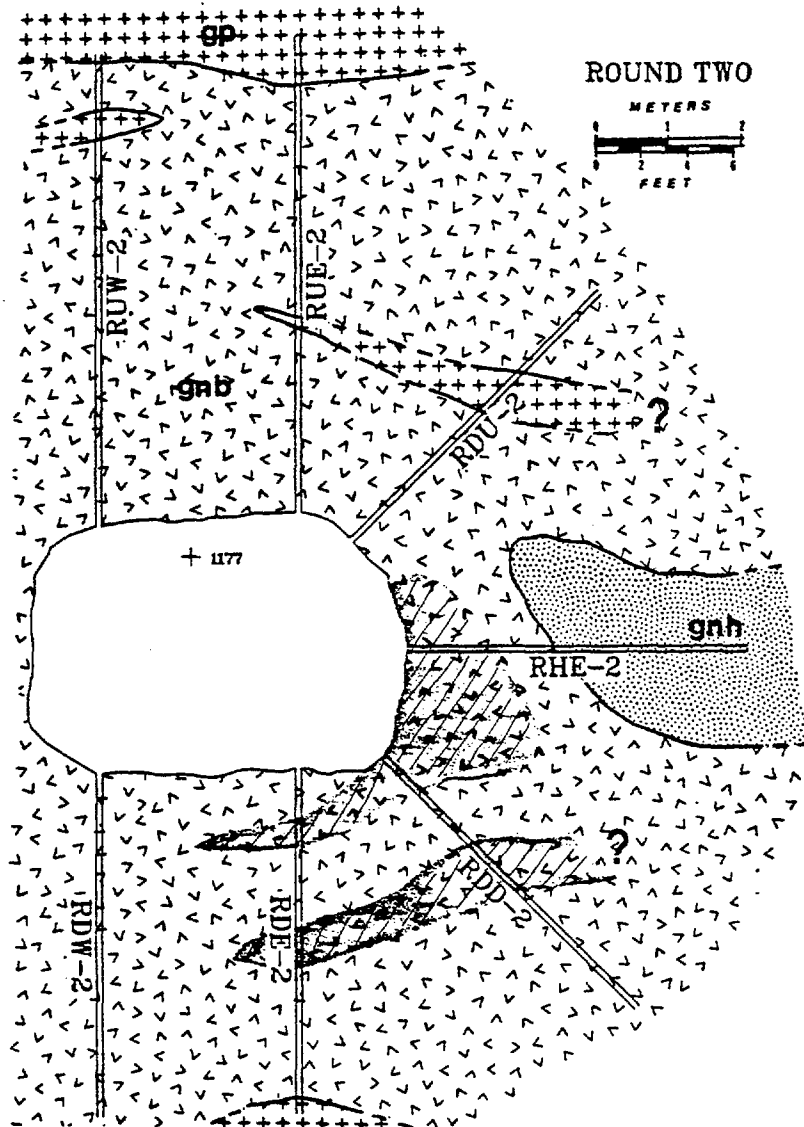


FIGURE 4.6. Geologic cross-section through the second round.

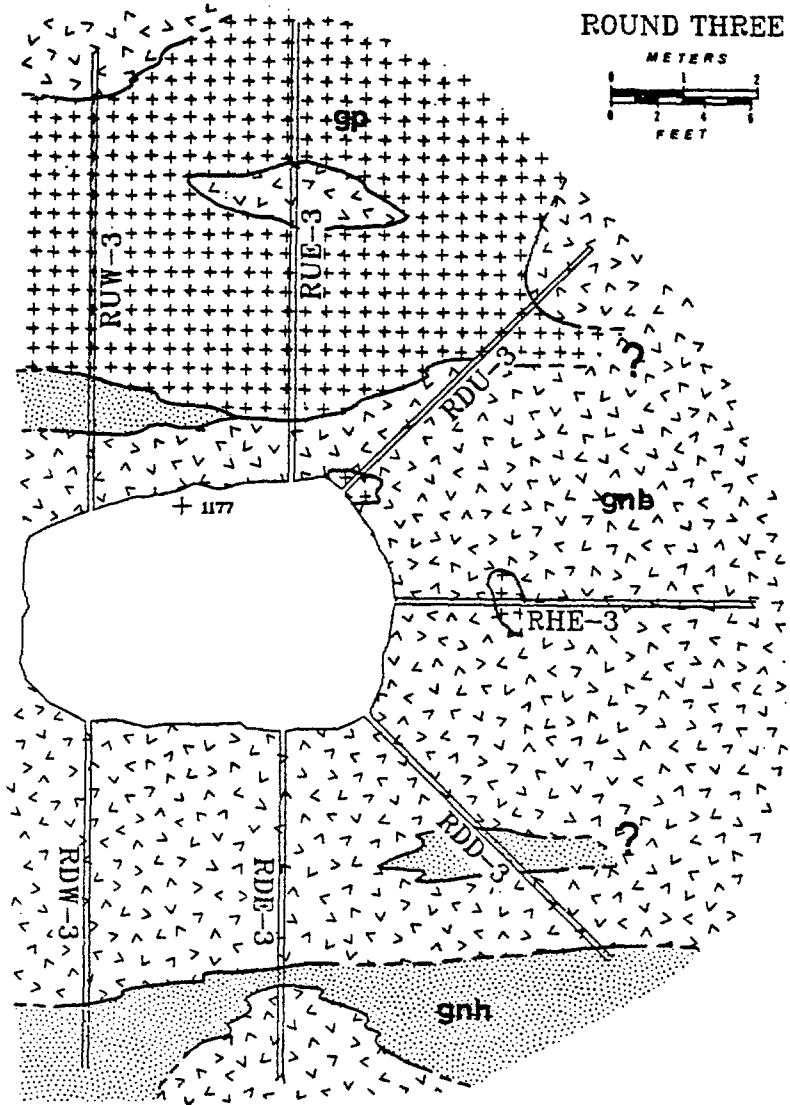


FIGURE 4.7. Geologic cross-section through the third round.

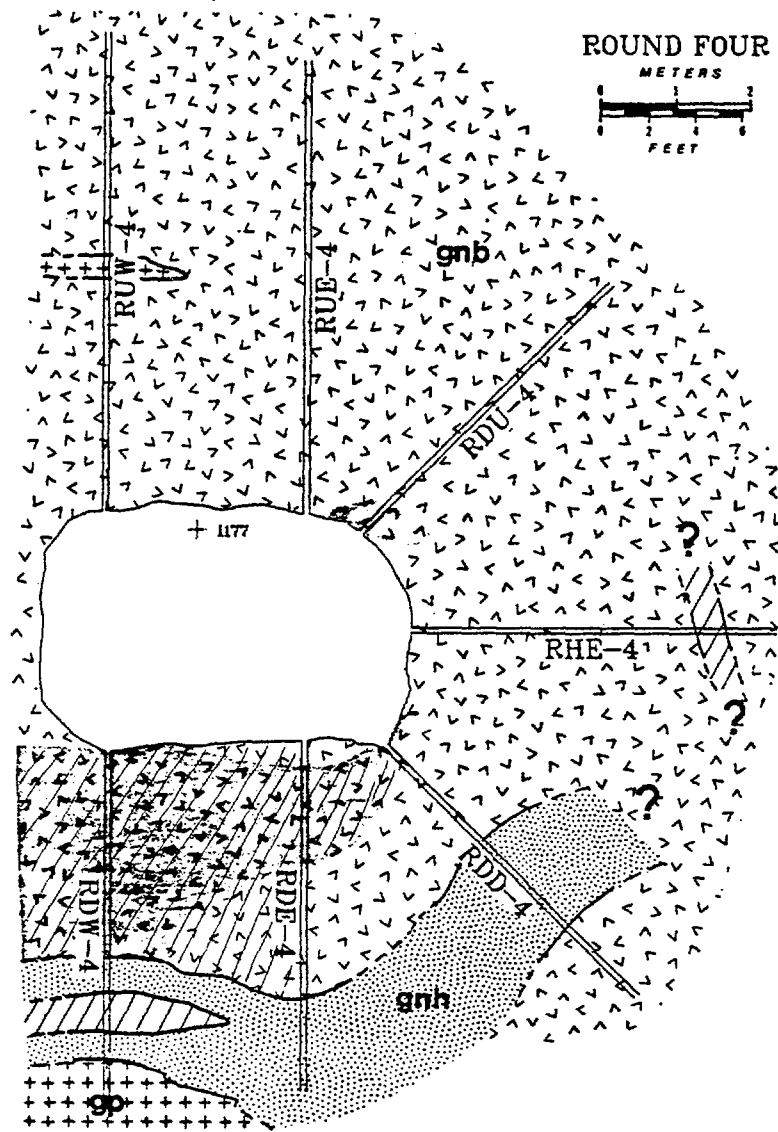


FIGURE 4.8. Geologic cross-section through the fourth round.

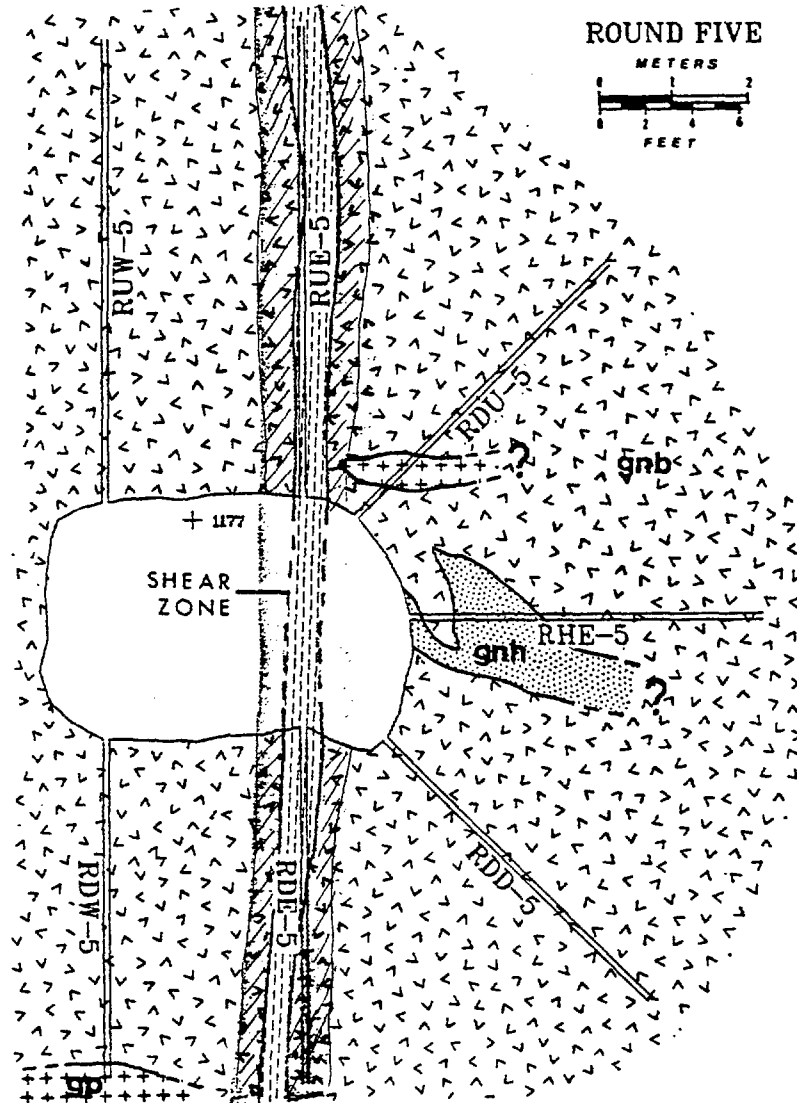


FIGURE 4.9. Geologic cross-section through the fifth round.

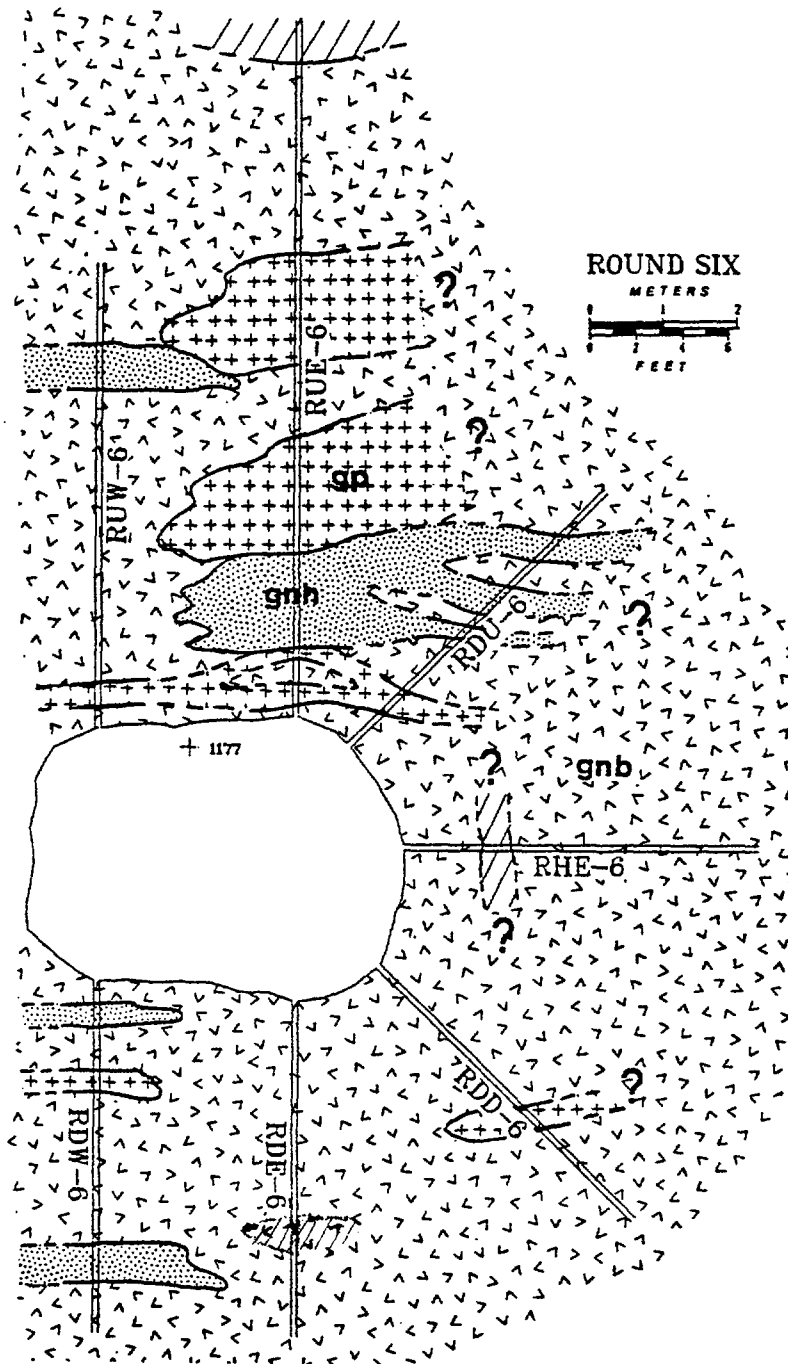


FIGURE 4.10. Geologic cross-section through the sixth round.

unknown. Closely associated with it is a fine- to very fine-grained, greenish-black hornblende biotite-gneiss which has a somewhat lenticular shape at its exposure on the west wall of the room and has a very poorly developed schistosity.

In the horizontal section (Figure 4.4), the contrast that can be seen in the vertical sections (Figures 4.5 to 4.10) cannot be seen. This is not a mapping problem, as equal efforts were spent in mapping all sections, rather it is the details of the variation in the horizontal direction that has caused the geologist to lump the rock type as a migmatite-biotite gneiss (gnb). In the horizontal interval between rounds one and six, there are hundreds of alternations between quartz-rich and biotite rich layers one to five cm thick. Therefore, in this interval this rock type may be classified as an anisotropic-homogeneous rock, whereas looking at the vertical sections one would definitely call the rock heterogeneous. This is of great significance in exploration drilling, especially for radioactive waste repository siting. Because the majority of the preliminary boreholes would be drilled vertically, great bias about the heterogeneity of the potential host rock may be introduced.

Another pegmatite body exists in the roof rock between rounds 2 and 3 (Figures 4.6 and 4.7). This body is richer in quartz and poorer in mafic minerals than the pegmatite

body to the south. However, its close association with a very fine-grained biotite gneiss is evident in these figures.

Heterogeneity of the rock can be clearly seen between the vertical sections (Figures 4.5 to 4.6) and the horizontal section (Figure 4.4). No smooth-gradual change in rock type can be seen from north to south. Round one (Figure 4.5) is closest to the A-left shear zone and the rock is more strongly altered. The percentage of the pegmatitic rock is higher in rounds two, three, and six. It should be noted that abundance of pegmatitic rock in one section does not necessarily mean that those areas of the room are richer in pegmatite. Most of the pegmatitic bodies are tabular in shape (a characteristic of migmatitic rocks), and lie nearly parallel to the plane of the radial boreholes. Therefore, it is possible that a radial borehole may follow such tabular bodies for a considerable distance. Nevertheless, these vertical sections may statistically represent the abundance or rareness of a rock type.

A near-vertical shear zone of about 3 m (10 ft.) width strikes parallel to A-left drift (N65E). The wall rock is slightly altered and chloritization can be observed in core from the longitudinal boreholes to a distance of about 5m (19 ft.) from the collar (Figure 4.4). Although considerable displacement may have occurred along this shear zone, no direct evidence of movement is apparent in the

work area. However, no continuity in geologic features can be seen from the shear zone.

A small shear zone crosses the middle of the room (Figure 4.4). Its extent to the west is unclear. A fracture zone in A-left spur, which coincides with the projected continuation of this shear zone (Figure 4.1), may indicate that it feathers out to the west. Its extension to the east coincides with the A-right shear. It is suspected that two separate vertical shear zones exist (one along the A-left and one along the A-right drift) forming a 35° intersection angle. It is further postulated that both shears feather out and become less distinct to the south.

4.4 Hydrogeologic Characteristics of the Mine.

Observations made by the writer from July, 1979 through January, 1982 suggest that generally there are three distinctive hydrogeological domains. These domains are referred to as (Figure 4.11):

- a) the zone of topographic gradient;
- b) the zone of vertical gradient; and
- c) the zone of regional gradient.

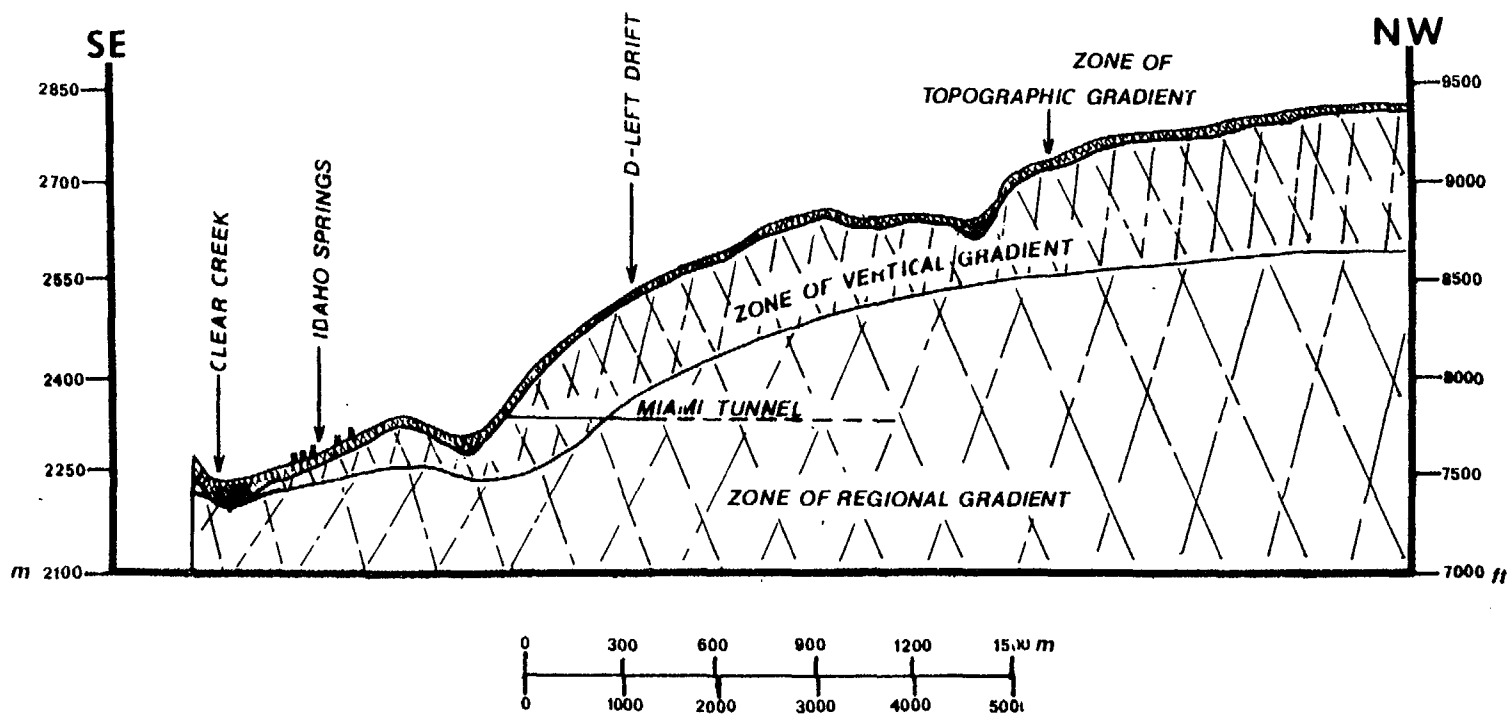


FIGURE 4.11. Schematic cross-section through the Miami Tunnel, showing the hydrogeological zonation of the fractured rocks.

The zones of topographic and vertical gradients define the active zone of Hurr and Richards (1974) and Robinson (1978), while the zone of regional gradient defines their passive zone. The terms used by these authors are somewhat misleading, as the "passive zone" contains active groundwater movements which, although very slow, are significant to underground storage of radioactive waste. On the other hand, the zone of vertical gradient, first used by Gale, et al. in 1977 and significant in evaluating nuclear waste repositories located in the unsaturated zone, is not defined by Hurr and Richards.

The zone of topographic gradient in this area is a thin veneer which may vary from a few meters on the steep slopes to more than 100m (300 ft.) in the valleys. This zone is exposed near the Miami portal (Figure 4.1) and extends about 30m (100 ft.) into the mine. It is also intersected by the A-left raise. This zone is highly permeable due to the enlargement of the fractures by weathering and stress relief. Depth to water table varies considerably during the year and is highly dependent on the meteorological conditions.

The Figure 4.12 photograph, taken early in June, 1980, shows the water flowing from the main portal. The water flow was seen only during months of May and June of 1980 and

FIGURE 4.12. View of the Miami portal showing water outflow during spring 1980. Note creek on left that is usually dry.

1981, with its peak flow occurring early in June. In order to compare this run-off with the precipitation pattern, the mean monthly precipitation at the Squaw Mountain station for the years 1979 through 1982 are plotted in Figure 4.13. The Squaw Mountain station is located approximately 15 km (10 miles aerial distance) to the south of Idaho Springs, and is at 3500m (11,500 ft.) elevation. This station was closed in July 1981 and after this date, data from Cabin Creek station, which is located approximately 50 km (31 miles) to the west, is used with some modification. Average ratios between the mean monthly precipitation of the Squaw Mountain and Cabin Creek stations were found for the years 1979 and 1981. This ratio was then used to estimate the monthly precipitation at the Squaw Mountain station for months following July 1981.

Figure 4.13 shows that the peak precipitation occurs in the month of May. This also happens to be when a warming trend starts in this area. Large amounts of precipitation, a large proportion of which is in the form of snow fall (Montazer, 1978) causes a peak runoff during the latter part of May and early June. This is the time when the out-flow from Miami portal was seen.

Only a few fractures within the first 30m of the Miami tunnel contribute to this flow. Figure 4.14 shows a fracture in this zone from which relatively large amounts of water

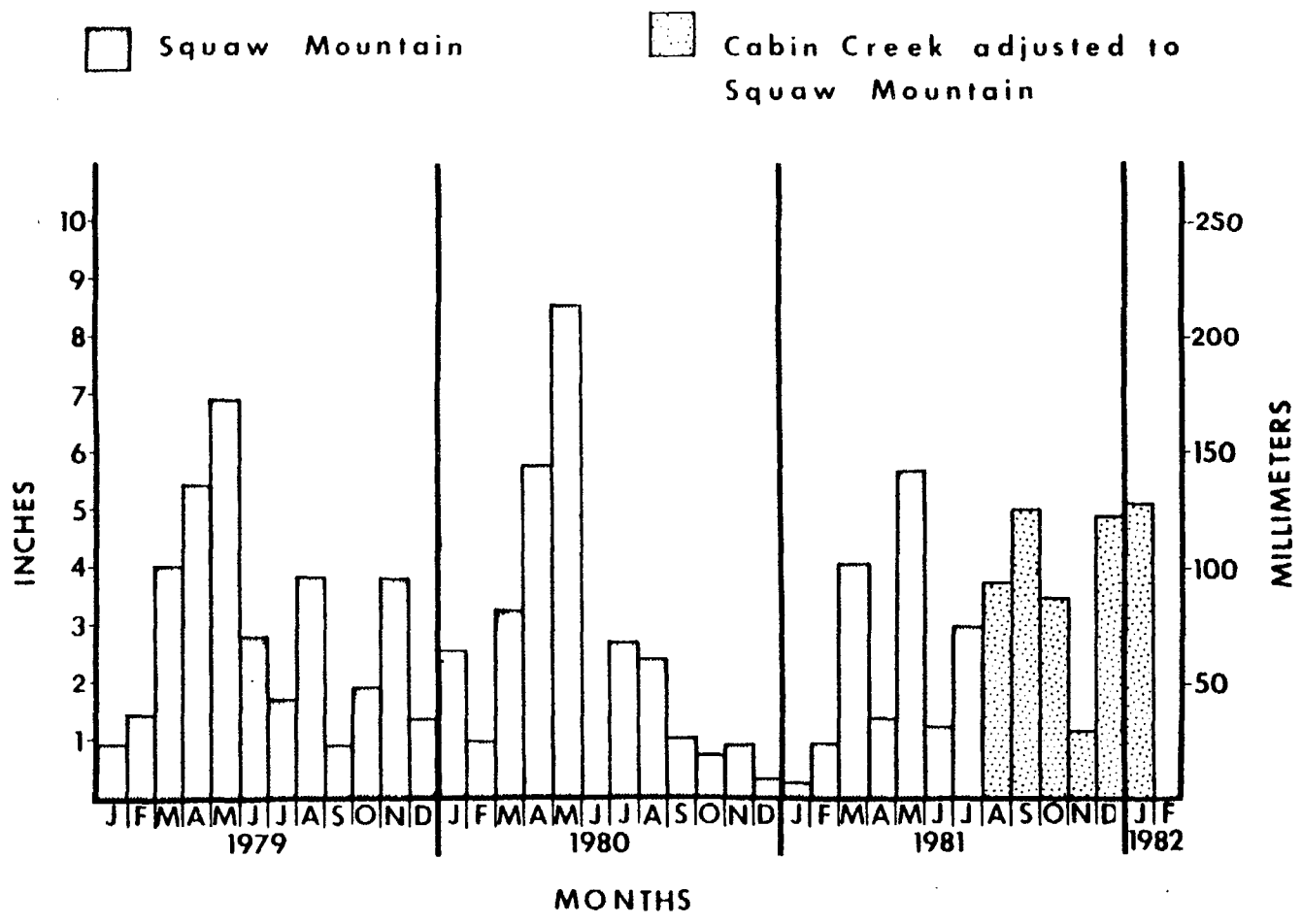


FIGURE 4.13. Monthly precipitation for the Squaw Mountain station. See text for method of converting the Cabin Creek data.

FIGURE 4.14. View 30m inside Miami tunnel showing water flowing from a usually dry fracture.

are being discharged into the mine. However, beyond 30m the mine is completely dry even though major fractures exist beyond this depth. During the time when water was flowing out of the Miami portal, small amounts were also observed flowing from A-left raise into the mine. This water, however, never reached the portal. Close examination of the shaft wall indicated that the seepage into the raise was only from the uppermost 20m immediately below the ground surface. No water was seen to flow from this raise throughout the rest of the year.

The rocks underlying the zone of topographic gradient are less weathered and vertical flow occurs only along major faults and shear zones. The thickness of this zone of vertical gradient may vary from zero beneath the stream valleys to several hundred meters beneath the high mountains. Around the experimental mine the zone of vertical gradient is estimated to be about 300m (1000 ft.) thick.

The permeability and porosity of this zone of vertical gradient decreases with depth. Generally, it has a much smaller permeability than the overlying zone of topographic gradient; therefore, it acts as a semi-permeable barrier. Major fractures in this zone are unsaturated, but the intact rock and fine cracks may be completely saturated. This is because the capillary attractive force in the small cracks and the matrix is greater than the gravitational force.

Therefore, water flow through the matrix and small cracks occurs mostly in saturated condition. This flow exists only when a potential gradient is imposed on these media through transient saturation and desaturation of the adjacent fractures.

The matrix saturation was shown by analysis of samples taken from the CSM/ONWI room (Voegle, 1980, private communication). In addition, whenever the pipes, used for extending the packers, were left inside the boreholes for a few days, water condensate was observed to form on the pipes. At first this was thought to indicate saturated conditions around the CSM/ONWI room; however, when the packers were set inside the boreholes for a few days, no pressure buildup was detectable with transducer sensitivity of 7 Pa (0.001 psi). Therefore, the rock matrix seems to be mostly saturated, while the fractures are unsaturated and drained by gravity.

The amount of flow in the zone of vertical gradient is so small that the rock surface in the mine is kept completely dry by normal evaporation aided by natural ventilation and weekly mechanical ventilation of the mine. In dead end drifts of the mine the rock surface is slightly wet but seepage can only be seen along major shear zones (such as the A-left shear). An indication of long time vertical flow in this zone is that the quartz needles formed along some fractures have hematite and clay residues only on the upper

FIGURE 4.15. Miami tunnel (to the left) and D-left drift (to the right) intersection showing water seepage.

faces of the crystals.

Beyond D-left drift (Figure 5.1) saturation of the rock mass is evidenced by the seepage that can be seen throughout the year. Figure 4.15 shows the wall of the mine in this area from which water flow was observed at all times. This flow is through almost all fractures large and small and does not vary noticeably by season. During the months of December 1981 and January 1982 this flow into the mine increased considerably and other areas that were previously dry showed noticeable water seepage. During these months considerable precipitation was recorded for the area (Figure 4.13). This area in the mine is where the transition occurs between the zone of vertical gradient and the zone of regional gradient. The water table in this zone may be irregular due to heterogeneity of the rock mass. It may vary in slope from near horizontal to near vertical. However, it is believed that a regional continuity in water table probably exists.

Interrelationships between the three zones discussed above is schematically shown in Figure 4.11. The zones of topographic gradient and regional gradient converge and the zone of vertical gradient disappears toward the stream valleys. It should be understood that this condition may not exist in areas with different hydrogeological conditions such as humid areas with rolling topography.

4.5 State of the Stress.

4.5.1 Stresses Around the CSM Experimental Mine.

Several in-situ stress measurements have been made in the past at various locations in the mine. No general agreement exists among the results of these measurements, which El Rabaa (1981) has summarized.

The magnitudes of the major principal stresses vary from 4.1 to more than 13 MPa (600 to 1900 psi) and the plunges are reported to vary from 16° to 53° , while the bearings assume almost any direction. Considering the complexity of the geologic structures existing near the measuring sites and the geometry of the mine workings, it is doubtful that any of these measurements represent the far field (undisturbed) state of stress.

In all cases horizontal stresses were reported to be greater than the vertical stresses by as much as 50%. It is interesting to note that the Clear Creek valley to the south of the portal is twice as deep as the level of the mine. Thus, if any horizontal compressive tectonic stresses exist at depth, their effect would not be detectable at this elevation due to the existence of unconfined (free moving) boundary conditions. In addition, as was noted earlier, it is doubtful that any stresses attributable to the Laramide Orogeny still exist .

Measurements made by El Rabaa (1981) suggest that a small shear zone may have considerable effect on the results of the overcoring stress measurements. It is suspected that gravity loading is predominant in this area and at this depth. Due to the rugged topography, the most probable orientation of the major principal stress axis plunges steeply to the south as shown by El Rabaa.

4.5.2 The State of Stress Around the CSM/ONWI Room.

The CSM/ONWI room is approximately 100m below the surface of the ground; therefore, stress due to gravity loading is expected to be in the neighborhood of 2MPa (300 psi). Results of overcoring of the west wall show a vertical stress of about 2.2MPa (320 psi) and horizontal stress of about 3.1MPa (450 psi) in what is believed to be the undisturbed stress state, since these values were obtained 9m or two room diameters from the wall (El Rabaa, 1981).

Stress elipsoids constructed from some of the overcoring data are shown in Figure 4.16. Note that these stresses are not necessarily the principal stresses, but are the projection of the principal stresses on to the horizontal plane. Directions of the principal stresses are shown in Figures 4.17a and 4.17b. The variation of horizontal stress parallel to the room axis is shown in Figure

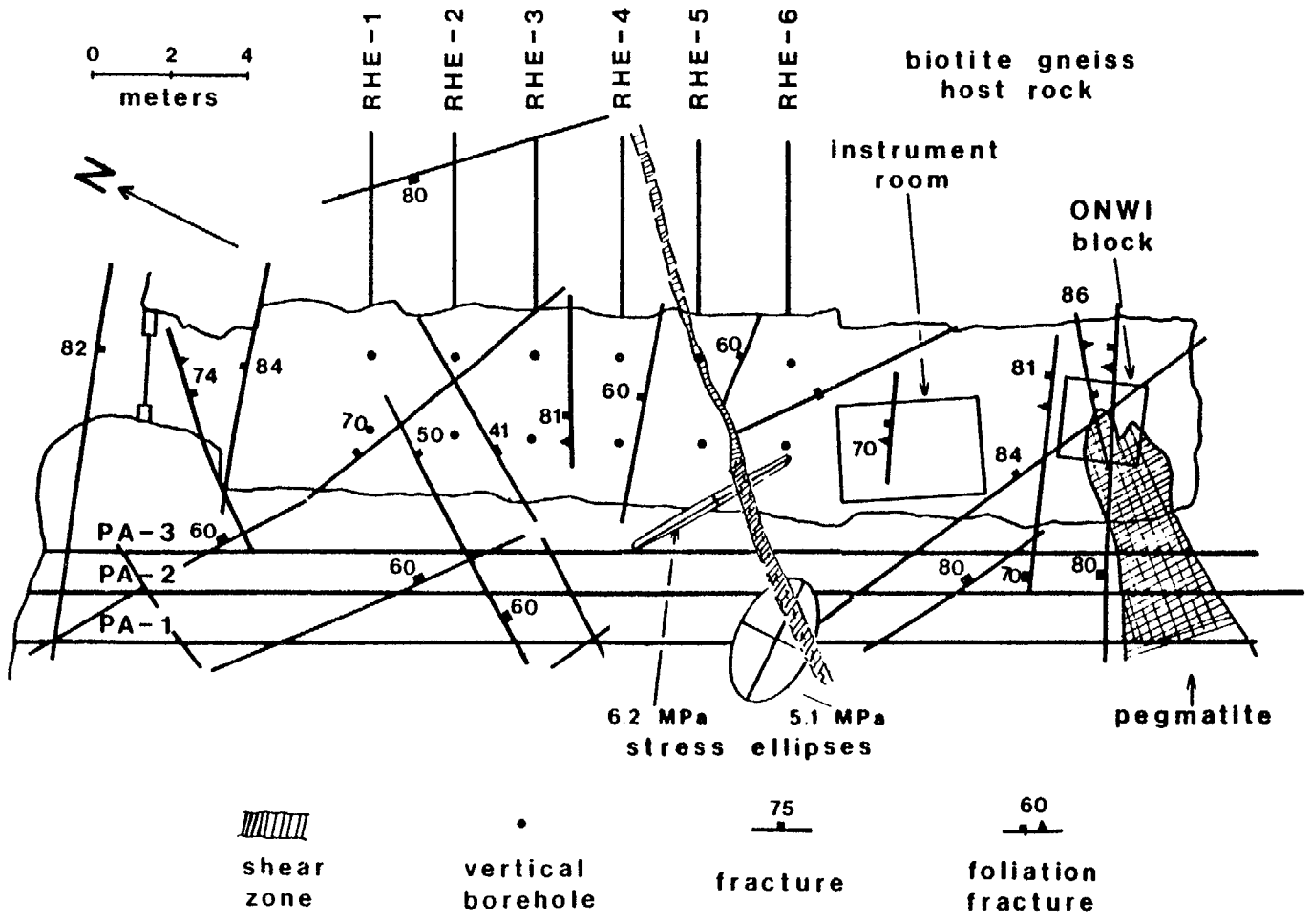


FIGURE 4.16. Simplified geologic map of the CSM/ONWI room showing stress ellipsoids near the shear zone.

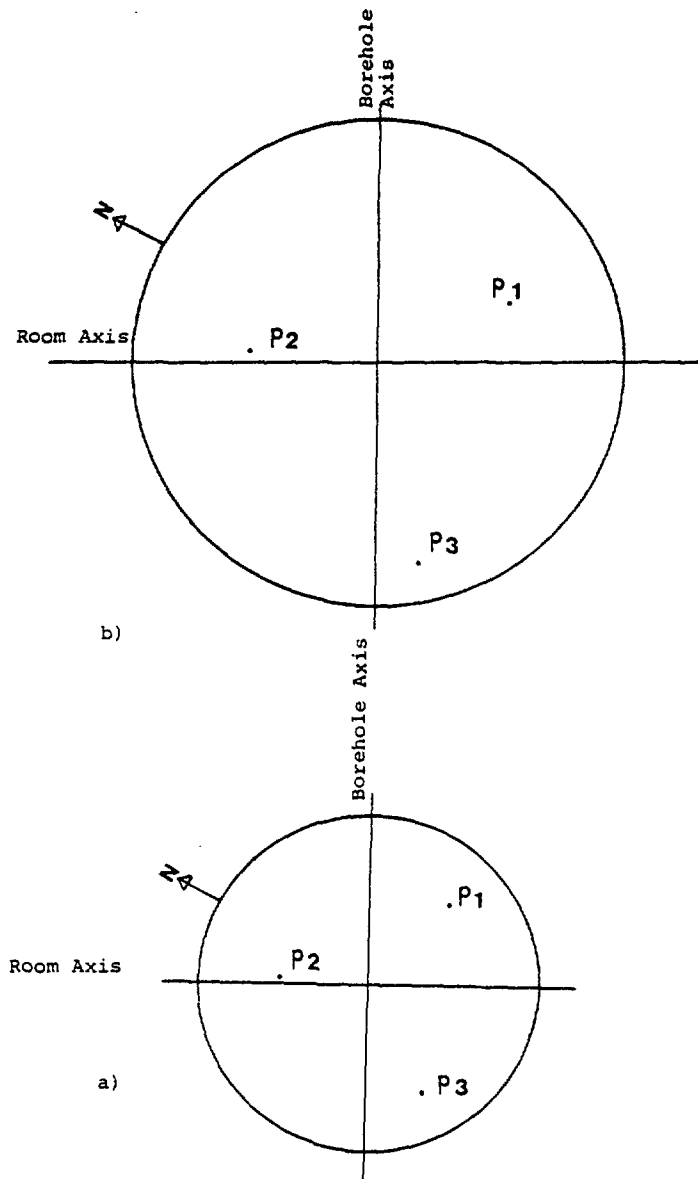


FIGURE 4.17. Stereographic projections of the principal axes of stresses in the west wall, $a = 30\text{cm}$, and $b = 4\text{m}$ from the wall. Radius of the sphere is proportional to the major principal stress. Data from El Rabaa, 1980.

4.18. This stress is normal to the foliation joints, which are the main fractures tested for permeability in the longitudinal boreholes. The stress close to the wall is approximately three times larger than the background stress. The significance of this trend will be discussed later.

4.6 Summary.

The CSM/ONWI room is excavated in migmatite-biotite gneisses of the Precambrian Idaho Springs Formation. The rock is heterogeneous and moderately fractured at the level of the room (100m or 300 ft. below ground surface). The rock is strongly foliated, with foliation striking N70E and dipping 70NW. The main fracture in the room is a near-vertical shear zone of about 30cm width. The rock in the vicinity of the Edgar Mine, in which the room is excavated, is characterized by three hydrogeologic zones:

1. zone of topographic gradient, which is a thin surficial layer of highly weathered and fractured rocks and is the main channel for interflow during the wet season;

2. zone of vertical gradient, which is mostly unsaturated and consists of moderately weathered and fractured rocks. Permeabilities are lower than the overlying zone 1 except along major fractures; and

3. zone of regional gradient, which is the downward continuation of zone 2 but is completely saturated.

At the room level, the virgin vertical stress is estimated to be about 2.2 MPa (320 psi), and the horizontal stress is estimated to be about 3.1 MPa (450 psi).

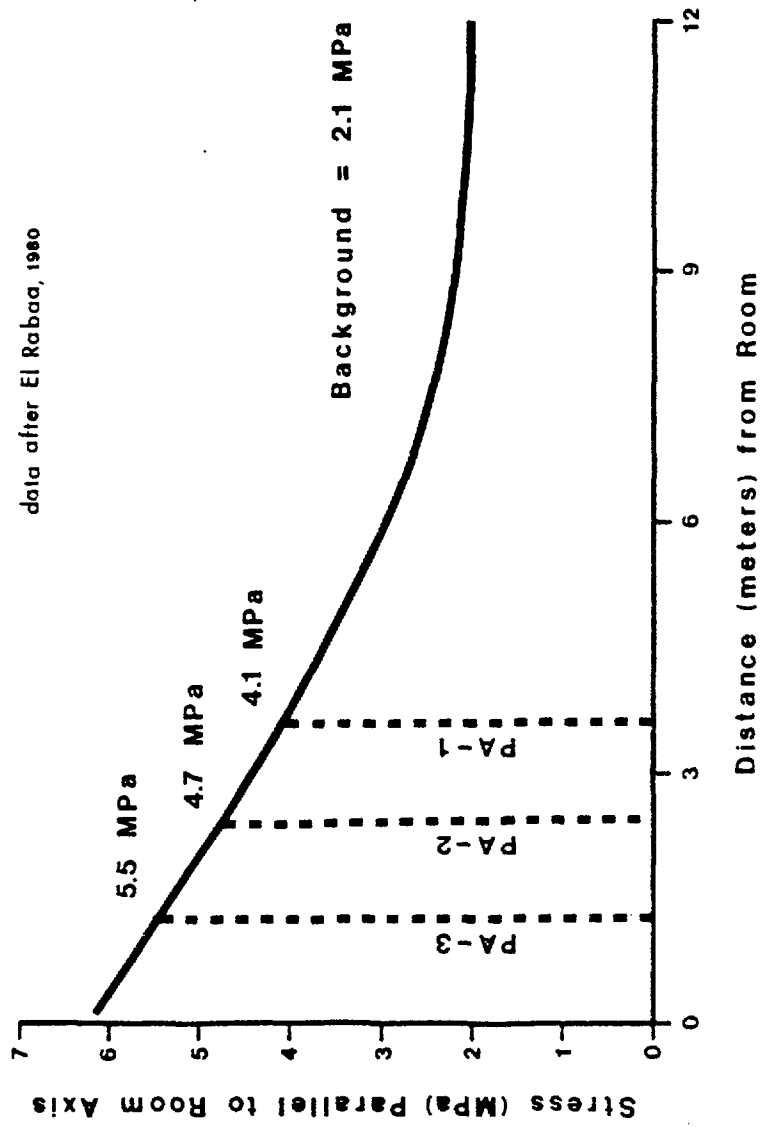


FIGURE 4.18. Variation of axial stress near the opening.

5. FRACTURE CHARACTERIZATION

5.1 A Requirement for Permeability Characterization.

In a situation where the opening already exists, assessment of the effect of underground excavation on the permeability of the fractured rock surrounding the cavity is complicated by the fact that very little information is available about the virgin state of the rock. Thus, one possible approach would be to analyze the trends of permeability along individual fractures or fracture sets. However, it is almost impossible to isolate a single fracture from the rest of the structural system when fluid flow is considered. That is, when sampling a borehole for permeability by injection techniques (which will be discussed in the following chapter), the only place that a single fracture may be isolated is within the borehole. As soon as the fluid flowing through the isolated fracture reaches another fracture that intersects it, the assumption of the singularity of the fracture is no longer valid.

Therefore, a three dimensional deterministic fracture map (as opposed to a statistical map) is required for delineation of the fracture network. Such deterministic maps are impossible to prepare with the true meaning of the word. This is because a great deal of uncertainty is involved

with extrapolation of the traces of the fractures mapped on the exposed faces of the rock or within boreholes. Here, a deterministic fracture map is referred to as a data base which can represent the position and orientation of every hydraulically significant fracture, assumed as a planar feature, within the rock. The most convenient method of compiling such a data base is by using the normal and position vectors to these planar features. Such a map can be used for statistical as well as deterministic (that is, where a fracture is located) analysis.

The problem with this approach is that the continuity of the fractures cannot be incorporated accurately. One way of incorporating continuity is by assuming that fracture planes are disc shaped around the point that the measurement is made.

In this chapter, the methodology used to prepare such a map is outlined. Nevertheless, this map was not effectively used for reduction of the permeability data, as this would require a complicated numerical model that was not available at this writing and its development was beyond the scope of this investigation. In any case, the information in this map was used manually to interpret the permeability results. This proved cumbersome. It is hoped that future development of a numerical model for the use of such maps will prove beneficial in permeability characterization of the rock mass.

5.2 Field and Laboratory Methods.

5.2.1 Drilling and Core Recovery Operations.

In this study a double tube wireline core barrel was used to recover the core. The emphasis during the drilling operation was on maximum possible core recovery rather than on speed. As the core was extracted it was boxed, photographed, and logged for recovery, rock quality designation (RQD, Deer, 1964), and rock type at the site (Figure 5.1 and Figure 5.2). The RQD was recorded as the recovered length rather than percentage of recovery.

Core from the three longitudinal boreholes was oriented using a core orienter developed for this purpose. The procedure was to take an impression of the core stub remaining in the borehole with plastic dough; simultaneously, a vertical line was marked on the dough with a plumb needle. The impression was matched to the core after the core was removed. The top of the core was then clearly marked (Figure 5.3). This procedure was repeated after each core removal (every three meters). Detailed description of the instrument and method is included as Appendix I.

Borehole no. RDE-1 Box no. 1 Dates 2/20/80 Interval 0 to 9'
 Bearing/Inc. _____ Core removal _____ Geologist T. Young
 depths.
 Collar elev. _____ Coord. _____ N _____ S Dpth. Oriented _____
 Remarks Recovery (0-9) - 111" RQD - 84"
 (RQD in percent = (RQD/Interval) *100.00)

From To	Rock Type	Texture	Structure	Integrity	Color/Alterath	Remarks
0 - 19	black & white qtz bio gneiss	gneiss		3-5" pieces		mostly dark
19 - 27	bio qtz mignatite			solid		lots of qtz
27 -	bio qtz mignatite	gneissic		some solid, some v. broken		some H & P highly meta.

Codes for fracture description: O = Open R = Rough P = Planar M = Mechanical-
 Prefix: SL = Slightly V = Very C = Closed S = Smooth I - Irregular break
 Fillings: CL: Clay H = Hematite Oriented Piece:

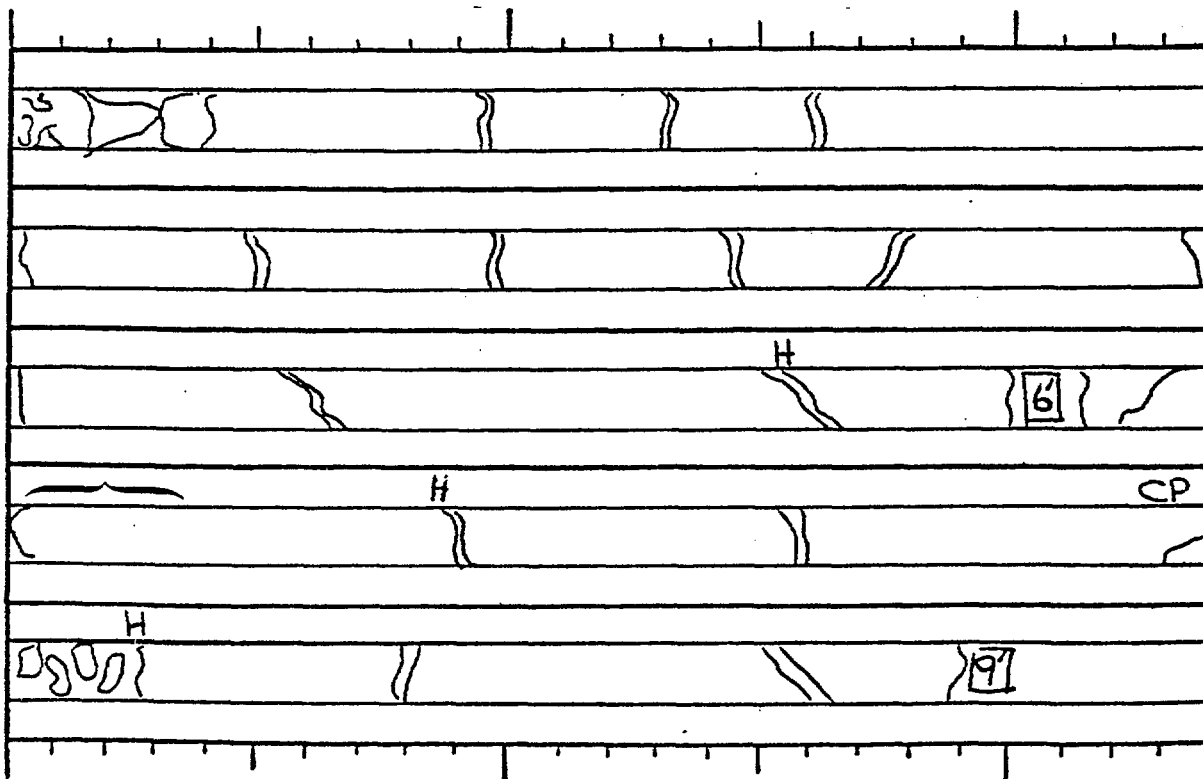


FIGURE 5.1. Facsimile of preliminary core log at the site.

FIGURE 5.2. Core immediately after removal from borehole.

FIGURE 5.3. Oriented core with the top line marked.

5.2.2 Core Logging Methods.

The main purpose of the core logging was to catalog fractures rather than mineralogy, petrology, or other structures, and the following procedures were developed with that goal in mind. However, significant petrological and structural variations were also recorded. The procedures outlined here for orientation are applicable to horizontal boreholes; however, with slight modification they can be applied to inclined boreholes (Goodman, 1976).

A total of 300 meters (1,000 ft.) of core was recovered and logged. Ninety meters of core came from 3 longitudinal holes; the remaining 210 meters of core came from a series of radial holes drilled in sets of seven holes (see chapter 4).

The equipment used for core logging was simple and basic; consisting of a Brunton compass, straight edge, protractor, measuring tape, and two-inch diameter conduit cut in half lengthwise. The conduit, wedged to prevent rolling, held the core in place. Fracture dips were measured with the Brunton; other angles, such as strikes and α angles (the maximum acute angle between the fracture and the axis), were measured with the straight edge and protractor.

For the purpose of logging, the longitudinal boreholes were assumed to be essentially horizontal. Their actual deviation of two degrees from the horizontal was within the

error of measurement. The orientation of the core was known for approximately sixty percent of the ninety meters of core taken from the longitudinal boreholes. This was achieved through close monitoring of the drilling process and careful matching of the broken pieces of core in the laboratory. However, for the remaining forty percent the orientation was far from precise, and considerable error could have occurred.

During the logging, the core was laid out and the pieces matched as closely as possible through refitting of broken ends and/or matching of foliation trends. It was then examined for fractures. When one was identified, the distance from the center of the fracture to the beginning of the core and the fracture's strike and dip were measured and recorded (Figure 5.4). The characteristics of the fracture were described in detail with respect to its overall geometry, surface type, aperture, and mineral filling, if any. Other traits, such as width of alteration surrounding the fracture, degree of branching, rock type, and foliation attitudes were also noted (Figure 5.5). Any detectable natural fracture was logged including healed fractures and veins.

The procedure was changed somewhat for core from the radial boreholes due to the fact that the orientation of the core from these boreholes was not known; therefore strike and dip of the fractures could not be measured directly. Instead, the maximum acute angle between the fracture plane



FIGURE 5.4. Matched pieces of core being logged for fractures.

LINE MAPPED: PA-1 GEOLOGIST: L. BrintonRECORDED: L. Sourp. 7-8

DISTANCE (cm)	FRACTURE CHARACTERISTICS												FOLIATION		REMARKS				
	STRIKE/DIP	PLANAR	IRREG.	CURVED	UNDUL.	SMOOTH	ROUGH	V. ROU	OPEN	S-OPEN	CLOSED	FILLING	CONTINUITY				STRIKE/DIP		
													- .5	.5-15		1.5-3		-3	
896.0																	N70E/30N	qtz vein	
906.0																		N70E/44N	bio. gneiss to 937.5
912.5	N70E/70N	X					X				X	C1, Ch							
918.0	N65E/70N	X					X				X	Ch							
925.0	N80E/43N	X				X					X	Ch							
935.5	N50E/30S	X				X			X			P							
941.0	N40E/83S	X						X			X								pos. healed frac.
944.0	N37W/5S	X				X				X		C1, gal							
956.3	N60E/75N	X					X				X	C1							
956.0	N55E/80N	X					X				X	C1							
958.5	N65E/25S	X					X	X				C1							

FIGURE 5.5. Facsimile of data for longitudinal boreholes.

and the axis of the core (the α angle) was measured. This information aided in correlating the core log data with fractures mapped in the borescope survey. In other respects the logging method was the same as that used for the longitudinal boreholes (Figure 5.6).

5.2.3 Fracture Mapping.

The purpose of this part of the investigation was to determine the spatial distribution, geometry, and characteristics of the fracture system around the ONWI room using a scanline mapping method. Seventy nine points were marked around the room about 1.5m (5 ft.) above the floor and at 1.0m horizontal spacings. These points were surveyed twice using a theodolite. A 3.0m (10 ft.) measuring tape, glued to a piece of aluminum pipe to avoid magnetic deflections on compass, was then laid along these points (Figure 5.7). All fractures greater than 50cm in trace were then mapped along this line 50cm above and below the pipe. Continuity of the fractures was recorded disregarding this limitation. All pertinent fracture characteristics such as surface roughness, opening, geometry of the plane, and nature of the filling material were recorded in addition to strike, dip and continuity measurements using the same format as in Figure 5.5. Some lines were mapped twice by different geologists

CORE FRACTURE LOG

BOREHOLE: RDE-1 DATE: 1-5-81 PAGE: 1GEOLOGIST: L. Sour RECORDER: M. Winter

Distance	α Angle	Planar	Irreg.	Curved	Smooth	Rough	V. Rough	Undul.	Open	Closed	Filling	Remarks
1.2	39	X				X			X		Cl	hi % bio. in qtz-felds gneiss (foliated)
0	54	X				X			X			folia. frac. (?), partially open
2.3	33	X				X			X		P, Cl, H	
65.8	33	X			X			X	X?		Ch, Cl(minor)	not continuous, in hi % bio. region
91.4	54	X				X			X		Ch, Cl	
135.3	36		X			X			X		Ch, Cl	pos. folia. frac.
157.4	16	X				X			X		P, qtz, Cl, Ch	partially open
161.4	20	X				X			X?		Cl, Ch, H	pos. folia. frac.
172.0	35, 26		X			X			X		Cl	frac. network, cuts folia., hi % bio., not continuous
180.6	37	X				X			X		P, qtz, Ch, H, Cl	3 mm wide to closed
194.5	66	X				X			X		H, Cl	intersects next frac.
197.5	32	X				X			X?		H	partially open, fine frac. network 4mm - .5mm wide

FIGURE 5.6. Facsimile of data from radial boreholes.

FIGURE 5.7. Line mapping of the walls.

to confirm observational accuracies and check on sampling bias. With this method of mapping, position and normal vectors for each fracture, along with its characteristics, were computed from which data for arbitrary scanlines such as boreholes were simulated. Predicted data were then compared with the mapped data.

5.2.4 Visual Examination of the Borehole Walls.

Raw data from borescope surveys was provided by Chitombo (1982) and for more detailed description of the methodology, the reader is referred to his report. A borescope with an angle of view of about 45° was used to examine the walls of the boreholes; wherever a fracture was seen its characteristics and the distance to three points on this fracture were recorded at three different angles from a predesignated axis. The aperture was estimated by comparing the distance between the walls of the fracture to a scale on the mirror, at three different points. Only relatively major features could be mapped and, unlike core logging, many details about the fracture characteristics could only be estimated.

Most borescopes cannot be used for depths of greater than a few meters. A few borescopes are available that can be used for depths of 30 meters (Gale, 1980).

During the exploration phase of a high level nuclear waste repository, boreholes with great depths are involved for which borescopes cannot be used. For this reason and the fact that the borescope available could not be extended to depths greater than 10 meters, a black and white borehole T.V. camera was used to map the walls of the longitudinal boreholes. This instrument is shown in Figure 5.8.

Aside from the applicability to greater depths, several other advantages were noticed over the borescope:

1. Fracture apertures can be measured more accurately and directly on the CRT screen with about seven times magnification (this can be increased to 20 times or more by changing the optical elements and/or the monitor).
2. the angles of rotation can be measured more reliably;
3. fracture attitudes can be approximated directly on the screen and compared with the computed results (see data analysis section in this chapter);
4. measurements of more than three points enables statistical averaging of the orientation data;

a. Accessories

b. Close-up of the Camera

FIGURE 5.8. Borehole T.V. camera and accessories used to map the borehole walls.

5. measurements of the relative distances to the points required for attitude calculations can be measured with much more accuracy;
6. relative ease of data collection speeds the operation and the cost of labor saved makes up for the initial investment made on the equipment; and
7. automation of the data collection and data processing can be developed as the electrical signals can be digitized and interfaced with a digital computer which is a great advantage when long intervals of borehole are being logged.

There are also other advantages, such as quality of the picture and high contrast, that are also of significance. The only disadvantage about the T.V. camera used is the lack of color which is of great help in identifying rock types and fracture filling material.

The procedures used for the borescope survey were modified to take advantage of the flexibility of the T.V. system. The method of using a tape or the pushing rod for measuring the distance to the points of the fracture was discontinued. Instead the relative distances of four points on a fracture, which were measured on the CRT screen, were used to calculate

the attitudes unless the angle between the fracture and the borehole axis (α -angle) was too small (see data analysis).

5.2.5 QUALITY CONTROL.

Several people were involved in the core logging process. Consistency and accuracy of observation were maintained in several ways; an important consideration when workers from different backgrounds obtain the same type of data.

Often two people worked as a team, a geologist and a recorder (also 2 geologists), freeing the geologist to concentrate on observation and allowing the recorder to independently check the reasonability of the data being recorded. They exchanged jobs at intervals, relieving any tendency to boredom. This also tended to increase the consistency of the data collection among workers.

Several boreholes were selected at random and relogged by different teams and the results were compared. Also, part of one borehole was relogged by the same geologist after several months had elapsed. All served as checks on the reproductibility of the data.

Within limits, the data produced from the same core by different geologists could be correlated. The α angle and mineral identification were the most consistent types of

data. Most of the differences were in measurement of distance and description of characteristics that were borderline between two categories. Also, judgment of which fractures are significant enough to be recorded varied among workers.

Agreement between two logs of the same core recorded by different workers varies between forty percent and seventy percent, computed on a number of fractures matched per total number logged basis. For the core relogged by the same person, agreement was approximately eighty percent.

5.3 Data Analysis.

5.3.1 Data Treatment.

Over 3,500 fractures were sampled on the walls and the boreholes. Data were coded and stored on magnetic tapes on the CSM Dec-10 computer system. In order to proof read the coded data, a program was written to decode and regenerate the information. Various programs were written and some existing ones were used for statistical analysis. Details of some of these programs are included in the Appendices and are briefly reviewed in the following sections.

5.3.2 Surveying Data.

In order to generate an easily correlated orientation data system, all surveying data were transformed into a standard right handed coordinate system with the origin located at the survey spad inside the room and with x positive to the north, y positive to the east and z positive downward. A position vector for the points at the beginning of each scanline (boreholes and detail lines) and the vector of the scanlines were calculated. The programs BORSUR and LINSUR were written for this purpose. The algorithm is briefly described in Appendix II.

5.3.3 Preparation of a Data Base.

A natural fracture may be assumed as a planar feature in most cases. This is due to the fact that the radius of curvature of most fractures is so large that it cannot be detected by conventional geological sampling techniques. In addition, from a mathematical point of view, any surface can be assumed planar at a point which here is considered to be the sampling (or measuring) point.

In geology it is convenient to represent a planar feature, such as a fracture, by its strike and dip (Figure 5.9). These orientations can be represented by unit vectors:

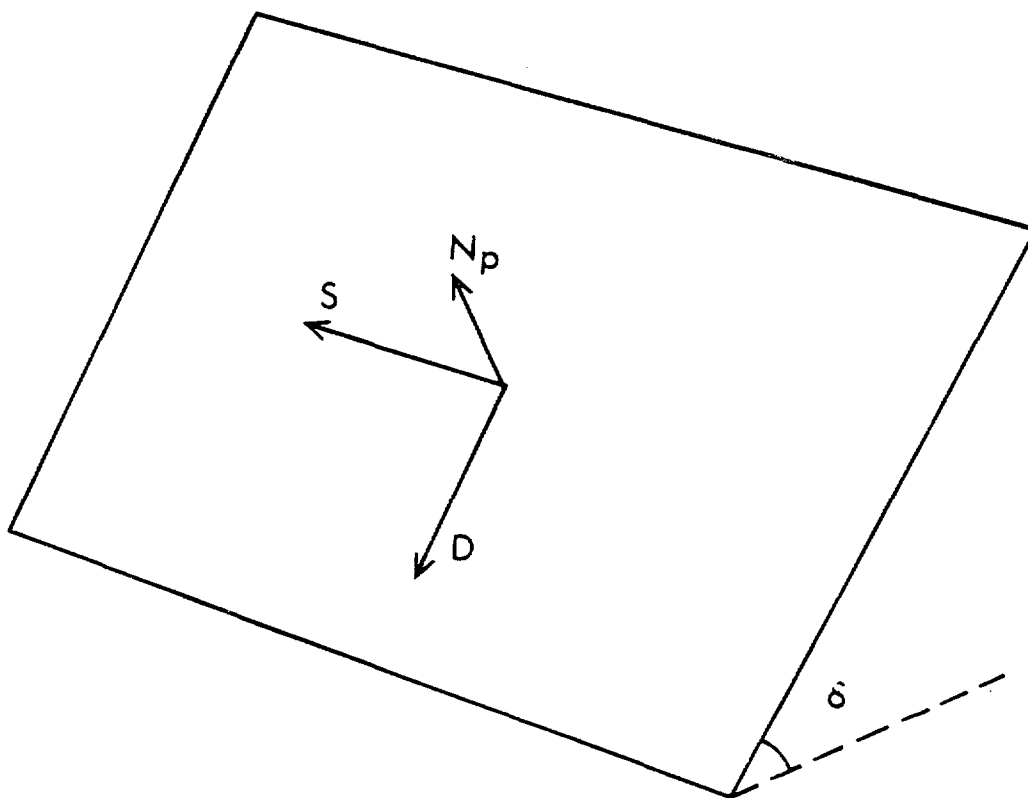


FIGURE 5.9. Relationship between strike, dip and normal vectors defining a planar feature.

$$S = s_1 i + s_2 j \quad (5.3.1)$$

$$D = d_1 i + d_2 j + d_3 k \quad (5.3.2)$$

where, S and D are strike and dip vectors respectively. In this section lower case letters are used to denote scalar variables and when subscripted they represent components of the vector. The unit normal vector to the plane is given by:

$$N_p = S \times D \quad (5.3.3)$$

where

$$N_p = n_1 i + n_2 j + n_3 k .$$

By convention N_p is always pointed upwards ($n_3 \leq 0$), S is defined by its azimuth (θ) and dip by its inclination (γ) which is always a positive acute angle measured from a horizontal datum.

Using equations 5.3.1 to 5.3.3 the normal vector can be given by:

$$N_p = (s_2 d_3) i - (s_1 d_3) j + (s_1 d_2 - s_2 d_1) k \quad (5.3.4)$$

where

$$s_1 d_2 \leq s_2 d_1 .$$

Because in geological sampling only the azimuth and dip are known the three vectors can be rewritten:

$$\begin{aligned} S &= (\cos\theta)i + (\sin\theta)j \\ D &= (\cos\gamma \sin\theta)i - (\cos\gamma \cos\theta)j - (\sin\gamma)k \\ N_p &= (\sin\theta/\sin\gamma)i + (\cos\theta \sin\gamma)j - (\cos \cos 2\theta)k \end{aligned} \tag{5.3.5}$$

Either S and D or N_p are sufficient to represent orientation of the plane. However, representation of the position of the plane in space and its extent require further information.

Using data provided by BORSUR and LINSUR computer codes and method of field data collection described earlier, a position vector (R_c) to every sampling point can be calculated (Figure 5.10):

$$R_c = R_b + \frac{d}{L_{sc}} R_{sc} \tag{5.3.6}$$

where:

R_b = position vector to the beginning of a scanline

R_c = position vector to the sampling point

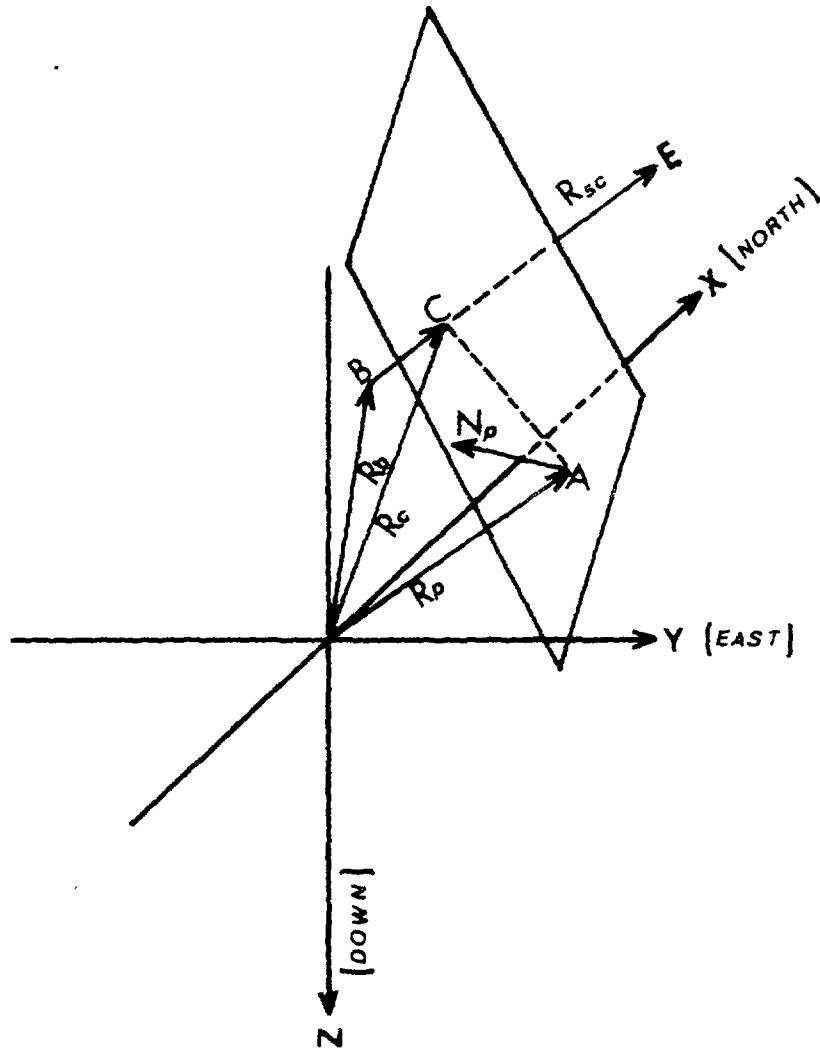


FIGURE 5.10. Vectors involved in defining a planar feature by sampling along a scanline.

R_{SC} = the scanline vector,

d = distance along the scanline to the sampling point (BC in Figure 5.10)

L_{SC} = total length of the scanline.

Continuity of a fracture cannot be effectively measured in the field and it is usually estimated along the traces of the fracture on the exposed surfaces. Commonly, it is expressed non-parametrically as ranges (ISRM, 1978). In this study this method of sampling was used. For this reason, continuity cannot be represented by a continuous variable and a discrete variable (c) is used. It is assumed that any fracture is a disc centered at the sampling point with c as its diameter. For fractures crossing the entire width of the underground opening, c was taken as twice the trace length. More detailed method of representing continuity is given by Pahl (1981).

It can be seen that the three quantities R_c , N_p and c along with the qualitative traits of the fracture (such as filling, aperture, etc.) can closely characterize a fracture in space. The usefulness of such a data base is only limited by the imagination of the user and a few examples given below will demonstrate this.

5.3.4 Generating Data Along a Scanline.

In this section it is shown how the data base can be used to generate data along a scanline for which no fracture information is available. From mapping nearby scanlines, not necessarily parallel to the unmapped scanline, we have the following (in Figure 5.10, BC is now the unmapped scanline):

$$N_p (n_1, n_2, n_3)$$

$$R_p (p_1, p_2, p_3)$$

$$R_b (b_1, b_2, b_3)$$

$$R_{sc} (e_1, e_2, e_3)$$

$$c \text{ (continuity)}$$

A scalar (d), which gives distance from the point (b_1, b_2, b_3) to where R_s (scanline) intersects the fracture plane (point C), and the position vector to C are required to transfer the data base from one scanline to another. Obviously, if the distance AC (Figure 5.10) is greater than the continuity no data transfer can be made. From Figure 5.10 it can be seen that:

$$\left(\frac{d}{L_{sc}} R_{sc} + R_b - R_p \right) \cdot N_p = 0 \quad (5.3.7)$$

from which d can be found easily. R_c is found from equation 5.3.6.

In Cartesian notation:

$$d = \left| \frac{(p_1 - b_1)n_1 + (p_2 - b_2)n_2 + (p_3 - b_3)n_3}{(e_1n_1 + e_2n_2 + e_3n_3)} \right| \times L_{sc} \quad (5.3.8)$$

5.3.5 Analysis of the Orientations.

The program QUAD (Call, 1971) was used for stereonet plotting and histogram preparation. Each scanline was first analyzed separately. Then, data from groups of scanlines were combined and analyzed. Several different combinations were used to study the effect of the orientation of the scanline on introduction of bias in the results to compare the variation of fracture distribution at different positions around the room.

5.3.6 Determination of True Spacing, Frequency and RQD.

For a set of parallel planes, equally spaced apart, the spacing is given by:

$$s = \frac{d}{L_{SC}} R_{SC} \cdot N_p \quad (5.3.9)$$

In nature, members of a fracture set are not exactly parallel to each other and spacing is uneven. In this case the normal to the set and its spacing are not well defined and equation 5.3.8 cannot be used. The computer code FRACTAN provides a mean normal vector (N_m) for each set. Using N_m , a mean spacing (s_m) for the set can be calculated as follows:

$$s_m = \frac{\sum_{i=1}^{m-1} d_i R_{SC} \cdot N_m}{n L_{SC}} \quad (5.3.10)$$

where n is the total number of fractures in a set. In equation 5.3.10 a normal distribution is presumed for the spacing.

A computer code was written to calculate the fracture frequency, the RQD (Rock Quality Designation) of Deere (1964), and the theoretical RQD of Priest and Hudson (1976 and 1981). This computer code (FRACTR) was written to handle the data collected on the site and from any, actual or simulated scanline.

The RQD is defined as

$$\text{RQD} = 100 \sum_{i=1}^n x_i / L_{\text{SC}} \quad (5.3.11)$$

where x_i is the length of the i th piece of core greater than twice the diameter of the core (0.1m or 4 inches for NX-core) and L_{SC} is the length of the core run (or scanline).

The theoretical RQD which was proposed by Priest and Hudson (1976) is defined as

$$\text{RQDT} = 100 e^{-0.1\lambda} \times (0.1\lambda + 1) \quad (5.3.12)$$

where λ is the fracture frequency per meter. Equation 5.3.12 is only applicable when the fracture frequency assumes a log normal distribution.

Both RQD's and fracture frequencies were determined for each meter of the scanlines logged. The fracture zones (or shear zones) were assigned a high fracture frequency (≈ 130 per meter) to emphasize their existence in the theoretical RQD evaluation. This did not affect the RQD calculated from Equation 5.3.11.

The frequency of fractures with certain characteristics was also evaluated separately. For example, frequencies of open or closed fractures, and those having various mineral

fillings, were calculated.

5.3.7 Analysis of Borescope and T.V. Camera Data.

Because the points measured on the fractures logged in the radial boreholes are at random angles, the techniques presented by Mahtab, et al. (1974); which require the points be measured at specific angles (-90, 0, 90 from the crest), could not be used to determine dip and strikes in this case. A computer code (BSCOPE) was, therefore, developed to calculate the position and normal vectors for each fracture.

In the BSCOPE, the azimuth and inclination of the borehole are needed to calculate the direction cosine of the z axis of the borehole coordinate system. Because this program was intended to be of general application, the azimuths and inclinations of the other two axes of the borehole coordinate system are required which are readily calculated knowing these parameters for the z-axis (the borehole axis).

It should be noted that one restriction in this program is that the borescope must be centered in the borehole. However, similar procedures used by Mahtab et al. (1974) can be followed for eccentric data. Otherwise there are several advantages in BSCOPE over that of Mahtab et al. Three (or

more) points can be measured at any arbitrary angle. This will enable measurement on a discontinuous fracture. In addition none of the axes of the borehole coordinate system (see Figure 5.11b) are restricted. For convenience of finding inclinations and azimuths of the x_b and y_b however, it is recommended to keep y_b always horizontal.

In this computation, the normal to the plane of fracture is found by the cross product of the two vectors in the plane. In order to find these vectors the coordinates of the three (or more) points measured on a fracture are first transformed from cylindrical coordinates to the Cartesian coordinate system by (Figure 5.11b):

$$\begin{aligned} p_{xi} &= r_b \times \cos (\alpha_i) \\ p_{yi} &= r_b \times \sin (\alpha_i) \\ p_{zi} &= d_i \end{aligned} \quad (5.3.13)$$

where p_{xi} , p_{yi} and p_{zi} are the coordinates of the three points, r_b is the radius of the borehole and α_i are the angles (measured clockwise from x_b) the borescope or T.V. camera was rotated and d_i are distances to the three points measured from a reference plane normal to the borehole axis.

The vectors in the plane are then calculated:

$$E_1 = (p_{x2} - p_{x1})i + (p_{y2} - p_{y1})j + (p_{z2} - p_{z1})k \quad (5.3.14)$$

$$E_2 = (p_{x3} - p_{x1})i + (p_{y3} - p_{y1})j + (p_{z3} - p_{z1})k \quad (5.3.15)$$

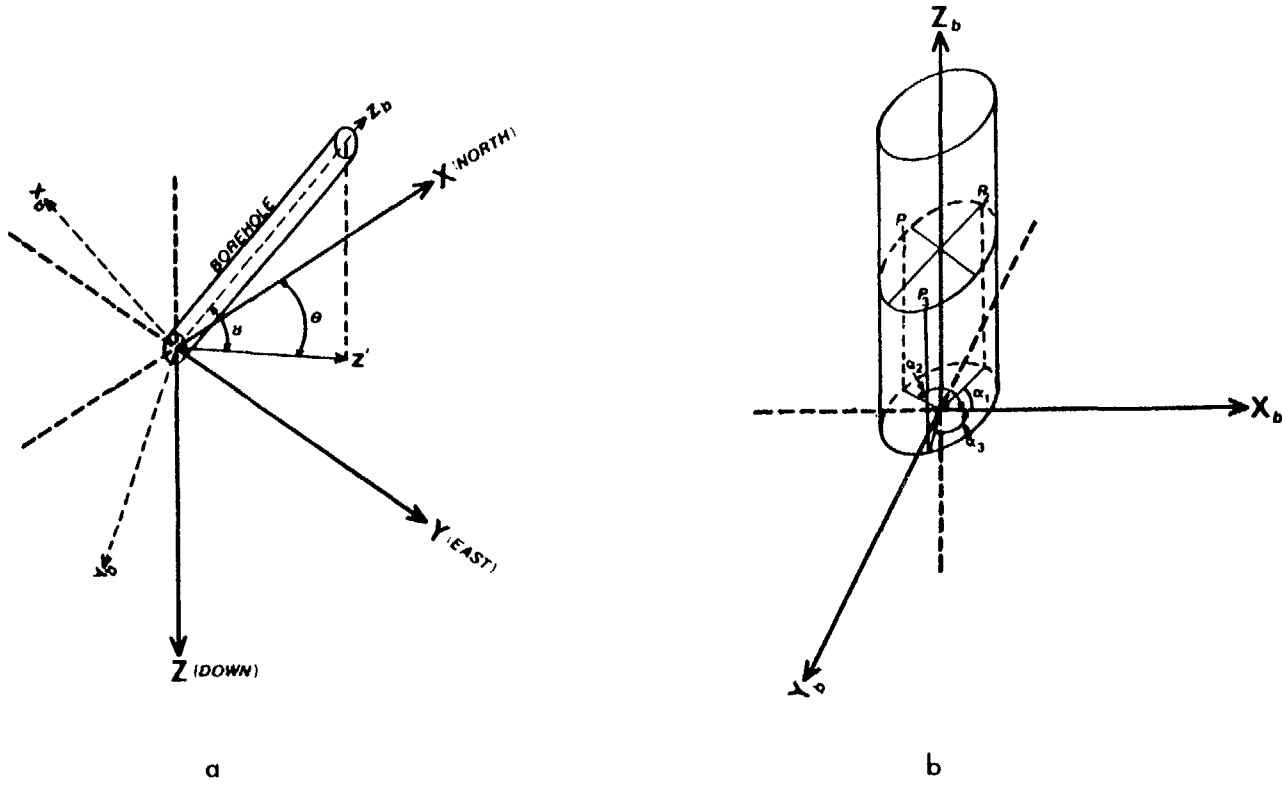


FIGURE 5.11. Borehole orientation in a) global system, b) local coordinate system.

The normal vector is then found by

$$N_b = E_1 \times E_2 \quad (5.3.16)$$

This normal is then transformed into the global coordinate system by

$$N_{gi} = n'_{ij} \times N_{bj} \quad (i \text{ and } j = 1, 2 \text{ and } 3) \quad (5.3.17)$$

where n' is the direction cosine matrix:

$$n'_{ij} = \begin{vmatrix} (\cos\gamma_1 \cos\theta_1) & (\cos\gamma_2 \cos\theta_2) & (\cos\gamma_3 \cos\theta_3) \\ (\cos\gamma_1 \sin\theta_1) & (\cos\gamma_2 \sin\theta_2) & (\cos\gamma_3 \sin\theta_3) \\ (\sin\gamma_1) & (\sin\gamma_2) & (\sin\gamma_3) \end{vmatrix} \quad (5.3.18)$$

where γ_i are the inclinations and θ_i are azimuths of the three axes of the borehole coordinate system with respect to the global system. It should be noted that inclinations are negative upwards.

After the normal is transformed into the global system the strike and dip are calculated with the quadrant determined from the sense of the normal:

$$\text{Strike} = \sin^{-1} \frac{|N_{g1}|}{\sqrt{|N_{g1}|^2 + |N_{g2}|^2}} \quad (5.3.19)$$

$$\text{Dip} = \cos^{-1} \left| \frac{N_{g3}}{N_g} \right| \quad (5.3.20)$$

Fracture characteristics are also decoded by BSCOPE and printed out along with the strike, dip and distance information. The program listing is given in Appendix III.

In surveying with the T.V. camera, four or more points, if possible, were measured on each fracture. This provides four or more possible planes for each fracture. The resultant normal vector of these four planes was used to calculate the strikes and dips.

A critical point in conducting borehole surveys using this method is the distance measured to each point on the fracture. A one centimeter error on the fracture can cause an error in dip and/or strike of as much as 30° in an NX-borehole. With a borescope, one cm is generally the minimum error. The error increases with depth as the measuring tape or rod is twisted or bent. With the T.V. camera the measurements can be made directly on the screen with accuracy of 1mm or less. This proved to be a significant advantage of the T.V. camera over the borescope.

In order to determine the coordinates of a point on a fracture directly on the screen a simple gnomonic projection (cylindrical) was used, assuming the CRT screen is a flat plane (Figure 5.12). From the figure it can be seen that:

$$\alpha = \tan^{-1} \left(\frac{X \times W_{sn}}{2 \tan \beta} \right) \quad (5.3.21)$$

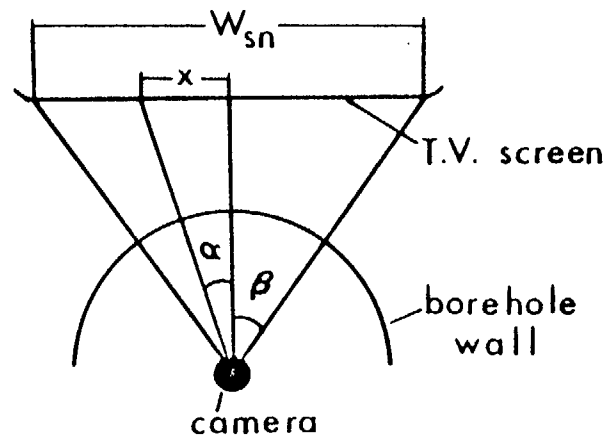


FIGURE 5.12. Relationship between the T.V. camera in the borehole and the CRT screen. Angles can be easily measured directly on the screen.

Distances can be directly measured in direction of the borehole axis (on the screen) and reduced by the magnification factor. A more accurate method of measuring α is to use a calibrated grid on the screen. This proved to be the most convenient method for measuring both angles and distances.

5.4 Results.

5.4.1 Overall Fracture Distribution

The general distribution of fracture orientations is shown in Plate 1 by means of lower hemisphere, Schmidt equal-area net plots of their poles. These plots are compiled from oriented core logs (longitudinal boreholes), borescope surveys (radial boreholes) and line mapping data (the walls of the room). Traces of major fractures shown in this map were drawn by observation and use of the line mapping data.

Along the longitudinal boreholes two vertical fracture sets are clearly shown toward the deeper one third: one with N50E to N60E strike and the other with N40W to N50W strike. Comparison of these with what is mapped in the room indicates reliable orientation of the core. The first set is what in this report is referred to as foliation fractures, because it is subparallel to the foliation. The latter set consists of the diagonal joints, forming an angle of about 60 degrees

with the foliation.

The diagonal joints are not as common to the north of the shear zone as to the south. Horizontal fracture sets are not detected by the line mapping which is partly due to the orientation of the sampling lines. The horizontal fractures shown in the longitudinal borehole logs are minor fractures and are mostly weak planes opened by the drilling operation. However, in radial boreholes, especially the vertical ones, a few horizontal fractures are found with the borescope.

5.4.2 Fracture Orientation.

5.4.2.1 Television and Borescope Surveys.

In the scanline mapping technique there is a great bias introduced into the sample. Every line is blind to any plane parallel to its direction. This is clearly shown in the results of the borescope survey from radial boreholes.

Horizontal radial boreholes, which have a bearing of N60E, are blind to any fracture striking in this direction (Figure 5.13a). They show high concentration for the diagonal joints, but do not reveal any significant new set to which the longitudinal boreholes and the walls of the room are blind. There is a very low concentration of foliation

fractures shown by these radial boreholes.

Figures 5.13b and 5.13c show the orientation of the fractures for the vertical boreholes. As can be seen, these sampling lines are blind to vertical fractures. New sets, not discovered by line mapping, do not have significant concentrations. Results of the diagonal boreholes are shown in Figures 5.13d and 5.13e.

Figure 5.13f shows the overall fracture orientations mapped by the borescope survey. A low concentration of foliation fractures is shown which would be expected since all boreholes are almost parallel to this set. The highest concentration is for the diagonal joints. No new set is identified except for some shallow dipping fractures, the concentration of which is very minor.

Comparison of the results of the borescope survey with the results of areal mapping of the blasting faces (Figure 5.14) reveals interesting relationships. The direction of the sampling plane in both cases is the same (radial boreholes are drilled parallel to blasting faces) and, therefore, one would expect to observe similar fracture orientations. This is true for all the important fracture sets except for the foliation fractures. The major set revealed by the mapping of the blasting faces is the foliation fracture set; whereas from the borescope survey this is a minor set. This shows the bias that is introduced by blasting of the

FIGURES 5.13. Fracture orientation patterns
from radial borehole logs.
Numbers in the circles are
per mil.

Fig. 5.13a

SCHMIDT EQUAL-AREA NET
LOWER HEMISPHERE

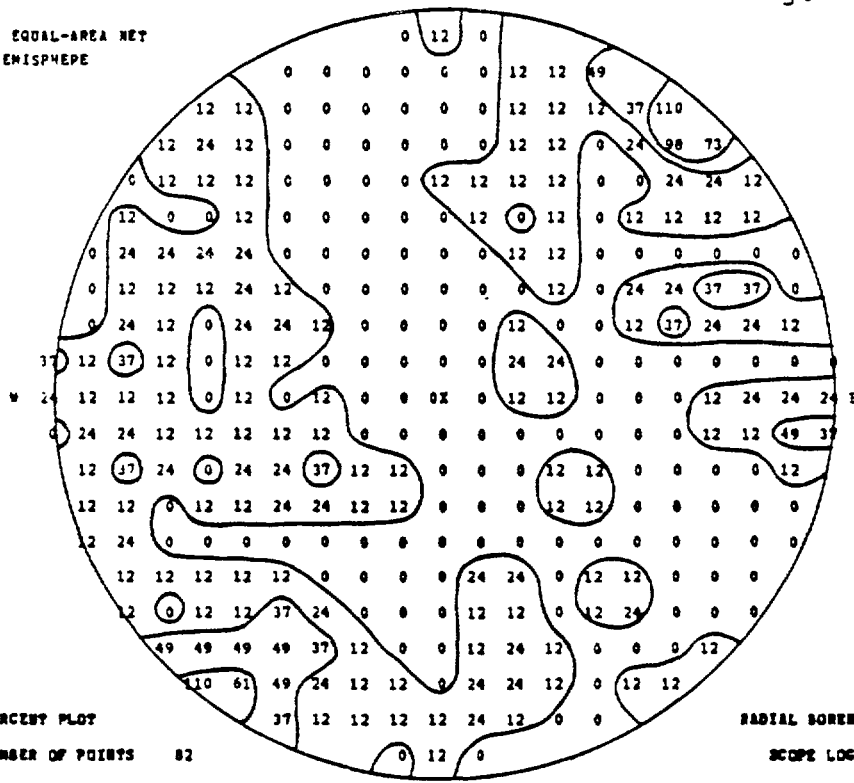


Fig. 5.13b

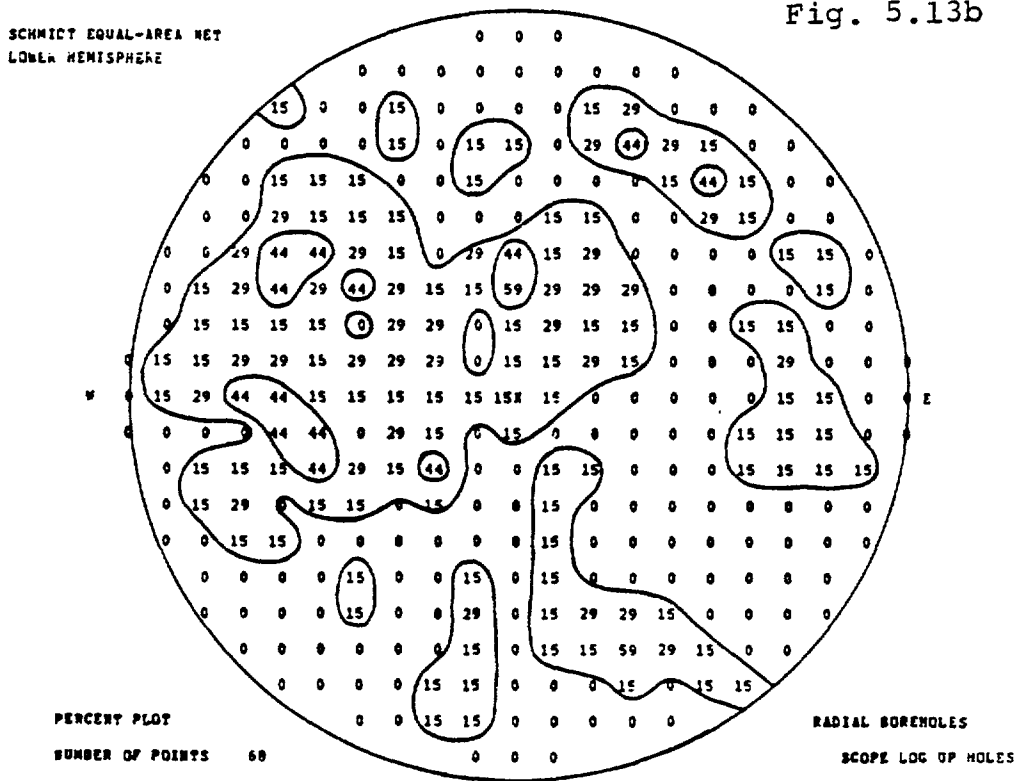
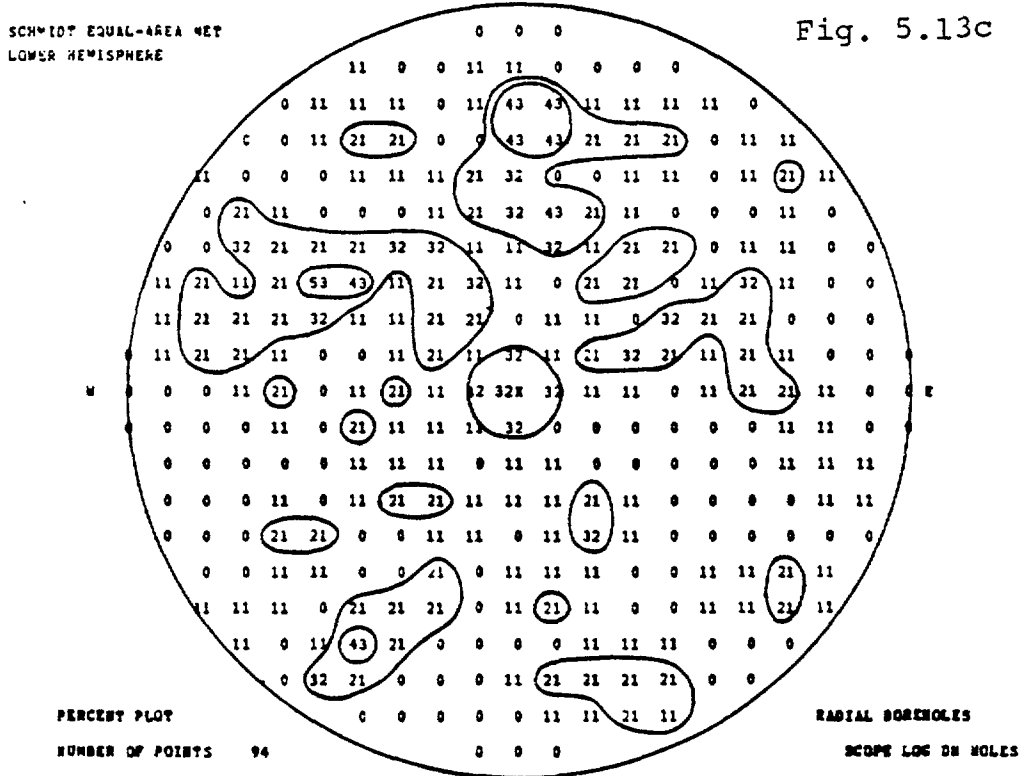
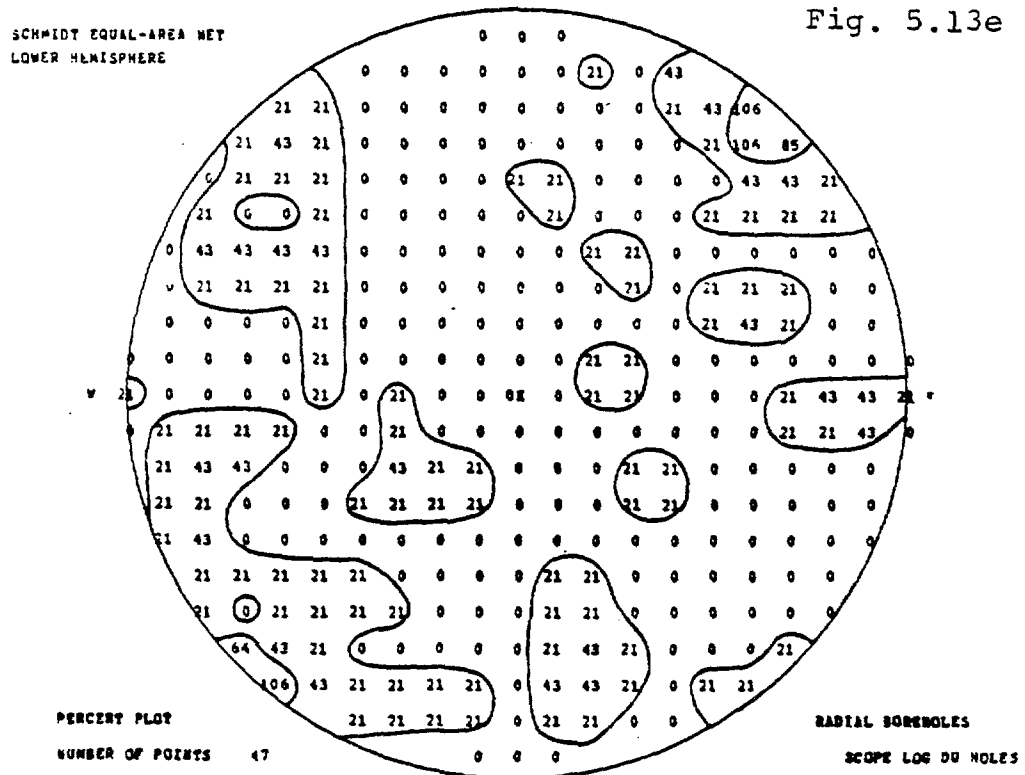
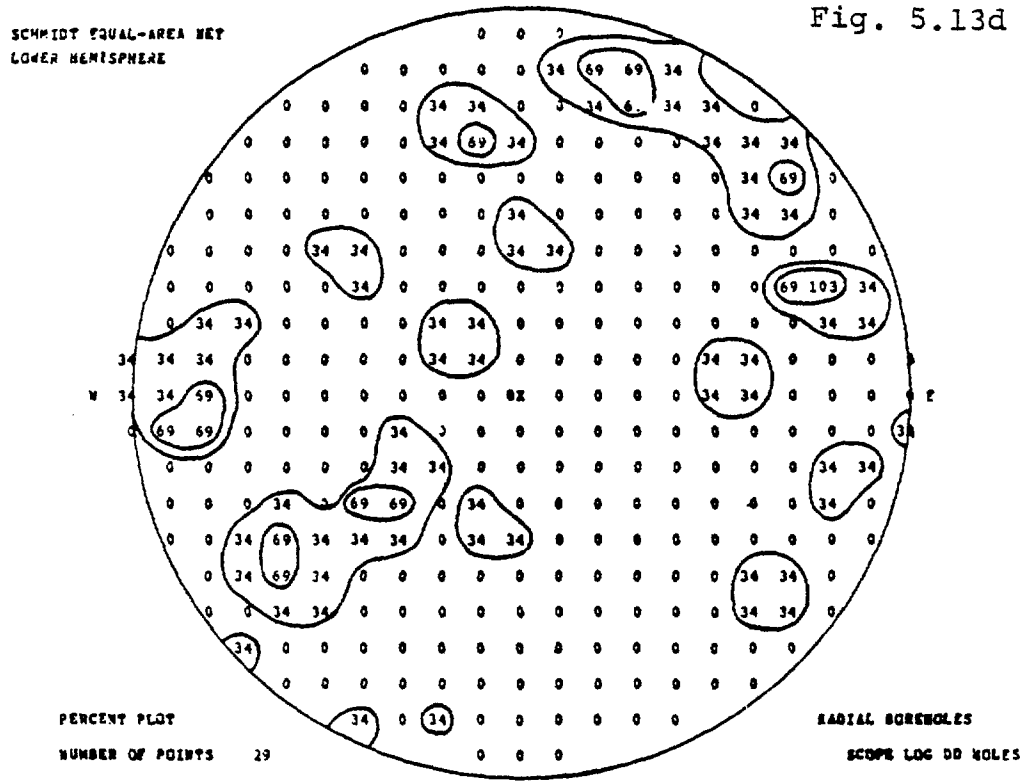


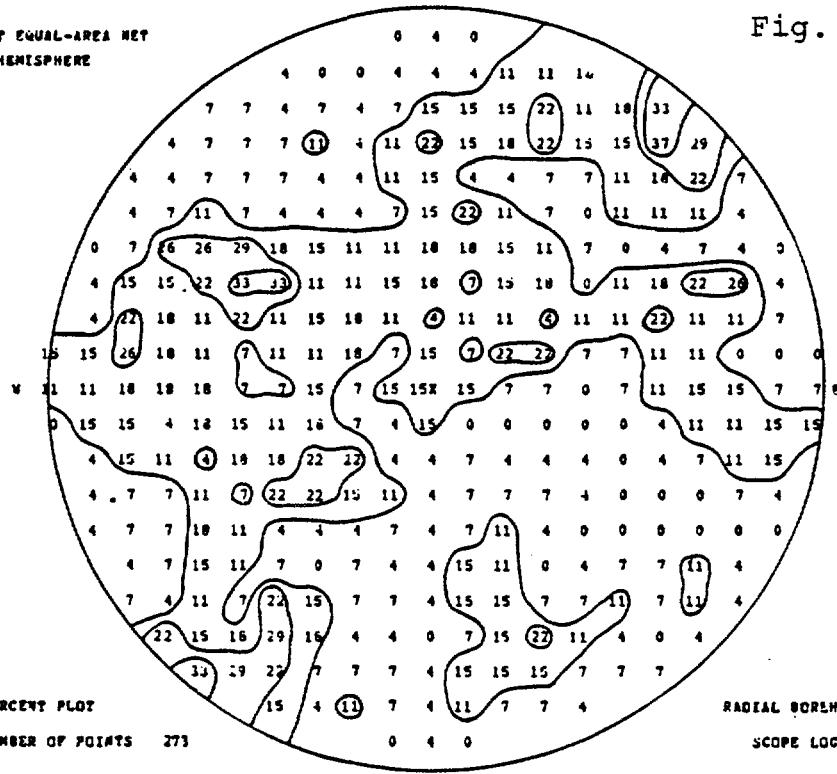
Fig. 5.13c





SCHMIDT EQUAL-AREA NET
LOWER HEMISPHERE

Fig. 5.13f



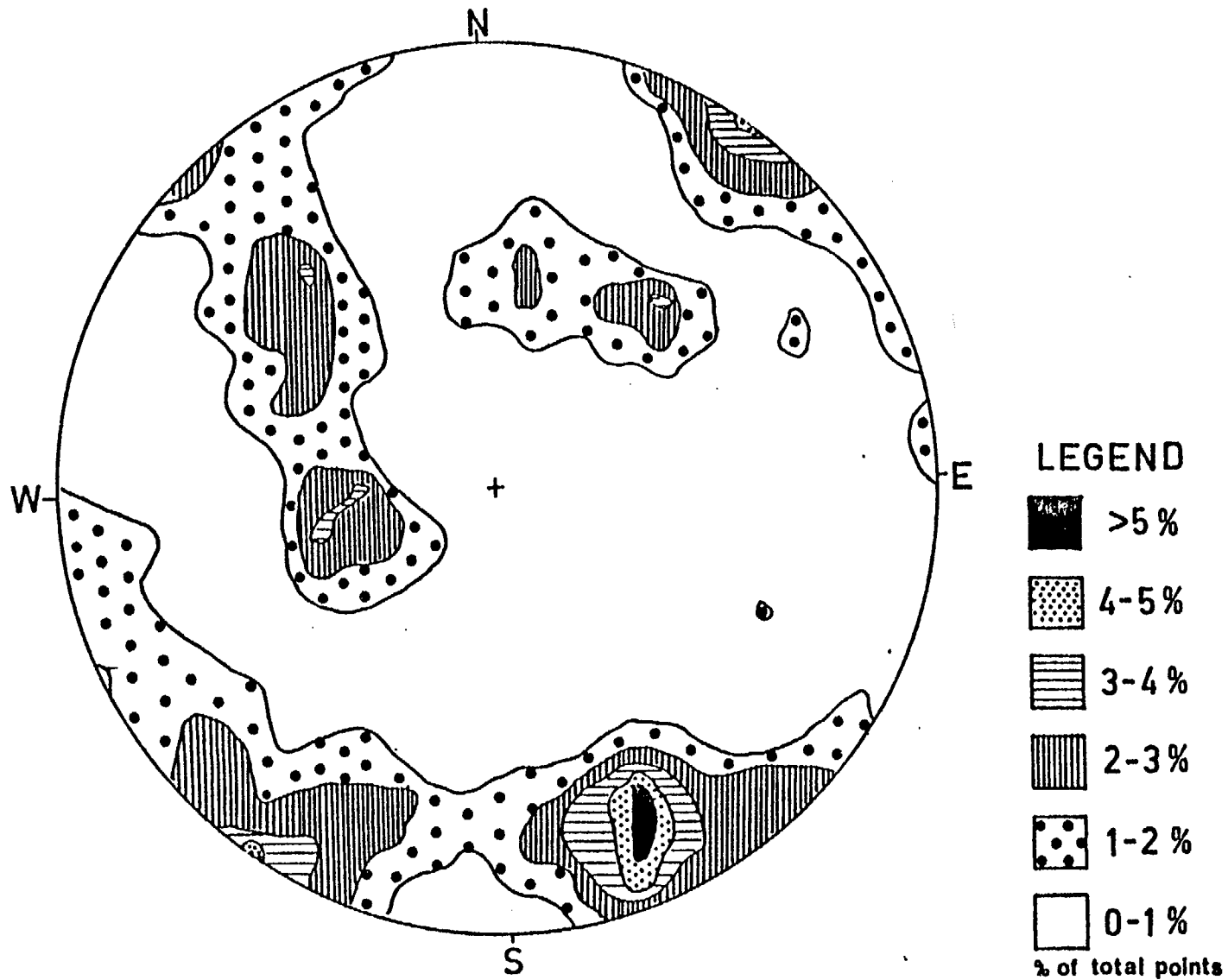


FIGURE 5.14. Contour diagram on lower hemisphere Schmidt equal-area net of 710 fracture orientations from the mapping of mining faces. (Hustrulid et al., 1980.)

rock. The foliation plane is a weak plane along which the rock breaks easiest, especially if there is little confining pressure normal to it (which is the case here). Similar reasoning may be applied to the results of the line mapping, in which the diagonal joints are exaggerated (in smooth wall blasting, when the peripheral drill holes are blasted there is little confining pressure normal to the wall).

5.4.2.2 Line Mapping.

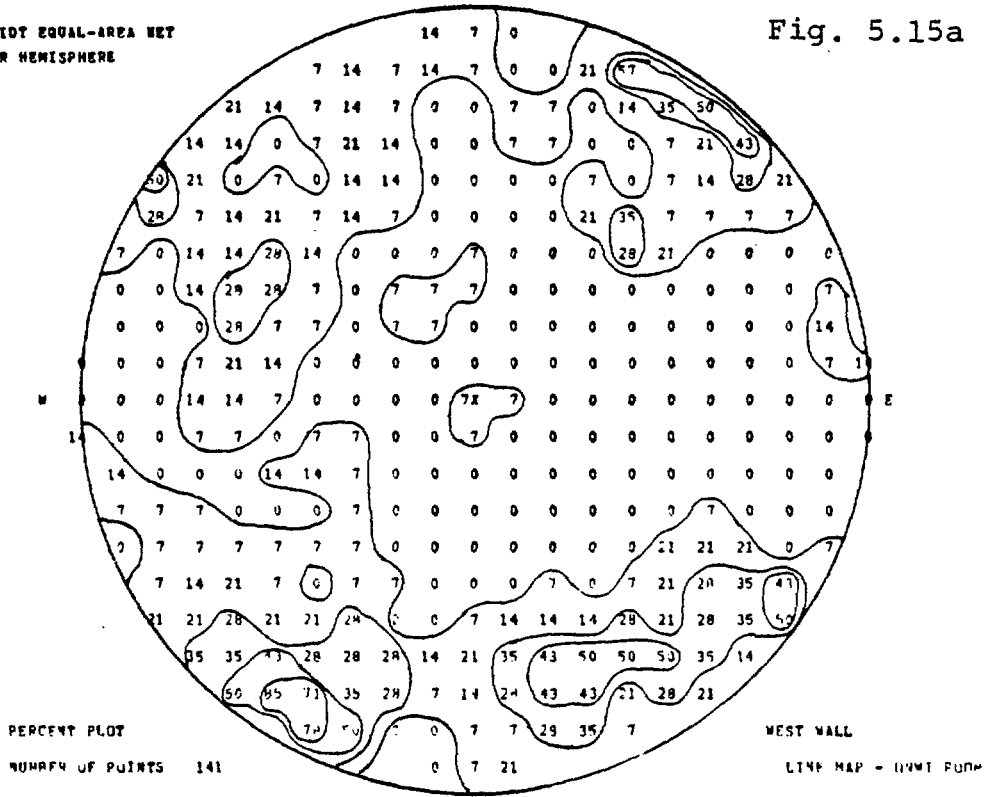
In order to compare the results of mapping of a wall by two different geologists, the west wall was mapped twice; once by a scanline method (laying a tape against the wall and mapping the entire line) and once by a systematic line mapping technique described in the previous section.

Figure 5.15a is the result of the systematic line mapping and Figure 5.15b shows the orientation of the fractures mapped by the earlier method. The higher number of fractures in Figure 5.15b is due to the lower cutoff limit for continuity (only fractures 30cm (1 ft.) or longer in trace were mapped). The cutoff limit for Figure 5.15a was 50cm (1.7 ft.). A close comparison indicates that all the orientation clusters are reproduced by both techniques, with only variations in their scatter, to within $\pm 5^\circ$ for both dip and strike.

FIGURES 5.15. Patterns of fracture orientation from mapping of the walls. Numbers in the circles are per mil.

SCHMIDT EQUAL-AREA NET
LOWER HEMISPHERE

Fig. 5.15a



SCHMIDT EQUAL-AREA NET
LOWER HEMISPHERE

Fig. 5.15b

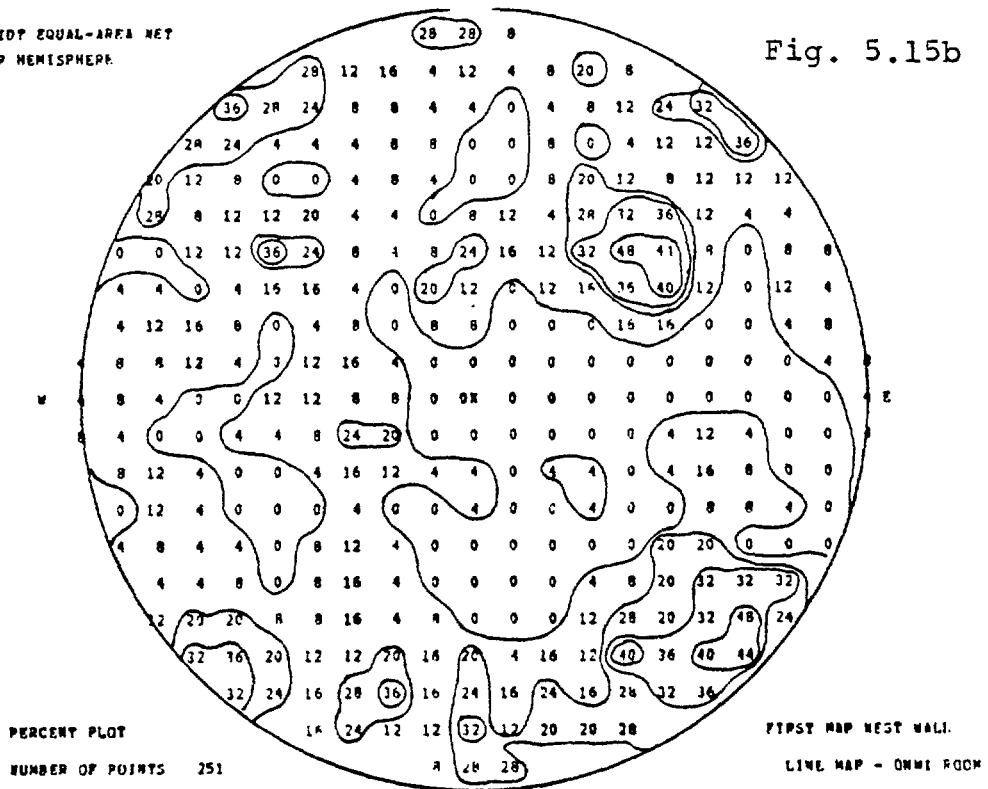


Fig. 5.15c

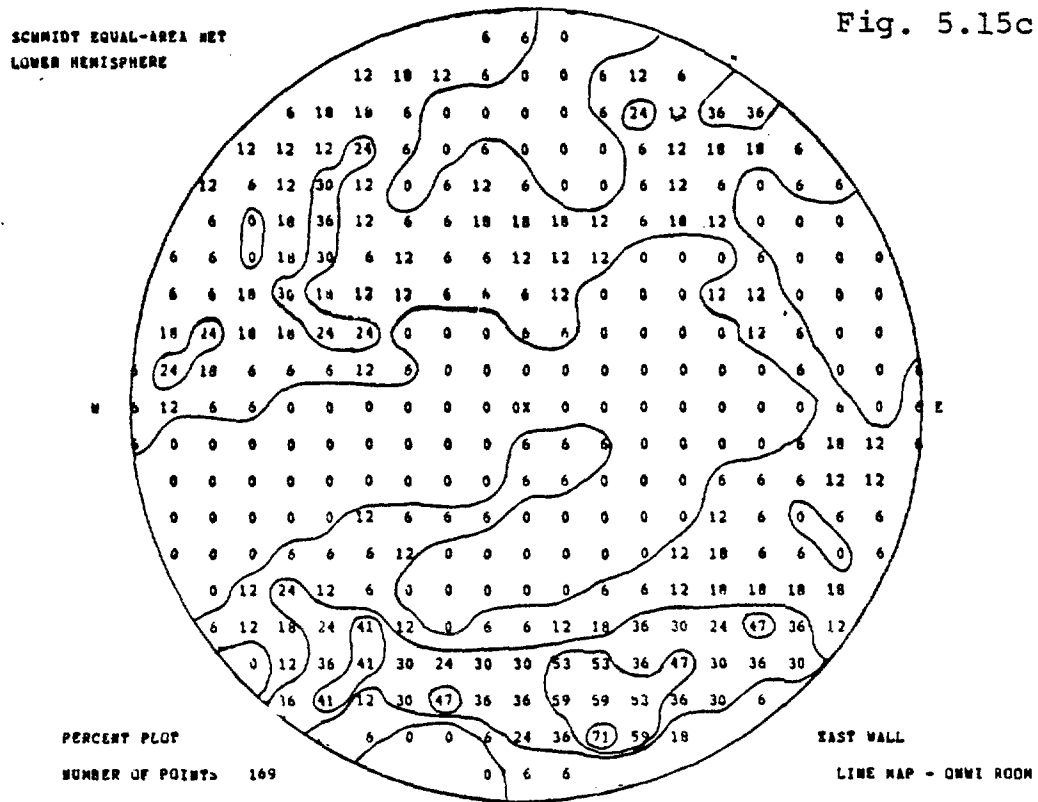
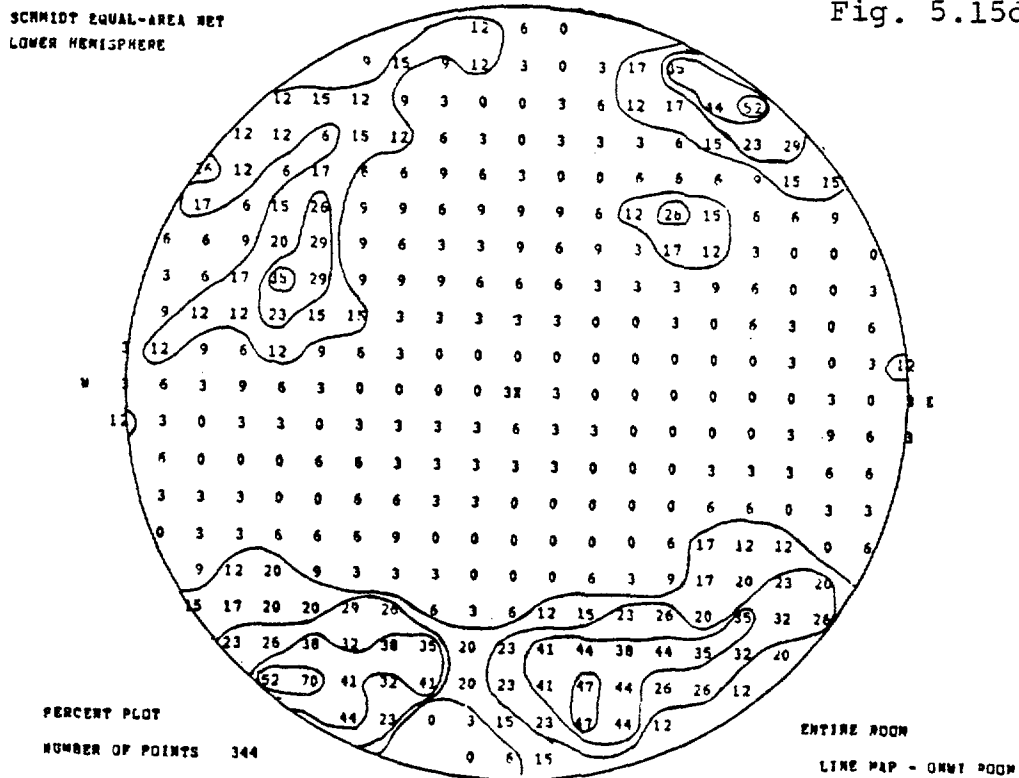
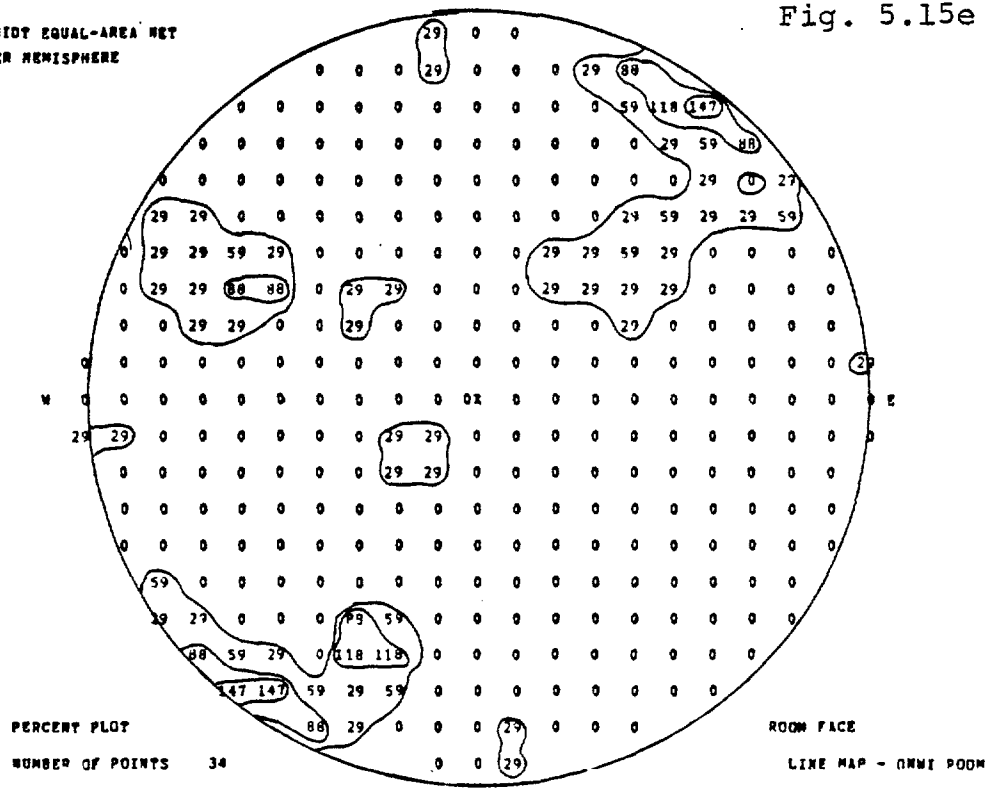


Fig. 5.15d



SCHMIDT EQUAL-AREA NET
LOWER HEMISPHERE

Fig. 5.15e



In addition, the plot for the entire room from line mapping (Figure 5.15d) was compared to the results of the areal mapping by Rosasco (1981, private communication), who in one method plotted fractures with trace length greater than 1m. Clusters in his plot are reproduced to within $\pm 5^\circ$, for both strikes and dips, with the scanline method used in the present study.

It should be noted that reproducibility of $\pm 5^\circ$ is better than one would expect, considering the use of different equipment and methods, mapping errors and errors introduced by fracture roughness and curvature.

Comparison of the results of mapping of the west wall (Figure 5.15a) with that of the east wall (Figure 5.15c) does not reveal significant variation in orientations of the fractures across the room. However, as may be seen on the map (Plate 1), the orientations as well as the frequencies vary both in the longitudinal direction and across the room, when individual sampling lines are compared to each other. This introduces local heterogeneity that affects small scale permeability tests.

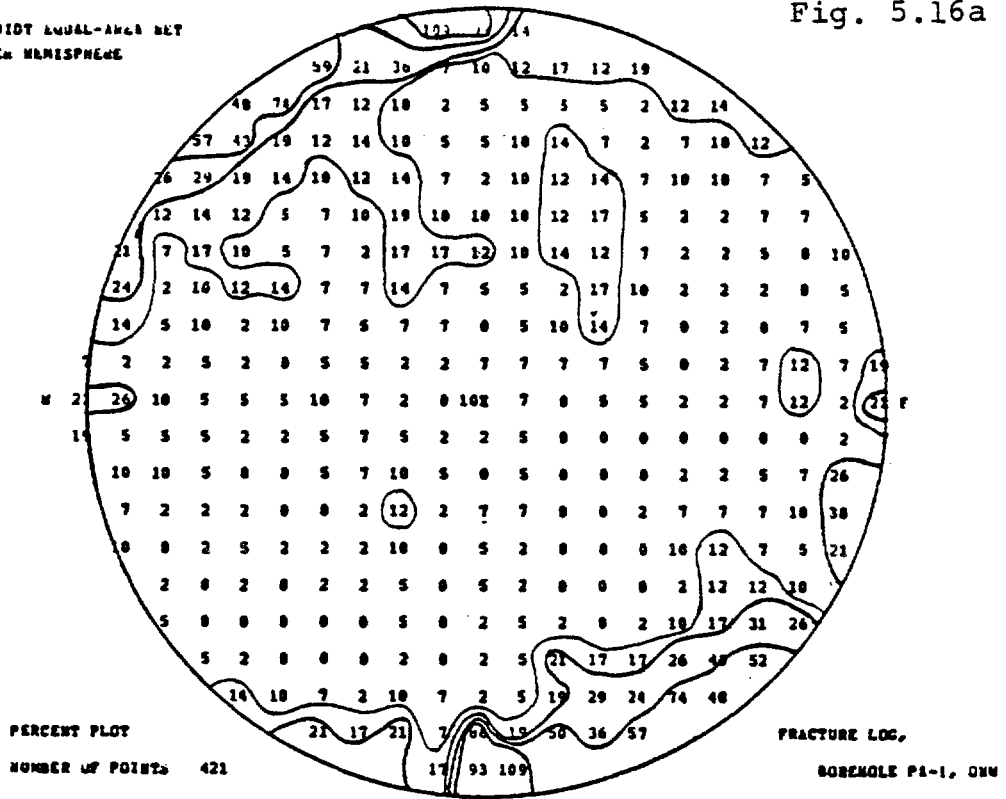
5.4.2.3 Core Logging.

The orientation data for the longitudinal boreholes is shown in Figures 5.16a through 5.16c. The high scatter of

FIGURES 5.16. Fracture orientation patterns from longitudinal borehole logs. Numbers in circles are per mil.

SCHMIDT EQUAL-AREA NET
LOWER HEMISPHERE

Fig. 5.16a



SCHMIDT EQUAL-AREA NET
LOWER HEMISPHERE

Fig. 5.16b

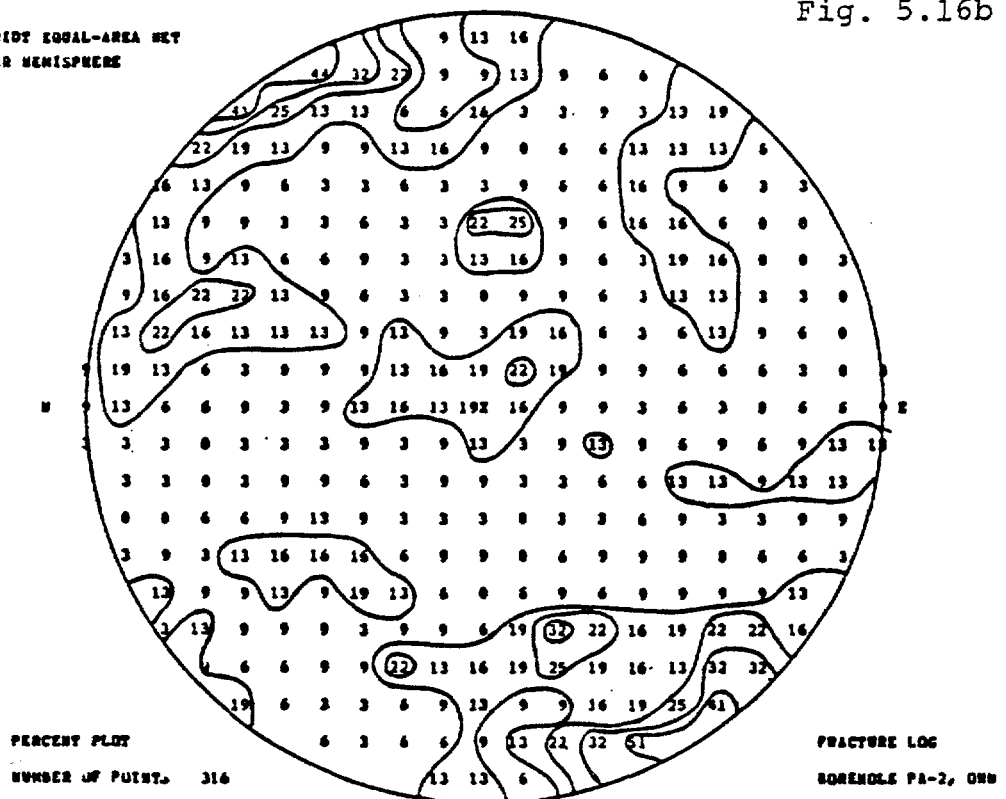
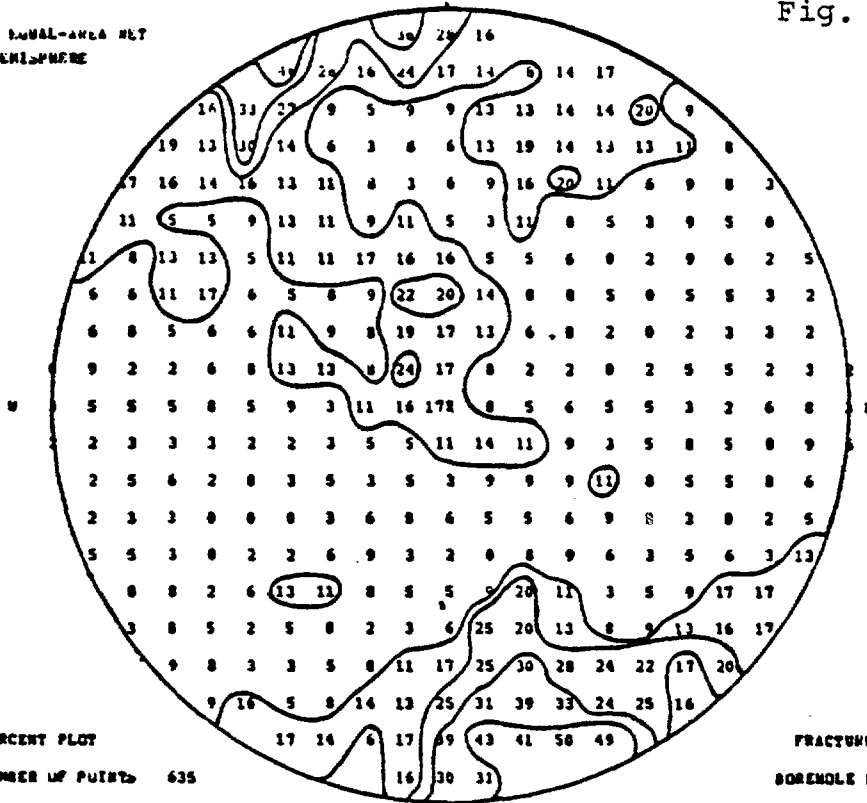


Fig. 5.16c

SCHMIDT EQUAL-AREA NET
LOWER HEMISPHERE



the points in these diagrams is due to the variations in accuracy of the core orientation. Despite this inaccuracy the attitudes of the foliation fractures agree to within $\pm 5^\circ$ with those from the line mapping (Figure 5.16d). Diagonal joints are not well sampled and a relatively low concentration is shown for this set. However, as can be seen in Plate 1, in some sections the diagonal joints are sampled with relatively high concentrations. Table 5.1 summarizes the significant fracture orientations along these scanlines.

5.4.3 Fracture Frequency, RQD and Spacing.

Prior to presentation of the results in this section it should be noted that two types of core logging are referred to: the field core logging which was completed on site immediately after removal of the core, and the detailed core logging which was carried out after completion of the drilling. In the field core logging, the purpose of which was mainly to preserve the initial arrangement of the pieces of the core, every break in the core, whether natural or artificial, was measured and recorded. In detailed core logging only natural fractures, disregarding the core integrity, were measured and described. Both results are presented here because it is believed that each contains information about different aspects of the rock properties.

Table 5.1- Summary of the significant fracture orientations.

Scanline(s)	strike/dip in decreasing order of significance				total no. of fractures
	1	2	3	4	
RH-boreholes	N50W/90 *				82
RU- ,,	N90E/30 S	N30E/60SE N00E/50 E N60W/60SW			68
RDE- ,,	N30E/50SE	N90E/60 S N60W/75NE*			94
RDD- ,,	N25W/75SW	N30W/60NE	N00E/75 S N05E/80NE		29
RDU- ,,	N50W/90 *				47
All radial boreholes	N50W/90 *	N30E/45SE			273
Mining faces	N65E/80NW+	N60W/90 *			710
West wall	N60W/90 *	N35E/90 N70E/70NW+	N45W/50SW	N25E/60SE	
West wall initial map	N45E/90 + N35W/50SW	N45W/90 * N70W/80NE* N35E/60SE	N60E/70NW	N90E/80 N	251
East wall	N75E/80NW+	N45E/75NW+ N75W/75NE*	N60W/90*	N40E/60SE	169
Room face	N50W/90	N65W/65NE	N30E/60SE		34
PA-1 borehole	N90E/90 *	N50E/85NW+			421
PA-2 ,,	N55E/90 +				316
PA-3 ,,	N70E/90 +				635

* Diagonal set
+ Foliation set

Figure 5.17a shows the frequency of breaks from the field logs. High frequencies are shown for the first meter of PA2 and PA3 and at several locations along the three longitudinal boreholes. The highest fracture frequency occurs near the shear zone (compare with Plate 1) for both PA2 and 3, whereas a lower frequency is shown in PA1. This does not necessarily indicate disappearance of the shear zone in PA1, rather it is indicative of excess core loss in PA1 at this depth. Examination of the RQD of detailed core logs (Figure 5.17b) shows very low values for this zone which confirms this. In addition T.V. camera survey clearly revealed the existence of the shear zone.

As a result of the treatment of the data, fracture frequencies calculated from detailed core logs (Figure 5.17c) are higher than those from field core logs (Figure 5.17a). The opposite is true for the RQD (Figures 5.17b and 5.17d). In locating significant fractures neither the frequencies nor the RQD values are completely reliable. However, by using all four in combination some trends can be correlated with the fractures mapped in the room. The frequency of open fractures along the PA-boreholes are plotted in Figure 5.17e.

For comparison the RQD's and frequencies are plotted for all the radial boreholes (Appendix IV). A significant anomaly can be seen in these figures. Most of the vertical boreholes show high frequency and low RQD for the beginning

FIGURES 5.17 - Fracture frequency and RQD
along longitudinal boreholes.

of the borehole, especially from the field core logging results. This may be due to several reasons:

- a - blast damage
- b - high stress concentrations
- c - drilling method

Because RQD from field core logs is more indicative of the rock strength than the fracture characteristics, low RQD near the opening could be due to the weakening of the rock by blast damage. High stress concentrations in the rock may also result in excessive core breakage. The beginning of each borehole is usually drilled with a started core barrel which is a single tube and does not provide any protection for the core. It is felt that the cause for the low initial RQD values is the combination of all three factors.

5.5 Summary.

Fractures and their significant characteristics were determined through logging of the cores from NX-boreholes, mapping of the walls of the boreholes by a borescope and a T.V. camera, and mapping of the walls of the room. Two major near-vertical fracture sets are identified, striking N50-60E and N40-50W. The first set is parallel and the

second is nearly perpendicular to the foliation. A third set, striking about N30E and dipping 60SE, also is present. Radial boreholes are found to be blind to the foliation fractures, but sample the oblique set very well. The longitudinal boreholes sample both sets, but are biased in favor of the foliation fractures. Only a few shallow dipping fractures are sampled in the vertical boreholes, showing their scarcity.

The shear zone crossing the room was found to be continuous across the three longitudinal boreholes and along one of the radial upholes with slight variations in minor details. Frequencies of the open fractures are comparable for the three longitudinal boreholes, except where excessive core loss has occurred. The high fracture frequencies at the proximal end of the radial boreholes are believed to be due to the combination of blast damage, high stress concentration, and drilling damage.

6. DESIGN, FABRICATION, AND CALIBRATION OF THE PERMEABILITY TESTING EQUIPMENT

6.1 Design Criteria.

The special hydrogeologic characteristics of the rock surrounding CSM/ONWI room:

- a) very low matrix permeability (10^{-15} cm²),
- b) unsaturated nature of the rock, and
- c) heterogeneous fracture distribution,

called for design of an instrument that could be used effectively and economically to characterize the permeability of the rock mass.

In addition, capability to measure small changes of permeability (Δk) at all ranges of expected permeabilities (10^{-8} to 10^{-15} cm²) was essential to assess modifications due to blasting and stress changes. It should be noted that equipment designed to measure high permeabilities are generally insensitive to small changes of permeability. In this latter category, whenever small permeabilities are encountered, the common practice is to increase the pressure which in some cases would require up to 2 MPa (300 psi) of injection pressure. It has been shown (Maini, et al.

1972) that, above about 0.2 MPa (30 psi) of excess pressure, fracture deformation and turbulence could introduce significant errors in the measured permeabilities.

In the present study, 0.2 MPa was set as the upper limit and it was not violated except in a few cases. In order to achieve the resolution required, the effort was concentrated on:

- a) increasing the resolution of pressure sensing devices,
- b) increasing the resolution of the flow rate measuring devices,
- c) providing a full control on detecting leakage, and
- d) developing reliable methods of calibration.

The unsaturated nature of the rock necessitated the applicability of both gas and water. This required a dual purpose flow metering system that could accurately measure flow rates of both water and gases. Also the flow and control devices had to be compatible to both phases.

In this chapter, the main components of the equipment are described briefly along with the calibration procedures. Both the equipment and the procedures were constantly upgraded during the course of the investigation. The effect of such modifications will be noted in Chapters 7 and 8.

6.2 Instrumentation.

6.2.1 Packer System.

Figure 6.1 shows the equipment for injection testing in an NX-borehole. The main injection probe, at area A (of Figure 6.1) consists of four packers and a transducer housing, spaced to create three chambers inside the borehole (Figure 6.2). The central chamber of the main probe is connected to the transducer through a short piece of steel tubing to reduce system compliance during transient testing. Each of the other chambers is connected to one transducer through plastic tubing. The central chamber can be pressurized with water or air; the pressure can be detected in all three chambers. There are two main advantages to having three chambers: any leakage around the packers is discovered immediately, and connected fractures and fractures striking parallel to the borehole can be detected. In

addition, in a homogeneous-anisotropic medium, directional permeabilities parallel and perpendicular to the borehole can be measured (Earlougher, 1979).

Water or air is injected into the central chamber (PT-2) through a continuous tubing. This greatly reduces the number of connections and, therefore, leakage possibilities. Pressure in the two end chambers is transmitted to the transducers, which are located immediately above the first packer, through plastic tubing. The transducer for measuring pressure in the central chamber is housed within the chamber. Placing the transducer housing inside the borehole results in a faster response due to closer proximity to the pressurized area. A greater distance between pressure chambers and transducer would delay transmission due to compressibility of the fluid and flexibility of the tubing. In fact, the delay to reach equilibrium may be up to several seconds for 30m of tubing. This is not desirable when transient testing is performed. Pressure in each chamber is sensed by transducers PT-1 through PT-3. A thermocouple is also housed in the central chamber to measure the temperature of the injection fluid.

Each monitoring probe consists of two packers forming a single chamber. This chamber can be pressurized with water or air or it can serve as a pressure observation chamber (Figures 6.1 and 6.3).

FIGURE 6.2a. The middle chamber of the main probe being tested for leaks.

FIGURE 6.2b. The pulse tester which is housed along with a transducer in the middle chamber.

FIGURE 6.2c. The outer pressure port of the main probe.

FIGURE 6.3. The monitoring probe .

6.2.2 Flowmetering System.

Four flow measuring devices were used simultaneously in order to observe and compare the accuracy and applicability of each system. These are shown in Figure 6.1 at areas B, C, D, and E.

The flow tank system (Figures 6.1B and 6.4) relies on the differential pressure across the transducer (DT-1), caused by the head of the water in the tank and a small friction loss across the fittings, to measure flow volume. The flow volume is linearly related to the rate of pressure drop assuming that the cross-sectional area remains constant throughout the tank. By reducing the diameter of the tanks the accuracy and sensitivity can be increased. This system cannot be used to measure the air flow rate.

The tracer line measures very small amounts of flow (Figures 6.1C and 6.5) by introducing a bubble or an electrolyte into the flowline. The time required for the pulse to travel between the two electrodes can be converted to flow rates.

A metering valve with a differential transducer (Figures 6.1 and 6.4) was also used. It is a very accurate and simple flow measuring device. However, the pressure behind the valve must be constant, which is accomplished with reducer valves and the flow tank system. In order to

FIGURE 6.4. The flow tank system. The upper row of valves selects the tank to be pressurized, the middle row selects the tank pressure to be read, and the lower row selects the outflow. Note the metering valve on the lower right.

FIGURE 6.5. The tracer line system.

be able to measure wide ranges of flows, two metering valves were used. The number of components required to construct this flow meter is fewer than all the others mentioned here. Therefore, it is the least expensive and most versatile.

Rotameters (Figures 6.1E and 6.6) also give accurate flow data and are simple and easy to use. However, they are sensitive and easily damaged. Each consists of a small sphere in a semiconical tube which moves as the flow rate changes. Five rotameters were used to obtain all possible ranges of flow. The advantage of the metering valve and rotameters is that they can be used for air flow rate as well as for water flow rate measurements.

6.2.3 Data Acquisition System

Figure 6.1 shows a very simplified schematic of the data acquisition system. All transducers are excited using a single 12V DC regulated power supply which is stable to 0.1mV. The output signals from the transducers are input into a 16 channel programmable Kays Instrument Digistrip II datalogger which is interfaced with a cassette tape recorder compatible with the CSM DEC-10 system computer (Figure 6.7).

Temperatures in the tanks and the injection zone originally were measured using YSI thermistors (T-1 and T-2) which later were replaced by type T thermocouples

FIGURE 6.6. The rotameter array, connected in series to provide a full range of 0.01 cc/min of water (1cc/min of air) to 25 lit/min of water (70 lit/min of air).

FIGURE 6.7. The data acquisition system. Above is the data logger, on the lower left the control terminal is located, and on the lower right the chart recorder and the cassette recorder can be seen.

(thermocouples being more compatible with the data logger). Conductivity meters were connected to a Schlumberger stripchart recorder and were powered separately.

6.2.4 Calibration.

One of the most important parts of injection testing of low permeability rock is calibration of the instruments. Calibration here refers to all the procedures that are necessary to increase accuracy of the results. Of major concern in using a packer system is the leakage in the flow system that occurs after the flow meter(s). The loss of fluid from the system may occur either from the tubing connections or from around the packers. If any flow occurs around those packers which isolate the main injection zone, it can be detected by a pressure response in the adjacent monitoring zones. This can be differentiated from the response due to fracture connections between the zones through the rock. In fractured rock the flow through the matrix is so slow that it would require a very long time for any flow path to be established between these zones. In case a high conductivity fracture connects these zones, its presence is usually detected easily during packer inflation.

A standard procedure has been developed to calibrate the permeability testing equipment at the CSM/ONWI test

site. The main probe is set inside a pipe with an inside diameter about the same as the borehole diameter (Figure 6.8). After calibration of all the measuring devices, a simulated injection test is conducted. The permeability obtained from such a test should be zero. If a zero permeability is not obtained, various sections of the flow system are isolated to locate the problem area. If the problem area cannot be found, the rock permeabilities obtained from the actual tests are corrected with the fictitious permeability.

6.3 Summary.

Multichamber-packer injection testing equipment was designed and assembled to assess the permeability of the fractured rock surrounding the CSM/ONWI room. The equipment consists of a main probe, which is a three chamber packer assembly and two monitoring probes, each of which is a single chamber-double packer assembly. Four different flow metering devices were used to measure flow rate of gases and water. Flow rates as small as 0.01 cc/min of water and one cc/min of nitrogen can be calibrated. Smaller flow rates can be sensed by the instrumentation, but cannot be calibrated easily. Pressures as low as 7 Pa (0.001 psi) can be sensed inside the boreholes. Combination of these allows measurement of permeabilities as small as $1.0E-17$ sq. cm., employing steady state tests. Using transient

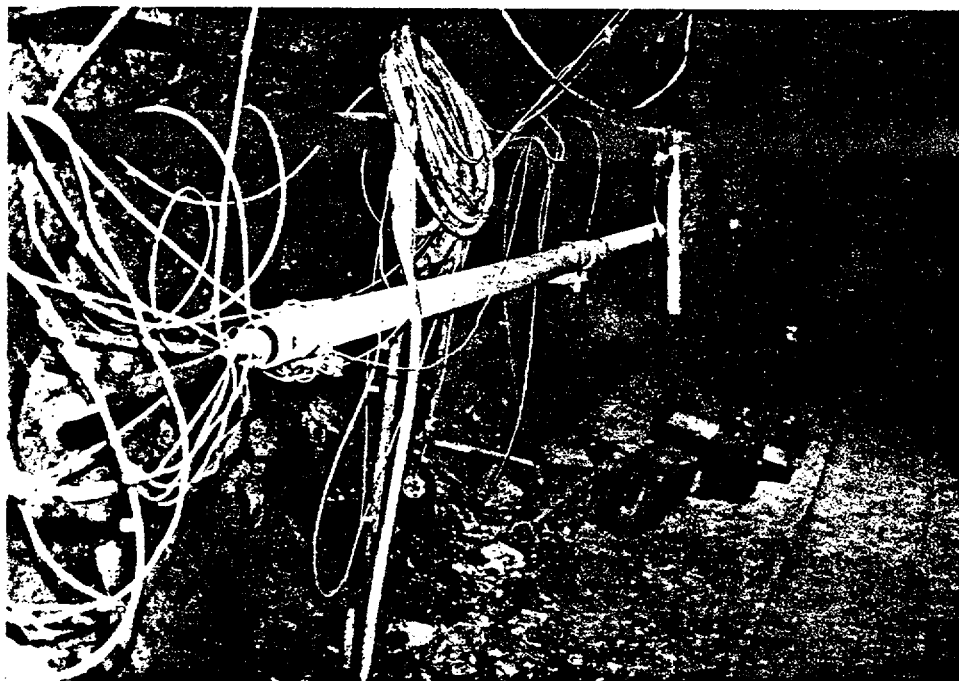


FIGURE 6.8. The main probe is inserted into a long piece of steel pipe for calibration.

tests, much smaller permeabilities can be measured, but the leakage around the packers should be reduced or corrected for. Values given here are for the minimum separation of the packers (1.2m or 4.0 ft.) and a maximum pressure of 0.25Mpa (35 psi). By increasing the length and or pressure, higher resolutions can be obtained.

7. TESTING OF PACKER EQUIPMENT IN A CONCRETE COLUMN MODEL.

Packer testing has been used in measuring permeability of rock formations for more than three decades. Many different equations with varying levels of complexity are now available to analyze data obtained from such tests. However, no attempt has been made to actually verify the applicability or accuracy of such analyses. The purpose of this part of the present investigation has been to determine the validity of the assumptions made in analysis of packer test data and to provide additional means of calibration.

7.1 Preparation of the Model.

A relatively large physical model was required for testing. A concrete column 3.7 m (12 ft.) long and .61 m (2 ft.) in diameter was prepared from silica sand (20-30 mesh) and portland cement (Figure 7.1). A mixture of 2 parts sand, 1 part cement and 1 part water was chosen on the basis of small test batches. This mixture produced the most uniform and lowest permeability concrete. Due to space restrictions and the large volume required it was not possible to pour the concrete in one batch. Several batches with a consistent mixture were poured in a period

FIGURE 7.1. The concrete column being tested with nitrogen with the main probe set in the center hole. In this picture the column is being prepared for water testing.

of four hours (setting time for the mixture was estimated to be 12 hours from the test batch). Uniformity was improved by vibration of the mixture inside the mold. A 7.4m (2.9 in.) hole was cast in the center along the axis of the column. This hole was reamed by an NX diamond bit to produce wall roughness similar to that of the boreholes.

7.2 Testing of the Model Using the Main Probe.

The column was allowed to cure inside the mine for about six months prior to testing. At the end of that time no visible cracks or imperfections were observed.

The testing equipment was at its final stage of development when used for testing the concrete column. All modifications that seemed necessary had been made during the systematic air injection testing (see following chapter). The only difference between the equipment used for the concrete column and that used for cross-hole testing was shortening of the length of the end chambers, so that the entire probe could fit inside the 3.7 m long center hole of the column.

The main probe was placed inside the hole and testing with nitrogen was conducted using the procedures outlined in the following chapter (see systematic nitrogen injection). Steady state points were obtained for 16 pressures ranging from about 0.03 to 0.3 Mpa (4 to 40 psi) at

two intervals: 1.2 to 2.4 m (4 to 8 ft.) and 0.4 to 1.6 m (1.3 to 5.3 ft.) from the end. Each test lasted from 5 to 24 hours. After each steady state test, a decay test, followed by a pulse test, was conducted. One major difference between these tests and the systematic tests was that in all cases the medium (concrete) was allowed to equilibrate with the mine pressure prior to initiation of another test.

Prior to water testing the center hole was pressurized with carbon dioxide to facilitate saturation. However, even after 30 days of water injection complete saturation was not achieved. Several water injection tests were conducted which were then followed by carbon dioxide and nitrogen injection tests.

7.3 Testing Samples of the Concrete Column

Two 15 cm (5.9 in.) diameter cores were obtained from the concrete column (Figure 7.2 and 7.3). From these several 5 cm (2 in.) diameter cores were prepared in the laboratory (Figure 7.4). One sample was tested with nitrogen and another with water in a modified triaxial cell (Figure 7.5 and 7.6). Three tests were conducted with nitrogen at 0.7 and 1.2 MPa (150 and 170 psi). Decay and pulse tests were also conducted on this sample. It should be noted that the flow metering system used during testing of the

FIGURE 7.2. Drilling of a 15 cm (5.9") core from the concrete column.

FIGURE 7.3. The 15 cm (5.9") diameter core. Note the high porosity of the sample.

FIGURE 7.4. Five cm (2 in.) diameter cores were obtained in the laboratory from the 15 cm core. The wax in the pores (white spots) are applied to protect the sleeve of the triaxial cell and prevent leakage.

FIGURE 7.5. A standard triaxial cell was modified to test the 5 cm cores. The piston is for measuring downstream flow or imposing a constant pressure at the downstream side. See Figure 7.6 for more details.

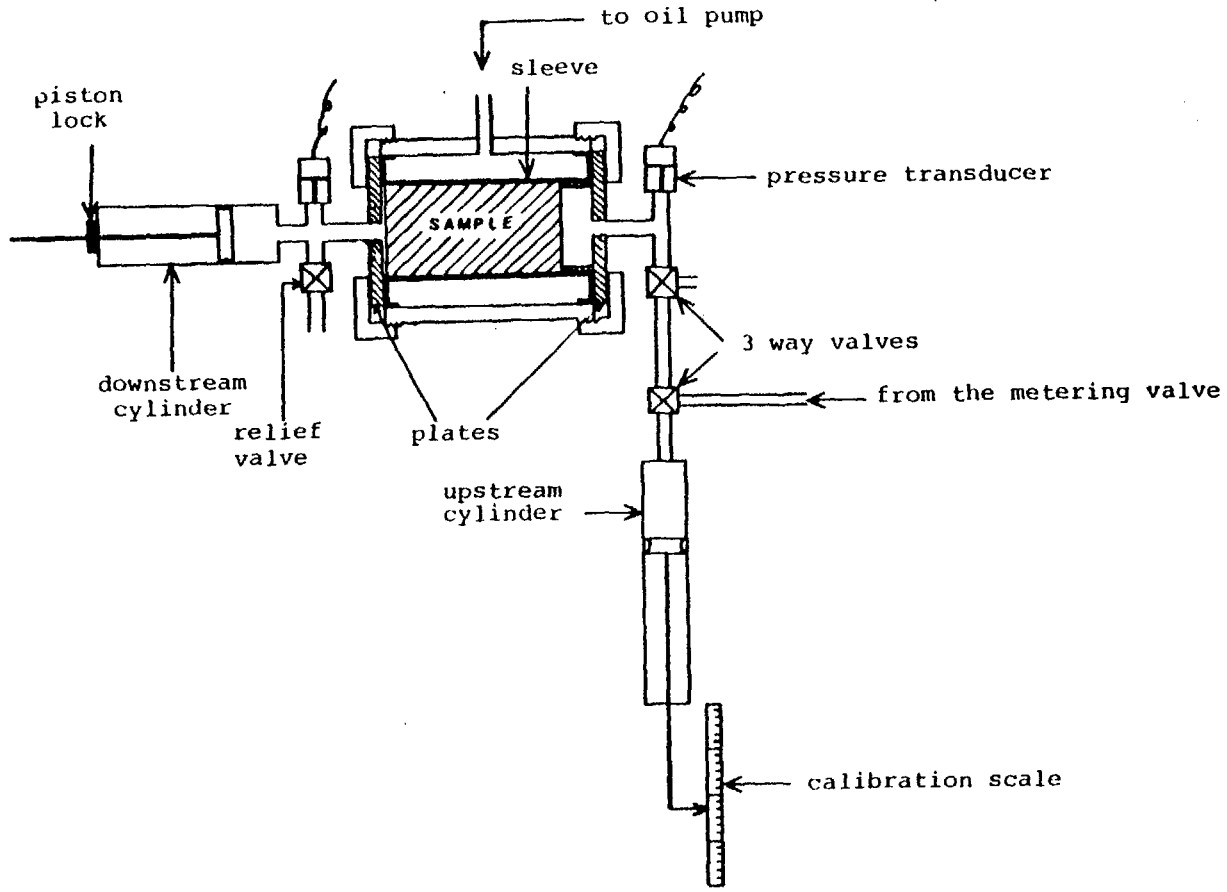


FIGURE 7.6. Schematic diagram showing the modified triaxial cell.

5 cm cores in the modified triaxial cell (Figure 7.6) was completely different from that used for the packer system.

The gas (nitrogen and carbon dioxide) flow rate was measured both on the downstream and upstream sides of the sample. On the upstream side it was measured by means of the fine metering valve. On the downstream side the flow rate was calculated from displacement of a piston, which also aided in keeping the downstream side at a constant pressure (constant friction between the piston and the cylinder). In calculating the permeability, the flow rate measured by the net piston displacement was used. Because the permeability of the sample was calculated on the basis of data collected by a completely different set of instruments than for the packer testing of the large concrete column model, comparison of the two is devoid of any bias.

Saturation of the second sample with water could not be achieved even after three weeks of maintaining an upstream pressure of 1.4 MPa (200 psi) and a downstream pressure of 0.5 Atm (-7.5 psi) vacuum (provided by the same piston mentioned above). Waterflow rate was attempted to be measured by a second piston (Figure 7.6). The amount of displacement was so small after five days that it could not be reliably used for steady state calculations. Therefore, only a pulse test could be conducted for this sample. It should be noted that carbon dioxide pressurization prior

to water injection also proved difficult.

7.4 Data Analysis.

7.4.1 Concrete Core Sample

7.4.1.1 Steady State Gas Injection.

The steady state one dimensional flow of an ideal gas through porous media is governed by (Collins, 1961):

$$\hat{V}_1 = k_\ell \times \delta \times (p + B) \frac{dp}{dx_1} \quad (7.4.1)$$

where k_ℓ is the permeability to a liquid and:

$$\delta = - \frac{M}{\mu RT}$$

\hat{V}_1 = specific mass flux (mean flow rate per unit area) (M/TL^2)

p = pressure (M/LT^2)

B = is a constant characteristic of the gas and the medium and has dimensions of pressure

M = molecular weight of the gas

R = the gas constant

T = temperature

μ = dynamic viscosity (M/LT).

Assuming that specific mass flux is invariable in the x_2 (perpendicular to the core axis, Figure 7.7) direction, equation 7.4.1 can be integrated throughout the length of the sample:

$$\hat{V}_1 = \frac{\hat{Q}}{A_s} = \frac{1}{2L_s} \delta k_\ell \frac{(p_u^2 - p_d^2)}{p_d} \left(1 + \frac{B}{(p_u + p_d)/2} \right) \quad (7.4.2)$$

Solving for k_ℓ :

$$k_\ell = \frac{2p_d Q_d L_s}{A_s (p_u^2 - p_d^2) \left(1 + \frac{B}{(p_u + p_d)/2} \right)} \quad (7.4.3)$$

where \hat{Q} is replaced by:

$$\hat{Q} = Q_d \rho_d$$

Since:

$$k_g = \left(1 + \frac{B}{(p_u + p_d)/2} \right) k_\ell \quad (7.4.4)$$

Then

$$k_g = \frac{2Q_d L_s p_d^\mu}{A_s (P_u^2 - p_d^2)} \quad (7.4.5)$$

where (see also Figure 7.7):

k_g = permeability to a gas

k_l = permeability to a liquid

p_u = upstream pressure

p_d = downstream pressure

Q_d = volume flow rate out of the downstream side

\hat{Q}_d = mass flow rate out of the downstream side

L_s = length of the sample

A_s = area of the sample

Equation 7.4.3 is the same as the Klinkenberg equation (see Chapter 3) and indicates the pressure dependence of gas permeability. The parameter B is difficult to find with a single test alone, however by using equation 7.4.5 and several tests, B can be found (see the results in this chapter).

7.4.1.2 Analysis of Decay and Pulse Tests.

Transient one dimensional flow of an ideal gas is governed by (Collins, 1961):

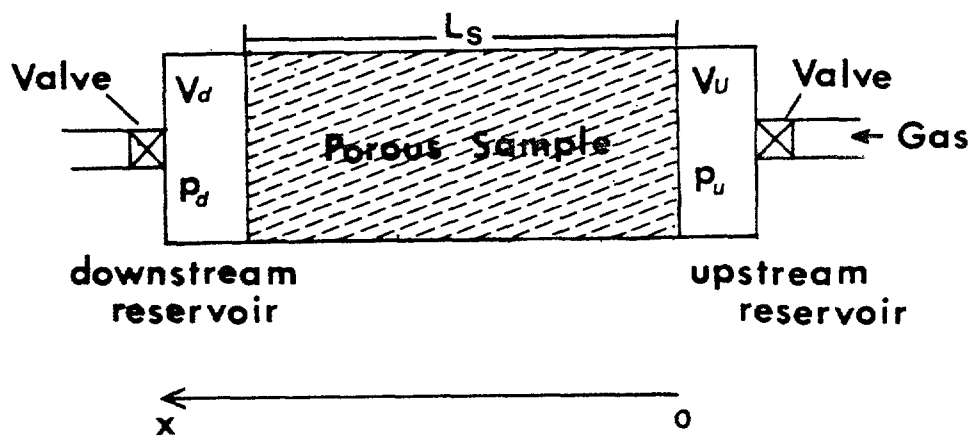


FIGURE 7.7. Schematic diagram showing the variables used for deriving flow equations.

$$\frac{\partial}{\partial x_1} \left(p \frac{\partial p}{\partial x_1} \right) - \frac{\phi \mu}{k_g} \frac{\partial p}{\partial t} = 0 \quad (7.4.6)$$

where ϕ is porosity. Two cases are needed to be considered:

- a) decay test, where the initial condition is the stabilized steady state condition and:

$$\frac{\partial}{\partial x_1} \left(p \frac{\partial p}{\partial x_1} \right) = 0 \quad (7.4.7)$$

- b) pulse test, where the initial condition is:

$$p = \text{constant (throughout the sample)} \quad (7.4.8)$$

Double integration of 7.4.7 yields:

$$p(x_1) = \left[\frac{x_1}{L_s} (p_d^2 - p_u^2) + p_u^2 \right]^{\frac{1}{2}} \quad (7.4.9)$$

where the symbols are as defined before.

It should be noted that (7.4.8) is a special case of (7.4.9). It is true when:

$$p_d = p_u$$

for this reason only the more general case (7.4.9) will be considered first.

The flow rate into the sample on the upstream side, after the input flow is shut, is given by

$$Q_u = \frac{-k_g}{\mu} A \left(\frac{\partial p_u}{\partial x_1} \right)_{x_1=0} \quad (7.4.10)$$

and (isothermal conditions)

$$Q_u = - \frac{v_u}{p_u} \frac{dp_u}{dt} \quad (7.4.11)$$

where v_u is the volume of the upper reservoir. Combining the latter two equations:

$$\frac{\mu v_u}{A_s k} \frac{dp_u}{dt} - \left(p_u \frac{\partial p_u}{\partial x_1} \right)_{x_1=0} = 0 \quad (7.4.12)$$

Similarly for the downstream side we have:

$$\frac{\mu v_d}{A_s k} \frac{dp_d}{dt} + \left(p_d \frac{\partial p_d}{\partial x_1} \right)_{x_1=L_s} = 0 \quad (7.4.13)$$

Following Bruce et al. (1953) in changing the variables:

$$x = \frac{x_1}{L_s}$$

$$P = \frac{p}{p_{u0}} \quad , \quad P_0 = \frac{p_{d0}}{p_{u0}}$$

$$\tau = \frac{p_{u0} k_g}{2L_s^2 \phi \mu} t$$

$$W_u = \frac{v_u}{v_p}$$

$$W_d = \frac{v_d}{v_p}$$

where:

p_{u0} = pressure in the upstream reservoir at time
($t = 0$)

$v_p = \phi A_s L_s$ = pore volume.

The equations to be solved are then reduced to:

$$\frac{\partial^2 P^2}{\partial x^2} - \frac{2\partial P}{\partial \tau} = 0 \quad (7.4.14a)$$

$$W_u \frac{2dP_u}{d\tau} - \left(\frac{\partial P_u^2}{\partial x} \right)_{x=0} = 0 \quad (7.4.14b)$$

$$W_d \frac{2dP_d}{d\tau} + \left(\frac{\partial P_d^2}{\partial x} \right)_{x=1} = 0 \quad (7.4.14c)$$

$$P(x,0) = \sqrt{x(P_0^2 - 1) + 1} \quad (7.4.14d)$$

Equation (7.4.14a) is a non-linear 2nd order partial differential equation which does not easily lend itself to analytical solution. Hsieh et al. (1981) have solved similar equations for a liquid of constant compressibility (water). Their method involves solving the diffusivity equation which is a linear partial differential equation. Even in the simplified case of Hsieh, the complexity of the analytical solution is evident. It is interesting to note that equations (7.4.6) and (7.4.14a) are of the same form as the Boussinesq equation describing the flow of groundwater with a free surface (Bear, 1972). Although Boussinesq (1904) as reported by Bear (1978) and some others (McWhorter and Duke, 1976; Schilfgaard, 1963; and Brooks, 1961) provided analytical solutions of this equation with simple boundary

conditions, no closed form solution was found to match the boundary and initial conditions described by equations 7.4.14b to d.

Finite difference techniques have been used frequently to solve this type of problem. Jenkins and Aronofsky (1953) and Bruce, et al. (1953) provided numerical solutions for equation (7.4.14a) with simple boundary conditions. Bruce, et al. (1953) specifically provided both implicit and explicit methods. Their explicit method was modified to include the boundary and initial conditions of the present study.

Application of Taylor's series expansion of P and P^2 about ΔX and $\Delta \tau$ will result in (in the same order as equations 7.4.14):

$$P_{i, k+1} = r (P_{i+1, k}^2 + P_{i+1, k}^2 - 2P_{i, k}^2) + P_{i, k} \quad (a)$$

$$P_{0, k+1} = \frac{1}{W_u} \frac{\Delta \tau}{\Delta x} (P_{i, k}^2 - P_{0, k}^2) + P_{0, k} \quad (b)$$

$$P_{n, k+1} = \frac{1}{W_d} \frac{\Delta \tau}{\Delta x} (P_{n-1, k}^2 - P_{n, k}^2) + P_{n, k} \quad (c)$$

$$P_{i, 0} = \sqrt{i \Delta x (P_0^2 - 1) + 1} \quad (d) \quad (7.4.15)$$

where:

$$r = \frac{\Delta T}{(\Delta X)^2} .$$

In equation (7.4.15d), the stability requirement is (Bruce, et al., 1953):

$$r \leq \frac{0.25}{P_k}$$

For this study 50,000 time steps were used to allow half the pressure to be decayed. The type curves produced by numerical solution are shown in Figure 7.8. The experimental results are shown in Figure 7.9 for comparison. In both the cases of the pulse and decay tests, the experimental results are reproduced by the numerical model.

The method of finding porosity and gas permeability is simply to find the W_u curve that fits the experimental results. The porosity (ϕ) is then found by:

$$\phi = \frac{W_u A_s L_s}{v_u}$$

and k_g from:

$$k_g = \frac{2\tau L^2 \phi \mu}{p_{u0} t}$$

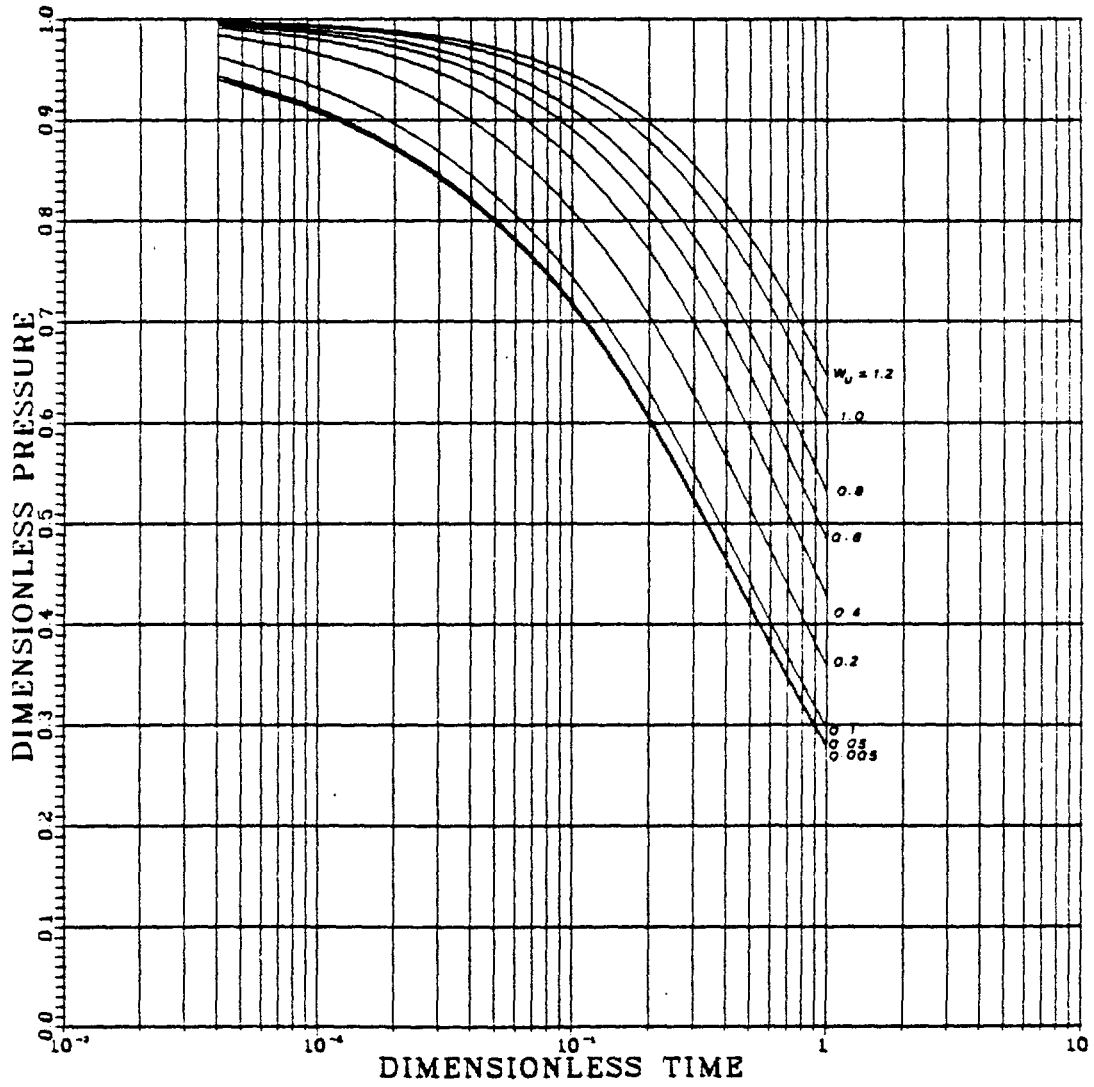


Figure 7.8. Type curve for pressure decay test of cylindrical core sample. Downstream pressure is constant.

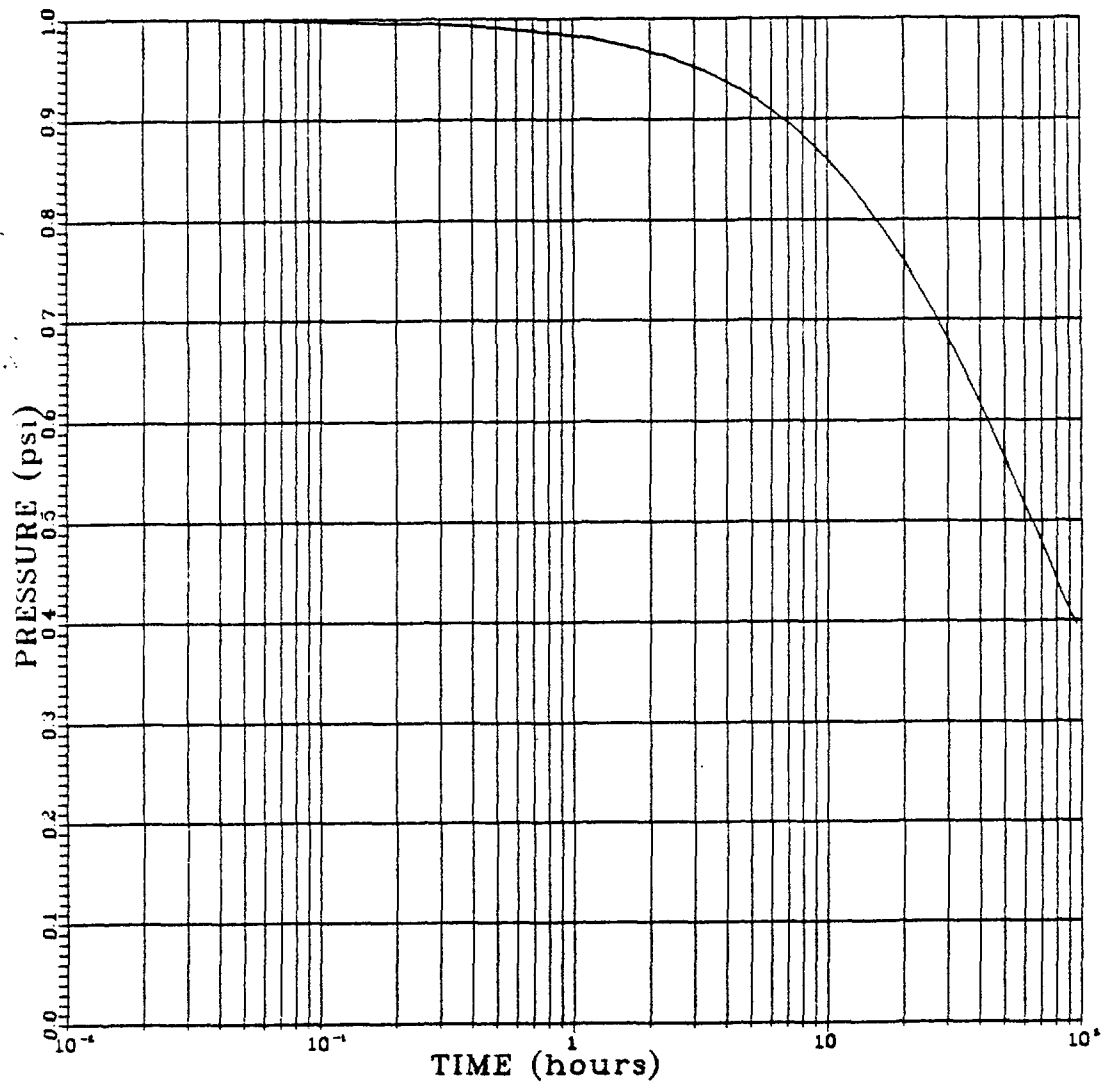


Figure 7.9. Sample 1 decay test no. 4 (carbon dioxide).
Downstream pressure = 1.51 psi.

where τ and t are found from a matching point.

7.4.2 Analysis of Column Test Results

Because the main interest, in conducting experiments involving the concrete model, was to verify the applicability of the steady state radial flow equation with ellipsoidal and cylindrical distribution of potentials (Zeigler, 1976), data from testing of the concrete column were analyzed using these equations.

Zeigler (1976) has extensively reviewed the packer testing methods and equations used to analyze the data. Since the potential distribution in the concrete column is nearly elliptical, the equation of Hvorslev (1951) was used for analysis of data. For an incompressible fluid this equation may be written as:

$$k = \frac{\mu Q}{L(p_i - p_w)} \left[\frac{1}{2\pi} \sinh^{-1} \left(\frac{\ell}{2r_w} \right) \right] \quad (7.4.16)$$

where:

k = permeability

μ = viscosity

Q = flow rate into the test zone

L = length of the test zone

p_i = initial aquifer pressure

p_w = steady state zone pressure

r_w = radius of the borehole

For compressible fluid and elliptical distribution of the potential, permeability may be calculated from (modified after Zeigler):

$$k = \frac{M_w}{\alpha \pi \ell} \frac{\sinh^{-1} \left(\frac{\ell}{2r_w} \right)}{(p_a^2 - p_w^2)} \quad (7.4.17)$$

where:

$\alpha = -m/\mu RT$

m = molecular weight of the gas

μ = viscosity

R = gas constant

T = absolute temperature

p_a = atmospheric pressure

M_w = mass flow rate in the borehole.

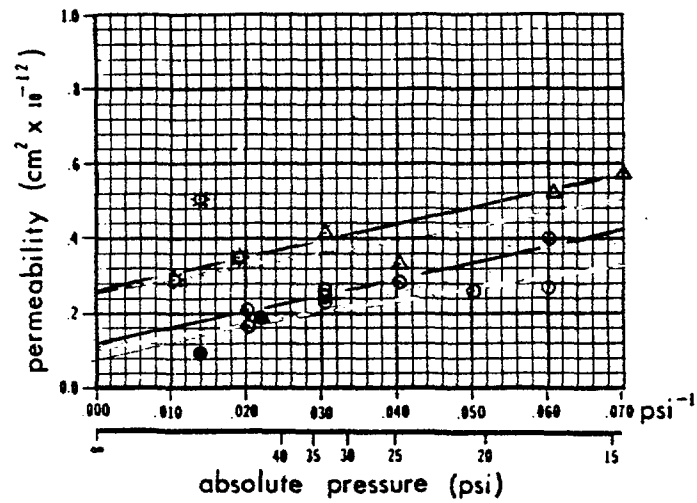
The above two equations were used to analyze the data from steady state testing of the concrete column. Equation 7.4.16 was used for analysis of the water test data and 7.4.17 was employed to analyze the nitrogen and carbon dioxide tests.

7.5 Results.

Figure 7.10 shows the plot of permeability versus the inverse of the pressure. In this figure, only permeabilities to nitrogen for both the sample and the concrete column are shown. The two straight lines are the least square fits to the permeabilities (calculated using the elliptical equation) obtained from packer testing of the concrete column. The lower line is fitted through the data from the 1.2 - 2.4 m interval and the upper line is for the data from the 0.4 - 1.6 m interval. From consideration of D'Arcy's Law a straight horizontal line is expected to be obtained. This deviation from D'Arcian flow may be explained by the Klinkenberg effect (see Chapter 3). In order to obtain the equivalent-liquid permeability (k_g), the permeability at infinite pressure should be determined. This may be accomplished by extrapolation of the straight lines in Figure 7.10 to infinite pressure.

In Figure 7.10 extrapolation to infinity of each set of tests is shown by dashed lines. The average permeability of the concrete was determined by regression of both data sets pooled. The equation describing the average gas permeability is

$$k_g = 0.126 \times 10^{-12} \left(1 + \frac{0.265}{p} \right)$$



- concrete column-interval 1.2-2.4m
- △ concrete column-interval .4-1.6m
- * concrete core sample-steady state tests
- concrete core sample-transient tests

FIGURE 7.10. Results of testing the concrete column and samples with nitrogen.

in which k_g is permeability to gas in cm^2 and p is the pressure in MPa. From this equation the permeability of the concrete to a liquid is expected to be $1.26 \times 10^{-13} \text{ cm}^2$ (when $p \rightarrow \infty$). Results of the testing of the 5cm (2 in.) core sample of the concrete from both steady state and transient tests are also shown in this diagram. The permeabilities measured by the decay tests are smaller than those determined from the steady state tests. In any case, the results obtained by the testing of the small samples agree very well with those of the 3.9m (12 ft.) long concrete column.

Two important conclusions can be drawn from these experiments. First, there is no apparent size effect; the permeability of the 5 cm core represents that of the 3.9m column. Second, permeabilities determined from packer testing are reliable even though simplified equations are used for permeability calculation. Moreover, the instrument is reliable at this level of permeability (10^{-13} cm^2).

Permeabilities of the concrete column measured at various pressures with water are plotted in Figure 7.11. In this case permeability increases with increase in pressure (or with decrease in inverse of pressure). In addition, permeabilities measured with water are two orders of magnitude smaller than those measured with nitrogen. This is believed to be due to the unsaturated nature of the concrete.

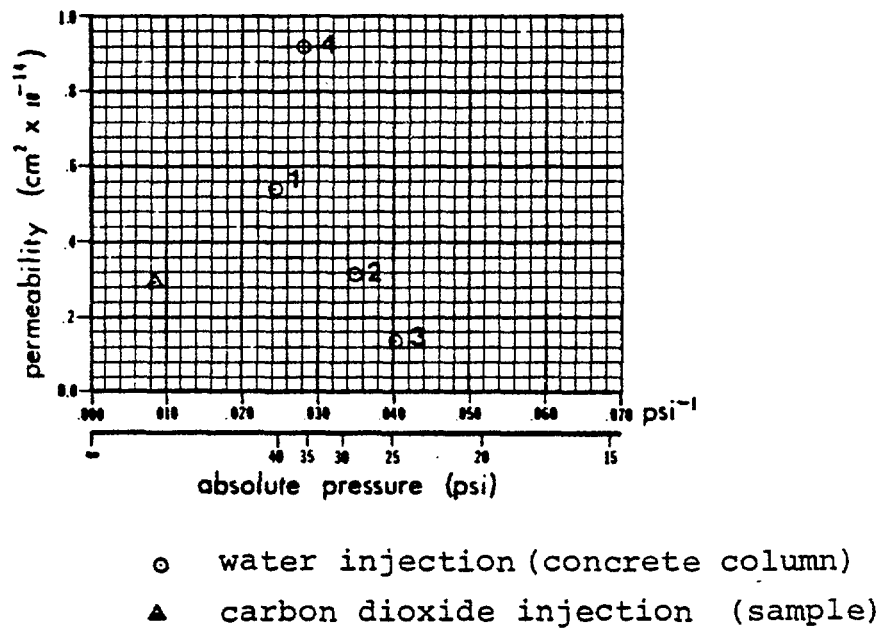


FIGURE 7.11. Results of testing the concrete column and sample with CO_2 and water.

The numbers in this diagram refer to the order of tests. Test number 4 was conducted after 20 days of water injection, whereas test number 1 is the result of 5 days of injection.

When a porous medium is saturated with a non-wetting phase (gas in this case), its total saturation with a wetting fluid (water in this case) is almost impossible with practically applicable pressures in relatively short times. In the present case it should have been increased to the level that would either dissolve any entrapped gas or overcome the capillary pressure (which can be in excess of several tens of MPa). The increase in permeability to water shown in Figure 7.11 may be attributed to the compressibility of the gas. As the pressure is increased the gas phase entrapped in the pores is compressed to smaller volumes. Therefore, a larger cross-sectional area is available for the flow of water.

For this reason it is suggested (Gale, 1980 private communication) that the medium should be saturated by a gas that is more soluble in water, for example carbon dioxide. Both the concrete core sample and the column were injected with carbon dioxide prior to injection with water. However, it was noticed that during displacement of nitrogen with carbon dioxide, in both the sample and the column, the flow

rate assumed a constantly decreasing trend. The permeability of the sample to CO_2 is also shown in Figure 7.11. It can be seen that permeability to CO_2 of the sample is in the same order of magnitude as permeability to water.

It should be noted that at the pressure and temperatures of the test, carbon dioxide is below its critical point (Barrow, 1973), that is both liquid and gas phases could exist simultaneously. It is suspected that the same phenomenon as described above for water controls the permeability of the sample to CO_2 . Under such conditions, injection of CO_2 causes an increase in the volume of the hygroscopic water held by the cement (Daniel Bass, 1982, private communication). The carbon dioxide-water mixture acts similar to the degased water. Therefore, no advantage is gained by presaturation of the medium with carbon dioxide.

It is concluded that the permeability obtained with nitrogen at infinite pressure can closely estimate the saturated permeability to liquid of the concrete. Furthermore, the packer testing equipment, developed for this research, can measure the permeability of a porous medium with an accuracy comparable to laboratory testing equipment.

7.6 Summary.

To assess the reliability of the injection testing equipment and the validity of the steady state radial flow equations, the packer testing equipment was tested in a simulated borehole made along the center line of a cylindrical concrete column 4m (12 ft.) long and 0.6m (2 ft.) in diameter. Numerous steady state tests with nitrogen and a few with water and carbon dioxide were conducted on the column. Steady state and transient tests were also conducted on 5 cm diameter cores from the column.

Permeabilities measured in the concrete column by the packer testing equipment using nitrogen are closely reproducible by the results of testing of the samples using steady state and transient tests ($1.3E-13$ sq. cm). Permeabilities from water testing of the concrete column are two orders of magnitude smaller than the results of nitrogen injection. Carbon dioxide testing of the core sample results in permeabilities in the same order of magnitude as that with water testing of the column.

I believe that the results of nitrogen injection testing of the concrete are more reliable than the results from the other two fluids, provided that correction is made for the Klinkenberg effect.

8. FRACTURE PERMEABILITY CHARACTERIZATION

8.1 Rationale.

The purpose of the series of experiments discussed in this chapter was to determine the extent of the modifications in the permeability of the rock mass due to the excavation of the CSM/ONWI room. This was made difficult by the lack of information about the virgin state of the rock mass permeability. Although some preliminary injection tests were conducted prior to the excavation of one of the faces of the CSM/ONWI room, instrumentation and procedures used for permeability testing were not well developed and the data were not considered reliable enough to draw any solid conclusions. Therefore, a program of data collection was designed and carried out, after the completion of the excavation, to try to delineate the induced changes (if any) in permeability of the host rock and their causes. This method is statistical in nature and is based on trend analysis.

The method of data collection consisted of two basic parts:

- a) systematic sampling of the permeability at pre-selected intervals in all boreholes, and
- b) sampling of the conductivity along preselected

fractures.

Several experiments were also conducted to study other possible factors, other than the excavation effect (such as variation in saturation in the rock or testing procedures), that may have been responsible for the observed permeability trends.

8.2 General Testing Procedures.

Three types of tests were used for measurements of permeability and/or conductivity:

- a) quasi-steady state
- b) decay after quasi-steady state equilibrium, and
- c) pulse test after natural or steady state equilibrium.

All three types of tests were employed. For systematic testing of the longitudinal boreholes only the results from the quasi-steady state tests were used for interpretation. The results of the quasi-steady state tests were also used for interpretation of the outcome of the systematic testing of the radial boreholes. In certain cases, however, instrumentation of the radial boreholes did not allow steady state testing. In such cases the results of pulse testing were used for presentation. This inconsistency does not affect the conclusions drawn since pulse testing was carried out for very low permeability zones in radial boreholes. A general description of the procedures used for each type of

test is outlined here.

8.2.1 Steady State.

In testing any natural media, the conditions of steady state equilibrium may be achieved only in rare circumstances (Earlougher, 1977). Normally, a source or a sink with a constant strength is introduced by either injection or withdrawal of a fluid at constant flow or constant pressure (Doe and Remer, 1981). The wave of the disturbance of the potential distribution within the medium travels indefinitely unless a boundary of no flow or constant pressure is reached. However, if axi-symmetric flow conditions are created by the pressure disturbance, the strength of the pressure wave decays very rapidly as it moves away from the source or sink. Therefore, after some time a state of quasi-steady equilibrium is reached when the continuation of the fluid injection or withdrawal does not significantly alter the state of the medium. This concept is discussed in mathematical terms by Earlougher (1977). In the discussions that will follow, the term "steady state" is used instead of the quasi-steady (or pseudo-steady) state for convenience.

Normally, either a single or a sequence of tests is conducted. After the packers are set in the selected zone, flow is opened at a predetermined pressure. Injection is

continued until flow becomes constant and the pressure inside zone #2 does not fluctuate more than 14 KPa (0.02 psi) for at least 15 minutes (this may require 24 hours of injection in some cases). Flow rate, pressures, and temperatures are recorded at short intervals. If a monitoring zone is also used, the equilibrium is judged from stabilization of both the injection and monitoring zones. This is the basic procedure for a single steady state test. In cases where multiple tests are required, two approaches may be used. One is to continue the testing by increasing the pressure in increments. This procedure is faster because no time is wasted by waiting for the test zone to reach its natural equilibrium. However, the biggest disadvantage is the interference of the multiple tests, one on another, which complicates the analysis.

The second method is to allow the zone pressure of each test to reach its original natural state before initiating a second test at a higher pressure. The problem with this type of testing is that in tight rocks the time required for the zone pressure to reach its natural equilibrium may be too long for practical purposes. In certain cases, where the rock has very low permeabilities, the half life of the zone pressure (that is the time required for the pressure to drop to half of its original value) may be more than 24 hours. When a large number of tests are to be conducted,

such long waiting times are impractical.

The first method is herein designated as "continuously incremented steady state test" (CISST) and the second is referred to as "incrementing after natural equilibrium steady state test", or, in short, "incrementing after equilibrium test" (IAET). The first type of test, that is CISST, was used more extensively for this study. However, in cases where critical data evaluation was needed, the second type of testing was used.

8.2.2 Decay After Steady State Test.

Following the highest testing pressure during CISST or after each of the IAET's, flow is stopped by means of a solenoid valve (area A, Figure 6.1) and a continuous record of the pressure decay is kept for every 1.4 KPa (0.2 psi) of pressure drop or every one minute, whichever occurs first, until the slope of the pressure decay curve approaches zero. This type of test will be referred to as "decay test" and should not be confused with decay after a pulse test. It should be noted that the decay test used here is similar to the Theis recovery test (Freeze and Cherry, 1979) and is the same as the pressure fall off test (Earlougher, 1977).

8.2.3 Pulse Test.

A pulse test is generally used for rapid permeability measurement of tight formations (Wang, et al., 1977). This type of test is normally conducted after the formation to be tested has reached its natural equilibrium. The procedure is then to introduce a small pulse of pressure to the packed-off zone in as short a time as possible. The pressure decay is then observed as mentioned in the previous section. For the present study, in addition to the conventional method, pulsing after a quasi-steady state equilibrium was also conducted.

It should be noted that the pulse test is practically the same as the slug test (Hvorslev, 1951; and Cooper, et al., 1967; also see Freeze and Cherry, 1979). However, the test known as the pulse test in ground water hydrology is completely different in principle and analysis from the "pulse test" known in the petroleum industry (Johnson, et al., 1966; and Earlougher, 1977) in which case a multiple of pulses are applied to the formation rather than just a single pulse. Because only one type of pulse testing is considered in the present study, no confusion should arise.

8.3 Systematic Injection Testing with Nitrogen.

8.3.1 Longitudinal Boreholes.

Steady state nitrogen injection in conjunction with pulse testing and decay tests were employed to sample all these boreholes for permeability. The CISST method was used for faster data collection for a range of pressure (0.01 to 0.3 MPa). Normally, four pressure increments were used prior to either decay or a pulse test. However, in certain cases more than five pressure increments were used. No pulse testing after natural equilibrium was used for the longitudinal boreholes.

A relatively long injection zone (L - 2.13m or 6.99 ft.) was used to test the longitudinal boreholes. The long interval was chosen to reduce the number of tests. However, in order to precisely locate a fracture and to isolate fractures within a group, a special testing method was required. If the length of the test chamber "L" (distance between packers) is longer than the apparent spacing of fractures, the permeability data from a single test may show the effects of numerous fractures, and their location within the tested interval cannot be determined precisely.

Consequently, the "sequentially overlapping interval" (SOI) method was developed. In this method, every test

interval was overlapped about 57% by another test. This allowed fracture location to within 14% and 25% of L in alternate test spacings. In this case where L was 2.13m and the packers were moved every 0.9m, 30 tests (covering 30m) provided information that would have required at least 90 tests employing side by side testing with an interval length of 0.3m. Therefore, testing effort was substantially reduced.

The significance of the SOI method may be realized when considering that more than 500 steady state tests and about 100 decay or pulse tests were required to cover the entire lengths of the three boreholes with the 2.13m length of the chamber. An average of 3 hours was spent for each test including calibration and maintenance. This means that (at 10 hours per day and 30 days per month) it would have required 18 months (instead of 6 months) to complete these tests, had 0.3m interval length and side by side testing been used instead of the SOI method.

During these sets of tests, the monitoring probes were set in adjacent boreholes and their interval span was adjusted to 3m (10 ft.). The centers of all three probes were approximately on a plane perpendicular to the axes of the three boreholes. This was done so that conductive fractures intersecting the three boreholes could be detected.

However, in only a few cases could good pressure communication between the three boreholes be established.

It should be noted that the equipment was constantly upgraded during these tests, and the quality of data was somewhat improved during the course of this set of tests. However, most of the major modifications were made during testing of the first borehole. The order in which the longitudinal boreholes were tested was PA-1, then PA-3 and finally PA-2. All boreholes were tested from the collar to end. About 3 meters near the collar and ends of these boreholes could not be tested due to the configuration of the main probe. Testing of these segments was carried out after the final version of the equipment was completed (after nitrogen testing of the concrete column). From some tests that overlapped previously tested intervals, it was noticed that there was little difference between the permeabilities measured by the preliminary and final versions of the equipment.

8.3.2 Radial Boreholes

Due to the enormous amount of data that was to be collected from the radial boreholes (total length of over 215m, 700 ft), the time-consuming method used for the longitudinal

boreholes proved impractical. In addition, because data acquisition was completely automated for the testing of the longitudinal boreholes, only occasional monitoring of the tests was required. For these reasons, a second, very simplified set of packer equipment was built for use in the radial boreholes, concurrent with the longitudinal boreholes.

A packer arrangement similar to that of a double packer monitoring assembly, using short interval of 0.75m (2.6 ft.) was used in order to obtain more complete coverage of the borehole. Boreholes were tested at intervals of 0.30m (1.0 ft.) with the SOI method. Each interval was tested at one equilibrated pressure and flow. If the flow was too small to be measured by the flowmeter, a pulse test was conducted. The flow rate was measured by a single rotameter and the sensitivity of the transducer used was only 0.7 KPa (0.1 psi). Therefore, permeabilities calculated for the radial boreholes are not entirely comparable with those of the longitudinal boreholes.

8.3.3 Data Analysis

8.3.3.a Steady State Radial Flow

Assuming that the Klinkenberg effect acts in the same

way in a single fracture as it does in a porous medium, it can be shown (Montazer and Hustrulid, 1981) that the conductivity of a single fracture from steady state injection test is given by (see Figure 8.1):

$$K_{\ell} = \frac{M_w}{2\alpha\pi\omega} \frac{\ln(r_e/r_w)}{(P_e - P_w) \left[\frac{P_e + P_w}{2} + B \right]} \quad (8.3.1)$$

where:

K = fracture conductivity

M_w = constant mass flow rate into the borehole

α = $-m/\mu RT$

m = molecular weight of the ideal gas

μ = absolute viscosity

R = gas constant

T = absolute temperature in the borehole

ω = equivalent fracture aperture

r_e = radial distance to some boundary

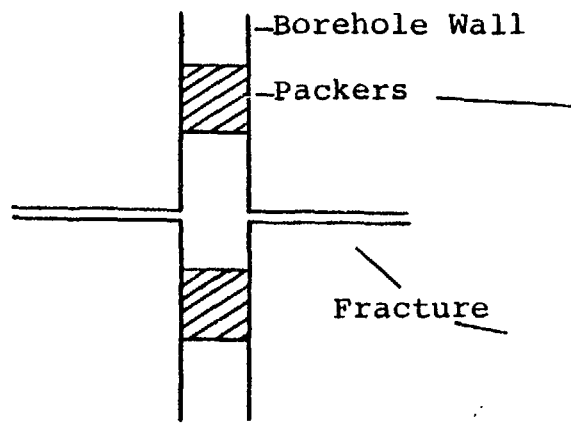
r_w = radius of the borehole

P_e = pressure at the boundary

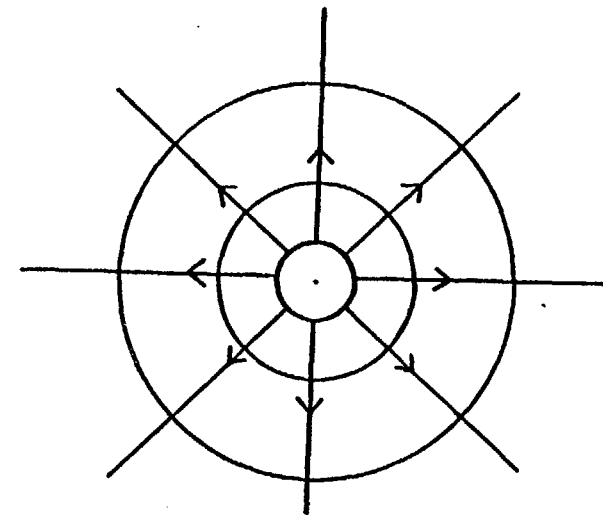
P_w = the steady injection pressure in the test chamber

B = the Klinkenberg constant.

The assumptions in deriving this equation are:



Longitudinal Section



Transverse Section

FIGURE 8.1. Theoretical flow pattern through a fracture at right angle to the borehole.

- a) the gas acts ideally (compressibility factor equals one)
- b) Fracture is isotropic.
- c) Fracture is perpendicular to the borehole axis.
- d) D'Arcy's law applies to the flow through the fracture, that is

$$V_i = K_\ell \frac{\partial \phi}{\partial x_i} \quad (8.3.2)$$

- e) A fictitious aperture can be assumed so that:

$$K_\ell = \frac{\omega^2}{12} \quad (8.3.3)$$

- f) Gravity effect is negligible.
- g) Isothermal condition.
- h) Axisymmetric flow.
- i) Matrix permeability is negligible.

Assumption (e) automatically follows assumption (d) above.

The significance of these two assumptions is that K_ℓ is taken as a constant.

Equation (8.3.1) has three unknowns: K_ℓ , ω and B ; however, by substituting $K_\ell = \omega^2/12$, this equation becomes

$$\frac{\omega^3}{12} = \frac{M_w}{2\alpha\pi} \frac{\ln(r_e/r_w)}{(P_e - P_w) \left(\frac{P_e + P_w}{2} + B \right)} \quad (8.3.4)$$

and, therefore, equation (8.3.1) becomes:

$$K_{\ell} = \frac{1}{12} \left\{ \frac{12 M_w}{2\alpha\pi} \frac{\ln (r_e/r_w)}{(P_e - P_w) \left[\frac{P_e + P_w}{2} + B \right]} \right\}^{2/3} \quad (8.3.5)$$

for which all parameters except B are known.

Disregarding the Klinkenberg effect ($B=0$) will result in an equation for K_g :

$$K_g = \frac{M_w}{\alpha\pi\omega} \frac{\ln (r_e/r_w)}{(p_e^2 - p_w^2)} \quad (8.3.6)$$

Where K_g is the fracture conductivity to a gas. Comparison between this equation and equation (8.3.1) shows that:

$$K_g = K_{\ell} \left\{ 1 + \frac{B}{(p_e + p_w)/2} \right\} \quad (8.3.7)$$

It should be noted that K_g is not equal to $\omega^2/12$, as K_g varies with pressure. K_g approaches K_{ℓ} when $(p_e + p_w) \rightarrow \infty$. However, as soon as the gas pressure exceeds the critical pressure, the gas will be converted to a liquid and the critical pressure may be assumed as the infinite pressure.

In the present study equation (7.4.17) is used to analyze the results of the steady state, systematic,

nitrogen injection tests. The length of the injection zone for these tests was about 2m. Considering a fracture frequency of 8 per meter, injection into such a relatively long packer interval influences a relatively large volume of the rock. Therefore, assumption of an elliptical distribution of the potential seems to be justified. The apertures reported in Appendix VI are calculated using equation (8.3.3) and may represent the effect of several fractures. Equation 8.3.6 is used to analyze the cross-hole test results. Zeigler (1976) showed that there is a small difference between permeabilities calculated from the radial flow and ellipsoidal equations.

By extrapolation of the pressure-permeability trends to infinite pressure, K_{ρ} is found using equation (8.3.7). Another method is by solving for B and K_{ρ} in equations (8.3.5) and (8.3.7). This method resulted in consistent answers when more than two values of K_g and p_w were available (see discussion).

In the previous discussion it was assumed that matrix permeability (k_m) is zero. The matrix permeability of the rock around the ONWI room is so small ($<10^{-15}$ cm²) that this assumption does not affect the results. Permeabilities presented in this report are the combination of k_m and k_f (assuming no interflow between the matrix and the

fracture):

$$k_t = \frac{n\omega k_\ell + (L - n\omega) k_m}{L} \quad (8.3.8)$$

where L is the length of the test interval, k_t the equivalent porous media permeability and n the number of fractures intersecting the borehole.

In case the fracture is not perpendicular to the borehole axis, Rocha and Franciss (1977) use the following expression:

$$k_t = \frac{K_\ell \omega}{L \cos\theta} \quad (8.3.9)$$

where θ is the angle between the normal to the fracture plane and the borehole axis.

8.3.3.2 Analysis of Pressure Pulse Tests.

During a pulse test, the main differential equation governing the flow is:

$$\frac{\partial^2 p^2}{\partial r^2} + \frac{1}{r} \frac{\partial p^2}{\partial r} = \frac{\phi \mu}{pK} \frac{\partial p^2}{\partial t} \quad (8.3.10)$$

where:

ϕ = porosity, equals one for the open fracture

$K = \frac{\omega^2}{12}$, the fracture conductivity.

The fracture is assumed to be perpendicular to the axis of the borehole. The boundary condition is:

$$\frac{Kw}{2\mu Lw} \left(\frac{\partial p^2}{\partial r} \right)_{r_w} = \frac{dp_w}{dt} \quad (8.3.11)$$

and the initial condition is:

$$p(r,0) = \begin{cases} p_0 & r > r_w \\ \delta p & r = r_w \end{cases} \quad (8.3.12)$$

where δp is the small pressure pulse applied to the packed-off chamber. This problem of solving a non-linear, 2nd order partial differential equation again arises. The numerical solution developed in section (7.4) can be easily extended to solve equations (8.3.10) 50 (8.3.12) with the results analyzed by curve matching. For analysis of

over 150 tests, this did not seem feasible. For this reason a simplified solution was sought.

If the pressure pulse (δp) applied is small compared to the initial pressure (p_0), the diffusivity equation describing the flow of slightly compressible fluid can be applied to this problem (Craft and Hawkins, 1959).

Wang, et al. (1977) presented a method of analyzing pulse tests using a solution to the diffusivity equation. The exact solution requires much computer time. Forster and Gale, 1979, have also pointed out the sensitivity of the method to equipment compliance and temperature. Therefore, the approximate method suggested by Wang, et al. (1977) was considered sufficient. This method has been modified to apply to isothermal flow of an ideal gas with variable compressibility.

Wang, et al. (1977) showed that for an infinite extent fracture the aperture can be closely approximated by:

$$\log (\omega) = -0.32 \log (t) + C + 0.32 \left(2.01 \log \frac{r_w}{0.04} + \log \frac{(\beta\mu)}{4.177 \times 10^{-13}} + \frac{1}{3} \log \frac{L}{2} \right) \quad (8.3.13)$$

where:

ω = fracture aperture (m)

t = time (sec.)

r_w = radius of the borehole (m)

β = compressibility (Pa^{-1})

μ = viscosity ($\text{Pa}^{-\text{sec}}$)

L = length of the test zone (m)

C = 1.09, 1.20, 1.27 for normalized pressures (PN) =
0.95, 0.9, 0.85, respectively.

Compressibility is defined as:

$$\beta = \frac{1}{\rho} \frac{d\rho}{dp} \quad . \quad (8.3.14)$$

For the case of an ideal gas:

$$\rho = \frac{Mp}{RT} \quad . \quad (8.3.15)$$

Substitution of this in equation (8.3.14) results in:

$$\beta = \frac{1}{p} \quad (8.3.16)$$

where ρ = density, R = gas constant and M molar mass. At 10°C , the compressibility of nitrogen is taken as $2/(2p_a + \delta p)$.

All the pressure pulse results were statistically analyzed to insure good consistency in relating time and pressure. All tests indicate a log-log correlation between pressure and time for at least the first five minutes of each test (Figure

8.2) with a correlation coefficient of 0.9 or greater.

An equation of the form:

$$t = \eta P^K \quad (8.3.17)$$

was derived by using linear regression analysis for each test. With equation (8.3.16) time at a normalized pressure (PN) of 0.85 was obtained and, using Equation (8.3.12), the aperture was calculated. Permeability was then calculated using Equations (8.3.3) and (8.3.8).

It is important to note that this method is very approximate since the diffusivity equation in the form used by Wang, et al. (1977) is not applicable to gas flow (Bruce, et al., 1953; Collins, 1961). However, because this method was only used for very small permeability zones in radial boreholes, the results obtained by using this approximation do not affect the conclusions drawn.

8.3.3.3 The Computer Code.

Data from the datalogger was continuously recorded on cassette tape. Initial conversion to engineering units was made by the datalogger. Information on the cassette tape was then loaded into the CSM DEC-10 computer and stored on magnetic tape. The program PERMEA (Appendix V) was developed

PULSE TEST ANALYSIS FOR
BOREHOLE NO. RDD-4, INTERVAL 9-11.5 FEET.

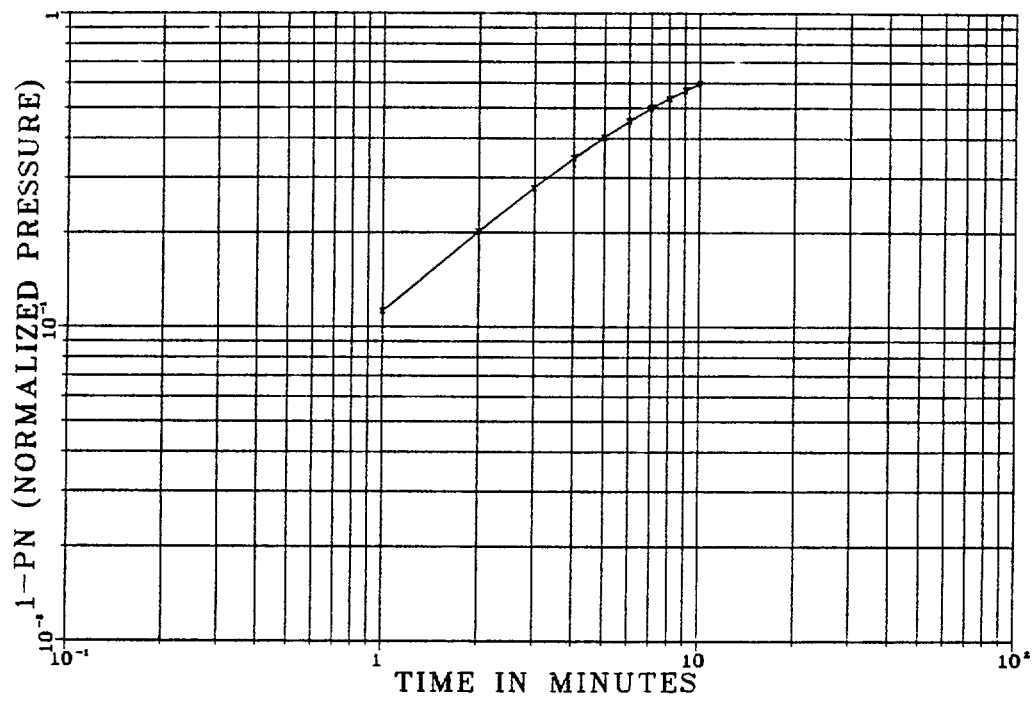


FIGURE 8.2. Pulse Test Analysis for Borehole No. RDD-4, Interval 9-11.5 Feet.

to:

- a) correct the data for any fluctuations in input voltage, zero drifts, and digital voltmeter drifts;
- b) calculate the flow rates by using various subroutines to correct for temperature and pressure variations;
- c) perform regression analysis of the calibration data, the output of which is then input into the program through a separate run for permeability calculations (Figure 8.3).

For steady state analysis, the pressure and flow are handsorted and input into the program. For transient decay and pulse tests the program performs regression analysis on the data and permeabilities are approximated by the simplified procedure of Wang, et al. (1977).

8.3.4 Results of Systematic Nitrogen Injection.

8.3.4.1 Longitudinal Boreholes.

A typical pressure-flow history during testing one of the intervals is shown in Figure 8.4. As previously noted, data were recorded for every 1.4 KPa (.1 psi) of pressure change or at one minute intervals. In this diagram only a few points are plotted to improve clarity. In this case, since permeability of the zone was relatively high (10^{-10} cm^2), pressure and flow stabilized very rapidly. In some cases testing had to be continued for 20 hours to reach a reasonably stable pressure and flow.

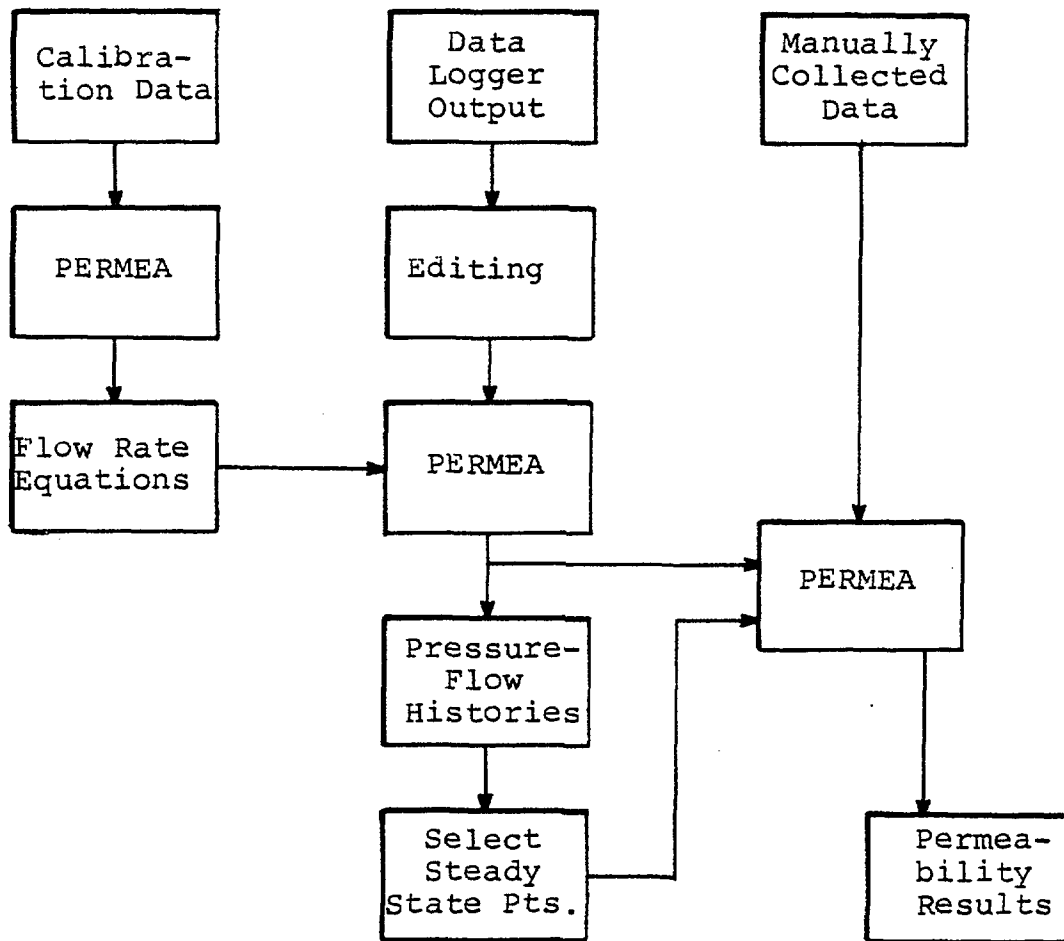
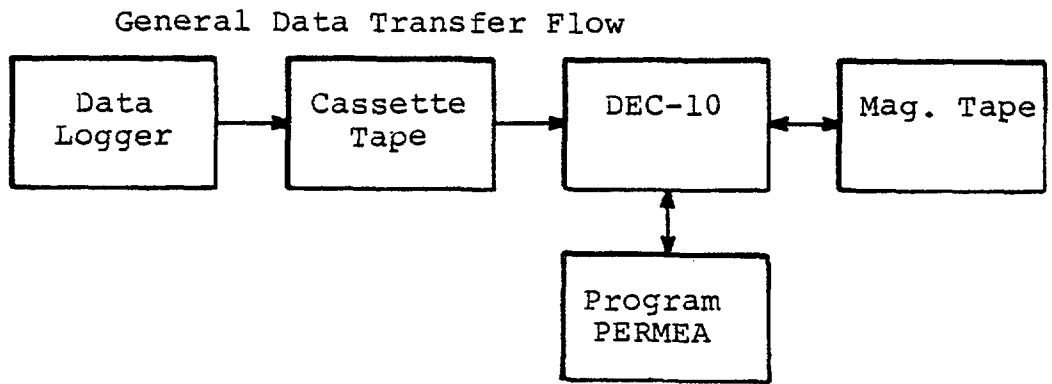


FIGURE 8.3. Flow chart showing the data handling and analysis by the computer code PERMEA.

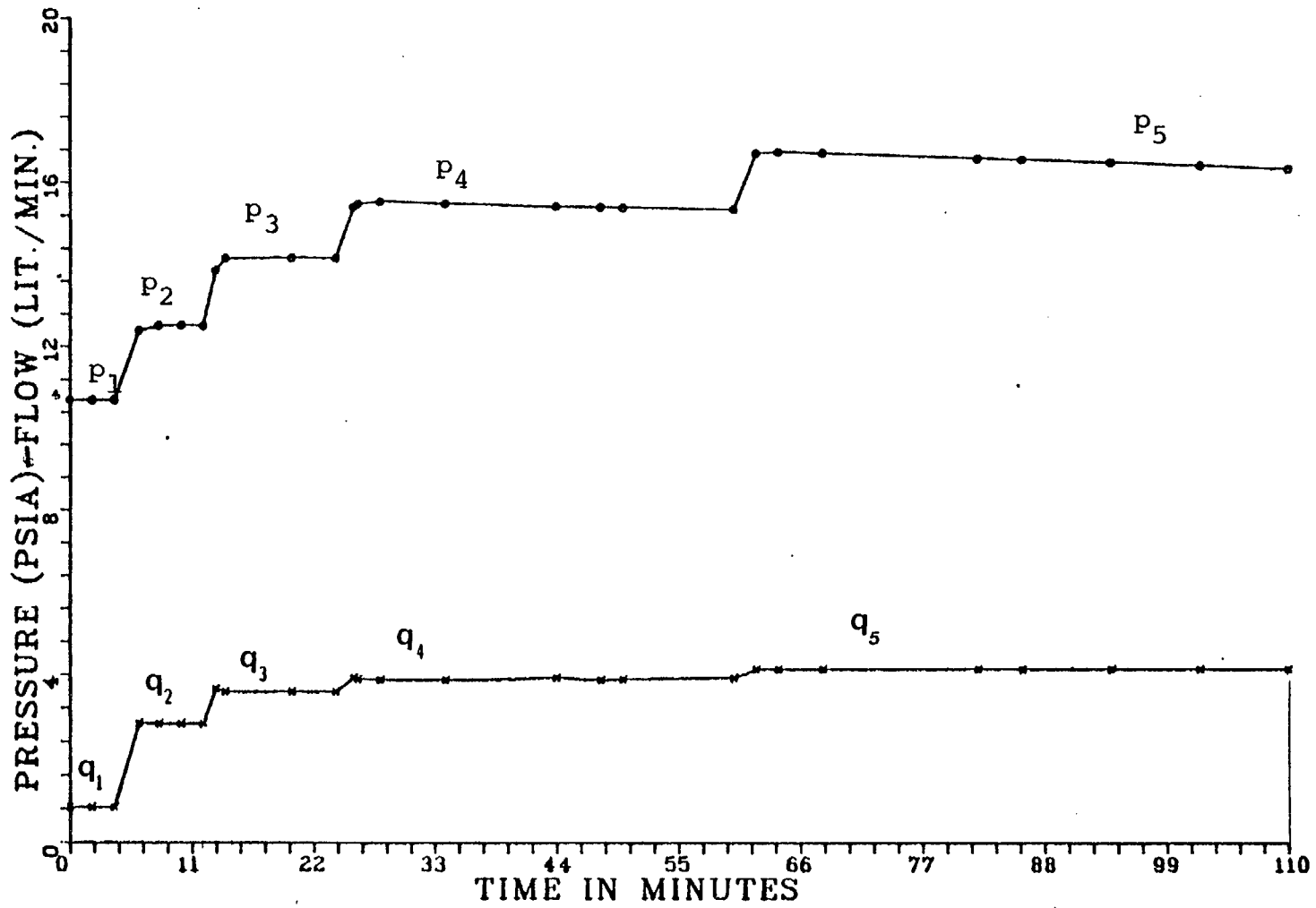


FIGURE 8.4. Pressure-flow history for BH. No. PA-2, Int. 47-54, X=Flow, O=Pressure.

For each tested interval, permeability versus inverse of pressure was plotted. This was done so that the comparison could be made between different fractures in adjacent holes on the basis of pressure-permeability trends rather than single values of permeabilities. The pressure-permeability plots are included in Appendix VI.

Single value permeabilities at infinite pressures are plotted along each borehole in Figure 8.5. Correlation of this diagram with the fracture map reveals the conductive fractures which are traced on this map (note that strikes are distorted due to exaggeration in distance between boreholes in this diagram).

Figures 8.6 through 8.10 show the pressure-permeability trends for probable single fractures encountered within two or three consecutive test intervals. As can be seen in some cases more than one fracture occurs in two or even three consecutive intervals (compare with Figure 8.5). It should be noted that "single fracture" is referred to a fracture only where it intersects the borehole. Obviously it is impossible to isolate a fracture in the rock mass.

Despite the frequent, stringent efforts of calibration, recalibration and checking for leakage, etc. straight horizontal lines are not obtained in the pressure-permeability plots, which contradicts the concept of "intrinsic permeability" and D'Arcy's law. Also, the pressure permeability

curves are not consistently the same shape which show that the effect is not the result of flow meter malfunctioning or flow rate calculation procedures. Therefore, it is concluded that the effect is due to the behavior of the fluid in the medium (fracture).

Fracture deformation during injection does not account for the observed anomaly, since the pressures of flow are far too small to cause any detectable fracture opening. Moreover, the pressure-permeability curves have different slope signs. That is, permeability in most cases decreases with increase in the pressure. If fracture deformation is the case, a consistent increase in permeability with pressure would be expected (and then only at pressures much higher than those used here).

Analysis of flow regimes using Louis's (1974) method indicates laminar flow in all cases with the possible exception of the shear zone. The geometrical boundary conditions also could not have been the cause, either because no detectable sharp anomaly was detected during steady-state injection. Rather, a very uniform and consistent transient behavior in flow and pressure was observed.

One interval (20.7-22.8m or 68-75 ft.) in BH PA-2 was randomly chosen for retests. Three sets of tests were conducted at different times (about 15 days apart). At permeability values of 10^{-13} cm^2 variations of $\pm 4\%$ of the range were indicative of the repeatability of the test results.

This repeatability was observed even at consecutive intervals as long as the same fracture was being tested (Figures 8.6-8.10).

Examinations of the pressure-permeability curves indicated that with an increase in test pressure (equilibrium pressure), either a systematic increase or systematic decrease in permeability existed (Appendix VI; e.g. BH PA-1, Int. 14-21 and Int. 26-33). It was also noted that, in the latter case, zone pressure and flow both rose until a steady state was reached.

The reduction of permeability with pressure increase is partially explained by the Klinkenberg effect as noted earlier:

$$k_g = k_l \left(1 + \frac{B}{p}\right) \quad (8.3.18)$$

where k_g is the permeability of the gas, k_l the permeability of a liquid, B a constant dependent on properties of the gas and medium, and p is the pressure. As the equation shows, the permeability of the gas (k_g) linearly decreases as the pressure increases. However, the characteristic of most of the higher-conductivity fractures has been non-linear. This indicates that either the Klinkenberg effect acts non-linearly in the fracture or some other phenomenon is responsible for the observed effects.

The case of increase of permeability with pressure coincides with a continuous increase in flow during a constant

pressure decline. This phenomenon is persistent for long periods of time while the pressure is stabilizing. In some cases, this effect is inconspicuous or nonexistent at low pressures. Further investigation has not indicated any correlation between this phenomenon and temperature variation. This effect was observed even though some of the tests were in operation continuously for 10-20 hours with a very slow decrease in rate of change of pressure and flow. If this is not a thermodynamic phenomenon, fracture conductivity apparently increases with time. This may be explained by the two-phase flow concept. This subject is discussed in further detail in the following chapter.

8.3.4.2 Radial Boreholes.

For each interval of the radial boreholes tested only a single value of permeability was obtained and these are plotted along the boreholes (Appendix VII). Although the rock matrix permeabilities observed during testing of the radial borehole are very low, the fracture permeabilities are several orders of magnitude larger than those calculated for fractures in the longitudinal boreholes. Such discrepancies are due to a combination of three potential reasons:

- 1) Blasting affected the conductivity of the fractures, but the affected depth in the rock was usually less than one meter.
- 2) Fractures near the beginning of the boreholes usually connect with the room, resulting in a shorter flow path to the large open space of the room and thus larger apparent permeability of the fractures.
- 3) Roughness of the boreholes in their beginning sections may provide leakage around the packers.

The packers used in testing the radial boreholes were shorter than those used in the longitudinal boreholes. This by itself exaggerates permeability. In addition, due to the less sophisticated instrumentation, there was no way of detecting packer leakage. However, prior to testing each borehole, the packer assembly was tested for leakage inside a 3 inch pipe and no leakage was observed.

The matrix permeabilities measured in the radial boreholes are also slightly larger than those measured in the longitudinal boreholes. This may be due in part to the method of analysis. In any case, none of these reasons, even combined, could be responsible for increase in

permeabilities of two to three orders of magnitude. This matter is discussed in more detail in the following chapter.

8.4 Variable Interval Testing.

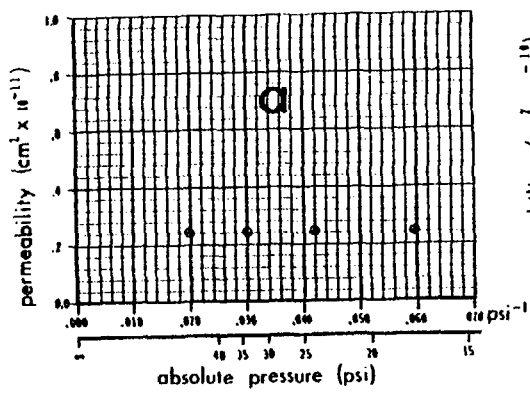
In order to examine the effect of sample size on the results of packer testing, a series of tests were conducted during which the length of the interval was increased gradually from 0.3m to 25m. One of the monitoring probes described in the systematic testing (section 8.3) was modified so that the end of the probe and the end of the borehole could form an injection chamber, and the first chamber (nearer to the collar of the borehole) could form a monitoring chamber. Testing procedures were similar to those used for systematic testing except that no monitoring probe was used in the adjacent boreholes.

Continuously incremented steady state tests (section 8.2.1) followed by decay tests were used. As the length of the interval was increased, the maximum pressure that could be applied to the injection zone became limited by the increase in the pressure loss in the flow system. For this reason, only two or three steady state tests could be conducted over long intervals. Data analysis was similar to that employed to reduce the data from systematic injection testing.

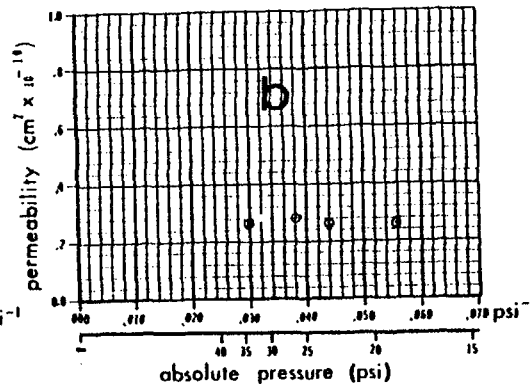
8.4.1 Scale Effects.

Results of testing by varying the length of the interval (VI method) provided some insight into the problem of sample size. Figure 8.11a to 8.11g are the pressure-permeability plots for the seven intervals selected for testing. It is apparent that in all cases the Klinkenberg effect is insignificant but increases as the length of the tested interval is increased. This is probably due to the inclusion of the shear zone in the longer intervals. It is also suspected that effusion of the nitrogen in the more complex fracture network is responsible for both the curvature and steepness of the pressure-permeability curves (see discussion).

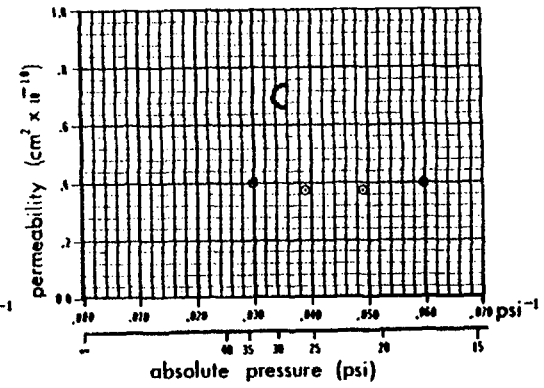
The permeabilities extrapolated to the infinite pressure are shown in Figure 8.12. It is evident that intervals longer than about 10m (33 ft.) have values of permeabilities that perturbate around a mean value of $5 \times 10^{-11} \text{ cm}^2$. This is the longitudinal scale effect which also bears some influence of the scale in radial direction (from the boreholes) as well. As the length of the interval is increased the probability that more fractures, belonging to the same sets parallel to the axis of the borehole (such as diagonal set), are included in the flow path of the fluid increases. Therefore, the flow through the fractured medium approaches that of a porous medium (Long et al., 1982; Snow, 1965). In Figure 8.12 fracture frequencies for the intervals tested with



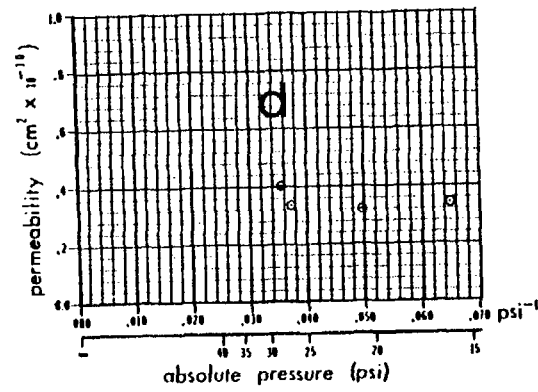
104.8 - 107



100 - 107



89 - 107



71 - 107

FIGURE 8.11. Pressure-permeability plots for the variable intervals in borehole PA-2.

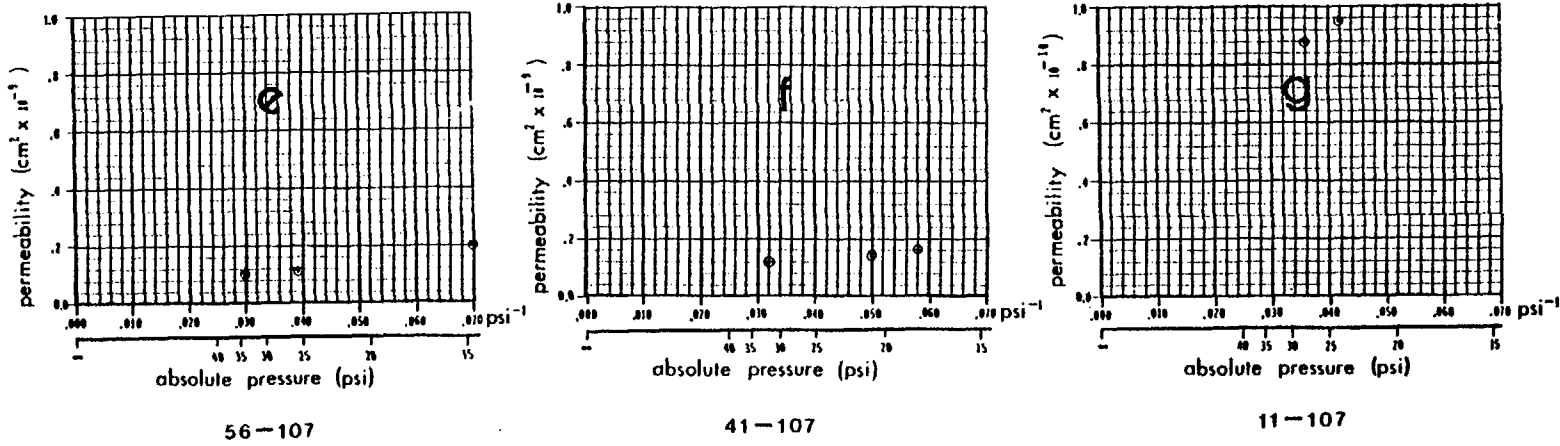


FIGURE 8.11. Pressure-permeability plots for the variable intervals in borehole PA-2.

PERMEABILITY ALONG BOREHOLE PA-2

T-2540

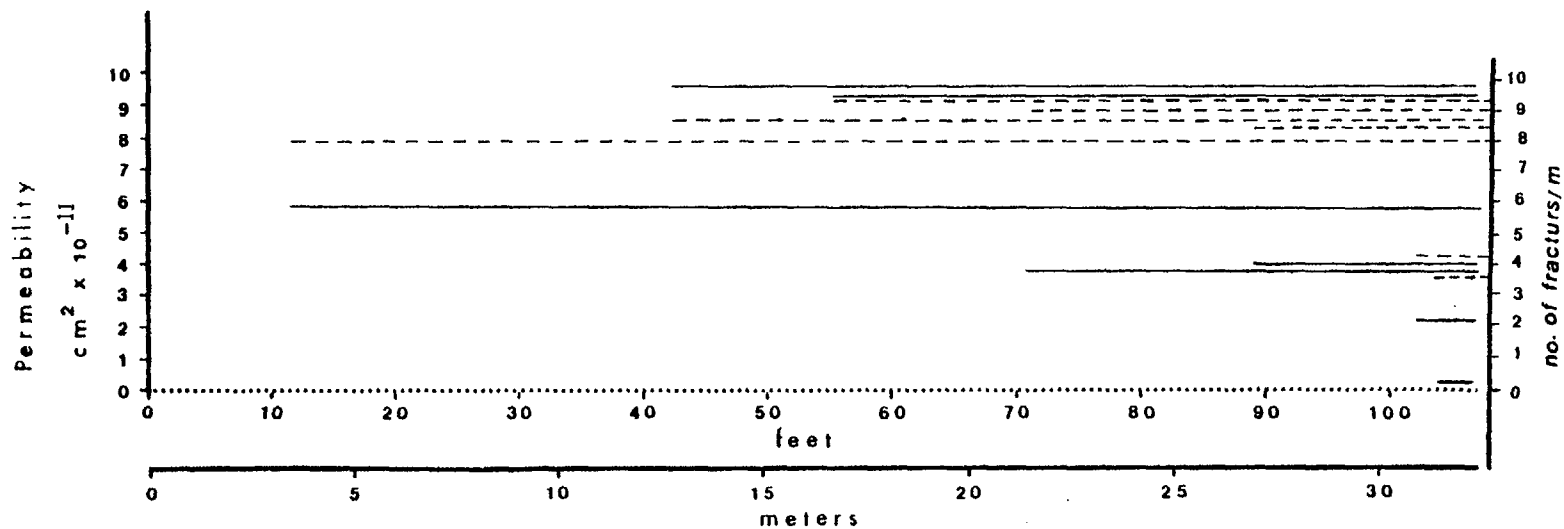


FIGURE 8.12. Permeabilities (solid lines) at infinite pressure for various intervals in borehole PA-2. Dashed lines show the fracture frequency (from detailed core logging) for the same intervals.

The VI method are also shown. The number of fractures per meter for these intervals also assumes a mean value for scanline lengths of ten meters or longer.

Permeability for the same tested intervals were also predicted from systematic nitrogen injection (SNI) testing using the sequentially overlapping intervals (SOI) technique of analysis. As was noted earlier, the length of the test section in SNI testing was 2.13m. Using the SOI method permeabilities for each 0.9m of the borehole were estimated and cumulated using the laws of flow through parallel layers (Craft and Hawkins, 1959) assuming that each fractured interval can be simulated by a single stratum to predict the permeabilities of the longer sections tested with the VI method. The results are presented in Figure 8.13. It is readily seen that the predicted permeabilities are within the same order of magnitude as those of the actual test results. In addition, distribution of the values has almost the same patterns.

Theoretically, the permeabilities extrapolated from the testing of the short sections to predict those for the longer intervals should be the same, provided that a homogeneous-isotropic porous medium is being tested and that the elliptical distribution of the equi-potentials is valid. By "homogeneous" the single phase state of the medium is also implied. As has been previously noted in several instances, the rocks around the ONWI room may be assumed

PERMEABILITY ALONG BOREHOLE PA-2

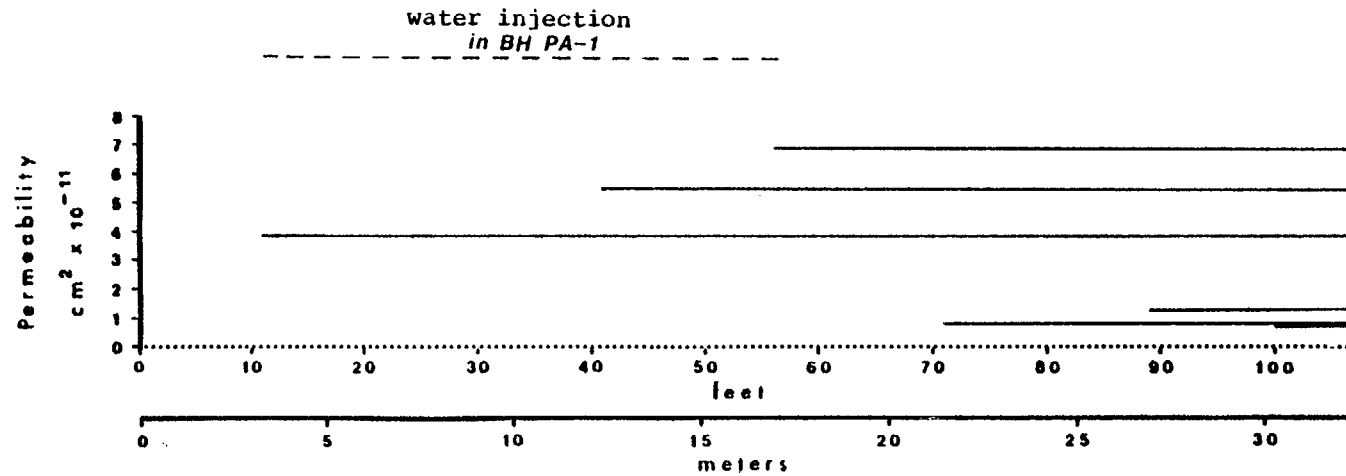


FIGURE 8.13. Permeabilities for various intervals predicted by the SOI method from systematic nitrogen testing.

to act as an anisotropic-porous medium if large enough of a sample is considered (Snow, 1965 and Wilson, 1970). The optimum size of this sample seems to be about ten meters, at least in the longitudinal direction. At this scale, uniformity is also demonstrated by the fracture frequency and permeabilities (Figure 8.12). Although the unsaturated nature of the rock inherently introduces some heterogeneity, it seems to have had negligible effects on the extrapolation of the permeabilities from the short intervals to the longer intervals. This occurs because, as was noted in section (8.3.4), the unsaturated nature of the rock has only affected the small permeability sections of the borehole in the SNI method, while the SOI method of combining the permeabilities of the shorter sections to obtain the permeability of a longer section is insensitive to the variations in the permeabilities of the tight intervals.

8.5 Cross-Hole Testing.

The main purpose of this set of tests was to determine the continuity and trends of conductivity variations along a few selected fractures. During systematic testing of the

longitudinal boreholes the monitoring probes were set in the adjacent boreholes at about the same depth. The pressure was monitored in these probes with a sensitivity of 7 Pa (0.001 psi). The length of the monitoring zones was 3 meters (10 ft.). Thus, any conductive fracture, crossing the main injection zone at an angle of 30° or more, would have established pressure communication with at least one of the adjacent monitoring zones. This information along with data from systematic testing, core logging, T.V. camera survey, and wall mapping was used to select individual fractures for detailed cross-hole testing. Only five such fractures along the longitudinal boreholes were found to be appropriate for such testing.

Comparison of the results of systematic nitrogen testing between boreholes along the selected fractures was criticized by P. A. Witherspoon (1981*) on the grounds that, effective conductivity to nitrogen varies along a fracture because of variation in water saturation of the fracture. Therefore, the trends delineated along the fractures by SNI may represent the trends of the effective rather than saturated conductivity. In order to resolve this problem alternate injections of nitrogen and water were conducted

*Open discussion at the 1981 Seminar on Flow and Transport in Fractured Rocks, held at the University of Waterloo, Waterloo, Ontario (April 24).

and the results were compared. Only two of the five fractures were found to be truly suitable for water testing. Pressure communication between boreholes along the other three fractures could not be established within a reasonable length of time.

8.5.1 Testing Procedures.

To prepare for profile testing, extremely careful calibration and system analysis methods were used to eliminate any misinterpretation of results. Leakage in the flow system was reduced to an undetectable level (less than 0.001 cc/min. of water). Leakage around the packers when set in the calibration pipe (7.62 cm or 3 in. diameter, slightly larger than NX-borehole diameter) were reduced to less than 0.01 cc/min. of water.

The testing procedures consisted of long time injections in one borehole and monitoring in the adjacent boreholes. Data collection was similar to that used during the systematic testing of longitudinal boreholes described in earlier sections. However, in this set of tests, all probes were used as both monitors and injectors interchangeably. Probes were moved back and forth to establish the best possible communication between boreholes. Air injection was conducted first, but only after the boreholes were allowed sufficient time to reach

natural equilibrium (12 months after the last water test and 60 days after the last nitrogen test). The results were used to find the best possible position of the probes during water injection.

During the water injection testing of low conductivity fractures, all three probes were pressurized to increase saturation efficiency. When equilibrium was established flow to one borehole was shut off and the pressure was allowed to reach equilibrium. Then flow to the second borehole was continued much longer to ensure equilibrium. After shutting off the flow to the last borehole, decay of pressure in all zones was recorded.

During the water saturation phase, the walls of the room were checked frequently for any sign of seepage. When seepage was observed, the time of its appearance and the rate of advance of the wetting front was recorded. When the rate of advance was undetectable, equilibrium was assumed. In some cases water flowed out of other boreholes. In those cases the location of the leaking fracture was determined by the T.V. camera. Attitude and characteristics of the fracture was noted. In one case it was possible to measure the flow rate out of one borehole.

8.5.2 Analysis of the Data.

Routine analysis, used for permeability calculations from systematic injection testing, was employed in reducing the results of cross-hole steady state tests. The main objective, however, was to compare the pressure and flow histories of the three boreholes during testing of each fracture. Therefore, the analysis of the data from cross-hole testing was mainly of a qualitative nature.

8.5.3 Results.

For the purpose of comparison the results of cross-hole (or profile) testing of two fractures are presented here. One of these fractures is the shear zone and the other belongs to the diagonal set which crosses the two radial-horizontal boreholes RHE-1 and RHE-2 in the northeastern corner of the room (Figure 8.17).

8.5.3.1 Pressure Profile Along the Shear Zone

Figure 8.14 is the pressure history during cross-hole testing of the shear zone at relatively high pressures with water. During the first hour, all three boreholes were injected simultaneously to saturate the fracture network connected to the shear zone. The packed-off zone in PA-3

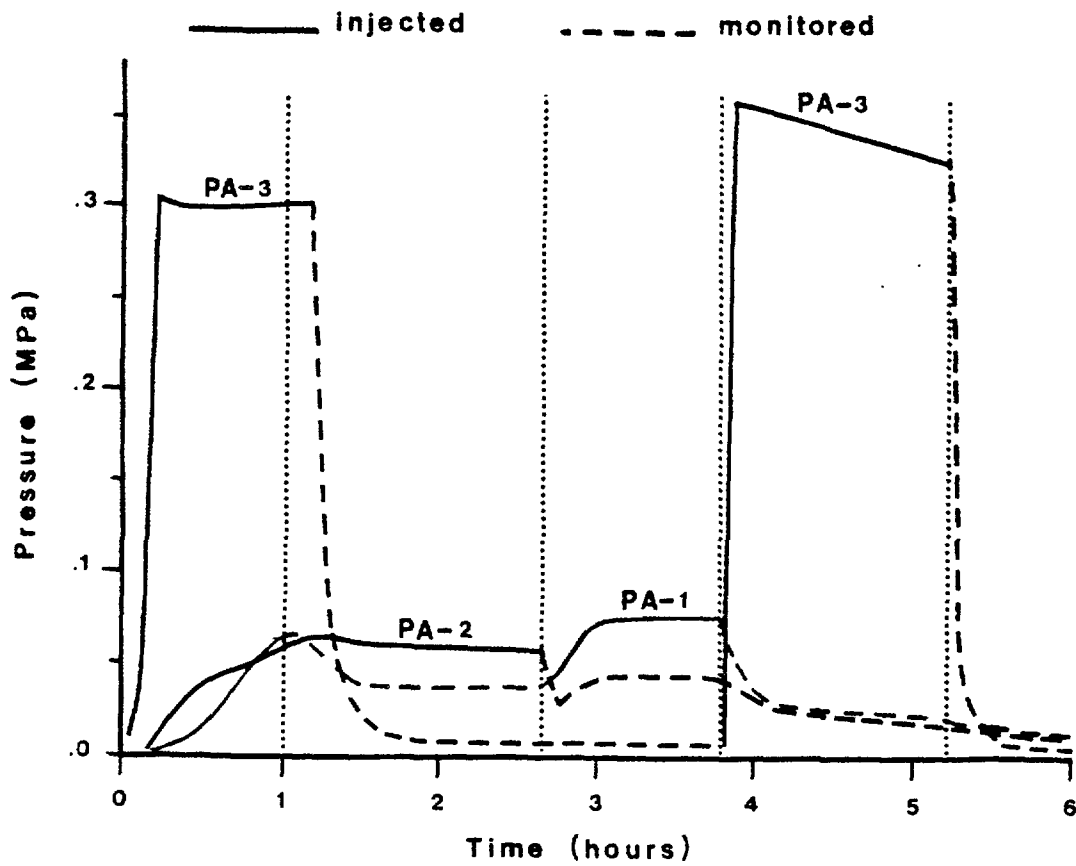


FIGURE 8.14. Pressure history during cross-hole testing of the shear zone. The vertical dotted lines are where the steady state points are measured.

(1.2m long) achieved the highest pressure in a short time. The zone in PA-2 (1.5m long) was the next to reach an initial peak. A second peak was observed after about one hour when the zone in PA-1 was filled and achieved its peak. At this point, when pressure continuity between the three boreholes was established, flow was shut to boreholes PA-1 and PA-3. A quasi-steady state was established at about 2.6 hours. At this time injection in PA-1 was initiated while flow to others was shut off. Finally after about 3.75 hours PA-3 alone was injected.

Continuity of the shear zone between these three boreholes is quite evident from the diagram in Figure 8.14. Any change in pressure in one borehole is clearly reflected in the others. It is also apparent that the shear zone has the smallest conductivity in PA-3 which is manifested by the pressure response in this borehole. This is also confirmed by the pressure profiles constructed from these tests at quasi-steady state points shown with dotted lines in this figure. Figure 8.15 shows the normalized pressure profiles at the steady state points. It is noticeable that the pressure drop across boreholes PA-2 and PA-3 is much greater than that between PA-2 and PA-1.

All of the observations noted in this set of tests point to the fact that the conductivity to water of the shear zone

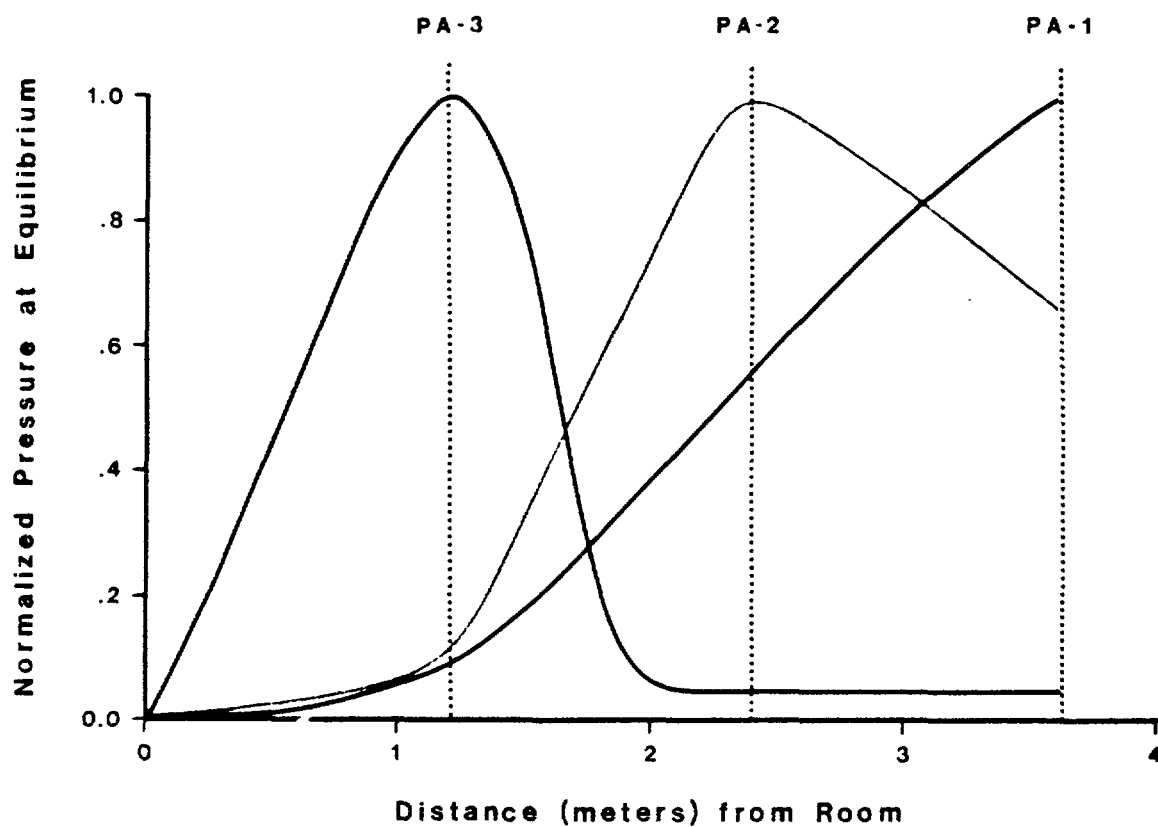


FIGURE 8.15. Normalized pressure profiles at the steady state points (see Figure 8.14) in the plane of the shear zone.

reduces toward the room as was concluded from systematic nitrogen injection testing. This proves that the effect cannot be due to the unsaturated nature of the rock. If such was the case, the trend of the effective conductivity of the fracture to water would have been opposite to that to nitrogen.

8.5.3.2 Cross-hole Testing of Boreholes RHE-1 and RHE-2.

During systematic injection testing of the boreholes RHE-1 and RHE-2 a fracture with relatively high conductivity was encountered (Figure 8.16). Continuity of this fracture was evident from the noise of the gas leakage in the adjacent borehole during injection testing of RHE-1 (Figure 8.17). The uniform appearance, lack of filling materials, and continuity made this fracture an excellent candidate for cross-hole testing. Several tests with nitrogen, carbon dioxide, and water were conducted to understand the nature of the unsaturated flow through a "single fracture."

The pressure-flow history during one of the nitrogen tests is plotted in Figure 8.18. Both pressure and flow reach a steady state condition after only a few minutes. It should be noted that there are as many flow measurements as there are pressure measurements (the log times are shown by plus signs for RHE-2 only for clarity). No data manipulation

FIGURE 8.16. T.V. camera view of the fracture selected for cross-hole testing in RHE-1. The camera is looking at the borehole wall. The width of the screen covers about 4cm of the borehole.

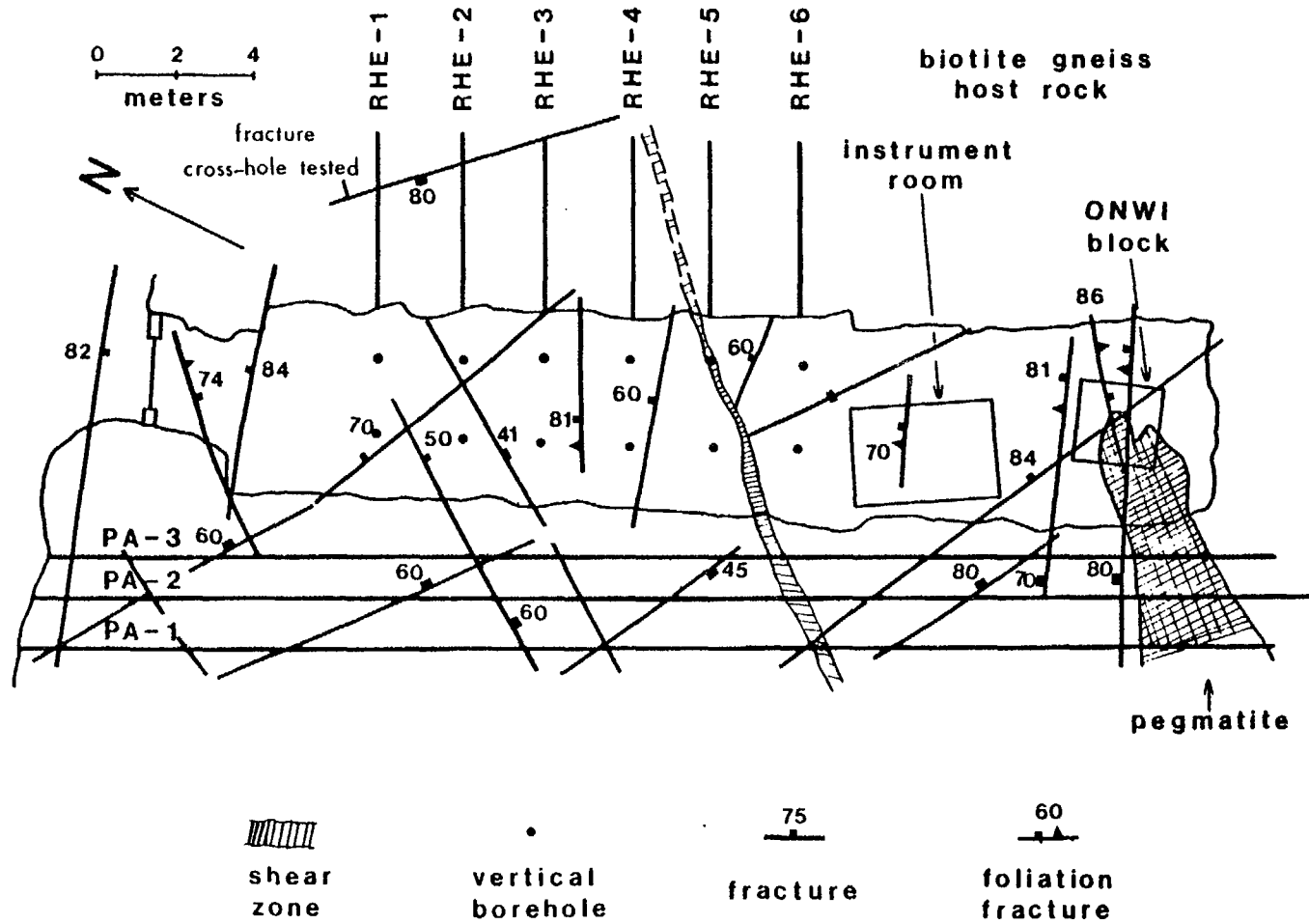


FIGURE 8.17. The simplified fracture map of the room showing a near vertical fracture crossing boreholes RHE-1 and RHE-2.

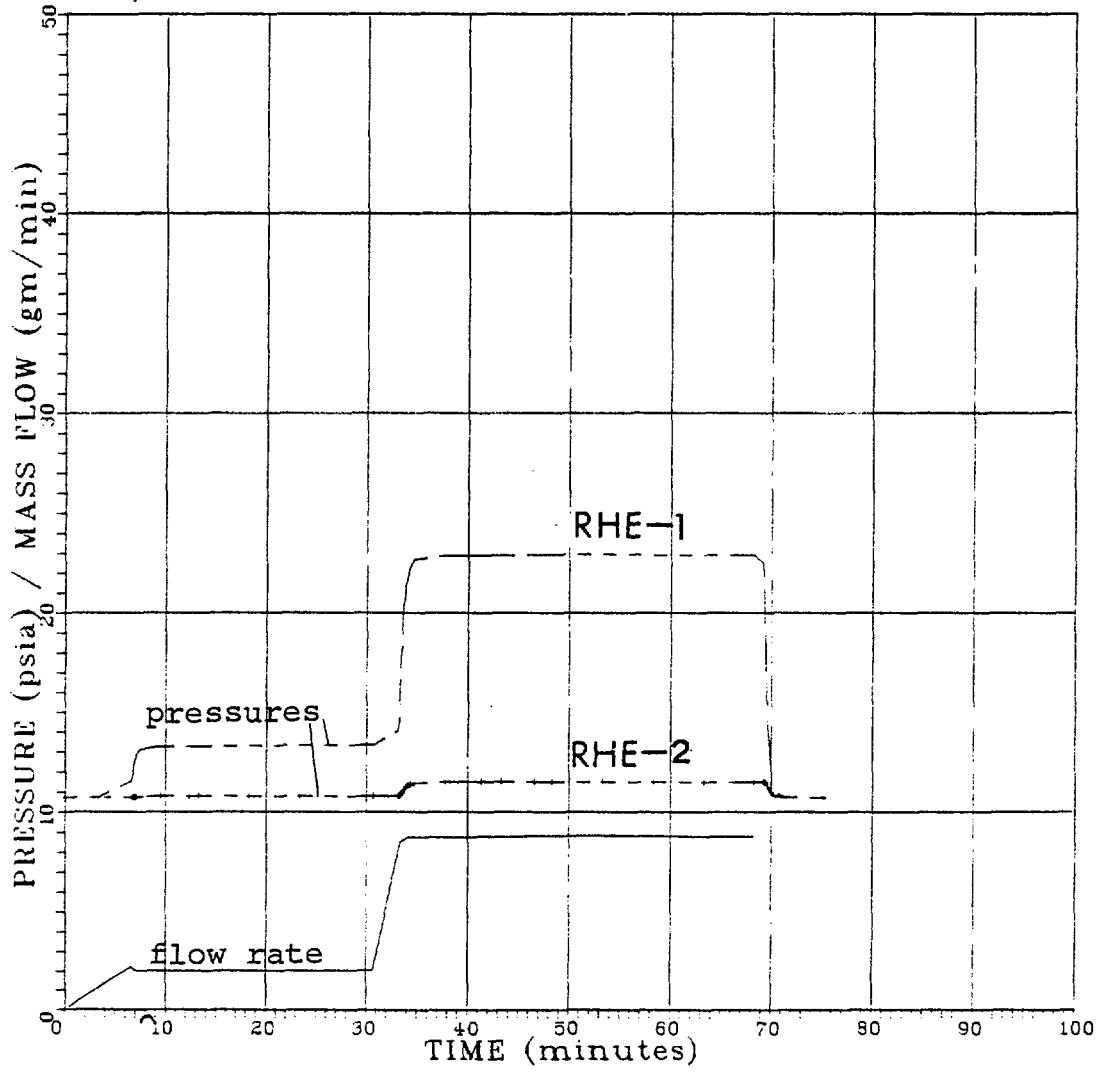


FIGURE 8.18. Pressure-flow history: Nitrogen Test No. 1 Boreholes RHE-1 and RHE-2.

or curve fitting are used to obtain the graphs. The stability of the pressure and flow are interpreted as prevailing single phase flow. This fracture had been exposed to the dry air of the mine through the two boreholes for more than 30 months prior to performance of these tests. Therefore, it is believed that evaporation must have maintained the water content below the residual water saturation. In such a condition, although two-phase condition exists in the fracture, the flow of non-wetting fluid (nitrogen in this case) is not significantly affected by the presence of the wetting phase.

Similar pressure and flow trends can be seen in Figure 8.19 for carbon dioxide displacing nitrogen. Two such tests were conducted to ensure saturation of the fracture with carbon dioxide prior to water testing. Higher pressures and flows were obtainable because of a slightly higher density.

Testing with water immediately followed the carbon dioxide injection. The pressure flow history for the first water test is shown in Figure 8.20. The smooth and steady behavior during testing with the non-wetting fluids cannot be seen in this test. Both flow and pressure are erratic and steady state condition is not established. In order to observe the effect of two-phase flow on the behavior of the flow and pressure, each of the boreholes were injected separately. This can only be explained by a piston displacement mechanism.

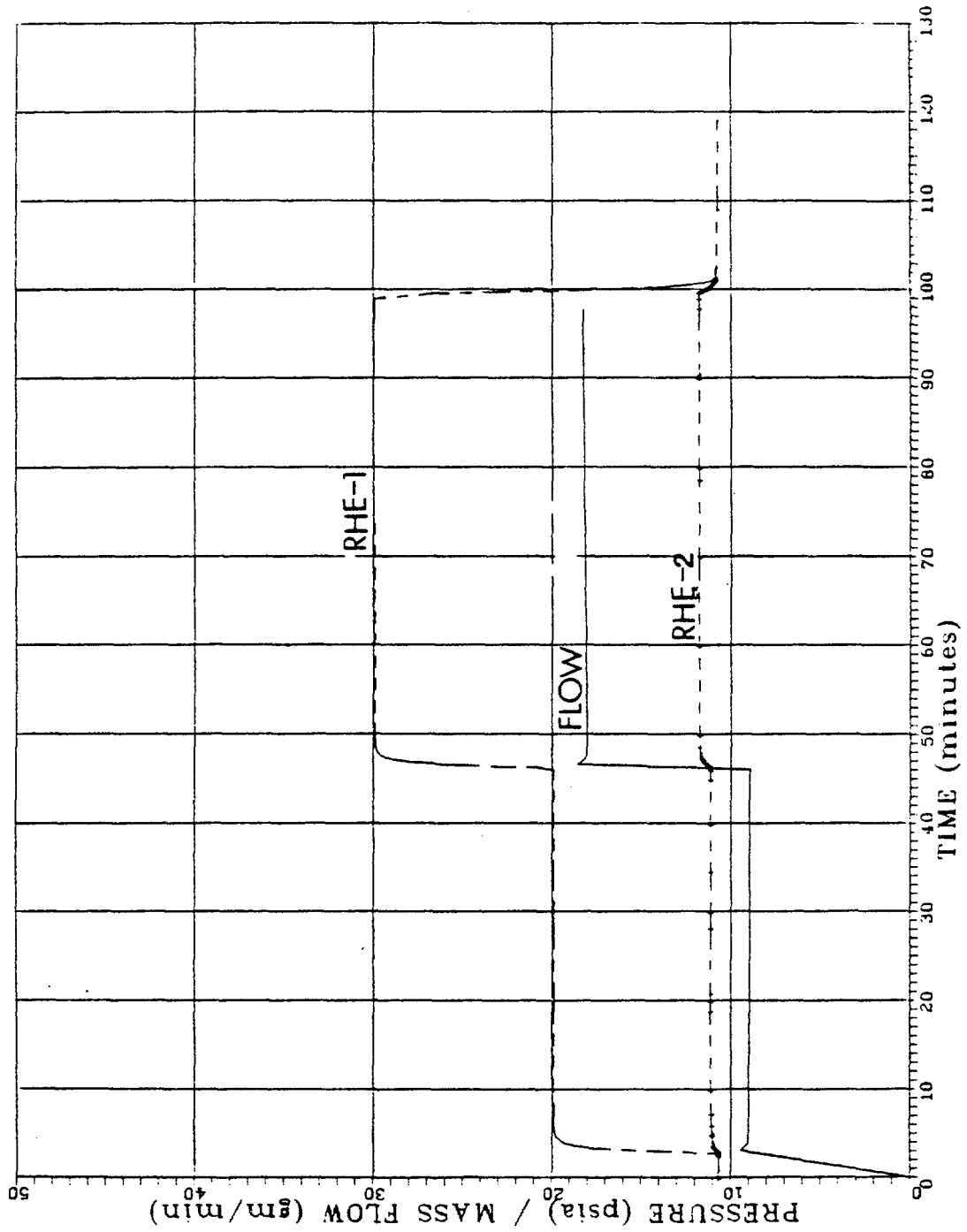


FIGURE 8.19. Pressure-flow history: carbon dioxide test no. 2.

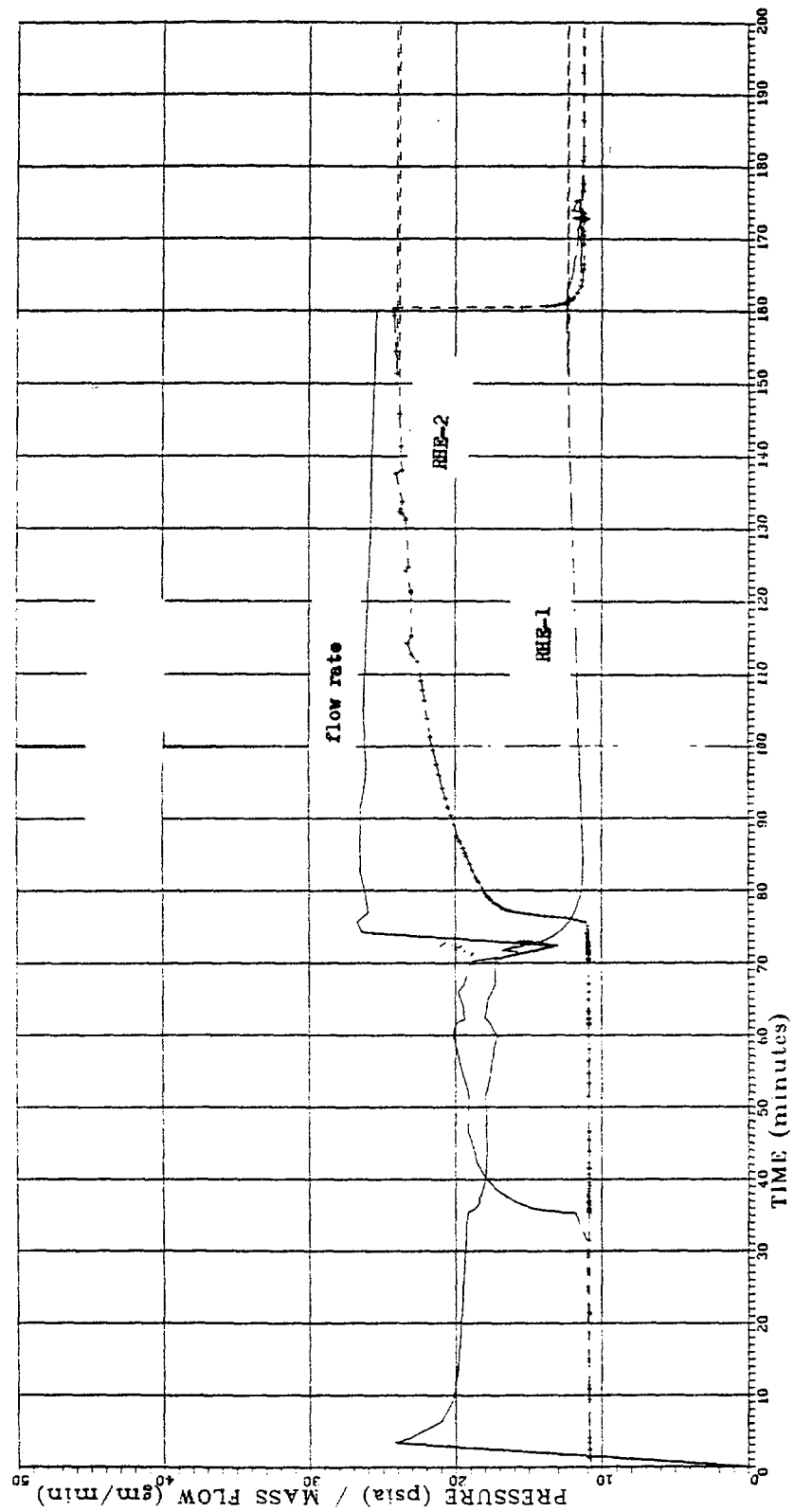


FIGURE 8.20. Pressure-flow history: water displacing carbon dioxide.

If fractional flow (see Collins, 1976) had been the case, the opposite would have been observed. In fractional flow, as the saturation to one fluid is increased, the effective permeability to that fluid will also be increased. In that case flow rate increases while the pressure drops with time.

When a fluid with smaller mobility ratio (like water) displaces a fluid with higher mobility ratio by piston displacement mechanism, the effective permeability to the former decreases with time because the overall mobility of the fluid system reduces as the saturation to the first fluid increases. The opposite is expected when the reverse condition prevails.

After the initial water injection, both boreholes were pressurized with water to attain the maximum possible saturation. The pressure flow history for this test is shown in Figure 8.21. Although smoother trends are produced by this test, the general decline of the flow rate and ascent of the pressure can be seen. The sudden jumps in pressure are probably due to the escape of entrapped gas either from the cavity or in the fracture. It is noticeable that decay of the pressure in both boreholes is much slower than that of the initial water injection test and that the final pressure falls below atmospheric (atmospheric pressure in the mine is about 0.074 MPa or 10.7 psi). This is due to the capillary attraction in the fracture. The stronger negative pressure in borehole RHE-1 is due to its smaller aperture

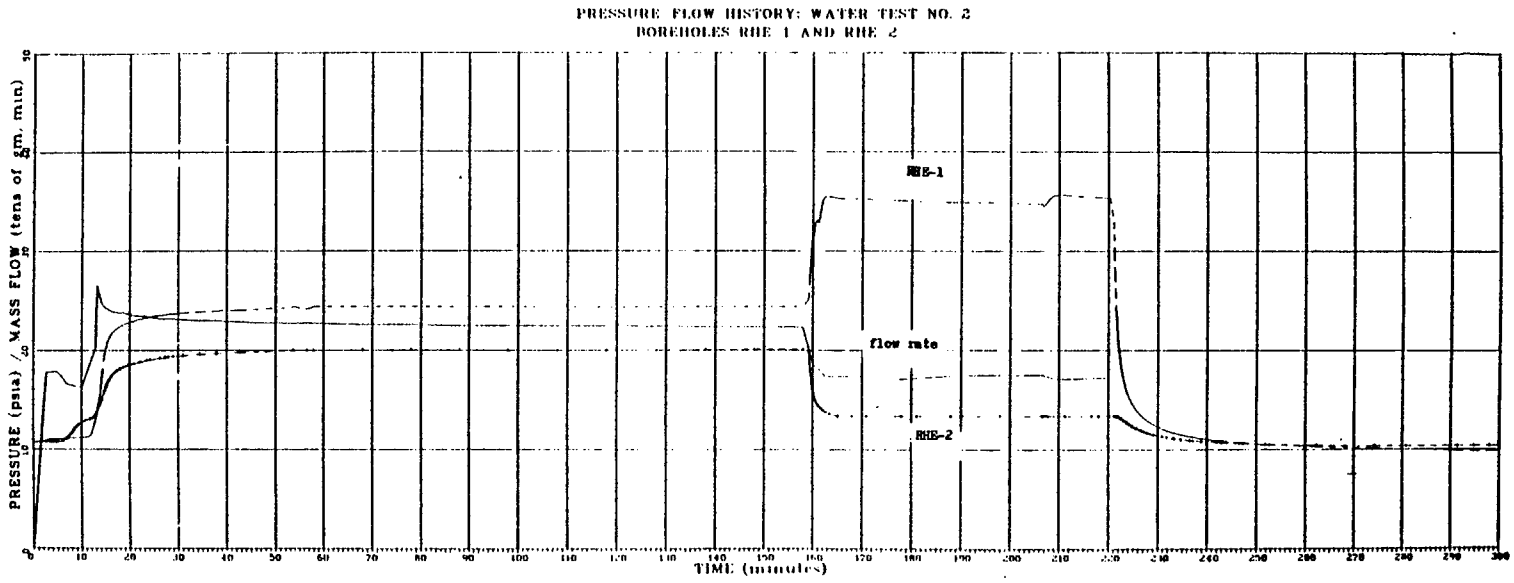


FIGURE 8.21. Pressure-flow history: water test no. 2.
Boreholes RHE-1 and RHE-2.

which is also shown by its lower conductivity.

Finally the water in the fracture was displaced with nitrogen as shown in Figure 8.22. During the first thirty minutes, the cavity is being filled with nitrogen after which a sudden pressure decline occurs. This pressure decline is consistent throughout the entire injection period and is accompanied by an upward trend in the flow rate. This is exactly opposite to that observed during the water test. In this case the overall mobility ratio of the system is increasing with time.

The equivalent permeabilities calculated from these tests are plotted versus the inverse of the pressure in Figure 8.23. Unlike the porous-concrete sample, permeabilities to all three fluids fall on the same line. Almost horizontal lines are obtained from these tests, unlike the results from testing the shear zone. The permeabilities obtained from these tests are in good agreement with those obtained, for the same zones, from systematic nitrogen injection testing after correction for difference in the lengths of the intervals is made.

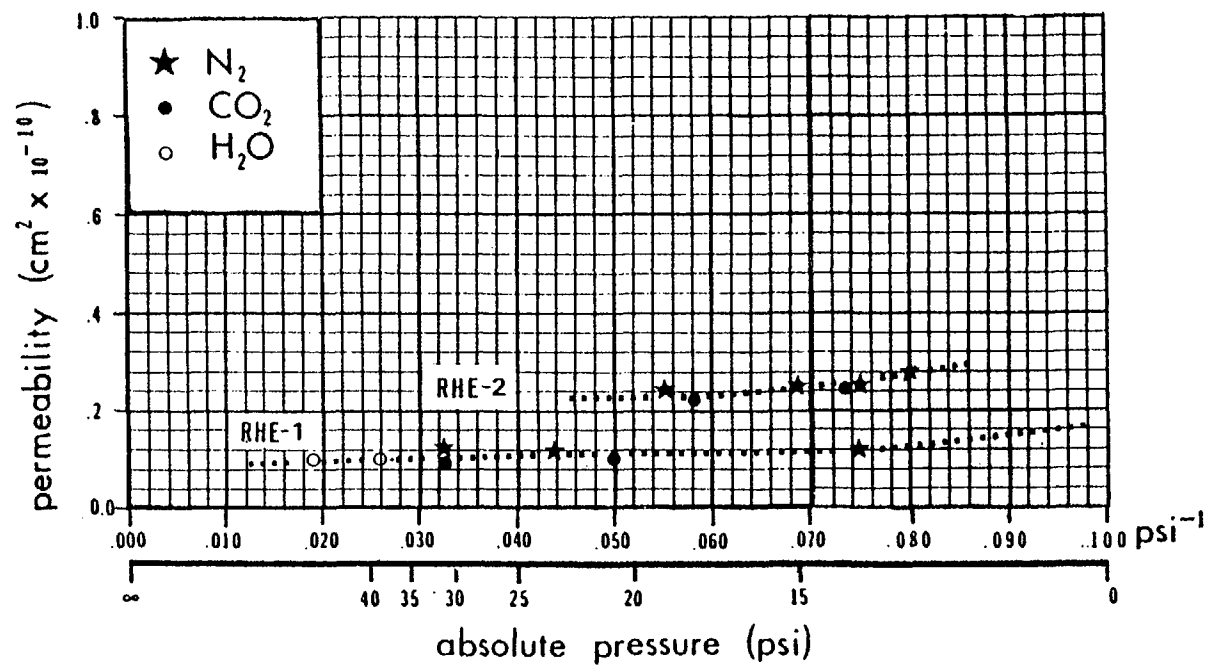


FIGURE 8.23. Pressure-permeability of the fracture shown in Figures 8.16 and 8.17.

8.6 Evaluation of the Preliminary Water Testing.

Early in this chapter, it was mentioned that the only direct evidence for the permeability modification after the construction of the CSM/ONWI room is the results of a series of water injection tests that were conducted before and after the excavation of one of the faces. However, the results were not considered reliable due to the preliminary configuration of the equipment used for conducting these tests. For this reason, the presentation of the results was held until this section so that comparison could be made between the data obtained by the initial equipment and that collected by the more sophisticated instrumentation developed later.

8.6.1 Original Instrumentation

The probe used for water injection tests was basically similar to the main probe described in Chapter Six except that no provision was made for the pulse testing and the pressure ports were made of modified pipe fittings. Only rotameters were used for flow rate measurements and the minimum flow rate that could be measured was about 20 cc/min. of water (compared with the 0.01 cc/min. of the later equipment design). The pressure transducer outputs were read on a digital voltmeter with resolution of 0.1 psi (0.7 KPa

as compared with 0.0007 KPa of the later equipment design).

The flow was regulated with a single reducer valve which was connected directly to the mine water pump. Water was injected into the main injection chamber through the short segments of connecting pipe and not continuous tubing. It is obvious that the accuracy of the data collected with this system was far inferior to the system developed later.

8.6.2 Data Analysis.

The permeabilities of the tested sections were calculated by the methods described by Zeigler (1976) which are basically employing equations developed by Hvorslev (1951). It should be noted, however, that injection of water into an unsaturated fractured rock from a horizontal borehole creates a non-radial flow domain. Therefore, strictly speaking, the radial flow equations of Hvorslev are not applicable to such tests.

The problem of steady state injection into a vertical fracture is similar to the problem of irrigation of an unsaturated porous medium with a drain pipe. The flow domain for such a system is shown in Figure 8.24. When water injection is initiated inside the borehole, a moving free surface (wetting front) is created within the fracture. If the injection rate is kept constant, a steady state condition

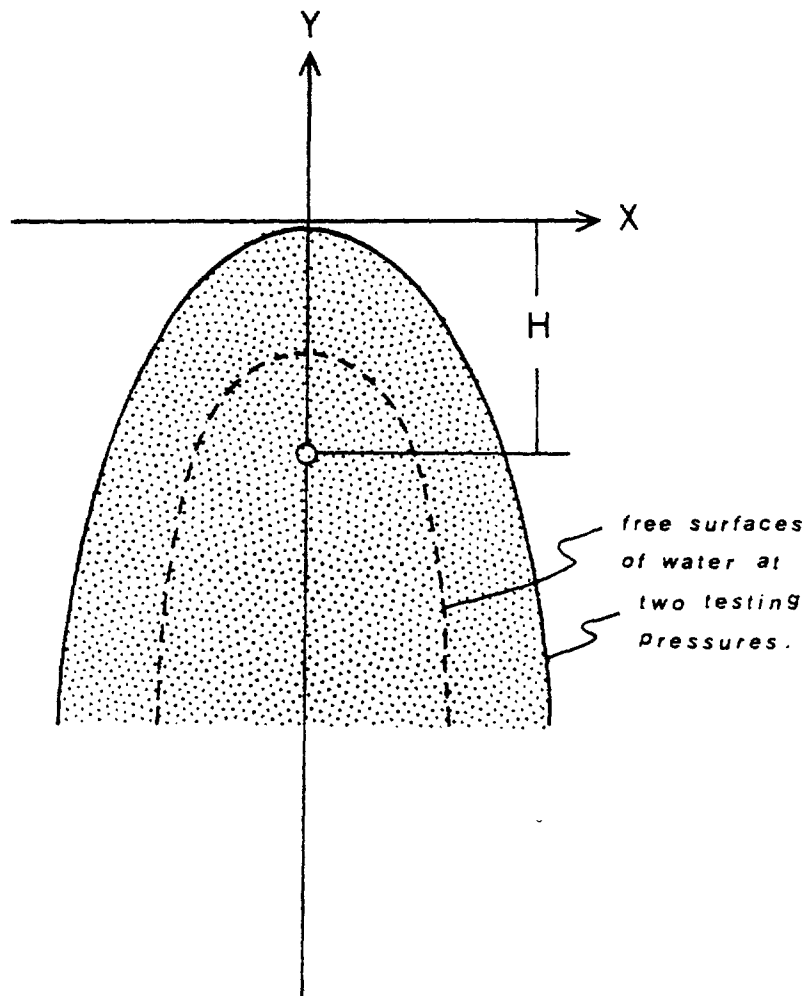


FIGURE 8.24. Schematic diagram showing the flow domain during injection into a vertical parallel plate model saturated with air. The shaded area is saturated with water. The solid curve corresponds to a higher injection pressure than the dashed curve.

will be reached after some time has elapsed. At this state, continuation of the injection will not affect the shape of the free surface. Polubarinova-Kochina (1962) has provided a solution for such a problem which, by using the similarity between the Hele-Shaw's parallel plate model and porous media, can be written as:

$$\frac{P_o}{\gamma} = A \left(\frac{1}{2\pi} \ln \frac{A}{4\pi r_w} + \frac{\ln 2}{\pi} \right) - h_c \quad (8.6.1)$$

where:

P_o = pressure in the borehole

γ = specific weight of water

h_c = capillary rise

$A = \frac{Q}{\omega} \times \frac{\mu}{\rho g}$

Q = injection flow rate

ω = fracture aperture

μ = viscosity

ρ = density

r_w = borehole radius.

The equation for the radial flow in a saturated fracture is (Zeigler, 1976):

$$\frac{P_o}{\gamma} = \frac{A}{2\pi} \ln \left(\frac{R}{r_w} \right) \quad (8.6.2)$$

in which R is the radius of influence. Figure 8.25 is the plot of P_o/γ versus the parameter A . The significant difference between the two types of flow renders equation (8.6.2) useless for unsaturated flow conditions. The fracture aperture is not an explicit term in equation 8.6.1 and should be determined by iteration.

When a system of fractures contribute to the flow in an unsaturated medium, the problem is extremely complicated by the fact that equations of flow leading to the solution given in equation 8.6.1 are non-linear. Due to this non-linearity of the differential equations, the principles of superposition cannot be used to apply equation 8.6.1 to a system of fractures. This means that the differential equations should be solved for every test. The number of unknowns and the labor involved in reducing the data makes the task of accurately calculating the permeabilities practically impossible. For these reasons air injection testing was chosen for the comprehensive investigation of the permeability distributions.

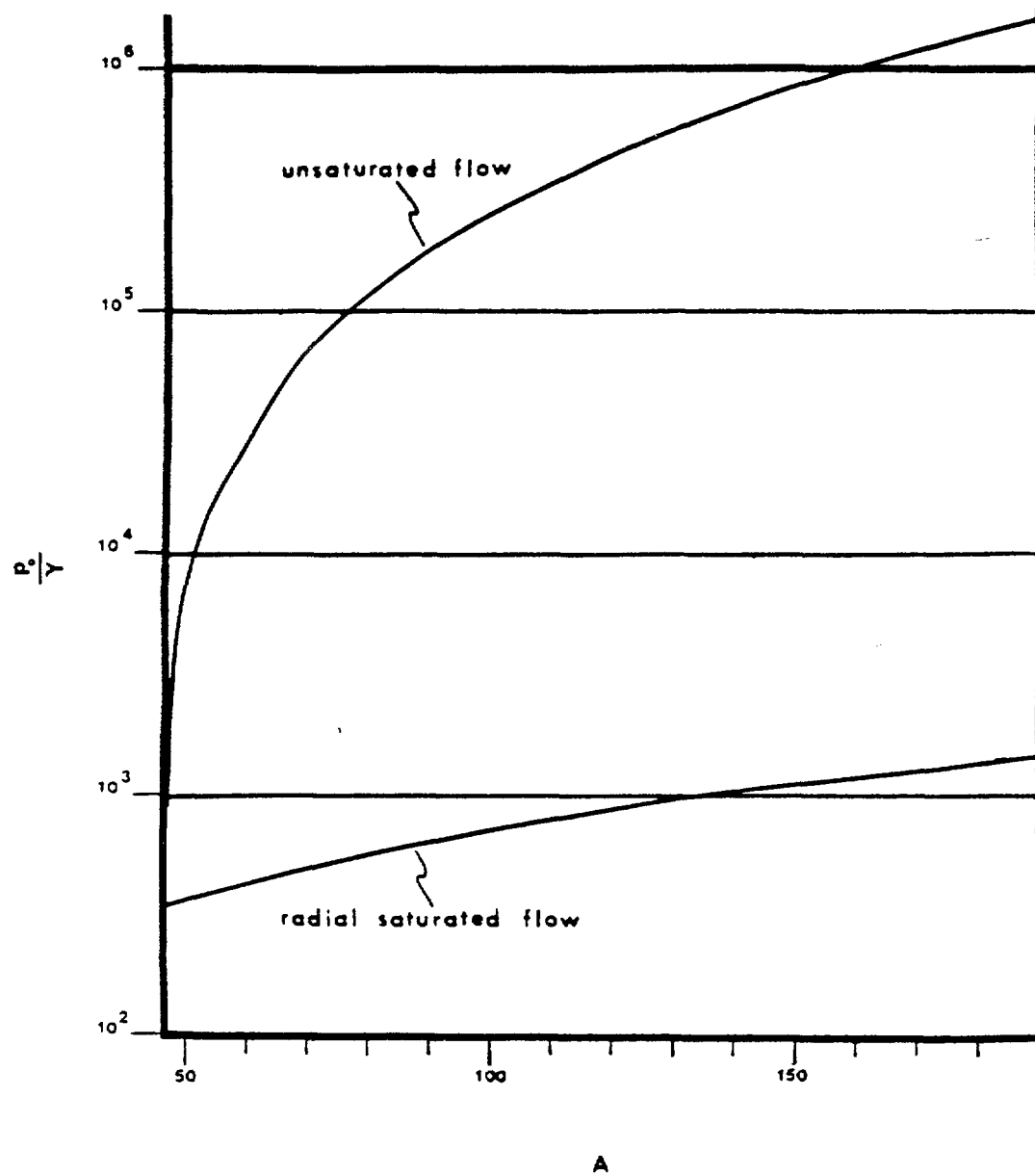


FIGURE 8.25. Graph of A versus $\frac{P_o}{\gamma}$ for the two conditions of radial flow and that shown in Figure 8.24. See text for definition of symbols ($r_w = 3.81\text{cm}$).

8.6.3 Results.

During the construction of the CSM/ONWI room the borehole PA-1 was drilled to about half of its final depth (Figure 8.26). This length of the borehole was tested before and after the blasting of one of the rounds shown in this figure. The results of these tests, using the radial flow equation, for this interval are shown in Figure 8.27. Two significant changes in permeability can be seen in this figure. First is that the slope of the pressure-permeability is substantially increased. Second is that the trend is shifted towards a lower permeability region in the graph.

The reason for a sloping pressure-permeability trend is the unsaturated nature of the fractures. Most of the fractures (if not all) intersecting the borehole are nearly vertical and unsaturated. Therefore, as the pressure increases a larger area of the fractures is affected by the water flow as shown in Figure (8.24). In other words, the effective conductivity of each fracture increases with pressure which is reflected in Figure 8.27. In case the apertures of the fractures decrease, parameter A in equation 8.6.1 and Figure 8.25 increases for each fracture. This means that at a given flow rate a larger area of the fractures with smaller aperture can be saturated. This is believed to be the cause of a steeper slope for the after

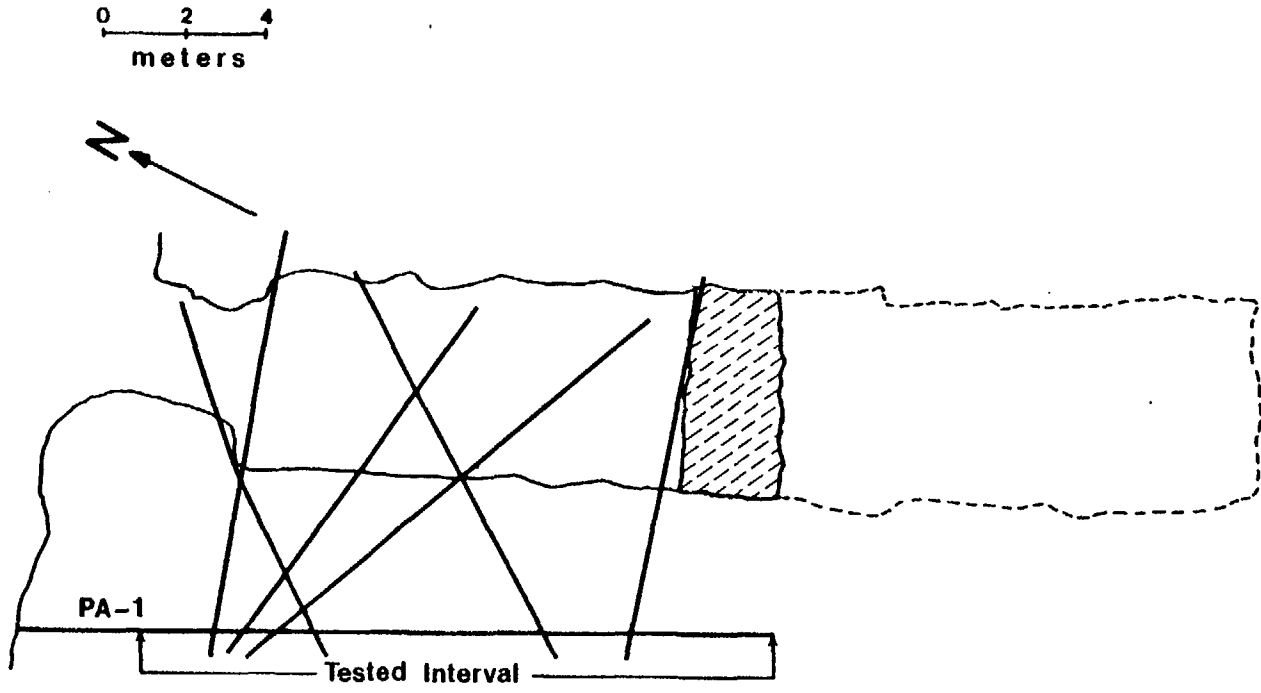


FIGURE 8.26. Plan view of the CSM/ONWI room during its construction. The interval shown was tested before and after the hatchured area was blasted.

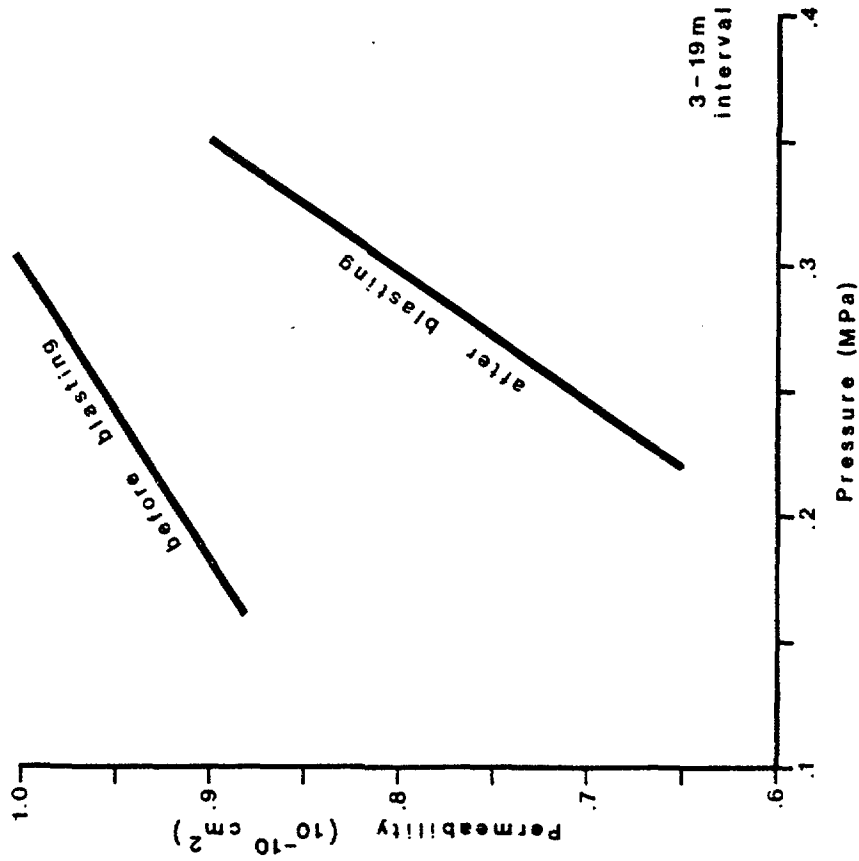


FIGURE 8.27. Pressure-permeability plot for water tests conducted before and after blasting of one of the faces (see Figure 8.26).

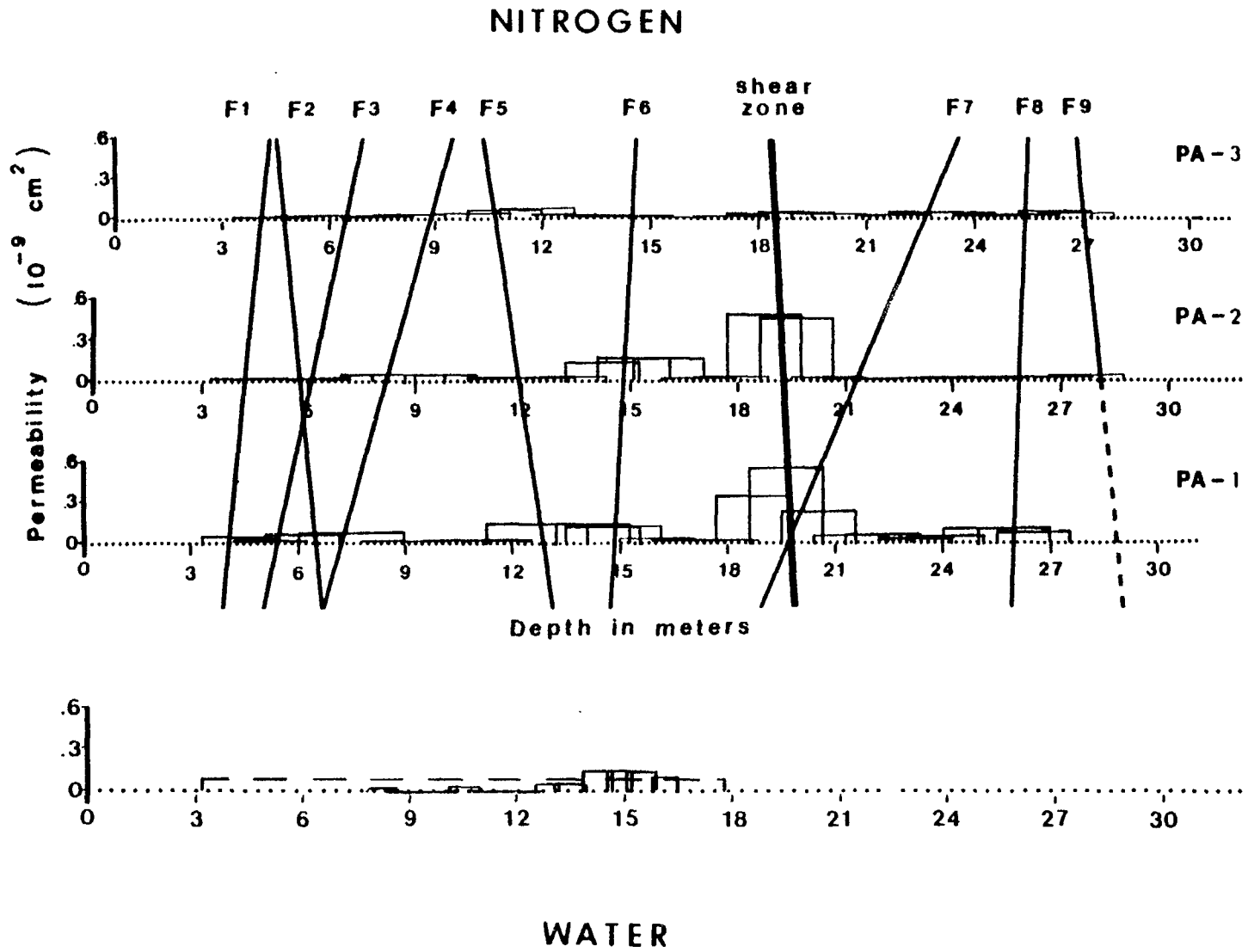


FIGURE 8.28. Comparison between injection testing with water and nitrogen for borehole PA-1.

blasting curve in Figure 8.27. Therefore, if these tests are considered reliable, the overall permeability of the tested section is reduced by about half an order of magnitude after the blasting.

After the blasting of this particular round, the entire length of PA-1 was tested with water at short intervals (0.76m) using the SOI method. The results are shown in Figure 8.28. At first glance it seems that the permeabilities of the tested sections are about the same for water and nitrogen. However, it should be noted that the shorter sections used during testing with water exaggerate the permeability. Therefore, if the permeabilities to water of the shorter sections are adjusted to correspond to the longer test sections (2.13m) used during nitrogen testing, it can be seen that the permeabilities to water are somewhat smaller. This also confirms the concept of the unsaturated flow discussed earlier in this section.

8.7 Summary of Results.

Systematic injection testing of the longitudinal boreholes with nitrogen revealed that the pressure-permeability relationship is non-linear and therefore, effects other than Klinkenberg's control the flow. Two types of pressure-permeability trends are delineated:

1. Permeability decreases with increase in the equilibrium pressure, and
2. Permeability increases with increase in the equilibrium pressure.

The first kind is seen mostly for high permeability zones and the second for low permeability zones. In both cases, extrapolation to infinite pressure was assumed reliable for comparison.

The overall permeability of the longitudinal borehole closest to the room is about 10^{-12} cm^2 and is one order of magnitude smaller than the overall permeability of the other two longitudinal boreholes. The highest permeability measured is $5 \times 10^{-10} \text{ cm}^2$ in the shear zone in the two boreholes farther from the room. The matrix permeability is estimated to be about 10^{-14} cm^2 . The permeability of the

shear zone is two orders of magnitude smaller in the borehole nearest the room. Similar reduction in permeability is clearly seen for two other fractures.

Along the radial boreholes, permeabilities range from $3E-13$ to $1.0E-6$ sq. cm. (corrected for the two meter interval). Large permeability values are recorded for the proximal 0.5m of the radial boreholes.

Variable interval testing of borehole PA-2 shows that there is a mean value for the permeability of the rock mass that is approached when the sample size becomes larger than 10m. This value is found to be about $5 \times 10^{-11} \text{cm}^2$ for this borehole.

Cross-hole testing of the shear zone with nitrogen and water confirms the significantly lower conductivity of this fracture near the room. Cross-hole testing of the fracture in radial boreholes shows that for high conductivity fractures, permeability values measured by water, carbon dioxide, and nitrogen are the same, provided the Klinkenberg effect for the gases is taken into account.

Evaluation of the preliminary water testing of borehole PA-1 shows that, after blasting of one of the mining faces, permeability of the rock mass may have been reduced.

9. DISCUSSION AND ANALYSIS OF THE RESULTS

The results presented thus far have revealed important insights into the problem of flow through fractured rocks, especially in relation to the excavation of an underground opening. This chapter derives some significant points from these results. The main questions are:

- 1) Using the techniques developed in this investigation, can one obtain an estimate of the intrinsic permeability of the fractured rock mass?
- 2) Is this value conservative as far as the contaminant transport through these rocks is concerned?
- 3) Which fluid is more appropriate for testing unsaturated fractured rock: nitrogen or water?
- 4) Are the pressure-permeability relationships useful to qualitatively compare permeabilities of various zones?
- 5) If so, what is the relationship between spatial variation of the permeabilities to the blasting techniques and stress distribution around the room?
- 6) Can these relationships be attributed to the excavation of the CSM/ONWI room?

There are still numerous uncertainties involved with

the conclusions being drawn in this chapter. These will require further, more rigorous analysis of the results and/or completion of a series of well designed experiments.

9.1 Analysis of the Pressure-Permeability Trends from Systematic Nitrogen Injection Tests.

There are two very common types of pressure-permeability trends that can be seen in the plots of Appendix VI:

- 1) A non-linear decrease in permeability with increase in pressure, and
- 2) an increase in permeability with increase in pressure which has somewhat an S-shaped (inverted) curve.

The first type is most commonly seen for intervals that include high conductivity fractures and show a permeability (for $L=2.13m$) of greater than 10^{-10} cm^2 . The second kind is mostly seen to be associated with the low permeability zones.

The characteristic of the pressure-flow histories of the first type is the rapid establishment of a steady state equilibrium in the test zone. A very small increase in pressure and decrease in flow is observed during initial stages of the equilibrium which vanishes as injection is continued. This type of behavior is very commonly observed in conventional packer testing with water in saturated zones.

In the second type, however, the equilibrium is almost

never reached. A decline in pressure and increase in flow is consistently observed, after the initial peak in pressure is reached. However, at low injection pressure (50 kPa or 7 psi) the steady state equilibrium behaviors of the first kind is most commonly encountered.

9.1.1 Causes for the Inverse Pressure-Permeability Relationship.

There are several factors that are probably combined to produce the trend of the first kind. Some of the more important factors are:

- 1) the gas slip phenomenon or Klinkenberg effect,
- 2) the lubrication effect of Rose (1960),
- 3) the interference of the subsequent steady state tests.

The Klinkenberg theory, which is reviewed in Chapter 3, predicts the decrease in permeability with increase in pressure. However, the relationship predicted by this theory is linear and the observed trends are highly nonlinear. The lubrication effect of Rose also exaggerates the permeability but it is insensitive to pressure.

The most probable cause for nonlinearity of the P-P curves appears to be the following: when a continuously

incremented steady state test is conducted, a pressure gradient is established in the fracture system during the first test. When the pressure is increased, without allowing this gradient to disappear, a new gradient is being imposed on the first one. As more and more pressure increments are imposed on the system, a step wise pressure gradient is formed in the fracture system. The result is that during the later stages of the test the permeabilities are underestimated. This problem has been discussed in more detail by Craft and Hawkins (1959) in relation to the gas reservoirs.

There are also other possible causes that may contribute to the deviation from Darcian flow of a gas through a fracture network. One example is the molecular diffusion (or effusion) of the gas in the fracture network. When gas is introduced into a fracture at low concentrations, as soon as the gas reaches another fracture intersecting the main flow path, considerable numbers of molecules may enter the second fracture. If the number of intersecting fractures is high, a significant amount of mass could be lost in the fracture network with little effect on the pressure gradient. One piece of supporting evidence for this is the noticeable difference between the pressure-permeability trends of the shear zone and the single fracture cross-hole tested in the radial boreholes (compare Figures 8.23 and 8.9). In the shear zone

which has a complicated network system the pressure-permeability trend is much steeper than that of the single fracture. This idea requires more detailed laboratory experiments and will not be given any further attention due to lack of sufficient evidence.

Due to a variety of the possible causes, no single method could be justified for determination of the absolute permeability (permeability to a liquid) of the tested zones. Nevertheless, it can be seen that all of the trends of the first kind can be extended to infinite pressure to obtain a single value of permeability. This was considered as the absolute permeability and this seems justified for the purpose of comparison and unification of the permeability data.

9.1.2 Causes for the Trends of the Second Kind.

9.1.2.1 Increase in Permeability With Time.

As is concluded in Chapter 4, it is suspected that the fractures are partially saturated with water. This is revealed by formation of a heavy condensate on pipes and other metal objects left inside the boreholes for any length of time. However, no pressure buildup is detected when the packers are left inflated in the borehole for a long time and

no actual water flow has been seen from any of the 45 boreholes (other than occasional dripping). These observations indicate that even though considerable amount of moisture is held by the rock mass, there is no hydrostatic pressure within the fractures. Moreover, many of the fractures are drained and unsaturated.

It appears probable that the flow of gas during nitrogen injection drives the water into the rock matrix and/or into deadend fractures by fractional flow or piston displacement mechanisms; the choice of mechanism depending upon the saturation state of the fractures. This flow of water is extremely slow, except in the latter case, as evidenced by the presence of the effect during very long tests. Isolated patches of water (pendular rings) in constricted areas of the fractures, where capillary attractive forces are high, are probably forced into the low permeability matrix by the gas flow. As the water moves away, the amount of air in the fracture (the air saturation) increases; therefore, the air permeability increases with time and pressure. Furthermore, if the pressure is high enough to overcome the capillary force in the largest pore of the matrix, the air may enter the matrix.

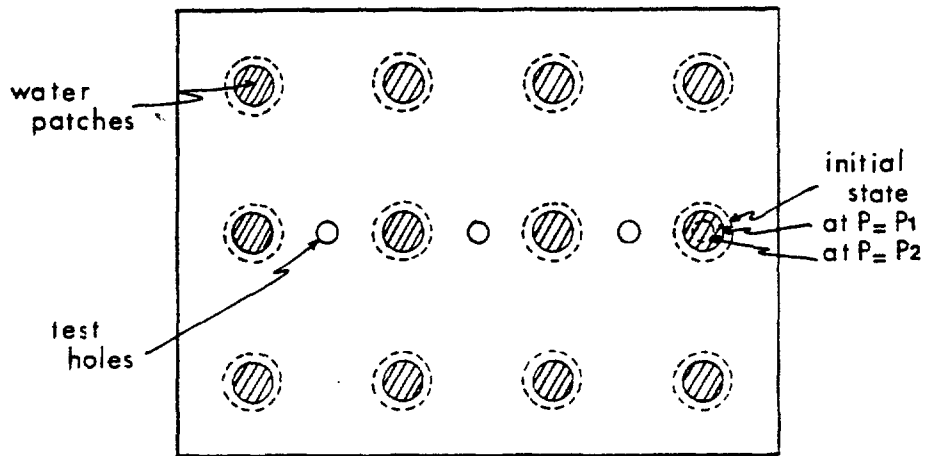
In high conductivity fractures this phenomenon is inconspicuous because the capillary attractive forces are small, fractures are already drained by gravity flow, and

low flow velocities are sufficient to quickly displace the water that is left in the fracture. In low conductivity fractures (where the capillary attractive forces are greater) higher pressures are required to reduce water saturation significantly.

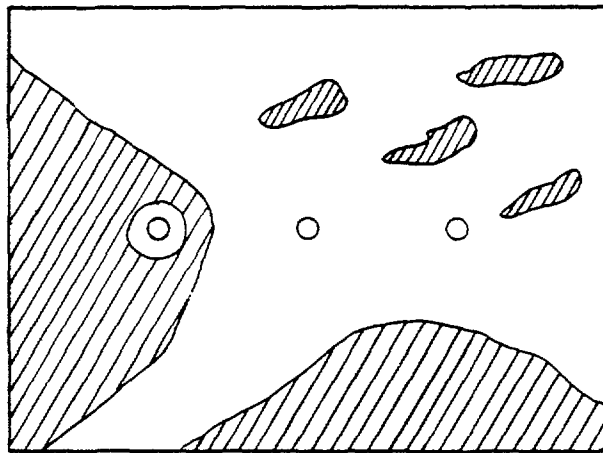
Therefore, the increase in the effective permeability with time is not observed in either the high conductivity fractures or when the low conductivity fractures are tested at low pressures.

9.1.2.2 Increase in Permeability with Pressure: A Conceptual Model.

The conditions described in the previous section may be visualized by the example shown in Figure 9.1a. The fracture considered here has uniform width distribution and is infinite in extent except that the width reduces at the points where the water patches are shown. It is further assumed (as is the case in this study) that the fracture is bounded on both sides by a saturated porous medium which holds water primarily due to capillary forces. Since the aperture of this fracture is larger than the largest pore size of the rock matrix and there is no pressure gradient, water does not stay in the fracture except in places where either the aperture is reduced to a small enough amount due to



- a. Looking in the plane of a hypothetical unsaturated fracture.



- b. Probable natural conditions.

FIGURE 9.1. Hypothetical unsaturated fracture during injection testing with a gas.

irregularities or by some fine grained infilling (circular hatched areas in Figure 9.1a).

When air is injected into one of the boreholes, the pressure around the water patches increases. The pressure increase, if in excess of the capillary pressure which holds the water in the areas, forces the water into the porous medium. The reduction in water content of the fracture causes an increase in the effective conductivity of the fracture. As may be visualized in this diagram, similar pressure-permeability trends should be observed for each borehole if the fracture characteristic is uniform (uniform aperture and uniform distribution of the water patches). In reality, the condition may be as shown in Figure 9.1b, in which case the pressure-permeability trends should be indicative of variations in fracture characteristics.

The flow of water into the rock matrix is extremely slow when testing such a fracture and depends on the permeability of the matrix. Therefore, a constant change in effective conductivity of the fracture would be expected. This change is not permanent because the unsaturated fracture has a memory. As soon as the boundary conditions return to their original natural state, the effective conductivity of the fracture will resume to the same value.

The same pressure permeability trends are observed

over and over. This may be because the conditions as explained above are reversible. As soon as the pressure in the fracture is brought to atmospheric, the water moves back into the restricted fracture areas in order to establish equilibrium according to the capillary pressure distribution. Similar effects are expected to be observed while testing the saturated matrix.

This conceptual model is partially supported by the results of cross-hole testing of the RHE-1 and RHE-2 (section 8.5.3.2). In these tests when nitrogen or carbon dioxide are injected into a relatively dry fracture, typical steady-state, pressure-flow histories are obtained. However, when nitrogen is injected into a wet fracture, the pressure-flow trends predicted by this model are observed (Figure 5.23), the pressure constantly decreases and the flow constantly increases, meaning that the effective permeability increases with time.

9.1.3 Rationale for Comparison of Permeabilities.

It is apparent that single values of permeabilities cannot be compared across the boreholes or along the identified fractures. Rather, the trends of pressure-permeability plots should be used for comparison between the three longitudinal boreholes.

This is considered reliable at least for the higher permeability zones ($\geq 10^{-1}$ cm²) because, as was noted above, the effect of unsaturation is overwhelmed by the stronger Klinkenberg effect in these zones. However, even for smaller permeability zones, variation of saturation in a 1.2m radius (i.e. between the three boreholes) is indicative of changes in fracture characteristics, because the pressure-permeability curves should be identical if the fracture characteristics remain unchanged and only the saturation level varies between the boreholes due to variation of boundary conditions. This is true because the effective conductivity of the fracture should remain constant at a given equilibrium condition, i.e. constant pressure, flow, temperature, fluid and medium properties.

Therefore, whenever a change in pressure-permeability trend along a fracture is observed, it is automatically concluded that a difference in the fracture characteristic must exist between the two measuring points.

9.2 Variation of Permeability Along Fractures.

In order to be able to compare the permeability of the fractures across the three boreholes, fractures had to be identified. This was accomplished by comparison of the fracture map (Plate 1) with the pressure-permeability results

for each fracture across the three boreholes (Figures 8.6 through 8.10). There were only five sufficiently distinct fractures (out of 12 identified) that could be isolated for the permeability comparisons. The other fractures were either isolated in one borehole but not in the other two, or their continuity was uncertain.

Three of these fractures (F3, FS4, and F12) show a strong diminishing trend in permeability towards the room (PA-3 is the borehole closest to the west wall of the room). FS4 is a 20 cm wide shear zone crossing the room with some change in appearance and opening. It is persistent and has also been identified in one of the radial boreholes showing large conductivities. Figure 8.5 shows that the equivalent porous media permeability of this fracture has reduced by more than one order of magnitude. F12 shows at least a one order of magnitude decline (at PA-3 isolation of F12 is uncertain), and F3 shows a two order of magnitude decline.

In contrast, the other two fractures (F1 and F5) do not show any detectable change in permeability. It can also be noted (in Figure 8.5) that the overall permeability of PA-3 is much less than the other two boreholes.

All of the above observations are the results of the nitrogen injection tests. Such tests have been criticized (Witherspoon, 1981, open discussion) on the grounds that the

effective conductivities of a fracture to nitrogen may not be compared across boreholes, due to the fact that variation in water content along a fracture causes changes in conductivity of the fracture. This statement, although valid, does not negate the conclusion that the conductivity of the fractures mentioned above are lower towards the room.

The reason for this is that the fracture conductivity is dependent on the fracture width. At the conditions of free gravitational flow the fractures with narrower width have higher water content (as expressed in percent of the saturated area). During injection testing with nitrogen, the residual-areal water saturation of the fracture is higher in more restricted areas of the fracture. Therefore, the observed effective conductivity trends along the fractures mentioned above are indicative of the absolute conductivity trends along these fractures. What remains uncertain is the actual difference, in the order of magnitudes in the conductivities, between the boreholes. The differences in the order of magnitudes shown by the effective conductivities may be highly exaggerated.

This problem is solved by the results of water profile testing which show the same order of magnitude difference between the conductivity of the shear zone in PA-3 and in PA-1 and PA-2. This not only proves that the trends

observed are those of the actual conductivities, but also indicates that the effect of unsaturation of this fracture on conductivity measurements has been negligible. This reasoning is also supported by the conceptual model; that the higher conductivity fractures are drained by gravity. Similarly, the results of profile testing of the RHE-1 and RHE-2 support the above conclusions.

9.3 Variation of Permeability Along Radial Boreholes.

In radial boreholes, only a single value of permeability is available for each tested section. The judgement on the trends of the permeability is based on the fact that the permeability values are all measured at narrow range of pressures ($0.24 \text{ MPa} \pm 0.014 \text{ MPa}$). However, there is still no guarantee that the pressure-permeability trends of various tested sections are the same. For this reason the results were statistically analyzed and compared with fracture indices reported for the same boreholes by Chitombo, et al. (1981). A brief description of the method follows.

The fracture index (FI) method, developed by Barrons (1978) is similar to pulse testing techniques (Wang, et al., 1977), except that in fracture index testing air is used instead of water and an external volume is provided to

increase the resolution of the pressure decay in high permeability zones. The test is based on the principle that when pressurized air is injected into a zone isolated by straddle packers, the rate of air flow will depend on the fracture characteristics and intensity. The FI, calculated from an approximate solution to the equation of flow of gas through porous media, is inversely proportional to the permeability of the medium. Therefore, test zones containing high conductivity fractures would show low FI values and vice versa.

Statistical analysis of the permeabilities calculated for each tested section indicates that they are both log-normally distributed. Regression analysis between the logarithm of the permeabilities and the logarithm of the inverse of the fracture index shows that at the 0.01 significance level they are related by ($r = 0.9333$):

$$\ln \left(\frac{1}{\text{FI}} \right) = 7.02 \times 10^9 \ln(k) + 0.279$$

where k is the permeability to nitrogen of a tested section in cm^2 . The means of the logarithm of permeabilities and inverse of the fracture index for four groups of boreholes are plotted in Figure 9.2. From this figure it is evident that a zone of high permeability (or low FI) exists in all

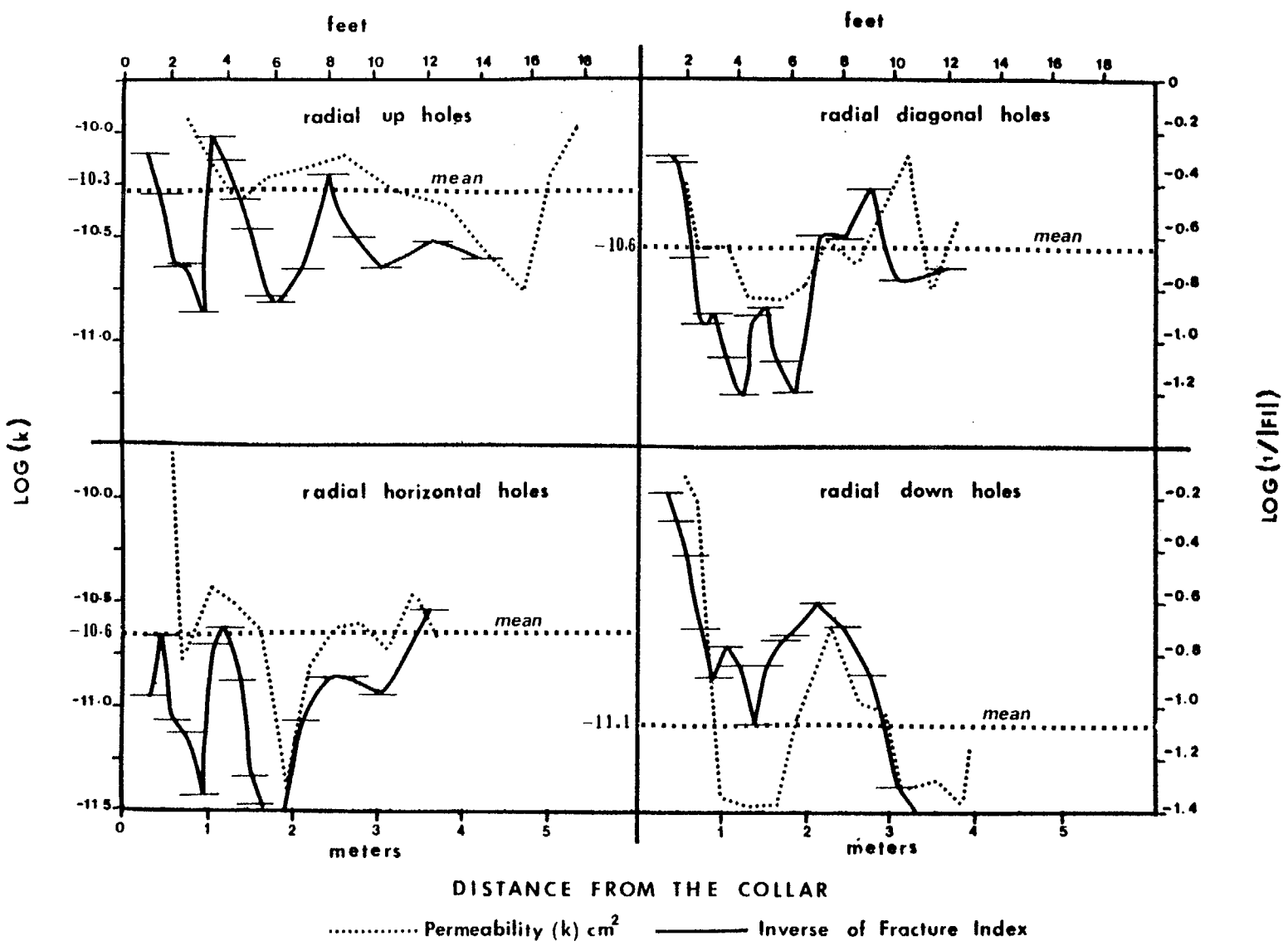


FIGURE 9.2. Distribution of the means of the logarithms of permeabilities and fracture indices along four groups of boreholes. Horizontal bars show the interval for which the fracture index is measured. Horizontal broken lines show the mean of the overall permeability of the borehole groups.

the boreholes within the first 0.5 meter.

9.4 Explanation for the Observed Spatial Trends.

From the discussions presented in the previous sections, it is clear that the spatial permeability trends are real and are not created by the unsaturated nature of the rock. Even if the absolute values of the permeabilities are to be considered unreliable, there is no doubt that the relative values of the permeabilities chosen from tests are significant and indicate variations in the transient properties of the medium, independent of the saturation state of the rock. Therefore, in this section we will explore the factors that may have caused these spatial trends.

9.4.1 Effects of Blasting.

El Rabaa and Hustrulid (1982), Chitombo (1982), Holmberg (1981) and Chitombo, et al. (1981) suggest that the blast damaged zone in the CSM/ONWI room is limited to the first 0.5m from the surface of the opening. Chitombo (1982) also suggests that the transient zone (zone of radial micro cracks from blasting) may have extended to 2m from the

opening walls. Although the permeability and fracture index results from radial boreholes support these suggestions, there are other factors that might have caused this high permeability envelope.

Fractures near the beginning of the boreholes are usually connected to the room which is a constant potential boundary condition. This may result in exaggeration of the permeabilities as the equations used to analyze the test data do not consider this effect. Also, the borehole walls near the collar are rough due to drilling methods used for the first one meter of the boreholes. The roughness of the borehole greatly increases the possibility of leakage around the packers.

It has been also noted that in some of the radial boreholes an apparent displacement along some fractures can be observed (Figure 9.3). This is inferred from the fact that step-like lips exist where these fractures intersect the borehole. It is very unlikely that deviation in drilling may have caused such unevenness in the borehole wall, as drilling deviation (especially in diamond drilling) is very gradual. Since these boreholes were drilled about two months after the excavation was completed, it is not clear whether this indicates a post-drilling displacement across these fractures, attributable to the continued

FIGURE 9.3. Looking into one of the radial horizontal boreholes. Note the offset along the fracture intersected by the borehole.

deformation of the rocks or whether it is damage due to drilling operation. El Rabaa (1981) shows that post-excavation deformation attenuated to an undetectable level in about two weeks after the completion of the excavation. However, drilling of the boreholes may have created new boundary conditions.

It seems that the most plausible explanation for the high permeability envelope may be the combined effects of stress concentration and blasting. Not all the radial boreholes have high permeability in the first .5m. More than 50% of the first 0.5m of all the radial boreholes have permeabilities equal to or smaller than the matrix permeabilities (Appendix VII). If other factors (roughness, etc.) were the cause, at least the majority of the boreholes should have shown high permeabilities at the beginning.

The fractures that are induced by blasting are generally parallel to the direction of the radial boreholes and therefore do not intersect them unless the blast holes intersect the radial boreholes (which is not the case). Deviating blast fractures may intersect the diamond drill holes. However, the estimated propagation distances of these fractures are relatively short. Those that do intersect the diamond drill holes would form undetectable microcracks which would not significantly increase the permeability of the rock.

It is suspected that detectable damage due to blasting or stress concentration occurs along pre-existing fractures. There are two extreme situations that may be considered with all the intermediate conditions possible:

- 1) Fractures that are perpendicular to the blast holes (and in this case perpendicular to the axis of the excavation).
- 2) Fractures that are parallel to the blast hole (and in this case parallel to the axis of the room).

The first set of fractures is intersected by the longitudinal boreholes and the latter by the radial ones.

In smooth wall blasting techniques (Holmberg, 1981), a series of peripheral boreholes is drilled and loaded to shape the outline of the opening. These percussion drilled holes are the last set to be detonated. At the instant that the charge in them is being fired, the confining stress in radial direction (perpendicular to the final room outline) is almost zero (Figure 9.4).

When the charge in these holes is detonated, the maximum distance of the induced crack extension (the transient zone) is half the distance between the blast holes ($0.5/2 = 0.25\text{m}$). In addition to creation of the cracks

radial to the axis of the opening, the compressive stress waves (which travel in radial direction) cause crushing of the rock and produce an envelope that is exposed to extremely high stresses. The propagation of the extremely high pressure gases into the natural fracture system tends to open these fractures which may close rapidly or stay open permanently, depending on the state of the stress across their plane.

For the first case (a fracture perpendicular to the room axis), then fractures will close very rapidly since the stress across their plane is increased (due to the creation of the opening). This opening and closure of the fracture causes the destruction of the asperates which in turn make the two faces fit together better than before. This causes a reduction in conductivity of these new fractures.

In the second case, the asperates are first crushed by the compression waves, but the fracture is re-opened by the high gas pressures and remains open by the high stresses that are created in its plane because of the opening.

Intermediate conditions between the two cases are far more complicated as the effect of shear displacement adds to the number of factors. Shear displacement generally

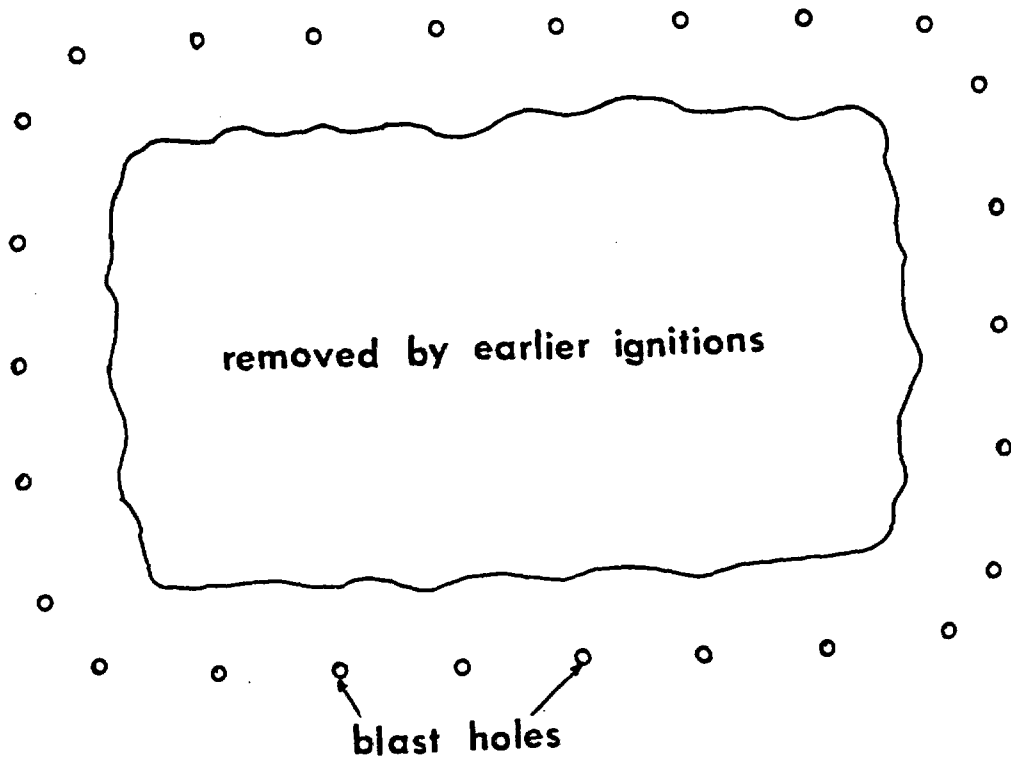


FIGURE 9.4. Schematic diagram showing the outline of the opening just before detonation of the peripheral blast holes.

causes reduction in conductivity of the fracture if the normal stress is high enough to prevent dilation, however it is the final orientation of the stress ellipsoid that determines the final conductivity of the fracture. Obviously, if the normal stress across the fracture is low or the fracture plane is irregular, dilation may cause an increase in conductivity.

In summary, here it is believed that there has been little (if any) blasting damage done to the matrix of the rock around the CSM/ONWI room, as far as the permeability of the rock is concerned. Nevertheless, blasting has modified the characteristics of the pre-existing fractures, which has been enhanced by the superposition of the new (post-excavation) stress system.

9.4.2 Effects of Stress Modification.

The stresses in the rock immediately adjacent to the room, as measured by overcoring, are plotted in Figures 4.16 through 4.18. The maximum principal stress is in a plane nearly perpendicular to the main fracture set - i.e., the set tested in the longitudinal boreholes, and plunges approximately 45° to the north. It has been shown by electron microscope studies (Batzel et al., 1980) that

cracks perpendicular to the applied compressive stress tend to close and those parallel to the applied stress tend to open. In addition, there are numerous examples showing closure of fractures with normal stress. In this particular fracture set (foliation fractures), the apertures would have decreased due to an increase in the normal stress across them, causing the considerable reduction in conductivity that was measured. The smaller the fracture stiffness, the more pronounced the effect.

This effect is believed to be the reason for the markedly lower permeabilities observed in borehole PA-3, which is closer to the room and where the highest stress exists across the fractures relative to PA-2 and PA-1, provided that blast damage has not affected this distance. If a similar stress distribution is assumed to exist all around the room, the exceptionally high fracture permeabilities observed in the radial boreholes, at depths greater than 0.5m, may be explained by fractures belonging to the diagonal sets. These fractures are oriented parallel to the maximum principal stress; a condition which would cause them to open. The fact that some fractures crossing the longitudinal boreholes do not show significant change in permeability may be because these fractures have high normal stiffnesses due to the nature of the filling material (such as pyrite).

In one borehole (RUE-5) high permeabilities were observed in a fracture oriented perpendicular to the axis of the room (perpendicular to the maximum principal stress). However, this fracture is parallel to the borehole and thus the radial flow equation does not apply; and estimated permeabilities tend to be exaggerated. This is due to the greater cross-sectional area of the fracture exposed at the wall of the borehole and also to the fact that the flow pattern is no longer radial.

9.4.3 Prediction of the Fracture Deformation.

In order to estimate the amount of aperture closure due to the increase in the stress across some of the fractures tested, a stress-deformation relationship is required for each fracture. This is not presently available for the fractures at the site. However, Shehata (1971) has presented the results of a series of laboratory tests on similar rock types near Idaho Springs. Although each fracture has its own characteristic stress-deformation relationship, a close approximation can be obtained from Shehata's experiments.

Shehata (1971) created tensile fractures in core samples and conducted uniaxial tests. He plotted the fracture

deformation ($\Delta 2b$) against the logarithm of the stress, obtaining a log-linear relationship:

$$\Delta 2b = \log (\sigma) / C \quad (9.4.1)$$

where $2b$ is the aperture, σ is the stress and C is the fracture modulus of elasticity.

In Figure 9.5 it can be seen that this relationship does not fit the test data. This equation is undefined for zero stress and would overestimate the deformation at large stresses.

A rigorous analysis of his data indicated that at low stresses there is little aperture deformation. This is probably due to the fact that the rock deformation is of the same order of magnitude as that of the fracture at small stresses. This may be due to the closure of micro-cracks in the rock matrix at small stresses. When the stress increases, the fracture deformation becomes more pronounced; however, the rate of change of deformation diminishes due to the increase in contact area (the number of asperities resisting the deformation increases). At high stresses when all the asperities are in contact (they also transfer stresses in a direction parallel to the fracture plane) the fracture begins to act as the rock itself. Statistical (non-linear regression) analysis of the data indicates that the equation defining the relationship between the fracture deformation

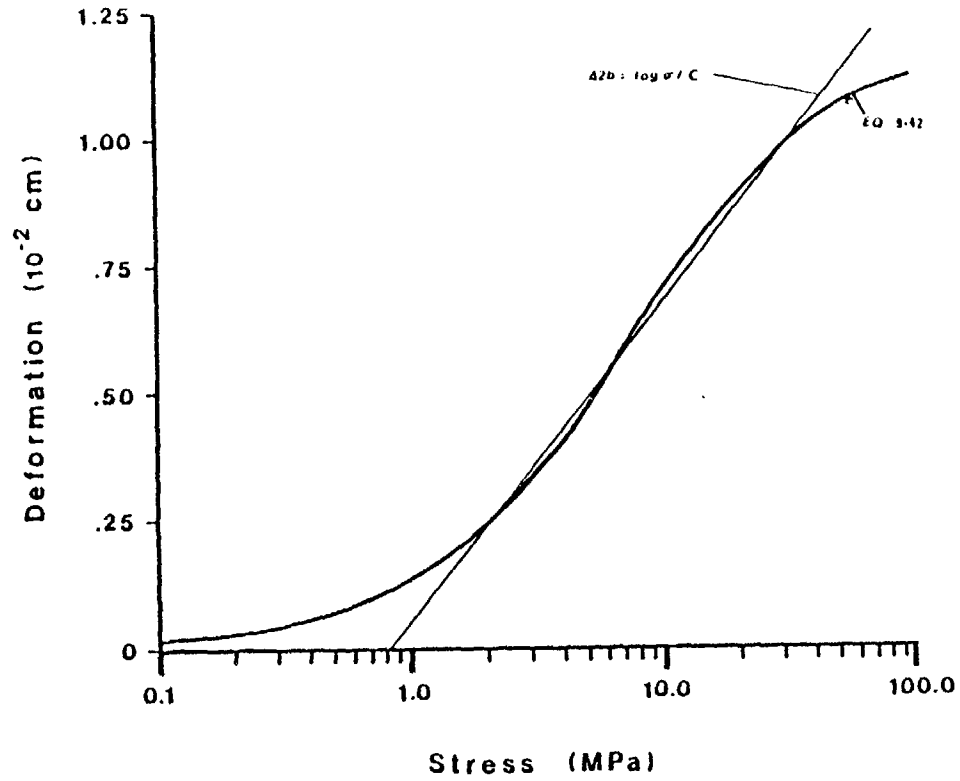


FIGURE 9.5. Stress deformation graph for a fracture induced in a sample from Idaho Springs formation (after Shehata, 1971).

and stress is of the form:

$$\Delta 2b = \left(\frac{2\sigma_n}{\sigma_n + \sigma_c} \right) (\Delta 2b)_c \quad (9.4.2)$$

where

- $\Delta 2b$ = the fracture deformation
- σ_n = the normal stress
- σ_c = the stress at the inflection point
- $(\Delta 2b)_c$ = the fracture deformation at the inflection point.

The equation indicates that fracture deformation is zero at zero stress and converges to a finite number ($\Delta 2b = 2(\Delta 2b)_c / \sigma_c$) at high stresses. This type of fracture behavior can be seen in data presented by Witherspoon, et al. (1977) (Figure 9.6). Note that these graphs show similar slow deformation at low stresses. Gale, et al. (1979a) have also conducted such tests, but they do not show slow deformation at low stresses. This may be due to the difference in instrumentation. It should be noted that these analyses are valid only for normal stresses acting on the fracture; shear stress would complicate this relationship.

The stresses parallel to the longitudinal boreholes are estimated from a curve that was fitted through the stress

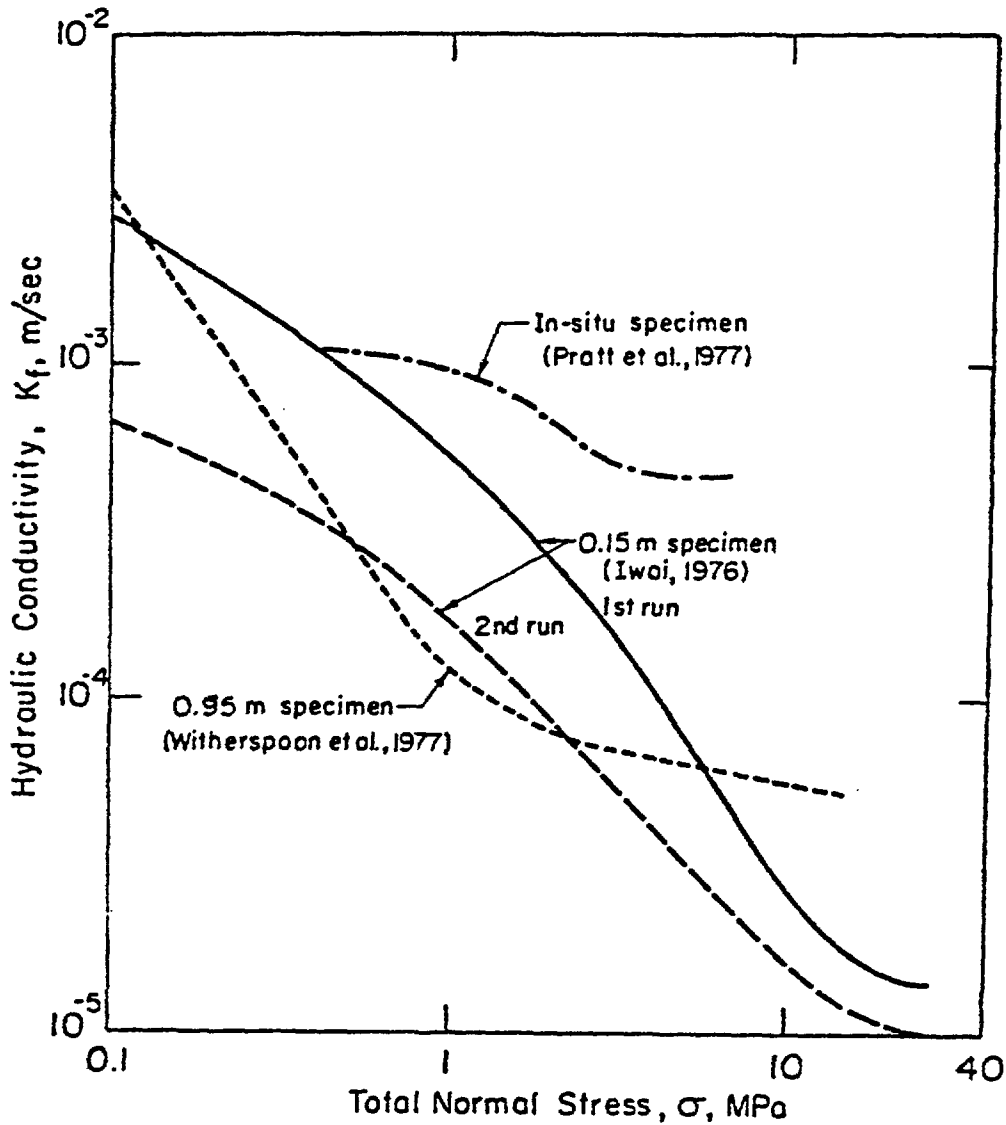


FIGURE 9.6. Variation of hydraulic conductivity in a fracture with increasing stress for three different-size rock samples. Results for the 0.15m and 0.95m specimens are with radial divergent flow. Results for the in situ specimen are with linear flow. (After Witherspoon, et al., 1977.)

data provided by El Rabaa (1981) (Figure 3.19). These values are used to calculate the deformation along a fracture perpendicular to the stresses. Fracture apertures are also estimated from permeability tests assuming a single fracture in the test zone and a parallel plate model (for fracture FS4, Figure 8.9) at a distance of about 65 ft. from the beginning of the boreholes).

The results are shown in Table 9.1. It can be seen that the two values agree very well. Therefore, it may be concluded that the permeability changes seen in the three boreholes along the same fracture may be explained by the stress modification caused by the excavation of the room. This conclusion drawn above is preliminary; more rigorous investigation of the stress-deformation relationship of fractures is required.

9.5 Anisotropy.

The generally high fracture permeabilities in the radial boreholes (normal to the room) in relation to the longitudinal boreholes (parallel to the room) indicate a strong anisotropy in fracture permeability in the vicinity of the room. Because the fractures tested in the radial boreholes are generally parallel or sub-parallel to the room (with the exception of borehole no. RUE-5), the maximum principal

TABLE 9.1

Comparison Between the Predicted and Calculated Values
Of Fracture Deformation

Borehole	Distance (meters & ft) from the West Wall.	Fracture Deformation Relative to Deformation at PA-1 Along the Same Fracture (cm).	
		Calculated from permeability.	Calculated from Equation 9.3.
PA-1	4.1 (12.5)	0	0
PA-2	2.7 (8.0)	-7×10^{-4}	-4×10^{-4}
PA-3	1.5 (4.5)	-70×10^{-4}	-10.4×10^{-4}

permeability around the opening is closely parallel to the room's long axis and the minimum principal permeability axis is perpendicular to that axis.

It is possible that such a strong anisotropy existed in the rock prior to the excavation of the room. However, the fracture frequency is much greater perpendicular to the axis of the room, and the conclusion drawn in the previous sections leads one to the belief that the anisotropy must have been enhanced by the superposition of the post-excavation stress conditions.

9.6 Summary.

The pressure-permeability trends are comparable, at least in a relative sense. They indicate the unsaturated state of the fractures, which in turn is indicative of the fracture characteristics. High permeability fractures show a decrease in permeability and low permeability fractures show an increase in permeability with increase in test pressure. Permeabilities measured by a single test pressure cannot be compared across boreholes.

On the basis of the comparison of the pressure-permeability trends, three fractures show a diminishing conductivity toward the room. These fractures, which are intersected by

the three longitudinal boreholes, have conductivities much higher than the rest of the fractures intersected by these three boreholes.

Comparisons made between permeabilities and fracture indices along the radial boreholes indicate that permeabilities can be compared, at least in a relative sense. In the first half meter of these boreholes, both parameters have values that are significantly higher than the mean calculated for boreholes having similar positions. This high permeability is suspected to be indicative of a damage envelope about a half meter thick, caused by blasting and/or stress concentration.

The reason for the near field high permeabilities in parallel direction and low permeabilities in radial direction is suggested to be the orientation of the stress ellipsoid with respect to the fracture system.

10. ENGINEERING IMPLICATIONS.

The instrumentation, methodology, and results of this investigation can be applied to solve a variety of engineering design problems in fractured rocks, especially those that involve excavation of underground openings. In this chapter general considerations are given to the design of tests in both saturated and unsaturated rocks. In addition, applications to design of underground openings are briefly discussed.

10.1 Fracture Sampling.

Scanlines to sample fracture characteristics should be selected carefully to acquire a representative three dimensional sample of the rock. The minimum requirement would be three nearly orthogonal sampling lines. Exposed surfaces of underground openings should be taken advantage of to estimate fracture continuity, fracture orientations and other fracture characteristics that are not obtainable from boreholes. Oriented core is useful in identification of major features and their correlation with those found on the surfaces of the excavation. However, detailed fracture logging of the core was found to be unnecessary for permeability

characterization purposes. Statistical sampling of the ubiquitous fractures and deterministic mapping of the more prominent features seem to be more feasible and sufficient for permeability characterization. A better approach would be to determine orientation and aperture of the fractures inside the boreholes by means of a T.V. camera, or a bore-scope or other geophysical means. Through correlation with the core, other characteristics are then obtained.

The apertures measured in the borehole are not the same as the equivalent parallel plate aperture. However, it seems reasonable to assume that the distribution function for the two is similar. If this is proven to be true, the task of equivalent parallel plate aperture measurement by indirect methods would be reduced substantially. Because, if the distribution function is found by sampling of a large number of apertures on the exposed surfaces of the rock, the distribution of the equivalent parallel plate aperture can be constructed from a small sample by Monte Carlo simulation or similar statistical methods.

Geologic continuity should be considered with reference to scale. Small fractures are found difficult to correlate across boreholes one meter apart. A 20 cm shear zone can be easily correlated across the room and through the boreholes in a distance of about 10 meters or more; but it is

difficult to find trace of this feature in drifts 50 m away. A 5 m wide shear zone, on the other hand, can be traced to the surface and along other drifts to distances of 100 m or more. It probably can be followed on the surface to at least a kilometer away. Therefore, geologic continuity requires a reference to the scale of study.

10.2 Testing Design.

10.2.1 Saturated Rocks.

Two types of information are sought when packer testing is used in fractured rocks: statistical and deterministic. In statistical sampling, the rock mass is assumed to behave as an equivalent porous medium. Therefore, a large sample would be required to approximate the equivalent porous medium properties.

In statistical sampling, the representative elemental volume (REV) can be determined by using the variable interval testing method described in section 8.4. This should be done for three nearly orthogonal directions.

Once the minimum size of the REV is estimated, the multichamber probes can be used to determine permeability. The packers separation must be equal or larger than the REV.

Testing can then be conducted with the main probe in

all the three orthogonal boreholes. It would be advantageous but not necessary to have a monitoring hole parallel to the main testing hole. The monitoring probe can be configured similar to the main probe for increase in the number of observation points. Directional permeabilities parallel and perpendicular to the borehole can be calculated with this method; unlike the method suggested by Snow (1965), the prior knowledge of the principal axes of the permeability tensor is not required because all the six components necessary to represent the permeability tensor can be estimated.

Deterministic sampling is impractical for large volumes of rock because large numbers of scanlines with varying orientations are required. The methods used for this investigation can be directly applied to characterize conductivity of a certain individual well defined fracture. In general, the best approach would be to evaluate only the relatively large features within the rock mass. After a large network is characterized in this manner, the blocks isolated between such large features can be statistically evaluated using similar methods as described above. Applicability of this method of coupled statistic-deterministic method depends on the site specific characteristics and in many cases may prove to be cost prohibitive. However, at

this state of the technology, it seems to be a possible solution for site characterization and modelling of the fractured rocks.

10.2.2 Unsaturated Rocks.

There are a great number of variables that control the flow through fractured unsaturated rocks. Here, it is assumed that only the state of saturation of the rock affects the permeabilities measured in an isothermal condition.

The most important component in testing of an unsaturated fractured medium is the injection fluid. Gases provide information about the natural state of the rock. Nitrogen seems to be an appropriate gas for injection testing. Air supplied from compressors should be avoided. It contains considerable amounts of moisture and some oil mist which are not desirable for testing purposes.

In case the rock is suspected to have high water saturation, both nitrogen and water testing are recommended. However, results of water testing cannot be analyzed by radial flow equations. In such a case permeabilities to both water and nitrogen, calculated by using radial flow equations, are underestimated. In both cases a wide range of test pressures should be used; however, test pressures should be kept low enough to avoid significant fracture

deformation. If a consistent pressure-permeability trend is obtained, extrapolation to infinite pressure should provide a good estimation of the saturated permeability.

10.3 Design of Underground Excavations

Although there are still some uncertainties, it seems reasonable to accept that the spatial permeability trends are, at least partially, formed by the post-excavational stress distribution. This concept, if accepted as a fact for this site, has a universal application in all hard rock and some soft rock excavations. Furthermore, if the mechanism of the fracture deformation-permeability relationship can be determined, this concept would become a useful tool in the design of the underground cavities for the isolation of hazardous or economical products, such as radioactive waste or liquid natural gas, respectively. In this section only the isolation problem will be discussed, because application of this concept to mineral exploitation would require economical justification, which is beyond the scope of this research.

The effectiveness of the immediate geologic barrier has great impact on the site selection and design of underground excavations for the storage of radioactive waste. Hard rocks, that is granitic and high grade meta-igneous rocks, are favorable geologic media for storage of radioactive

waste because of their extremely low matrix permeability; but are looked upon very cautiously because of the contaminant transport potential of the fractures. If the contribution to the permeability by these fractures can be reduced to negligible limits, the problem of the immediate geologic barrier would be solved.

According to the concept hypothesized in this study, we have been able to reduce the radial permeability of the rock mass one order of magnitude. If we can discover some design method by which the near-field rock mass permeability can be reduced to its minimal limit, the problem of the immediate geologic barrier would be at least partially solved.

The orientation of the opening with respect to the virgin stress, the fracture system, the shape of the opening, and mechanical properties of the rock determine the final near-field stress distribution. Orientation and shape are designable factors. It is believed that, depending on the site specific characteristics, underground excavations can be designed to maximize the number of fractures intersecting the long axis of the opening perpendicularly. The shape of the opening can be designed to increase the stresses across these fractures. The outcome would be an opening with minimal near-field radial permeabilities and maximal

near-field longitudinal permeabilities. The increase in longitudinal permeability facilitates grouting of the rock, because longitudinal fractures are more favorable for drilling purposes, and the enhanced permeability increases the grout take and, therefore, reduces the grouting effort.

11. CONCLUSIONS

The migmatite-biotite gneiss hosting the CSM/ONWI room is a heterogeneous, moderately fractured rock. In the vicinity of the Edgar Mine, within which the room is located, the rock consists of three distinct hydrogeologic zones:

- a) zone of topographic gradient, a shallow-surficial zone of highly fractured rock in which most of the interflow occurs and is underlain by;
- b) the zone of vertical gradient, which is unsaturated and the flow of moisture is mostly vertical; and
- c) the zone of regional gradient, which is saturated and is overlain by the zone of vertical gradient.

The following conclusions have been reached from the results of this study:

1. The fracture characterization technique used for this study is believed to be applicable to radioactive waste repository site characterization.
2. Detailed fracture mapping used here seems to be unnecessary. Statistical sampling of small fractures combined with deterministic mapping of the

more prominent features is more practical.

3. Apertures measured in boreholes are not the same as the equivalent parallel plate apertures and are much exaggerated.
4. Estimation of the equivalent aperture by injection testing may be used, along with borehole surveys, to better understand the distribution of the aperture for specific fracture sets.
5. Permeability testing methods used here are applicable to characterization of unsaturated fractured hard rocks.
6. Although in situ permeabilities smaller than 10^{-14} cm^2 were not encountered in this investigation, the instrument is capable of detecting permeabilities of 10^{-17} cm^2 by the steady state injection. More resolution but less accuracy is gained employing transient testing and/or by increasing the pressure and distance between the packers.
7. The instrument produces results comparable in accuracy to laboratory permeability testing results.
8. For porous material, the steady radial flow equations can be used reliably to estimate the permeabilities in the order of 10^{-13} cm^2 . When such materials are dry or have low water content, nitrogen seems to

be a suitable testing fluid.

9. Water and carbon dioxide underestimate the permeability.
10. Tests with nitrogen would require wide ranges of pressures to delineate the Klinkenberg effect.
11. The sequentially overlapping interval method of borehole injection testing significantly increases spatial resolution and reduces testing efforts. However, analysis of the data to obtain permeabilities of the overlapped intervals requires numerical techniques.
12. Pressure-permeability relationships from systematic injection testing of the longitudinal boreholes are non-linear and are due to a combination of effects of unsaturated nature of the rock and gas slip phenomenon.
13. These relationships are valuable in comparison between permeabilities of various zones and estimation of the saturated permeability. Employing these relationships and comparison with the result of cross-hole testing with water and nitrogen along a few fractures indicate that permeabilities along some of the high conductivity fractures is smaller near the room.
14. The overall permeability of PA-3 (nearest the room)

is about $1.0E-12$ and is one order of magnitude smaller than the overall permeability along the other two longitudinal boreholes.

15. The permeability of the shear zone is almost two orders of magnitudes smaller in PA-3 than the other two boreholes.
16. Conclusions 13 to 15 are suspected to be due to an increase in the normal stress in the plane of the fractures perpendicular to the room axis.
17. Large permeability values are recorded for the first 0.5 meter of 50 percent of the radial boreholes.
18. Conclusion 17 is probably due to a combination effect of blasting and an increase in the component of the stress in the plane of fractures parallel to the room axis.
19. If Conclusions 16 to 18 are true, a significant change in the orientation and magnitude of the permeability tensor in the 1.5m envelope must have occurred. The increase in ratio of longitudinal to radial permeability may have been as much as 100.
20. If Conclusion 19 is proven to be the case for the CSM/ONWI room, it can be used advantageously to design underground storage rooms so that the radial

permeability after the excavation would be almost as low as the matrix permeability. This would significantly reduce the rate of leakage of the stored substances, the rate of escape of radio nuclides, and the drainage problem.

12. RECOMMENDATIONS

For future work on this specific site the following tasks are suggested:

1. Intact-fracture samples of some of the identified fractures should be taken from the room. These samples can then be tested to study stress-permeability relationships as well as unsaturated flow investigations.
2. A three-dimensional finite element stress-flow model should be set up for the ONWI Room.
3. The present packer system is capable of measuring large-scale anisotropic permeabilities of the rock; this capability should be used to calibrate the finite element computer modeling.
4. A large-scale permeability test is suggested for the entire room. This may be accomplished by injecting air into the room blocked at the entrance. Analysis of the transients observed in the instrumented boreholes would provide the skin factor

which is indicative of either blast damage and/or stress effects. This method would clearly estimate the zone of influence.

5. An instrument should be developed to measure in situ stiffness properties of the fractures in the exploratory boreholes. This is a necessity in predicting the behavior of the fractures prior to excavation of an actual repository.

Investigation on this subject can be duplicated at a different site in this mine or another underground location to simulate other repository conditions. The difference would be that the new site should be completely instrumented, tested for permeabilities, and mapped for fractures prior to excavation. Then the post-excavation modification of the stress and permeability could be predicted by the methods and theories presented here, and the predictions could then be compared with the actual post-excavation conditions.

VOLUME 2

BIBLIOGRAPHY OF FLOW THROUGH FRACTURED MEDIA

BIBLIOGRAPHY OF FLOW THROUGH FRACTURED MEDIA

ASTM, 1954, Symposium on permeability of soils: 57th Ann. Mtg. of Am. Soc. for Testing Materials, Chicago, Ill, spec Publ. no. 163.

ASTM, 1972, Standard method test for permeability of granular solids (constant head): Am. Natl Stan Inst.

Aberg, B., 1969, Lavera Project hydraulic calculations on storage of gas in underground rock chambers: Stockholm, Sweden (internal report).

Aberg, B., 1969, Model test on oil storage in unlined rock chambers: Proc. 13th Congr. of the Int. Assoc. for Hydraulic Res., Kyoto.

Aberg, B., 1969, Theoretical investigation on methods to prevent leakage of oil through a fracture between caverns in rock: Internal Report (in Swedish).

Aberg, B., 1977, Model tests on oil storage in unlined rock caverns: Proc. 1st Int. Symp. on Storage in Excavated Rock Caverns, vol. 2, Pergamon Press, N.Y., p. 517.

Aberg, B., 1978, Prevention of gas leakage from unlined reservoirs in rock: Proc. 1st Int. Symp. on Storage in Excavated Rock Caverns, vol. 2, Pergamon Press, N.Y., p. 399-413.

Adams, A.R., Ramey, H.J., Jr., and R.J. Burgess, 1968, Gas well testing in a fractured carbonate reservoir: Jour. Pet. Tech. (Oct. 1968), p. 1187-1194.

Aguiera, R. and H.K. Van Poolen, 1977, Current status on the study of naturally fractured reservoirs: The Log Analyst, May-June.

Aitken, Janet M., 1969, Relation of bedrock fracture systems to underground water supplies in the Stafford Spgs, South Coventry, Spring Hill, and Westford Quadrangles: Conn Univ., Storrs.

Aladiev, I.T., Trusov, V.P., Peredery, A.D., Strign, E.M., Saperov, E.V., and V.K. Fardzinov, 1976, Heat and mass transfer processes in aquifer systems with artificially increased fracturing: Proc. 2nd U.N. Symp. on Devel. and Use of Geothermal Energy, p. 1529-1535.

Allen, Martin J. and S.M. Morrison, 1973, Bacterial movement through fractured bedrock: Ground Water, vol. 11, n. 2, p. 6-10.

Alpay, O.A., 1973, Application of aerial photographic interpretation to the study of reservoir natural fracture systems: Jour. Pet. Tech. (Jan., 1973), p. 37-45.

Ando, Takeshi and Toshinobu Itoh, 1973, Formation fracture detection by the sonic shear wave logging: Laboratory studies: SPWLA Logging Symp., 14th, Ann., Trans., Lafayette, La., Pap. C, 10 p.

Andrews, J. N., and D.F. Wood, 1972, Mechanism of radon release in rock matrices and entry into groundwaters: Trans. Inst. Mining Metall., Sec. B., vol. 81, n. 792, p. 8198-8209.

Anonymous, 1976, Developments in theoretical and applied mechanics: Proc. of the Southeastern Conf. on Theoretical and Applied Mechanics, 8th, 1976, Va. Polytech. Inst. and State Univ., Blacksburg, Va., vol. 8, 612 p.

Anonymous, 1973, International symposium on development of ground water resources, Proc., volumes 1 through 4, 1974: Counc. of Sci. and Ind. Res., New Delhi, for Nat'l. Comm. for IHD, India, 4 vol.

Anonymous, 1977, International symposium on innovative numerical analysis in applied engineering science: Publ. by Cent Tech. des Ind Mec, Senlis, France.

Apps, J.A., Cook, N.G.W., and P.A. Witherspoon, 1978, An appraisal of underground radioactive waste disposal in argillaceous and crystalline rocks: Some geochemical, geomechanical, and hydrological questions: Lawrence Berkeley Lab report LBL-7047, 50 p

Arihara, N., Ramey, H.J., Jr., and W.E. Brigham, 1976, Nonisothermal single- and two-phase flow through consolidated sandstones: spe/A.I.M.E.

Aronofsky, J.S., Masse, L., and S.G. Natanson, 1958, A model for the mechanism of oil recovery from porous matrix due to water invasion in fractured reservoir: Trans. A.I.M.E., vol. 213, p. 17-19.

Aronova, L.A. and S.N. Chernyshev, 1967, Planning of filtration sampling of a rock massif with the account of heterogeneity: Proc. of Sci. Tech. Conf. on Eng. Investigations, May 11-15, PNIIS (in Russian)

Asher, J.M., 1978, National waste terminal storage program progress report: Office of Nuclear Waste Isolation, Union Carbide Corp., 403 p.

Azarkovich, A.E., and Shuifer, M.I., 1965, Influence of natural jointing of ledge rock on the radius of crack formation during an explosion: Fiziko-Tekhnicheskie Problemy Razrabotki Poleznykh Iskopaemykh, no. 1, Jan.-Feb., p. 33-44.

Bagir-Zade, S.N. and G.P. Guseinov, 1973, Nonstationary fluid seepage in fissured porous layer toward oil well with semispherical end face: PMTF, Ah Prikl Mekh Tekh Fiz, n. 6, p. 115-123.

Baker, W.J., 1955, Flow in fissured formations: Proc. 4th World Petr Cong, Sect II, p. 379

Ballance, W.C. and G.A. Dinwiddie, 1972, Hydraulic testing of hole UA-1-HTH-1, Amchitka Island, Alaska: U.S.G.S. report no. 474-144.

Banks, D.C., 1972, In situ measurements of permeability in basalt: Proc. Symp. Percolation Through Fissured Rock, Int. Soc. Rock Mech., TI-A:1-6.

Barelli, A., Manetti, G., Celati, R., and G. Neri, 1976, Build up and back up pressure tests on Italian geothermal wells: Proc. 2nd U.N. Symp. on Devel. and Use of Geothermal Energy, p. 1537-1546

Barenblatt, G.I., 1963, On certain boundary value problems for the equation of seepage of a liquid in fissured rocks: Prikl Matem Mekh, vol. 27, no. 2, p.

348-350 (in Russian).

Barenblatt, G.I., Zheltov, U.P., and G.H. Kochina, 1960, Basic concepts in the theory of seepage of homogeneous liquids in fissured rocks: Prikl Matem Mekh, vol. 24, pt 5, p. 852-864 (in Russian).

Barfield, E.C., Jordan, J.K., and W.D. Moore, 1959, An analysis of large scale flooding in the fractured Spraberry Trend Area Reservoir: Jour. Pet. Tech. (April, 1959), p. 15-19.

Barron, K., 1978, An air injection technique for investigating the integrity of pillars and ribs in coal mines: Int. Jour. Rock Mech. Min. Sci. and Geomech Abstr, vol. 15, no. 2, p. 69-76,

Barrow, G.M., 1973, Physical chemistry: Mc Graw-Hill book Co., 787 p.

Barr, M.V. and G. Hocking, 1976, Borehole structural logging employing a pneumatically inflatable impression packer: Proc. Symp. on Exploration for Rock Eng., Johannesburg.

Barton, N.R., 1972, The problem of joint shearing in coupled stress-flow analysis: Proc. Symp. Percolation Through Fissured Rock, Int. Soc. Rock Mech., D4: 14-16

Bathe, K.J., Bolourchi, S., Ramaswamy, S., and M. Snyder, 1977, Some recent developments in computational capabilities for nonlinear finite element analysis: Comof the Eur. Communities, Luxembourg, pap 4/1, 4 p.

Batu, Vedat, 1977, Steady infiltration from a ditch: Theory and experiment: Soil Sci. Soc. Am. J., vol. 41.

Batu, Vedat, 1978, Steady infiltration from single and periodic strip sources: Soil Sci. Soc. Am. J., vol. 42.

Batzel, M.I., Simmon, G., and Robert, S., 1980, Microcrack closure in rocks under stress: J. Geophys. Res., Paper no. 80b1244.

Bearinger, B.D., 1980, Procedures for lab study of stress-permeability characteristics of natural rock fractures: Univ. of Waterloo, Waterloo, Ont, Can.

Bear, J., 1978, Hydraulics of ground wter: Mc Graw-Hill Book Co., 569 p.

Bear, J., 1972, Dynamics of fluids in porous media: Amer. Elsevier Pub. Inc., N.Y., 764 p.

Benko, K.F., 1966, Instrumentation in rock grouting for Postage Mountain Dam: Water Power, vol. 18, no. 10, p. 407-415.

Bentsen, N. W. and J.N. Veny, 1976, Prefomed stable foam performance in drilling and evaluating shallow gas wells in Alberta: JPT J. Pet. Technol., vol. 28, p. 1237-1240.

Bergman, S.M., 1978, Groundwater leakage into tunnels and storage caverns: A documentation of factual conditions at 73 caverns and tunnels in Sweden: Proc. 1st Int. Symp. on Storage in Excavated Rock Caverns, Pergamon Press, N.Y., p. 267-273.

Bergman, M. and H. Helfrich, 1976, Geotechnical logging of boreholes and cores: Swedish Rock Mech. Res. Found., BeFo, report no. 22, Stockholm (summary in English).

Bernaix, Jean, 1974, Properties of rock and rock masses: Int. Soc. for Rock Mech., 3rd Congr., Proc., Denver, vol. 1, Part A., p. 9-38.

Bernaix, J., 1967, Etude geotechnique la roche de malpasset, Dunod, Paris, 215 p.

Bernaix, J., 1969, New laboratory methods of studying the mechanical properties of rock: Int. Jour. Rock Mech. Min. Sci., vol. 6, p43-90.

Bernard, J. and J. Evano, 1976, Specification of a model applicable to offshore geothermal sources with nuclear fracturing: Proc. 2nd U.N. Symp. on Develop. and Use of Geothermal Energy, p. 1554-58

Bianchi, L., and Snow, D.T., 1969, Permeability of crystalline rock interpreted from measured orientation and apertures of fractures: *Annals of Arid Zone*, Jodhpur, India, v. 8, no. 2, p. 231-245.

Bianchi, L., 1968, *Geology of the Manitou Springs-Cascade area, El Paso Co., Colo, with a study of the permeability of its crystalline rocks*: unpubl. MS thesis, Colo. Sch. Mines, Golden, Colo, 197 p.

Bieniawski, Z. T., 1974, Geomechanics classification of rock masses and its application in tunnelling: *Int. Soc. for Rock Mech., 3rd Congr., Proc., Pap., Denver, vol. 2, Part A., p. 27-32.*

Biot, M. A., 1973, Nonlinear effect of initial stress on crack propagation between similar and dissimilar orthotropic media: *Applied Math*, vol. 30, n. 4, p. 379-406.

Bjerrum, L., Nash, J. K. T. L., Kennard, R. M., and R.E. Gibson, 1972, Hydraulic fracturing in field permeability testing: *Norg. Geotek. Inst., Publ., n. 94, 12 p.*

Bjurstrom, S., 1978, Transport and storage of heated water in unlined rock openings: *Proc. 1st Int. Symp. on Storage in Excavated Rock Caverns*, Pergamon Press, N.Y., vol. 2, p. 433-440

Blank, Horace R. and Melvin C. Schroeder, 1973, *Geologic classification of aquifers*: *Ground Water*, vol. 11, n. 2, p. 3-5.

Boardman, C.R., and J. Shrove, 1965, Changes in the fracture permeability of a granite rock mass resulting from contained nuclear explosion: *Univ. Calif., Livermore Rad Lab Publ. UCRL 14292, 21 p*

Bodvarsson, G., 1969, On the temperature of water flowing through fractures: *J. Geophys. Res.*, vol. 74, n. 8, p. 1987-92.

Bodvarsson, Gunnar, Shi-Ming Lu, Richard, and Robert P. Lowell, 1974, Temperature transients in flowing boreholes: *Geothermics*, vol. 3, no. 1.

Bodvarsson, G., 1976, Thermoelastic phenomena in geothermal systems: Proc. 2nd U.N. Symp. on Develop. and Use of Geothermal Energy, p. 903-907.

Bogoslovsky, V. A. and A.A. Ogilvy, 1973, Electrometric observations of antifiltrational cementation curtains: Geophys. Prospect., vol. 21, n. 2, p. 296-314.

Bogoslovsky, V. A. and A.A. Ogilvy, 1972, Study of streaming potentials of fissured media models: J. Pet. Technol., vol. 24, p. 1063-1072.

Bonetskii, V. A., Bogatyrev, V. D., Bogatyreva, A. S., and V.P. Sadokhin, 1976, Assessment of the air permeability of the rock between openings during mining of contiguous seams: Sov. Min. Sci., vol. 12, n. 2, p. 201-203.

Booker, John R., 1973, Pore pressure and strain: Stanford Univ., Sch. of Earth Sci., Calif. (Geol. Sci., vol. 13).

Boos, M.F., 1954, Genesis of Precambrian granitic pegmatites in the Denver Mountain Parks area, Colorado: Geol. Soc. Amer. Bull., v. 65, p. 115-142.

Boreli, M. and B. Pavlin, 1967, Approach to the problem of the underground water leakage from storage in karst regions: Hydrology of Fractured Rocks, Proc. Dubrovnik Symp. (Oct. 1965), vol. 1, p. 32-62.

Borg, S.F., 1963, Matrix tensor methods in continuum mechanics: D Van Nostrand, N.Y., 313 p

Bortoli, M. de and P. Gaglione, 1974, Environmental radioactivity, Espra 1972: Commission of the Eur. Communities, Espra, Italy.

Boulton, N.S. and T.D. Streltsova, 1977, Unsteady flow to a pumped well in a fissured water-bearing formation: Jour. Hydrol, vol. 35, no. 3-4, p. 257-269.

Boulton, N.S. and T.D. Streltsova-Adams, 1978, Unsteady flow to a pumped well in an unconfined fissured aquifer: Jour. Hydrology, vol. 37, no. 3-4, p. 349-363.

Brace, W.F., 1976, Permeability from resistivity and pore shape: Industrial Liason Program, MIT, 25 p

Brace, W.F. and R.J. Martin, 1968, A test of the law of effective stress for crystalline rocks of low porosity: Int. Jour. of Rock Mech. Min. Sci., vol. 5, p. 615-626

Brace, W.F. and A.S. Orange, 1968, Electrical resistivity changes in saturated rocks during fracture and frictional sliding: Jour. Geophys. Res., vol. 73, no. 4, p. 1433-1445.

Brace, W.F., Orange, A.S., and T.R. Madden, 1965, The effect of pressure on the electrical resistivity of water-saturated crystalline rocks: Jour. Geophys. Res., vol. 70, no. 22, p. 5669-5678.

Brace, W.F., Pauling, B.W., Jr., and C. Scholtz, 1966, Dilatancy in the fracture of crystalline rocks: Jour. Geophys. Res., vol. 71, no. 16, p. 3934-3953

Brace, W.F., Walsh, J.B. and W.T. Fraces, 1968, Permeability of granite under high pressure: Jour. Geophys. Res., vol. 73, p. 2225-2236.

Brace, W.F., 1968, Theoretical and experimental studies of mechanical properties of rock: MIT Dept. of Geol. and Geophys, Cambridge, Mass.

Braester, C., Larsson, I., Rosen, B., and Thunvik, 1978, Depression of groundwater around rock storage: Proc. 1st Int. Symp. Storage in Excavated Rock Caverns, Pergamon Press, vol. 2, p. 691-696.

Brandt, H. W., 1974, Man-made oil field: Trans. Soc. Min. Eng. A.I.M.E., vol. 256, n. 3, p. 252-259.

Brekke, T.L., Noorishad, J., Witherspoon, P.A., and Y.N.T. Maini, 1972, Coupled stress and flow analysis of fractured dam foundations and rock slopes: Proc. Symp. Percolation Through Fissured Rock, Int. Soc. Rock Mech., T4-J:1-7

Brereton, N. R. and A.C. Skinner, 1974, Groundwater flow characteristics in the Triassic sandstone in the Fylde area of Lancashire: Water Serv.,

vol. 78, n. 942, p. 275-279.

Bresler, Eshel, 1973, Anion exclusion and coupling effects in nonsteady transport through unsaturated soils -- I. Theory: Soil Sci. Soc. Am., Proc., vol. 37, n. 5, p. 663-669.

Brigham, W.E., 1970, Planning and analysis of pulse tests: Jour. of Petrol Tech, spe/A.I.M.E.

Brooks, R.H., 1961, Unsteady flow of ground water into drain tiles: Jour. Irrig. and Drainage Division, Am. Soc. Civ. Eng., no. IR2, p. 27-37.

Bruce, G.H., Peaceman, D.W., Rachford, H.H., Rice, J.D., 1953, Calculations of unsteady-state gas flow through porous media: Trans. AIME, v. 198, p. 79-92.

Bruhn, R.W., 1972, A study of the effects of the pore pressure on the strength and deformability of Berea Sandstone in triaxial compression: 3rd Interim Report, Missouri River Division, Corps of Eng., Omaha, Neb.

Budiansky, Bernard and Richard J. O'Connell, 1976, Elastic moduli of a cracked solid: Int. J. Solids Struct., vol. 12, n. 2, p. 81-97.

Burford, A.E. and J.M. Dixon, 1978, Systematic fracturing in young clay of the Cuyahoga River Valley, Ohio and its relation to bedrock jointing and drainage segments: Geotechnique, vol. 28, no. 2, p. 201-206.

Burton, D.E., Lettis, L.A., Bryan, J.B., Butkovich, T.R., and A.L. Bruce, 1977, Anisotropic creation and closure of tension induced fractures: Calif. Univ., Livermore, presented at Amer Nuclear Soc. topical Mtg. on Energy and Mineral Recovery Research, Golden, April 1977.

Butkovich, T.R., Burton, D.E., and J.B. Bryan, 1977, Computational modeling of explosive fracture and permeability enhancement: Calif. Univ., Livermore, presented at Amer Nuclear Soc. topical Mtg. on Energy and Mineral Recovery Research, Golden, April 1977.

Butkovich, T.R., 1976, Calculation of fracture and permeability enhancement from underground explosions in coal: Calif. Univ., Livermore.

Butkovich, T.R., 1976, Calculation of fracture and permeability enhancement from underground explosions in coal: Calif. Univ., Livermore.

Byerlee, J.D., Wilson, M.G., and L. Peselnick, 1972, Elastic shock activity and fluid injection (abstract): Geol. Soc. Am., Abstracts with Programs, vol. 4, p. 135.

Caldwell, J.A., 1972, The theoretical determination of the permeability tensor for jointed rocks: Proc. Symp. Percolation Through Fissured Rock, Int. Soc. Rock Mech., T1-C:1-6

Call, R.D., 1971, Quad a computer code for Schmidt net diagrams: Univ. of Arizona.

Cardew, G. E. and I.C. Howard, 1976, Edge-crack in an elastic strip and related problems in fracture mechanics and viscous flow: Int. J. Eng. Sci., vol. 14, n. 4, p. 403-414.

Carlsson, Leif and Anders Carlstedt, 1977, Estimation of transmissivity and permeability in Swedish bedrock: Nord. Hydrol., vol. 8, no. 2, p. 103-116.

Carlsson, A. and T. Olsson, 1976, Bestamning av berggrundens permeabilitet genom vattenforlustmatning: Vannet i Norden, no. 3, vol. 9, Oslo, p. 29-35.

Carlsson, L. and Carlstedt, A., 1976, Estimation of transmissivity and permeability in Swedish bedrock: Nordic Hydrological Conf., Session III, vol. 8, no. 2, p. 103-116, Reykjarik, p. 27-39.

Carlsson, A. and T. Olsson, 1977, Water leakage in the Forsmark Tunnel, Uppland, Sweden: Geol. Surv. of Sweden, Ser C, no. 734.

Carter, Melvin W., Moghissi, A. Alan, and Bernd Kahn, 1979, Management of low-level radioactive waste (vol 2): Pergamon Press Inc, Maxwell House, Fairview Park, Elmsford, NY 10523.

Casagrande, Arthur, 1937, Seepage through dams: New Eng. Water Works Assoc., vol. 51, no. 2.

Cassagrande, A., 1961, Control of seepage through foundations and abutments of dams: Geotechnique, Inst. Civ Eng., London, vol. 11, no. 3, p. 161-181.

Castillo, E., 1972, Dispersion of a contaminant in jointed rock: PhD thesis, Northwestern Univ., Evanston, Ill.

Castillo, E., Karadi, G.M., and R.J. Krizek, 1972, Unconfined flow through jointed rock: Water Res. Bull., v.8, no.2, p. 266-281.

Castillo, E., 1972, Mathematical model for two-dimensional percolation through fissured rock: Proc. Symp. Percolation Through Fissured Rock, Int. Soc. Rock Mech., T1-D: 1-7.

Cervik, J., Sainato, A., and Maurice Deul, 1977, Water infusion of coalbeds for methane and dust control: U.S. Bur Mines Rep Invest, no. 8241, 31 p.

Cervik, J., 1969, Behavior of coal-gas reservoirs: U.S. Bur. Mines-Tech. Progress Report 10, 10 p.

Charlwood, R.G., Mahtab, M.A., Burgess, A.S., McCreath, D.R., Gnirk, P.F., and J.L. Ratigan, 1978, Geological engineering factors in the design of a radioactive waste repository in hard crystalline rock (preliminary): Can. Geosci Council, Niagara Falls, Ont, Can.

Charlwood, R.G. and P.F. Gnirk, 1978, Conceptual design studies for a high-level waste repository in igneous rock: Proc. 1st Int. Symp. on Storage in Excavated Rock Caverns, vol. 3, Pergamon Press, N.Y., p. 781-788.

Chatterji, P.C., 1966, A study of the joint pattern and groundwater movement in Jalore Granite, Rajasthan, India: Mineral, geological, and metallurgical: Inst. of India Trans., vol. 63, p. 45-53.

Chernyshev, S.N., 1966, Statistical examination of fracturing and permeability of intrusive massives: Bull Moscow Soc. of Nat Scientists, Geol. Dept., issue 5, Moscow (in Russian)

Chernyshev, S.N., 1972, Estimation of the permeability of the jointed rock in massif: Proc. Symp. Percolation Through Fissured Rock, Int. Soc. Rock Mech., T1-G:1-11

Cheung, Y.K. and S.G. Hutton, (ed.), 1976, Finite element methods in engineering: Univ. of Adelaide, South Aust.,.

Childs, E.C., 1952, The measurement of the hydraulic permeability of saturated soil in situ (part I): Proc. Royal Soc. of London, Ser A, vol. 215, p. 525-535.

Childs, E.C., Cole, A.H. and D.H. Edwards, 1953, The measurement of the hydraulic permeability of saturated soil in situ (part II): Proc. Royal Soc. of London.

Childs, E.C. and N. Collis-George, 1949, The permeability of porous materials: Proc. Royal Soc. of London.

Childs, E.C., 1957, The physics of land drainage, in drainage of agricultural lands: Luthin, J.N. (ed.), Madison, Wisc, Am. Soc. Agriculture, p1-78

Chitombo, G.P.F., 1982, Blast damage assessment using ultrasonic cross-hole measurements: M.S. Thesis, Colorado School of Mines, Golden, Colorado, 211 p.

Chitombo, G.P.F., Hustrulid, W.A., and King, R.M., 1981, An investigation of blast damage extent around an underground opening in metamorphic rocks using a transient air injection technique and a borehole petroscope: Battelle/ONWI subcontract no. EY-76-c-06-1830, Draft Topical Report, no. 140(6).

Christl, R.J., 1964, Storage of radioactive waste in basement rock beneath the Savannah River Plant: EI Du Pont de Nemours and Co, Savannah River Laboratory, DP-844, 106 p.

Cinco-Ley, H. and F. Samaniego-V., 1977, Effect of wellbore storage and damage on the transient pressure behavior of vertically fractured wells: 52nd Ann. Fall Technical Conf. Exhibition of SPE/A.I.M.E.

Cinco-Ley, Heber and Fernando Samaniego-V., 1978, Transient pressure analysis for fractured wells: 53rd Ann. Fall Technical Conf. Exhibition of spe/A.I.M.E.

Claassen, Hans C. and Edwin H. Cordes, 1975, Two-well recirculating tracer test in fractured carbonate rock, Nevada: Hydrol. Sci. Bull., vol. 20, n. 3, p. 367-382.

Claesson, A., 1975, Storage of liquified gas in mined caverns: Congress Paper Gastech 75, Paris, France.

Clark, K.K., 1968, Transient pressure testing of fractured water injection wells: Jour. Pet. Tech, p. 639.

Clayton, N., 1978, Fluid-pressure testing of concrete cylinders: Mag Concr Res., vol. 30, no. 102, p. 26-30.

Cleary, Michael P., 1977, Fundamental solutions for a fluid-saturated porous solid: Int. Jour. Solids Struct, vol. 13, no. 9, p. 785-806.

Closmann, Philip J., 1975, Aquifer model for fissured reservoirs: Soc. Pet. Eng. A.I.M.E. J., vol. 15, n. 5, p. 385-398.

Clough, Ray W., 1974, Areas of application of the finite element method: Comput. Struct., vol. 4, n. 1, p. 17-40.

Cobb, W.M., Ramey, H.J., Jr., and Frank G. Miller, 1972, Well-test analysis for wells producing commingled zones: Jour. of Pet. Tech.

Cobb, W.M. and J.T. Smith, 1975, An investigation of pressure buildup tests in bounded reservoirs: Jour. of Pet. Tech., AIME, v.259, p.991-996

Colgate, S.A., Petschek, A.G., Browning, R.V., and N.K. Bowers, 1977, Underground stress engineering: The lifting and stabilization of underground voids: Los Alamos Sci. Lab, New Mex, presented at Amer Nuclear Soc. topical Mtg. on Energy and Mineral Recovery Research, Golden, 12 April 1977.

Collins, R.E., 1961, Flow of fluids through porous materials: The Petroleum Publishing Co., 270 p.

Cooper, H.H. Jr., Bredhoeft, J.D., Papadopoulos, I.S., 1967, Response of a finite - diameter well to an instantaneous charge of water: Water Res. Resch., v. 3, no.1, p. 263-269.

Cooper, H. H., Jr., Bredehoeft, J.D., and I. S. Papadopoulos, 1967, Response of a finite-diameter well to an instantaneous charge of water: Water Res. Res., vol. 3, no. 1, p. 263-269.

Cornet, F. and C. Fairhurst, 1972, Variation of pore volume in disintegrating rock: Proc. Symp. Percolation Through Fissured Rock, Int. Soc. Rock Mech., T2-A: 1-8.

Craft, B.C., and Hawkins, M. F., 1959, Petroleum reservoir engineering: Prentice-Hall, Inc., Englewood Cliffs, N.J., 437 p.

Crawford, G. E., Hagedorn, A. R., and A. E. Pierce, 1976, Analysis of pressure buildup tests in a naturally fractured reservoir: JPT J. Pet. Technol., vol. 28, p. 1295-1300.

Crawford, P.B. and R.E. Collins, 1954, Estimating effects of vertical fractures on secondary recovery: Trans. A.I.M.E., vol. 201, p. 192.

Crawford, P.B. and B.L. Landrum, 1955, Effect of unsymmetrical vertical fractures on production capacity: Trans. A.I.M.E., vol. 204, p. 251.

Croft, H.O., 1938, Thermodynamics, fluid flow and heat transmission: McGraw Hill Book Co, Inc, N.Y., 312 p.

Crook, J. M. and F.T. Howell, 1977, Some field permeation properties of fractured Permian and Triassic sandstones in Northwest England: J. Pressure Vessel Technol. Trans. ASME, vol. 99, Ser. J., n. 1, p. 187-191.

Crosby, W.O., 1981, On the absence of joint-structure at great depths, and its relation to the forms of coarsely crystalline eruptive masses: Geol.

Mag (decade 2), 8.

Currey, D.T., 1977, Deeply weathered rock at Victorian damsites: Eng. Geol., vol. 11, no. 4, p. 341-363.

Currie, J.B. and G.A. Reik, 1977, Method of distinguishing regional directions of jointing and of identifying joint sets associated with individual geologic structures: Can. Jour. Earth Sci., vol. 14, no. 6, p. 1211-1228.

Currie, J. B. and S.O. Nwachukuwu, 1974, Evidence of incipient fracture porosity in reservoir rocks at depth: Bull. Can. Pet. Geol., vol. 22, n. 1, p. 42-58.

D'Andrea, Dennis V., Larson, Wm.C., Chamberlain, Peter G., and James J. Olson, 1976, Some considerations in the design of blasts for in situ copper leaching: Univ. of Utah, Utah Eng. Exp Stn, Salt Lake City, Pap 1, 4 p.

Dabbous, M. K., Reznik, A. A., Mody, B. G., Fulton, P. F., and J.J. Taber, 1976, Gas-water capillary pressure in coal at various overburden pressures: Soc. Pet. Eng. A.I.M.E. J., vol. 16, n. 5, p. 261-268.

Daneshy, A.A., 1978, Hydraulic fracture propagation in layered formations: Soc. Pet. Eng. A.I.M.E. J., vol. 18, no. 1, p. 33-41.

Davis, S.N., 1963, Hydrologic and geologic evaluation-Nevada Test Site: Interim Report, Hazleton Nuclear Sci. Corp, Palo Alto, Calif., unpubl, 25 p.

Davis, S.N., Peterson, F.L., and A.D. Halderman, 1969, Measurement of small surface displacement induced by fluid flow: Water Resources Res., vol. 5, no. 1, p. 129-138.

Davis, S.N. and L.J. Turk, 1963, Some hydrologic characteristics of crystalline rocks: Private Report Hazleton Nuclear Sci. Corp, HNS 38.

Davis, S.N., and L.J. Turk, 1964, Optimum depth of wells in crystalline rocks: Groundwater, vol. 2, no. 2, p. 6-11.

Davis, S.N., and G.W. Moore, 1965, Semidiurnal movement along a bedrock joint in Wool Hollow Cave, Calif: Nat speleological Soc. Bull., vol. 27, no. 4, p. 133-142.

De Ridder, N.A. and A. Erez, 1977, Optimum use of water resources: Int. Inst. Land Reclam Improv Neth Publ, no. 21, 258 p.

De Swaan, Abraham O., 1977, Analytical solutions for determining the properties of naturally fractured reservoirs by employing pressure buildup tests: Rev Inst. Mex Pet, vol. 9, no. 4, p. 41-48.

De Wiest, R.J.M., 1965, Geohydrology: John Wiley, N.Y., 366 p.

Debacker, Louis W., 1967, Measurement of entrapped gas in the study of unsaturated flow phenomena: Water Res. Res., vol. 3, no. 1, p. 245-249.

Deere, D.V., 1964, Technical description of rock cores for engineering purposes: Rock Mech. Eng. Geol., v. 1, p. 17-22.

Deere, D. U., Merritt, A. H., and R.F. Coon, 1969, Engineering classification of in situ rock: U.S. Air Force Systems Command-Air Force Weapons Lab-Tech. Report AFWL-TR-67-144, 296 p.

Deere, Don U., Coon, Richard R., and Andrew H. Merritt, 1969, Engineering classification of in situ rock: Ill Univ., Urbana, Ill, Dept. of Civil Eng.

Deju, R.A., 1978, Feasibility of storing radioactive waste in Columbia River Basalt: Proc. 1st Int. Symp. on Storage in Excavated Rock Caverns, Pergamon Press, N.Y., vol. 3, p. 747-754.

Deniel, E.J., 1954, Fractured reservoirs of the Middle East: Bull A.A.P.G., vol. 38, p. 774.

Desai, C. S. (ed.), 1972, Applications of the finite element method in geotechnical engineering, Proc. of the symposium: U. S. Army Eng. Water Exp. Stn., Soil Mech. Inf. Anal. Cent., Vicksburg, Miss., 1227 p.

Detzlhofer, H., 1969, Influence of rock fissures water on tunnel construction: Rock Mech., Felsmech., Mec. Roches, vol. 1, n. 4, p. 207-40.

DiBiagio, E., and F. Myrvoll, 1972, In-situ tests for predicting the air and water permeability of rock masses adjacent to underground openings: Proc. Symp. Percolation through Fissured Rock, Int. Soc. Rock Mech., T1-B: p. 1-15.

Diadkin, Y.D., Witherspoon, P.A., Tsiviritsyna, V.V., and T. Lasseter, 1973, Temperature regime of underground boilers in fractured masses with non-uniform permeability: Problems of Mining Thermophysics, presented at 200th Ann. Mtg. of Leningrad Mining Inst., Leningrad, U.S.S.R., Oct. 30-Nov 2, 1973, p. 104-107 (in Russian).

Diamond, W. P., McCulloch, C. M., and B.M. Bench, 1976, Use of surface joint and photolinear data for predicting subsurface coal cleat orientation: U.S. Bur. Mines Rep. Invest., n. 8120, 16 p.

Dieterich, J.H., Raleigh, C.B., and J.D. Bredehoeft, 1972, Earthquake triggering by fluid injection at Rangely, Colo.: Proc. Symp. Percolation Through Fissured Rock, Int. Soc. Rock Mech., T2-B: 1-12.

Dobrynin, V.M., 1962, Effect of overburden pressure on some properties of sandstone: Soc. Pet. Eng. J., vol. 2, p. 360-366.

Doe, T., and Remer, J., 1981, Analysis of constant-head well tests in nonporous fractured rock: In Testing in Low Permeability environments, 3rd LBL invitational well testing symposium, p. 84-89.

Dontsov, K.M., 1967, Inertial resistance in a fractured reservoir: Neft'i Gaz, vol. 10, no. 3, p. 55-59.

Dubinchuk, V. T., Polyakov, V. A., Kuptsov, V. M., Seletskii, Yu. B., Karasev, B. V., Nechaev, V. I., Babushkin, V. D., and G.N. Kashkovskii, 1974, Conditions for groundwater recharge using natural stable and radioactive isotopes together with analog simulation: Int. Atomic Energy Agency, Vienna, Aust., Isot Tech. in Groundwater Hydrol, Symp. Proc., paper and discuss., vol. 1, Pap IAEA-SM-182/52, p. 399-429.

Duckworth, H.E., Duckworth, H.W., Porter, Arthur, and J.S. Rogers, 1977, Environmental aspects of nuclear power development in Canada -- Adequacy of the information available: Can. Environ Advisory Council, Occasional Paper no. 2, Ottawa, Ont, Can.

Duguid, James O. and P.C.Y. Lee, 1977, Flow in fractured porous media: Water Res. Res., vol. 13, no. 3, p. 558-566.

Duguid, J.O., 1973, Flow in fractured porous media: PhD thesis, Princeton Univ., 111p.

Duncan, J.M., Witherspoon, P.A., Mitchell, J.K., Watkins, D.J., Hardcastle, J.H., and J.C. Chen, 1972, explosive cratering: Report no. TE-72-2, Univ. Calif., Berkeley.

Dunmore, R., 1969, Gas flow through underground strata: Min. Engr., n. 100, p. 193-199.

Dunn, D.E., LaFountain, L.T., and R.E. Jackson, 1973, Porosity dependence and mechanism of brittle fracture in sandstone: Jour. Geophys. Res., vol. 78, p. 2403-2417.

Dyes, A.B., Kemp, C.E., and B.H. Caudle, 1958, Effect of fracture on sweep-out pattern: Trans. A.I.M.E., vol. 213, p. 245-249.

Dzeban, I.P., 1970, Elastic wave propagation in fractured and vuggy media: I.Z.V. Earth Phys. trans. by D.G. Fry, no. 10, p. 31-38.

Earlougher, R.C., Jr., 1977, Advances in well test analysis: Soc. Petr. Eng. of AIME, N.Y., p.

Earlougher, Robert C., Jr., 1979, Analysis and design methods for vertical well testing: spe no. 8038.

Earl, K.D. and W.A. Jury, 1977, Water movement in bare and cropped soil under isolated trickle emitters: II. Analysis of cropped soil experiments: Soil Sci. Soc. Am. J., vol. 41.

Eggers, Dwight E., 1976, Application of borehole geophysics to the selection and monitoring of nuclear waste disposal sites: Univ. of Utah, Utah Eng. Exp Stn, Salt Lake City, Pap 3, 7 p.

El Rabaa, A.W.M.A., Hustrulid, W.A., Ubbes, W.F., 1982, Spatial distribution of deformation moduli around the CSM/ NWI room, Edgar Mine, Idaho Springs, Colorado: 23rd U.S. Symp. on Rock Mech. "Issues in Rock Mech.", Preprint, 12 p.

El Rabaa, A.W.M.A., 1981, Measurements and modeling of rock mass response to underground excavation: M.S. Thesis, Colorado School of Mines, Golden, Colo., 217 p.

El Shazly, E. M., Abdel-Hady, M. A., El Ghawaby, M. A., and I.A. El Kassas, 1974, Geologic interpretation of ERTS-1 satellite images for west Aswan area, Egypt: Environ. Res. Inst. of Mich., Willow Run Lab, Ann. Arbor, vol. 1, p. 119-131.

Elkins, L.F., 1969, Internal anatomy of a tight fractured Hunton Lime Reservoir revealed by performance, west Edmond Field: Jour. Pet. Tech, p. 221-232.

Elkins, L.F., and A.M. Skov, 1960a, Anisotropic spread of pressure transients delineates Spraberry fracture orientation: Trans. A.I.M.E., vol. 219, p. 407.

Elkins, L.F., and A.M. Skov, 1960b, Determination of fracture orientation from pressure interference: Trans. A.I.M.E., vol. 219, p. 301.

Ellis, E.E., 1906, Occurrence of water in crystalline rocks: Underground Water Paper 160, U.S.G.S., p. 19-29.

Ellis, E.E., 1909, Groundwater in crystalline rocks of Connecticut: U.S.G.S., Water Supply Paper 232, p. 54-103.

Engelder, T. and C. Scholz, 1978, Fluid transport properties of rock fractures at high pressure and temperature. Progress report. July 1, 1977-June 30, 1978: Dept. of Energy (1877000).

Eriksson, A., 1975, Groundvatteninläckning i bergtunnlar: Seminarium om hydrogeologisk undersökningsmetodik, 21 May 1975, BFR, Göteborg, p. 1-32.

Esbeckplaten, H.H.V., 1972, Permeability and grouting measures in the construction of the Tinajones Reservoir in Northern Peru: Proc. Symp. Percolation Through Fissured Rock, Int. Soc. Rock Mech., T4-B: 1-10 (in German).

Esmiol, E.E., 1957, Seepage through foundations containing discontinuities: Jour. Soil Mech. and Found. Eng., vol. 83, p1-17.

Everell, M. D., Herget, G., Sage, R., and D.F. Coates, 1974, Mechanical properties of rocks and rock masses: Int. Soc. for Rock Mech., 3rd Congr., Proc., Pap., vol. 1, Part A, p. 101-108.

Ewert, F.K., 1972, Investigations into the permeability of Tertiary Rock at the Tavera Dam (Dominican Republic): Proc. Symp. Percolation Through Fissured Rock, Int. Soc. Rock Mech., T4-C: 1-20 (in German).

Fairhurst, C. and N.G.W. Cook, 1966, The phenomenon of rock splitting parallel to the direction of maximum compression in the neighbourhood of a surface: Proc. 1st Int. Congr. of Rock Mech., Lisbon.

Fairhurst, C. and J.C. Roegiers, 1972, Estimation of rock mass permeability by hydraulic fracturing -- A suggestion: Proc. Symp. Percolation Through Fissured Rock, Int. Soc. Rock Mech., D2: 1-5.

Fatt, I. and D.H. Davis, 1952, Reduction in permeability with confining pressure: Am. Inst. Mech. Eng. Trans., vol. 195, p. 329.

Faust, C.R., and J.W. Mercer, 1976, Mathematical modeling of geothermal systems: Proc. 2nd U.N. Symp. on Develop. and Use of Geothermal Energy, p. 1635-1641.

Fetkovich, M.J., 1973, The isochronal testing of oil wells: Am. Inst. of Mining, Met, and Petrol Engineers, Inc, paper no. spe 4529.

Fisekci, M. Y. and K. Barron, 1975, Methane pressure and flow measurements in coal in surrounding strata: CIM Bull., vol. 68, n. 762, p. 91-98.

Fisher, Henry N., 1977, Interpretation of the pressure and flow data for the two fractures of the Los Alamos hot dry rock geothermal system: Colo. Sch. Mines Press, Golden, Colo, vol. 1, p. 1B4.

Fisher, Sir Ronald, F.R.S., 1952, Dispersion on a sphere: Proc. Royal Soc. of London, Ser A, vol. 217, p. 295-305.

Fraser, C.D. and B.E. Pettit, 1962, Results of a field test to determine the type and orientation of a hydraulically induced formation fracture: Jour. Pet. Tech. (May, 1962).

Fredrickson, S. E. and G.C. Broaddus, 1976, Selective placement of fluids in a fracture by controlling density and viscosity: J. Pet. Technol., vol. 28, p. 597-602.

Freedman, H.A. and S.G. Natanson, 1959, Recovery problems in a fractured-pore system, Kirkuk Field: Proc. 5th World Pet. Cong, vol. 2, p. 297.

Freeze, R.A., and Cherry, J.A., 1979, Ground water: Prentice-Hall Inc., N.J., 604 p.

Freeze, R. Allan and P.A. Witherspoon, 1966, Theoretical analysis of regional groundwater flow: 1. Analytical and numerical solutions to the mathematical model: Water Res. Res., vol. 2, no. 4, p. 641-656.

Frost, N.E. and J.K. Sharples, 1978, Prediction of the fatigue behaviour of cylinders subjected to a repeated internal fluid pressure: Eng. Fract Mech., vol. 10, no. 2, p. 371-379.

Gale, J. E. and P.A. Witherspoon, 1977, Effect of fracture deformation on fluid pressure distribution -- An indicator of slope instability: Can. Geotech. J., vol. 14, no. 3, p. 302-309.

Gale, J. E., Raven, K., Dugal, J., and P. Brown, 1976, Subsurface containment of solid radioactive wastes: Geol. Surv. of Canada, Ottawa, Ontario, Pap. 76-1B: Rep. of Act., Pt. B p. 147-150.

Gale, J.E., 1980, Assessing the permeability characteristics of fractured rock: in Recent Trends In Hydrology, Spec. Publ., Geol. Soc. Am., 55 p.

Gale, J.E., and Forster, C., 1979, A laboratory assessment of the use of borehole pressure transients to measure the permeability of fractured rock masses: Univ. of Waterloo Research Institute, Contract no. WRI 708-04, 99 p.

Gale, J.E., Rouleau, A., Fritz, P., and Witherspoon, P.A., 1981, The fracture hydrology program at Stripa, Sweden: 1981 Seminar on Flow and Transport in Fractured Rocks, April 24, Univ. Waterloo, Ontario, Canada.

Gale, J.E., 1977-1978, Subsurface containment of solid radioactive waste -- Proposed program: Eng. and Environ Geol. Sect, Terrain Sci. Div., Geol. Surv. of Can, Dept. of Energy, Mines, and Resources.

Gale, J.E., Brown, P.A., Raven, K.G., Dugal, J.J.B., and J. Lau, 1976, Subsurface containment of solid radioactive waste -- Progress report: Eng. and Environ Geol. Sect, Terrain Sci. Div., Geol. Surv. of Can, Dept. of Energy, Mines, and Resources.

Gale, J.E. and K.G. Raven, 1979, An assessment and evaluation of compliance effects of borehole transient test equipment (final report): Off of Res. Admin, Univ. of Waterloo, Waterloo, Ont., Can.

Gale, J.E., Schmitke, B.W., and R. Nadon, 1979a, Assessment of stress-permeability characteristics of natural fractures from the Chalk River area: Dept. of Earth Sci., Off. of Res. Admin., Univ. of Waterloo, Waterloo, Ont., Can.

Gale, J.E., Schmitke, B.W., and R. Nadon, 1979b, Stress-permeability characteristics of induced tension fractures in Chalk River cores: Univ. of Waterloo Res. Inst., Univ. of Waterloo, Waterloo, Ont., Can.

Gale, J.E., 1975, A numerical field laboratory study of flow in rocks with deformable fractures: PhD Thesis, Univ. Calif., Berkely, 255 p.

Gale, J.E., Taylor, R.L., Witherspoon, P.A., and Ayatollahi, 1973, Investigations of fluid injection in fractured rock and effect on stress distribution: Ann. Report, U.S.G.S. Contract no. 14-08-001-12727, ARPA contract no. 1648, Univ. Calif., Berkeley.

Gale, J.E., Taylor, R.L., Witherspoon, P.A., and Mi.S. Ayatollahi, 1974, Flow in rocks with deformable fractures: J.T. Oden, D.C. Zienkiewicz, R.H. Gallagher, and C. Taylor (ed.), Finite Element Methods in Flow Problems, UAH Press, Univ. of Alabama, Huntsville, Ala., p. 583-598.

Gale, J.E., 1977, Numerical, field and laboratory study of flow in rocks with deformable fractures: Canadian Inland Waters Branch Sci. Ser, no. 72, 145 p.

Gale, J.E., 1982, The effects of fracture type (induced versus natural) on the stress-fracture closure-fracture permeability relationships: Proc., 23rd Symposium on Rock Mechanics, Berkeley, California., p.290:298.

Gates, C.F. and G.G. Brown, 1951, Production engineering aspects of Shannon Reservoir-Cole Creek Field -- Wyoming: Petrol Branch, A.I.M.E., paper no. 449-G.

Ghaboussi, J., Wilson, E.L., and J. Isenberg, 1973, Finite element for rock joints and interfaces: Jour. Soil Mech. and Found. Div., A.S.C.E., vol. 99, no. SM10, p. 833-848.

Glenn, H.D., 1975, Technique to enhance crack growth and increase permeability in geological media: Calif. Univ., Livermore, Lawrence Livermore Lab.

Gloyna, E.F. and T.D. Reynolds, 1961, Permeability measurements of rock salt: Jour. Geophys. Res., vol. 66.

Gomez-Rivero, Orlando, 1978, Formation resistivity factor -- A qualitative permeability tool: Pet. Eng., vol. 50, no. 1, p. 91-98

Goodman, R.E., 1976, Methods of geological engineering in discontinuous rocks, West Publ. Co., N.Y., 472 p.

Goodman, Richard E. and Yuzo Ohnishi, 1973, Undrained shear testing of jointed rock: Rock Mech., Felsmech., Mec. Roches, vol. 5, n. 3, p. 129-149.

Goodman, R.E., 1970, The deformability of joints: Determination of the in-situ modulus of deformation of rock: ASTM, STP477, p. 174-196.

Goodman, R.E., 1974, The mechanical properties of joints: Proc. 3rd Congr. of Int. Soc. Rock Mech., vol. 1, p. 127-140.

Goodman, R.E. and J. Dubois, 1972, Duplication of dilatancy of jointed rocks: Jour. Soil Mech. and Found. Div., A.S.C.E., vol. 98, no. SM4.

Gowd, T.N. and F. Rummel, 1977, Effect of fluid injection on the fracture behavior of porous rock: Int. Jour. Rock Mech. Min. Sci. Geomech Abstr, vol. 14, no. 4, p. 203-208.

Grant, M.A., 1977, Permeability reduction factors at Wairakei: A.S.M.E. Pap no. 77-HT-52 for Mtg., 4 p.

Gray, D.M., Fatt, I., and G. Bergamini, 1963, The effect of stress on permeability of sandstone cores: Soc. Pet. Eng. Jour., vol. 3, p. 95-100.

Gretener, P. E., 1969, Fluid pressure in porous media. Its importance in geology: Bull. Can. Petrol. Geol., vol. 17, n. 3, p. 255-95.

Grindley, G.W. and P.R.L. Browne, 1976, Structural and hydrological factors controlling the permeabilities of some hot-water geothermal fields: Proc. 2nd U.N. Symp. on Develop. and Use of Geothermal Energy, p. 377-386.

Gringarten, A.C. and H.J. Ramey, Jr., 1974, Unsteady-state pressure distributions created by a well with a single horizontal fracture, partial penetration, or restricted entry: Soc. Pet. Eng. Jour. (Aug, 1974), p. 413-426.

Gringarten, A.C., Ramey, H.J., Jr., and R. Raghavan, 1972, Pressure analysis for fractured wells: Soc. Pet. Eng. 47th Ann. Fall Mtg., San Antonio, Tex.

Gringarten, A.C., Ramey, H.J., and R. Raghavan, 1974, Unsteady-state pressure distributions created by a well with a single infinite-conductivity vertical fracture: Soc. Pet. Eng. Jour. (Aug, 1974), p. 347-360.

Gringarten, A.C. and P.A. Witherspoon, 1972, A method of analyzing pump test data from fractured aquifers: Proc. Symp. Percolation Through Fissured Rock, Int. Soc. Rock Mech., T3-B: 1-9.

Grose, T.L.T., 1972, Tectonics: in Geologic Atlas of the Rocky Mountain Region, Rocky Mountain Assoc. Geol., p.35-44.

Haberland, C. and F. Koehler, 1977, Semi-analytical calculation of temperature transients in jointed structures: Waerme Stoffuebertrag Thermo Fluid Dyn, vol. 10, no. 3, p. 153-158.

Hagerman, T.H., 1970, Groundwater problems in underground construction: Proc. Int. Sym in Oslo (1969), Large Permanent Underground Openings, Universitatforlaget, Oslo.

Haimson, B. C., 1974, Determination of stresses in deep holes and around tunnels by hydraulic fracturing: Soc. of Min. Eng. of A.I.M.E., N.Y., N.Y., Rapid Excavation and Tunnelling Conf., Proc., San Francisco, Calif., vol. 2, p. 1539-1560.

Haimson, B., 1968, Hydraulic fracturing in porous and nonporous rock and its potential for determining in-situ stresses at great depth: PhD dissertation, Univ. of Minnesota.

Haimson, B. and C. Fairhurst, 1970, In-situ stress determination at great depth by means of hydraulic fracturing: Rock Mech., Theory and Practice, Somerton (ed.), 11th Symp. on Rock Mech., p. 559-584.

Halligan, B. D., 1971, Stress relaxation. A problem in reciprocating shaft seal design: Automot Des. Eng., vol. 10, p. 20-1.

Handin, J.T. and R.V. Hager, Jr., 1963, Experimental deformation of sedimentary rocks under confining pressure: Pore pressure tests: Bull A.A.P.G., vol. 47, p. 717.

Handin, J. and C.B. Raleigh, 1972, Man-made earthquakes and earthquake control: Proc. Symp. Percolation Through Fissured Rock, Int. Symp. Rock Mech., T2-D: 1-10.

Hantush, Mahdi S. and Robert G. Thomas, 1965, Method for analyzing a drawdown test in anisotropic aquifers: Water Res. Res., vol. 2, no. 2.

Hardy, Michael P. and Charles Fairhurst, 1974, Analysis of fracture in rock and rock masses: NM Sect., ASME, Eng. for the Matter/Energy Challenge, p. 73-80.

Harper, T.R., 1972, Some observations of the influence of geological environment upon groundwater: Proc. Symp. Percolation Through Fissured Rock, Int. Soc. Rock Mech., T4-D: 1-10.

Harper, T.R. and Hinds, 1978, The impression packer: A tool for recovery of rock mass fracture geometry: Proc. 1st Int. Symp. on Storage in Excavated Rock Caverns, Pergamon Press, N.Y., p. 259-266.

Harrison, J.E. and Moench, R.H., 1961, Joints in Precambrian rocks of the Central City-Idaho Springs area, Colorado., : U.S. Geol. Survey Prof. Pap. 374-B, 14 p.

Harrison, J.E., and Wells, J.D., 1959, Geology and Ore deposits of the Chicago Creek area, Clear Creek County, Colorado: U.S. Geol. Survey Prof. Pap. 319.

Harsford, J.T., and D.A.T. Donohue, 1967, The relation of multi-well vertical fractures to five-spot sweep efficiency at breakthrough: Prod. Monthly (Jan., 1967), vol. 31, p. 2.

Haswell, C. K., 1975, Problems of tunnelling in chalk: Tunnels Tunnelling, vol. 7, n. 6, p. 40-43.

Haynes, Charles D., 1974, Pressure-fracture gradient problems in deep well waste disposal: Ala Univ.

Healy, J.H., Ruby, W.W., Griggs, D.T., and C.B. Raleigh, 1968, The Denver earthquakes: Science, vol. 161, p. 1301-1310.

Healy, J. and M.P. Hochstein, 1973, Horizontal flow in hydrothermal systems: Jour. Hydrology (NZ), vol. 12, p71-81.

Heard, H.C. and A. Duba, 1978, Capabilities for measuring physiocochemical properties at high pressure: Calif. Univ., Livermore.

Heidecker, E. J., and T. Supajanya, 1975, Simple optical method for routine analyses of fracture traces: Trans. Inst. Min. Metall. Sect. B, vol. 84, n. 822, p. 856-858.

Heindl, L.A., 1967, Groundwater in fractured volcanic rocks in southern Arizona: Proc. Dubrovnik Symp. on Hydrology of Fractured Rocks, vol. 2, p. 503-516.

Hele-Shaw, H.S., 1898, Investigation of the nature of surface resistance of water and of streamline motion under certain experimental conditions: Trans. Inst. Nav Architects, vol. 40, p. 21-46.

Henriet, J. P., 1976, Direct applications of the Dar Zarrouk parameters in groundwater surveys: Geophys. Prospect, vol. 24, n. 2, p. 344-353.

Herper, H. and H.C. Barksdale, 1951, Preliminary report on the geology and groundwater supply of the Newark, New Jersey area: New Jersey Dept. of Cons and Econ Dev, spec Report no. 10.

Heuze, Francois E. and Richard E. Goodman, 1971, A design procedure for high cuts in jointed hard rock -- Three dimensional solutions (Vol I): Calif. Univ., Berkeley.

Hilber, Hans M. and Robert L. Taylor, 1976, A finite element model of fluid flow in systems of deformable fractured rock: Calif. Univ. Berkeley.

Hinds, D.V., 1974, A method of taking an impression of a borehole wall: Rock Mech. Res. Report, no. 28, Imperial College, London.

Ho, Teh Chung and Morton M. Denn, 1977, Stability of plane Poiseuille flow of a highly elastic liquid: Jour. Non Newtonian Fluid Mech., vol. 3, no. 2, p. 179-195.

Holcomb, David L., 1975, Low surface tension hydrochloric-hydrofluoric acid mixtures in low porosity, low permeability sandstones: A.I.M.E., N.Y., N.Y., Pap spe 5411, p. 149-158.

Holmberg, R., 1981, Hardrock excavation at the CSM/ONWI test site using Swedish blast design techniques: Battelle/ONWI subcontract no. E512-04800, Draft Topical Report no. 140(3), 140 p.

Horner, D.R., 1951, Pressure buildup in wells: Proc. of 3rd World Petrol Congress -- Sect II, p. 503-521.

Houlsby, Adam Clive, 1977, Engineering of grout curtains to standards: ASCE Jour. Geotech. Eng. Div., vol. 103, no. 9, p. 953-970.

Howard, G.C. and C.R. Fox, 1970, Hydraulic fracturing: Monograph, vol. 2, A.I.M.E. Series.

Howard, J. Hatten III and V.J. Hurst, 1972, Studies of sapolite and its relation to the migration and occurrence of groundwater in crystalline rocks: Georgia Univ., Athens, Ga, Dept. of Geo.

Howells, D.A., 1972, Manmade earthquakes; the reservoir designer's problem: Proc. Symp. Percolation Through Fissured Rock, Int. Soc. Rock Mech., T2-E: 1-5.

Hsieh, P.A., Tracy, J.V., Neuzil, C.E., Bredhoeft, J.D., and Silliman, S.E., 1981, A transient laboratory method for determining the hydraulic properties of tight rocks- I. Theory: Int. Jour. Rock Mech. Min. Sci. and Geomech. Abst., v. 18, p. 245-252.

Hsu, Kenneth J., 1977, Studies of Ventura Field, Calif., II: Lithology, compaction, permeability of sands: A.A.P.G., vol. 61/2.

Hsu, Y.C., 1975, Forced oscillations of the Los Alamos Sci. Lab's dry hot rock geothermal reservoir: Los Alamos Sci. Lab, New Mex.

Hubbert, M. King, 1953, Entrapment of petroleum under hydrodynamic conditions: Bull of Am. Assoc. of Petrol Geol., vol. 37, no. 8, p. 1954-2026.

Hubbert, M.K. and D.G. Willis, 1957, Mechanics of hydraulic fracturing: Trans. A.I.M.E., vol. 210, p. 153-166.

Huitt, J.L., 1956, Fluid flow in simulated fractures, Am. Inst. Chem Eng. Jour, vol. 2, p. 259.

Hunsbedt, Anstein, Kruger, Paul, and A.L. London, 1977, Laboratory studies of non-isothermal fluid production from fractured geothermal reservoirs: A.S.M.E. Pap no. 77-HT-53 for Mtg., 8 p.

Hunsbedt, Anstein, Kruger, Paul, and A.L. London, 1978, Energy extraction from a laboratory model fractured geothermal reservoir: spe/A.I.M.E.

Huntoon, Peter W., 1974, Karstic groundwater basins of the Kaibab Plateau, Arizona: Water Res. Res., vol. 10, n. 3, p. 579-590.

Hurr, R.T. and Richards, D.B., 1974, Hydrologic investigations: U.S. Geol. Surv. Prof. Pap. 815, p 79-92.

Hurr, R.T. and D.B. Richards, 1966, Groundwater engineering of the Straight Creek Tunnel (Pilot bore), Colo: Eng. Geol., vol. 3, no. 2, p. 80-90.

Huskey, W.L. and P.B. Crawford, 1967, Performance of petroleum reservoir containing vertical fractures in the matrix: Soc. Pet. Eng. Jour., p. 221.

Hustrulid, W.M., Cudnick, R., Trent, R., Holmberg, R., Sperry, } P.E., Hutchinson, R., and p. Rosasco
1980, mining technology development for hard rock
Excavation: Rockstore '80, Stockholm, Sweden.

Hutchinson, R.M., 1981, Geological and structural setting of the CSM/ONWI Test Site, CSM Experimental Mine, Idaho Springs, Colorado: Batelle/ONWI subcontract no. E512-4800, Draft Topical Report no. 140(2), 56 p.

Hvorslev, M.J., 1951, Time lag and soil permeability in ground water observations: U.S. Army Eng. Waterways Experiment Station, Bull. no. 36, p.

Iffly, R., Rousselet, D., and J.L. Vermeulen, 1974, Basic investigation of the imbibition in a fractured reservoir: Rev. Inst. Fr. Pet. Ann. Combust. Liq., vol. 29, n. 2, p. 217-241.

Illingsworth, C.R., 1950, Some Solutions of the equations of flow of a viscous compressible fluid: Proc. Cambridge Phil. Soc., v. 46, p. 469-478.

Ilyin, N.I., Chernyshev, S.N., Dzektser, E.S., and V.S. Zilberg, 1967, Estimation of accuracy of determining the permeability of rocks: Publ. Nauka, Moscow (in Russian).

International Society for Rock Mechanics, 1978, Suggested methods for the quantitative description of discontinuities in rock masses: Int. J. Rock Mech. Sci. and Geomech. Abstr., vol. 15, p.319-368.

International Society for Rock Mechanics, 1972, Percolation through fissured rocks: Proc. Symp., Stuttgart.

Iwai, K., 1976, Fundamental studies of fluid flow through a single fracture: Ph.D. thesis, Univ. of Calif., Berkley, 208 p.

James, R., 1976, Drawdown test results differentiate between crack flow and porous bed permeability: Proc. 2nd U.N. Symp. on Develop. and Use of Geothermal Energy, p. 1693-1696.

Jansson, G., 1968, Petroleum products in unlined rock chambers (Petroleumprodukt i oinklada berggrum): Teknisk Tidskrift, H 21 (in Swedish).

Jenkins, R. and Aronofsky, J.S., 1953, Unsteady flow of gas through porous media--one dimensional case: Proc. 1st U.S. National Cong. Appl. Mech., J. Edwards, Inc.

Jensen, M., Smith, M., and R.J. Rogers, 1973, Fracture trends identified by ERTS-1 imagery in Utah and Nevada: Utah Univ., Salt Lake City, Dept. of Geol. and Geophys Sci.

Johansson, S. and R. Lahtinen, 1976, Oil storage in rock caverns in Finland: Tunnelling, Paper 13.

Johnson, C.R., Greenkorn, R.A., and Woods, E.G., 1966, Pulse testing: anew method for describing reservoir flow properties between wells: Jour. Pet. Teck., v. 237, p. 1599-1604.

Johnson, H.H., 1975, Environment and fracture -- Technical progress report: Cornell Univ., Ithaca, N.Y., Materials Sci. Center.

Johnston, J. E., Miller, R. L., and K.J. Englund, 1975, Applications of remote sensing to structural interpretations in the southern Appalachians: J. Res. U.S. Geol. Surv., vol. 3, n. 3, p. 285-293.

Johnston, Kenneth H., 1968, Performance of a low-permeability sandstone oil reservoir, West Avant Field, Osage Co, Okla: Bur of Mines, Wash DC.

Jones, Elmer E., Jr. and Charles M. Murray, 1977, Improving the sanitary protection of ground water in severely folded, fractured, and creviced limestone: Ground Water, vol. 15, n. 1, spec. issue vol. 2, p. 66-74.

Jones, F.O., 1975, A laboratory study of the effects of confining pressure on fracture flow and storage capacity in carbonate rocks: Jour. Pet. Tech. (Jan., 1975), p. 21-27.

Jones, Frank O., Jr., 1975, Laboratory study of the effects of confining pressure on fracture flow and storage capacity in carbonate rocks: JPT J. Pet. Technol., vol. 27, p. 21-27.

Jouanna, P., 1972, In situ permeability tests under applied stresses: Proc. Symp. Percolation Through Fissured Rock, Int. Soc. Rock Mech., T2-G: 1-6 (in French).

Jury, W.A. and K.D. Earl, 1977, Water movement in bare and cropped soil under isolated trickle emitters: I. Analysis of bare soil experiments: Soil Sci. Soc. Am. J., vol. 41.

Karadi, Gabor M., Krizek, Raymond J., and Enrique Castillo, 1972, Hydrodynamic dispersion in a single rock joint: J. Appl. Phys., vol. 43, n. 12, p. 5013-5021.

Karunaratne, G. P., 1975, Examination and identification of some permeable natural soil fabrics: Inst. of Eng., Malays, Kuala Lumpur, p. 1.

Kasameyer, P.W. and R.C. Schroeder, 1976, Thermal depletion of a geothermal reservoir with both fracture and pore permeability: Calif Univ., Livermore.

Kazemi, Hossein, Merrill, L. S., Porterfield, K. L., and P.R. Zeman, 1976, Numerical simulation of water-oil flow in naturally fractured reservoirs: spe/A.I.M.E., N.Y., N.Y., Symp. on Numer. Simul. of Reservoir Perform., 4th, Proc., Los Angeles, Calif., Pap. spe 5719, p. 7-30.

Kazemi, Hossein, and John F. McElhiney, 1974, Fluid flow and mass transport in fractured rocks: A.I.M.E., N.Y., Solution Min. Symp., Proc., 103rd Meet., p. 98.

Kazemi, H., Merrill, L. S., Jr., Porterfield, K. L., and P.R. Zeman, 1976, Numerical simulation of water-oil flow in naturally fractured reservoirs: Soc. Pet. Eng. A.I.M.E. J., vol. 16, n. 6, p. 317-326.

Kazemi, H., 1969, Pressure transient analysis of naturally fractured reservoirs with uniform fracture distribution: S.P.E.J. (Dec, 1969), p. 451-462.

Kazemi, H., Thomas, G.W., and M.S. Seth, 1969, The interpretation of interference tests in naturally fractured reservoirs with uniform fracture distribution: S.P.E.J. (Dec, 1969), p. 463-472.

Keck, L.J., 1977, Shallow formation hydrofracture mapping experiment: A.S.M.E. Pap no. 77-Pet-51 for Mtg. Sept 18-22, 1977, 4 p.

Kehle, R.O., 1964, Determination of tectonic stress through analysis of hydraulic well fracturing: Jour. Geophys. Res., vol. 69, p. 259-274.

Kendall, H.A., 1977, Fundamentals of pressure control -- Anatomy of a kick: Pet. Eng., vol. 49, no. 2, p. 64,66,70,72.

Kennedy, T.B., 1958, Pressure-grouting fine fissures: Jour. Soil Mech. and Found. Div. A.S.C.E., vol. 84, no. SM3, Proc. Paper 1731, p. 1-30.

Khalevin, N.I., 1960, Measurement of rock porosity by sonic well logging: Razvedochnaya i Promyslovaya Geofizika, vol. 30, p. 39.

Kiraly, L., 1971, Groundwater flow in heterogeneous, anisotropic fractured media: A simple two-dimensional electric analog: J. Hydrol., vol. 12, n. 3, p. 255-261.

Kiraly, L., 1969, Statistical analysis of fractures, orientation and density: Geol. Rundsch, vol. 59, no. 1, p. 125-151.

Klinkenberg, H.J., 1941, The permeability of porous media to liquids and gases: Drilling and Production Practice, v. , p. 200-213.

Klopp, K., 1972, Significance of geological conditions at the percolation of fissured bedrock of dams: Proc. Symp. Percolation Through Fissured Rock, Int. Soc. Rock Mech., T4-E: 1-7.

Knutson, C. F., 1976, Modeling of noncontinuous Fort Union and Mesaverde sandstone reservoirs, Piceance Basin, Northwestern Colorado: Soc. Pet. Eng. A.I.M.E. J., vol. 16, n. 4, p. 175-188.

Knutson, C.F. and B.F. Bohor, 1963, Reservoir rock behaviour under moderate confining pressure: 5th Symp. on Rock Mech., Univ. Minnesota, 1962, N.Y., Macmillan Co, p. 627-659.

Koerperich, E.A., 1975, Evaluation of the circumferential microsonic log -- A fracture detection device: Trans. SPWLA (June 1975).

Koerperich, E.A., 1978, Investigation of acoustic boundary waves and interference patterns as techniques for detecting fractures: Jour. Pet. Tech. (Aug, 1978), p. 1199-1207.

Koide, H. and S. Bhattacharji, 1975, Formation of fractures around magmatic intrusions and their role in ore localization: Econ. Geol., vol. 70, n. 4, p. 781-799.

Komar, C. A., Overbey, W. K., Jr., and J. Pasini III, 1973, Directional properties of coal and their utilization in underground gasification experiments: U.S. Bur. Mines Tech. Prog. Rep., n. 73, 11 p.

Kouzov, D. P., 1969, Diffraction of a cylindrical hydroacoustic wave at the joint of two semi-infinite plates: Prikladnaya Matematika i Mekhanika, vol. 33, n. 2, p. 240-50.

Kreft, A., Lenda, A., Turek, B., Zuber, A., and K. Czauderna, 1974, Determination of effective porosities by the two-well pulse method: IAEA, Vienna, Austria, Isot. Tech. in Groundwater Hydrol., Symp. Proc., Pap. and Discuss., vol. 2, Pap. IAEA-SM-182/46, p. 295-312.

Krinari, A.I., 1958, Relationship between specific resistivity and reservoir properties of water-bearing terrestrial rocks: Geol. Nefti, no. 7, p. 668-673.

Krizek, R.J., Karadi, G.M. and E. Socias, 1972, Dispersion of a contaminant in fissured rock: Proc. Symp. Percolation Through Fissured Rock, Int. Soc. Rock Mech., T3-C: 1-15.

Kuo, Ming-Ching T., Kruger, Paul, and W.E. Brigham, 1975, Heat and mass transfer in porous rock fragments: Stanford Univ., Calif.

Lachenbruch, A.H., 1961, Depth and spacing of tension cracks: Jour. Geophys. Res., vol. 66.

Lakner, John F., 1968, A new apparatus for permeability measurements under lithostatic conditions and results on drop fractured and high explosive fractured oil shale: Calif. Univ., Livermore, Lawrence Rad Lab.

Lamb, H., 1932, Hydrodynamics: 6th Ed, Cambridge Univ. Press, N.Y., 738 p.

Landers, R. A. and L.J. Turk, 1973, Occurrence and quality of ground water in crystalline rocks of the Llano Area, Texas: Ground Water, vol. 11, n. 1, p. 5-10.

Lane, K.S., 1969, Engineering problems due to fluid pressure in rock: Proc. 11th Symp. Rock Mech., A.I.M.E., p. 501-540.

Larson, J.D. and J.E. Weir, Jr., 1969, Inventory of springs in the Morey Peak area of central Nevada: U.S.G.S., Denver, Colo.

Larsson, Ingemar, Flexer, Akiva, and Bengt Rosen, 1977, Effects on groundwater caused by excavation of rock store caverns: Eng. Geol., vol. 11, no. 4, p. 279-294.

Laubscher, D.H. and H.W. Taylor, 1977, Importance of geomechanics classification of jointed rock masses in mining operations: A. A. Balkema, Cape Town, S. Afr., for S. Afr. Inst. of Civ. Eng., Geotech. Div., Marshalltown, Transvaal, vol. 1, p. 119-128.

Lawson, D. W., 1968, Groundwater flow systems in crystalline rocks of Okanagan Highland, British Columbia: Can. J. Earth Sciences, vol. 5, n. 4, pt. 1, p. 813-24.

Lebedinets, N. P. and A.Z. Istomin, 1975, Oil flow to a well from a fissiporous stratum in the presence of top gas: Izv Vyssh Uchebn Zaved, Neft. i. Gaz, n. 4, p. 46-50.

Lee, Michael C. H. and Michael C. Williams, 1976, Radial flow of viscoelastic liquids -- 1. Theoretical: J. Non Newtonian Fluid Mech., vol. 1, n. 4, p. 323-341.

Leeman, E.R., 1958, Some underground observations relating to the extent of the fracture-zone around excavations in some Central Rand Mines: Assoc. Mine Managers, Transvaal and Orange Free State Chamber of Mines, Johannesburg, S. Africa, p. 357-384.

Lefebvre du Prey, E., 1976, Cascade drainage of blocks in a fissured reservoir: Rev. Inst. Fr. Pet., vol. 31, n. 1, p. 173-178.

Lenda, A. and A. Zuber, 1970, Isotope hydrology -- Proc. of a symposium: Int. Atomic Energy Agency, Vienna.

Lergrand, H.E., 1949, Sheet structure, a major factor in the occurrence of groundwater in granites of Georgia: Econ Geol., vol. 44, no. 2, p. 110-118.

Lewis, D.J., 1977, Development of computer methods to study fractures in hot rocks: Commission of Eur. Communities, Dir-Gen Sci. and Tech. Inf. and Inf. Manage, Luxembourg, vol. 2, p. 693-705.

Lewis, D.C., and R.H. Burgy, 1964, Hydraulic characteristics of fractured and jointed rock: Groundwater, vol. 2, no. 3, p. 4-9.

Lindhom, U.E., Janelid, I., and T. Forselles, 1978, Tightness test of an underground cavern for LPG: Proc. 1st Int. Symp. on Storage in Excavated Rock Caverns, Pergamon Press, N.Y., vol. 2, p. 415-422.

Lister, C.R.B., 1976, Qualitative theory on the deep end of geothermal systems: Proc. 2nd U.N. Symp. on Develop. and Use of Geothermal Energy, p. 459-463.

Lister, D.R.B., 1974, On the penetration of water into hot rock: Royal Astron Soc. Geophys Jour, vol. 39, p. 465-506.

Lomenick, T.F., 1978, General geology and general hydrology: National Waste Management Program Report: Office of Waste Isolation, Union Carbide Corp, p. 111-112.

Lomize, G.M., 1951, Fluid flow in fractured rocks: Goseneroizdat, Moscow (in Russian).

Londe, P., 1971, The flow of water in rock: Univ. of Alberta, Edmonton, Alberta, Canada.

Londe, P. and F. Sabarlay, 1966, Permeability distribution in arch dam foundations as a function of the stress field: Proc. 1st Congr. Int. Soc. Rock Mech., Lisbon.

Long, J. and C. Wilson (ed.), 1978, Recommended well drilling and testing program: Lawrence Berkeley Lab, Univ. of Calif., Berkeley.

Long, J.C.S., Remer, J.S., Wilson, C.R., Witherspoon, P.A., 1982, Porous media equivalent for networks of discontinuous fractures: Water Resources Res., v. 18, no. 3, p. 645-658.

Long, R.R., 1961, Mechanics of solids and fluids: Prentice-Hall, Englewood Cliffs, NJ, 156 p.

Louis, C., 1969, Study of groundwater flow in jointed rock and its influence on the stability of rock masses: Imp. Coll. Sci. Technol., Rock Mech. Res. Rep. 10, 90 p.

Louis, C., 1968, Study of groundwater flow in jointed rocks and its influence on stability of rock masses: Electricite de France-Bull. de la Direction des Etudes et Recherches Ser A, n. 3, p. 5-131.

Louis, C., 1967, Stromungsvorgange in Kluftigem Medien und ihre Wirkung auf die Standsicherheit von Bauwerken und Boscungen im Fels: Report, Research Inst. for Hydraulic Structures and Agricultural Eng., Univ. of Karlsruhe, Karlsruhe, Germany.

Louis, C., 1968, Etude des ecoulements d'eau dans les roches fissurees et leurs influences sur la stabilite des massifs rocheux: PhD thesis Univ. Karlsruhe, Karlsruhe, Germany, Electr Fr Bull Dir Et Rech. (A), no. 3, 132 p.

Louis, C., 1969, A study of groundwater flow in jointed rock and its influence on the stability of rock masses: Rock Mech. Res. Report, vol.10, Imperial College of Science and Technology, London, 90 p.

Louis, C., 1970, Ecoulement a trois dimensions dans les roches fissurees: Res. Ind. Miner., Fr., no spec, p. 73-93.

Louis, C., 1970, Hydraulic triple probe to determine the directional hydraulic conductivity of porous or jointed rock: report D12, Imperial College, London.

Louis, C., 1972, Hydraulique de roches: PhD thesis, Univ. of Paris.

Louis, C., 1974, Rock hydraulics: Bur Rech Geol. Min, Orleans, France, 107 p.

Louis, C. and Y.N.T. Maini, 1970, Determination of in-situ hydraulic parameters in jointed rock: Proc. 2nd Congr. Int. Soc. Rock Mech., Belgrade, T1, no. 1-32, p. 235-245.

Louis, C. and Perrot, 1972, Three-dimensional investigation of flow conditions at Grand Maison Damsite: Proc. Symp. Percolation Through Fissured Rock, Int. Soc. Rock Mech., T4-F: 1-16.

Louis, C. and B. Ricome, 1972, Comportment hydromecanique de materieux fissures: Report B.R.G.M.

Louis, C. and Wittke, 1971, Etude experimentale des ecoulements d'eau dans un massif rocheux fissure: Geotechnique, Instn. C.E., vol. 21, no. 1.

Lovelock, P.E.R., Price, M., and T.K. Tate, 1975, Groundwater conditions in the Penrith Sandstone at Cliburn, Westmoreland: J. Inst. Water Eng. Sci., vol. 29, n. 4, p. 157-174.

Lovering, T.S., and Goddard, E.N., 1950, Geology and ore deposits of the Front Range, Colo., USGS Prof. Paper 223, 319 p.

Lowell, R.P., 1975, Circulation in fractures, hot springs and convective transport on mid-ocean ridge crests: Royal Astron Soc. Geophys Jour, vol. 40, n3, p. 351-366.

Loy, LeRoy D., Jr., 1974, Description of new, innovative and theoretical mine drainage abatement techniques: Symp. on Coal Mine Drain Res., 5th, Coal and the Environ. Tech. Conf., Louisville, KY, p. 146-159.

Lucas, Peter T. and James M. Drexler, 1976, Altamont-Bluebell -- A major, naturally fractured stratigraphic trap, Uinta Basin, Utah: Am. Assoc. of Pet. Geol., Tulsa, Okla., North Am. Oil and Gas Fields, p. 121-135.

Lundstrom, L., Stille, H., and Karnbranslesakerhet, 1980, Large scale permeability test of the granite in the Stripa mine and thermal conductivity test: Lawrence Berkeley Laboratory, Report LBL-7052.

Mahtab, M.A., Bolstad, D.D. and Pulse, R.R., 1974, Determination of attitudes of joints surveyed with a borescope in inclined boreholes: U.S. Bureau of Mines Information Circular no. 8615, 12 p.

Mahtab, M.A., 1970, Three-dimensional finite element analysis of jointed rock slopes: PhD dissertation, Univ. Calif., Berkeley.

Mahtab, M.A., Bolstad, D.D., Alldredge, J.R., and R.J. Shanely, 1973, Analysis of fracture orientations for input to structural models of discontinuous rock: U.S. Bur Mines Rep Invest, 7669.

Maini, Y.N.T., 1971, Interpretation and design of in situ hydraulic testing in jointed rock: PhD thesis, Imperial College, London.

Maini, Y.N.T., 1971, In-situ hydraulic parameters in jointed rock: Their measurement and interpretation: PhD thesis, Imperial College, Univ., London, 312 p.

Maini, Y.N.T., Noorishad, J., and J.C. Sharp, 1972, Theoretical and field considerations on the determination of in-situ hydraulic parameters in fractured rock: Proc. Symp. Percolation Through Fissured Rock, Int. Soc. Rock Mech., T1-E: 1-8.

Malofeev, G.E. and F.A. Kennabi, 1978, Coefficient of heat transfer from a heat carrier to fissured layer blocks: Izv Vyssh Uchebn Zaved Neft Gaz, no. 1, p. 29-35.

Mangushev, K.I. and E.A. Zolotovitskaya, 1969, Prospects of using nuclear explosions in developing oil and gas deposits: Trans. of Geologiya Nefti i Gaza (USSR), vol. 13, no. 4, p. 20-24.

Marine, I.W., 1967, The permeability of fractured crystalline rock at the Savannah River Plant near Aiken, S Carolina: U.S.G.S. Prof. Paper 575-B, p. B203-211.

Marine, I.W., 1966, Correlation and water-transmitting properties of fractures: A.I.M.E., Soc. Pet. Eng., Preprint paper no. S.P.E. 1280, 7 p.

Marine, I.W., 1964, Hydrology of crystalline rocks beneath the Atlantic Coastal Plain at the Savannah River Plant, S Carolina (abstract): Geol. Soc. Am. Program, Ann. Mtg., Miami Beach, Fla, p. 128.

Marine, I.W., 1975, Water-level fluctuations due to earth tides in a well pumping from slightly fractured crystalline rock: Water Res. Res., vol. 11, no. 1, p. 165-173.

Marsell, R.E., 1964, Groundwater in bedrock in Utah: Utah Water and Power Board, 9th Bienn Report.

Martin, John C., 1959, Simplified equations of flow in gas drive reservoirs and the theoretical foundation of multiphase pressure buildup analyses: spe, Petrol

Trans.

Masch, Frank D. and Kleber J. Denny, 1965, Grain size distribution and its effect on permeability of unconsolidated sands: Water Res. Res., vol. 2, no. 4.

Massarsch, Karl Rainer, 1978, New aspects of soil fracturing in clay: ASCE Jour. Geotech. Eng. Div., vol. 104, no. 8, p. 1109-1123.

Matthess, Georg, 1972, Permeability and yields of wells in the Bunter of Hesse in comparison with other rocks: Dtsch Ges fuer Erd- und Grundbau, Essen, Ger, Symp. on Percolation through Fissured Rock, Proc., Stuttgart, Ger., Pap. T-3E, 12 p.

Matthess, G., 1972, Permeability and yield of wells in the Bunter of Hesse in comparison with other rocks: Proc. Symp. Percolation Through Fissured Rock, Int. Soc. Rock Mech., T3-E: 1-12 (in German).

Matthews, C.S. and D.G. Russell, 1967, Pressure buildup and flow tests in wells: Soc. Pet. Eng. Monograph Series, vol. 1, spe, Dallas, Texas.

McCreath, Dougal R., 1976, Energy related underground storage: A.I.M.E., N.Y., N.Y., p. 240-256.

McKee, C.R., Hanson, M.E., and R.W. Terhune, 1977, Permeability from single and multiple detonations in boreholes: In Situ Oil Coal Shale Miner, vol. 1, no. 1, p. 37-73.

McKee, C. R. and M.E. Hanson, 1975, Explosively created permeability from single charges: Soc. Pet. Eng. A.I.M.E. J., vol. 15, n. 6, p. 495-501.

McKee, C.R. and M.E. Hanson, 1976, Predicting explosion-generated permeability around geothermal wells: Calif. Univ., Livermore, Lawrence Livermore Lab.

McKinley, R.M., Vela, Saul, and L.A. Carlton, 1968, A field application of pulse-testing for detailed reservoir description: Jour. of Petrol Tech, spe Trans., vol. 243.

McLatchie, A.S., Hemstock, R.A., and J.W. Young, 1958, The effect of compressibility of reservoir rock and its effect on permeability: Am. Inst. Mech. Eng. Trans., vol. 213, p. 386-388.

McMahon, Barry K., 1974, Design of rock slopes against sliding on pre-existing fractures: Int. Soc. for Rock Mech., 3rd Congr., Proc., Pap., Denver, Colo., vol. 2, Part B., p. 803-808.

McMullen, E.T. and A.D. Pasternak, 1970, Field measurements of fracture permeability in granodiorite: Calif. Univ., Livermore, Lawrence Livermore Lab.

Mc Whorter, D.B. and Duke, H.R., 1976, Transient drainage with nonlinearity and capillarity: Jour. Irrigation and Drainage Division, Am. Soc. Civil Eng., v. , p. 193-204.

Means, Jeffrey, Crerar, David A., Borcsik, Maria P., and James O. Duguid, 1978, Adsorption of Co and selected actinides by Mn and Fe oxides in soils and sediments: Geochimica et Cosmochimica Acta, vol. 42, p. 1763-1773, Pergamon Press Ltd, Great Britain.

Menard, L. and Y. Broise, 1975, Theoretical and practical aspects of dynamic consolidation: Geotechnique, vol. 25, n. 1, p. 3-18.

Merkel, R. H., MacCary, L. M., and R.S. Chico, 1976, Computer techniques applied to formation evaluation: Log Anal., vol. 17, n. 3, p. 3-10.

Michel, G., 1972, Knowledge of the groundwater conductivity of Mesozoic Rock of East Westphalia from experience in well sinkings: Proc. Symp. Percolation Through Fissured Rock, Int. Soc. Rock Mech., T3-F: 1-7 (in German).

Miletich, Anton Fedorovich, 1969, Air leakage and air leakage calculations in mine ventilation: Joint Publ. Res. Serv, Wash DC., Trans. of monograph Utechki Vozdukha i ikh Raschet pri Provetrivanii Shakht, Moscow, 1968, 146 p.

Moench, R.H., Harrison, J.E., and Sims, P.K., 1962, Precambrian folding in the Idaho Springs area, Front Range, Colorado: Geol. Soc. Amer. Bull., v. 73, p.

35-58.

Moench, S.P., Sheridan, D.M., 1976, Geology and resources of titanium in The United States: U.S. Geol. Surv., Prof. Pap. 959-G, 17 p.

Montazer, p., Chitombo, G., King, R.M., and Ubbes, W., 1982, Spatial distribution of permeability around CSM/ONWI room, Edgar Mine, Idaho Springs, Colorado: 23rd U.S. Symp. on Rock Mech., "Issues in Rock Mech.", preprint, 10 p.

Montazer, P. and Hustrulid, W.A., 1981, An investigation of fracture permeability around an underground opening in metamorphic rocks: Battelle/ONWI subcontract no. EY-76-C-06-1830, 140(5), 200 p.

Montazer, P., Sour, L.E., King, R.M., and Hustrulid, W.A., 1981, Results of Core logging and fracture mapping in CSM/ONWI room: Battelle/ONWI subcontract no. E512-04800, Draft Topical Report no. 140(6), 200 p.

Montazer, P., 1978, Engineering geology of Upper Bear Creek area, Clear Creeek County, Colorado: M.S. Thesis, Colorado School of Mines, Golden, Colo., 229 p.

Mordecai, M., and L.H. Morris, 1970, Investigation into the changes of permeability occurring in a sandstone when failed under triaxial stress conditions: Soc. Mining Eng., A.I.M.E., Proc. 12th Symp. on Rock Mechanics, p. 221-39.

Mordecai, M., and L.H. Morris, 1971, An investigation into the changes of permeability occurring in a sandstone when failed under triaxial stress conditions: Dynamic Rock Mechanics, 12th Symp. Rock Mech., Rolla, Missouri, Proc., p. 221-239.

Morel-Seytoux, H.J., 1969, Introduction to flow of immiscible liquids: in Flow Through Porous Media, R.J.M. Dewiest ed., Academic Press, N.Y., p. 456-516.

Morfeltdt, C.O., 1972, Drainage problems in connection with tunnel construction in Precambrian granitic bedrock (in Sweden): Proc. Symp. Percolation Through Fractured Rock, Int. Soc. Rock Mech., T4-G:

1-9.

Morfeltdt, C.O., 1972, Storage of oil in unlined caverns in different types of rock: 14th Symp. on Rock Mech., Penna State Univ., U.S. Natl Comm for Rock Mech.

Morgenstern, N.R., 1971, The influence of groundwater on stability: Stability in Open Pit Mining, C.O. Brawner and V. Milligan (ed.), A.I.M.E., p. 65-81.

Morgenstern, N.R. and H. Guther, 1972, Seepage into an excavation in a medium possessing stress dependent permeability: Proc. Symp. Percolation Through Fissured Rock, Int. Soc. Rock Mech., T2-C: 1-15.

Morland, L.W., 1977, Oscillatory flows in a porous thermoelastic matrix due to earth tides: Geothermics, vol. 6, p. 107-116, printed in Great Britain.

Morlier, P., 1971, Description of rock-fissuration state by means of simple, NDT testing: Rock Mech., Felsmech., Mec. Roches, vol. 3, n. 3., p. 125-38.

Morris, R.L., Grine, D.R., and T.E. Arkfeld, 1964, Using compressional and shear acoustic amplitudes for the location of fractures: Jour. Petrol Tech. (June, 1964), p. 623-632.

Morrison, S.M. and Martin J. Allen, 1972, Bacterial movement through fractured bedrock: CSU, Ft Collins, Colo., Environ Res. Center.

Morton, Douglas M., 1977, Surface deformation in part of the San Jacinto Valley, Southern California: J. Res. U.S. Geol. Sur., vol. 5, n. 1, p. 117-124

Muffler, L.J.P., 1976, Geology, hydrology, and geothermal systems: Summary of Sect II, Proc. 2nd U.N. Symp. on Devel. and Use of Geothermal Resources, p. xlv-lii.

Mundi, E. Kengnjisu and James R. Wallace, 1973, Field permeability measurements in fractured rocks: Law Eng. Testing Co., Denver, Colo.

Murphy, H.D., 1978, Thermal stress cracking and the enhancement of heat extraction from fractured geothermal reservoirs: Los Alamos Sci. Lab, New Mex.

Murphy, H.D., 1977, Fluid injection profiles: Modern analysis of wellbore temperature survey: Los Alamos Sci. Lab, New Mex, presented at Ann. Mtg. of Soc. Pet. Eng., Oct. 1977, Denver, Colo.

Myung, J.I. and R.W. Baltosse, 1971, Fracture evaluation by the borehole logging method: 13th Symp. U.S. Natl Comm for Rock Mech., Univ. of Illinois, Urbana, Ill (Aug-Sept 1971).

Myung, John I., and Donald P. Helander, 1974, Borehole investigation of rock quality and deformation using the three-dimensional velocity log: North Ohio Geol. Soc., Cleveland, Ohio, Symp. on Salt, 4th Proc., Houston, Tex., vol. 2, p. 141-152.

Narasimhan, T.N. and P.A. Witherspoon, 1977, Numerical model for saturated-unsaturated flow in deformable porous media: 1. Theory: Water Res. Res., vol. 13, no. 3, paper no. 7W0004.

Narasimhan, T.N., Witherspoon, P.A., and A.L. Edwards, 1978, Numerical model for saturated-unsaturated flow in deformable porous media: 2. The algorithm: Water Res. Res., vol. 14, no. 2, paper no. 7W0962.

Nathenson, M., 1976, Production technology, reservoir engineering, and field management: Summary of Sec VII, Proc. 2nd U.N. Symp. on Develop and Use of Geothermal Resources, p. xvii-ci.

Neale, Graham and Walter Nader, 1974, Formulation of boundary conditions at the surface of a porous medium: Soc. Pet. Eng. A.I.M.E. J., vol. 14, n. 5, p. 434-436.

Nelson, Ronald A., 1976, Experimental study of fracture permeability in porous rock: Univ. of Utah, Utah Eng. Exp Stn, Salt Lake City, Pap 6, 8 p.

Nelson, Ronald A. and John Handin, 1977, Experimental study of fracture permeability in porous rock: A.A.P.G. Bull., vol. 61, no. 2, p. 227-236.

Nelson, R.A., 1975, Fracture permeability in porous reservoirs, and experimental and field approach: PhD thesis, Texas AM Univ., 171 p.

Nelson, R.A. and Handin, 1977, Experimental study of fracture permeability in porous rock: A.A.P.G., vol. 61, no. 2, p. 227-236.

Nemat-Nasser, S. and H. Ohtsubo, 1978, Fluid flow and heat transfer through hydraulically induced fractures in hot, dry rock masses: Jour. Pressure Vessel Tech. Trans. ASME, vol. 100, no. 3, p. 277-284.

Neuman, Shlomo P., 1976, Wetting front pressure head in the infiltration model of Green and Ampt: Water Res. Res., vol. 12, no. 3.

Neuman, Shlomo P., Feddes, Reinder A., and Eshel Bresler, 1975, Finite element analysis of two-dimensional flow in soils considering water uptake by roots: I. Theory: Soil Sci. Soc. Am. Proc., vol. 39.

Neuman, Shlomo P. and P.A. Witherspoon, 1971, Analysis of nonsteady flow with a free surface using the finite element method: Water Res. Res., vol. 7, no. 3, p. 611-623.

Nonvieller, E., 1970, Grouted cut-off curtains in fissured rocks: 2nd Congr. Int. Soc. Rock Mech., Belgrade, Yugoslavia.

Noorishad, J., Witherspoon, P.A., and Y.N.T. Maini, 1972, Investigation of fluid injection and effect on stress distribution: Ann. Report, U.S.G.S. Contract no. 14-08-001-12727, ARPA contract no. 1648, Univ. Calif., Berkeley.

Noorishad, J., Witherspoon, P.A., and Y.N.T. Maini, 1972, The influence of fluid injection on the state of stress in the earth's crust: Proc. Symp. Percolation Through Fissured Rock, Int. Soc. Rock Mech., T2-H: 1-11.

Noorishad, J., Witherspoon, P.A., and T.L. Brekke, 1971, A method for coupled stress and flow analysis of fractured rock masses: Univ Calif., Berkeley, Geotech. Eng. Publ. 71-76, 128 p.

Norton, D., 1976, Transport phenomena in hydrothermal systems: The Nature of Porosity, Am. Jour. Sci.

O'Connell, Richard J. and Bernard Budiansky, 1977, Viscoelastic properties of fluid-saturated cracked solids: Jour. of Geophys Res., vol. 82, no. 36.

O'Neill, A.L. and M.S. Lyon, 1964, Test grouting for Oroville Dam: Eng. Geol., vol. 1, no. 1, p. 1-13.

Odeh, A.S. and F. Selig, 1963, Pressure buildup analysis, variable-rate case: spe.

Odeh, A.S., 1965, Unsteady-state behaviour of naturally fractured reservoirs: Soc. Pet. Eng. Jour. (March 1965), p. 60-66.

Office of Waste Isolation, 1977, Movement of fluid in largely impermeable rocks: Seminar held at Univ. Texas at Austin, Jan 27-29, Y/OWI/SUB-77/14223, 56 p.

Ohnishi, Y., 1973, Lab measurement of induced water pressures in jointed rocks: PhD thesis, Univ. Calif., Berkeley, 277 p.

Ohnishi, Y., and R.E. Goodman, 1974, Results of lab tests on water pressure and flow in joints: Proc. 3rd Congr. Int. Soc. Rock Mech., Denver, IIA, p. 660-666.

Olmstead, F.H., Glancy, P.A., Harril, J.R., Rush, F.E., and A.S. Van Denburgh, 1975, Preliminary hydrogeologic appraisal of selected hydrothermal systems in northern and central Nevada: U.S.G.S. Open-file Report, 75-56, 267 p.

Osgood, John O., 1974, Hydrocarbon dispersion in ground water significance and characteristics: Ground Water, vol. 12, n. 6, p. 427-438.

Overbery, W.K., Jr., and R.L. Rough, 1968, Surface studies predict orientation of induced formation fractures: Prod. Monthly, vol. 32, p. 16.

Overbey, W. K., Jr., Komar, C. A. and J. Pasini III, 1973, Predicting probable roof fall areas in advance of mining by geological analysis: U. S. Bur. Mines, Tech. Progr. Rep., n. 70, 19 p.

Pahl, P.J., 1981, Estimating the mean length of discontinuity traces: Int. Jour. Rock Mech. Min. Sci. Geomech. Abstr., v. 18, p. 221-228.

Pai, S.I., 1956, Viscous flow theory; I- Laminar flow: D. Vannastrand Co., Inc., Princeton, N.J., 384 p.

Papadopoulos, Istavros S. and Hilton H. Cooper, Jr., 1967, Drawdown in a well of large diameter: Water Res. Res., vol. 3, no. 1, p. 241-244.

Papadopoulos, Istavros S., Bredehoeft, John D., and Hilton H. Cooper, Jr., 1973, On the analysis of 'slug test' data: Water Res. Res., vol. 9, no. 4, p. 1087-1089.

Papadopoulos, I.S., 1967, Nonsteady flow to a well in an infinite anisotropic aquifer: Hydrology of Fractured Rocks, Proc. Dubrovnik Symp. (Oct. 1965), v.1, p.21-31

Parizek, R. R. and S.H. Siddiqui, 1970, Determining the sustained yields of wells in carbonate and fractured aquifers: Ground Water, vol. 8, n. 5, p. 12-20.

Parizek, R. and S.H. Siddiqui, 1970, Determining the sustained yield of wells in carbonate and fractured aquifers: Groundwater, vol. 8, no. 5.

Parker, Frank L. and James L. Grant, 1978, Migration of radioactive material in soil: Dept. of Environ and Water Resources Eng., Vanderbilt Univ., and Nuclear Eng. Co, Inc.

Parrish, D.R., 1963, Fluid flow in rough fractures: Soc. Pet. Eng. Production Research Symp, Univ. Okla.

Parsons, R.W., 1966, Permeability of idealized fractured rocks: Soc. Pet. Eng. Jour., vol. 6, no. 1, p126-136,

Parsons, M. L., 1972, Determination of Hydraulic properties of fissured rocks: Proc. 24th Geol. Cong., Montreal, Section II, Hydrogeology, p. 89-99.

Patching, T.H., 1965, Variations in permeability of coal: Proc. Toronto Rock Mech. Symp, Dept. of Mines and Technical Surv., Ottawa, Canada, p. 185-199.

Pavlenko, V. V., 1974, Method of elimination of seepage through expansion joints of a concrete dam: Gidrotekh Stroit, n. 5, p. 32-34.

Pertsovsky, V.V., 1967, Application of a theory of measurements to estimation of accuracy of the permeability parameters: Izvestia of the High School, Geol. and Reconnaissance (in Russian).

Petrovic, Z., 1976, Types of hydrogeological structures and possible hydrogeochemical provinces of thermomineral waters of Serbia: Proc. 2nd U.N. Symp. on Develop. and Use of Geothermal Energy, p. 531-537.

Philip, J.R. and R.I. Forrester, 1975, Steady infiltration from buried, surface, and perched point and line sources in heterogeneous soils: II. Flow details and discussion: Soil Sci. Soc. Am. Proc., vol. 39.

Phipps, S.C. and John N. Khalil, 1975, A method for determining the exponent value in a Forchheimer-type flow equation: JPT Forum, A.I.M.E.

Pickens, John F. and Gerald E. Grisak, 1979, Finite element analysis of liquid flow, heat transport, and solute transport in a groundwater flow system: Governing equations and model formulation: Contaminant Hydrogeo Sect, Hydrol Res. Div., Inland Waters Direct, Environment Can. for Atomic Energy of Can. Res. Co, Storage and Disposal Branch, Pinawa, Manitoba.

Picket, G.R., 1968, Properties of the Rocky Mountain Arsenal disposal reservoir and their relation to Derby earthquake: Quarterly, Colo. Sch. Mines, vol. 63, no. 1, p. 73-100.

Pickett, G. R., 1969, Evaluation of fractured reservoirs: Soc. Pet. Eng. J., vol. 9, n. 1, p. 28-38.

Pincus, H.J., 1951, Statistical methods applied to the study of rock fractures: Geol. Soc. Am. Bull., vol. 62, p. 81-130.

Pincus, H.J., 1953, The analysis of aggregate of orientation data in the earth sciences: Jour. Geol., vol. 61, no. 6, p. 482-509.

Podwysocki, Melvin H., 1977, Some computer-based methods for the analysis of geologic fracture information: A.I.M.E., Soc. of Min. Eng., p. 880-892.

Pogrebiskiy, M.I. and S.N. Chernyshev, 1977, Determination of the permeability of the frozen fissured rock massif in the vicinity of the Kilyma Hydroelectric Power Station: Cold Regions Res. and Eng. Lab, Hanover, New Hamp, draft Trans. of Kolyma (USSR), vol. 39, no. 1, p. 28-31 (Jan. 1975).

Pollard, P., 1959, Evaluation of acid treatment from pressure build-up analysis: Trans. A.I.M.E., vol. 216, p. 38-43.

Polubarinova-Kockina, P.YA., 1962, Theory of ground water movement: J.M.R. De Wiest translation, Princeton Univ. Press, Princeton, N.J., 613 p.

Popilack, Romman, 1979, Field and laboratory programs: D'Appolonia Consulting Engineers, Denver, Colo. , internal report.

Poth, C. W., 1968, Hydrology of the metamorphic and igneous rocks of central Chester Co., Penna: Penna. Topo Geol. Surv-Bull., vol. 25, 84 p.

Potter, J.M., 1978, Experimental permeability studies at elevated temperatures and pressures of granitic rocks: Los Alamos Sci. Lab, New Mex.

Pratt, H.R., Swolfs, H.S., Brace, W.F., Black, A.D., and J. W. Handin, 1977, Elastic and transport properties of an in situ jointed granite: Int. Jour. Rock Mech. Min. Sci. Geomech. Abstr, vol. 14, n.

1, p. 35-45.

Pratt, H.R., Swolfs, H.S., and A.D. Black, 1974, Properties of in-situ jointed rock: Final Technical report no. TR 54-57, Terra Tek, Salt Lake City, Utah, submitted to Environmental Sciences Div., U.S. Army Res. Office, Durham, North Carolina, contract no. DAH CO4 72C0049.

Price, V., 1976, Raw data from orientation studies in crystalline rock areas of the southeastern US: Du Pont de Nemours and Co, Aiken, S Carol.

Priest, S.D. and Hudson, J.A., 1976, Discontinuity spacing in rock: Int. Jour. Rock Mech. Min. Sci. Geomech. Abst., v. 13, p. 135-148.

Priest, S.D. and Hudson, J.A., 1981, Estimation of discontinuity spacing and trace length using scanline surveys: Int. Jour. Rock Mech. Min. Sci. Geomech. Abst., v. 18, p. 183-197.

Proctor, J.F. and I.W. Marine, 1965, Geologic, hydrologic, and safety considerations in the storage of radioactive wastes in a vault excavated in crystalline rock: Nuclear Sci. and Eng., vol. 22, p. 350-365.

Quong, R., 1969, Permeability increases in Hardhat Granodiorite samples fractured by exploding foils: Calif. Univ., Livermore, Lawrence Rad Lab.

Raghavan, R., 1977, Pressure transient analysis of a vertically fractured well produced by solution gas drive: Soc. Pet. Eng. A.I.M.E. J., vol. 17, no. 5, p. 369-376.

Raghavan, Raj and Nico Hadinoto, 1978, Analysis of pressure data for fractured wells: The constant-pressure outer boundary: Soc. Pet. Eng. A.I.M.E. J., vol. 18, no. 2, p. 139-150.

Raghavan, Raj, Uraiet, A., and G.W. Thomas, 1978, Vertical fracture height: Effect on transient flow behavior: spe/A.I.M.E.

Raghavan, R., 1977, Pulse test analysis of vertically fractured wells: thesis, Tulsa Univ., Okla.

Raleigh, C.B., 1972, Mechanical behaviour of fissured rock due to percolation: Man-made earthquake: Proc. Symp. Percolation Through Fissured Rock, Int. Soc. Rock Mech., G2:1-9.

Raleigh, C.B., Healy, J.H., and J.D. Bredehoeft, 1972, Faulting and crustal stress at Rangely, Colo.: Flow and Fracture of Rocks, A.G.U. Geophys. Monogr., vol. 16, p. 275-284.

Ramey, H.J., Jr., 1964, Rapid methods for estimating reservoir compressibilities: spe/A.I.M.E.

Ramey, H.J., Jr., 1976, Practical use of modern well test analysis: A.I.M.E., paper no. spe-5878.

Ramey, H.J., Jr. and W.M. Cobb, 1971, A general pressure buildup theory for a well in a closed drainage area: Jour. of Pet. Tech. Trans., vol. 251.

Ramey, H.J., 1970, Short-time well test data interpretation in the presence of skin effect and wellbore storage: Jour. Pet. Tech. (Jan. 1970), p. 97-104.

Rats, M.V., 1967, Heterogeneity of rocks and their physical properties: Pub Nauka (in Russian).

Rats, M.V., 1967, Statistical aspect of the problem on the jointy rocks: Hydrology of Fractured Rocks, Proc. Dubrovnik Symp, Oct. 1965, vol. 1, UNESCO 1967.

Rausch, R.W. and K.W. Beaver, 1964, Case history of successfully water flooding a fractured sandstone: Jour. Pet. Tech. (Nov 1964), p. 1233-1237.

Raven, K.G., 1977-1979, Studies in fracture hydrology at Chalk River Nuclear Laboratories -- Report on part of the hydrogeologic research activities conducted by Contaminant Hydrogeology Section Inland Waters Directorate Environment Canada in support of the Program for Geologic Disposal of Radioactive Wastes: Univ. of Waterloo, Waterloo, Ont, Can.

Raven, K.G. and J.E. Gale, 1977, Project 740057: Subsurface containment of solid radioactive waste: A study of the surface and subsurface structural and groundwater conditions at selected underground mines and

excavations: EMR-GSC-RW Internal Report no. 1-77, Library of Geol. Surv. of Canada, Ottawa, Canada.

Reed, J.E. and M.S. Bedinger, 1962, Estimating the effects of stream impoundment on groundwater levels: Geol. Surv. Research, p. 450B.

Reeves, M. J., Skinner, A. C., and W.B. Wilkinson, 1975, Relevance of aquifer-flow mechanisms to exploration and development of groundwater resources: J. Hydrol., vol. 25, n. 1-2, p. 1-21.

Reinius, E., 1977, Groundwater flow to rock caverns: Rockstore, 1977, Stockholm.

Reinius, E., 1978, Groundwater flow to rock caverns: Proc. 1st Symp. on Storage in Excavated Rock Caverns, vol. 2, Pergamon Press, N.Y., p. 343-348.

Remson, Irwin and J.R. Randolph, 1962, Review of some elements of soil-moisture theory -- Fluid movement in earth materials: Geol. Surv. Prof. Paper 411-D.

Remson, I., Hornberger, G.M., and F.J. Molz, 1971, Numerical methods in subsurface hydrology: John Wiley.

Rice, James R., 1977, Pore pressure effects in inelastic constitutive formulations for fissured rock masses: A.S.C.E., p. 295-297.

Rice, James R. and Donald A. Simons, 1976, Stabilization of spreading shear faults by coupled deformation-diffusion effects in fluid-infiltrated porous materials: J. Geophys. Res., vol. 81, n. 29, p. 5322-5334.

Rice, James R. and Michael P. Cleary, 1976, Some basic stress diffusion solutions for fluid-saturation elastic porous media with compressible constituents: Rev. Geophys. Space Phys., vol. 14, n. 2, p. 227-241.

Richardson, J.T., 1948, Summary of uplift pressure at Bureau of Reclamation dams: U.S. Bur of Reclam, Tech. Memo636, p. 16.

Rinehart, J.S., 1976, Alteration of flow characteristics within geothermal area by tidal forces: Proc. 2nd U.N. Symp. on Develop. and Use of Geothermal Energy, p. 549-551.

Rivera, R.A., 1964, Faults as possible suppliers of groundwater: Unpub Report Min. Eng. 229, Univ. of Calif., Berkeley.

Robertson, A. MacG., and D.R. Piteau, 1973, Determination of joint populations and their significance for tunnel stability: Trans. Soc.

Mining Eng. A.I.M.E., vol. 254, n. 2, p. 135-139.

Robinson, C.J., 1978, Hydrology of fractured crystalline rocks, Henderson Mine, Colorado: Mining Engineering, v. , p. 1185-1194.

Rocha, M., 1972, Discussion: Proc. Symp. Percolation Through Fissured Rock, Int. Soc. Rock Mech., D1:11-15.

Rocha, Manuel and Fernando Franciss, 1977, Determination of permeability in anisotropic rock -- Masses from integral samples: Rock Mech. Felsmech Mec Roches, vol. 9, no. 2-3, p. 67-93.

Rodatz, W. and W. Wittke, 1972, Interaction between deformation and percolation in fissured anisotropic rock: Proc. Symp. Percolation Through Fissured Rock, Int. Soc. Rock Mech., T2-I: 1-8 (in German).

Rodinov, V.N., Spivak, A.A., Tsvetkov, V.M., and Sizov, I.A., 1981, Changes in permeability in the zone of inelastic deformations due to underground blasting: Fiziko- Tekhnicheskie Problemy Razrabotki Poleznykh Isokopaemykh, no. 1, Jan-Feb., p. 27-33.

Rofail, N., 1965, Analysis of pumping tests in fractured rocks: Proc. Dubrovnik Symp. on Hydrology of Fractured Rocks, p. 81.

Romagnoli, P., Cuellar, G., Jimenez, M., and G. Ghezzi, 1976, Hydrogeological characteristics of geothermal field of Ahuachapan, El Salvador: Proc. 2nd

U.N. Symp. on Develop. and Use of Geothermal Energy, p. 571-574.

Romm, E.S., 1966, Fluid flow in fractured rocks: Nedra, Moscow (in Russian).

Romm, E.S., and B.V. Pozinenko, 1963, Investigation of seepage in fractured rocks: Tr VNIGRI, 214 p. (in Russian).

Rosenbaum, J.H., 1974, Synthetic microseismograms: Logging in porous formations: Geophysics, vol. 39, no. 1.

Rose, W., 1960, Fluid flow in petroleum reservoirs, III- Effect of fluid-fluid boundary condition: Illinois State Geol. Surv., Circular no. 291, 18 p.

Rossen, Robert H., 1977, Simulation of naturally fractured reservoirs with semi-implicit source terms: Soc. Pet. Eng. A.I.M.E. J., vol. 17, no. 3, p. 201-210.

Rossen, Robert H., 1976, Simulation of naturally fractured reservoirs with semi-implicit source terms: spe/A.I.M.E., N.Y., N.Y., Symp. on Numer. Simul. of Reservoir Perform., 4th, Proc., Los Angeles, Calif., Pap. spe 5737, p. 271-283.

Rothfus, R.R., Archer, D.H., Klimas, I.C., and K.G. Sikchi, 1957, Simplified flow calculations for tubes and parallel plates: Amer Inst. Chem Eng. Jour, vol. 3, p. 208.

Rousseau, Joe, 1976, Soil moisture theory and the unsaturated flow equation (lecture outline).

Rowe, R.I., 1943, Faults as a source of water supply: BS Thesis in Irrig, Univ. Calif., Berkeley.

Rowland, D.A., 1962, Initial fluid injection characteristics Precambrian interval pressure injection disposal well Rocky Mountain Arsenal, Denver, Colo: Polumbus, Jr. and Assoc. Inc, Denver, Colo.

Rowlands, D., 1974, Diamond drilling with soluble oils: Trans. Inst. Min. Metall., Sect. A., vol. 83, n. 815, p. A127-A132.

Rummel, F. and C. Fairhurst, 1970, Determination of the post-failure behavior of brittle rock using a servo-controlled testing machine: *Rock Mech., Felsmech., Mec. Roches*, vol. 2, n. 4, p. 189-204.

Russell, D.G. and M. Prats, 1962, Practical aspects of interlayer cross flow: *Jour. Pet. Tech.* (June 1962), p. 589-594.

Saad, K.F., 1967, Determination of the vertical and horizontal permeabilities of fractured water-bearing formations: *Bull. I.A.S.H.*, vol. 3, p. 22.

Saad, K.F., 1967, Effect of impervious barriers of deep-seated fractures on groundwater flow: *Hydrology of Fractured Rocks, Proc. Dubrovnik Symp. Oct. 1965*, vol. 1, p. 76-80.

Sabarly, F., 1968, Les injection et les drainages de foundation de barrages: *Geotechnique*, vol. 18-2.

Saidi, A. M., 1974, Effect of gas pressure maintenance on the recovery of the Iranian fractured limestone reservoirs: *U. S. Nat'l. Comm. of the World Energy Conf., N.Y., N.Y.*, vol. 4, p. 224-236.

Saidi, A. M., 1974, Gas injection will hike recovery in Iran's gravity-drainage fields: *Oil Gas J.*, vol. 72, n. 42, p. 110-113.

Samsonov, B.G. and V.V. Chizhikov, Hydrochemical zonation in fracture waters of North Kazakhstan and production of fresh water: *Int. Geol. Rev.*, vol. 7, no. 10, p1789-1793.

Sandquist, G., Swanson, S., Stoker, R., and J. Kunze, 1977, On evaluating the energy capacity and lifetime of fracture-dominated geothermal reservoirs: *Proc. Intersoc Energy Convers Eng. Conf. 12th, Publ. by ANS, LaGrange Park, Ill*, vol. 1, pap 779123, p. 804-809.

Sanyal, S.K., Marsden, S.S., Jr., and H.J. Ramey, Jr., 1974, Effect of temperature on petrophysical properties of reservoir rocks: *A.I.M.E. Soc. Pet. Eng. Paper 4898*, 23 p.

Sarda, J.P., Le Tirant, P., and G. Baron, 1974, Influence des contraintes et de la pression de fluide sur l'écoulement dans les roches fissure: Proc. 3rd Congr. Int. Soc. Rock Mech., vol. II-A, p. 667-673.

Sato, K. and T. Ide, 1976, On structural characters and simulation of rock fracturing of geothermal areas in northeastern Japan: Proc. 2nd U.N. Symp. on Develop. and Use of Geothermal Energy, p. 575-581.

Sawhney, B.L. and J.Y. Parlange, 1974, Two-dimensional water infiltration from a trench in unsaturated soils: Soil Sci. Soc. Am. Proc., vol. 38.

Sawhney, B.L. and J.Y. Parlange, 1976, Radial movement of saturated zone under constant flux: Theory and application to the determination of soil-water diffusivity: Soil Sci. Soc. Am. J., vol. 40.

Sawyer, Walter K. and L.Z. Shuck, 1976, Numerical simulation of mass and energy transfer in the Longwall process of underground gasification of coal: spe/A.I.M.E., N.Y., N.Y., Symp. on Numer. Simul. of Reservoir Perform, 4th, Proc., Los Angeles, Calif., Pap. spe 5743, p. 355-370.

Sawyer, W.K. and J.C. Mercer, 1977, Diffusivity model for fluid flow and heat conduction in porous media: Energy Research and Develop Admin, Morgantown, W Va.

Sawyer, W.K., Mercer, J.C., and K.H. Frohne, 1976, Prediction of fracture extent by simulation of gas well pressure and production behavior: Energy Res. and Develop Admin, Morgantown, W Va.

Schatz, J., Kusubov, A., Hearst, J., Abey, A., and C. Snell, 1977, Rock mechanics project progress and results: Rock fracture and pore collapse: Calif. Univ., Livermore.

Scheidegger, A.E., 1960, The physics of flow through porous media: The Macmillan Co., N.Y., 228p.

Schilfgaard, J.V., 1963, Design of tile drainage for falling water tables: Jour. Irrigation and Drainage Division, Am. Soc. Civil Eng., IR2, p. 1-11.

Schmieder, A., 1976, Development in time of water diffusibility in water reservoirs consisting of fissured and stratified rocks of loose structure: Publ. of Hungarian Min. Res. Inst., no. 19, p. 21-29.

Schoeller, 1967, Hydrodynamique dans le karst: Hydrology of Fractured Rocks, Proc. of Dubrovnik Symp, Oct. 1965, vol. 1, p. 3-20.

Scopel, L.J., 1964, Pressure injection disposal well, Rocky Mtn Arsenal, Denver, Colo: The Mountain Geologist, vol. 1, no. 1, p. 35-2

Serafin, J.L. and A. del Campo, 1965, Interstitial pressures on rock foundations of dams: Proc. A.S.C.E., vol. 91, no. SM5

Serafin, J.L., 1968, Influence of interstitial water on the behaviour of rock masses: Chap 3 of Rock Mech. in Eng. Practice, John Wiley and Sons, London, K.G. Stagg and O.C. Zienkiewicz (ed.).

Serafin, J.L., 1972, Influence of joint water on the stability of structures in rock: Drainage measures: Proc. Symp. Percolation Through Fissured Rock, Int. Soc. Rock Mech., G4: 1-17.

Sever, C.W., 1964, Groundwater conduits in the Ashland Mica Schist, Northern Georgia: U.S.G.S. Prof. Paper 501-D, p. D141-143.

Shanley, R.J. and Mahtab, M.A., 1975, FRACTAN; a computer code for analysis of clusters defined on the unit hemisphere: U.S. Bureau of Mines information Circular 8671, 49 p.

Sharp, J. C., Maini, Y. N. T., and T.R. Harper, 1972, Influence of groundwater on the stability of rock masses -- 1. Hydraulics within rock masses: Trans. Inst. Min. Metall., Sect. A, vol. 81, n. 782, p. A 13-20.

Sharp, J.C., 1970, Fluid flow through fissured media: PhD thesis, Imperial College Sci. Tech, London, 200 p.

Sharp, J.C. and C.O. Brawner, 1972, Prediction of the drainage properties of rock masses: Proc. Symp. Percolation Through Fissured Rock, Int. Soc. Rock Mech., Theme 4.

Sharp, J.C. and Y.N.T. Maini, 1972, Fundamental consideration on the hydraulic characteristics of joints in rock: Proc. Symp. Percolation Through Fissured Rock, Int. Soc. Rock Mech., T1-F: 1-15.

Shehata, W.M., 1971, Geohydrology of Mount Vernon Canyon Area, Jefferson County, Colo: PhD thesis, Colo. Sch. Mines, Golden, Colo, 164 p.

Sheridan, D.M. and Marsh, Sh. P., 1976, Geologic map of the Squaw Pass Quadrangle, Clear Creek, Jefferson, and Gilpin Counties, Colorado: U.S. Geol. Surv., 7.5 minute geologic quadrangle map, GQ-1337.

Sherman, W.C. and D.C. Banks, 1970, Seepage characteristics of explosively produced waters in soil and rock: U.S. Waterways Expt Station, NCG Tech. Report no. 27, Vicksburg, Miss.

Sherwood, A.E., Quong, R., and D.F. Snoeberger, 1977, Permeability of explosive-fractured-coal aquifer modeling and analysis of field hydraulic tests: Calif. Univ., Livermore.

Shvidler, M.I., 1966, On solving a type of spring in the problem of non-stable permeability of liquids in the medium with random heterogeneity: Izvestia A.S. U.S.S.R., Mech. Liquid and Gas, no. 4, (in Russian).

Sibley, W. P., 1970, Method for handling spatially varying fluid properties in a simulation model for a fissured reservoir: Soc. Petrol. Eng. J., vol. 10, n. 1, p. 25-32.

Silveria, A.F., Rodrigues, F.P., Grossman, N.F., and F.M. Mendes, 1966, Quantitative characterization of the geometric parameters of jointing in rock masses: Proc. 1st Int. Congr. on Rock Mech., Lisbon, Portugal, p. 225-233.

Simmons, J., Landrum, B.L., Pinston, J.M. and P.B. Crawford, 1959, Swept areas after breakthrough in vertically fractured five-spot patterns: Trans. A.I.M.E., vol. 216, p. 73-77.

Simmons, Gene, 1977, Microcrack technology for geothermal exploration and assessment: MIT, Cambridge, Mass.

Simpson, Frank, 1976, Monitoring of subsurface waste-disposal operations: A generalized systems approach with examples from Canadian case histories: IEEE, N.Y., N.Y., vol. 1, Pap. 9-7, 4 p.

Sims, P.K. and Harrison, J.E., 1958, Summary of geology of Precambrian rocks in the Central City- Idaho Springs area, Front Range, Colorado: Precambrian field trip guidebook, Ann. Mtg. Rocky Mtn. Sect., Geol. Soc. Amer., Golden, Colorado, p. 15-23.

Siple, G.E., 1964, Geohydrology of storage of radioactive waste in crystalline rocks at the AEC Savannah River Plant, S Carolina: U.S.G.S. Prof. Paper 501-C, p. C180-184.

Siqueira, L., 1965, Contribution of geology to the research of groundwater in crystalline rocks: Departamento Technco, Recife, Brasil, 34 p. (trans. from Portuguese).

Siskind, David E., and Robert R. Fumanti, 1974, Blast-produced fractures in Lithonia Granite: U.S. Bur. Mines Rep. Invest., n. 7901, 38 p.

Skibitzke, H.E., 1964, Extending Darcy's concept of groundwater motion -- Fluid movement in earth materials: U.S.G.S. Prof. Paper 411-F.

Smith, D. G. and M. Chowdary, 1975, Fracture toughness of slip-cast fused silica: Materials Sci. Eng. vol. 20, n. 1, p. 83-88.

Smith, L. R., Fast, C. R., and O.R. Wagner, 1969, Development and field testing of large volume remedial treatments for gross water channeling: J. Pet. Technol., vol. 21, n. 8, p. 1015-25.

Smith, M.B., Holman, G.B., Fast, C.R., and R.J. Covlin, 1978, Azimuth of deep, penetrating fractures in the Wattenberg Field: JPT Jour. Pet. Technol, vol. 30, p. 185-193.

Smith, M.C., 1975, The Los Alamos Scientific Lab Dry Hot Rock Geothermal Project (LASL Group Q-22): Geothermics, vol. 4, no. 51-4, p. 27-39.

Smith, M.C., Aamodt, R.L., Potter, R.M. and D.W.Brown, 1976, Manmade geothermal reservoirs: Proc. 2nd U.N. Symp. on Develop. and Use of Geothermal Energy, p. 1781.

Smith, M.C., 1978, Initial results from the first Los Alamos hot dry rock energy system: Los Alamos Sci. Lab, New Mex, Symposium on Geothermal Energy, Gothenburg, Sweden.

Smith, R.C. and R.A. Greenkorn, 1969, An investigation of the flow regime for Hele-Shaw flow: Soc. of Pet. Eng., vol. 246.

Smolen, J.J. and L.R. Litsey, 1979, Formation evaluation using wireline formation tester pressure data: spe/A.I.M.E.

Snow, D.T., 1970, The frequency and apertures of fractures in rock: Int. Jour. Rock Mech. Min. Sci., vol. 7, p. 23-40, Pergamon Press, Great Britain.

Snow, D.T., 1965, A parallel plate model of fractured permeable media: unpubl. PhD thesis, Univ. of Calif. at Berkeley, 331 p.

Snow, D.T. and R. Karol, 1965, Estimation of fracture porosity in crystalline rock: Chemical Grouting Topics, no. 5, American Cyanamid Co, Princeton, New Jersey.

Snow, D.T., 1966, Threehole pressure test for anisotropic foundation permeability: Fels U Ing Geol., vol. 4, p. 298.

Snow, D.T., 1967a, Anisotropy of permeable fractured media: Hydrology and Flow Through Porous Media, The Muskat vol, R.J.M. De Wiest (ed.), Academic Press, N.Y., 86 p.

Snow, D.T., 1967b, Discussion: Proc. 1st Int. Congr. Rock Mech., p. 243-244.

Snow, D.T., 1968a, Discussion of transmissibility as function of scale: Proc. Natl Symp. on Analysis of Water Resources Systems, Am. Water Res. Assoc., Denver, Colo, p. 141.

Snow, D.T., 1968b, Fracture deformation and changes of permeability and storage upon changes of fluid pressure: Quart of Colo. Sch. Mines, vol. 63, no. 1, p. 201-244.

Snow, D.T., 1968c, Hydraulic character of fractured metamorphic rocks of the Front Range and implications to the Rocky Mountain Arsenal Well: Quart of Colo. Sch. of Mines, vol. 63, no.1, p. 167-199.

Snow, D.T., 1968d, Rock fracture spacing, opening, and porosities: Jour. of Soil Mech. and Found Div., Proc. A.S.C.E., p. 73-91.

Snow, D.T., 1969a, Anisotropic permeability of fractured media: Water Resources Res., vol. 5, no. 6, p. 1273-1289.

Snow, D.T., 1969b, Closure to discussions, rock fracture spacings, opening and porosities: Jour. Soil Mech. and Found. Div. A.S.C.E., vol. 95, no. 3, p. 880-883.

Snow, D.T., 1970, The frequency and apertures of fractures in rock: Int. Jour. Rock Mech. and Min. Sci., vol. 7, no. 1, p. 23.

Snow, D.T., 1972a, Fundamentals and in situ determination of permeability: Proc. Symp. Percolation Through Fissured Rock, Int. Soc. Rock Mech., G1:1-6.

Snow, D.T., 1972b, Discussion: Proc. Symp. Percolation Through Fissured Rock, Int. Soc. Rock Mech., D1:18-22.

Snow, D.T., 1972c, Geodynamics of seismic reservoirs: Proc. Symp. Percolation Through Fissured Rock, Int. Soc. Rock Mech., T2-J: 1-19.

Snow, D.T., 1972d, Mountain groundwater supplies: Mountain Geologist, vol. 10, no. 1, p. 19-24.

Sobolevskii, V. V., Myasnikov, B. I., Shevchenko, Yu. M., and B.I. Mitel'man, 1975, Effect of the properties of rocks on their fracture by high-pressure jets: Neft Khoz, n. 4, p. 9-10.

Sohns, H. W., 1972, Feasibility of in situ retorting of Green River Oil Shale, utilizing nuclear explosives for fracturing: Int. Atomic Energy Agency, Vienna, Austria, Pap. IAEA-PL-388-3/6, p. 99-121.

Somerton, W. H., Soylemezoglu, I. M., and R.C. Dudley, 1975, Effect of stress on permeability of coal: Int. J. Rock Mech. Min. Sci. Geomech. Abstr., vol. 12, n. 5-6, p. 129-145.

Somerton, Wilbur H., 1958, Some thermal characteristics of porous rocks: SPE Trans., Technical Note 2008.

Somerton, W.H., Soylemezoglu, I.M., and R.C. Dudley, 1974, Effect of stress on permeability of coal: Calif. Univ., Berkeley, Petr Eng. Lab.

Sowers, George F., 1976, Dewatering rock for construction: Rock Eng. for Found and Slopes, Proc. of a spec Conf., Publ. by A.S.C.E., N.Y., vol. 1, p. 20-21

Sowers, George F., 1973, Remote sensing for water resources: Civ. Eng. (NY), vol. 43, n. 2, p. 35-39.

Spangler, 1970, Gravitational water and seepage: Soil Engineering, 3rd edition, Int. Textbook Co, Scranton, Pa., Chap. 10.

Springer, T.D., 1977, Hybrid computers for simulation of gas diffusion in fractured shale: Los Alamos Sci. Lab, New Mex, Eastern Gas Shale Program Conf., Morgantown, W Va, Oct. 1977.

Sprunt, E. and W.F. Brace, 1974, Direct observation of microcavities in crystalline rocks: Int. Jour. Rock Mech. Min. Sci., vol. 11, no. 4, p. 139-150.

Stearns, Richard G., 1974, Porosity and hydrology of jointed Middle Ordovician Limestones in the J. Percy Priest Dam areas of central Tenn: Tenn Univ., Knoxville, Tenn, and Vanderbilt Univ., Nashville, Tenn.

Stearns, D.W. and M. Friedman, 1972, Reservoirs in fractured rocks: Stratigraphic oil and gas fields, A.A.P.G. Mem 16, p. 82-106.

Stein, R., 1976, Hydrogeology of the Edmonton area (northeast segment), Alberta: Rep Alberta Res., no. 76-1, 24 p.

Stephens, D.R., 1974, Fracture-induced permeability: Present situation and prospects for coal: Calif. Univ., Livermore, Lawrence Livermore Lab.

Stewart, J.W., 1962a, Water-yielding potential of weathered crystalline rocks at the Georgia Nuclear Lab: U.S.G.S. Prof. Paper 450-B.

Stewart, J.W., 1962b, Relation of permeability and jointing in crystalline metamorphic rocks near Jonesboro, Georgia: U.S.G.S. Prof. Paper 450-D, p. D168-170.

Stewart, J.W., 1964, Infiltration and permeability of weathered crystalline rocks, Georgia Nuclear Lab, Dawson County, Georgia: U.S.G.S. Bull., 1133-D, 59 p.

Stewart, G., 1971, Occurrence and characteristics of fractures in the crystalline rocks of southeastern New Hamp and their relationship to the yield of drilled water wells: New Hamp Univ., Durham, New Hamp.

Storage in Excavated Rock Caverns, Rockstore 77: Proc. 1st. Int. Symp., Stockholm, Sweden, 832 p.

Streltsova, T. D., 1976, Hydrodynamics of groundwater flow in a fractured formation: Water Res. Res., vol. 12, n. 3, p. 405-414.

Strobel, C. J., Gulati, M. S., and H.J. Ramey, Jr., 1976, Reservoir limit tests in a naturally fractured reservoir -- A field case study using type curves: JPT J. Pet. Technol., vol. 28, p. 1097-1106.

Sulla, M.B., Tsoi, P.I., and Baranov, V.P., Migration of gas through seams with different physical properties: Fiziko-Tekhnicheskie Problemy Razrabotki Poleznykh Iskopaemykh, no. 2, Jan-Feb., p. 67-71.

Summers, W.K., 1972, Specific capacities of wells in crystalline rocks: Groundwater, vol. 10, no. 6, p. 37-47.

Sun, R. J., 1977, Possibility of triggering earthquakes by injection of radioactive wastes in shale at Oak Ridge National Lab., Tenn: J. Res. U.S. Geol. Surv., vol. 5, n. 2, p. 253-262.

Sundrani, G. and S.H. Nagaraja, 1970, The effect of a fissure in the permeable foundation on the uplift pressure beneath a hydraulic structure: Proc. 2nd Conf. Fluid Mech. and Fluid Power, vol. 1, paper H12, 14 p.

Szilas, A.P. and F. Patsch, 1975, Flow in geothermal hot water wells: Geothermics, vol. 4, no. 1-4.

Tabary, J., 1978, Monitored impermeability for petroleum storage and other underground works: Proc. 1st Int. Symp. on Storage in Excavated Rock Caverns, Pergamon Press, N.Y., p. 507-516.

Teltamanti, T., 1967, Hydrologic and hydraulic characteristics of water flowing from fissured carbonated rocks into mines: Proc. Dubrovnik Symp. on Hydrology of Fractured Rocks, vol. 1, p. 106-119.

Terhune, R. W. and J.G. Shaw, 1972, Calculations of rock fracturing from multiple nuclear explosive sources: Int. Atomic Energy Agency, Vienna, Austria, Pap. IAEA-PL-388-3/10, p. 251-275.

Terman, Maurice J., 1970, Environments at U.S. and U.S.S.R. nuclear explosion sites: Petroleum-simulation projects: U.S.G.S., Wash DC.

Terzaghi, K., 1962, Does dam foundation engineering really lag?: Eng. News Record, p. 58.

Terzaghi, R., 1965, Sources of error in joint survey: London, Inst. Civil Eng., Geotechnique, vol. 15, p. 287-304.

Thayer, D.P., 1962, Interim report, Permeability study, Underground power plant, Oroville Dam, Calif.: Dept. Water Resources, 14 p.

Thomas, Adrian W., Duke, Harold R., Zachmann, David W., and E. Gordon Kruse, 1976, Comparisons of calculated and measured capillary potentials from line sources: Soil Sci. Soc. Am. J., vol. 40.

Thomas, Harold E., 1974, Air injection to evaluate mine rock fractures: U.S. Bur. of Mines, Compressed Air, vol. 79, n. 8, p. 12-13.

Thomas, L. Kent and Ray G. Pierson, 1978, Three-dimensional geothermal reservoir simulation: SPE/A.I.M.E.

Thompson, T.W., Sen, S., Gray, K.W., and T.F. Edgar, 1977, Influence of drying and stress on the permeability of Texas Lignite: A.S.M.E. Pap no. 77-Pet-26 for Mtg., Sept 18-22, 1977, 7 p.

Tirant, P. and G. Baron, 1972, Flow in fissured rocks and effective stresses: Proc. Symp. Percolation Through Fissured Rock, Int. Soc. Rock Mech., T2-K: 1-24 (in French).

Tisot, Peter R. and H.W. Sohns, 1971, Structural deformation of Green River Oil Shale as it is related to in situ retorting: U.S. Bur of Mines.

Toki, Takashi, Okada, Katsuya, and Yukio Kamiyama, 1977, Some experiments on the permeability of concrete: Takenaka Tech. Res. Rep, no. 18, p. 74-82.

Tomasson, J., Fridleifsson, I.B., and V. Stefansson, 1976, A hydrological model for the flow of thermal water in southwestern Iceland, with special reference to the Reykiv and Reykjavik thermal areas: Proc. 2nd U.N. Symp. on Develop. and Use of Geothermal Energy, p. 643-648.

Tomasson, J. and T. Thorsteinsson, 1976, Use of injection packer for hydrothermal drillhole stimulation in Iceland: Proc. 2nd U.N. Symp. on Develop. and Use of Geothermal Energy, p. 1821-1827.

Trainer, F.W., 1968, Temperature profile in water wells as indicator of bedrock fractures: U.S.G.S. Prof. Paper 600-B, p. B210-214.

Tremblay, J. J., D'Cruz, J., and H. Anger, 1973, Salt water intrusion in the Summerside area, P.E.I.: Ground Water, vol. 11, n. 2, p. 21-27.

Tullis, Jan and Richard A. Yund, 1977, Experimental deformation of Westerly Granite: Jour. of Geophys Res., vol. 82, no. 36.

Tuncer, E. and S. Simsek, 1976, Geology of Izmir-Seferihisar geothermal area western Anatolia of Turkey: Determination of reservoir by means of gradient drilling: Proc. 2nd U.N. Symp. on Develop. and Use of Geothermal Energy, p. 349-361.

Turcotte, D.L. and E.R. Oxburgh, 1968, A fluid theory for the deep structure of dip-slip fault zones: Phys Earth Planet Interiors, vol. 1, p. 381-386.

Turk, J.L., 1963, The occurrence of groundwater in crystalline rocks: MS Report, Stanford Univ.

United Nation, 1976, 2nd Symposium on Development and Use of Geothermal Energy.

US National Bureau of Standards, 1951, Monte Carlo method: Applied Math Ser 12, 42 p.

Van Der Ploeg, R.R. and F. Beese, 1977, Model calculations for the extraction of soil water by ceramic cups and plates: Soil Sci. Soc. Am. J., vol. 41.

Van Everdingen, A.F. and W. Hurst, 1949, The application of the LaPlace Transformation to flow problems in reservoirs: SPE/A.I.M.E. Ann. Mtg., San Francisco, Calif.

Van Huffel, G., 1975, Geologic map of the Edgar Mine: Colorado School of Mines, Senior Thesis, 1 map.

Van Poolen, H.K., 1960, Status of drill-stem testing techniques and analysis: SPE/A.I.M.E.

Vecchioli, John, 1967, Directional hydraulic behaviour of a fractured shale aquifer in New Jersey: Int. Assoc. Sci. Hyd. Publ. 73, p. 318-326.

Vecchioli, J., Carlswell, L.D., and H.F. Kasabach, 1969, Occurrence and movement of groundwater in the Brunswick Shale at a site near Trenton, New Jersey: U.S.G.S. Prof. Paper 650-B, p. B154-157.

Versluys, J., 1915, De onbepaalde vergelijking der permanente beweging van het grondwater: Verk Geol. Mijnbouw Genoot Ned en Kolonien, Geol. Serie 1S, p. 349-360.

Villas, R.N.N., 1975, Fracture analysis, hydrodynamic properties and mineral abundance in the altered igneous wall rocks of the Mayflower mine, Park City District, Utah: PhD dissertation, Univ. of Utah, 254 p.

Vogel, C.B., 1973, Method and apparatus for detecting fractures: U.S. Patent no. 3,775,739 (Nov 27, 1973).

Volkov, S. A., Solov'eva, I. V., and V.A. Globa, 1976, Leakage of washing fluid in drilling rig joints: Razved Okhr. Nedr., n. 10, p. 21-24.

Von Thun, J. Lawrence, 1976, Stability analysis of cut slopes at Auburn Dam: A.S.C.E., vol. 1, p. 349-360.

Walker, T., 1962, Fracture zones vary acoustic signal amplitudes: World Oil (May 1962).

Wallner, Manfred and Walter Wittke, 1976, Finite element analysis of grout propagation: A.S.C.E., New York, N.Y., vol. 2, p. 1119-1132.

Wallner, M. and W. Wittke, 1972, Water break-ins during construction of underground opening in rock: Proc. Symp. Percolation Through Fissured Rock, Int. Soc. Rock Mech., T4-I: 1-15 (in German).

Walsh, J.B., 1965, The effect of cracks on the compressibility of rock: Jour. Geophys. Res., vol. 70, no. 20, p. 381-389.

Walsh, J.B., and W.F. Brace, 1966, Cracks and pores in rocks: Proc. 1st Int. Congr. on Rock Mech., Lisbon, Portugal, vol. 1, p. 643-646.

Wang, J.S.Y., Narasimhan, T.N., Tsang, C.F., and Witherspoon, P.A., 1977, Transient flow in tight fractures: 1st Invitational well testing symposium, Proc. Lawrence Berkeley Lab., p. 103-116.

Wantland, D., 1964, Geophysical measurements of rock properties in situ: State of Stress in the Earth's Crust, Am. Elsevier Pub Co, Inc, W.R. Judd (ed.), p. 409-448.

Warren, J.E., Dougherty, E.L., and Price, 1960, Reservoir simulation on a digital computer: The differential equation program: Proj 5219, Calif. Res. Corp, La Habra, Calif.

Warren, J.E. and H.S. Price, 1961, Flow in heterogeneous porous media: Soc. Pet. Eng. Jour. (Sept 1961), p. 153-169.

Warren, J.E. and P.J. Root, 1963, The behaviour of naturally fractured reservoirs: Soc. Pet. Eng. Jour. (Sept 1963), p. 245-255.

Warren, J.E. and P.J. Root, 1965, Discussion: Soc. Pet. Eng. Jour. (March 1965), p. 64-65.

Warrick, A.W. and A. Amoozegar-Fard, 1977, Soil water regimes near porous cup water samplers: Water Res. Res., vol. 13, no. 1, p. 203-207.

Warrick, A.W. and D.O. Lomen, 1976, Time-dependent linearized infiltration: III. Strip and disc sources: Soil Sci. Soc. Am. J., vol. 40.

Watson, Geoffrey, 1966, The statistics of orientation data: Jour. of Geol., vol. 74, p. 786-797.

Weir-Jones, Iain, 1977, Current methods for rock slope stability evaluation: Idaho Transp Dept., Div of Highways, Boise, Idaho, p. 107-119.

Weller, W.T., 1965, Reservoir performance during two-phase flow: SPE, Jour. of Pet. Tech.

Werneck, M.L.G., Costa Filho, L.M., and H. Franca, 1977, In situ permeability and hydraulic fracture tests in Guanabara Bay Clay: Asian Inst. of Technol, Bangkok, Thailand, p. 399-416.

Wesslon, A., Gustafson, G., and P. Maripuu, 1977, Groundwater and storage in rock caverns, pumping tests as an investigation method: Proc. 1st Int. Symp. on Storage in Excavated Rock Caverns, vol. 2, Pergamon Press, N.Y., p. 359-365.

White, D.E., 1968, Hydrology, activity, and heat flow of the Steamboat Springs thermal system, Washoe County, Nevada: U.S.G.S. Prof. Paper 458-C, 109 p.

Widmer, K., 1959, Jointing with relation to groundwater movement in Triassic rocks of New Jersey: Geol. Soc. Am. Bull., vol. 70, no. 12, p. 1697-1698.

Wilhelmi, B. and W. H. Somerton, 1967, Simultaneous measurement of pore and elastic properties of rocks under triaxial stress conditions: Soc. Pet. Eng. Jour., vol. 7, p. 283-294.

Wilkes, P. F., 1974, Permeability tests in alluvial deposits and the determination of K/O: Geotechnique, vol. 24, n. 1, p. 1-11.

Williams, R.E., and R.N. Farvolden, 1967, The influence of joints on the movement of groundwater through glacial till: Jour. of Hydrology, vol. 5, p. 163.

Wilson, Charles R. and P.A. Witherspoon, 1974, Steady state flow in rigid networks of fractures: Water Res. Res., vol. 10, n. 2, p. 328-335.

Wilson, C.R., 1970, Flow in jointed rock: PhD thesis, Univ. Calif., Berkeley.

Wilson, C.R. and P.A. Witherspoon, 1970, An investigation of laminar flow in fractured rocks: Geotech. Rep, 70-6, Univ. Calif., Berkeley, Calif., 178 p.

Winter, Thomas C., 1978, Numerical simulation of steady state three-dimensional groundwater flow near lakes: Water Res. Res., vol. 14, no. 2.

Witherspoon, P.A., and Gale, J.E., 1977, Mechanical and hydraulic properties of rocks related to induced seismicity: Eng. Geol., V. 11, p. 23-55.

Witherspoon, P.A., 1978, Radioactive waste storage in crystalline and argillaceous rocks: National Waste Management Program Report, Office of Waste Isolation, Union Carbide Corp, p. 83-87.

Witherspoon, P.A., 1978, Introduction: spec Session, Underground Storage of Nuclear Waste, Proc. 1st Int. Symp. on Storage in Excavated Rock Caverns, Pergamon Press, vol. 3, p. 721.

Witherspoon, P.A., Amick, C.H., and J.E. Gale, 1976, Observations on stress dependent fracture permeability using large diameter granite core: Abstract E.O.S. Trans., Ann. Mtg., Fall 1976.

Witherspoon, P.A., Amick, C.H., and J.E. Gale, 1977, Stress-flow behaviour of a fault zone with fluid injection and withdrawal: Report to U.S.G.S. Contract no. 14-08-001-14583, Report no. 77-1.

Witherspoon, P.A., Cook, N.G.W., and J.E. Gale, 1978, Cooperative work program with Swedish Nuclear Fuel Supply Company on radioactive waste storage in mined caverns: Natl Waste Management Program Report, Office of Waste Isolation, Union Carbide Corp, p. 87-100.

Witherspoon, P.A. and O. Degerman, 1978, Swedish-American Cooperative program on radioactive waste storage in mined caverns: Program summary: Lawrence Berkeley Lab Report LBL-7049.

Witherspoon, P.A. and D.L. DePasquale, 1968, Feasibility of storing natural gas in underground chambers constructed with nuclear explosives: Trans. Am. Nuclear Soc., 1968 Winter Mtg., Wash. D.C., Nov 10-15.

Witherspoon, P.A., Diadkin, Y.D., Tsiviritsyna, V.V., and Lasseter, 1974, Influence of permeability distribution of hot dry rock in underground boilers on their thermal regime: Problems of Mining Thermophysics, Leningrad Mining Inst., Leningrad, p. 71-76 (in Russian).

Witherspoon, P.A. and J.E. Gale, 1976, Effect of fracture deformation on fluid pressure distribution -- An indicator of slope instability: 29th Canadian Geotech. Conf., Vancouver, British Columbia, Oct. 13-15.

Witherspoon, P.A. and J.E. Gale, 1977, Mechanical and hydraulic properties of rocks related to induced seismicity: Eng. Geol., vol. 11, p. 23-55.

Witherspoon, P.A., Gale, J.E., and N.G.W. Cook, 1978, Radioactive waste storage in argillaceous and crystalline rock masses: Proc. 1st Int. Symp. on Storage in Excavated Rock Caverns, vol. 3, Pergamon Press, N.Y., p. 805-811.

Witherspoon, P.A., Gale, J.E., Taylor, R.L., and M.S. Ayatollahi, 1974, Effect of permeability anisotropy and tectonic stress orientation on fluid injection in a fault zone: E.O.S. Trans., vol. 55, no. 12, p. 1191 (Dec. 1974).

Witherspoon, P.A., Gale, J.E., Taylor, R.L., and M.S. Ayatollahi, 1974, Investigation of fluid injection in fractured rock and effect on stress distribution: Ann. Report Period March 13, 1973, through June 12, 1974, to U.S.G.S., contract 14-08-001-12727, A.R.P.A. order 1648, 96 p.

Witherspoon, P.A., Gale, J.E., Taylor, R.L., and M.S. Ayatollahi, 1974, Fluid injection and withdrawal in a fault zone with deformable fractures: E.O.S. Trans., vol. 55, no. 4, p. 353.

Witherspoon, P.A. and A.C. Gringarten, 1973, Extraction of heat from multiply-fractured dry hot rock: Geothermics, vol. 2, no. 3-4, p. 119-122.

Witherspoon, P.A., Gringarten, A.C., and Ohnishi, 1975, Theory of heat extraction from fractured hot dry rock: Jour. Geophys. Res., vol. 80, no. 8, p. 1120-1124, (March 10).

Witherspoon, P.A. and I. Javandel, 1968, Analysis of transient fluid flow in multi-layered systems: Water Resources Center Contribution no. 124, Water Res. Center, Univ. Calif. at Los Angeles (March 1968), 119 p.

Witherspoon, P.A., Javandel, I., Neuman, S.P., and R.A. Freeze, 1967, Interpretation of aquifer gas storage conditions from water pumping tests: Am. Gas Assoc. Monograph (June 1967), 273 p.

Witherspoon, P.A., Lindblom, U., Morfeldt, C.O., and I. Janelid, 1974, Gas storage in mined caverns: Proc. Operating Section, Am. Gas Assoc., p. T154-161.

Witherspoon, P.A. and Y.N.T. Maini, 1973, Influence of fluid injection on stress in the earth's crust: Proc. 5th World Conf. on Earthquake Eng., Rome, Italy (June 25-29).

Witherspoon, P.A., Mueller, T.D., and R.W. Donovan, 1962, Evaluation of underground gas storage conditions in aquifers through investigations of groundwater hydrology: Jour. Petr. Tech. (May 1962), p. 555-561.

Witherspoon, P.A. and S.P. Neuman, 1972, Hydrodynamics of fluid injection: Underground Waste Management and Environmental Implications, T.D. Cook (ed.), Am. Assoc. Petrol. Geol. Mem. 18, p. 258-272.

Witherspoon, P.A., Noorishad, J., and C.R. Wilson, 1971, Mathematical modeling of flow in fractures: Abst with Programs, Geol. Soc. Am. 1971 Ann. Mtg., Wash, D.C., Nov 1-3.

Witherspoon, P.A., Raleigh, C.B., Gringarten, A.C., and Y. Ohnishi, 1974, Multiple hydraulic fracturing for recovery of geothermal energy: E.O.S. Trans., vol. 55, no. 4, p. 426.

Witherspoon, P.A. and C.R. Wilson, 1974, Steady state flow in rigid network of fractures: Water Resources Res., vol. 10, no. 2, p. 328-335.

Witherspoon, P.A., Taylor, R.L., Maini, Y.N.T., Gale, J.E., and M.S. Ayatollahi, 1973, A coupled stress-flow method of analyzing effect of fluid injection on stress distribution in fractured rocks: E.O.S. Trans., vol. 54, no. 4, p. 369.

Witherspoon, P.A., 1977, Summary review of workshop on movement of fluids in largely impermeable rocks: Texas Univ., Austin.

Wittke, W.K., 1969, Durchstromung von Kluftigem Fels: Report Res. Inst. for Hydraulic Structures and Agri Eng., Univ. of Karlsruhe, Karlsruhe, Germany.

Wittke, W.K., and C. Louis, 1966, Determination of the influence of groundwater flow on the stability of slopes and structures in jointed rock: 1st Int. Congr. on Rock Mech., Lisbon, Portugal, Proc., vol. 2, p. 201-206.

Wittke, W., Rissler, P. and S. Semprich, 1972, Three-dimensional laminar and turbulent flow through fissured rock according to discontinuous and continuous models: Proc. Symp. Percolation Through Fissured Rock, Int. Soc. Rock Mech., T1-H: 1-18.

Wittke, W., 1976, A new design concept for underground opening in jointed rock: Pub Inst. Foundation Eng., Soil Mech., Rock Mech. and Water Ways Const, RWTH Aachen, vol. 1, p. 46-117.

Wittke, W., Pierau, B., and K. Schetelig, 1978, Planning of a compressed air pumped storage scheme at Vinden/Luxembourg: Proc. 1st Int. Symp. on Storage in Excavated Rock Caverns, vol. 2, Pergamon Press, N.Y., p. 367.

Wolff, R. G., Bredehoeft, J. D., Keys, W. S., and Eugene Shuter, 1975, Stress determination by hydraulic fracturing in subsurface waste injection: J. Am. Water Works Assoc., vol. 67, n. 9, p. 519-523.

Wolters, R., Reinhardt, M., and B. Jager, 1972, Observations on the openings of fissures, their arrangement and their extension: Proc. Symp. Percolation Through Fissured Rock, Int. Soc. Rock Mech., T1-J: 1-13 (in German).

Wong, H. Y. and I.W. Farmer, 1973, Hydrofracture mechanisms in rock during pressure grouting: Rock Mech., Felsmech., Mec. Roches, vol. 5, n. 1, p. 21-41.

Wood, Leonard A., 1973, Use of underground space for waste storage through injection wells: Ann. Arbor Sci. Publ., Inc., Mich., Extr. of Miner and Energy: Today's Dilemmas, Int. Workshop on Environ. Probl. of the Extr. Ind., Pap. 16, p. 193-202.

Yardley, D.H., 1975, Hydrology of some deep mines in Precambrian rocks: Office of Waste Isolation Report Y/OWI/SUB-4367/1 (Oct. 1975).

Yuster, S.T. and J.C. Calhoun, 1945, Pressure parting of formations in water flood operations: Oil Weekly, vol. 117, no. 2, p. 38.

Zanger, C.N., 1953, Theory and problems of water percolation: Eng. Monograph 8, U.S. Bur Reclam, Denver, Colo.

Zeigler, Timothy W., 1976, Determination of rock mass permeability: U.S. Waterw. Exp. Stn. Tech. Rep., S-76-2, 112 p.

Zhel'tov, U.P., 1961, On single phase liquid flow through deformed fractured non-porous rocks: Appl Math Tech. Phys, U.S.S.R., 6.

Zienkiewicz, O.C. and K.G. Stagg, 1966, The cable method of in-situ testing: Proc. 1st Congr. Int. Soc. Rock Mech., 1: 667-672.

Zoback, M.D. and Byerlee, J.D., 1976, The effect of microcrack dilatancy on the permeability of Westerly Granite, Geology.

Zohnishi, Yuzo, and Richard E. Goodman, 1974, Results of laboratory tests on water pressure and flow in joints: Int. Soc. for Rock Mech., 3rd Congr., Proc., Pap., Denver, vol. 2, Part A., p. 660-666.

Zuppi, G. M., Fontes, J. Ch., and R. Letolle, 1974, Environmental isotopes and movements of sulfated water in Latium, Italy: IAEA, Vienna, Austria, Isot. Tech. in Groundwater Hydrol., Symp. Proc. Pap and Discuss., vol. 1, Pap. IAEA-SM-182/16, p. 341-361.

VOLUME 3

APPENDIX I
DESCRIPTION OF
PLASTIC DOUGH CORE ORIENTER

APPENDIX I
DESCRIPTION OF
PLASTIC DOUGH CORE ORIENTER

Orientation of the core obtained from diamond drill holes is an integral part of any detailed engineering geology study. Oriented cores are used in areas such as fracture hydrology (Gale, 1980), rock slope stability and rock mechanics studies of fractured rock (Goodman, 1976), and many other geological engineering projects (Robinson, 1980). Many devices have been used in obtaining oriented core which are either very expensive or inaccurate. A relatively simple and inexpensive device was developed for this project. It has been used successfully in orienting core in horizontal and slightly inclined ($\pm 10^\circ$) holes at the Colorado School of Mines Experimental Mine. This device can be used in either wireline or conventional core drilling operations. In most cases an accuracy of $\pm 5^\circ$ can be obtained in orienting the core.

General Description.

The plastic dough core orienter is a device which can be inserted inside a core hole to obtain an oriented impression

of the in situ end of the core stub. In diamond core drilling operations after the core is broken and removed, usually a piece of core about 4 in. (10 cm) long remains at the bottom of the hole (Figure I-1). Of course there are circumstances where a fracture intersects the hole at the bottom and the core is entirely removed but this is usually rare in hard rock. This piece can be oriented by taking an impression of the end of the hole. Plastic dough which is readily available is a perfect and inexpensive substance for taking impressions of the core. It does not stick to the rock and preserves the shape indefinitely unless disturbed. The only problem is to orient the plastic dough simultaneously with taking impressions, since in long holes it is almost impossible to insert a string of pipes without losing the orientation, especially underground where room is usually limited. This is done by using a pendulum to mark the other end of the plastic dough cylinder, thereby making a vertical reference line. Upon removal of the next core barrel the first piece can be matched with the impression on the plastic dough and, therefore, be oriented (Figure I-2).

This system can be used inside a wireline rod when the inner barrel is removed or in conventional core drilling when the entire string is removed. Figure I-3 is a photograph of a core orienter assembled for a wireline rod string. Note the yellow plastic dough at the end of the instrument. The

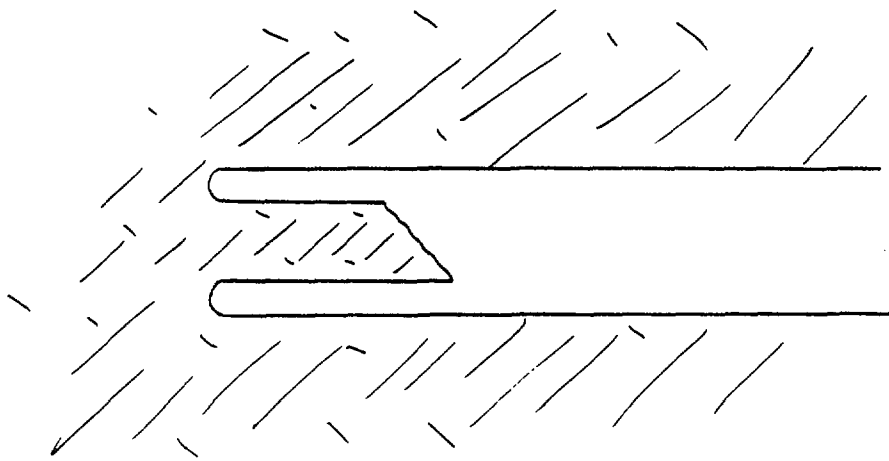


FIGURE I-1. A diamond drill hole after removal of the core.

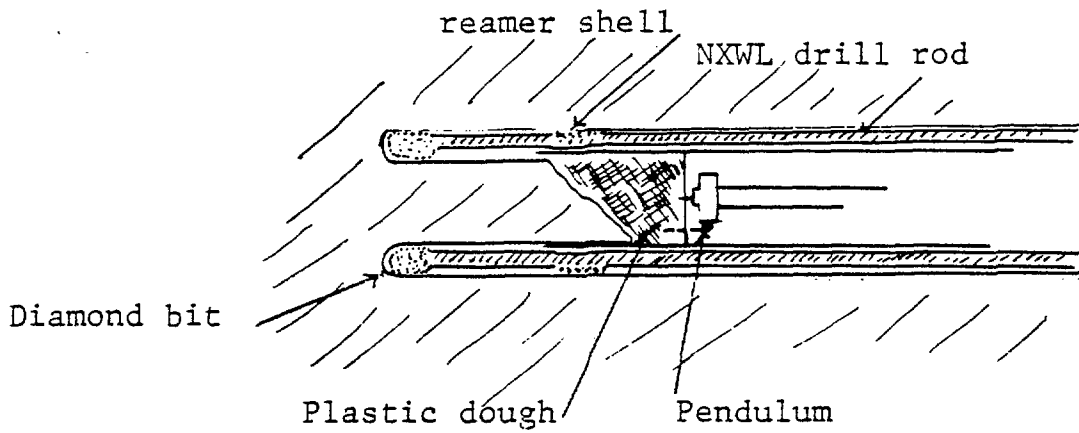


FIGURE I-2. A core orienter positioned to take impression.

same system can be inserted and secured inside a piece of short NX-core barrel or a piece of NX-rod to be used inside the borehole when the string is removed (Figure I-4). This instrument can be constructed for different size boreholes and cores; however, it is unlikely that the pendulum would be practicable for the smaller EX or even AX holes.

In Figure I-5 the end of the impressed cylinder of plastic dough is shown. Note how details of the core end can be seen on the end of the cylinder. Figure I-6 is the other end of the same cylinder with a central mark and a smaller off center mark which makes a vertical reference line. Finally, Figure I-7 shows how the core stub is matched to the plastic dough cylinder after removal. Even in flat vertical core ends the plastic dough can pick up details that other more expensive core orienters cannot (c.f. Carlius core orienter; Goodman, 1976).

The instrument shown here was made from material that can be obtained from most hardware stores with a total cost of less than \$50. However, for more precise orientation a machined version of this core orienter can be made for \$200 to \$250, which is still less expensive than a week's rent of some of the current core orienters. Details of this version are given below.

FIGURE I-3. Core orienter assembled for inside wireline drill rods.

FIGURE I-4. Core orienter with a wireline rod as outer casing for inside the hole.

FIGURE I-7. Core end matched with the impression.

Detailed Description.

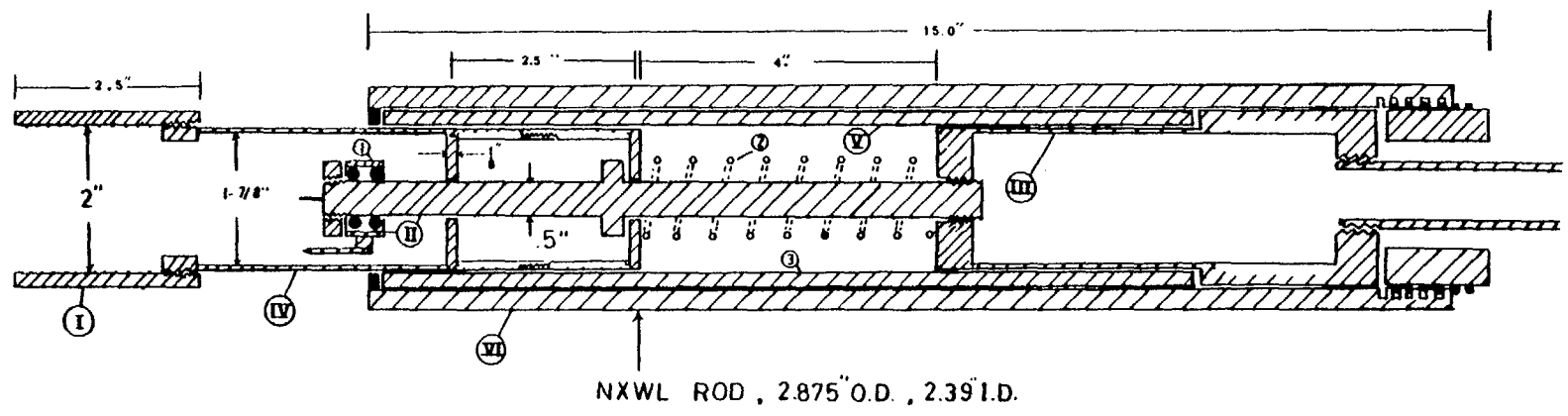
Figure I-8 shows a detailed cross section through the center line of a core orienter. Some construction detail on this diagram may seem unnecessary; however, they are unavoidable due to machining problems. Aluminum is recommended for material as the excess weight of steel would cause difficulties in a horizontal hole. The instrument consists of the following parts:

- I. - Plastic dough tube
- II. - Pendulum and pendulum rod
- III. - Pusher assembly and spring
- IV. - Pendulum rod guide
- V. - Inner casing
- VI. - Outer casing

These parts are identified by roman numerals in Figure 8.

I. Plastic Dough Tube

This tube is simply a 2.5" long piece of 2" pipe, preferably plastic, which can be removed easily. Several of these tubes should be made available because once the plastic dough is impressed and removed it has to wait within its tube until the stub is drilled and removed before it can be used for core orientation. A second tube can be used to take an



- ① 1" diameter ball bearing
- ② .5" I.D. compression spring
- ③ 2" pipe machined to O.D. of 2.38"

FIGURE I-8. Details of a plastic dough core orienter.

impression of the second stub at this time, in preparation for orienting the next core run. This would save some drilling time. The interior of the tube should be rough or, even better threaded, to prevent the dough from sliding.

II. Pendulum and Pendulum Rod

The pendulum consists of a light-weight shielded ball bearing with great ease of movement. On a point on the periphery a small pin and a relatively heavy piece of lead are attached. Care should be taken in having the pin straight. A nut at the end of a $\frac{1}{2}$ in. solid rod would protect the ball bearing. However, the ball bearing should be affixed to the rod independent of the nut. A projection of of 4" from the end of the rod limits the longitudinal movement of the pendulum during insertion and removal.

III. Pusher Assembly and Spring

As the name implies its function is to insert the instrument inside the hole without causing the pendulum to contact the end of the plastic dough. It is made of a hollow tube (for weight purposes) which is threaded on both sides to accommodate a $\frac{3}{4}$ " pipe on one side (outer) and the pendulum rod on the other side (inner). The spring's function is to keep the pendulum separated from the end of the plastic dough until the end of the tube touches the bottom of the hole at

which time a slight excess force to compress the spring will cause the pendulum to move towards the dough. It should be noted that the stiffness of the spring should be such that the resisting force of the spring is less than either the shear force developed between plastic dough and the wall of the tube or the plastic strength of the dough. A spring stiffness of .25 to .5 lb/in. is acceptable for this spring.

IV. Pendulum Rod Guide

The pendulum rod guide is a thin walled tube with two 1/8" thick washers installed inside it. The rod clearance should be small to prevent any slack in the rod.

V. Inner Casing

The inner casing is a 2" I.D. and 2.35" O.D. pipe which fits inside a NX wireline rod. This size is currently most common and has the advantage that the drill rods are usually clean inside and there is no danger of losing the instrument.

VI. The Outer Casing

The outer casing is simply a short piece of NX wireline rod fabricated to enclose the above described assembly. This enables one to use the instrument inside the diamond drill holes with the drill string pulled out.

Possible Improvements

One major modification that can be made is to use a small gyroscope instead of a pendulum. This would make the instrument applicable for steeper holes of up to probably 50° inclination.

APPENDIX II

ANALYSIS OF BOREHOLE SURVEYING DATA

APPENDIX II

ANALYSIS OF BOREHOLE SURVEY DATA

In order to be able to analyze the borescope data, the position in space of each borehole is needed. In this project, because boreholes are relatively short, they are assumed to be straight lines. A 3m (10 ft.) steel pipe of the same diameter (close fit) of the borehole (old core barrels are ideal) is inserted into the borehole to a depth of about 1.5m (5 ft.). Two points on the pipe are then surveyed at the end of the pipe (P_e) and at the collar of the borehole (P_b).

In general surveying, spherical coordinates (R_s, ω, ϕ) are used. To obtain Cartesian coordinates of a points, the following transformation is used.

$$Y_s = R_s \sin \omega \cos \phi \quad (\text{II.1})$$

$$X_s = R_s \sin \omega \sin \phi \quad (\text{II.2})$$

$$Z_s = R_s \cos \omega - H \quad (\text{II.3})$$

where X_s, Y_s and Z_s are Cartesian coordinates of a point in surveying coordinate system, R_s is the distance to the point, ω is the inclination measured from Z_s , ϕ is the azimuth and H is the height of the instrument from the global origin.

The vector \vec{R}_s calculated in this fashion is then transformed into the global coordinate system by:

$$R_i = n_{ij} R_{sj} \quad (\text{II.4})$$

where R_i are the global components of the vector, n_{ij} are the components of a 3 x 3 direction cosine matrix and R_{sj} are the components of the vector in surveying coordinate system. The direction cosine matrix is given by:

$$n_{ij} = \begin{bmatrix} \cos\beta & \sin\beta & 0 \\ -\sin\beta & \cos\beta & 0 \\ 0 & 0 & 1 \end{bmatrix} \quad (\text{II.5})$$

where β is the rotation angle. Inclination and azimuth of the borehole are calculated as follows:

$$\theta = \tan^{-1} (R_2/R_1) \quad (\text{II.6})$$

$$\gamma = \cos^{-1} (R_3/R)$$

where θ is the azimuth, and γ the inclination (from vertical).

The computer code BORSUR was written for analysis of the borehole orientation data. It should be noted that this program can also be used for reducing surveying data for any other line, such as detail lines used for fracture mapping. This program, however, is specifically designed so that its output can be directly used as an input for the BSCOPE computer code (see the following appendix). The input

format into the computer program is as follows:

<u>Record#</u>	<u>Variable</u>	<u>Description</u>	<u>Format</u>
1	BORENO	Borehole number	A10
2	HITE	Height of the instrument from the global origin	free
	XDEV	Azimuth of the line from the instrument to the reference point	"
	BLENGT	Length of the borehole	"
3	AZIMB	Azimuth of the beginning	free
	INCLB	Inclination of the begin- ning	"
	DISTB	Distance to " "	"
	AZIME	Azimuth to the end	"
	INCLE	Inclination the the end	"

Records 1 to 3 can be repeated for as many boreholes as desired. The program listing is included in the following pages.

Listing of BORSUR

```

00100 C
00200 C THIS PROGRAM REDUCES SURVEY DATA FROM THE ONWI ROOM
00300 C
00400 DOUBLE PRECISION BORENO
00500 REAL INCL,INCLB,INCLE
00600 OPEN(UNIT=10,FILE='BORSUR.DAT')
00700 OPEN(UNIT=11,FILE='BORSUR.OUT')
00800 IN=10
00900 IQUT=11
01000 WRITE(IQUT,1000)
01100 1 READ(IN,100,END=99) BORENO
01200 READ(IN,*) HITE,XDEV,BLENGT
01300 READ(IN,*) AZIMB,INCLB,DISTB,AZIME,INCLE,DISTE
01400 C
01500 C
01600 AZIMB=ANGLF(AZIMB)
01700 AZIME=ANGLF(AZIME)
01800 INCLB=ANGLF(INCLB)
01900 INCLE=ANGLF(INCLE)
02000 100 FORMAT(A10)
03000 C
03100 CONST=57.29577951
03200 C
03300 XBEGIN=XCORD(AZIMB,DISTB,INCLB,XDEV)
03400 YBEGIN=YCORD(AZIMB,DISTB,INCLB,XDEV)
03500 ZBEGIN=ZCORD(DISTB,INCLB,HITE)
03600 XEND=XCORD(AZIME,DISTE,INCLE,XDEV)
03700 YEND=YCORD(AZIME,DISTE,INCLE,XDEV)
03800 ZEND=ZCORD(DISTE,INCLE,HITE)
03900 C
04000 XBORE=XEND-XBEGIN
04100 YBORE=YEND-YBEGIN
04200 ZBORE=ZEND-ZBEGIN
04300 C
04400 BORLNG=SQRT(XBORE**2+YBORE**2+ZBORE**2)
04500 C
04600 BORAZ=ATAN(YBORE/XBORE)*CONST
04700 BORINC=ACOS(ZBORE/BORLNG)*CONST
04800 C
04900 WRITE(IQUT,1100) BORENO,XBORE,YBORE,ZBORE,BLENGT,BORAZ,
05000 1 BORINC
05100 GO TO 1
05200 99 STOP
05300 1000 FORMAT(5X,'BORE NO.',7X,'X-COORD',3X,'Y-COORD',3X,
05400 1 'Z-COORD',3X,'LENGTH',4X,'AZIMUTH',3X,'INCLINATION')
05500 1100 FORMAT(3X,A10,4X,6F10.3)
05600 END
05700 C
05800 C A SUBPROGRAM TO CONVERT DEG.MIN.SEC TO FRACTIONAL ANGLES
05900 C
06000 FUNCTION ANGLF(ANGLD)
06100 DEG=AINTE(ANGLD)
06200 ANGLD2=ANGLD-DEG
06300 CMIN=AINTE(ANGLD2*100.0)/60.0
06400 SEC=(ANGLD2*100.0-CMIN*60.0)/36.0
06450 ANGLF=DEG+CMIN+SEC
06500 RETURN
06600 END
06700 C
06800 C FUNCTION TO FIND X-COMPONENT OF VECTORS TO THE SURVEYED

```

```
06900 C POINT (INCLINATION MEASURED FROM VERTICAL)
07000 C
07100 FUNCTION XCORD(AZIM,DIST,INCL,XDEV)
07150 REAL INCL
07200 XCORD=DIST*SIND(INCL)*(COSD(AZIM)
07300 1 *COSD(XDEV)+SIND(AZIM)*SIND(XDEV))
07400 RETURN
07500 END
07600 C
07700 C FUNCTION TO FIND Y-COMPONENT OF VECTOR TO THE SURVEYED
07800 C POINT (INCLINATION MEASURED FROM VERTICAL)
07900 C
08000 FUNCTION YCORD(AZIM,DIST,INCL,XDEV)
08050 REAL INCL
08100 YCORD=DIST*SIND(INCL)*(COSD(AZIM)
08200 1 *SIND(XDEV)+SIND(AZIM)*COSD(XDEV))
08300 RETURN
08400 END
08500 C
08600 C FUNCTION TO FIND Z-COMPONENT OF VECTOR TO THE SURVEYED
08700 C POINT (INCLINATION MEASURED FROM VERTICAL)
08800 C
08900 FUNCTION ZCORD(DIST,INCL,HITE)
08950 REAL INCL
09000 ZCORD=DIST*COSD(INCL)+HITE
09100 RETURN
09200 END
```

RUW-1
-206.7,27.,652.78
348.0640,81.2810,540.5,348.1520,69.0400,572.8
RUW-2
-206.7,27.,624.84
337.4130,73.0215,312.5,337.4350,54.2340,368.7
RUW-3
-206.7,27.,604.52
302.5000,50.4640,142.2,302.3820,32.3730,148.3
RUW-4
-206.7,27.,632.46
210.1000,68.2000,198.3,209.4800,43.0910,267.5
RUW-5
-206.7,27.,612.14
193.2550,73.4310,355.5,193.0200,60.2800,391.6
RUW-6
-206.7,27.,614.68
191.4050,82.4430,604.5,191.3740,72.2540,631.3
RUE-1
-213.4,27.,619.76
12.3605,79.2115,518.8,12.4015,66.5020,554.23
RUE-2
-206.7,27.,629.92
21.4340,73.5122,328.6,21.4530,56.5525,376.7
RUE-3
-206.7,27.,604.52
59.2900,55.5225,165.9,58.2820,33.3705,250.
RUE-4
-206.7,27.,599.44
141.5000,67.1540,204.7,141.3620,44.2020,270.8
RUE-5
-206.7,27.,622.3
161.2700,76.3825,379.,161.2645,61.1840,421.6

EXAMPLE INPUT TO BORSUR PROGRAM

APPENDIX III

BSCOPE, A COMPUTER CODE FOR REDUCING DATA
FROM BOREHOLE SURVEYS WITH T.V. CAMERA AND
OTHER VISUAL INSTRUMENTS

APPENDIX III

BSCOPE, A COMPUTER CODE FOR REDUCING DATA
FROM BOREHOLE SURVEYS WITH T.V. CAMERA
AND OTHER VISUAL INSTRUMENTS

In situations where the oriented core (see Appendix I) does not provide accurate data about the fracture orientation, an alternative would be to map the borehole walls with some kind of visual or sensor device. The common visual aids for mapping borehole walls are T.V. camera, borescope (also known as petroscope or periscope), and borehole photographic camera. Some of the sensor instruments that can be used to map boreholes for fractures are borehole seisviewer (a sounding device) and dip meter. All these devices provide information about the position of the trace of the fracture on the borehole wall. This information can be used to compute the orientation of the fracture in space. Details of the algorithm are presented in section 5.3.6. The computer code BSCOPE was written on the basis of this algorithm. Following is a description for the use of this program.

It should be noted that there are two versions of the program. BSCOPE is written specifically to analyze data provided by Chitombo, et al (1981). They measured only three

points on each fracture. This code was later revised for a more general use where several points are measured on the same fracture. This code is named BSCTV. Following, instruction for use of the BSCOPE is provided which is similar to that for BSCTV.

Both programs were developed for use on the DEC-10 computer and are in DEC FORTRAN-10 language. For use with other computer systems, certain statements may need to be modified or replaced by proper statements. The OPEN statement is unfamiliar to most other machines, however, it can be easily replaced by DEFINE FILE statement which is standard in WATFIV computer language and is available in most advanced machines (such as IBM 360/370).

Two input files are required for both programs. The programs will ask for the file containing borescope (or T.V. camera) data, the output file name and the file containing borehole axes data. An auxiliary output file is also created that contains dip and strikes without any heading, to be used by other programs such as QUAD and FRACTAN (see section 5.3.5). The format for the input file containing the borescope data is as follows (see section 5.3.6 for description of the symbols):

Record #1 Borehole No. (A10) 10 characters

Record #2 Joint no., d_1 , d_2 , d_3 , Angle 1, Angle 2, Angle 3, Plane, surface, opening, aperture, filling 1 through 6 (free format)

Record #n repeat record number 2 for as many fractures in the same borehole as necessary

Record #n+1 -1
repeat records number 1 through n + 1 for different boreholes as many times as necessary.

If desired the characteristics may be left blank. Following codes are used for characteristics:

Plane

0 = blank
1 = planar
2 = irregular
3 = curved
4 = undulating
5 = bifurcates
6 = fracture zone

Opening: always < 0

- 0 = blank
- 1 = open
- 2 = semi open
- 3 = closed

Aperture = the actual measurement of the aperture.

Surface:

- 0 = blank
- 1 = smooth
- 2 = rough
- 3 = very rough

Filling:

- 0 = blank
- 1 = hematite
- 2 = pyrite
- 3 = clay
- 4 = chlorite
- 5 = quartz
- 1 = no filling

The format for the borehole orientation data file is:

- 1 Title (4A10) 40 characters title
 - 2 'RADII', 0, 0, 0, 0, 0, 0, 0, 0, 0, 0 (dummy card)
 - 3 Radius (decimal free format)
 - 4 'Borehole no.', X_b , Y_b , z_b , borehole length, AZ_1 , AZ_2 ,
 AZ_3 (azimuths), $Incl_1$, $Incl_2$, $Incl_3$
- o
- o
- n Repeat for all boreholes having same diameter.
If borehole diameter changes repeat dummy card no. 2,
then card no. 3 and continue as above. It should be
noted that BORSUR

It is important that Borehole number be enclosed in quotation marks and all zeroes be present in record number 2. Following is the program listing and input output samples.

Program listing of the BSCOPE

```

00010 C-----
00020 C PROGRAM TO FIND STRIKE AND DIP OF FRACTURE PLANE DETERMINED
00030 C BY THREE GENERAL POINTS MEASURED ON A BOREHOLE WALL
00040 C
00050 C-----
00060 C
00070 C BY PARVIZ MONTAZER
00080 C COLO. SCH. OF MINES 1981
00090 C-----
00100 DIMENSION DIRCOS(3,3),DIST(3),ANGL(3),PTCJOR(3,3),
00110 1 VEC(3),IFILL(6),FILL(6),AZIM(3),INCL(3)
00120 REAL NORMAL(3,1),NORMAG,INCL,NORMA(3,1)
00130 DOUBLE PRECISION PLANE,IAPER,SURF,BURENG
00140 1 ,BOREN2,TITLE(4,2)
00150 LOGICAL NPOS1,NPOS2,NPOS3,NNEG1,NNEG2,NNEG3
00160 OPEN(UNIT=12,FILE='BSCOP.IN',DIALOG)
00170 OPEN(UNIT=13,FILE='BSCOP.OUT',DIALOG)
00180 OPEN(UNIT=14,FILE='BORDIR.DAT',DIALOG)
00182 OPEN(UNIT=15,FILE='BSCOPI.OUT')
00190 IN1=12
00200 IN2=14
00210 IOUT=13
00215 IOUT2=15
00220 WRITE(IOUT,1200)
00230 DO 4 J=1,2
00240 READ(IN2,300)(TITLE(I,J),I=1,4)
00250 300 FORMAT(4A10)
00260 4 WRITE(IOUT,1300)(TITLE(I,J),I=1,4)
00270 1200 FORMAT(/////////37X,'FRACTURE CHARACTERISTICS FROM
00280 1 BOREHOLE SURVEY'/)
00290 1300 FORMAT(40X,4A10)
00300 1 READ (IN2,*,END=99)BORENO,XBORE,YBORE,ZBORE,BLENGT,
00310 1 (AZIM(I),I=1,3),(INCL(I),I=1,3)
00320 IF(BLENGT.LE.0.0)READ(IN2,*)BORAD
00330 CC TYPE *,BORAD
00340 IF(BLENGT.LE.0.0)GO TO 1
00350 READ(IN1,100) BOREN2
00360 IF(BOREN2.NE.BORENO)TYPE 1125
00370 WRITE(IOUT,1000) BORENG
00375 WRITE(IOUT2,1111)BORENG
00377 1111 FORMAT(1X,A10)
00380 100 FORMAT(A10)
00390 2 READ(IN1,200,END=99) JOING,(DIST(I),I=1,3),(ANGL(I),
00400 1 I=1,3),IPLANE,ISURF,IOPEN,APER,(IFILL(I),I=1,6)
00410 200 FORMAT(1,6F,3I,F,6I)
00420 IF(JOING.LT.0) GO TO 1
00430 C
00440 C FIND DIRECTION COSINES FOR BOREHOLE COORDINATE SYSTEM
00450 C
00460 DO 5 J=1,3
00470 DIRCOS(1,J)=COSD(INCL(J))*COSD(AZIM(J))
00480 DIRCOS(2,J)=COSD(INCL(J))*SIND(AZIM(J))
00490 DIRCOS(3,J)=SIND(INCL(J))
00500 5 CONTINUE
00510 C
00520 C
00530 C
00540 C
00550 C
00560 C TRANSFORM CYLINDRICAL TO RECTANGULAR COORDINATES FOR THE

```

```

00570 C THREE POINTS
00580 C
00590 DO 50 I=1,3
00600 PTCOOR(I,1)=BORAD*COSD(ANGL(I))
00610 PTCOOR(I,2)=BORAD*SIND(ANGL(I))
00620 PTCOOR(I,3)=DIST(I)
00630 50 CONTINUE
00640 C
00650 C
00660 TYPE 1100,JOIND
00670 TYPE 9900,PTCOOR
00680 C
00690 DO 145 I=1,3
00700 145 TYPE 9900,(DIRCOS(I,J),J=1,3)
00710 ANO=PTCOOR(1,2)-PTCOOR(3,2)
00720 BNO=PTCOOR(1,3)-PTCOOR(2,3)
00730 CNO=PTCOOR(1,3)-PTCOOR(3,3)
00740 DNO=PTCOOR(1,2)-PTCOOR(2,2)
00750 ENO=PTCOOR(1,1)-PTCOOR(3,1)
00760 FNO=PTCOOR(1,1)-PTCOOR(2,1)
00770 C
00780 NORMAL(1,1)=ANO*BNO-CNO*DNO
00790 NORMAL(2,1)=CNO*FNO-ENO*BNO
00800 NJRMAL(3,1)=ENO*DNO-ANO*FNO
00810 TYPE 9900,NORMAL
00820 CALL MATMUL(3,1,3,DIRCOS,NORMAL,NORMA)
00830 TYPE 9900,NORMA
00840 9900 FORMAT(IX,3F10.3)
00850 C
00860 CONST=57.29577951
00870 C
00880 NORMMAG=SQRT(NORMA(1,1)**2+NORMA(2,1)**2+NORMA(3,1)**2)
00890 C
00900 DIP=ACOS(ABS(NORMA(3,1)/NORMMAG))*CONST
00910 IF(NORMA(1,1).EQ.0.0)STRDIR='N'
00920 IF(NORMA(2,1).EQ.0.0)STRDIR='E'
00930 IF(NORMA(2,1)+NORMA(1,1).NE.0.0)GO TO 35
00940 STRDIR='N'
00950 STRIKE=0.0
00960 GO TO 37
00970 35 STRIKE=ABS(ASIN(NORMA(1,1)/SQRT(NORMA(1,1)**2+NORMA(2,1)**2)))
00980 1 *CONST
00990 STRDIR='E'
01000 IF(NORMA(1,1)*NORMA(2,1).GT.0.0) STRDIR='W'
01010 C
01020 37 AN=NORMA(1,1)
01030 BN=NORMA(2,1)
01040 CN=NORMA(3,1)
01050 TYPE *,AN,BN,CN
01060 NPOS1=(AN.GE.0.0)
01070 NPOS2=(BN.GE.0.0)
01080 NPOS3=(CN.GE.0.0)
01090 NNEG1=(AN.LT.0.0)
01100 NNEG2=(BN.LT.0.0)
01110 NNEG3=(CN.LT.0.0)
01120 IF((NPOS1.AND.NPOS2.AND.NPOS3).OR.(NNEG1.AND.NNEG2.AND.
01130 1 NNEG3)) DIPDIR='SW'
01140 IF((NNEG1.AND.NPOS2.AND.NPOS3).OR.(NPOS1.AND.NNEG2.AND.
01150 1 NNEG3)) DIPDIR='NW'
01160 IF((NNEG1.AND.NNEG2.AND.NPOS3).OR.(NPOS1.AND.NPOS2.AND.

```

```

01170      1          NNEG3)) DIPDIR="NE"
01180      IF((NPOS1.AND.NNEG2.AND.NPOS3).OR.(NNEG1.AND.NPOS2.AND.
01190      1          NNEG3)) DIPDIR="SE"
01200      IF(CN.EQ.0.0)DIPDIR=" "
01210      IF(DIP.EQ.0.0)DIPDIR=" "
01220      DISTAN=(DIST(1)+DIST(2)+DIST(3))/3.0
01230      C
01240      C
01245      IF(IPLANE.EQ.0)PLANE="-----"
01250      IF(IPLANE.EQ.1) PLANE="PLANAR"
01260      IF(IPLANE.EQ.2) PLANE="IRREGULAR"
01270      IF(IPLANE.EQ.3) PLANE="CURVED"
01280      IF(IPLANE.EQ.5) PLANE="BIFURCATED"
01290      IF(IPLANE.EQ.4) PLANE="UNDULATING"
01300      IF(IPLANE.EQ.6.OR.DIST(1).LT.0.0.OR.DIST(2).LT.0.0.OR.
01310      1          DIST(3).LT.0.0) PLANE="FRAC ZONE"
01315      IF(IOPEN.EQ.0)IAPER="-----"
01320      IF(IOPEN.EQ.-1.0) IAPER="OPEN"
01330      IF(IOPEN.EQ.-2.0) IAPER="SEMI OPEN"
01340      IF(IOPEN.EQ.-3.0) IAPER="CLOSED"
01345      IF(ISURF.EQ.0)SURF="-----"
01350      IF(ISURF.EQ.1) SURF="SMOOTH"
01360      IF(ISURF.EQ.2) SURF="ROUGH"
01370      IF(ISURF.EQ.3) SURF="VERY ROUGH"
01380      DO 55 I=1,6
01385      IF(IFILL(I).EQ.0)FILL(I)=" "
01390      IF(IFILL(I).EQ.1) FILL(I)="HEMA."
01400      IF(IFILL(I).EQ.2) FILL(I)="PYRI."
01410      IF(IFILL(I).EQ.3) FILL(I)="CLAY"
01420      IF(IFILL(I).EQ.4) FILL(I)="CHLO."
01430      IF(IFILL(I).EQ.5) FILL(I)="QUAR."
01435      IF(IFILL(I).EQ.-1)FILL(I)="NO FIL"
01440      55      CONTINUE
01450      C
01460      C
01462      C      WRITE(IOUT2,1350)JOINC,(DIST(I),I=1,3),(ANGL(I),I=1,3)
01464      C      1 ,PLANE,SURF,IAPER,APER,(FILL(I),I=1,6)
01466      1350  FORMAT(1X,I3,6F8.3,2X,3A10,6F8.4,2X,6A5)
01470      WRITE(IOUT,1100) JOINC,DISTAN,DIP,DIPDIR,STRIKE,STRDIR,
01480      1  APER,PLANE,SURF,(FILL(I),I=1,6),IAPER
01482      WRITE(IOUT2,1100) JOINC,DISTAN,DIP,DIPDIR,STRIKE,STRDIR,
01484      1  APER,PLANE,SURF,(FILL(I),I=1,6),IAPER
01490      GO TO 2
01500      1000  FORMAT(1H1///50X,"BOPEHOLE NO.:"A10//2X,"JOINT",2X,"DIST",
01510      1  2X,"DIP",5X,
01520      1  "STRIKE",3X,"APER",4X,"PLANE",5X,"SURFACE",17X,"FILLING",
01530      2  25X,/4X,"NO.",2X,"ANGLE",19X,"TURE"/9X,"(M.)",19X,"(CM.)"/)
01540      1100  FORMAT(2X,I3,F8.2,F5.1,A2,3X,"N",F4.1,A1,F8.3,3X,2(A10,2X)
01550      1  ,6(A5,2X),A10)
01560      1125  FORMAT(5X,"THE TWO FILES ARE NOT IN THE SAME ORDER")
01570      99      STOP
01580      END
01590      SUBROUTINE MATMUL(M,N,L,A,B,C)
01600      DIMENSION A(M,L),B(L,N),C(M,N)
01610      TYPE 9900,A,B,C
01620      DO 10 I=1,M
01630      DO 10 J=1,N
01640      CIJ=0.0
01650      DO 5 K=1,L
01660      CIJ=A(I,K)*B(K,J)+CIJ

```

```
01670  CC      TYPE *,I,J,K
01680  CC      TYPE 9900,A(I,K),B(K,J),CIJ
01690  5        CONTINUE
01700                C(I,J)=CIJ
01710  CC      TYPE 9900,CIJ
01720  10      CONTINUE
01730                RETURN
01740  9900    FORMAT(1X,3F10.3)
01750                END
```


RDW-1

1,2.22,2.13,2.15,0,-90,-45,0,2,-1,.5,0
 2,2.06,2.00,2.01,180,-90,-135,0,2,-1,.175,0
 3,1.91,1.89,1.92,0,-90,90,0,2,-3,.09,1
 4,1.75,1.75,1.74,90,45,0,1,0,-2,.175,1
 5,1.37,1.32,1.35,0,-90,-45,1,0,-1,.375,0
 6,1.30,1.3,1.3,0,-45,-90,1,0,-1,.55,0
 7,1.14,1.17,1.03,0,90,-90,0,2,-2,.625,2
 8,.98,1.01,.89,-90,-45,-135,1,0,-2,.175,1
 9,.86,.87,.83,90,0,-90,1,0,-1,.375,0
 10,.82,.8,.73,90,0,-90,1,0,-1,1.25,0
 11,.7,.69,.73,-45,0,45,0,2,-1,1.25,0
 -1

RDE-1

1,2.35,2.35,2.32,-45,0,45,0,2,-1,.375,0
 4,1.22,1.23,1.21,-135,180,90,1,0,-1,1.5,0
 7,1.85,1.81,1.86,-90,0,45,0,2,-2,.5,1
 8,1.8,1.71,1.68,-90,-135,-45,1,0,-1,.375,0
 9,1.68,1.65,1.62,45,-90,0,1,0,-2,.75,2
 10,1.55,1.59,1.6,-45,0,90,2,0,-1,.875,0
 11,1.42,1.39,1.35,-45,0,45,1,0,-2,.25,1
 12,1.09,1.12,1.13,45,0,90,0,2,-1,.5,0
 13,.915,.92,.9,45,0,-45,1,0,-3,.5,2
 15,.42,.38,.46,-45,0,-90,0,2,-1,.375,0
 16,.09,.05,.23,45,0,-90,1,0,-1,.25,0
 -1

RDD-1

1,1.93,1.94,1.93,-90,180,-135,1,0,-1,.625,0
 2,1.85,1.85,1.89,90,0,-45,1,0,-1,.425,0
 3,1.54,1.55,1.38,0,90,180,1,0,-3,1.05,2
 4,1.34,1.3,1.3,0,45,-45,0,2,-1,.175,0
 5,1.28,1.2,1.19,-90,180,0,0,2,-2,.55,1
 6,.6,.59,.58,90,45,135,0,2,-1,.175,0
 7,.5,.49,.47,90,45,135,0,2,-1,.625,0
 8,.5,.55,.53,0,-90,-45,0,2,-1,.175,0
 9,.37,.33,.4,90,135,45,1,0,-1,.375,0
 10,.14,.08,.07,90,0,-90,1,0,-1,1.5,0
 -1

RHE-1

1,2.64,2.61,2.59,90,0,-90,1,0,-1,.625,0
 2,1.19,1.2,1.12,0,-90,-45,0,2,-1,.175,0
 3,1.18,1.17,1.13,90,180,0,1,0,-1,1.5,0
 4,1.1,1.02,1.02,0,90,45,1,0,-1,.625,0
 5,.03,.01,.02,90,180,0,1,0,-1,.3,0
 -1

RDU-1

1,2.55,2.52,2.57,90,135,45,1,0,-1,.175,0
 2,2.24,2.22,2.19,0,90,-90,1,0,-1,.75,0
 3,1.85,1.84,1.77,0,90,-90,1,0,-1,.175,0
 4,1.73,1.69,1.71,90,180,135,0,2,-2,.09,1
 5,.38,.4,.28,0,90,-90,1,0,-1,1.5,0
 6,.2,.2,.18,0,90,-90,1,0,-1,.625,0
 7,.16,.08,.01,90,45,0,1,0,-1,.175,0
 -1

RUE-1

1,2.54,2.49,2.35,-45,0,90,1,0,-2,1.25,1
 2,2.27,2.39,2.35,-45,0,45,1,0,-2,.625,2
 12,1.09,1.1,1.1,45,0,90,0,2,-2,.625,2
 15,.91,.95,.92,45,0,90,1,0,-2,1.25,2
 16,.75,.97,.75,-45,0,-90,1,0,-2,1.,2

Input file to BSCOPE containing fracture data from boreholes.

EXPERIMENTAL MINE OF COLO. SCH. OF MINES
UN#1 ROOM

RADII,0,0,0,0,0,0,0,0,0,0
0.0381

RDW-1	-0.380	-1.523	-114.536	454.660	60.000	150.000	-120.000	0.000	0.000	90.000
RDE-1	0.479	0.337	-114.541	467.360	60.000	150.000	-120.000	0.000	0.000	90.000
RDD-1	44.756	75.999	-80.869	464.820	59.506	149.506	59.506	-47.482	0.000	42.518
RHE-1	67.153	113.856	0.174	480.060	-120.532	149.468	59.468	-89.925	0.000	-0.075
RDU-1	50.192	83.553	82.886	464.820	-120.994	149.006	59.006	-49.623	0.000	-40.377
RUE-1	-0.147	0.278	122.147	619.760	-120.000	150.000	60.000	0.000	0.000	-90.000
RUW-1	1.245	1.435	124.371	652.780	-120.000	150.000	60.000	0.000	0.000	-90.000
RDW-2	-0.252	-0.648	-114.472	457.200	60.000	150.000	-120.000	0.000	0.000	90.000
RDE-2	0.102	-0.067	-114.531	459.740	60.000	150.000	-120.000	0.000	0.000	90.000
RDD-2	39.588	72.192	-83.113	472.440	61.261	151.261	61.261	-44.730	0.000	45.270
RHE-2	60.427	108.752	0.111	447.040	-119.058	150.942	60.942	-89.949	0.000	-0.051
RDU-2	39.596	74.839	88.298	461.010	-117.882	152.118	62.118	-43.798	0.000	-46.202
RUE-2	0.027	0.119	114.219	629.920	-120.000	150.000	60.000	0.000	0.000	-90.000
RUW-2	0.718	0.274	123.487	624.840	-120.000	150.000	60.000	0.000	0.000	-90.000
RDW-3	0.636	-0.851	-115.473	462.280	60.000	150.000	240.000	0.000	0.000	90.000
RDE-3	-0.977	-0.535	-115.527	464.820	60.000	150.000	-120.000	0.000	0.000	90.000
RDD-3	39.252	74.251	-80.711	457.200	62.137	152.137	62.137	-46.140	0.000	43.860
RHE-3	58.226	109.862	0.951	472.440	-117.923	152.077	62.077	-89.562	0.000	-0.438
RDU-3	40.354	74.818	87.582	457.200	-118.341	151.000	659.000	61.659	-44.145	0.000
RUE-3	2.220	0.906	115.113	604.520	-120.000	150.000	60.000	0.000	0.000	-90.000
RUW-3	-1.221	4.045	68.672	604.520	-120.000	150.000	60.000	0.000	0.000	-90.000
RDW-4	0.773	-0.056	-115.121	462.280	60.000	150.000	240.000	0.000	0.000	90.000
RDE-4	1.183	1.296	-114.513	464.820	60.000	150.000	-120.000	0.000	0.000	90.000
RDD-4	42.701	62.899	-124.964	467.360	55.828	145.828	55.828	-31.315	0.000	58.685
RHE-4	63.849	112.800	0.397	474.980	-119.512	150.488	60.488	-89.824	0.000	-0.176
RDU-4	44.161	77.322	87.737	464.820	-119.732	150.268	60.268	-45.424	0.000	-44.576
RUE-4	0.485	0.829	114.558	599.440	-120.000	150.000	60.000	0.000	0.000	-90.000
RUW-4	1.287	1.751	121.972	632.460	-120.000	150.000	60.000	0.000	0.000	-90.000
RDW-5	-0.918	-0.578	-114.575	447.040	60.000	150.000	240.000	0.000	0.000	90.000
RDE-5	0.098	0.728	-88.513	474.980	60.000	150.000	-120.000	0.000	0.000	90.000
RDD-5	41.511	74.607	-80.637	492.760	60.909	150.909	60.909	-46.636	0.000	43.364
RHE-5	61.020	111.313	0.489	459.740	-118.731	151.269	61.269	-89.779	0.000	-0.221
RDU-5	42.101	75.578	88.963	469.900	-119.120	150.880	60.880	-44.200	0.000	-45.800
RUE-5	-0.751	-0.135	114.817	622.300	-120.000	150.000	60.000	0.000	0.000	-90.000
RUW-5	1.073	2.144	93.370	612.140	-120.000	150.000	60.000	0.000	0.000	-90.000
RDW-6	2.730	1.468	-114.461	467.360	60.000	150.000	240.000	0.000	0.000	90.000
RDE-6	0.521	1.069	-56.747	447.040	60.000	150.000	-120.000	0.000	0.000	90.000
RDD-6	42.532	75.213	-80.662	477.520	60.512	150.512	60.512	-46.000	969.000	0.000
RHE-6	63.676	112.435	-1.740	464.820	60.475	150.475	60.475	-89.228	0.000	0.772
RDU-6	42.641	76.535	88.975	477.520	-119.124	150.876	60.876	-44.558	0.000	-45.442
RUE-6	1.106	0.497	114.574	619.480	-120.000	150.000	60.000	0.000	0.000	-90.000
RUW-6	-1.961	-0.933	114.220	614.680	-120.000	150.000	60.000	0.000	0.000	-90.000

Input file to BSCOPE containing information about borehole orientation.

APPENDIX IV

FRACTURE FREQUENCY AND RQD

APPENDIX IV

FRACTURE FREQUENCY AND RQD

In order to calculate fracture frequency and RQD for the data obtained from core logging (see sections 5.2.2 and 5.4.3), the computer code FRACTR was written. This program was written in a general form so that it can be employed to analyze data from any kind of scanline fracture mapping. Details of the calculations involved are presented in section 5.4.3 of the main text. Here, a brief description of the program and a brief instruction for its application is provided.

The input into the program is simply the distances to the fractures along a scanline. The program interactively asks for the option (on the terminal). There are four options that can be chosen:

1. All distances for each scanline are on the same record (free format).
2. All distances are in column. This option is useful for files that contain records of fracture characteristics and begin with the distance.
3. The source file contains distances to the fractures in an increasing order.

4. Same as 3 except that data are not in order.

It is recommended that option 3 be used if possible as other options are somewhat complicated. Options one and two require certain code numbers in the data file that should be carefully inserted. These options are most useful for data that are in segments, for example data that are obtained from core logging in the field which are usually separated for each box. Examples for each types of optional file formats are provided in the following pages along with the program listing and a sample output. The output information from FRACTR was plotted along the boreholes around the CSM/ONWI room using a plotting routine written for this purpose by Manouch Bahavar (1981, personal communication). The results for the radial boreholes follow the program listing.

```

00100 CCCCCCCCCCCCCCCCCCCCCCCCCCCCCCCCCCCCCCCCCCCCCCCCCCCCCCCCCCCCC
00200 C
00300 C
00400 C
00500 C
00600 C
00700 C
00800 C
00900 C
01000 C
01100 C
01200 C
01300 CCCCCCCCCCCCCCCCCCCCCCCCCCCCCCCCCCCCCCCCCCCCCCCCCCCCCCCCC
01400 C
01500 C
01600 C
01700 C
01800 C
01900 C
02000 C
02100 C
02200 C
02300 C
02400 C
02500 C
02600 CCCCCCCCCCCCCCCCCCCCCCCCCCCCCCCCCCCCCCCCCCCCCCCCCCCCCCCCC
02700 C
02800 C
02900 C
03000 C
03100 C
03200 C
03300 C
03400 C
03500 C
03600 C
03700 CCCCCCCCCCCCCCCCCCCCCCCCCCCCCCCCCCCCCCCCCCCCCCCCCCCCCCCCC
03800 C
03900 C
04000 C
04100 C
04200 C
04300 C
04400 C
04500 C
04600 CCCCCCCCCCCCCCCCCCCCCCCCCCCCCCCCCCCCCCCCCCCCCCCCCCCCCCCCC
04700 C
04800 C
04900 C-----INITIALIZATION
05000 C
05100 C
05200 C
05300 C
05400 C
05500 C
05600 C-----UNIT 8 IS THE INPUT FILE
05700 C
05800 C
05900 C
06000 C-----UNIT 9 IS THE MAIN OUTPUT FILE

```

FRACTR.FOR

SEPTEMBER, 1981
COLORADO SCHOOL OF MINES, GOLDEN, COLO.
PARVIZ M. MONTAZER LESLIE SOUR

THIS PROGRAM CALCULATES FRACTURE FREQUENCY, ACTUAL RQD,
THEJRETICAL RQD, AND RECOVERY FOR CORE LOG AND LINE MAP
FRACTURE DATA.

- AR = INITIAL DATA ARRAY, INCLUDES CODES (SEE NOTE)
DIST = FINAL DATA ARRAY, IS DISTANCE TO EACH FRACTURE
FRJM ORIGIN (BEGINNING OF BOREHOLE OR BASELINE)
NUMFRA = TOTAL NUMBER OF FRACTURES
FREQ = FRACTURE FREQUENCY PER METER
RQD = % OF METER INTERVAL IN PIECES > TWICE THE CORE
DIAMETER IN LENGTH
RQDA = RQD ADJUSTED FOR THE CORE RECOVERY
TRQD = THEJRETICAL RQD (EQUATION FROM PRIEST AND HUDSON,
1976)

INPUT CODES:

- 1 = DATA FOR EACH BOREHOLE OR BASELINE IS IN A SINGLE
LINE IN THE DATA FILE. IF THERE IS TOO MUCH DATA
FOR ONE LINE, A -99 CODE INDICATES CONTINUATION
2 = SAME AS # 1, BUT THE FORMAT IS COLUMN
3 = DATA FOR EACH BOREHOLE OR BASELINE IS IN A SEPARATE
DATA FILE, AND DISTANCES ARE IN ORDER FROM ORIGIN
4 = SAME AS # 3, BUT DISTANCES ARE NOT IN ORDER

DATA CODES FOR #1 AND #2:

- 1 = END OF CORE BOX DIVISION
-2 = FRACTURE ZONE FROM PREVIOUS DISTANCE TO FOLLOWING
DISTANCE
-3 = FOLLOWING DISTANCE IS A FOOT MARKER
-99 = DATA ON NEXT LINE IS CONTINUATION OF BOREHOLE

DOUBLE PRECISION NAME
DIMENSION AR(1500),DIST(2000),RQD(50),FREQ(50),RQDA(50)
1,RQDT(50)
COMMON DIST

UNIT 8 IS THE INPUT FILE

OPEN(UNIT=8,DIALOG)

UNIT 9 IS THE MAIN OUTPUT FILE

```

06100 C
06200 OPEN(UNIT=9,DIALOG)
06300 C
06400 C-----UNIT 10 IS THE RQD OUTPUT FILE FOR MAPLOT.FOR
06500 C
06600 OPEN(UNIT=10,DIALOG)
06700 C
06800 C-----UNIT 11 IS THE FRACTURE FREQUENCY OUTPUT FILE FOR MAPLOT.FOR
06900 C
07000 OPEN(UNIT=11,DIALOG)
07100 IN=8
07200 IOUT=9
07300 IFILE=0
07400 C
07500 C-----NAME IS THE BOREHOLE LABEL, AND IS THE FIRST PIECE OF DATA
07600 C-----IN THE INPUT FILE
07700 C
07800 15 CJNTINUE
07900 READ(IN,100,END=99)NAME
08000 100 FORMAT(A10)
08100 C WRITE(IOUT,100)NAME
08200 C
08300 C-----CHECK THE INPUT FILE TYPE
08400 C
08500 IF(IFILE.EQ.1)GO TO 23
08600 TYPE 106
08700 106 FORMAT(1X,"TYPE IN THE FILE TYPE"/
08800 11X,"(LINE DATA=1,COLUMN=2,ORDERED=3,UNORDERED COLUMN=4)")
08900 ACCEPT *,IFILE
09000 IF(IFILE.EQ.1)GO TO 23
09100 IF(IFILE.EQ.3)GO TO 56
09200 C IF(IFILE.EQ.4)GJ TO 52
09300 C
09400 C-----FILE CODE 2
09500 C
09600 DO 22 I=1,1500
09700 22 READ(IN,*,END=8)AR(I)
09800 C
09900 C-----FILE CODE 1
10000 C
10100 23 CONTINUE
10200 READ(IN,300,END=99)AR
10300 NUM=1
10400 2 CJNTINUE
10500 IDUM=NUM
10600 DO 16 II=IDUM,1500
10700 IF(AR(II).EQ.0.0)GO TO 17
10800 NUM=II
10900 16 CJNTINUE
11000 17 CJNTINUE
11100 IF(AR(NUM).GT.-99)GO TO 8
11200 READ(IN,300,END=99) (AR(I),I=NUM,1500)
11300 GO TO 2
11400 8 CJNTINUE
11500 C
11600 C-----LOOP TO CONVERT INITIAL, CODED ARRAY TO ARRAY CONTAINING
11700 C-----ONLY DISTANCES TO FRACTURES
11800 C
11900 DO 5 I=1,1500
12000 IF(AR(I).EQ.0.0)GO TO 7

```

```

12100      NUM=I
12200      5      CONTINUE
12300      7      CONTINUE
12400      300    FORMAT(1500F)
12500      FRDIST=0.0
12600      NUMFRA=0
12700      DO 55 I=1,NUM
12800      NQFRAZ=0
12900      IFLAG=0
13000      IF(AR(I).LT.0.0)IFLAG=INT(AR(I))
13100      IF(IFLAG.GT.-3)GO TO 10
13200      FTMARK=AR(I+1)
13300      GO TO 55
13400      10     CONTINUE
13500      IF(IFLAG.NE.-2)GO TO 20
13600      IF(I.EQ.1)X=0.0
13700      IF(I.GT.1)X=AR(I-1)
13800      IF(INT(AR(I-2)).EQ.-3)X=AR(I-3)
13900      IF(INT(AR(I-1)).EQ.-1)X=0.0
14000      NJFRAZ=INT((AR(I+1)-X)/0.5-0.001)
14100      IF(NQFRAZ.EQ.0)GO TO 40
14200      DO 40 J=NUMFRA+1,NUMFRA+NQFRAZ
14300      DIST(J)=X+(J-NUMFRA)*0.5+FRDIST
14400      40     CONTINUE
14500      NUMFRA=NUMFRA+NQFRAZ
14600      GO TO 55
14700      20     CONTINUE
14800      IF(IFLAG.NE.-1) GO TO 30
14900      Y=AR(I-1)
15000      IF(INT(AR(I-2)).EQ.-3)Y=AR(I-3)
15100      FRDIST=Y+FRDIST
15200      IF(AR(I+1).GT.1.0) GO TO 55
15300      FRDIST=FRDIST-AR(I+1)
15400      NUMFRA=NUMFRA-1
15500      GO TO 55
15600      30     CONTINUE
15700      IF(INT(AR(I-1)).EQ.-3)GO TO 55
15800      IF(I.LT.3)GO TO 31
15900      IF(INT(AR(I-2)).NE.-3)GO TO 31
16000      FRDIST=FRDIST-AR(I)+AR(I-3)
16100      GO TO 55
16200      31     CONTINUE
16300      NUMFRA=NUMFRA+1
16400      DIST(NUMFRA)=AR(I)+FRDIST
16500      55     CONTINUE
16600      C      DO 60 I=1,NUMFRA
16700      C60    WRITE(10UT,400) DIST(I),I
16800      400    FORMAT(1X,F7.2,16)
16900      C
17000      C
17100      GO TO 59
17200      C
17300      C-----FILE CODE 3
17400      C
17500      56     CONTINUE
17600      DO 57 I=1,2000
17700      READ(IN,*,END=58)DIST(I)
17800      IF(DIST(I).LT.0)GO TO 58
17900      NUMFRA=I-1
18000      57     CONTINUE

```



```

18100 58      FIMARK=DIST(NUMFRA+1)
18200 C      NUMFRA=NUMFRA-1
18300 C
18400 C-----FILE CODE 4
18500 C
18600 C52      IF(IFILE.EQ.4)CALL ORDER
18700 C
18800 C-----INPUT HAS BEEN DECODED, NOW FRACTURE FREQUENCY AND
18900 C-----RQD WILL BE CALCULATED
19000 C
19100 59      CONTINUE
19200      MM=1
19300      NN=NUMFRA/20
19400 C
19500 C-----THE DISTANCE ARRAY IS OUTPUT TO CHECK IN A SEPARATE
19600 C-----LPT FILE
19700 C
19800      DO 691 I=1,NN+1
19900 C      PRINT 690,(DIST(II),II=MM,20*I)
20000 691      MM=20*I+1
20100 690      FORMAT(2X,20F6.1)
20200 C
20300 C-----INITIALIZATION FOR MAIN CALCULATION LOOP
20400 C
20500      DATA RQDA/50*000.00/
20600      KJUNT=0
20700      TSUM=0.0
20800      SUM=0.0
20900      INCRE=1
21000      TESTI=1.0
21100      TEST=TESTI
21200 C
21300 C-----THRVLU (THRESHOLD VALUE) IS TWICE THE CORE DIAMETER
21400 C-----EXPRESSED IN METERS
21500 C
21600      THRVLU=0.10795
21700 C
21800 C-----MAIN CALCULATION LOOP
21900 C
22000      DO 70 K=1,NUMFRA
22100          J=K
22200 C
22300 C-----KJUNT IS THE FRACTURE COUNTER
22400 C
22500      KOUNT=KOUNT+1
22600 C
22700 C-----CONVERTING DISTANCES TO METERS
22800 C
22900      DIST(J)=DIST(J)*.0254
23000      T=0.0
23100      IF(J.GT.1)T=DIST(J-1)
23200 C
23300 C-----DIF IS THE LENGTH OF THE CORE PIECE BETWEEN 2 FRACTURES
23400 C
23500      DIF=DIST(J)-T
23600      IF(DIF.GE.THRVLU)SUM=SUM+DIF
23700      IF((DIST(J).GE.TEST).OR.(J.EQ.NUMFRA))GO TO 105
23800 C
23900 C-----AT THE END OF A METER INTERVAL, GO TO STATEMENT 105 TO
24000 C-----CALCULATE RQD AND FREQUENCY FOR THE INTERVAL

```

```

24100 C
24200 GO TO 70
24300 105 CONTINUE
24400 C
24500 C-----DENOM IS THE LENGTH OF THE INTERVAL FOR WHICH FREQUENCY
24600 C-----IS CALCULATED. IT IS 1 METER EXCEPT AT THE END OF THE
24700 C-----BOREHOLE.
24800 C
24900 DENOM=1.0
25000 IF((J.EQ.NUMFRA).AND.(DIST(NUMFRA).LT.TEST))
25100 1 DENOM=DIST(NUMFRA)-(TEST-1)
25200 C
25300 C-----CALCULATION OF FREQUENCY
25400 C
25500 FREQ(INCRE)=(KOUNT-1)/DENOM
25600 C
25700 C-----IF THE METER MARK IS WITHIN A PIECE > 4.25" (.10795 M)
25800 C-----LONG, SUM IS CORRECTED TO INCLUDE ONLY THAT PORTION OF
25900 C-----THE PIECE THAT IS INSIDE THE INTERVAL. THE REMAINDER
26000 C-----OF THE LENGTH OF THE PIECE IS THE "ZERO" OF THE SUM
26100 C-----FOR THE NEXT INTERVAL.
26200 C
26300 IF((J.EQ.NUMFRA).AND.(DIST(NUMFRA).LT.TEST))
26400 1 GO TO 107
26500 IF(DIF.GT.THRVLU)SUM=SUM-(DIST(J)-TEST)
26600 C
26700 C-----CALCULATION OF RQD (SUM IS TOTAL LENGTH OF PIECES IN THE
26800 C-----INTERVAL WITH INDIVIDUAL LENGTHS > 4.25")
26900 C
27000 107 RQD(INCRE)=SUM*100.0/DENOM
27100 TSUM=TSUM+SUM
27200 C
27300 C-----ZEROING COUNTERS FOR NEXT METER INTERVAL
27400 C
27500 SUM=0.0
27600 IF(DIF.GE.THRVLU)SUM=DIST(J)-TEST
27700 INCRE=INCRE+1
27800 TEST=TEST+INCRE
27900 KOUNT=1
28000 IF((J.EQ.NUMFRA).AND.(DIST(J).GT.(TEST-1.)))
28100 1 RQD(INCRE)=100.0
28200 70 CONTINUE
28300 XMTMRK=FTMARK*.3048
28400 C
28500 C-----CALCULATION OF RECOVERY, AVG FREQUENCY, & AVG RQD FOR BOREHOLE
28600 C
28700 RECOV=DIST(NUMFRA)/XMTMRK*100.0
28800 IFREQ=(NUMFRA-1)/XMTMRK
28900 TRQD=TSUM/XMTMRK*100.0
29000 C
29100 C-----ADJUSTMENT OF FREQUENCY & RQD FOR RECOVERY
29200 C
29300 ADJUST=RECOV/100.0
29400 DJ 90 MM=1,INCRE
29500 M=MM
29600 RQDT(M)=100.0*EXP(-THRVLU*FREQ(M))*(FREQ(M)*THRVLU+1)
29700 FREQ(M)=FREQ(M)*ADJUST
29800 C IF(RECOV.GT.100.0)GO TO 90
29900 RQDA(M)=RQD(M)*ADJUST
30000 IF(RECOV.GE.100.0)RQDA(M)=RQD(M)

```

```

30100 90      CONTINUE
30200 C      TRQD=TRQD*ADJUST
30300      IF(RECOV.GT.100.0)RECOV=100.0
30400 125     CONTINUE
30500 C
30600 C-----OUTPUT
30700 C
30800      WRITE(10,1300)NAME
30900      WRITE(11,1300)NAME
31000 1300    FORMAT(25X,A10)
31100      WRITE(IQUT,1000)NAME
31200 1000    FORMAT(1H1,///5X,"FRACTURE FREQUENCY AND RQD FOR ",
31300      1 "SCANLINE NO. ",A10//1X,"INTERVAL",6X,"RQD",7X,
31400      1 "ADJ RQD",5X,"THEO RQD",5X,
31500 1 "FREQUENCY"/3X,"(M)",10X,"%",11X,"%",11X,"%",10X,"(FRAC/M)")
31600 C      INCRE=INCRE-1
31700      DO 110 NN=1,INCRE-1
31800          D2=NN
31900          D1=D2-1.0
32000          IF(D2.LE.DIST(NUMFRA))GO TO 113
32100          D2=DIST(NUMFRA)
32200          D1=FLOAT(INT(D2))
32300 113      CONTINUE
32400          WRITE(10,1400)RQD(NN)
32500          WRITE(11,1400)FREQ(NN)
32600 1400    FORMAT(1X,F7.2,"-1")
32700          WRITE(IQUT,1100)D1,D2,RQD(NN),RQDA(NN),
32800      1 RQDT(NN),FREQ(NN)
32900 1100    FORMAT(1X,F3.0,"-",F4.1,3X,F7.2,5X,F7.2,
33000      1 5X,F7.2,7X,F7.2)
33100          IF(D2.GT.DIST(NUMFRA))GO TO 111
33200 110      CONTINUE
33300 111      NUMFRA=NUMFRA-1
33400          WRITE(IQUT,1200)XMTMRK,RECOV,TRQD,TFREQ,NUMFRA
33500 1200    FORMAT(/5X,"BOREHOLE LENGTH =",F7.2,1X,"M"/
33600 1 5X,"RECOVERY =",F7.2,1X,"%/5X,"AVERAGE RQD =",F7.2,1X,
33700 2 "%/5X,"AVERAGE FREQUENCY =",F7.2,1X,"FRAC/M"/5X,
33800 3 "TOTAL NUMBER OF FRACTURES =",1X,I5)
33900      GO TO 15
34000 C      IF(IFILE.GT.1)STOP
34100 99      STOP
34200      END

```

```

00100 CCCCCCCCCCCCCCCCCCCCCCCCCCCCCCCCCCCCCCCCCCCCCCCCCCCCCCCCCCCCCCCCC
00200 C
00300 C ORDER.FOR C
00400 C C
00500 C SEPTEMBER, 1981 LESLIE SOUR C
00600 C COLORADO SCHOOL OF MINES, GOLDEN, COLO. C
00700 C C
00800 C THIS SUBPROGRAM READS A FILE WITH UNORDERED DATA IN COLUMNS C
00900 C AND ORDERS IT. ONLY THE FIRST PIECE OF DATA PER LINE IS C
01000 C ORDERED, BUT THE LINE STAYS INTACT DURING THE SHUFFLING C
01100 C PROCESS. C
01200 C C
01300 CCCCCCCCCCCCCCCCCCCCCCCCCCCCCCCCCCCCCCCCCCCCCCCCCCCCCCCCCCCCCCCCC
01400 C
01500 C SUBROUTINE ORDER
01600 C COMMON D
01700 C DOUBLE PRECISION NAMEIN,NAMOUT,M1,M2,M3,M4,L1,L2,L3,L4,L5,L6,L7,
01800 C 1 L8
01900 C DIMENSION D(1000),IDUM(6),IFIL(5),M1(1000),M2(1000),M3(1000),
02000 C 1 M4(1000)
02100 C OPEN(UNIT=18,DIALOG)
02200 C OPEN(UNIT=19,DIALOG)
02300 C
02400 C-----INPUT
02500 C
02600 C DO 10 II=1,1000
02700 C READ(18,100,END=99)D(II),M1(II),M2(II),M3(II),M4(II)
02800 C 100 FORMAT(F,4A10)
02900 C NUM=II
03000 C 10 CONTINUE
03100 C 99 CJNTINUE
03200 C
03300 C-----ORDERING LOOP
03400 C
03500 C DO 20 J=1,NUM
03600 C L=J
03700 C DO 30 K=L,NUM
03800 C IF(D(K).GT.D(J))GO TO 30
03900 C DUM1=D(K)
04000 C DUM2=D(J)
04100 C D(K)=DUM2
04200 C D(J)=DUM1
04300 C
04400 C-----TRANSFERING THE REST OF THE LINE
04500 C
04600 C L1=M1(K)
04700 C L2=M1(J)
04800 C M1(K)=L2
04900 C M1(J)=L1
05000 C L3=M2(K)
05100 C L4=M2(J)
05200 C M2(K)=L4
05300 C M2(J)=L3
05400 C L5=M3(K)
05500 C L6=M3(J)
05600 C M3(K)=L6
05700 C M3(J)=L5
05800 C L7=M4(K)
05900 C L8=M4(J)
06000 C M4(K)=L8

```

```
06100                                M4(J)=L7
06200    30                          CONTINUE
06300    20                          CONTINUE
06400    C
06500    C-----OUTPUT
06600    C
06700                                DJ 40 NM=1,NUM
06800                                WRITE(19,300)D(NM),M1(NM),M2(NM),M3(NM),M4(NM)
06900                                FORMAT(1X,F7.2,"",",",4A10)
07000    300
07100    40                          CONTINUE
07200    999                          RETURN
                                END
```

AN EXAMPLE INPUT TO FRACTR

```

RUE-6 CORE
0.00,88, , , , 1, 2,-1, 0, 3, 1
7.99, , , , 0, 0, 0, 0
8.27
9.54
17.16
18.43
19.7
20.97
22.00,75, , , , 1, 2,-1, 0, 1, 3, 2
22.24
23.51
24.78
25
32.00,87, , , , 1, 2,-1, 0, 1, 3, 2
37.00,60, , , , 1, 2,-1, 0, 4, 3, 1
57.50,88, , , , 1, 2,-1, 0, 3
75.00,30, , , , 1, 2,-1, 0, 1, 4, 3
432.00,21, , , , 1, 2,-1, 0, 3
445.00,99, , , , 0, 0, 0, 0
446.30,
447.50,
448.80,
450.10,
451.40,
452.60,
453.00,
455.00,37, , , , 1, 2,-2, 0, 2, 3, 1
541.50,31, , , , 1, 2,-2, 0, 5, 2, 1
545.10,47, , , , 1, 3,-1, 0, 3, 1
545.60,15, , , , 1, 2,-1, 0, 2, 3, 1
553.30,40, , , , 1, 2,-1, 0, 2, 5, 1
555.00,12, , , , 1, 2,-1, 0, 1, 2, 5, 3
561.70,23, , , , 1, 2,-2, 0, 2
565.70,57, , , , 1, 2,-1, 0, 1, 3
577.50,26, , , , 1, 2,-1, 0, 3, 2
586.90,35, , , , 1, 2,-2, 0, 3
596.90,59, , , , 1, 2,-1, 0, 2
602.70,12, , , , 1, 2,-1, 0, 1
30.17
-5
RDU-6 CORE
55.00,51, , , , 1, 3,-1, 0, 3, 5, 4
56.50,58, , , , 1, 2,-1, 0, 3, 2, 1
58.00,40, , , , 1, 2,-1, 0, 2, 1, 4
126.50,19, , , , 1, 2,-1, 0, 2, 1, 4, 3
129.00,32, , , , 1, 3,-2, 0, 2, 1, 5
135.40,47, , , , 1, 2,-2, 0, 2
137.00,38, , , , 5, 2,-2, 0, 3, 5
137.90,34, , , , 1, 2,-2, 0, 4, 3
15.67
-5

```

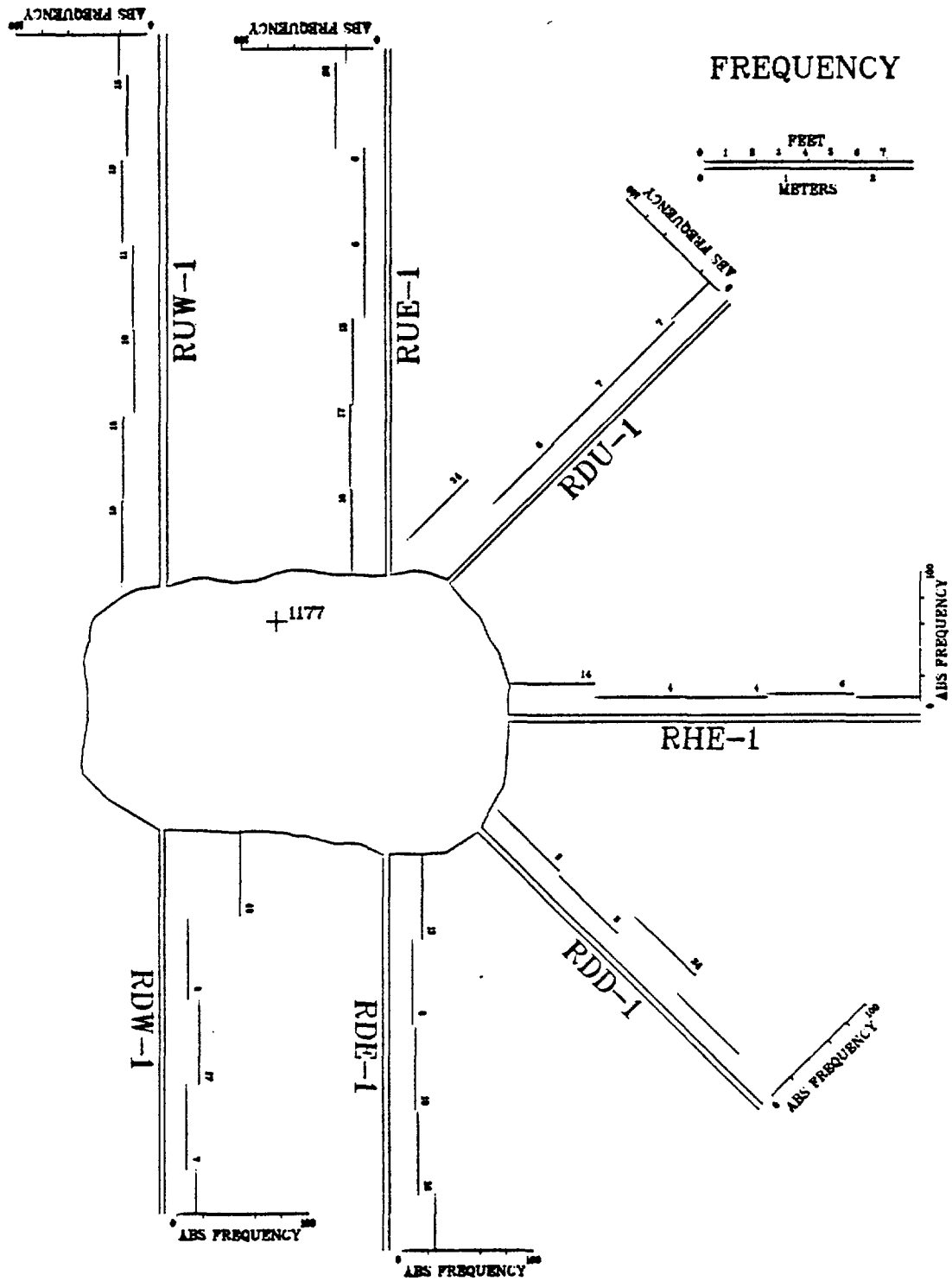
Example output from FRACTR

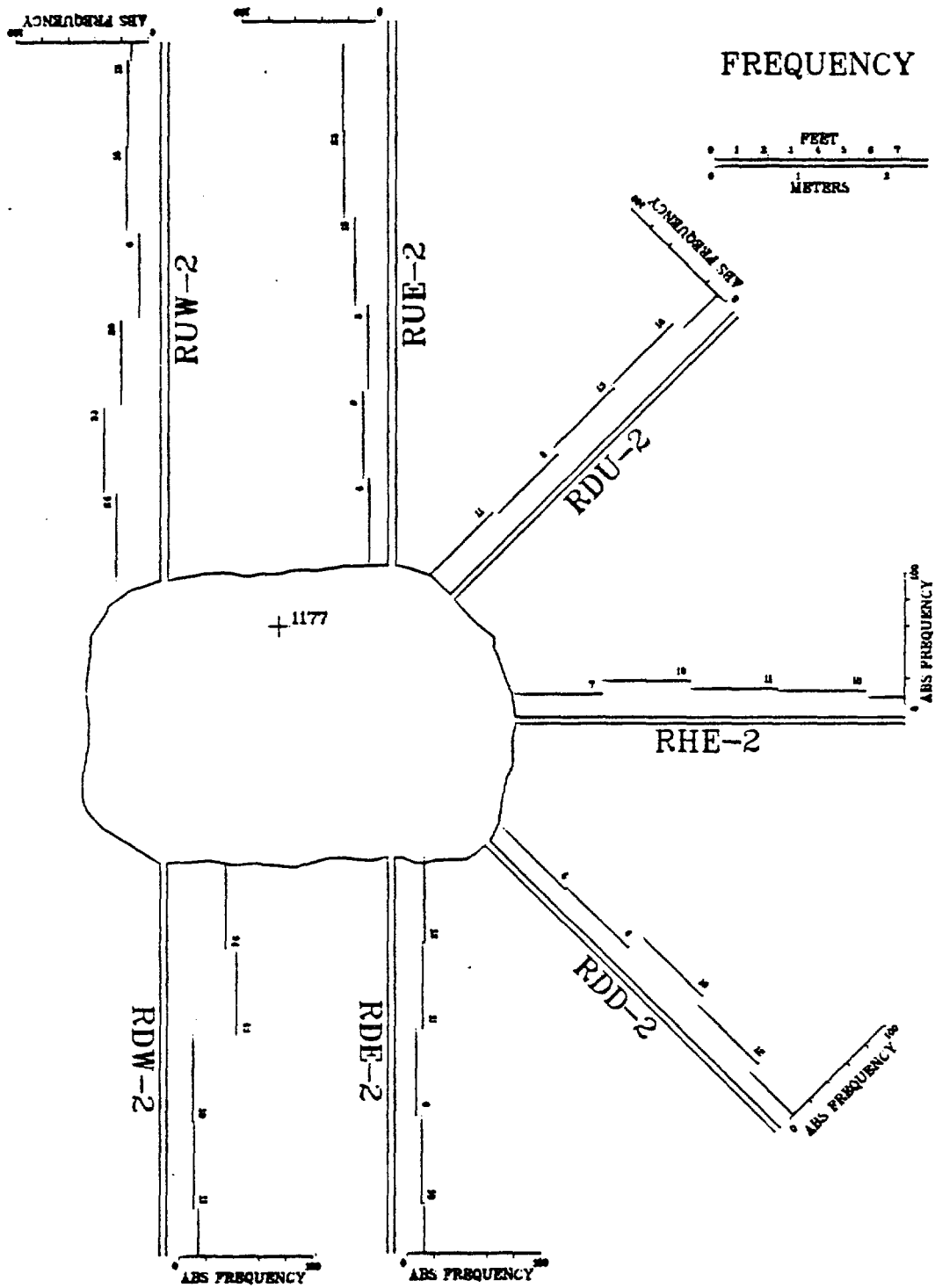
FRACTURE FREQUENCY AND RQD FOR SCANLINE NO. RUW-2 CORE

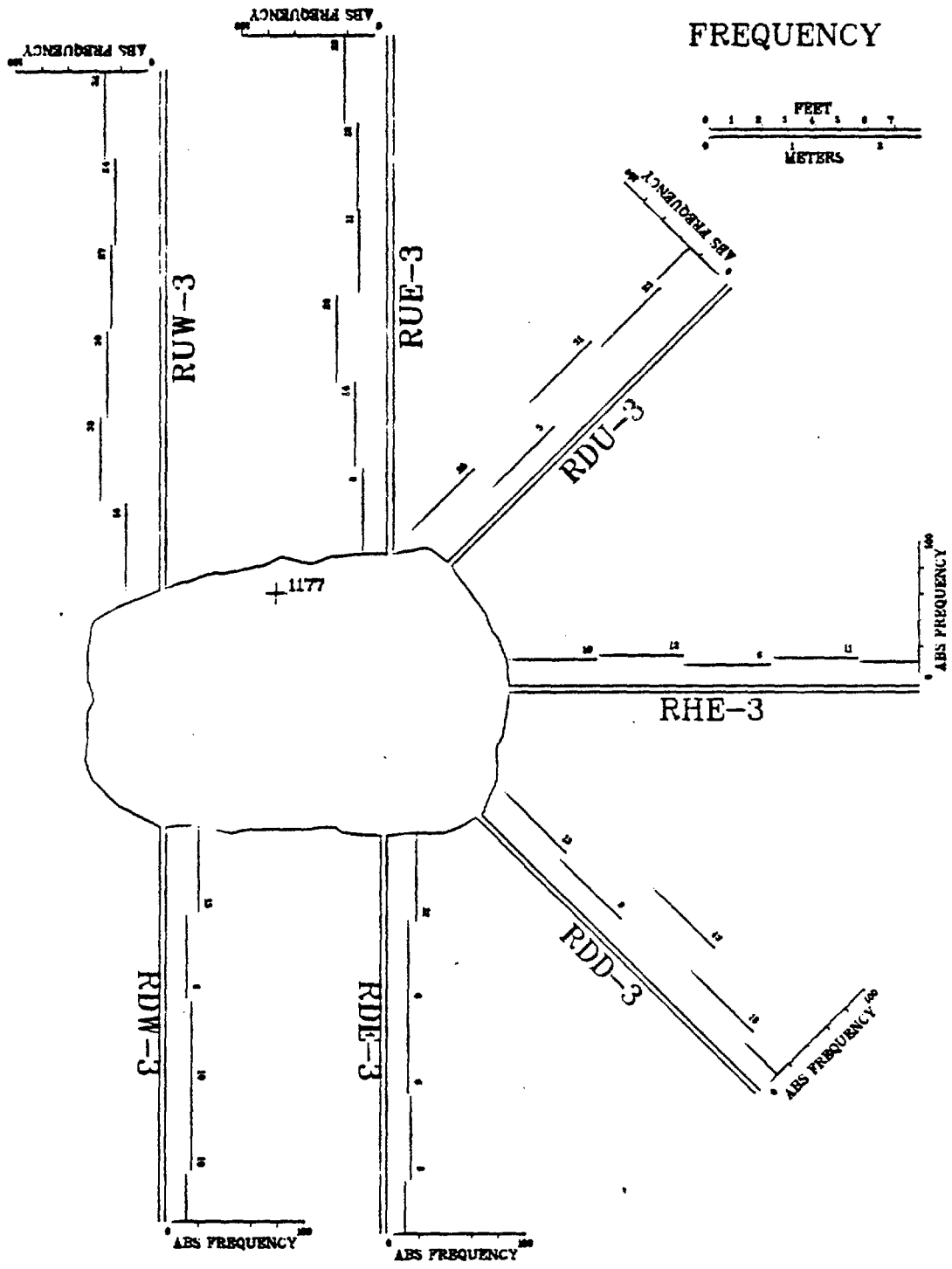
INTERVAL (M)	RQD %	ADJ RQD %	THEO RQD %	FREQUENCY (FRAC/M)
0.- 1.0	100.00	97.69	97.98	1.95
1.- 2.0	90.40	88.31	86.22	5.86
2.- 3.0	100.00	97.69	92.97	3.91
3.- 4.0	81.50	79.62	82.46	6.84
4.- 5.0	78.20	76.39	82.46	6.84
5.- 6.0	74.30	72.58	74.62	8.79

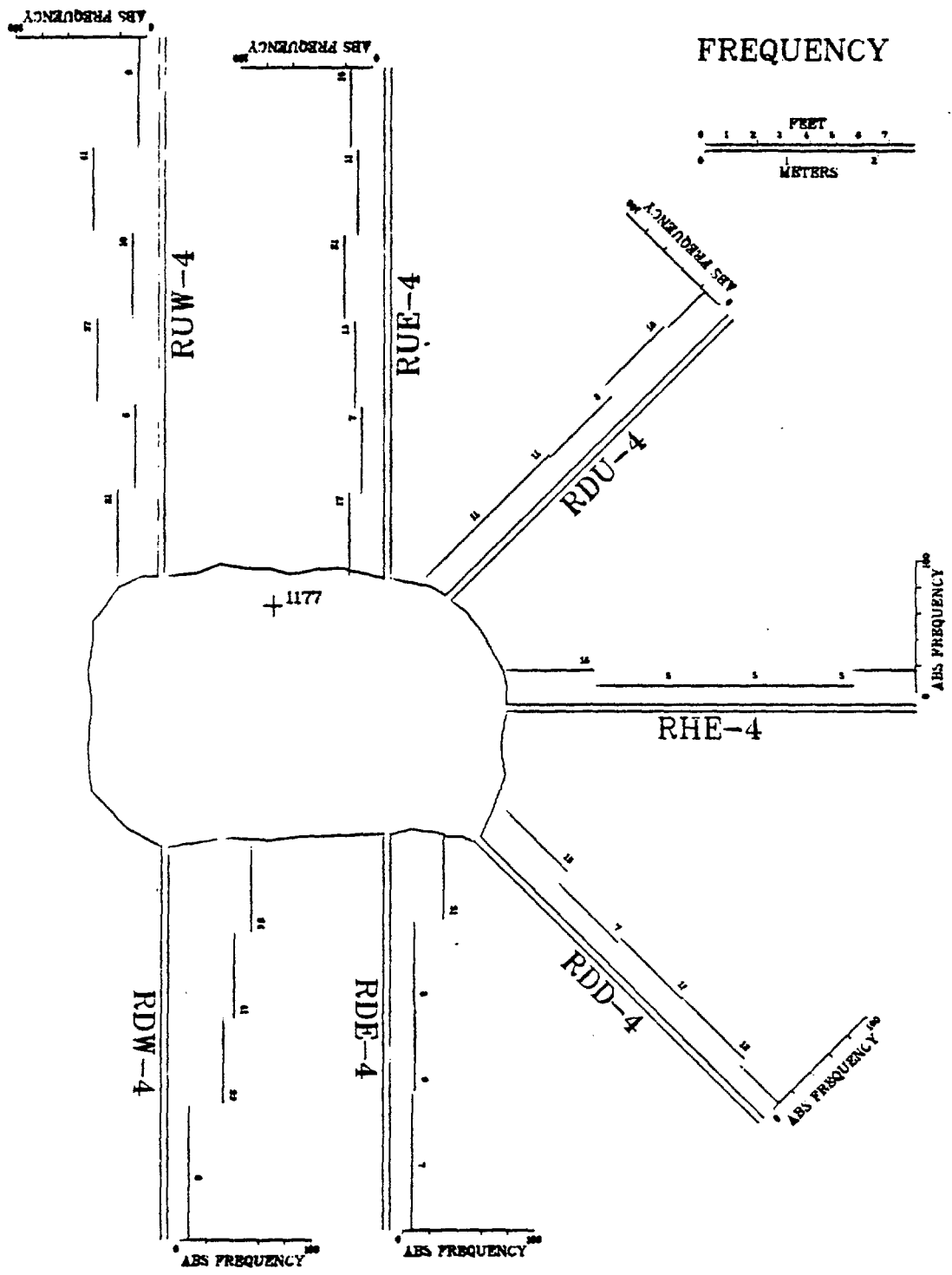
BOREHOLE LENGTH = 6.25 M
 RECOVERY = 97.69 %
 AVERAGE RQD = 83.93 %
 AVERAGE FREQUENCY = 5.60 FRAC/M
 TOTAL NUMBER OF FRACTURES = 35

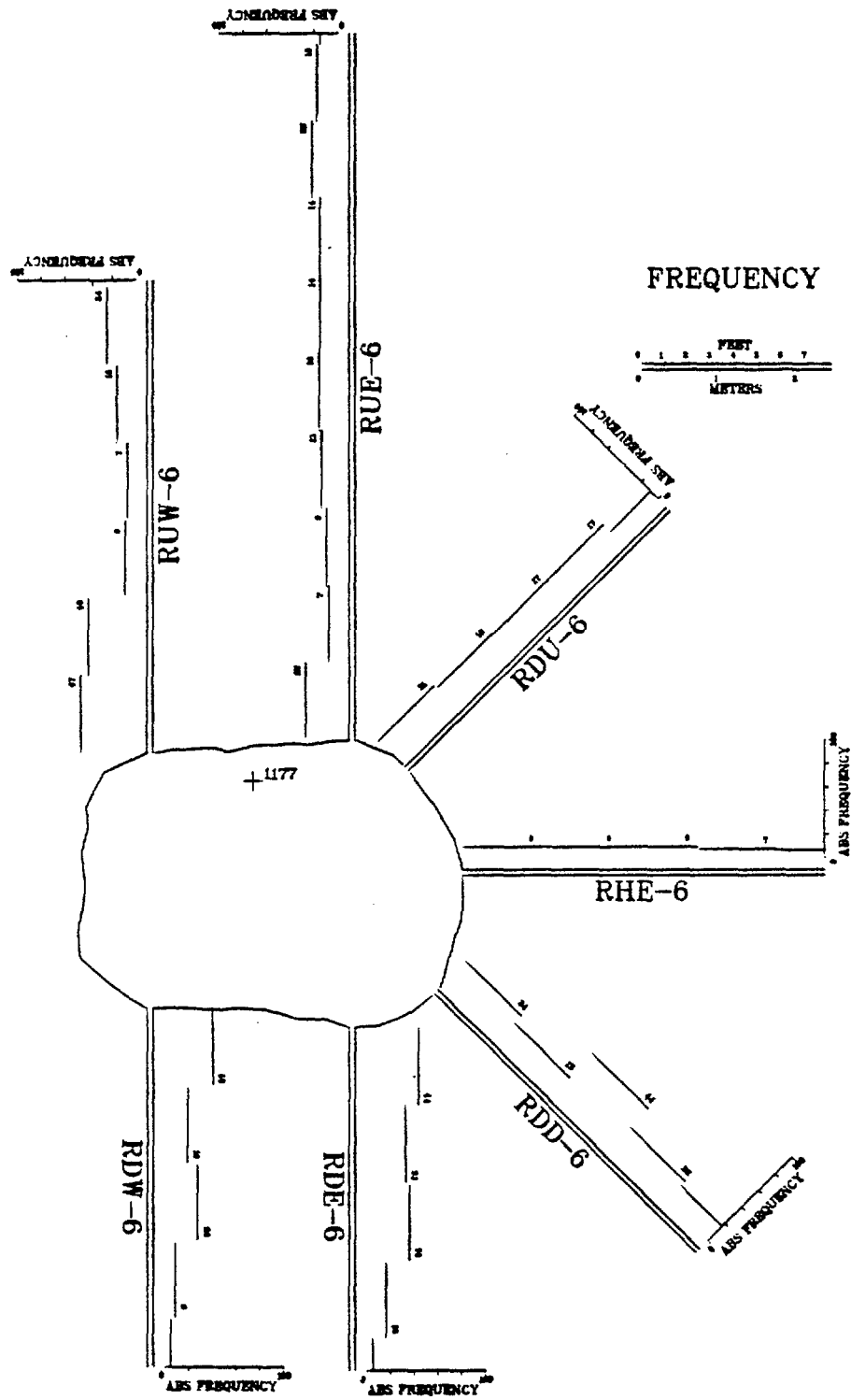
FRACTURE FREQUENCY ALONG THE RADIAL
BOREHOLES FROM FIELD CORE LOGS.

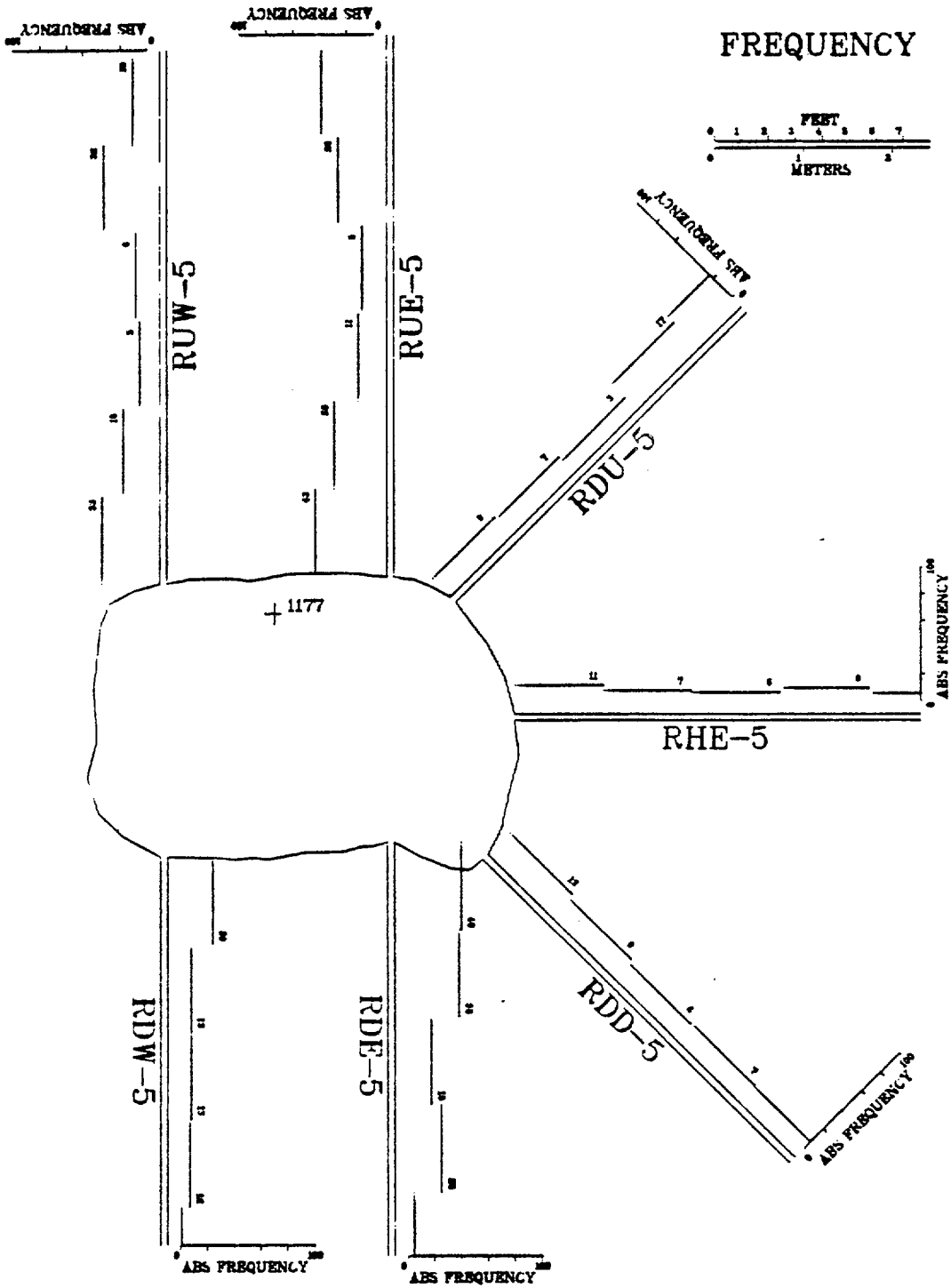






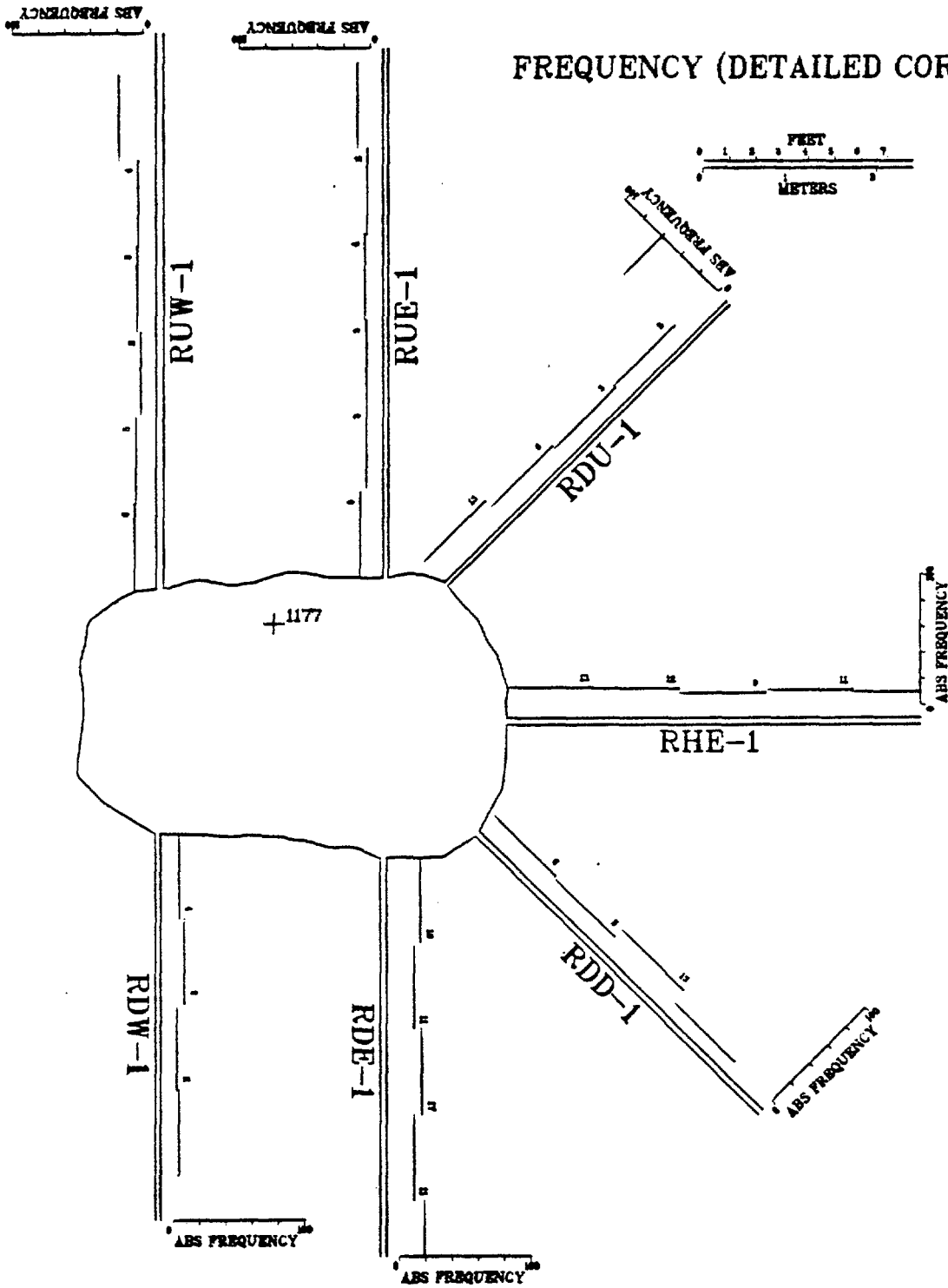


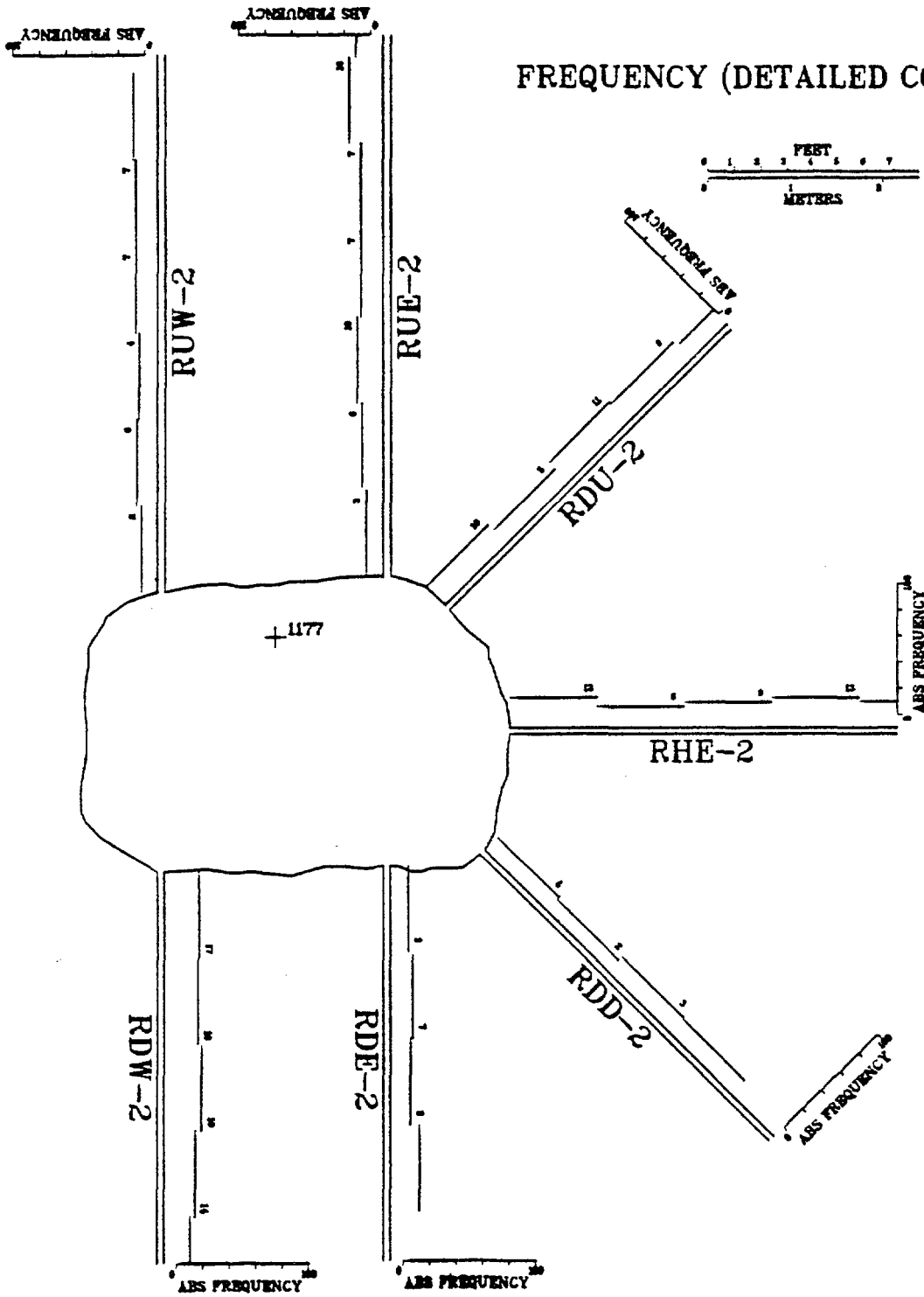




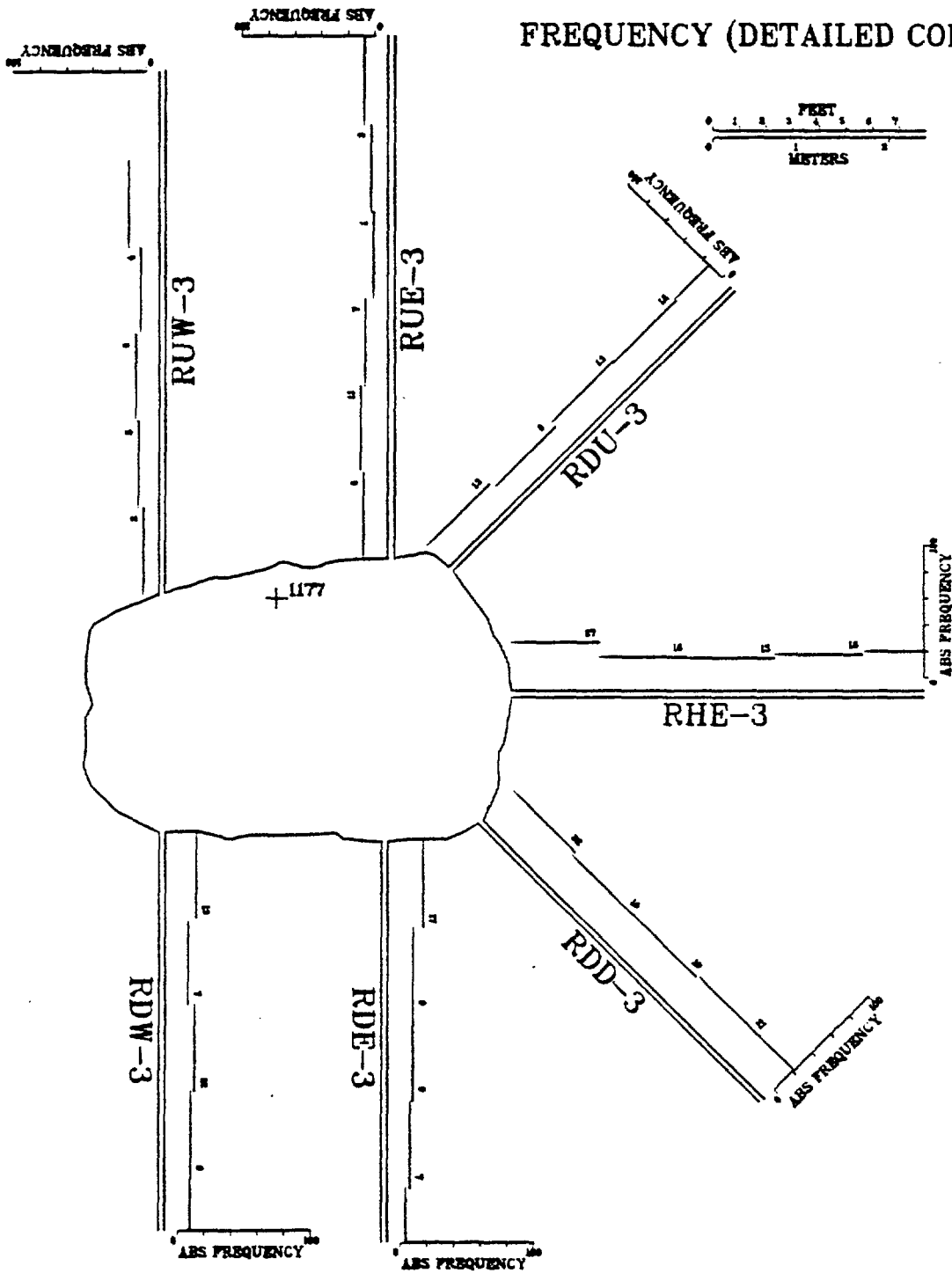
FRACTURE FREQUENCY ALONG RADIAL BOREHOLES
FROM DETAILED CORE LOGS.

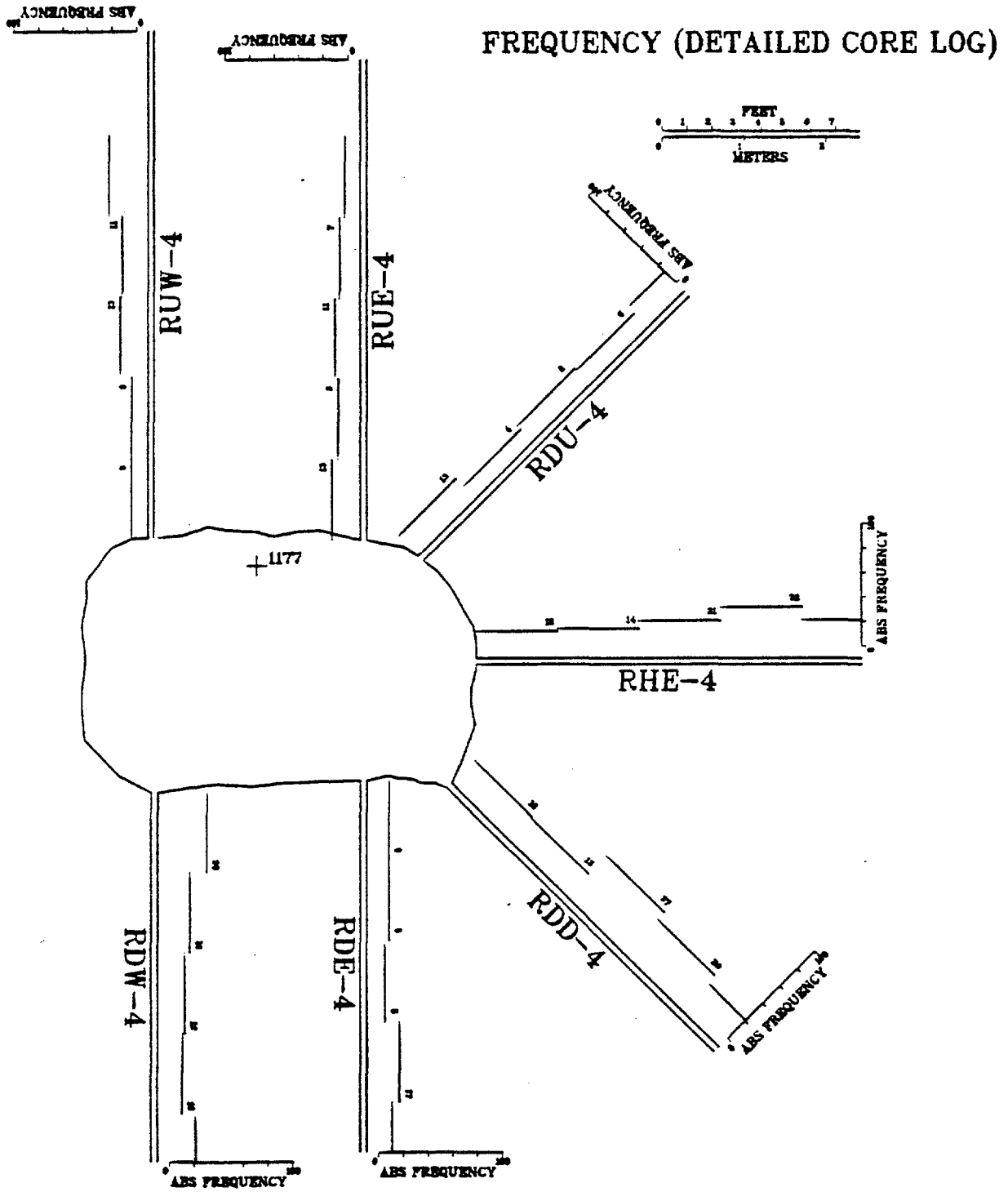
FREQUENCY (DETAILED CORE LOG)



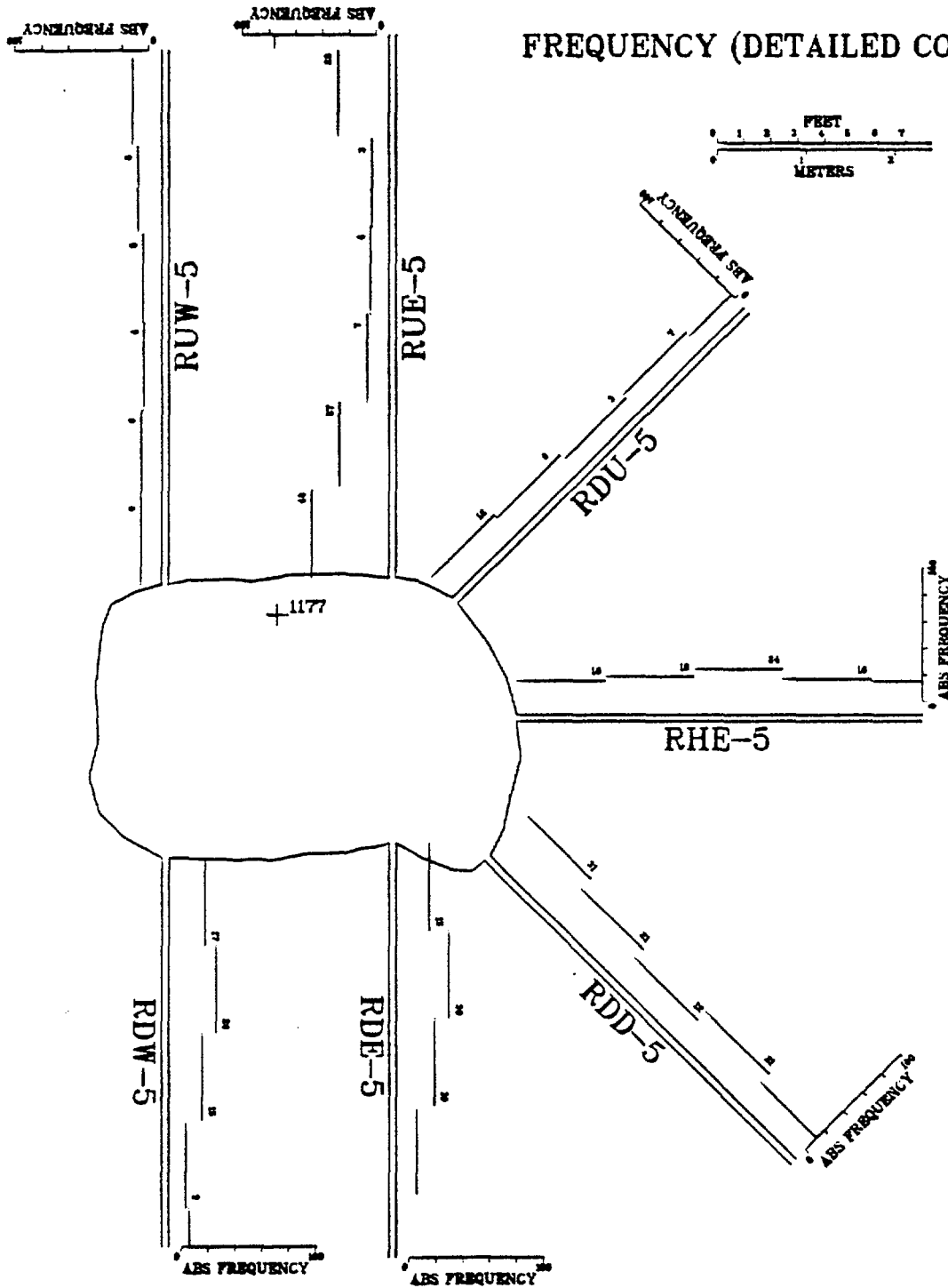


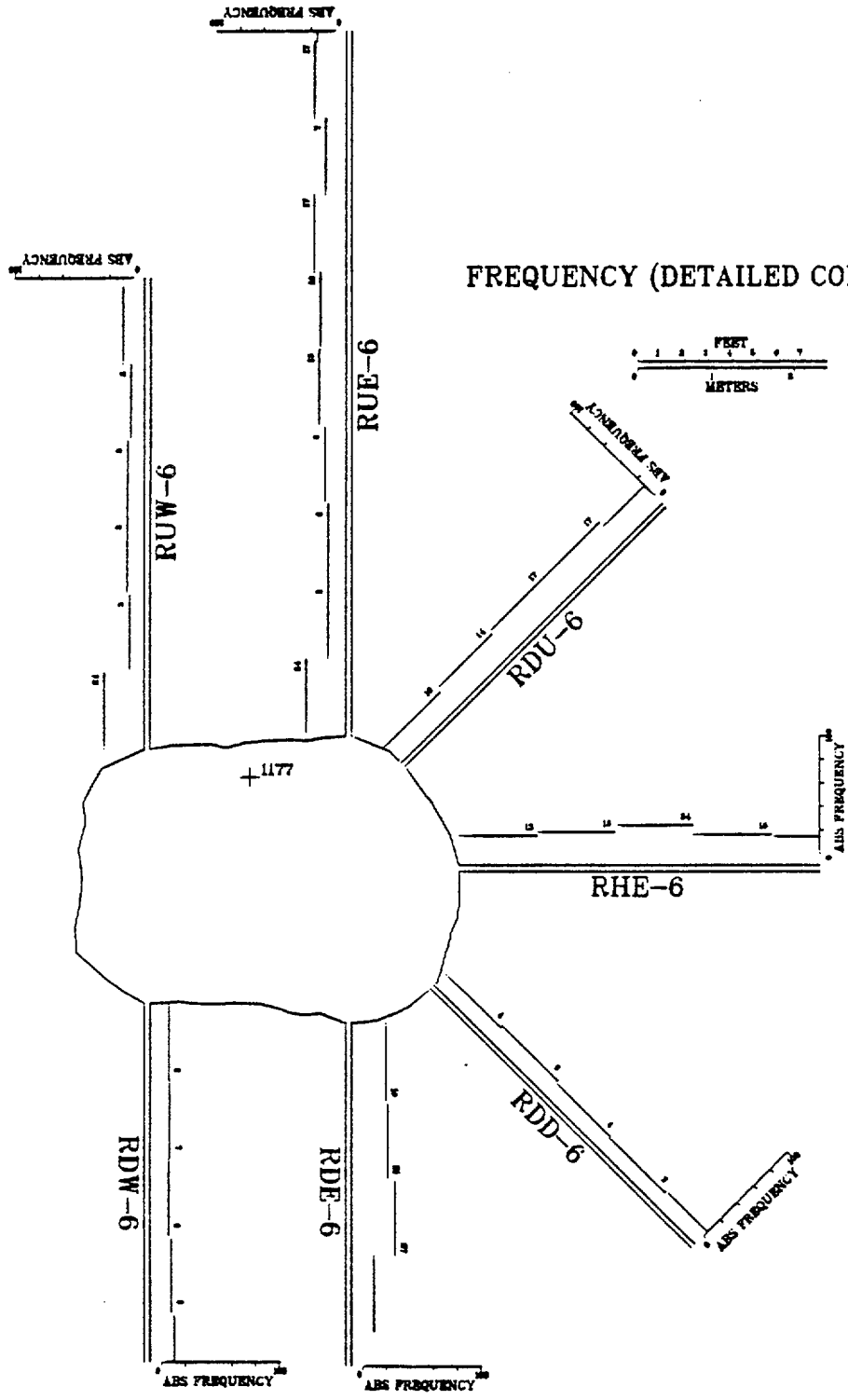
FREQUENCY (DETAILED CORE LOG)





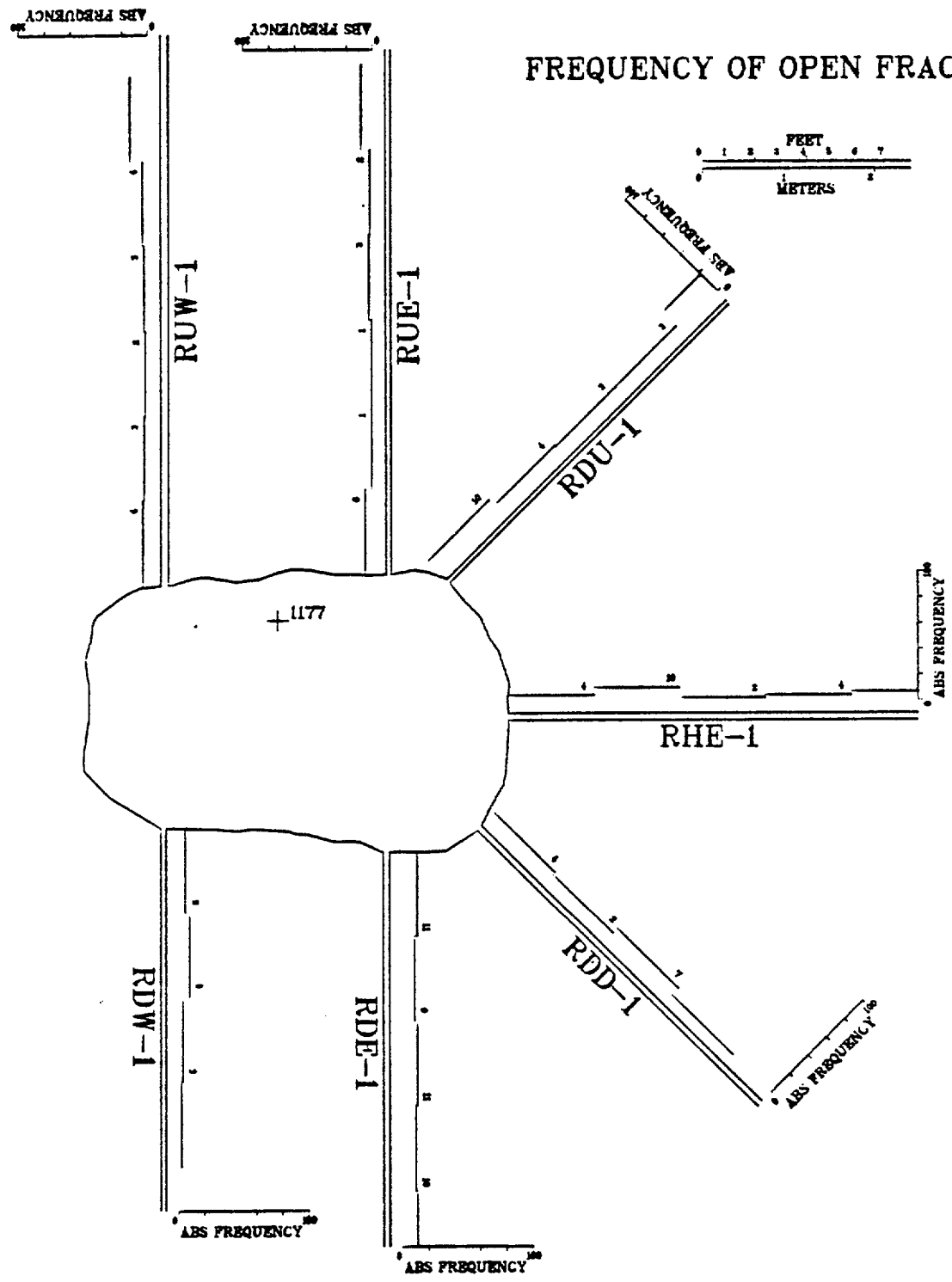
FREQUENCY (DETAILED CORE LOG)

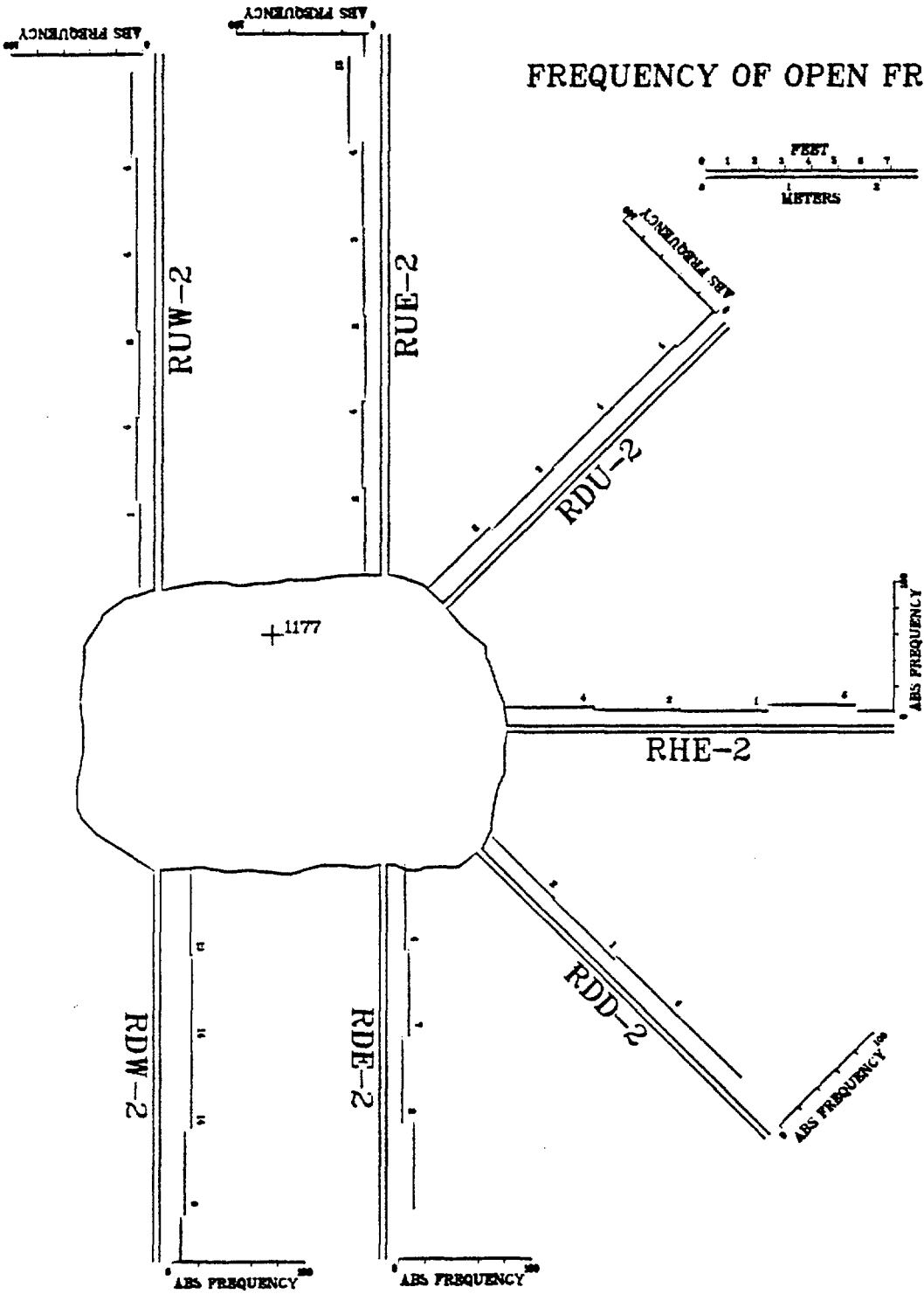




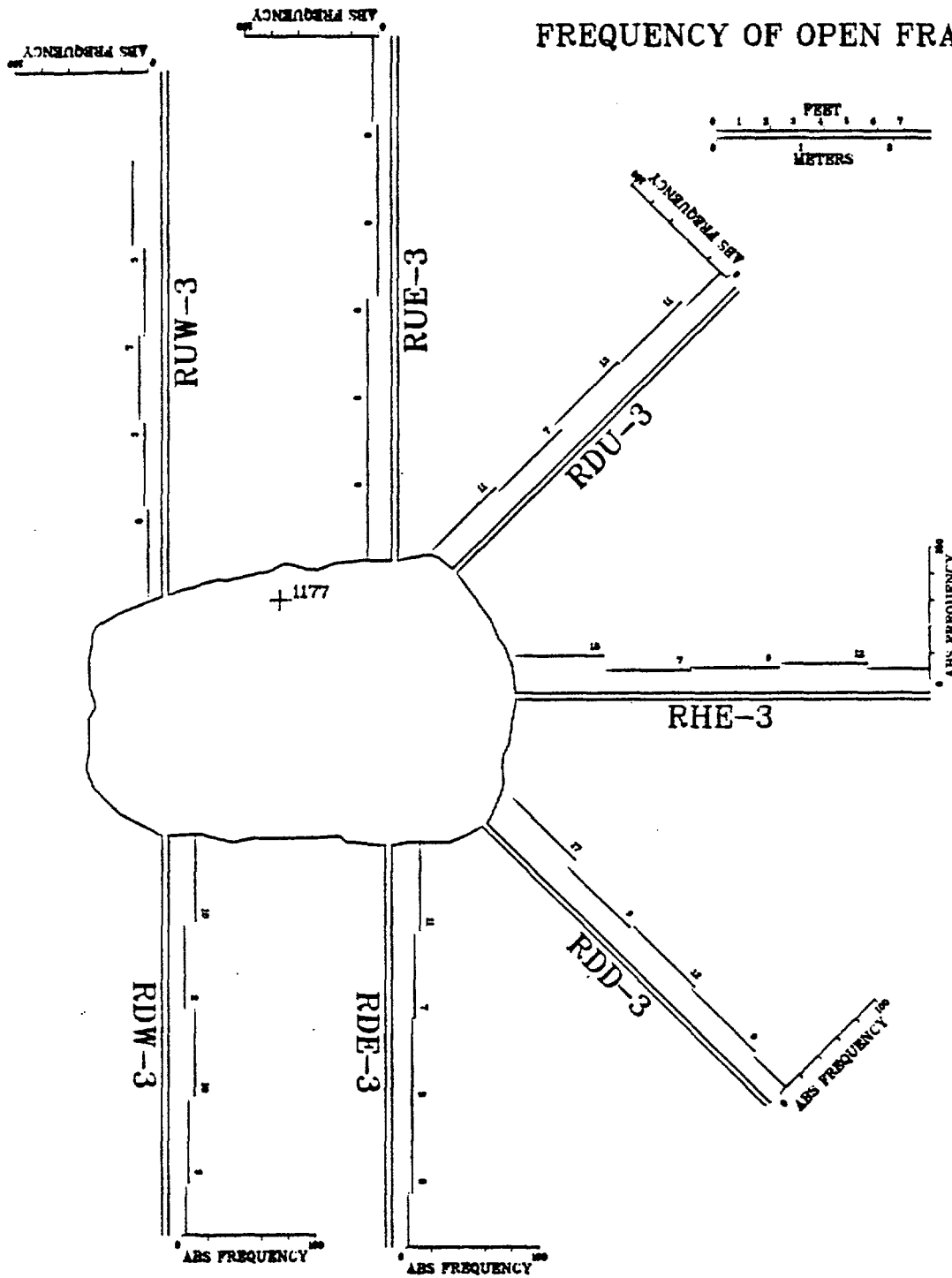
FREQUENCY OF OPEN FRACTURES
ALONG RADIAL BOREHOLES.

FREQUENCY OF OPEN FRACTURES

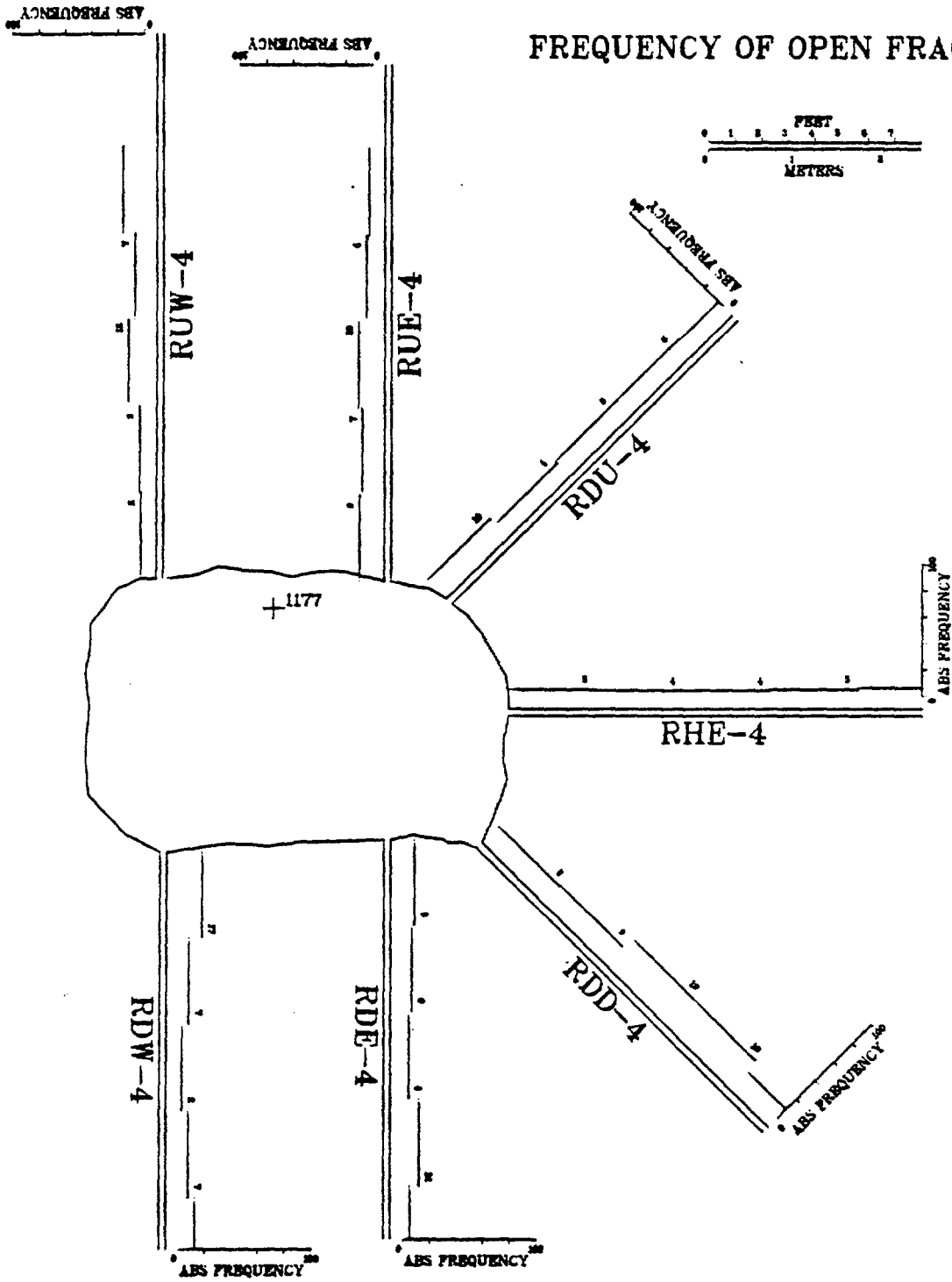




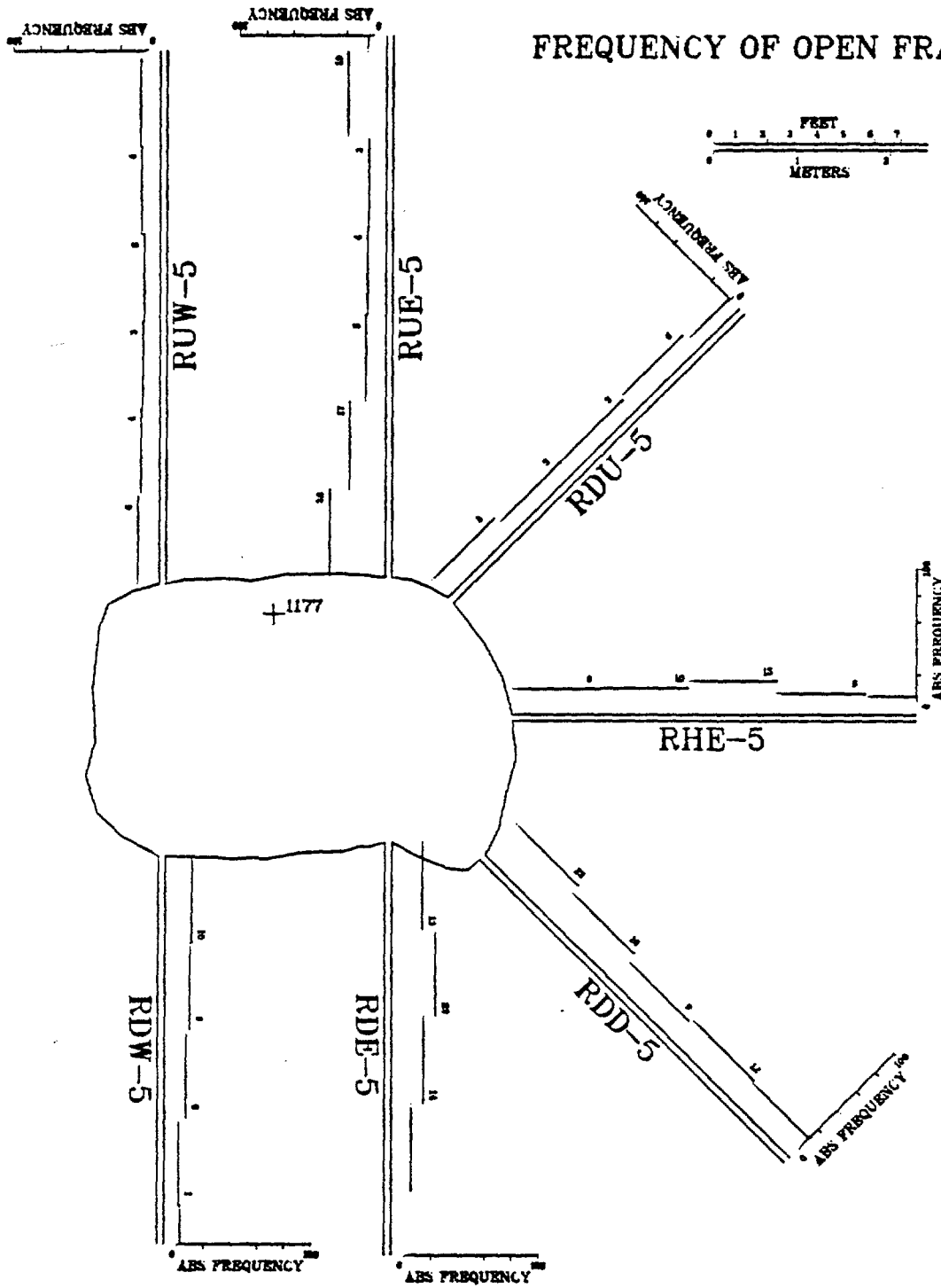
FREQUENCY OF OPEN FRACTURES

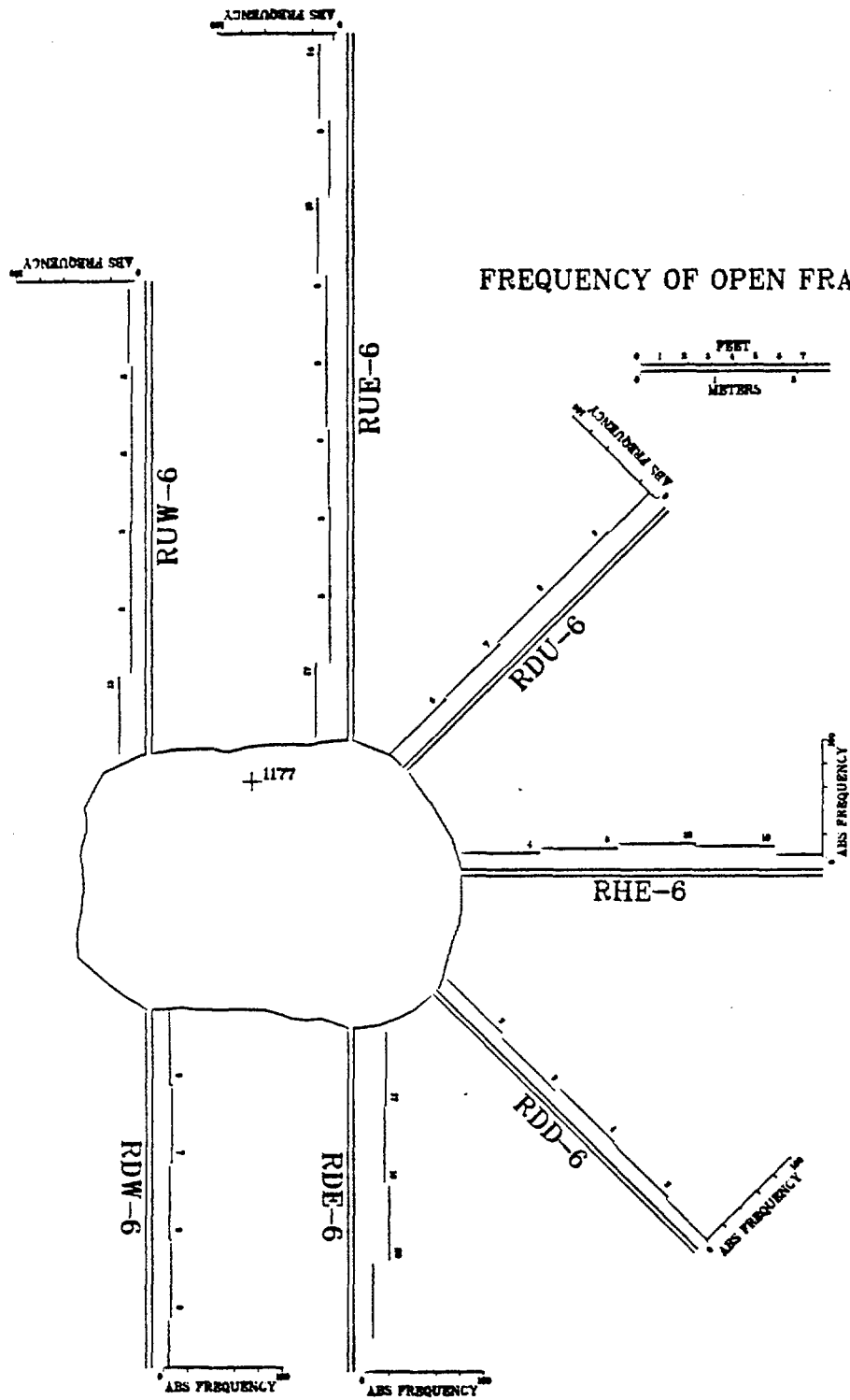


FREQUENCY OF OPEN FRACTURES

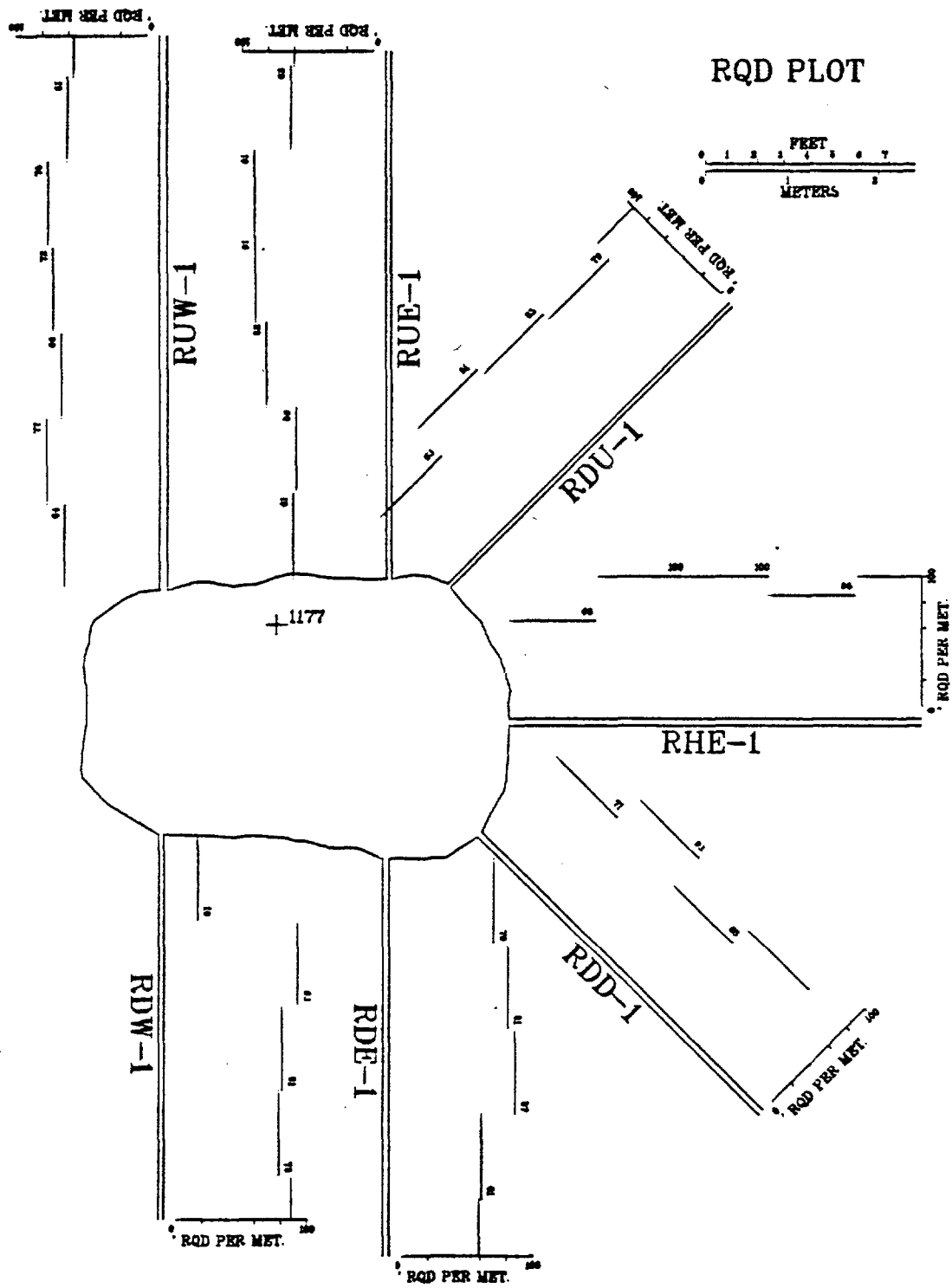


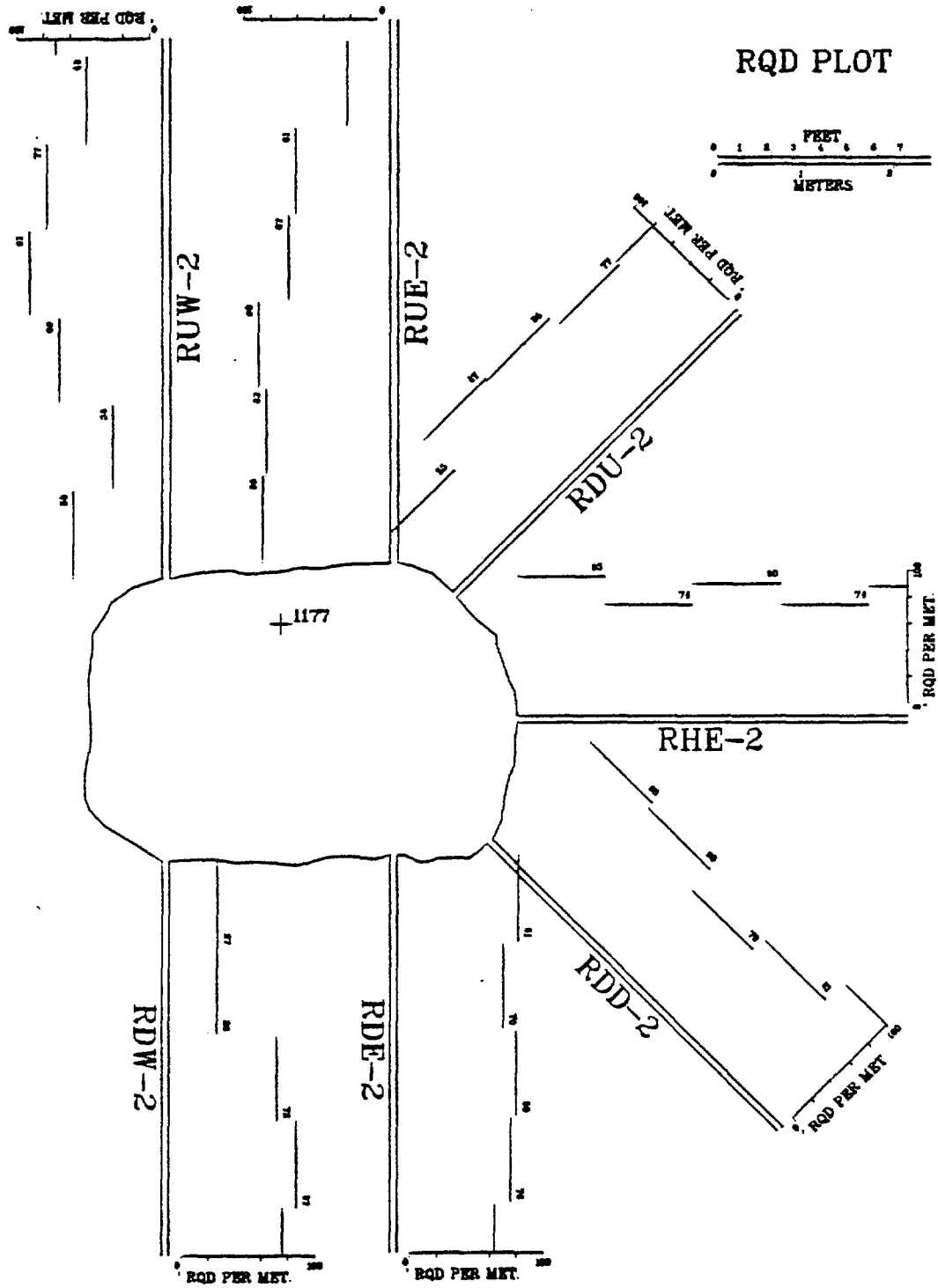
FREQUENCY OF OPEN FRACTURES

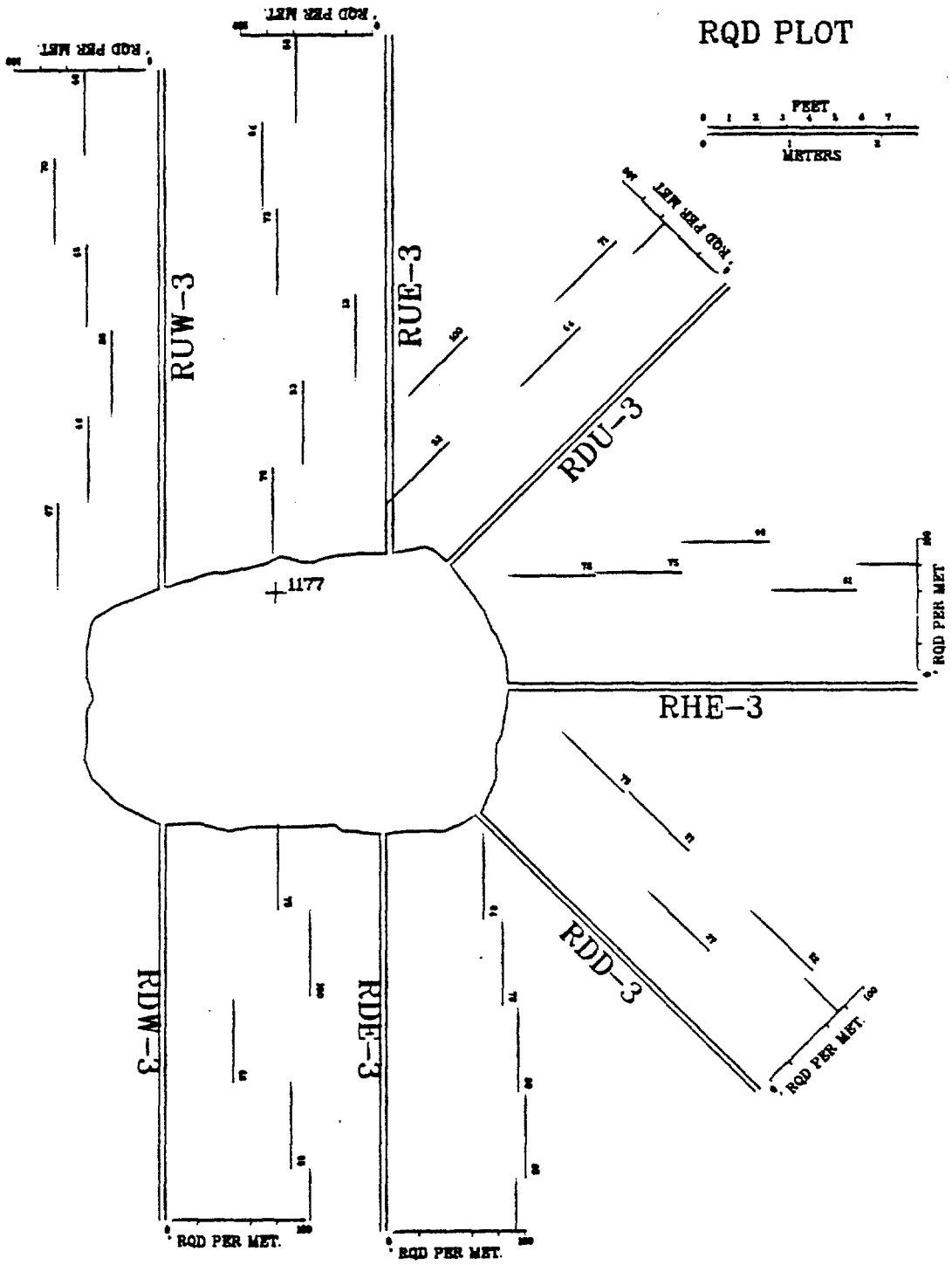


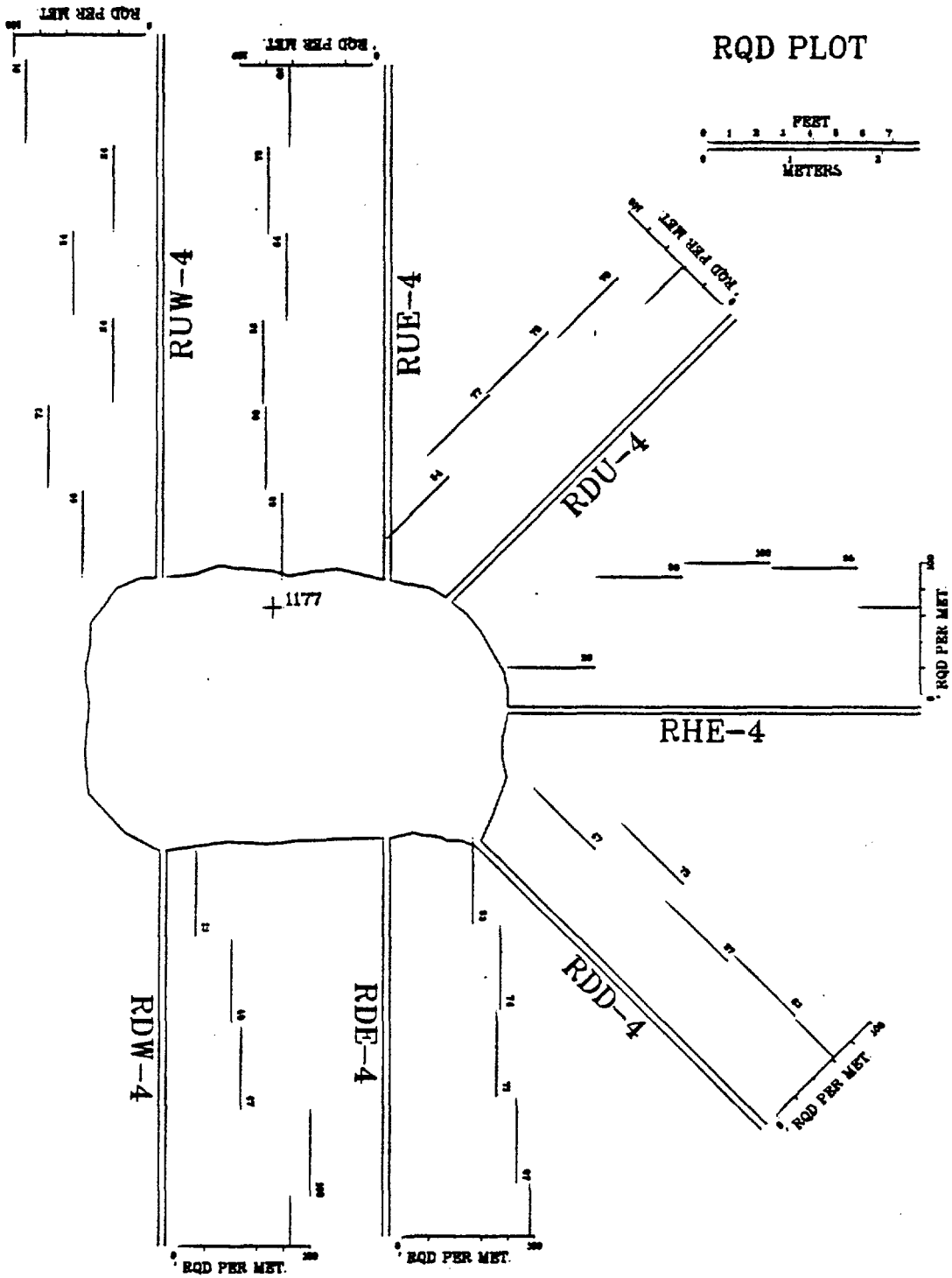


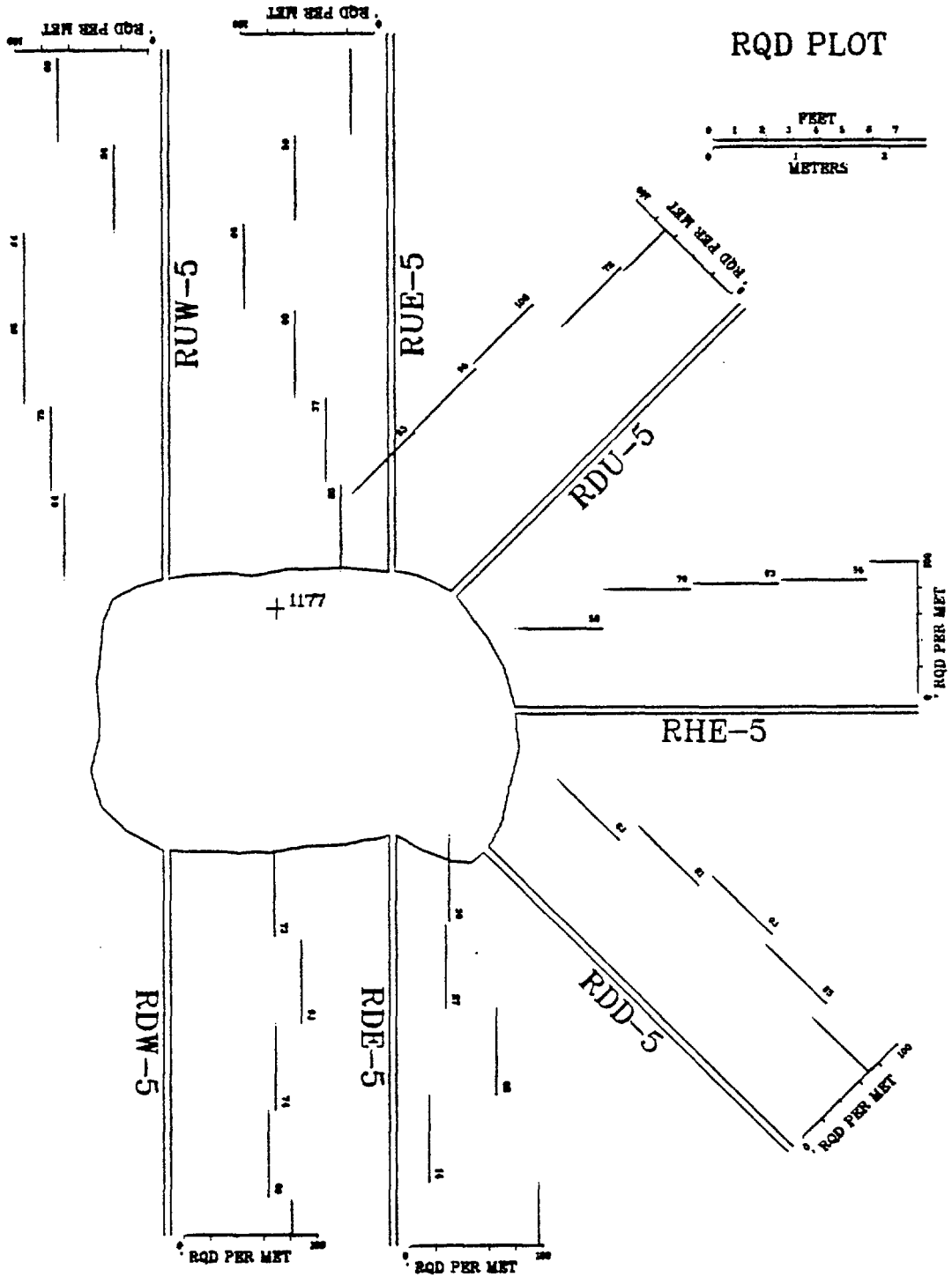
RQD ALONG RADIAL BOREHOLES
FROM FIELD LOGS.





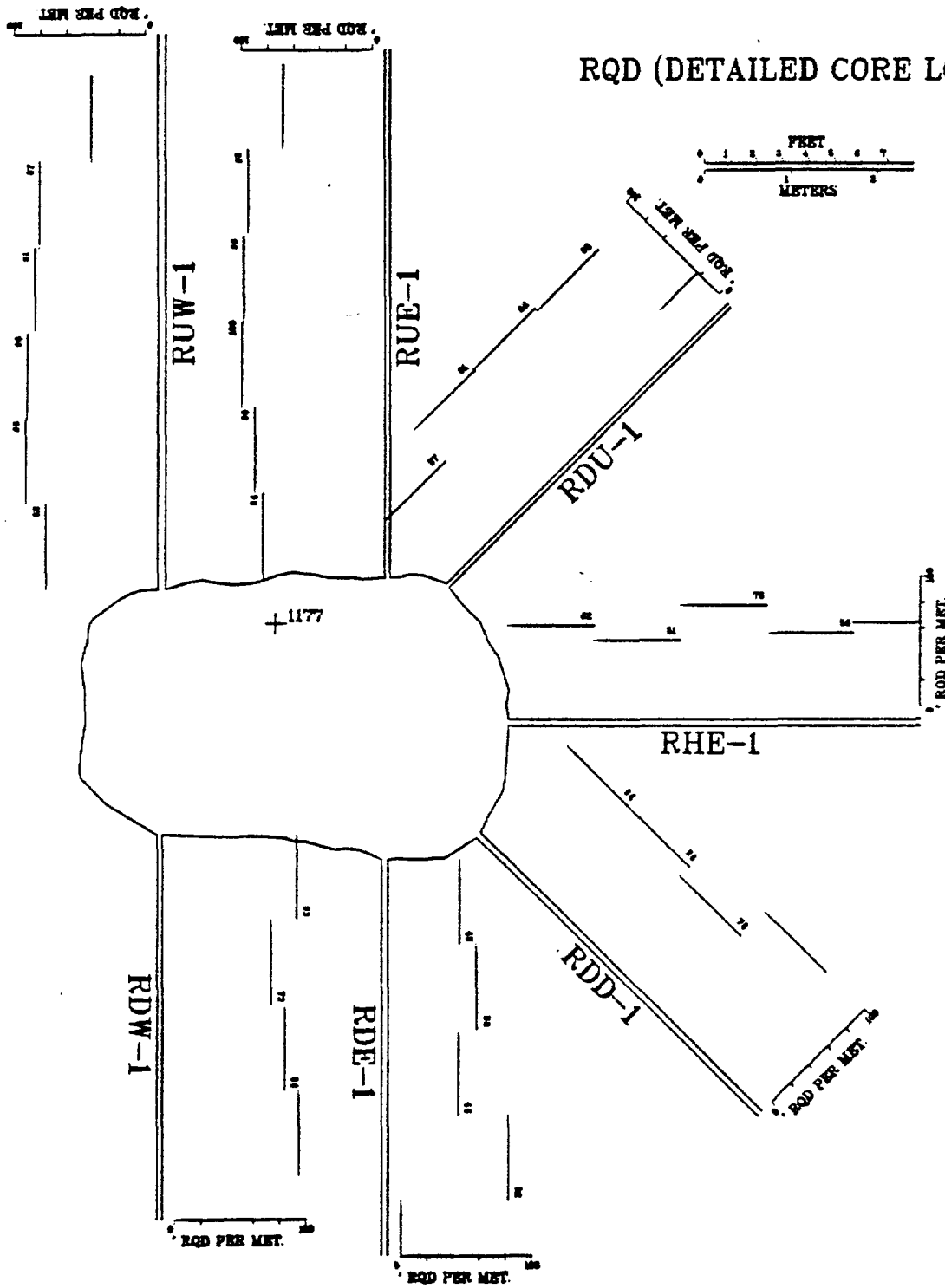




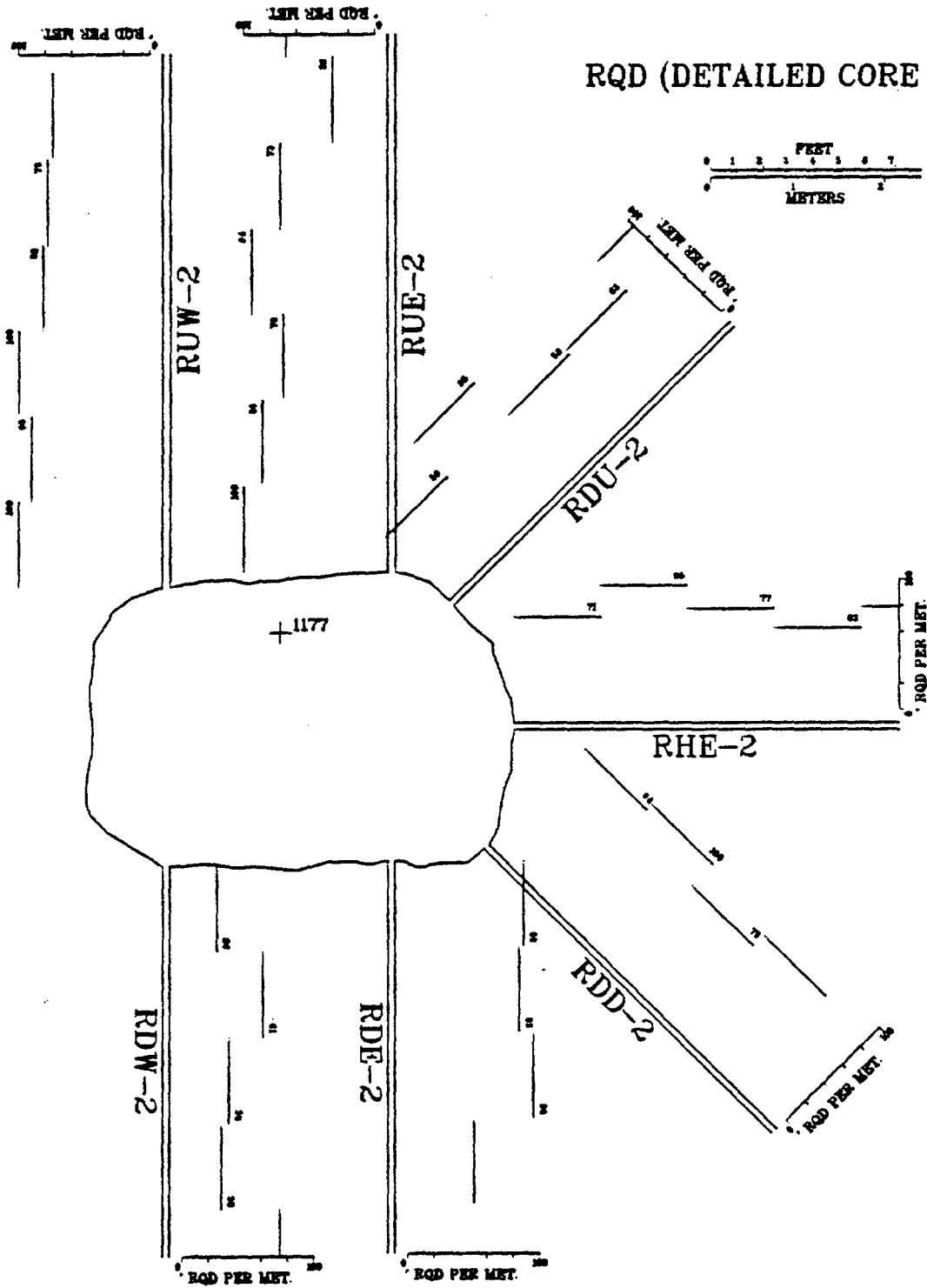


RQD ALONG RADIAL BOREHOLES
FROM DETAILED CORE LOGS.

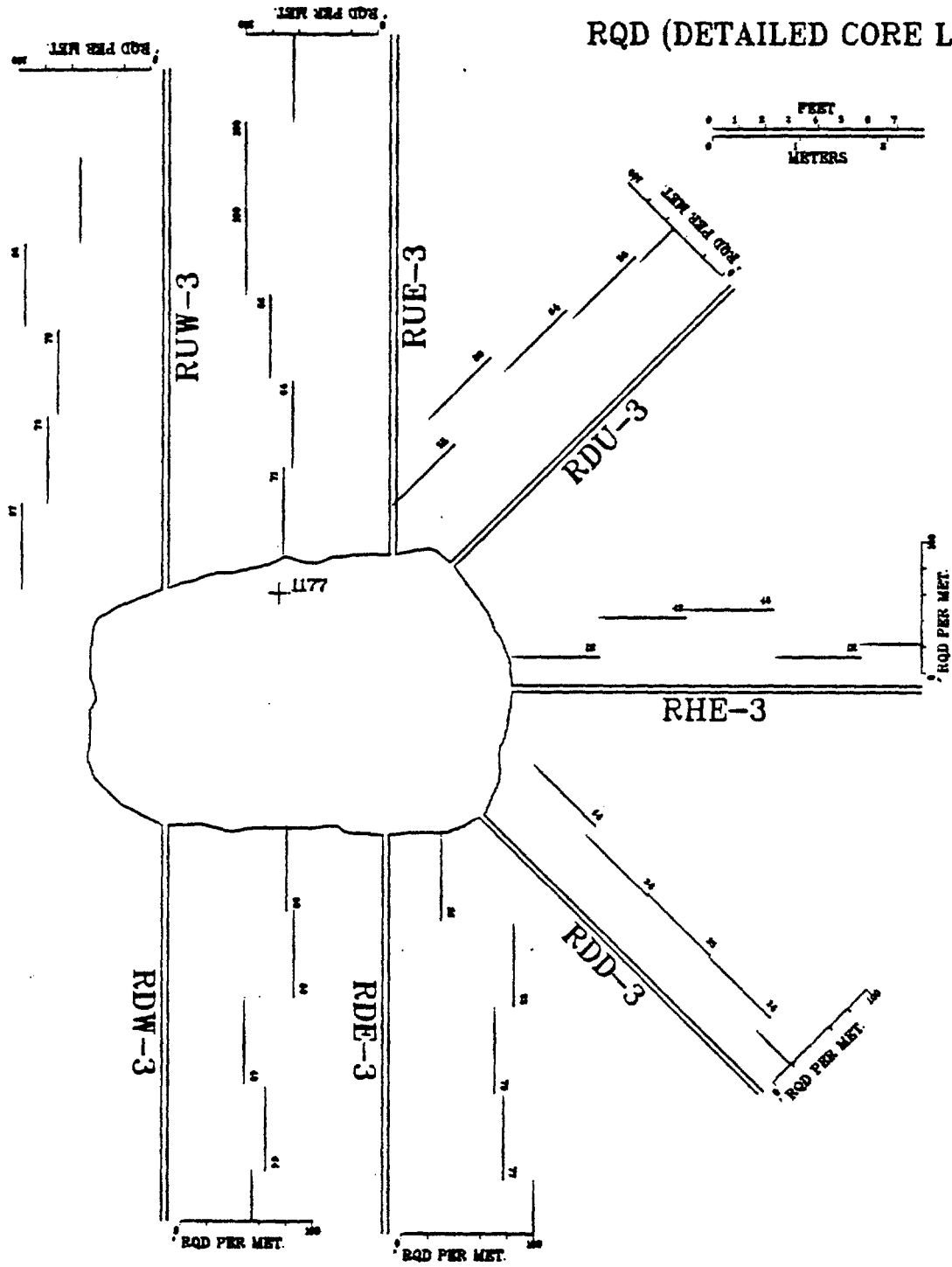
RQD (DETAILED CORE LOG)



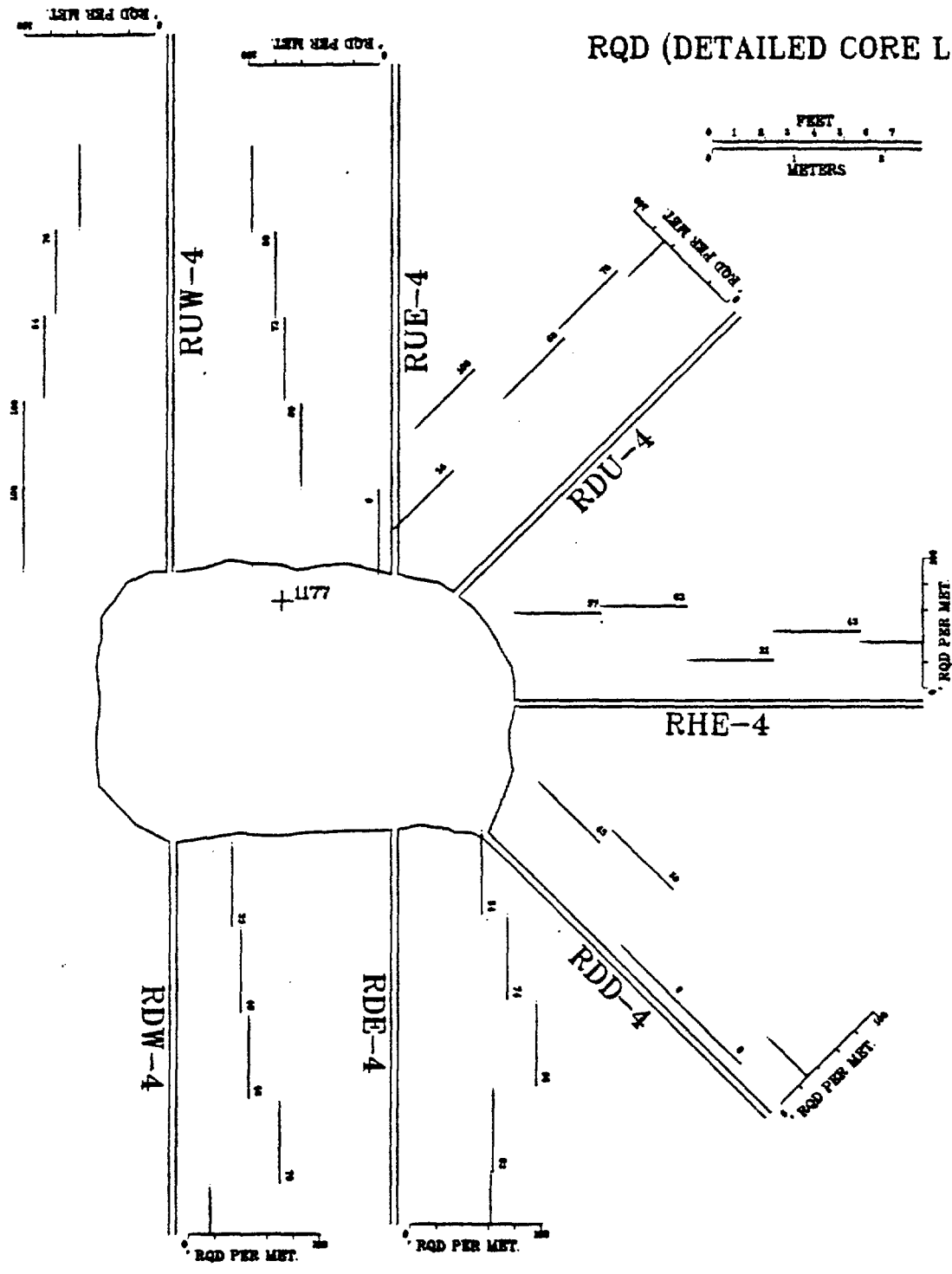
RQD (DETAILED CORE LOG)



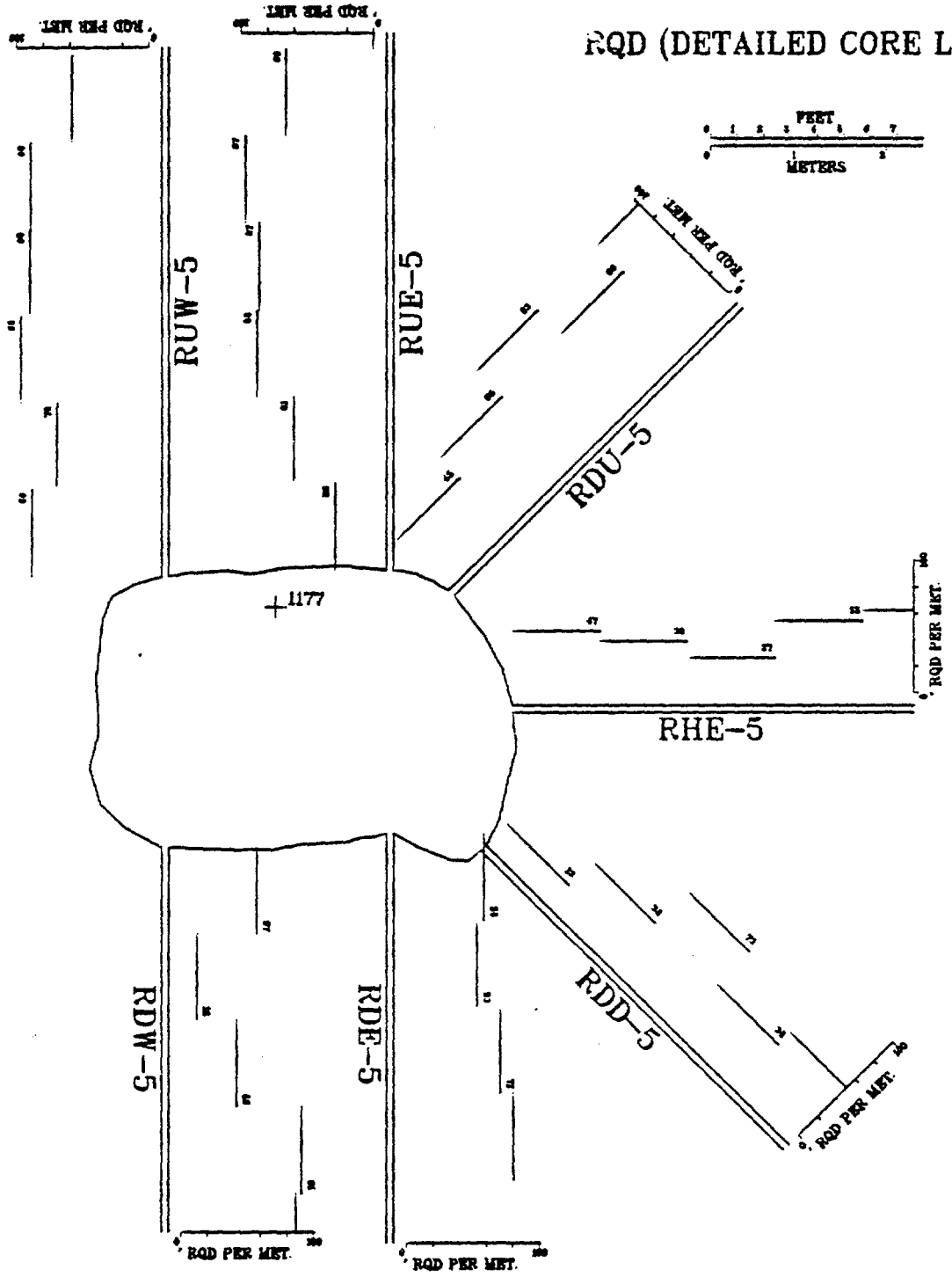
RQD (DETAILED CORE LOG)

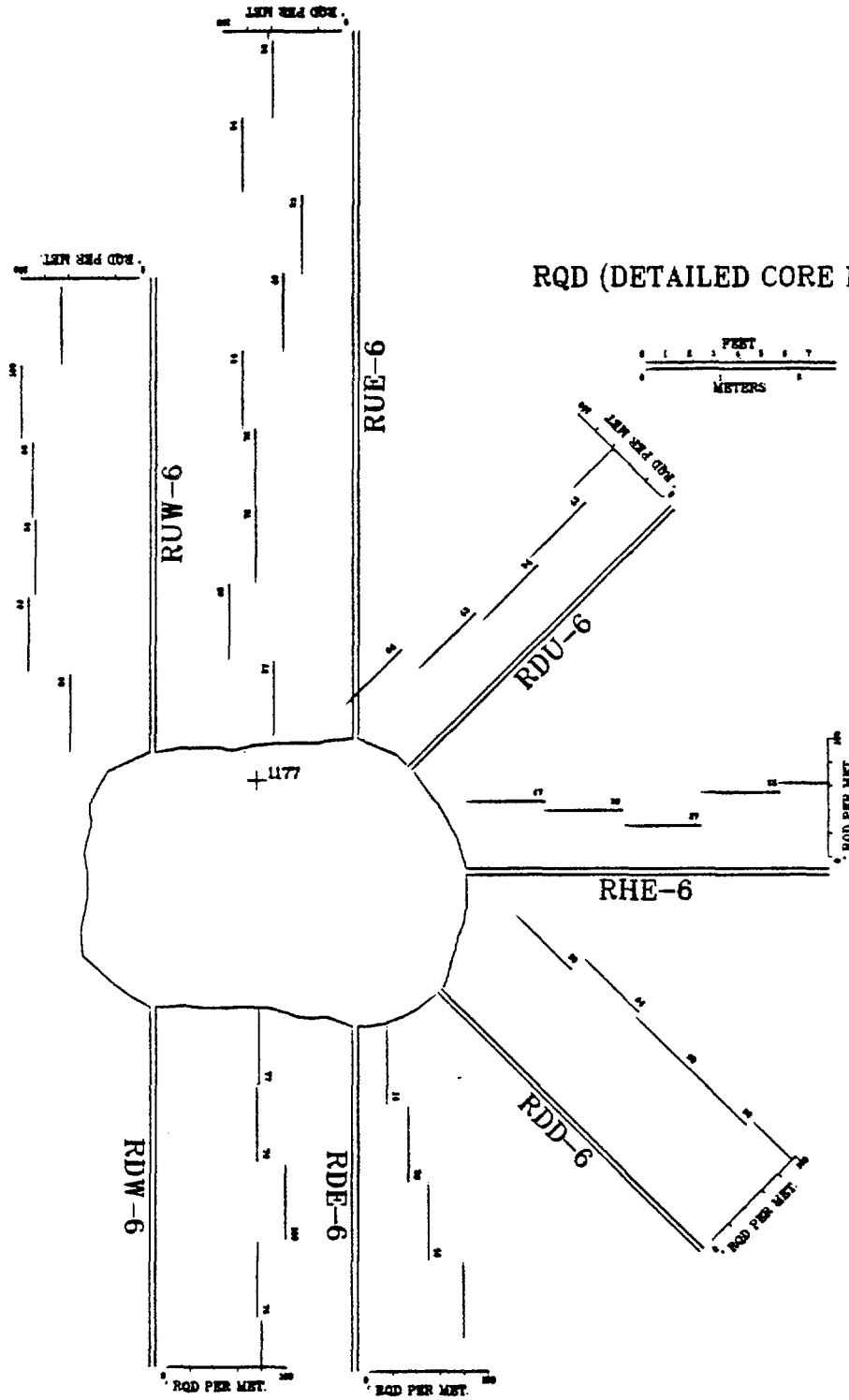


RQD (DETAILED CORE LOG)



RQD (DETAILED CORE LOG)





FRACTURE FREQUENCY AND RQD FOR SCANLINE NO. RUW-1

INTERVAL (M)	RQD %	ADJ RQD %	THEO RQD %	FREQUENCY (FRAC/M)
0.- 1.0	63.50	63.50	42.16	19.02
1.- 2.0	77.47	77.47	45.25	17.96
2.- 3.0	65.81	65.81	74.62	9.51
3.- 4.0	72.36	72.06	70.65	10.57
4.- 5.0	75.87	75.87	42.16	19.02
5.- 6.0	60.88	60.88	55.41	14.79
6.- 6.9	55.91	55.91	36.39	21.16

BOREHOLE LENGTH = 6.53 M
 RECOVERY = 100.00 %
 AVERAGE RQD = 71.35 %
 AVERAGE FREQUENCY = 15.93 FRAC/M
 TOTAL NUMBER OF FRACTURES = 104

FRACTURE FREQUENCY AND RQD FOR SCANLINE NO. RUE-1

INTERVAL (M)	RQD %	ADJ RQD %	THEO RQD %	FREQUENCY (FRAC/M)
0.- 1.0	61.39	61.39	48.48	16.15
1.- 2.0	59.36	59.36	45.25	17.16
2.- 3.0	81.97	81.97	51.87	15.14
3.- 4.0	90.86	90.86	86.22	6.06
4.- 5.0	91.11	91.11	86.22	6.06
5.- 6.0	62.92	62.92	19.58	28.26
6.- 6.3	59.92	59.92	37.21	19.91

BOREHOLE LENGTH = 6.20 M
 RECOVERY = 100.00 %
 AVERAGE RQD = 74.68 %
 AVERAGE FREQUENCY = 15.01 FRAC/M
 TOTAL NUMBER OF FRACTURES = 93

FRACTURE FREQUENCY AND RQD FOR SCANLINE NO. RDU-1

INTERVAL (M)	RQD %	ADJ RQD %	THEJ RQD %	FREQUENCY (FRAC/M)
0.- 1.0	62.92	62.92	12.94	33.52
1.- 2.0	90.86	90.86	86.22	6.10
2.- 3.0	84.76	84.76	82.46	7.11
3.- 4.0	79.17	79.17	82.46	7.11
4.- 4.7	94.02	94.02	71.85	9.85

BOREHOLE LENGTH = 4.65 M
 RECOVERY = 100.00 %
 AVERAGE RQD = 82.95 %
 AVERAGE FREQUENCY = 12.91 FRAC/M
 TOTAL NUMBER OF FRACTURES = 60

FRACTURE FREQUENCY AND RQD FOR SCANLINE NO. RHE-1

INTERVAL (M)	RQD %	ADJ RQD %	THEJ RQD %	FREQUENCY (FRAC/M)
0.- 1.0	65.71	59.30	48.48	14.20
1.- 2.0	100.00	88.73	92.97	3.55
2.- 3.0	100.00	88.73	92.97	3.55
3.- 4.0	85.52	75.98	82.46	6.21
4.- 4.3	100.00	88.73	93.41	3.42

BOREHOLE LENGTH = 4.80 M
 RECOVERY = 88.73 %
 AVERAGE RQD = 78.57 %
 AVERAGE FREQUENCY = 6.67 FRAC/M
 TOTAL NUMBER OF FRACTURES = 32

FRACTURE FREQUENCY AND RQD FOR SCANLINE NO. RDD-1

INTERVAL (M)	RQD %	ADJ RQD %	THEO RQD %	FREQUENCY (FRAC/M)
0.- 1.0	71.30	64.29	74.62	8.11
1.- 2.0	93.29	84.12	86.22	5.41
2.- 3.0	64.77	58.40	21.23	24.34
3.- 4.0	76.40	68.89	86.22	5.41

BOREHOLE LENGTH = 4.65 M
 RECOVERY = 90.16 %
 AVERAGE RQD = 65.78 %
 AVERAGE FREQUENCY = 10.33 FRAC/M
 TOTAL NUMBER OF FRACTURES = 48

FRACTURE FREQUENCY AND RQD FOR SCANLINE NO. RDE-1

INTERVAL (M)	RQD %	ADJ RQD %	THEO RQD %	FREQUENCY (FRAC/M)
0.- 1.0	70.35	70.36	55.41	15.08
1.- 2.0	81.13	81.13	82.46	7.54
2.- 3.0	86.79	86.79	74.62	9.70
3.- 4.0	60.53	60.63	66.72	11.85
4.- 5.0	57.33	57.33	26.92	25.86

BOREHOLE LENGTH = 4.67 M
 RECOVERY = 100.00 %
 AVERAGE RQD = 76.24 %
 AVERAGE FREQUENCY = 13.91 FRAC/M
 TOTAL NUMBER OF FRACTURES = 65

FRACTURE FREQUENCY AND RQD FOR SCANLINE NO. RDW-1

INTERVAL (M)	RQD %	ADJ RQD %	THEO RQD %	FREQUENCY (FRAC/M)
0.- 1.0	16.18	16.18	3.47	48.26
1.- 2.0	92.39	92.39	78.58	8.04
2.- 3.0	80.92	80.92	45.25	17.09
3.- 4.0	78.18	78.18	82.46	7.04
4.- 4.6	88.01	88.01	55.46	14.06

BOREHOLE LENGTH = 4.55 M
RECOVERY = 100.00 %
AVERAGE RQD = 70.04 %
AVERAGE FREQUENCY = 19.35 FRAC/M
TOTAL NUMBER OF FRACTURES = 88

FRACTURE FREQUENCY AND RQD FOR SCANLINE NO. RUW-2

INTERVAL (M)	RQD %	ADJ RQD %	THEO RQD %	FREQUENCY (FRAC/M)
0.- 1.0	57.58	57.58	31.39	23.51
1.- 2.0	27.76	27.76	15.30	33.13
2.- 3.0	68.86	68.86	39.24	20.31
3.- 4.0	91.11	91.11	86.22	6.41
4.- 5.0	77.39	77.39	51.87	16.03
5.- 6.0	47.62	47.62	55.41	14.96
6.- 6.7	71.22	71.22	63.59	12.62

BOREHOLE LENGTH = 6.25 M
 RECOVERY = 100.00 %
 AVERAGE RQD = 66.99 %
 AVERAGE FREQUENCY = 18.40 FRAC/M
 TOTAL NUMBER OF FRACTURES = 115

FRACTURE FREQUENCY AND RQD FOR SCANLINE NO. RUE-2

INTERVAL (M)	RQD %	ADJ RQD %	THEO RQD %	FREQUENCY (FRAC/M)
0.- 1.0	86.28	77.02	89.75	4.46
1.- 2.0	83.49	74.52	70.65	8.93
2.- 3.0	89.59	79.96	86.22	5.36
3.- 4.0	66.78	59.60	45.25	15.17
4.- 5.0	61.34	54.75	22.99	23.21
5.- 5.6	22.20	19.81	20.78	24.33

BOREHOLE LENGTH = 6.30 M
 RECOVERY = 39.26 %
 AVERAGE RQD = 63.70 %
 AVERAGE FREQUENCY = 12.86 FRAC/M
 TOTAL NUMBER OF FRACTURES = 81

FRACTURE FREQUENCY AND RQD FOR SCANLINE NO. RDU-2

INTERVAL (M)	RQD %	ADJ RQD %	THEO RQD %	FREQUENCY (FRAC/M)
0.- 1.0	54.79	51.69	62.85	11.32
1.- 2.0	87.30	82.37	78.58	7.55
2.- 3.0	85.52	80.69	55.41	13.21
3.- 4.0	77.14	72.78	45.25	16.04
4.- 4.4	79.74	75.23	76.42	8.06

BOREHOLE LENGTH = 4.61 M
 RECOVERY = 94.35 %
 AVERAGE RQD = 72.15 %
 AVERAGE FREQUENCY = 11.71 FRAC/M
 TOTAL NUMBER OF FRACTURES = 54

FRACTURE FREQUENCY AND RQD FOR SCANLINE NO. RHE-2

INTERVAL (M)	RQD %	ADJ RQD %	THEO RQD %	FREQUENCY (FRAC/M)
0.- 1.0	95.25	95.25	82.46	7.25
1.- 2.0	74.27	74.27	45.25	17.60
2.- 3.0	90.35	90.35	66.72	11.39
3.- 4.0	74.35	74.35	70.65	10.36
4.- 4.6	87.91	87.91	90.56	4.93

BOREHOLE LENGTH = 4.47 M
 RECOVERY = 100.00 %
 AVERAGE RQD = 87.14 %
 AVERAGE FREQUENCY = 10.73 FRAC/M
 TOTAL NUMBER OF FRACTURES = 48

FRACTURE FREQUENCY AND RQD FOR SCANLINE NO. RDD-2

INTERVAL (M)	RQD %	ADJ RQD %	THEO RQD %	FREQUENCY (FRAC/M)
0.- 1.0	94.74	94.74	92.97	4.05
1.- 2.0	90.02	90.02	86.22	6.07
2.- 3.0	69.52	69.52	39.24	19.21
3.- 4.0	80.70	80.70	62.85	12.14
4.- 4.8	100.00	100.00	93.40	3.90

BOREHOLE LENGTH = 4.72 M
 RECOVERY = 100.00 %
 AVERAGE RQD = 87.37 %
 AVERAGE FREQUENCY = 9.31 FRAC/M
 TOTAL NUMBER OF FRACTURES = 44

FRACTURE FREQUENCY AND RQD FOR SCANLINE NO. RDE-2

INTERVAL (M)	RQD %	ADJ RQD %	THEO RQD %	FREQUENCY (FRAC/M)
0.- 1.0	81.46	81.46	62.85	12.16
1.- 2.0	69.93	69.93	66.72	11.14
2.- 3.0	80.04	80.04	66.22	6.08
3.- 4.0	75.67	75.67	70.65	10.13
4.- 4.7	63.52	63.52	62.09	12.36

BOREHOLE LENGTH = 4.60 M
 RECOVERY = 100.00 %
 AVERAGE RQD = 75.87 %
 AVERAGE FREQUENCY = 10.23 FRAC/M
 TOTAL NUMBER OF FRACTURES = 47

FRACTURE FREQUENCY AND RQD FOR SCANLINE NO. RDW-2

INTERVAL (M)	RQD %	ADJ RQD %	THEO RQD %	FREQUENCY (FRAC/M)
0.- 1.0	26.92	26.92	14.08	34.45
1.- 2.0	26.42	26.42	7.09	43.07
2.- 3.0	71.65	71.65	74.62	9.69
3.- 4.0	86.54	86.54	70.65	10.77
4.- 4.9	75.77	75.77	59.04	14.01

BOREHOLE LENGTH = 4.57 M
 RECOVERY = 100.00 %
 AVERAGE RQD = 61.56 %
 AVERAGE FREQUENCY = 22.53 FRAC/M
 TOTAL NUMBER OF FRACTURES = 103

FRACTURE FREQUENCY AND RQD FOR SCANLINE NO. RUW-3

INTERVAL (M)	RQD %	ADJ RQD %	THEO RQD %	FREQUENCY (FRAC/M)
0.- 1.0	66.68	66.68	51.87	15.65
1.- 2.0	43.81	43.81	11.89	35.47
2.- 3.0	26.03	26.03	18.05	30.25
3.- 4.0	45.19	45.09	22.99	27.12
4.- 5.0	69.85	69.85	29.08	23.99
5.- 6.0	46.28	46.28	15.30	32.34
6.- 6.3	64.57	64.67	84.19	6.83

BOREHOLE LENGTH = 6.04 M
 RECOVERY = 100.00 %
 AVERAGE RQD = 52.53 %
 AVERAGE FREQUENCY = 26.47 FRAC/M
 TOTAL NUMBER OF FRACTURES = 160

FRACTURE FREQUENCY AND RQD FOR SCANLINE NO. RUE-3

INTERVAL (M)	RQD %	ADJ RQD %	THEO RQD %	FREQUENCY (FRAC/M)
0.- 1.0	76.20	75.20	78.58	8.18
1.- 2.0	53.34	53.34	55.41	14.31
2.- 3.0	13.33	13.33	19.58	28.62
3.- 4.0	73.03	73.03	66.72	11.24
4.- 5.0	84.07	84.07	62.85	12.27
5.- 6.0	58.09	58.09	31.39	22.49
6.- 6.2	7.53	7.53	0.99	62.98

BOREHOLE LENGTH = 6.04 M
 RECOVERY = 100.00 %
 AVERAGE RQD = 59.46 %
 AVERAGE FREQUENCY = 17.54 FRAC/M
 TOTAL NUMBER OF FRACTURES = 106

FRACTURE FREQUENCY AND RQD FOR SCANLINE NO. RDU-3

INTERVAL (M)	RQD %	ADJ RQD %	THEO RQD %	FREQUENCY (FRAC/M)
0.- 1.0	53.01	52.79	24.89	24.90
1.- 2.0	100.00	99.58	89.75	4.98
2.- 3.0	44.12	43.94	15.30	30.87
3.- 4.0	71.48	71.18	29.08	22.90
4.- 4.6	55.12	54.89	18.14	28.82

BOREHOLE LENGTH = 4.57 M
 RECOVERY = 99.58 %
 AVERAGE RQD = 65.42 %
 AVERAGE FREQUENCY = 21.87 FRAC/M
 TOTAL NUMBER OF FRACTURES = 100

FRACTURE FREQUENCY AND RQD FOR SCANLINE NO. RHE-3

INTERVAL (M)	RQD %	ADJ RQD %	THEO RQD %	FREQUENCY (FRAC/M)
0.- 1.0	72.06	72.06	70.65	10.00
1.- 2.0	74.60	74.60	59.07	13.00
2.- 3.0	98.10	98.10	86.22	6.00
3.- 4.0	60.53	60.63	66.72	11.00
4.- 4.7	80.72	80.72	77.46	8.28

BOREHOLE LENGTH = 4.72 M
 RECOVERY = 100.00 %
 AVERAGE RQD = 77.02 %
 AVERAGE FREQUENCY = 9.74 FRAC/M
 TOTAL NUMBER OF FRACTURES = 46

FRACTURE FREQUENCY AND RQD FOR SCANLINE NO. RDD-3

INTERVAL (M)	RQD %	ADJ RQD %	THEO RQD %	FREQUENCY (FRAC/M)
0.- 1.0	77.77	77.02	51.87	14.85
1.- 2.0	80.98	80.19	78.58	7.92
2.- 3.0	37.47	37.10	5.44	42.58
3.- 4.0	81.87	81.07	42.16	17.82
4.- 4.5	73.52	72.90	80.21	7.51

BOREHOLE LENGTH = 4.57 M
 RECOVERY = 99.03 %
 AVERAGE RQD = 69.31 %
 AVERAGE FREQUENCY = 19.25 FRAC/M
 TOTAL NUMBER OF FRACTURES = 88

FRACTURE FREQUENCY AND RQD FOR SCANLINE NO. RDE-3

INTERVAL (M)	RQD %	ADJ RQD %	THEO RQD %	FREQUENCY (FRAC/M)
0.- 1.0	63.81	63.81	62.85	12.28
1.- 2.0	78.41	78.41	86.22	6.14
2.- 3.0	90.20	90.20	86.22	6.14
3.- 4.0	95.20	95.20	78.58	8.19
4.- 4.8	88.24	88.24	93.07	4.06

BOREHOLE LENGTH = 4.65 M
 RECOVERY = 100.00 %
 AVERAGE RQD = 84.84 %
 AVERAGE FREQUENCY = 7.53 FRAC/M
 TOTAL NUMBER OF FRACTURES = 35

FRACTURE FREQUENCY AND RQD FOR SCANLINE NO. RDW-3

INTERVAL (M)	RQD %	ADJ RQD %	THEO RQD %	FREQUENCY (FRAC/M)
0.- 1.0	75.24	73.57	51.87	14.67
1.- 2.0	100.00	97.78	66.22	5.87
2.- 3.0	41.58	40.66	70.65	9.78
3.- 4.0	85.40	83.50	70.65	9.78
4.- 4.5	100.00	97.78	87.10	5.63

BOREHOLE LENGTH = 4.62 M
 RECOVERY = 97.78 %
 AVERAGE RQD = 76.63 %
 AVERAGE FREQUENCY = 9.52 FRAC/M
 TOTAL NUMBER OF FRACTURES = 44

FRACTURE FREQUENCY AND RQD FOR SCANLINE NO. RUW-4

INTERVAL (M)	RQD %	ADJ RQD %	THEO RQD %	FREQUENCY (FRAC/M)
0.- 1.0	46.23	46.23	33.85	21.27
1.- 2.0	72.75	72.75	78.58	8.10
2.- 3.0	23.90	23.80	9.20	37.48
3.- 4.0	54.33	54.33	70.65	10.13
4.- 5.0	23.50	23.50	7.09	40.51
5.- 6.0	90.60	90.60	86.22	6.08
6.- 6.4	100.00	100.00	90.00	4.99

BUREHOLE LENGTH = 6.32 M
 RECOVERY = 100.00 %
 AVERAGE RQD = 55.62 %
 AVERAGE FREQUENCY = 19.61 FRAC/M
 TOTAL NUMBER OF FRACTURES = 124

FRACTURE FREQUENCY AND RQD FOR SCANLINE NO. RUE-4

INTERVAL (M)	RQD %	ADJ RQD %	THEO RQD %	FREQUENCY (FRAC/M)
0.- 1.0	67.56	67.56	48.48	16.80
1.- 2.0	80.11	80.11	82.46	7.35
2.- 3.0	81.97	81.97	62.95	12.60
3.- 4.0	64.19	64.19	36.47	21.00
4.- 5.0	78.16	78.16	70.65	10.50
5.- 6.0	62.15	62.15	51.87	15.75
6.- 6.3	85.32	85.32	45.25	17.85

BOPEHOLE LENGTH = 6.00 M
 RECOVERY = 100.00 %
 AVERAGE RQD = 76.60 %
 AVERAGE FREQUENCY = 14.18 FRAC/M
 TOTAL NUMBER OF FRACTURES = 85

FRACTURE FREQUENCY AND RQD FOR SCANLINE NO. RDU-4

INTERVAL (M)	RQD %	ADJ RQD %	THEO RQD %	FREQUENCY (FRAC/M)
0.- 1.0	53.77	53.77	70.65	10.54
1.- 2.0	76.53	76.63	70.65	10.54
2.- 3.0	78.38	78.38	78.58	8.43
3.- 4.0	70.31	70.31	45.25	17.91
4.- 4.9	41.11	41.11	53.65	15.27

BOREHOLE LENGTH = 4.65 M
 RECOVERY = 100.00 %
 AVERAGE RQD = 67.98 %
 AVERAGE FREQUENCY = 12.48 FRAC/M
 TOTAL NUMBER OF FRACTURES = 58

FRACTURE FREQUENCY AND RQD FOR SCANLINE NO. RHE-4

INTERVAL (M)	RQD %	ADJ RQD %	THEO RQD %	FREQUENCY (FRAC/M)
0.- 1.0	19.99	19.27	45.25	16.39
1.- 2.0	89.33	86.10	89.75	4.82
2.- 3.0	100.00	96.33	89.75	4.82
3.- 4.0	96.19	92.71	89.75	4.82
4.- 4.6	66.55	64.14	44.22	16.70

BOREHOLE LENGTH = 4.75 M
 RECOVERY = 96.38 %
 AVERAGE RQD = 72.42 %
 AVERAGE FREQUENCY = 8.84 FRAC/M
 TOTAL NUMBER OF FRACTURES = 42

FRACTURE FREQUENCY AND RQD FOR SCANLINE NO. RDD-4

INTERVAL (M)	RQD %	ADJ RQD %	THEO RQD %	FREQUENCY (FRAC/M)
0.- 1.0	46.55	44.92	39.24	18.29
1.- 2.0	75.26	72.45	82.46	6.74
2.- 3.0	56.67	54.55	66.72	10.59
3.- 4.0	63.42	61.06	62.95	11.55
4.- 4.5	61.77	59.47	66.14	5.80

BOREHOLE LENGTH = 4.67 M
 RECOVERY = 96.27 %
 AVERAGE RQD = 58.38 %
 AVERAGE FREQUENCY = 11.13 FRAC/M
 TOTAL NUMBER OF FRACTURES = 52

FRACTURE FREQUENCY AND RQD FOR SCANLINE NO. RDE-4

INTERVAL (M)	RQD %	ADJ RQD %	THEO RQD %	FREQUENCY (FRAC/M)
0.- 1.0	53.09	53.09	16.62	30.80
1.- 2.0	74.02	74.02	78.58	8.21
2.- 3.0	71.27	71.27	74.62	9.24
3.- 4.0	86.56	86.56	82.46	7.19
4.- 4.8	96.71	96.71	84.47	6.64

BOREHOLE LENGTH = 4.65 M
 RECOVERY = 100.00 %
 AVERAGE RQD = 77.38 %
 AVERAGE FREQUENCY = 12.69 FRAC/M
 TOTAL NUMBER OF FRACTURES = 59

FRACTURE FREQUENCY AND RQD FOR SCANLINE NO. RDW-4

INTERVAL (M)	RQD %	ADJ RQD %	THEO RQD %	FREQUENCY (FRAC/M)
0.- 1.0	12.70	12.70	2.64	53.68
1.- 2.0	39.98	39.98	7.73	41.05
2.- 3.0	47.17	47.17	15.30	32.63
3.- 4.0	100.00	100.00	86.22	6.32
4.- 4.9	85.05	85.05	87.05	6.07

BOREHOLE LENGTH = 4.62 M
 RECOVERY = 100.00 %
 AVERAGE RQD = 59.16 %
 AVERAGE FREQUENCY = 28.55 FRAC/M
 TOTAL NUMBER OF FRACTURES = 132

FRACTURE FREQUENCY AND RQD FOR SCANLINE NO. RUW-5

INTERVAL (M)	RQD %	ADJ RQD %	THEO RQD %	FREQUENCY (FRAC/M)
0.- 1.0	63.93	63.93	14.08	33.40
1.- 2.0	74.75	74.75	45.25	17.74
2.- 3.0	94.77	94.77	89.75	5.22
3.- 4.0	94.41	94.41	78.58	8.35
4.- 5.0	26.21	26.21	15.30	32.36
5.- 6.0	68.83	68.83	70.65	10.44
6.- 6.4	0.00	0.00	4.02	48.41

BOPEHOLE LENGTH = 6.12 M
 RECOVERY = 100.00 %
 AVERAGE RQD = 69.10 %
 AVERAGE FREQUENCY = 19.77 FRAC/M
 TOTAL NUMBER OF FRACTURES = 121

FRACTURE FREQUENCY AND RQD FOR SCANLINE NO. RUE-5

INTERVAL (M)	RQD %	ADJ RQD %	THEO RQD %	FREQUENCY (FRAC/M)
0.- 1.0	25.40	23.97	4.16	43.40
1.- 2.0	36.93	34.85	15.30	29.25
2.- 3.0	60.12	56.73	62.85	11.32
3.- 4.0	97.97	92.43	74.62	8.49
4.- 5.0	59.35	55.01	19.58	26.42
5.- 5.9	17.32	16.34	6.34	38.93

BOPEHOLE LENGTH = 6.22 M
 RECOVERY = 94.35 %
 AVERAGE RQD = 47.38 %
 AVERAGE FREQUENCY = 26.03 FRAC/M
 TOTAL NUMBER OF FRACTURES = 162

FRACTURE FREQUENCY AND RQD FOR SCANLINE NO. RDU-5

INTERVAL (M)	RQD %	ADJ RQD %	THEO RQD %	FREQUENCY (FRAC/M)
0.- 1.0	94.92	94.92	74.62	9.04
1.- 2.0	96.19	96.19	82.46	7.03
2.- 3.0	100.00	100.00	95.76	3.01
3.- 4.0	72.31	72.31	45.25	17.07
4.- 4.7	68.93	68.93	27.69	23.73

BOREHOLE LENGTH = 4.73 M
 RECOVERY = 100.00 %
 AVERAGE RQD = 87.87 %
 AVERAGE FREQUENCY = 11.28 FRAC/M
 TOTAL NUMBER OF FRACTURES = 53

FRACTURE FREQUENCY AND RQD FOR SCANLINE NO. RHE-5

INTERVAL (M)	RQD %	ADJ RQD %	THEO RQD %	FREQUENCY (FRAC/M)
0.- 1.0	49.53	49.53	66.72	11.05
1.- 2.0	79.35	79.35	82.46	7.03
2.- 3.0	83.49	83.49	86.22	6.03
3.- 4.0	86.03	86.03	74.62	9.04
4.- 4.6	100.00	100.00	90.23	4.88

BOREHOLE LENGTH = 4.60 M
 RECOVERY = 100.00 %
 AVERAGE RQD = 78.36 %
 AVERAGE FREQUENCY = 7.83 FRAC/M
 TOTAL NUMBER OF FRACTURES = 36

FRACTURE FREQUENCY AND RQD FOR SCANLINE NO. RDD-5

INTERVAL (M)	RQD %	ADJ RQD %	THEO RQD %	FREQUENCY (FRAC/M)
0.- 1.0	62.66	62.66	59.07	13.03
1.- 2.0	80.70	80.70	74.62	9.02
2.- 3.0	93.40	93.40	86.22	6.01
3.- 4.0	84.51	84.51	82.46	7.02
4.- 4.9	69.75	69.75	84.81	6.40

BOREHOLE LENGTH = 4.93 M
 RECOVERY = 100.00 %
 AVERAGE RQD = 78.49 %
 AVERAGE FREQUENCY = 8.32 FRAC/M
 TOTAL NUMBER OF FRACTURES = 41

FRACTURE FREQUENCY AND RQD FOR SCANLINE NO. RDE-5

INTERVAL (M)	RQD %	ADJ RQD %	THEO RQD %	FREQUENCY (FRAC/M)
0.- 1.0	29.72	27.55	5.44	39.86
1.- 2.0	27.28	25.29	6.49	38.00
2.- 3.0	65.46	60.67	39.24	17.61
3.- 4.0	14.45	13.40	21.23	25.03
4.- 4.4	97.35	90.23	89.83	4.61

BOREHOLE LENGTH = 4.75 M
 RECOVERY = 92.69 %
 AVERAGE RQD = 37.07 %
 AVERAGE FREQUENCY = 27.80 FRAC/M
 TOTAL NUMBER OF FRACTURES = 132

FRACTURE FREQUENCY AND RQD FOR SCANLINE NO. RDW-5

INTERVAL (M)	RQD %	ADJ RQD %	THEO RQD %	FREQUENCY (FRAC/M)
0.- 1.0	73.33	73.33	24.99	29.08
1.- 2.0	93.40	93.40	66.72	12.80
2.- 3.0	74.35	74.35	66.72	12.80
3.- 4.0	68.76	68.76	70.65	11.63
4.- 5.0	83.74	83.74	86.22	6.98

BOREHOLE LENGTH = 4.47 M
 RECOVERY = 100.00 %
 AVERAGE RQD = 88.02 %
 AVERAGE FREQUENCY = 14.09 FRAC/M
 TOTAL NUMBER OF FRACTURES = 63

FRACTURE FREQUENCY AND RQD FOR SCANLINE NO. RUW-6

INTERVAL (M)	RQD %	ADJ RQD %	THEO RQD %	FREQUENCY (FRAC/M)
0.- 1.0	19.74	19.74	5.94	46.59
1.- 2.0	61.65	61.65	10.03	39.94
2.- 3.0	73.84	73.84	78.58	8.87
3.- 4.0	91.52	91.62	86.22	6.66
4.- 5.0	81.84	81.84	55.41	15.53
5.- 6.0	26.72	26.72	31.39	24.41
6.- 6.8	57.87	57.87	13.02	36.53

BOREHOLE LENGTH = 6.15 M
 RECOVERY = 100.00 %
 AVERAGE RQD = 65.53 %
 AVERAGE FREQUENCY = 25.21 FRAC/M
 TOTAL NUMBER OF FRACTURES = 155

FRACTURE FREQUENCY AND RQD FOR SCANLINE NO. RUE-6

INTERVAL (M)	RQD %	ADJ RQD %	THEO RQD %	FREQUENCY (FRAC/M)
0.- 1.0	52.83	52.93	22.99	26.87
1.- 2.0	75.54	75.54	82.46	7.23
2.- 3.0	83.74	83.74	74.62	9.30
3.- 4.0	72.57	72.57	59.07	13.43
4.- 5.0	76.38	76.38	51.87	15.50
5.- 6.0	62.10	62.10	55.41	14.47
6.- 7.0	89.64	89.64	55.41	14.47
7.- 8.0	74.95	74.95	33.85	21.70
8.- 9.0	54.36	54.36	45.25	17.57
9.- 9.5	71.33	71.33	55.62	14.40

BOREHOLE LENGTH = 9.20 M
 RECOVERY = 100.00 %
 AVERAGE RQD = 73.75 %
 AVERAGE FREQUENCY = 15.55 FRAC/M
 TOTAL NUMBER OF FRACTURES = 143

FRACTURE FREQUENCY AND RQD FOR SCANLINE NO. RDU-6

INTERVAL (M)	RQD %	ADJ RQD %	THEO RQD %	FREQUENCY (FRAC/M)
0.- 1.0	56.64	56.64	36.47	21.44
1.- 2.0	52.83	52.83	45.25	18.23
2.- 3.0	62.76	62.76	48.48	17.15
3.- 4.0	66.73	66.73	48.48	17.15
4.- 5.0	82.22	82.22	74.62	9.65

BOREHOLE LENGTH = 4.78 M
 RECOVERY = 100.00 %
 AVERAGE RQD = 67.25 %
 AVERAGE FREQUENCY = 16.33 FRAC/M
 TOTAL NUMBER OF FRACTURES = 78

FRACTURE FREQUENCY AND RQD FOR SCANLINE NO. RHE-6

INTERVAL (M)	RQD %	ADJ RQD %	THEO RQD %	FREQUENCY (FRAC/M)
0.- 1.0	73.94	73.60	74.62	8.97
1.- 2.0	74.95	74.61	74.62	8.97
2.- 3.0	80.44	80.18	74.62	8.97
3.- 4.0	79.93	79.67	82.46	6.98
4.- 4.6	91.97	91.67	85.04	6.30

BOREHOLE LENGTH = 4.65 M
 RECOVERY = 99.67 %
 AVERAGE RQD = 79.02 %
 AVERAGE FREQUENCY = 8.18 FRAC/M
 TOTAL NUMBER OF FRACTURES = 38

FRACTURE FREQUENCY AND RQD FOR SCANLINE NO. RDD-6

INTERVAL (M)	RQD %	ADJ RQD %	THEO RQD %	FREQUENCY (FRAC/M)
0.- 1.0	37.52	37.52	31.39	24.15
1.- 2.0	79.68	79.68	55.41	15.37
2.- 3.0	35.97	35.97	7.09	43.91
3.- 4.0	65.23	65.23	36.47	21.96
4.- 4.9	66.64	86.64	50.69	16.85

BOREHOLE LENGTH = 4.47 M
 RECOVERY = 100.00 %
 AVERAGE RQD = 66.47 %
 AVERAGE FREQUENCY = 24.58 FRAC/M
 TOTAL NUMBER OF FRACTURES = 110

FRACTURE FREQUENCY AND RQD FOR SCANLINE NO. RDE-6

INTERVAL (M)	RQD %	ADJ RQD %	THEO RQD %	FREQUENCY (FRAC/M)
0.- 1.0	14.66	14.66	7.09	43.54
1.- 2.0	39.70	39.70	16.62	32.65
2.- 3.0	52.10	52.10	12.94	35.92
3.- 4.0	62.41	62.41	51.97	16.33
4.- 4.9	96.48	96.48	91.03	5.02

BOREHOLE LENGTH = 4.47 M
 RECOVERY = 100.00 %
 AVERAGE RQD = 56.46 %
 AVERAGE FREQUENCY = 27.26 FRAC/M
 TOTAL NUMBER OF FRACTURES = 122

FRACTURE FREQUENCY AND RQD FOR SCANLINE NO. RDW-6

INTERVAL (M)	RQD %	ADJ RQD %	THEO RQD %	FREQUENCY (FRAC/M)
0.- 1.0	41.66	41.66	8.44	40.40
1.- 2.0	75.95	75.95	42.16	19.14
2.- 3.0	43.18	43.18	22.99	27.65
3.- 4.0	72.09	72.09	78.58	8.51
4.- 5.0	100.00	100.00	92.57	4.39

BOPEHOLE LENGTH = 4.67 M
 RECOVERY = 100.00 %
 AVERAGE RQD = 70.56 %
 AVERAGE FREQUENCY = 20.12 FRAC/M
 TOTAL NUMBER OF FRACTURES = 94

FRACTURE FREQUENCY AND RQD FOR SCANLINE NO. RUW-1 CORE

INTERVAL (M)	RQD %	ADJ RQD %	THEO RQD %	FREQUENCY (FRAC/M)
0.- 1.0	82.30	75.09	82.46	6.39
1.- 2.0	97.50	89.96	86.22	5.47
2.- 3.0	96.30	87.87	97.98	1.82
3.- 4.0	90.70	82.76	89.75	4.56
4.- 5.0	87.20	79.56	92.97	3.65
5.- 6.0	47.23	43.09	34.11	19.07

BOREHOLE LENGTH = 6.53 M
 RECOVERY = 91.24 %
 AVERAGE RQD = 76.46 %
 AVERAGE FREQUENCY = 6.74 FRAC/M
 TOTAL NUMBER OF FRACTURES = 44

FRACTURE FREQUENCY AND RQD FOR SCANLINE NO. RUE-1 .

INTERVAL (M)	RQD %	ADJ RQD %	THEO RQD %	FREQUENCY (FRAC/M)
0.- 1.0	83.50	82.05	78.58	7.86
1.- 2.0	90.00	88.44	95.76	2.95
2.- 3.0	100.00	98.26	95.76	2.95
3.- 4.0	98.50	96.79	92.97	3.93
4.- 5.0	95.00	93.35	97.98	1.97
5.- 6.0	68.00	66.82	70.65	9.83

BOREHOLE LENGTH = 6.20 M
 RECOVERY = 95.26 %
 AVERAGE RQD = 86.34 %
 AVERAGE FREQUENCY = 4.84 FRAC/M
 TOTAL NUMBER OF FRACTURES = 30

FRACTURE FREQUENCY AND RQD FOR SCANLINE NO. RDU-1 CORE

INTERVAL (M)	RQD %	ADJ RQD %	THEO RQD %	FREQUENCY (FRAC/M)
0.- 1.0	57.00	55.86	59.07	12.74
1.- 2.0	91.10	89.27	86.22	5.88
2.- 3.0	92.20	90.35	95.76	2.94
3.- 4.0	89.50	87.71	89.75	4.90
4.- 4.6	22.86	22.42	1.02	60.03

BOREHOLE LENGTH = 4.65 M
 RECOVERY = 97.99 %
 AVERAGE RQD = 73.68 %
 AVERAGE FREQUENCY = 13.12 FRAC/M
 TOTAL NUMBER OF FRACTURES = 61

FRACTURE FREQUENCY AND RQD FOR SCANLINE NO. RHE-1 CORE

INTERVAL (M)	RQD %	ADJ RQD %	THEO RQD %	FREQUENCY (FRAC/M)
0.- 1.0	62.30	62.30	59.07	13.45
1.- 2.0	50.30	50.80	62.85	12.41
2.- 3.0	78.10	78.10	74.62	9.31
3.- 4.0	56.40	55.40	66.72	11.38
4.- 5.0	64.70	64.70	73.36	9.64

BOREHOLE LENGTH = 4.30 M
 RECOVERY = 100.00 %
 AVERAGE RQD = 64.60 %
 AVERAGE FREQUENCY = 11.25 FRAC/M
 TOTAL NUMBER OF FRACTURES = 54

FRACTURE FREQUENCY AND RQD FOR SCANLINE NO. RDD-1 CORE

INTERVAL (M)	RQD %	ADJ RQD %	THEO RQD %	FREQUENCY (FRAC/M)
0.- 1.0	84.00	76.80	82.46	6.40
1.- 2.0	84.10	76.90	89.75	4.57
2.- 3.0	73.70	67.39	55.41	12.80
3.- 4.0	100.00	91.43	99.46	0.91

BOREHOLE LENGTH = 4.65 M
 RECOVERY = 91.43 %
 AVERAGE RQD = 73.53 %
 AVERAGE FREQUENCY = 5.81 FRAC/M
 TOTAL NUMBER OF FRACTURES = 27

FRACTURE FREQUENCY AND RQD FOR SCANLINE NO. RDE-1 CORE

INTERVAL (M)	RQD %	ADJ RQD %	THEO RQD %	FREQUENCY (FRAC/M)
0.- 1.0	44.70	43.73	48.46	15.65
1.- 2.0	57.80	56.54	66.72	10.76
2.- 3.0	44.10	43.14	45.25	16.63
3.- 4.0	82.20	80.41	66.72	10.76
4.- 4.6	0.00	0.00	38.49	18.85

BOREHOLE LENGTH = 4.67 M
 RECOVERY = 97.83 %
 AVERAGE RQD = 48.97 %
 AVERAGE FREQUENCY = 14.12 FRAC/M
 TOTAL NUMBER OF FRACTURES = 66

FRACTURE FREQUENCY AND RQD FOR SCANLINE NO. RDW-1 CORE

INTERVAL (M)	RQD %	ADJ RQD %	THEO RQD %	FREQUENCY (FRAC/M)
0.- 1.0	93.00	73.66	89.75	3.96
1.- 2.0	73.40	58.14	70.65	7.92
2.- 3.0	84.00	66.53	95.76	2.38
3.- 3.6	94.68	75.00	89.81	3.95

BOREHOLE LENGTH = 4.55 M
 RECOVERY = 79.21 %
 AVERAGE RQD = 67.60 %
 AVERAGE FREQUENCY = 4.62 FRAC/M
 TOTAL NUMBER OF FRACTURES = 21

FRACTURE FREQUENCY AND RQD FOR SCANLINE NO. RUW-2 CORE

INTERVAL (M)	RQD %	ADJ RQD %	THEO RQD %	FREQUENCY (FRAC/M)
0.- 1.0	100.00	97.69	97.98	1.95
1.- 2.0	90.40	88.31	86.22	5.86
2.- 3.0	100.00	97.69	92.97	3.91
3.- 4.0	81.50	79.62	82.46	6.84
4.- 5.0	78.20	76.39	82.46	6.84
5.- 6.0	74.30	72.58	74.62	8.79

BOREHOLE LENGTH = 6.25 M
 RECOVERY = 97.69 %
 AVERAGE RQD = 83.93 %
 AVERAGE FREQUENCY = 5.60 FRAC/M
 TOTAL NUMBER OF FRACTURES = 35

FRACTURE FREQUENCY AND RQD FOR SCANLINE NO. RUE-2 CORE

INTERVAL (M)	RQD %	ADJ RQD %	THEO RQD %	FREQUENCY (FRAC/M)
0.- 1.0	100.00	98.22	95.76	2.95
1.- 2.0	86.10	84.57	86.22	5.89
2.- 3.0	70.00	68.75	70.65	9.82
3.- 4.0	94.40	92.72	82.46	6.88
4.- 5.0	72.60	71.31	82.46	6.88
5.- 6.0	32.20	31.63	48.48	15.72
6.- 6.2	68.09	66.87	68.14	10.45

BOREHOLE LENGTH = 6.30 M
 RECOVERY = 98.22 %
 AVERAGE RQD = 74.30 %
 AVERAGE FREQUENCY = 8.09 FRAC/M
 TOTAL NUMBER OF FRACTURES = 51

FRACTURE FREQUENCY AND RQD FOR SCANLINE NO. RDU-2 CORE

INTERVAL (M)	RQD %	ADJ RQD %	THEO RQD %	FREQUENCY (FRAC/M)
0.- 1.0	59.00	53.53	66.72	9.98
1.- 2.0	94.90	86.10	89.75	4.54
2.- 3.0	58.80	53.35	62.85	10.89
3.- 4.0	62.70	56.89	70.65	9.07
4.- 4.2	94.02	85.30	88.25	4.93

BOREHOLE LENGTH = 4.61 M
 RECOVERY = 90.73 %
 AVERAGE RQD = 63.47 %
 AVERAGE FREQUENCY = 8.46 FRAC/M
 TOTAL NUMBER OF FRACTURES = 39

FRACTURE FREQUENCY AND RQD FOR SCANLINE NO. RHE-2 CORE

INTERVAL (M)	RQD %	ADJ RQD %	THEO RQD %	FREQUENCY (FRAC/M)
0.- 1.0	70.90	70.07	59.07	12.85
1.- 2.0	95.50	94.38	86.22	5.93
2.- 3.0	77.40	76.49	74.62	8.89
3.- 4.0	62.50	61.77	59.07	12.85
4.- 4.4	78.75	77.84	72.45	9.43

BOREHOLE LENGTH = 4.47 M
 RECOVERY = 98.83 %
 AVERAGE RQD = 75.88 %
 AVERAGE FREQUENCY = 10.06 FRAC/M
 TOTAL NUMBER OF FRACTURES = 45

FRACTURE FREQUENCY AND RQD FOR SCANLINE NO. RDD-2 CORE

INTERVAL (M)	RQD %	ADJ RQD %	THEO RQD %	FREQUENCY (FRAC/M)
0.- 1.0	93.90	85.01	92.97	3.62
1.- 2.0	100.00	90.53	97.98	1.81
2.- 3.0	77.50	70.16	86.22	5.43
3.- 4.0	88.50	80.12	89.75	4.53

BOREHOLE LENGTH = 4.72 M
 RECOVERY = 90.53 %
 AVERAGE RQD = 76.18 %
 AVERAGE FREQUENCY = 3.60 FRAC/M
 TOTAL NUMBER OF FRACTURES = 17

FRACTURE FREQUENCY AND RQD FOR SCANLINE NO. RDE-2 CORE

INTERVAL (M)	RQD %	ADJ RQD %	THEO RQD %	FREQUENCY (FRAC/M)
0.- 1.0	88.00	76.54	92.97	3.48
1.- 2.0	84.80	73.76	78.58	6.96
2.- 3.0	95.80	83.33	86.22	5.22
3.- 4.0	50.20	43.67	55.30	12.20

BOREHOLE LENGTH = 4.60 M
 RECOVERY = 80.98 %
 AVERAGE RQD = 69.34 %
 AVERAGE FREQUENCY = 6.96 FRAC/M
 TOTAL NUMBER OF FRACTURES = 32

FRACTURE FREQUENCY AND RQD FOR SCANLINE NO. RDW-2 CORE

INTERVAL (M)	RQD %	ADJ RQD %	THEO RQD %	FREQUENCY (FRAC/M)
0.- 1.0	25.90	25.49	45.25	16.73
1.- 2.0	61.40	60.42	48.48	15.74
2.- 3.0	35.60	35.03	39.24	18.70
3.- 4.0	29.70	29.23	55.41	13.78
4.- 4.5	74.15	72.96	70.57	9.86

BOREHOLE LENGTH = 4.57 M
RECOVERY = 98.40 %
AVERAGE RQD = 41.47 %
AVERAGE FREQUENCY = 15.53 FRAC/M
TOTAL NUMBER OF FRACTURES = 71

FRACTURE FREQUENCY AND RQD FOR SCANLINE NO. RUW-3 CORE

INTERVAL (M)	RQD %	ADJ RQD %	THEO RQD %	FREQUENCY (FRAC/M)
0.- 1.0	96.70	75.55	97.98	1.56
1.- 2.0	77.60	60.62	62.46	5.47
2.- 3.0	69.90	54.61	70.65	7.81
3.- 4.0	95.40	74.53	89.75	3.91
4.- 4.7	53.32	41.66	46.46	12.98

BOREHOLE LENGTH = 6.04 M
 RECOVERY = 78.12 %
 AVERAGE RQD = 62.56 %
 AVERAGE FREQUENCY = 5.96 FRAC/M
 TOTAL NUMBER OF FRACTURES = 36

FRACTURE FREQUENCY AND RQD FOR SCANLINE NO. RUE-3 CORE

INTERVAL (M)	RQD %	ADJ RQD %	THEO RQD %	FREQUENCY (FRAC/M)
0.- 1.0	71.00	64.16	74.62	8.13
1.- 2.0	64.00	57.84	62.85	10.84
2.- 3.0	81.50	73.65	78.58	7.23
3.- 4.0	100.00	90.37	99.46	0.90
4.- 5.0	100.00	90.37	95.76	2.71
5.- 5.5	63.85	57.70	75.98	7.82

BOREHOLE LENGTH = 6.04 M
 RECOVERY = 90.37 %
 AVERAGE RQD = 73.79 %
 AVERAGE FREQUENCY = 6.12 FRAC/M
 TOTAL NUMBER OF FRACTURES = 37

FRACTURE FREQUENCY AND RQD FOR SCANLINE NO. RDU-3 CORE

INTERVAL (M)	RQD %	ADJ RQD %	THEO RQD %	FREQUENCY (FRAC/M)
0.- 1.0	51.90	51.22	59.07	12.85
1.- 2.0	79.50	78.61	74.62	8.90
2.- 3.0	64.20	63.48	59.07	12.85
3.- 4.0	56.20	55.57	62.85	11.87
4.- 4.5	50.86	50.30	57.46	13.29

BOREHOLE LENGTH = 4.57 M
 RECOVERY = 98.89 %
 AVERAGE RQD = 60.85 %
 AVERAGE FREQUENCY = 11.81 FRAC/M
 TOTAL NUMBER OF FRACTURES = 54

FRACTURE FREQUENCY AND RQD FOR SCANLINE NO. RHE-3 CORE

INTERVAL (M)	RQD %	ADJ RQD %	THEO RQD %	FREQUENCY (FRAC/M)
0.- 1.0	11.70	11.50	21.23	26.53
1.- 2.0	41.90	41.17	48.48	15.72
2.- 3.0	47.90	46.97	51.87	14.74
3.- 4.0	12.10	11.89	42.16	17.69
4.- 4.6	21.96	21.58	35.80	19.90

BOREHOLE LENGTH = 4.72 M
 RECOVERY = 98.26 %
 AVERAGE RQD = 27.01 %
 AVERAGE FREQUENCY = 18.84 FRAC/M
 TOTAL NUMBER OF FRACTURES = 89

FRACTURE FREQUENCY AND RQD FOR SCANLINE NO. RDD-3 CORE

INTERVAL (M)	RQD %	ADJ RQD %	THEO RQD %	FREQUENCY (FRAC/M)
0.- 1.0	43.70	43.70	31.39	22.22
1.- 2.0	33.70	33.70	39.24	19.19
2.- 3.0	35.00	35.00	39.24	19.19
3.- 4.0	33.50	33.50	33.85	21.21
4.- 4.6	19.09	19.09	33.76	21.25

BOREHOLE LENGTH = 4.57 M
 RECOVERY = 100.00 %
 AVERAGE RQD = 34.49 %
 AVERAGE FREQUENCY = 20.56 FRAC/M
 TOTAL NUMBER OF FRACTURES = 94

FRACTURE FREQUENCY AND RQD FOR SCANLINE NO. RDE-3 COR

INTERVAL (M)	RQD %	ADJ RQD %	THEO RQD %	FREQUENCY (FRAC/M)
0.- 1.0	29.30	28.46	45.25	16.51
1.- 2.0	84.70	82.27	74.62	8.74
2.- 3.0	70.30	68.29	74.62	8.74
3.- 4.0	76.80	74.60	62.46	6.80
4.- 4.5	100.00	97.13	93.32	3.77

BOREHOLE LENGTH = 4.65 M
 RECOVERY = 97.13 %
 AVERAGE RQD = 67.25 %
 AVERAGE FREQUENCY = 9.47 FRAC/M
 TOTAL NUMBER OF FRACTURES = 44

FRACTURE FREQUENCY AND RQD FOR SCANLINE NO. RDW-3 CORE

INTERVAL (M)	RQD %	ADJ RQD %	THEO RQD %	FREQUENCY (FRAC/M)
0.- 1.0	80.00	80.00	59.07	13.18
1.- 2.0	85.50	85.50	82.46	7.10
2.- 3.0	48.00	48.00	62.85	12.17
3.- 4.0	64.40	64.40	74.62	9.13
4.- 4.7	54.28	54.28	75.78	8.83

BOREHOLE LENGTH = 4.62 M
 RECOVERY = 100.00 %
 AVERAGE RQD = 68.19 %
 AVERAGE FREQUENCY = 10.16 FRAC/M
 TOTAL NUMBER OF FRACTURES = 47

FRACTURE FREQUENCY AND RQD FOR SCANLINE NO. RUW-4 CORE

INTERVAL (M)	RQD %	ADJ RQD %	THEO RQD %	FREQUENCY (FRAC/M)
0.- 1.0	100.00	79.25	92.97	3.17
1.- 2.0	100.00	79.25	92.97	3.17
2.- 3.0	84.40	66.88	48.48	12.66
3.- 4.0	75.90	60.15	55.41	11.09
4.- 5.0	57.70	45.73	19.58	22.19

BOREHOLE LENGTH = 6.32 M
 RECOVERY = 79.25 %
 AVERAGE RQD = 66.09 %
 AVERAGE FREQUENCY = 10.44 FRAC/M
 TOTAL NUMBER OF FRACTURES = 66

FRACTURE FREQUENCY AND RQD FOR SCANLINE NO. RUE-4 CORE

INTERVAL (M)	RQD %	ADJ RQD %	THEO RQD %	FREQUENCY (FRAC/M)
0.- 1.0	0.00	0.00	51.87	13.32
1.- 2.0	60.10	53.35	74.62	7.99
2.- 3.0	73.00	64.80	62.95	10.65
3.- 4.0	79.80	70.84	78.58	7.10
4.- 5.0	97.30	86.81	95.76	2.66

BOREHOLE LENGTH = 6.00 M
 RECOVERY = 88.77 %
 AVERAGE RQD = 51.82 %
 AVERAGE FREQUENCY = 7.84 FRAC/M
 TOTAL NUMBER OF FRACTURES = 47

FRACTURE FREQUENCY AND RQD FOR SCANLINE NO. RDU-4 CORE

INTERVAL (M)	RQD %	ADJ RQD %	THEO RQD %	FREQUENCY (FRAC/M)
0.- 1.0	56.30	56.30	59.07	13.13
1.- 2.0	100.00	100.00	92.97	4.04
2.- 3.0	68.00	68.00	78.58	6.08
3.- 4.0	76.20	76.20	86.22	6.06
4.- 4.7	67.10	67.10	59.12	13.11

BOREHOLE LENGTH = 4.65 M
 RECOVERY = 100.00 %
 AVERAGE RQD = 74.65 %
 AVERAGE FREQUENCY = 8.61 FRAC/M
 TOTAL NUMBER OF FRACTURES = 40

FRACTURE FREQUENCY AND RQD FOR SCANLINE NO. RHE-4 CORE

INTERVAL (M)	RQD %	ADJ RQD %	THEO RQD %	FREQUENCY (FRAC/M)
0.- 1.0	57.00	56.50	62.85	11.89
1.- 2.0	62.50	61.95	55.41	13.88
2.- 3.0	21.20	21.01	33.95	20.82
3.- 4.0	43.20	42.92	14.08	31.72
4.- 4.7	35.08	34.77	33.31	21.03

BOREHOLE LENGTH = 4.75 M
 RECOVERY = 99.12 %
 AVERAGE RQD = 43.95 %
 AVERAGE FREQUENCY = 19.79 FRAC/M
 TOTAL NUMBER OF FRACTURES = 94

FRACTURE FREQUENCY AND RQD FOR SCANLINE NO. RDD-4 CORE

INTERVAL (M)	RQD %	ADJ RQD %	THEO RQD %	FREQUENCY (FRAC/M)
0.- 1.0	44.80	43.24	45.25	16.41
1.- 2.0	58.50	56.46	48.48	15.44
2.- 3.0	0.00	0.00	8.44	36.68
3.- 4.0	0.00	0.00	16.62	28.96
4.- 4.5	29.22	28.20	32.44	20.82

BOREHOLE LENGTH = 4.67 M
 RECOVERY = 96.52 %
 AVERAGE RQD = 25.30 %
 AVERAGE FREQUENCY = 23.97 FRAC/M
 TOTAL NUMBER OF FRACTURES = 112

FRACTURE FREQUENCY AND RQD FOR SCANLINE NO. RDE-4 CORE

INTERVAL (M)	RQD %	ADJ RQD %	THEO RQD %	FREQUENCY (FRAC/M)
0.- 1.0	53.90	53.90	78.58	8.01
1.- 2.0	74.00	74.00	78.58	8.01
2.- 3.0	96.10	96.10	89.75	5.01
3.- 4.0	63.00	63.00	45.25	17.03
4.- 4.7	61.13	61.13	68.01	10.69

BOREHOLE LENGTH = 4.65 M
 RECOVERY = 100.00 %
 AVERAGE RQD = 70.37 %
 AVERAGE FREQUENCY = 9.68 FRAC/M
 TOTAL NUMBER OF FRACTURES = 45

FRACTURE FREQUENCY AND RQD FOR SCANLINE NO. RDW-4 CORE

INTERVAL (M)	RQD %	ADJ RQD %	THEQ RQD %	FREQUENCY (FRAC/M)
0.- 1.0	32.50	32.50	18.05	29.89
1.- 2.0	39.50	39.50	48.48	16.49
2.- 3.0	45.50	45.50	62.85	12.37
3.- 4.0	69.50	69.50	70.65	10.31
4.- 4.8	16.34	16.34	34.07	21.55

BOREHOLE LENGTH = 4.62 M
RECOVERY = 100.00 %
AVERAGE RQD = 43.15 %
AVERAGE FREQUENCY = 17.95 FRAC/M
TOTAL NUMBER OF FRACTURES = 83

FRACTURE FREQUENCY AND RQD FOR SCANLINE NO. RUW-5 CORE

INTERVAL (M)	RQD %	ADJ RQD %	THEO RQD %	FREQUENCY (FRAC/M)
0.- 1.0	88.60	81.18	86.22	5.50
1.- 2.0	69.90	63.96	86.22	5.50
2.- 3.0	97.50	89.34	92.97	3.67
3.- 4.0	90.30	82.74	89.75	4.58
4.- 5.0	89.70	82.19	74.62	8.25
5.- 5.6	58.39	53.50	58.48	12.06

BOREHOLE LENGTH = 6.12 M
 RECOVERY = 91.63 %
 AVERAGE RQD = 77.02 %
 AVERAGE FREQUENCY = 6.21 FRAC/M
 TOTAL NUMBER OF FRACTURES = 38

FRACTURE FREQUENCY AND RQD FOR SCANLINE NO. RUE-5 CORE

INTERVAL (M)	RQD %	ADJ RQD %	THEO RQD %	FREQUENCY (FRAC/M)
0.- 1.0	29.00	28.38	3.17	47.94
1.- 2.0	60.50	59.30	19.58	27.40
2.- 3.0	88.30	86.40	82.46	6.85
3.- 4.0	86.50	84.64	92.97	3.91
4.- 5.0	97.00	94.91	95.76	2.94
5.- 6.0	66.00	64.58	18.05	28.38
6.- 6.1	0.00	0.00	0.21	76.10

BOREHOLE LENGTH = 6.22 M
 RECOVERY = 97.85 %
 AVERAGE RQD = 68.67 %
 AVERAGE FREQUENCY = 20.40 FRAC/M
 TOTAL NUMBER OF FRACTURES = 127

FRACTURE FREQUENCY AND RQD FOR SCANLINE NO. RDU-5 CORE

INTERVAL (M)	RQD %	ADJ RQD %	THEO RQD %	FREQUENCY (FRAC/M)
0.- 1.0	44.60	40.54	59.07	11.82
1.- 2.0	65.50	59.54	70.65	9.09
2.- 3.0	92.80	84.35	89.75	4.54
3.- 4.0	67.50	61.35	78.58	7.27
4.- 4.3	95.22	86.55	93.93	3.34

BOREHOLE LENGTH = 4.70 M
 RECOVERY = 90.89 %
 AVERAGE RQD = 63.04 %
 AVERAGE FREQUENCY = 7.87 FRAC/M
 TOTAL NUMBER OF FRACTURES = 37

FRACTURE FREQUENCY AND RQD FOR SCANLINE NO. RHE-5 CORE

INTERVAL (M)	RQD %	ADJ RQD %	THEO RQD %	FREQUENCY (FRAC/M)
0.- 1.0	47.10	45.66	48.48	15.51
1.- 2.0	39.30	38.10	39.24	18.42
2.- 3.0	26.60	25.79	24.89	24.24
3.- 4.0	54.70	53.03	45.25	16.48
4.- 4.5	62.50	60.59	50.67	14.88

BOREHOLE LENGTH = 4.60 M
 RECOVERY = 96.95 %
 AVERAGE RQD = 42.59 %
 AVERAGE FREQUENCY = 18.28 FRAC/M
 TOTAL NUMBER OF FRACTURES = 84

FRACTURE FREQUENCY AND RQD FOR SCANLINE NO. RDD-5 CORE

INTERVAL (M)	RQD %	ADJ RQD %	THEO RQD %	FREQUENCY (FRAC/M)
0.- 1.0	12.70	12.65	15.30	30.89
1.- 2.0	38.40	38.26	33.85	20.92
2.- 3.0	73.20	72.94	62.85	11.96
3.- 4.0	38.00	37.86	33.85	20.92
4.- 4.9	51.04	50.86	62.56	12.03

BOREHOLE LENGTH = 4.93 M
 RECOVERY = 99.64 %
 AVERAGE RQD = 42.36 %
 AVERAGE FREQUENCY = 19.48 FRAC/M
 TOTAL NUMBER OF FRACTURES = 96

FRACTURE FREQUENCY AND RQD FOR SCANLINE NO. RDE-5 CORE

INTERVAL (M)	RQD %	ADJ RQD %	THEO RQD %	FREQUENCY (FRAC/M)
0.- 1.0	57.90	45.14	39.24	14.81
1.- 2.0	53.00	41.32	8.44	29.62
2.- 3.0	70.90	55.19	26.92	18.71
3.- 3.7	80.77	62.97	81.99	5.55

BOREHOLE LENGTH = 4.75 M
 RECOVERY = 77.96 %
 AVERAGE RQD = 50.20 %
 AVERAGE FREQUENCY = 19.11 FRAC/M
 TOTAL NUMBER OF FRACTURES = 86

FRACTURE FREQUENCY AND RQD FOR SCANLINE NO. RDW-5 CORE

INTERVAL (M)	RQD %	ADJ RQD %	THEO RQD %	FREQUENCY (FRAC/M)
0.- 1.0	56.50	56.50	45.25	17.34
1.- 2.0	11.50	11.50	24.89	25.50
2.- 3.0	41.70	41.70	51.87	15.30
3.- 4.0	91.00	91.00	95.76	3.06
4.- 4.6	86.61	86.61	88.52	5.46

BOREHOLE LENGTH = 4.47 M
RECOVERY = 100.00 %
AVERAGE RQD = 55.73 %
AVERAGE FREQUENCY = 14.09 FRAC/M
TOTAL NUMBER OF FRACTURES = 63

FRACTURE FREQUENCY AND RQD FOR SCANLINE NO. RUW-6 CORE

INTERVAL (M)	RQD %	ADJ RQD %	THEO RQD %	FREQUENCY (FRAC/M)
0.- 1.0	58.10	54.34	22.99	24.32
1.- 2.0	93.20	87.17	95.76	2.81
2.- 3.0	87.60	81.93	89.75	4.68
3.- 4.0	90.00	84.18	89.75	4.68
4.- 5.0	100.00	93.53	97.98	1.87
5.- 5.8	65.73	61.48	73.30	8.73

BOREHOLE LENGTH = 6.15 M
 RECOVERY = 93.53 %
 AVERAGE RQD = 77.78 %
 AVERAGE FREQUENCY = 7.81 FRAC/M
 TOTAL NUMBER OF FRACTURES = 48

FRACTURE FREQUENCY AND RQD FOR SCANLINE NO. RUE-6 CORE

INTERVAL (M)	RQD %	ADJ RQD %	THEO RQD %	FREQUENCY (FRAC/M)
0.- 1.0	56.50	55.71	26.92	23.67
1.- 2.0	94.50	93.19	89.75	4.93
2.- 3.0	72.00	71.00	89.75	4.93
3.- 4.0	72.40	71.39	78.58	7.89
4.- 5.0	63.50	82.34	59.07	12.82
5.- 6.0	48.80	48.12	62.85	11.83
6.- 7.0	33.00	32.54	45.25	16.76
7.- 8.0	83.70	82.54	82.46	6.90
8.- 9.0	58.10	57.29	45.25	16.76
9.- 9.1	61.76	50.91	52.90	14.50

BOREHOLE LENGTH = 9.20 M
 RECOVERY = 98.61 %
 AVERAGE RQD = 65.98 %
 AVERAGE FREQUENCY = 11.85 FRAC/M
 TOTAL NUMBER OF FRACTURES = 109

FRACTURE FREQUENCY AND RQD FOR SCANLINE NO. RDU-6 CORE

INTERVAL (M)	RQD %	ADJ RQD %	THEO RQD %	FREQUENCY (FRAC/M)
0.- 1.0	64.10	62.62	70.65	9.77
1.- 2.0	42.50	41.52	55.41	13.68
2.- 3.0	33.50	32.73	45.25	16.61
3.- 4.0	42.60	41.62	45.25	16.61
4.- 4.7	58.71	57.35	62.80	11.73

BOPEHOLE LENGTH = 4.73 M
 RECOVERY = 97.69 %
 AVERAGE RQD = 46.44 %
 AVERAGE FREQUENCY = 13.82 FRAC/M
 TOTAL NUMBER OF FRACTURES = 66

FRACTURE FREQUENCY AND RQD FOR SCANLINE NO. RHE-6 CORE

INTERVAL (M)	RQD %	ADJ RQD %	THEO RQD %	FREQUENCY (FRAC/M)
0.- 1.0	47.10	45.15	48.48	15.34
1.- 2.0	39.30	37.67	39.24	18.21
2.- 3.0	26.60	25.50	24.89	23.97
3.- 4.0	54.70	52.44	45.25	16.30
4.- 4.5	62.50	59.92	50.67	14.72

BOPEHOLE LENGTH = 4.65 M
 RECOVERY = 95.87 %
 AVERAGE RQD = 42.21 %
 AVERAGE FREQUENCY = 18.07 FRAC/M
 TOTAL NUMBER OF FRACTURES = 84

FRACTURE FREQUENCY AND RQD FOR SCANLINE NO. RDD-6 CORE

INTERVAL (M)	RQD %	ADJ RQD %	THEO RQD %	FREQUENCY (FRAC/M)
0.- 1.0	79.80	79.80	92.97	4.14
1.- 2.0	94.40	94.40	86.22	6.21
2.- 3.0	89.80	89.80	92.97	4.14
3.- 4.0	90.00	90.00	95.76	3.11
4.- 4.6	95.90	95.90	90.65	4.90

BOREHOLE LENGTH = 4.47 M
 RECOVERY = 100.00 %
 AVERAGE RQD = 92.70 %
 AVERAGE FREQUENCY = 4.47 FRAC/M
 TOTAL NUMBER OF FRACTURES = 20

FRACTURE FREQUENCY AND RQD FOR SCANLINE NO. RDE-6 CORE

INTERVAL (M)	RQD %	ADJ RQD %	THEO RQD %	FREQUENCY (FRAC/M)
0.- 1.0	14.40	12.49	31.39	19.08
1.- 2.0	32.80	28.45	26.92	20.81
2.- 3.0	49.40	42.84	15.30	26.89
3.- 3.9	79.16	68.65	69.66	8.89

BOREHOLE LENGTH = 4.47 M
 RECOVERY = 86.73 %
 AVERAGE RQD = 37.15 %
 AVERAGE FREQUENCY = 19.23 FRAC/M
 TOTAL NUMBER OF FRACTURES = 86

FRACTURE FREQUENCY AND RQD FOR SCANLINE NO. RDW-6 CORE

INTERVAL (M)	RQD %	ADJ RQD %	THEO RQD %	FREQUENCY (FRAC/M)
0.- 1.0	77.00	77.00	86.22	6.11
1.- 2.0	75.30	75.80	82.46	7.12
2.- 3.0	100.00	100.00	86.22	6.11
3.- 4.0	75.90	75.90	78.58	8.14
4.- 4.8	79.87	79.87	68.30	10.78

BOREHOLE LENGTH = 4.67 M
 RECOVERY = 100.00 %
 AVERAGE RQD = 83.25 %
 AVERAGE FREQUENCY = 7.49 FRAC/M
 TOTAL NUMBER OF FRACTURES = 35

FRACTURE FREQUENCY AND RQD FOR SCANLINE NO. PA-1

INTERVAL (M)	RQD %	ADJ RQD %	THEO RQD %	FREQUENCY (FRAC/M)
0.- 1.0	77.14	77.14	82.46	7.34
1.- 2.0	89.84	89.84	86.22	6.29
2.- 3.0	78.41	78.41	59.07	13.63
3.- 4.0	100.00	100.00	92.97	4.19
4.- 5.0	91.11	91.11	82.46	7.34
5.- 6.0	16.89	16.89	59.07	13.63
6.- 7.0	51.67	51.67	78.58	8.39
7.- 8.0	82.22	82.22	62.85	12.56
8.- 9.0	92.38	92.38	70.65	10.48
9.-10.0	58.09	58.09	33.85	22.02
10.-11.0	95.56	95.56	92.97	4.19
11.-12.0	100.00	100.00	95.76	3.15
12.-13.0	96.19	96.19	78.58	8.39
13.-14.0	98.73	98.73	89.75	5.24
14.-14.8	100.00	100.00	96.68	2.75

BOREHOLE LENGTH = 14.08 M
 RECOVERY = 100.00 %
 AVERAGE RQD = 85.54 %
 AVERAGE FREQUENCY = 8.73 FRAC/M
 TOTAL NUMBER OF FRACTURES = 123

FRACTURE FREQUENCY AND RQD FOR SCANLINE NO. PA-2

INTERVAL (M)	RQD %	ADJ RQD %	THEO RQD %	FREQUENCY (FRAC/M)
0.- 1.0	68.89	68.89	26.92	24.32
1.- 2.0	80.34	80.34	78.58	8.11
2.- 3.0	42.54	42.54	48.48	16.21
3.- 4.0	80.01	80.01	66.22	6.08
4.- 5.0	51.06	51.06	48.48	16.21
5.- 6.0	65.03	65.08	62.85	12.16
6.- 7.0	87.93	87.93	66.22	6.08
7.- 8.0	100.00	100.00	92.97	4.05
8.- 9.0	59.15	59.15	66.72	11.15
9.-10.0	90.68	90.68	86.22	6.08
10.-11.0	89.84	89.84	89.75	5.07
11.-12.0	92.38	92.38	95.76	3.04
12.-13.0	100.00	100.00	92.97	4.05
13.-14.0	80.95	80.95	82.46	7.09
14.-15.0	59.36	59.36	59.07	13.17
15.-16.0	77.78	77.78	74.62	9.12
16.-17.0	90.48	90.48	86.22	6.08
17.-18.0	94.28	94.26	86.22	6.08
18.-19.0	89.21	89.21	86.22	6.08
19.-20.0	66.93	65.98	31.39	22.29
20.-21.0	84.12	84.12	59.07	13.17
21.-22.0	100.00	100.00	89.75	5.07
22.-23.0	96.79	96.79	89.75	5.07
23.-24.0	32.38	32.38	66.72	11.15
24.-25.0	74.29	74.29	86.22	6.08
25.-26.0	76.51	76.51	82.46	7.09
26.-27.0	69.52	69.52	48.48	16.21
27.-28.0	83.49	83.49	86.22	6.08
28.-29.0	80.32	80.32	86.22	6.08
29.-30.0	73.33	73.33	26.92	24.32
30.-31.0	90.48	90.48	82.46	7.09
31.-32.0	100.00	100.00	95.76	3.04
32.-33.0	100.00	100.00	92.97	4.05

BOREHOLE LENGTH = 32.74 M
 RECOVERY = 100.00 %
 AVERAGE RQD = 80.28 %
 AVERAGE FREQUENCY = 9.26 FRAC/M
 TOTAL NUMBER OF FRACTURES = 303

FRACTURE FREQUENCY AND RQD FOR SCANLINE NO. PA-3

INTERVAL (M)	RQD %	ADJ RQD %	THEO RQD %	FREQUENCY (FRAC/M)
0.- 1.0	45.39	43.96	36.47	19.37
1.- 2.0	65.74	63.56	62.46	6.78
2.- 3.0	84.74	82.06	78.58	7.75
3.- 4.0	80.36	77.83	78.56	7.75
4.- 5.0	50.29	48.71	51.87	14.53
5.- 6.0	79.12	76.63	82.46	6.78
6.- 7.0	87.86	85.09	74.62	8.72
7.- 8.0	50.47	48.88	66.72	10.65
8.- 9.0	60.95	78.40	82.46	6.78
9.-10.0	72.70	70.40	66.72	10.65
10.-11.0	64.44	62.41	51.87	14.53
11.-12.0	80.95	78.40	55.41	13.56
12.-13.0	82.95	80.24	82.46	6.78
13.-14.0	86.55	83.93	78.58	7.75
14.-15.0	77.64	75.20	86.22	5.81
15.-16.0	96.36	93.90	89.75	4.84
16.-17.0	92.38	89.47	86.22	5.81
17.-18.0	74.32	72.47	29.08	22.28
18.-19.0	82.55	79.95	82.46	6.78
19.-20.0	97.54	94.47	89.75	4.84
20.-21.0	100.00	96.85	89.75	4.84
21.-22.0	73.97	71.63	55.41	13.56
22.-23.0	58.72	56.87	48.48	15.50
23.-24.0	100.00	96.85	95.76	2.91
24.-25.0	94.31	91.92	82.46	6.78
25.-26.0	87.00	84.25	86.22	5.81
26.-27.0	85.70	83.00	86.22	5.81
27.-28.0	65.43	63.36	78.58	7.75
28.-29.0	68.54	65.38	82.46	6.78
29.-30.0	90.47	87.62	89.75	4.84
30.-30.2	39.93	38.57	86.50	5.74

BOREHOLE LENGTH = 31.15 M

RECOVERY = 96.85 %

AVERAGE RQD = 75.95 %

AVERAGE FREQUENCY = 8.89 FRAC/M

TOTAL NUMBER OF FRACTURES = 277

FRACTURE FREQUENCY AND RQD FOR SCANLINE NO. PA-1 CORE

INTERVAL (M)	RQD %	ADJ RQD %	THEO RQD %	FREQUENCY (FRAC/M)
0.- 1.0	41.50	41.50	55.41	14.65
1.- 2.0	94.00	94.00	95.76	3.14
2.- 3.0	100.00	100.00	99.46	1.05
3.- 4.0	15.20	15.20	22.99	27.21
4.- 5.0	22.30	22.30	22.99	27.21
5.- 6.0	31.00	31.00	26.92	25.12
6.- 7.0	37.70	37.70	51.87	15.70
7.- 8.0	49.40	49.40	55.41	14.65
8.- 9.0	52.80	52.80	59.07	13.61
9.-10.0	67.90	67.90	62.85	12.56
10.-11.0	78.30	78.30	78.58	8.37
11.-12.0	74.50	74.50	70.65	10.47
12.-13.0	70.80	70.80	74.62	9.42
13.-14.0	76.60	76.60	66.72	11.51
14.-15.0	70.00	70.00	74.62	9.42
15.-16.0	100.00	100.00	89.75	5.23
16.-17.0	77.10	77.10	74.62	9.42
17.-18.0	91.10	91.10	95.76	3.14
18.-19.0	100.00	100.00	99.46	1.05
19.-20.0	96.00	96.00	92.97	4.19
20.-21.0	49.00	49.00	51.87	15.70
21.-22.0	64.50	64.50	45.25	17.79
22.-23.0	55.50	55.50	55.41	14.65
23.-24.0	29.50	29.50	42.16	18.84
24.-25.0	26.30	26.30	45.25	17.79
25.-26.0	13.40	13.40	45.25	17.79
26.-27.0	26.50	26.50	36.47	20.93
27.-28.0	12.20	12.20	12.94	34.54
28.-29.0	46.50	46.50	36.47	20.93
29.-30.0	63.50	63.50	59.07	13.61
30.-31.0	50.20	50.20	45.25	17.79
31.-32.0	85.80	85.80	89.75	5.23

BOREHOLE LENGTH = 31.76 M
 RECOVERY = 100.00 %
 AVERAGE RQD = 58.85 %
 AVERAGE FREQUENCY = 13.32 FRAC/M
 TOTAL NUMBER OF FRACTURES = 423

FRACTURE FREQUENCY AND RQD FOR SCANLINE NO. PA-2 CORE

INTERVAL (M)	RQD %	ADJ RQD %	THEO RQD %	FREQUENCY (FRAC/M)
0.- 1.0	45.00	44.72	24.89	24.85
1.- 2.0	96.00	95.41	95.76	2.98
2.- 3.0	84.00	83.48	82.46	6.96
3.- 4.0	84.00	83.48	92.97	3.98
4.- 5.0	52.70	52.37	36.47	19.88
5.- 6.0	78.00	77.52	74.62	8.94
6.- 7.0	84.50	83.98	92.97	3.98
7.- 8.0	88.00	87.46	86.22	5.96
8.- 9.0	77.90	77.42	66.72	10.93
9.-10.0	88.50	87.95	92.97	3.98
10.-11.0	78.80	78.31	74.62	8.94
11.-12.0	73.20	72.75	74.62	8.94
12.-13.0	78.70	78.21	74.62	8.94
13.-14.0	65.00	64.60	66.72	10.93
14.-15.0	54.50	54.16	51.87	14.91
15.-16.0	100.00	99.38	92.97	3.98
16.-17.0	63.10	62.71	62.85	11.93
17.-18.0	95.20	94.61	66.72	10.93
18.-19.0	73.80	73.34	70.65	9.94
19.-20.0	63.40	63.01	29.08	22.86
20.-21.0	47.30	47.01	74.62	8.94
21.-22.0	88.40	87.85	89.75	4.97
22.-23.0	91.30	90.74	89.75	4.97
23.-24.0	76.50	76.03	82.46	6.96
24.-25.0	67.90	67.48	70.65	9.94
25.-26.0	17.00	16.89	18.05	28.82
26.-27.0	0.00	0.00	31.39	21.86
27.-28.0	49.00	48.70	26.92	23.85
28.-29.0	6.40	6.36	26.92	23.85
29.-30.0	73.40	72.95	62.85	11.93
30.-31.0	55.50	55.16	62.85	11.93
31.-32.0	92.10	91.53	69.75	4.97
32.-32.5	82.18	81.67	87.56	5.59

BOPEHOLE LENGTH = 32.74 M

RECOVERY = 99.38 %

AVERAGE RQD = 68.21 %

AVERAGE FREQUENCY = 11.39 FRAC/M

TOTAL NUMBER OF FRACTURES = 373

FRACTURE FREQUENCY AND RQD FOR SCANLINE NO. PA-3 CORE

INTERVAL (M)	RQD %	ADJ RQD %	THEO RQD %	FREQUENCY (FRAC/M)
0.- 1.0	26.10	25.05	24.89	24.00
1.- 2.0	41.50	39.93	36.47	19.20
2.- 3.0	0.00	0.00	7.73	37.43
3.- 4.0	0.00	0.00	0.49	66.23
4.- 5.0	24.40	23.42	5.44	41.27
5.- 6.0	13.30	12.77	16.62	28.79
6.- 7.0	0.00	0.00	19.58	26.88
7.- 8.0	32.80	31.48	15.30	29.75
8.- 9.0	41.60	39.93	26.92	23.04
9.-10.0	6.30	6.05	10.03	34.55
10.-11.0	17.00	16.32	1.05	58.55
11.-12.0	24.30	23.32	5.94	40.31
12.-13.0	28.50	27.35	39.24	18.24
13.-14.0	68.50	65.75	62.85	11.52
14.-15.0	45.00	43.19	62.85	11.52
15.-16.0	85.80	82.35	62.85	11.52
16.-17.0	66.27	63.61	59.07	12.48
17.-18.0	68.70	65.94	62.85	11.52
18.-19.0	52.60	50.49	22.99	24.96
19.-20.0	67.50	64.79	66.72	10.56
20.-21.0	72.00	69.11	70.65	9.60
21.-22.0	93.20	89.46	82.46	6.72
22.-23.0	37.50	36.09	16.62	28.79
23.-24.0	24.50	23.52	10.92	33.59
24.-25.0	15.50	14.88	29.08	22.06
25.-26.0	15.70	15.07	7.09	38.39
26.-27.0	49.50	47.61	39.24	18.24
27.-28.0	18.30	17.56	15.30	29.75
28.-29.0	24.50	23.52	21.23	25.92
29.-29.9	27.70	26.58	15.12	29.89

BOREHOLE LENGTH = 31.15 M
 RECOVERY = 95.98 %
 AVERAGE RQD = 34.87 %
 AVERAGE FREQUENCY = 26.16 FRAC/M
 TOTAL NUMBER OF FRACTURES = 815

APPENDIX V

COMPUTER CODE PERMEA

APPENDIX V

COMPUTER CODE PERMEA

The computer program PERMEA was written specifically for the purpose of handling data that was collected by the data acquisition system described in section 6.2.3. Its purpose is somewhat diverse but it may be modified with little difficulty for processing of data from other data acquisition systems designed for permeability measurement. This version of the program provides calculation of permeability from ideal gas injection tests only. However, for water injection tests it provides the pressure-flow histories and can process data from the data acquisition system described in section 6.2.3. In order to avoid wasted computer storage during compilation and loading processes a small routine similar to the subroutine PERMEA was written for calculation of permeabilities from steady state water injection tests.

This program performs several different calculations, the type of which is chosen by the user in the main input file. Three extra input files can also be specified. The type of analysis is determined by the first character of the first record in a data set. Following is a brief description of these features.

The program will interactively ask for an input file. This input file must have the first three records as follows:

<u>Record #</u>	<u>Variables</u>	<u>Format</u>
#1	INFIL2, OUTFIL, OUTFI2	3A10
#2	VISC, LENGTH, RAD	"
#3	ITYPE, BORNUM, NUMREC	(A1, A5, I2)

These three records are control data and are always required to execute the program. Description of the variables is as follows:

INFIL2	The name of the second input file (see ITYPE)
OUTFIL	" " " " main output file
OUTFI2	" " " " second " "
VISC	Viscosity in centipoise
LENTH	Length of the test section in cm
RAD	Radius of the borehole in cm
ITYPE	A single character that determines the actions to be taken as follows:

- R: Flow pressure and temperatures are not available so approximate.
- D: Analyze pulse test.
- P: All pertinent data about flow are present and complete.

V: Calculate the metering valve coefficient.

L: Prepare pressure flow histories.

BORNUM Five character borehole designation.

NUMREC Number of records before data for a new borehole is to be read.

The ITYPE also determines what kind of files and the formats within those files. Various cases are described below.

ITYPE = R: In this case the program knows that data are incomplete as far as the temperature at the flowmeter and inside the test zone are concerned. This was the case for systematic testing of the radial boreholes. In this case following the three records in the main input file data should be entered as follows:

	<u>Variables</u>	<u>Format</u>
Record #4	INTR1,PERFLW,PRESS(2)	,PRESS(7)

where:

INTR1 = the beginning of the tested interval

PERFLW = percent flow read on the rotameter

PRESS(2) = zone pressure at steady state

PRESS(7) = flow pressure at the rotameter.

Record 4 can be repeated as many times as the NUMREC allows. To enter data for a new borehole record number #3 should be repeated followed by a series of records similar to record #4. In this type of file, because there only one input and output files are needed, the INFIL2 and OUTFI2 should be entered as NONE.

ITYPE = P: In this case all data are present and there is only one input file and one output file. The records following the 3rd control record have the following format:

	<u>Variables</u>	<u>Format</u>
Record #4	PRESS(2), ZONET, FLOWT, PRESS(6) PRESS(7), POW, PERFLW, METNO, INTR1, FLO2, MET2.	free

This record can be repeated for as many times as necessary. The variables are:

ZONET	Temperature in the test zone
FLOWT	" at the rotameter
PRESS(2)	Pressure in the test zone
PRESS(6)	" at the metering valve
PRESS(7)	" " " rotameter
POW	Exitation voltage

PERFLW	Rotameter reading
METNO	Rotameter I.D. number
INTR1	Beginning of the test section
FLO2	Second rotameter reading (if two are simultaneously used)
MET2	The second rotameter I.D. number

ITYPE = D: In this case analysis of the pulse test is initiated. In this case also only an input and an output is required. The main input file format is the same for the first 3 records. The following records have the following format:

	<u>Variables</u>	<u>Format</u>
Record #4	INTR1,PRESS(1) to PRESS(20)	Free

This record can be repeated for as many times as the NUMREC allows. It should be noted that records of the type R, P and D can be intermixed as long as record number 3 precedes the data (see example inputs).

ITYPE = V: In this case the program is asked to carry out a regression analysis to find the valve coefficient of the metering valves. In this case two input files are required: a main input file (which contains the control cards and is exactly the same as in case of ITYPE = P), and an

auxiliary input file which contains the metering valve status information in following format:

	<u>Variables</u>	<u>Format</u>
Record #1	VI	A1
#2	VLVFLW (I,J)	9F

VI is the valve type and refers to fine regulating valve when it is equal to "F" and to the coarse regulating valve when it is equal to "C". VLVFLW is the valve status at the time when data in the main file are recorded. It refers to the number of turns that a valve was opened to permit flow through the valve. Record number 2 is repeated to include all data.

ITYPE = L: In this case the pressure flow history will be computed by the program. Two input and two output files must be defined. The main input file, which is specified during the run time, contains the control records followed by the data about the rotameter reading:

	<u>Variables</u>	<u>Format</u>
Record #4	TIMEF,PERFLW,METNO,IVALV, FLO2,MET2	(2F,2I,F,I)

where: TIMEF is the flow time which is written in decimal as follows:

HH.MMSS

HH = hours

MM = minutes

SS = seconds

These time correspond to the times recorded by the data logger at which a rotameter reading is taken. IVALV is the valve identification number. Other variables are as defined in case ITYPE = P.

The second input file in this case is the output of the datalogger without any modifications other than correction of the noise data.

In general option "V" is used first so that valve coefficients can be calculated. This is required only once after every recalibration of the system. Then using this valve coefficient, the "L" option is used to obtain flow histories from which steady state points can be obtained. Using this then other options can be used to calculate permeability. Example input outputs and the program listing is included in the followings.


```

00100 CCCCCCCCCCCCCCCCCCCCCCCCCCCCCCCCCCCCCCCCCCCCCCCCCCCCCCCCCCCCCCCCCCCCC
00200 CCCCCCCCCCCCCCCCCCCCCCCCCCCCCCCCCCCCCCCCCCCCCCCCCCCCCCCCCCCCCCCCCCCCC
00300 CCCCCCCCCCCCCCCCCCCCCCCCCCCCCCCCCCCCCCCCCCCCCCCCCCCCCCCCCCCCCCCCCCCCC
00400 CCCCCCCCCCCCCCCCCCCCCCCCCCCCCCCCCCCCCCCCCCCCCCCCCCCCCCCCCCCCCCCCCCCCC
00500 CCCCCC A PROGRAM TO CALCULATE PERMEABILITIES FROM DOUBLE PACKER
00600 CCCCCC INJECTION TESTS.
00700 C
00800 CCCCCC THIS PROGRAM USES THE STEADY STATE RADIAL, ISOTHERMAL
00900 CCCCCC FLOW OF COMPRESSIBLE FLUIDS. THIS PROGRAM CORRECTS FOR
01000 CCCCCC SMALL VARIATIONS OF TEMPRATURE ALONG THE FLOW PATH.
01100 CCCCCC FLOW METER READINGS ARE CORRECTED FOR PRESSURE AND
01200 CCCCCC TEMPERATURE VARIATIONS.
01300 CCCCCCCCCCCCCCCCCCCCCCCCCCCCCCCCCCCCCCCCCCCCCCCCCCCCCCCCCCCCCCCCCCCCC
01400 CCCCCC
01500 CCCCCC
01600 CCCCCC
01700 CCCCCC
01800 CCCCCC DIAMF = DIAMETER OF THE FLOAT
01900 CCCCCC WF = WEIGHT OF THE FLOAT (GM)
02000 CCCCCC DF = DENSITY OF THE FLOAT (GM/ML)
02100 CCCCCC R = DIAMETER RATIO OF THE FLOWMETER
02200 CCCCCC PERFLW = SCALE READING OF THE FLOWMETER
02300 CCCCCC R = PERFLW*SLOPE+YINTER
02400 CCCCCC VISC = VISCOSITY AT STP
02500 CCCCCC LENTH = DISTANCE BETWEEN THE PACKERS (CM)
02600 CCCCCC RAD = RADIUS OF THE BOREHOLE (CM)
02700 CCCCCC PRESS(2) = INJECTION PRESSURE AT EQUILIBRIUM (PSIG)
02800 CCCCCC ZONET = ZONE TEMPERATURE (DEG. CENTIGRADE)
02900 CCCCCC FLOWT = FLOW TEMPERATURE AT THE FLOWMETER (DEG. C)
03000 CCCCCC PRESS(6) = PRESSURE AT THE REGULATING VALVE (PSIG)
03100 CCCCCC PRESS(7) = " " " " FLOWMETER (PSIG)
03200 CCCCCC POW = POWER SUPPLIED TO THE TRANSDUCERS (VOLTS)
03300 CCCCCC METNO = FLOWMETER NUMBER
03400 CCCCCC INTR1 = BEGINNING OF THE INTERVAL TESTED (FEET)
03500 CCCCCC FLO2 = FLOW AT THE SECOND FLOWMETER (3)
03600 CCCCCC MET2 = THE SECOND FLOWMETER NUMBER
03700 CCCCCC VISCO = VISCOSITY AT TEST P & T (CP)
03800 CCCCCC DEN = DENSITY AT TEST P & T
03900 CCCCCC FLOW = VOLUMETPIC FLOWRATE (ML/MIN)
04000 CCCCCC FLOWMAS = MASS FLOWRATE (GM/MIN)
04100 CCCCCC PERM(1) = INTRINSIC PERMEABILITY IN CENTIMETERS SQUARED
04200 CCCCCC PERM(4) = EQUIVALENT HYDRAULIC CONDUCTIVITY AT STP (CM/SEC)
04300 CCCCCCCCCCCCCCCCCCCCCCCCCCCCCCCCCCCCCCCCCCCCCCCCCCCCCCCCCCCCCCCCCCCCC
04400 C
04500 C
04600 DIMENSION DIAMF(4),WF(4),SLOPE(4),YINTER(4),VLVFLW(200,2),
04700 1 FLOWI(200),PRSVLV(200),POWER(200),TEMP(200)
04800 2 ,PRESS(7),FRSPRS(7),PERM(6)
04900 REAL INTR1,INTR2,LENTH
05000 DOUBLE PRECISION INFILE, OUTFIL,INFIL2,OUTF12
05100 COMMON WTHOLE
05200 C
05300 CCCCCC INITIALIZE
05400 C
05500 C
05600 IN=14
05650 IDUM=18
05700 IOUT=15
05800 INFILE='INPUT'
05900 OUTFIL='OUTPUT'

```

```

06000      INCOMP='R'
06100      IDECAY='D'
06200      ICOMP='P'
06300      IVLVCO='V'
06400      ATMOSP=10.7
06500      ILOGGR='L'
06600      M=1
06700      IKOUNT=0
06800      OPEN(UNIT=IN,ACCESS='SEQIN',FILE=INFILE,DIALOG)
06900      LDUM=0
07000      READ(IN,455)INFIL2,OUTFIL,OUTFI2,VISC,WTMOLE,LENTH,RAD
07100      LDUM=LENTH
07200      OPEN(UNIT=IOUT,ACCESS='SEQOUT',FILE=OUTFIL)
07300      IF(OUTFI2.EQ.'NONE')GO TO 11
07400      IOUT2=17
07500      OPEN(UNIT=IOUT2,ACCESS='SEQOUT',FILE=OUTFI2)
07600      11 CONTINUE
07700      IF(INFIL2.EQ.'NONE')GO TO 12
07800      IN2=16
07900      OPEN(UNIT=IN2,ACCESS='SEQIN',FILE=INFIL2)
08000      12 READ(IN,450,END=15)ITYPE,BORNUM,NUMREC
08100      IF(ITYPE.EQ.IVLVCO)GO TO 4
08200      IF(ITYPE.EQ.ILOGGR)GO TO 61
08300      WRITE(IOUT,1000)BORNUM
08400      IF(IKOUNT.NE.0)GO TO 13
08500      455 FORMAT(3A10/4F)
08600      13 CONTINUE
08700      MET1=0
08800      CONTINUE
08900      C
09000      C
09100      C      ANALYSIS OF DECAY TEST STARTS HERE
09200      C
09300      C
09400      DO 10 I=1,NUMREC
09500      IKOUNT=I
09600      C
09700      IF(ITYPE.NE.ILOGGR)GO TO 62
09800      61 CALL LOGGER(IN2,IN,IOUT,IOUT2,PRESS,VISC,ATMOSP)
09900      62 CONTINUE
10000      C
10100      IF(ITYPE.EQ.IDECAY)CALL DECAY(PERM(1),IN,IKOUNT,INTR1,INTR2
10200      1 ,APERTR,IOUT,RAD,LENTH,VISC,NUMREC)
10300      IF(PERM(1).EQ.-90.0)GO TO 10
10400      IF(ITYPE.EQ.IDECAY)GO TO 14
10500      IF(ITYPE.EQ.ICOMP)GO TO 4
10600      C
10700      C
10800      C      ANALYSIS OF DATA WITHOUT P & T INFORMATION
10900      C
11000      C
11100      READ(IN,500,END=15)INTR1,PERFLW,PRESS(2),PRESS(7)
11200      DATA ZONET,FLOWT,PRESS(6),POW,METNO/9.0,11.0,0.0,1.0,7/
11300      GO TO 7
11400      C
11500      C
11600      CCCCC READ IN DATA
11700      C
11800      C
11900      4 CONTINUE

```

```

12000      READ(IN,400,END=15)PRESS(2),ZONET,FLOWT,PRESS(6),PRESS(7),
12100      1 POW,PERFLW,METNO,INTR1,FLO2,MET2
12200      IF(KOUNT.EQ.0)TEST=INTR1
12205      IF(INTR1.EQ.TEST)GO TO 107
12210      C      IDUM=IDUM+1
12215      TEST=INTR1
12220      107      CONTINUE
12300      IF(LDUM.LT.0)INTR2=ABS(LDUM)
12400      IF(LDUM.LT.0)LENTH=(INTR2-INTR1)*30.48
12500      CTYPE *,LENTH
12600      KOUNT=KOUNT+1
12700      C      PRINT 103,KOUNT,ITYPE,NUMREC
12800      103      FORMAT(I,A5,I)
12900      IF(KOUNT.EQ.1)POW1=POW
13000      PRESS(2)=PRESS(2)*POW1/POW
13100      PRESS(7)=PRESS(7)*POW1/POW
13200      PRESS(6)=PRESS(6)*POW1/POW
13300      7      INTR2=INTR1+LENTH/30.48
13400      PRESS(2)=PRESS(2)+ATMOSP
13500      PRESS(7)=PRESS(7)+ATMOSP
13600      PRESS(6)=PRESS(6)+ATMOSP
13700      C
13800      C
13900      CALL ROTAME(METNO,MET2,PERFLW,FLO2,VISC,FLOW,PRESS,
14000      1 FLOMAS,FLOWT,ZONET)
14100      FLOWI(KOUNT)=FLOMAS
14200      PRSVLV(KOUNT)=PRESS(6)
14300      POWER(KOUNT)=POW
14400      TEMP(KOUNT)=FLOWT
14500      IF(ITYPE.EQ.IVLVCO)GO TO 4
14600      CALL PERMEA(PRESS,PERM,LENTH,VISC,ZONET,FLOMAS,APERTR
14700      1 ,RAD,ATMOSP, IDUM)
14800      14      PERM(4)=PERM(1)*9.7694611E4
14900      PERM(2)=PERM(1)*1.01325E8
15000      PERM(3)=PERM(1)*1.076391E-3
15100      PERM(5)=PERM(4)/30.48
15200      PERM(6)=PERM(5)*6.46317E5
15300      443      FORMAT(1X,10F10.3)
15400      WRITE(IOUT,1100)INTR1,INTR2,PRESS(2),APERTR,FLOW,
15500      1 (PERM(IP),IP=1,6)
15600      IF(ITYPE.EQ."P")GO TO 4
15700      10      CONTINUE
15800      15      CONTINUE
15900      IF(ITYPE.NE.IVLVCO)GO TO 77
16000      IF(ITYPE.EQ.IVLVCO)
16100      1 CALL FLWCOF(FLOWI,KOUNT,POWER,TEMP,VLVFLW,PRSVLV
16200      2 ,IN2,IOUT,IOUT2)
16300      IF(ITYPE.EQ.IVLVCO)STOP
16400      IF(ITYPE.EQ.INCOMP.OR.ITYPE.EQ.IDECAY)GO TO 12
16500      IF(ITYPE.EQ.ICOMP)GO TO 4
16600      77      CONTINUE
16700      IF(ITYPE.NE.IVLVCO)STOP
16800      100      FORMAT(A5)
16900      1000      FORMAT(1H1,41X,"AIR INJECTION TESTING RESULTS FOR BOREHOLE NO ",
17000      1 A5///3X,"INTERVAL",4X,"ZONE ",4X,"APER-",4X,"VOLUME "
17100      2 ,20X,"EQUIVALENT POROUS MEDIA PERMEABILITY"//
17200      3 15X,"PRESS",4X,"TURE ",4X,"FLOW."
17300      4 ,20X,"INTRINSIC",20X,"HYDRAULIC CONDUCTIVITY"//
17400      5 5X,"FEET"
17500      6 ,6X,"PSIA",5X,"CM. ",5X,"ML/M",9X,"SQUAR CM.",5X,"DARCY",

```

```

17600      7 10X,'SQUAR FT.',5X,'CM/SEC',8X,'FT/SEC',6X,'GAL/D FT**2/')
17700      1100  FORMAT(1X,F5.1,'-',F5.1,1X,F6.2,1X,E8.2,2X,F8.2,4X,6E14.5)
17800      200   FORMAT(2I)
17900      1200  FORMAT(1X,'TYPE IN INPUT,OUTPUT UNITS-FORMAT=2I')
18000      1300  FORMAT(1X,'TYPE IN INPUT ,OUTPUT FILE NAMES-FORAMT 2A10')
18100      1400  FORMAT(1X,6E15.5//1X,6E15.5)
18200      300   FORMAT(12A10)
18300      400   FORMAT(7F,I,2F,I)
18400      450   FORMAT(A1,A5,I2)
18500      500   FORMAT(4F)
18600      1150  FORMAT(1X,'TYPE IN BOREHOLE NO ')
18700      STOP
18800      END
18900      C
19000      C-----
19100      CCCCCC A SUBPROGRAM TO CALCULATE DENSITY AT THE TEST
19200      CCCCCC TEMPERATURE AND PRESSURE
19300      C-----
19400      C
19500      FUNCTION DENSTY(P,T,WM)
19600      DENSTY=8.283E-4*WM*P/(T+273.16)
19700      IF(WM.LT.0.0)DENSTY=1.0
19800      RETURN
19900      END
20000      C
20100      C
20200      C
20300      C-----
20400      C
20500      CCCCCCC SUBROUTINE TO ANALYZE DECAY TESTS
20600      C
20700      C-----
20800      C
20900      CCCCCC THIS SUBROUTINE USES APPROXIMATION OF THE SOLUTION
21000      C TO THE DIFFUSIVITY EQUATION FOR INFINITE FRACTURE
21100      C-----
21200      C
21300      SUBROUTINE DECAY(PERM,IN,IKOUNT,INTR1,INTR2,APERTR,IOUT
21400      1 ,RADIUS,LENGTH,VISC,NUMREC)
21500      DIMENSION TIME(20),PRESS(20),PERM(6)
21600      REAL INTR1 ,LENGTH,INTR2
21700      COMMON WITHOLE
21800      COMP=5.8589E-6
21900      1 READ(IN,100)INTR1,(PRESS(I),I=1,20)
22000      PRESO=PRESS(1)
22100      INTR2=INTR1+(LENGTH/0.3048)
22200      DO 5 I=1,20
22300      IF(PRESS(I).EQ.0.0)GO TO 5
22400      IF(PRESS(I).LE.PRESS(I+1))GO TO 99
22500      5 CONTINUE
22600      DO 10 I=1,20
22700      IF(PRESS(I).EQ.0.0)GO TO 10
22800      TIME(I)=ALOG10(FLOAT(I)*60.0)
22900      C PRINT 100, INTR1,PRESS(I),PRESS(I+1),PRESS(1)
23000      PRESS(I)=ALOG10(1.0-PRESS(I+1)/PRESO)
23100      N=I
23200      10 CONTINUE
23300      C
23400      C
23500      CCCCCC CALCULATING TIME AT 85% NORMALIZED PRESSURE

```

```

23600 C
23700 C
23800 CALL LINREG(PRESS,TIME,N,SLOPE,YINTER,REGCOF)
23900 PRINT *,REGCOF,SLOPE,YINTER,N
24000 TIMLOG=SLOPE*-.82391+YINTER
24100 C PRINT *,TIMLOG
24200 APERLG=-.32*TIMLOG+1.27+.32*(2*ALOG10(RADIUS/.04)
24300 1 +ALOG10(COMP*VISC*2.3941E9))+ALOG10(LENGTH/2)/3.0
24400 C PRINT *,APERLG
24500 APERTR=10.0**APERLG*1.0E-4
24600 C PRINT *,APERTR
24700 PERM(1)=APERTR**3/(12.0*LENGTH*100.0)
24800 C PRINT *,PERM(1),LENGTH
24900 RETURN
25000 99 WRITE(IOUT,200)INTR1,INTR2
25100 100 FORMAT(21F)
25200 200 FORMAT(1X,F5.1,"-",F5.1," DECADE TOO SLOW DUE TO EXTREMELY LOW
25300 1 PERMEABILITY")
25400 PERM(1)=-90.0
25500 RETURN
25600 END
-----
25700 C-----
25800 CCCCC SUBROUTINE TO PERFORM LINEAR REGRESSION
25900 CCCCC ANALYSIS
-----
26000 C
26100 C
26200 C
26300 SUBROUTINE LINREG(X,Y,N,S,B,R)
26400 DIMENSION X(N),Y(N)
26500 REAL NUMB
26600 SUMXY=0.0
26700 SUMX=0.0
26800 SUMY=0.0
26900 SUMXX=0.0
27000 SUMYY=0.0
27100 C
27200 C
27300 DO 10 I=1,N
27400 XY=X(I)*Y(I)
27500 SUMXY=XY+SUMXY
27600 SUMX=X(I)+SUMX
27700 SUMY=Y(I)+SUMY
27800 SUMXX=X(I)**2+SUMXX
27900 SUMYY=Y(I)**2+SUMYY
28000 10 CONTINUE
28100 NUMB=FLOAT(N)
28200 C
28300 C
28400 CCCCC CALCULATION OF SLOPE
28500 C
28600 C
28700 S=(SUMXY-(SUMX*SUMY)/NUMB)/(SUMXX-SUMX**2/NUMB)
28800 B=(SUMY-S*SUMX)/NUMB
28900 C
29000 C
29100 CCCCC FINDING REGRESSION COEFFICIENT
29200 C
29300 C
29400 STDEVX=SQRT(SUMXX-SUMX**2/NUMB)/(NUMB-1)
29500 STDEVY=SQRT(SUMYY-SUMY**2/NUMB)/(NUMB-1)

```

```

29600      R=S*STDEVX/STDEVY
29700      R=S*STDEVX/STDEVY
29800      RETURN
29900      END
30000      C
-----
30100      C
30200      C
30300      CCCCCC      SUBROUTINE TO CALCULATE FLOW COEFFICIENT
30400      CCCCCC      FOR THE METERING VALVE
30500      C
-----
30600      C
30700      C
30800      SUBROUTINE FLWCOF(FLOWI,KOUNT,POWER,TEMP,VLVFLW
30900      1 ,PRSVLV,IN2,IOUT,IOUT2)
31000      DIMENSION VLVFLW(KOUNT,2),FLOWI(KOUNT),PRSVLV(KOUNT)
31100      1 ,P1(200),PRSLG(200),COEFF(200),VLVSTA(6),ICOFF(6)
31200      2 ,TEMP(KOUNT),COFF(200),POWER(200),CVALV(200),SUMC(6)
31300      COMMON WTHOLE
31400      DOUBLEPRECISION VLVSTA
31500      C
31600      C
31700      READ(IN2,230)VI
31800      230      FORMAT(A1)
31900      DO 21 I=1,50
32000      N=M+3
32100      READ(IN2,600,END=22)ATNT,((VLVFLW(K,J),J=1,2),K=M,N)
32200      600      FORMAT(9F)
32300      M=4*I+1
32400      21      CONTINUE
32500      22      KV=0
32600      C      PRINT 443,VLVFLW,POWER
32700      DO 24 I=1,N-3
32800      IF(VLVFLW(I,2).EQ.0.0)GO TO 24
32900      KV=KV+1
33000      C      PRINT *,KV
33100      VLVFLW(KV,1)=VLVFLW(I,1)
33200      24      CONTINUE
33300      DO 25 I=1,200
33400      IF(VLVFLW(I,2).EQ.0.0)GO TO 25
33500      KV=KV+1
33600      VLVFLW(KV,1)=VLVFLW(I,2)+.065
33700      25      CONTINUE
33800      C      PRINT 443,VLVFLW,POWER
33900      443      FORMAT(1X,10F10.3)
34000      DO 10 I=1,KOUNT
34100      DIFPRS=1.915561*VLVFLW(I,2)/POWER(I)
34200      C      PRINT 100,DIFPRS
34300      P1(I)=PRSVLV(I)+DIFPRS
34400      PRSLG(I)=ALOG(P1(I)/PRSVLV(I))
34500      TEMP(I)=TEMP(I)+273.16
34600      COEFF(I)=(P1(I)**2-PRSVLV(I)**2)/(FLOWI(I)**2*TEMP(I))
34700      TEMP(I)=TEMP(I)-273.16
34800      10      CONTINUE
34900      VLVSTA(1)="FRV 10/10"
35000      VLVSTA(2)="FRV 5/5"
35100      VLVSTA(3)="FRV 5/10"
35200      VLVSTA(4)="FRV 10/5"
35300      VLVSTA(5)="CRV 1/4"
35400      VLVSTA(6)="CRV 1/2"
35500      C

```

```

35600 C
35700 C
35800 C
35900 DO 30 JC=1,6
36000 WRITE(IOUT,150)VLVSTA(JC)
36100 AJ=FLOAT(JC)
36200 KCOFF=0
36300 C
36400 SUMC(JC)=0.0
36500 NUMB=0
36600 DO 20 I=1,KOUNT
36700 IF(VLVFLW(I,1).NE.AJ)GO TO 20
36800 KCOFF=KCOFF+1
36900 COFF(KCOFF)=1.0/COEFF(I)
37000 PRSLOG(KCOFF)=PRSLOG(I)
37100 TEM=TEMP(I)+273.16
37200 DEN=DENSTY(PRSVLV(I),TEM,WTMOLE)
37300 TEM1=283.16
37400 DEN1=DENSTY(P1(I),TEM1,WTMOLE)
37500 C FLOCAL=55.0029*DEN*SQRT(P1(I)*DEN1/(DEN1**2-DEN**2))
37600 C 1*(1.0-(PRSVLV(I)/P1(I))**(1.0/3.5))
37700 CVALV(KCOFF)=FLOWI(I)/28316.847*SQRT(DEN*TEM/(.001201
37800 1*(P1(I)**2-PRSVLV(I)**2)))/0.00116
37900 PRSQR=P1(I)**2-PRSVLV(I)**2
38000 IF(VLVFLW(I,1).EQ.1.0)FLOCAL=SQRT(PRSQR
38100 1*(0.982*ALOG(P1(I)/PRSVLV(I))-0.02)/TEM)
38200 IF(VLVFLW(I,1).EQ.5.0)FLOCAL=0.209390*SQRT(PRSQR/(TEM*DEN))
38300 SUMC(JC)=SUMC(JC)+CVALV(KCOFF)
38400 WRITE(IOUT,100)P1(I),PRSVLV(I),FLOWI(I),FLOCAL,TEMP(I),
38500 1 COEFF(I),COFF(KCOFF),PRSLOG(I),CVALV(KCOFF)
38600 NUMB=NUMB+1
38700 20 CONTINUE
38800 IF(KCOFF.EQ.0)GO TO 30
38900 CALL LINREG(PRSLOG,COFF,KCOFF,SLOPE,BSEPT,R)
39000 CVMEAN=SUMC(JC)/FLOAT(NUMB)
39100 WRITE(IOUT,200)SLOPE,BSEPT,R,CVMEAN,NUMB
39200 30 CONTINUE
39300 C
39400 C
39500 100 FORMAT(9F10.4)
39600 150 FORMAT(1H1//,25X,"FLOW COEFFICIENT FOR",A10//
39700 1 5X,"P1",13X,"P2",13X,"MASS FLOW",5X,"TEMPERATURE"
39800 2 ,4X,"COEFFICIENT"/)
39900 200 FORMAT(/5X,"VLV COEFF.=",F8.3,"*LOG(P1/P2)+",F8.3,
40000 1 12X,"CORRELATION COEFF=",F8.5,E15.5,I4)
40100 C
40200 RETURN
40300 END
40400 C
40500 C
40600 C-----
40700 C
40800 CCCCCC SUBROUTINE TO CALCULATE FLOW FROM ROTAMETER DATA
40900 C
41000 C-----
41100 C
41200 C
41300 SUBROUTINE ROTAME(METNO,MET2,PERFLW,FLO2,VISC,FLOW,PRESS,
41400 1 FLOMAS,FLOWT,ZONET)
41500 DIMENSION DIAMF(4),PRESS(7),WF(4),SLOPE(4),YINTER(4)

```

```

41600      COMMON WTMOLE
41700      C
41800      C
41900      C
42000      C          IF 2ND FLOWMETER USED SIMULTANEOUSLY DO THIS PART
42100      C
42200      FLOW=0.0
42300      FLOWMAS=0.0
42400      IF (PERFLW.LE.0.0) RETURN
42500      DATA (DIAMF(I),I=1,4),(WF(I),I=1,4),DF,(SLOPE(I),I=1,4),
42600      1 (YINTER(I),I=1,4)
42700      2 /.25,.125,.0625,.375,.339,.0424,.0053,1.142,2.53
42800      3 /.261,.200,.250,.2501,-.85,.7745,1.475,1.0/
42900      C
43000      FLOW1=0.0
43100      KO=0
43200      GO TO 7
43300      8      METNO=MET2
43400      FLOW1=FLOW
43500      PERFLW=FLOW2
43600      MET2=?
43700      KO=KO+1
43800      7      CONTINUE
43900      IF (KO.GT.0) GO TO 5
44000      VISCO=VISC+(6.111E-5*FLOWT)
44100      IF (WTMOLE.LT.0.0) VISCO=1.0
44200      IF (ZONET.EQ.0.0) ZONET=FLOWT-2.0
44300      IF (PRESS(7).EQ.0.0) PRESS(7)=PRESS(2)
44400      C
44500      C
44600      CCCCC  CALCULATION OF FLOW BEGINS HERE
44700      C
44800      C
44900      5      DEN=DENSTY(PRESS(7),FLOWT,WTMOLE)
45000      M=METNO-3
45100      R=SLOPE(M)*PERFLW+YINTER(M)
45200      STOKE=1.042*WF(M)*(DF-DEN)*DEN**3/(VISCO**2*DF)
45300      IF (STOKE.LT.5.0) CR=.0852*SQRT(STOKE)
45400      IF (STOKE.LT.5.0) GO TO 2
45500      A=3.09*ALOG10(R)-1.25
45600      B=3.83-1.17*ALOG10(R)
45700      C=ALOG10(STOKE)-.111*ALOG10(R)
45800      CR=(SQRT(B**2+4*A*C)-B)/(2*A)
45900      2      FLOW=59.8*DIAMF(M)*CR*SQRT(WF(M)*(DF-DEN)/(DF*DEN))
46000      1 *R*(R/100.+2.)
46100      IF (MET2.GT.0) GO TO 8
46200      FLOW=FLOW+FLOW1
46300      FLOWMAS=FLOW*DEN
46400      CTYPE *,DEN
46500      IF (PRESS(7).NE.PRESS(2)) GO TO 6
46600      C      PRESS(7)=SQRT(PRESS(2)**2+(FLOWMAS**2+2.17)/.31)
46700      CTYPE *,PRESS(7)
46800      C      GO TO 5
46900      6      CONTINUE
47000      C      IF (PRESS(6).EQ.ATMOSP) PRESS(6)=SQRT(PRESS(7)**2+2*
47100      1 (FLOWMAS**2+2.17))
47200      C      PRINT *,KOUNT
47300      C      RETURN
47400      C      END
47500      C-----

```



```

47600 CCCCCC      SUBROUTINE TO CALCULATE PERMEABILITY
47700 CCCCCC      USING ELLIPTICAL POTENTIAL DISTRIBUTION
47800 -----
47900 C
48000      SUBROUTINE PERMEA(PRESS,PERM,LENTH,VISC,ZONET,FLOMAS,APERTR
48100      1 ,RAD,ATMOSP,IDUM)
48200 C
48300 C
48400 C
48500 C----- CALCULATION OF PERMEABILITY
48600 C
48700      DIMENSION PRESS(7),PERM(6)
48800      COMMON WTMOLE
48900      REAL LENTH
49000      AL=LENTH/(2*RAD)
49100      VISCO=VISC+(6.6111E-5*ZONET)
49200 C----- ZONE PRESSURE IN PASCALS -----
49300      PB=PRESS(2)*6.894757E3
49400      ATMO=ATMOSP*6.894757E3
49500      DEN=DENSTY(PRESS(2),ZONET,WTMOLE)
49600      PERM(1)=FLOMAS*VISCO*ALOG(AL+SQRT(1.+AL**2))*PB
49700      1 /((PB**2-ATMO**2)*LENTH*188495.5592*DEN)
49800 CTYPE 13
49900 13      FORMAT(1X,'FLMAS,VIS,AL,L,PB,AT,DEN')
50000 CTYPE *,FLOMAS,VISCO,AL,LENTH,PB,ATMO,DEN
50100      APERTR=(PERM(1)*12.0*LENTH)**(1.0/3.0)
50105      PINV=(1.0/PB)*1.0E6
50110      BORFLW=FLOMAS/DEN
50115      PBSQ=(PB**2-ATMO**2)/PB*1.0E-6
50130      WRITE(IDUM,1013)PBSQ,BORFLW,PINV,PERM(1),APERTR
50132 1013      FORMAT(5(E14.5,' '))
50135      TYPE *,IDUM
50200      RETURN
50300      END
50400 C
50500 C
50600 C-----
50700 CCCCCC      SUBROUTINE TO READ DATA FROM DATA LOGGER
50800 CCCCCC      OUT PUT AND TO CALCULATE THE FLOW HISTORY
50900 -----
51000 C
51100 C
51200      SUBROUTINE LOGGER(IN2,IN,IOUT,IOUT2,PRESS,VISC
51300      1 ,ATMOSP)
51400      DIMENSION PRESS(7),FRSPRS(7),HEAD(30)
51500      COMMON WTMOLE
51600      KTIME=0
51700      KFTIME=0
51800 52      READ(IN,100,END=54)TIMEF,PERFLW,METNO,IVALV,FLO2
51900      1 ,MET2
52000 CTYPE *,PERFLW,TIMEF
52100 100      FORMAT(2F,2I,F,I)
52200      TIMFLW=TIMEF
52300      KFTIME=KFTIME+1
52400      TI=AIN(TIMEF)
52500      IF((TIMEF-TI).GT.0.5959)TI=TI+1.0
52600      TIMEF1=TI*60.0
52700      TI2=(TIMEF-TI)*100.0
52800      TI3=AIN(TI2)
52900      IF((TI2-TI3).GT.0.59)TI3=TI3+1.0

```

```

59000      1 ,FLOW,PRESS,FLOMAS,FLOWT,ZONET)
59100 CTYPE *,KTIME
59200      IF(ITIME.GT.ITIMEF)GO TO 52
59300      IF(WTMOLE.LT.0.0)FLOMAS=FLOMAS/100.0
59400      WRITE(IOUT,*)TIMEFT,FLOMAS,PRESS(2)
59500      GO TO 52
59600      65      STOP
59700      200     FORMAT(1X,6(F8.3,', '),2(F10.5,', '))
59800
59900      END
60000 C
60100 C
60200 C-----
60300 C
60400 CCCCC      SUBROUTINE TO CALCULATE FLOW FROM REGULATING
60500 CCCCC      VALVES AND OTHER FLOW CONDITIONS
60600 C
60700 C-----
60800 C
60900 C
61000      SUBROUTINE VALVEF(FLOWT,PRESS,FLOMAS,FLOW,IVALV,POW
61100      1 ,VLVOLT,VLV)
61200      DIMENSION PRESS(7),CV(10,2)
61300      COMMON WTMOLE
61400      J=2
61500      IF(VLV.GT.50.0)J=1
61600      FLOWT=FLOWT+273.16
61700      DATA ((CV(M,N),M=1,7),N=1,2)/.27038657,.8517177,1.771032,
61800      1 3.1905615,4.9886322,6.9218962,8.8281216,9.46353,17.3372,
61900      2 31.6839,44.7852,56.7812,71.5064,86.2317/
62000      DIFPRS=VLVOLT
62100 CCTYPE *,DIFPRS,IVALV,CV(IVALV,J)
62200      DEN=DENSITY(PRESS(6),FLOWT,WTMOLE)
62300      P2=PRESS(6)-DIFPRS
62400      PRSQR=PRESS(6)**2-P2**2
62500      IF(PRSQR.LE.0.0)PRSQR=0.0
62600      IF(WTMOLE.LT.0.0)FLOW=2.18*CV(IVALV,J)*SQRT(DIFPRS)
62700      IF(WTMOLE.GT.0.0)FLOW=0.41458*CV(IVALV,J)*SQRT(PRSQR/DEN/FLOWT)
62800      FLOW=6.666666*FLOW
62900      FLOMAS=FLOW*DEN
63000      RETURN
63100      END

```

AN EXAMPLE OF THE MAIN INPUT FILE FOR PERMEA

This format applies for the cases when ITYPE is set equal to P,
V, or R.

```
NONE      PA1.PER  NONE
.01708,28,213.06,3.81
PPA-1
4.24,8.73,10.73,0,0,6.2899,11,4,11
12.49,8.93,10.93,0,0,6.2900,25.0,4,11
7.59,9.04,11.04,0,0,6.2899,11.0,4,11
16.66,8.43,10.43,0,0,6.2898,21.0,4,11
24.31,8.36,10.36,0,0,6.2897,31,4,11
28.73,6.63,8.63,0,0,6.2893,41,4,11
5.65,10.28,12.28,0,0,6.2876,9.0,5,14
11.71,10.21,12.21,0,0,6.2874,21.0,5,14
17.69,10.21,12.21,0,0,6.2876,33.0,5,14
24.61,9.99,11.99,0,0,6.2873,49.5,5,14
5.24,8.88,10.88,0,0,6.2874,45.1,5,17
9.56,8.70,10.70,0,0,6.2876,74,5,17
14.28,8.37,10.37,0,0,6.2873,22.5,4,17
```

```
WPRF02.DATWPRF02.OT1WPRF02.OT2
1.0,-1,0,0
LOGGER
13.1826,0,7
13.3135,23.2,7,7
13.3500,23.3,7
13.4000,23.3,7
13.4500,23.1,7
13.5000,23.1,7
13.5223,23,7
13.5306,23,7
13.5422,23,7
13.5500,23,7
13.5642,23,7
14.0000,22.8,7
14.0326,22.8,7
14.0500,22.7,7
14.0635,22.7,7
14.0906,22.6,7
14.1000,22.5,7
14.1441,22.4,7
14.1801,59.9,4
14.2243,59,4
14.2500,58.8,4
14.2752,58.8,4
14.3000,58.8,4
14.3500,58.6,4
14.4000,58.4,4
14.4500,58.2,4
14.5000,58.1,4
15.2709,57,4
15.3500,57,4
15.4344,56.7,4
15.5044,56.2,4
16.0500,56.1,4
16.1500,56,4
16.3000,55.6,4
17.0417,55,4
17.1600,55.2,4
```

An example input to PERMEA with option "L".

An example of the datalogger output which is used as input to PERMEA

ADV	PROFILE TESTING MAIN IN PA-1										PA1 64.	PA2*62.	PA3 59.	FERT	VLV SET	CRV. 7	TANK NO.	PUMP	WATER	1992	STE
0119	01	02	03	04	05	06	07	08	09	10	11	12	13	14	15						
16	CPT-1	PA-1	CPT-3	PA-2	PA-3	MET.VLV.	FLW.TNK	ZFRD	FLW T	ZONF-T	M-VLV			VLV PHS	FLN PRS	PO					
13.17.26 856V	0.24P	0.24P	0.77P	-0.04P	-0.27P	4.953P	12.566M	-0.001M	9.9C	10.8C	-0.1			54.85	8.82	11.					
13.27.03 856V	0.23P	0.24P	0.78P	-0.03P	-0.27P	5.046P	12.472M	0.000M	9.7C	10.8C	-0.1			54.64	8.66	11.					
13.30.00 856V	0.39P	0.25P	0.86P	-0.02P	-0.18P	-0.163P	12.461M	0.001M	9.7C	10.8C	-0.1			57.68	-0.27	11.					
13.31.35 856V	0.47P	0.24P	0.79P	-0.02P	-0.26P	5.740P	12.433M	-0.001M	9.7C	10.8C	-0.1			54.25	9.49	11.					
13.35.00 856V	0.37P	0.22P	0.82P	-0.03P	-0.27P	5.888P	12.375M	0.001M	9.7C	10.8C	0.0			54.29	9.67	11.					
13.40.00 856V	0.29P	0.22P	0.82P	-0.00P	-0.27P	5.868P	12.296M	0.001M	9.6C	10.8C	-0.1			54.30	9.65	11.					
13.45.00 856V	0.26P	0.22P	0.82P	0.02P	-0.27P	5.849P	12.367M	0.001M	9.6C	10.9C	-0.1			54.29	9.63	11.					
13.50.00 856V	0.24P	0.22P	0.83P	0.04P	-0.27P	5.858P	12.316M	0.001M	9.7C	10.9C	-0.1			54.29	9.60	11.					
13.52.23A 856V	0.24P	0.22P	0.83P	0.25P*	-0.27P	5.819P	12.297M	0.001M	9.7C	10.8C	-0.1			54.29	9.77	11.					
13.53.06A 856V	0.23P	0.21P	0.83P	0.46P*	-0.27P	5.814P	12.291M	0.001M	9.7C	10.8C	-0.1			54.30	9.94	11.					
13.54.22A 856V	0.23P	0.22P	0.83P	0.67P*	-0.27P	5.778P	12.287M	0.001M	9.7C	10.8C	-0.1			54.34	10.11	11.					
13.55.00 856V	0.23P	0.22P	0.83P	0.76P	-0.27P	5.752P	12.275M	0.001M	9.7C	10.8C	-0.1			54.33	10.20	11.					
13.56.42A 856V	0.23P	0.22P	0.83P	0.87P*	-0.27P	5.746P	12.262M	0.001M	9.7C	10.8C	-0.1			54.32	10.29	11.					
13.59.47A 856V	0.23P	0.22P	0.83P	1.07P*	-0.27P	5.693P	12.401M	0.001M	9.7C	10.9C	-0.1			54.32	10.44	11.					
14.00.00 856V	0.23P	0.22P	0.83P	1.09P	-0.27P	5.675P	12.400M	0.001M	9.7C	10.8C	-0.1			54.33	10.45	11.					
14.03.26A 856V	0.23P	0.22P	0.84P	1.27P*	-0.27P	5.658P	12.395M	0.001M	9.7C	10.8C	-0.1			54.35	10.59	11.					
14.05.00 856V	0.23P	0.22P	0.84P	1.35P	-0.27P	5.645P	12.393M	0.000M	9.8C	10.9C	-0.1			54.33	10.65	11.					
14.06.53A 856V	0.23P	0.22P	0.84P	1.47P*	-0.27P	5.618P	12.392M	0.002M	9.8C	10.8C	-0.1			54.35	10.73	11.					

T-2540

543

AIR INJECTION TESTING RESULTS FOR BOREHOLE NO PA-1

INTERVAL	ZONE	APER- TURE	VOLUME FLOW.	EQUIVALENT POROUS MEDIA PERMEABILITY					
				INTRINSIC			HYDRAULIC CONDUCTIVITY		
				FEET	PSIA	CM.	ML/H	SQUAR CM.	DARCY
11.0- 10.0	14.94	.41E-02	1074.46	0.26947E-10	0.27304E-02	0.29005E-13	0.26325E-05	0.06369E-07	0.55022E-01
11.0- 10.0	23.19	.37E-02	2991.86	0.19286E-10	0.19542E-02	0.20759E-13	0.18041E-05	0.61016E-07	0.39952E-01
11.0- 10.0	18.29	.32E-02	1074.19	0.13326E-10	0.13502E-02	0.14344E-13	0.13019E-05	0.42712E-07	0.27606E-01
11.0- 10.0	27.36	.30E-02	2423.63	0.10409E-10	0.10547E-02	0.11204E-13	0.10169E-05	0.33364E-07	0.21564E-01
11.0- 10.0	35.01	.29E-02	3065.09	0.94697E-11	0.95951E-03	0.10193E-13	0.92514E-06	0.30352E-07	0.19617E-01
11.0- 10.0	39.43	.30E-02	5366.25	0.10077E-10	0.10210E-02	0.10046E-13	0.98444E-06	0.32298E-07	0.20075E-01
14.0- 21.0	16.35	.14E-02	65.35	0.11722E-11	0.11077E-03	0.12617E-14	0.11451E-06	0.37570E-08	0.24202E-02
14.0- 21.0	22.41	.18E-02	320.40	0.22645E-11	0.22945E-03	0.24374E-14	0.22122E-06	0.72500E-08	0.46910E-02
14.0- 21.0	28.40	.18E-02	616.94	0.24447E-11	0.24771E-03	0.26315E-14	0.23804E-06	0.78359E-08	0.50645E-02
14.0- 21.0	35.32	.19E-02	1060.01	0.25640E-11	0.25988E-03	0.27607E-14	0.25057E-06	0.82208E-08	0.53132E-02
17.0- 24.0	15.94	.36E-02	930.63	0.18334E-10	0.18577E-02	0.19735E-13	0.17912E-05	0.58765E-07	0.37981E-01
17.0- 24.0	20.26	.35E-02	1777.41	0.16363E-10	0.16500E-02	0.17613E-13	0.15986E-05	0.52448E-07	0.33898E-01
17.0- 24.0	24.99	.33E-02	2634.99	0.14073E-10	0.14259E-02	0.15140E-13	0.13748E-05	0.45106E-07	0.29153E-01
17.0- 24.0	29.31	.35E-02	4461.00	0.16341E-10	0.16557E-02	0.17509E-13	0.15964E-05	0.52376E-07	0.33851E-01
20.0- 27.0	15.20	.43E-02	1330.74	0.31141E-10	0.31553E-02	0.33520E-13	0.30423E-05	0.99012E-07	0.64510E-01
20.0- 27.0	18.96	.41E-02	2392.22	0.26595E-10	0.26947E-02	0.28627E-13	0.25982E-05	0.85242E-07	0.55094E-01
20.0- 27.0	23.07	.38E-02	3265.65	0.21296E-10	0.21578E-02	0.22923E-13	0.20005E-05	0.68250E-07	0.44117E-01
20.0- 27.0	27.00	.37E-02	4612.71	0.20337E-10	0.20607E-02	0.21091E-13	0.19069E-05	0.65105E-07	0.42130E-01
23.0- 30.0	15.10	.44E-02	1360.42	0.32762E-10	0.33196E-02	0.35264E-13	0.32006E-05	0.10501E-06	0.67868E-01
23.0- 30.0	19.05	.40E-02	2325.89	0.25600E-10	0.25947E-02	0.27564E-13	0.25010E-05	0.82079E-07	0.53049E-01

AN EXAMPLE OUTPUT FROM PERMEA

AIR INJECTION TESTING RESULTS FOR BOREHOLE NO RDU-1

INTERVAL	ZONE	APER- PRESS	VOLUME FLOW.	EQUIVALENT POROUS MEDIA PERMEABILITY					
				INTRINSIC			HYDRAULIC CONDUCTIVITY		
				FEET	PSIA	CM.	ML/M	SQUAR CM.	DARCY
1.5-4.5	27.10	.49	4986.60	0.12900E-09	0.13879E-01	0.13894E-12	0.12610E-04	0.41373E-06	0.26740E+00
5.0-7.0	33.10	.50	2299.61	0.38732E-10	0.39245E-02	0.41691E-13	0.37839E-05	0.12414E-06	0.80237E-01
6.0-7.0	33.00	.50	2177.84	0.36933E-10	0.37419E-02	0.39751E-13	0.36879E-05	0.11837E-06	0.76504E-01
7.0-8.0	32.90	.50	2294.63	0.39427E-10	0.39950E-02	0.42439E-13	0.38518E-05	0.12637E-06	0.81677E-01
8.0-9.0	16.20	.90	7739.70	0.82828E-08	0.83926E-01	0.89156E-12	0.80919E-04	0.26548E-05	0.17159E+01
9.0-11.0	15.80	1.00	7931.52	0.11403E-08	0.11554E+00	0.12274E-11	0.11140E-03	0.36548E-05	0.23622E+01

AIR INJECTION TESTING RESULTS FOR BOREHOLE NO RDU-2

INTERVAL	ZONE	APER- PRESS	VOLUME FLOW.	EQUIVALENT POROUS MEDIA PERMEABILITY					
				INTRINSIC			HYDRAULIC CONDUCTIVITY		
				FEET	PSIA	CM.	ML/M	SQUAR CM.	DARCY
0.5-1.5	23.70	.50	6275.34	0.22704E-09	0.23805E-01	0.24438E-12	0.22181E-04	0.72771E-06	0.47033E+00
1.5-2.0	23.50	.50	6279.31	0.34554E-09	0.35812E-01	0.37194E-12	0.33757E-04	0.11075E-05	0.71581E+00
2.0-3.0	23.50	.50	6944.90	0.98820E-10	0.91989E-02	0.97637E-13	0.88616E-05	0.29074E-06	0.17991E+00
3.0-4.0	23.50	.50	6978.55	0.35344E-10	0.35701E-01	0.37926E-13	0.34422E-04	0.11293E-05	0.73991E+00
4.0-5.0	23.50	.50	6938.86	0.35344E-10	0.35995E-01	0.38238E-13	0.34406E-04	0.11386E-05	0.73592E+00
5.0-6.0	23.50	.50	4108.44	0.87314E-10	0.88532E-02	0.94849E-13	0.85360E-05	0.28085E-06	0.18100E+00
6.0-7.0	23.50	.50	4105.44	0.73143E-10	0.74388E-01	0.78950E-13	0.73383E-05	0.32606E-06	0.21074E+00
7.0-8.0	23.50	.50	4116.61	0.19313E-10	0.19388E-01	0.19556E-13	0.19383E-05	0.32606E-06	0.21074E+00
8.0-9.0	23.50	.50	883.26	0.13523E-10	0.13702E-02	0.14556E-13	0.13211E-05	0.43343E-07	0.28014E-01

AIR INJECTION TESTING RESULTS FOR BOREHOLE NO RDU-3

INTERVAL	ZONE	APER- PRESS	VOLUME FLOW.	EQUIVALENT POROUS MEDIA PERMEABILITY					
				INTRINSIC			HYDRAULIC CONDUCTIVITY		
				FEET	PSIA	CM.	ML/M	SQUAR CM.	DARCY
0.5-1.5	25.80	.51	5871.37	0.14619E-09	0.14812E-01	0.15735E-12	0.14282E-04	0.46856E-06	0.30284E+00
1.5-2.0	26.20	.51	4947.53	0.13697E-09	0.13879E-01	0.14743E-12	0.13381E-04	0.43902E-06	0.28375E+00
2.0-3.0	33.50	.50	359.55	0.58200E-11	0.58971E-03	0.62645E-14	0.56858E-06	0.18654E-07	0.12056E-01
3.0-4.0	33.50	.50	1769.46	0.38672E-11	0.31878E-02	0.33915E-13	0.29965E-05	0.98310E-07	0.63539E-01
4.0-5.0	32.60	.50	11648.00	0.27990E-09	0.28361E-02	0.30028E-13	0.27345E-05	0.89714E-07	0.57984E-01
5.0-6.0	32.80	.50	68873.07	0.23644E-09	0.23957E-01	0.25450E-12	0.23099E-04	0.75783E-06	0.48980E+00
6.0-7.0	33.00	.50	68866.76	0.22617E-09	0.22917E-01	0.24345E-12	0.22096E-04	0.72493E-06	0.46853E+00
7.0-8.0	33.00	.50	6338.92	0.22617E-09	0.22917E-01	0.24345E-12	0.22096E-04	0.72493E-06	0.46853E+00
8.0-9.0	26.10	.50	5129.88	0.14429E-09	0.14620E-01	0.15531E-12	0.14096E-04	0.46248E-06	0.29891E+00
9.0-10.0	26.10	.50	5398.08	0.16880E-09	0.17088E-01	0.18083E-12	0.16412E-04	0.53847E-06	0.34802E+00
10.0-11.0	21.00	.50	6623.06	0.31799E-09	0.32221E-01	0.34228E-12	0.31066E-04	0.10192E-05	0.65875E+00
11.0-12.0	20.90	.50	6695.52	0.32506E-09	0.32937E-01	0.34989E-12	0.31757E-04	0.10419E-05	0.67339E+00

AIR INJECTION TESTING RESULTS FOR BOREHOLE NO RDU-4

INTERVAL FEET	ZONE PRESS PSIA	APER- TURE CM.	VOLUME FLOW. ML/M	EQUIVALENT POROUS MEDIA PERMEABILITY					
				INTRINSIC			HYDRAULIC CONDUCTIVITY		
				SQUAR CM.	DARCY	SQUAR FT.	CM/SEC	FT/SEC	GAL/D FT**2
0.5-3.0	32.70	.228E-02	1345.85	0.222919E-10	0.232222E-02	0.24669E-13	0.22390E-05	0.73459E-07	0.47478E-01
1.0-4.0	32.90	.228E-02	1348.32	0.225011E-10	0.22799E-02	0.24220E-13	0.21983E-05	0.72121E-07	0.46613E-01
2.0-5.0	28.10	.448E-02	4223.44	0.99721E-10	0.10104E-01	0.10734E-12	0.97422E-05	0.31963E-06	0.20658E+00
3.0-6.0	28.20	.448E-02	4159.19	0.97392E-10	0.98682E-02	0.10483E-12	0.95147E-05	0.31216E-06	0.20175E+00
4.0-7.0	27.50	.448E-02	4410.95	0.10993E-09	0.11138E-01	0.11033E-12	0.10739E-04	0.35234E-06	0.22772E+00
5.0-8.0	24.70	.558E-02	5485.77	0.17409E-09	0.17640E-01	0.17739E-12	0.17008E-04	0.55800E-06	0.36065E+00
6.0-9.0	25.20	.558E-02	5398.28	0.16476E-09	0.16694E-01	0.17734E-12	0.16096E-04	0.52808E-06	0.34131E+00
7.0-10.0	25.20	.558E-02	2696.35	0.51028E-10	0.51705E-02	0.54927E-13	0.49852E-05	0.16356E-06	0.10657E+00
8.0-11.0	31.70	.338E-02	2137.71	0.38526E-10	0.39036E-02	0.41469E-13	0.37638E-05	0.12348E-06	0.79809E-01
9.0-12.0	31.00	.338E-02	2137.71	0.38253E-10	0.38760E-02	0.41175E-13	0.37371E-05	0.12261E-06	0.79244E-01
10.0-13.0	29.90	.558E-02	3332.21	0.68027E-10	0.68929E-02	0.73224E-13	0.66459E-05	0.21804E-06	0.14092E+00
11.0-13.5	25.00	.558E-02	5412.66	0.16732E-09	0.16954E-01	0.18010E-12	0.16346E-04	0.53629E-06	0.34661E+00

AIR INJECTION TESTING RESULTS FOR BOREHOLE NO RDU-5

INTERVAL FEET	ZONE PRESS PSIA	APER- TURE CM.	VOLUME FLOW. ML/M	EQUIVALENT POROUS MEDIA PERMEABILITY					
				INTRINSIC			HYDRAULIC CONDUCTIVITY		
				SQUAR CM.	DARCY	SQUAR FT.	CM/SEC	FT/SEC	GAL/D FT**2
7.0-9.5	27.50	.44E-02	4445.30	0.10858E-09	0.11001E-01	0.11687E-12	0.10607E-04	0.34801E-06	0.22492E+00
8.0-10.5	27.30	.44E-02	4613.35	0.11639E-09	0.11793E-01	0.12528E-12	0.11370E-04	0.37304E-06	0.24110E+00
9.0-11.5	26.90	.44E-02	4693.38	0.12160E-09	0.12321E-01	0.13089E-12	0.11879E-04	0.38974E-06	0.25190E+00

AIR INJECTION TESTING RESULTS FOR BOREHOLE NO RDU-6

INTERVAL FEET	ZONE PRESS PSIA	APER- TURE CM.	VOLUME FLOW. ML/M	EQUIVALENT POROUS MEDIA PERMEABILITY					
				INTRINSIC			HYDRAULIC CONDUCTIVITY		
				SQUAR CM.	DARCY	SQUAR FT.	CM/SEC	FT/SEC	GAL/D FT**2
0.5-3.0	31.45	.34E-02	2376.33	0.44032E-10	0.44616E-02	0.47396E-13	0.43017E-05	0.14113E-06	0.91216E-01
1.0-4.0	29.20	.44E-02	3704.39	0.80397E-10	0.81462E-02	0.86633E-13	0.78834E-05	0.25760E-06	0.16755E+00
2.0-5.0	28.70	.44E-02	3838.93	0.86287E-10	0.87430E-02	0.92897E-13	0.84429E-05	0.27607E-06	0.18075E+00
3.0-6.0	27.20	.44E-02	4448.13	0.11423E-09	0.11574E-01	0.12249E-12	0.11113E-04	0.36657E-06	0.24063E+00
4.0-7.0	27.00	.44E-02	1458.89	0.29023E-10	0.29387E-02	0.31244E-12	0.28355E-05	0.91222E-07	0.60122E-01
5.0-8.0	30.90	.33E-02	1807.91	0.29878E-10	0.29387E-02	0.31244E-12	0.28355E-05	0.91222E-07	0.60122E-01
6.0-9.0	30.90	.33E-02	1807.91	0.35878E-10	0.36353E-02	0.38619E-12	0.35854E-05	0.11564E-06	0.74324E-01
7.0-10.0	25.95	.55E-02	4441.36	0.12296E-09	0.13134E-01	0.13953E-12	0.12066E-04	0.41549E-06	0.28093E+00
8.0-11.0	25.50	.55E-02	4572.17	0.13898E-09	0.14088E-01	0.14960E-12	0.13578E-04	0.44527E-06	0.29593E+00
9.0-12.0	24.70	.55E-02	4957.72	0.16292E-09	0.16507E-01	0.17456E-12	0.15916E-04	0.52218E-06	0.35174E+00
10.0-13.0	29.50	.39E-02	2848.87	0.62492E-10	0.63320E-02	0.67206E-13	0.61051E-05	0.20030E-06	0.12940E+00

AIR INJECTION TESTING RESULTS FOR BOREHOLE NO RDD-1

INTERVAL FEET	ZONE PSIA	APER- TURE CM.	VOLUME FLOW. ML/M	EQUIVALENT POROUS MEDIA PERMEABILITY					
				INTRINSIC		HYDRAULIC CONDUCTIVITY			
				SQUAR CM.	DARCY	SQUAR FT.	CM/SEC	FT/SEC	GAL/D FT**2
0.7- 3.2	12.30	.15E-01	7893.04	0.33691E-08	0.34138E+00	0.36265E-11	0.32915E-03	0.10799E-04	0.69794E+01

AIR INJECTION TESTING RESULTS FOR BOREHOLE NO RDD-2

INTERVAL FEET	ZONE PSIA	APER- TURE CM.	VOLUME FLOW. ML/M	EQUIVALENT POROUS MEDIA PERMEABILITY					
				INTRINSIC		HYDRAULIC CONDUCTIVITY			
				SQUAR CM.	DARCY	SQUAR FT.	CM/SEC	FT/SEC	GAL/D FT**2
1.0- 3.2	30.15	.23E-02	1186.30	0.23171E-10	0.23478E-02	0.24941E-13	0.22637E-05	0.74268E-07	0.48001E-01
1.0- 4.4	30.15	.23E-02	1878.00	0.17850E-10	0.18086E-02	0.19213E-13	0.17430E-05	0.57512E-07	0.36577E-01
1.0- 5.6	30.15	.23E-02	1222.10	0.25689E-10	0.26030E-02	0.27657E-13	0.25007E-05	0.82340E-07	0.54821E-01
1.0- 7.0	30.15	.23E-02	933.70	0.40943E-10	0.41486E-02	0.44071E-13	0.39999E-05	0.13123E-06	0.84817E-01
1.0- 8.4	30.15	.23E-02	2030.71	0.44494E-10	0.45084E-02	0.47893E-13	0.43468E-05	0.14261E-06	0.92113E-01
1.0- 11.5	29.30	.35E-02	2065.22	0.45281E-10	0.45881E-02	0.48740E-13	0.44237E-05	0.14513E-06	0.93802E-01

AIR INJECTION TESTING RESULTS FOR BOREHOLE NO RDD-3

INTERVAL FEET	ZONE PSIA	APER- TURE CM.	VOLUME FLOW. ML/M	EQUIVALENT POROUS MEDIA PERMEABILITY					
				INTRINSIC		HYDRAULIC CONDUCTIVITY			
				SQUAR CM.	DARCY	SQUAR FT.	CM/SEC	FT/SEC	GAL/D FT**2
0.7- 3.2	30.15	.23E-02	597.07	0.12249E-08	0.12664E-02	0.13453E-11	0.12210E-05	0.40059E-07	0.25891E-01
1.0- 4.4	30.15	.23E-02	454.09	0.09065E-08	0.09322E-02	0.10233E-11	0.92874E-05	0.30470E-07	0.19693E-01
1.0- 5.6	30.15	.23E-02	902.43	0.23317E-08	0.23599E-02	0.24941E-11	0.22882E-05	0.68325E-07	0.44160E-01
1.0- 7.0	30.15	.23E-02	284.04	0.73389E-08	0.73389E-02	0.77877E-11	0.70682E-05	0.23190E-06	0.14988E+00
1.0- 8.4	30.15	.23E-02	101.11	0.86900E-08	0.86900E-02	0.92331E-11	0.83786E-05	0.27489E-06	0.17767E+00
1.0- 9.8	30.15	.23E-02	690.97	0.16133E-08	0.16133E-02	0.17133E-11	0.15554E-05	0.51029E-07	0.32981E-01
1.0- 11.5	30.15	.23E-02	697.90	0.15959E-08	0.15959E-02	0.17133E-11	0.16681E-05	0.21659E-06	0.13999E+01
1.0- 14.8	30.15	.23E-02	808.08	0.35964E-08	0.35964E-02	0.38788E-11	0.27940E-05	0.91666E-06	0.59245E+00
1.0- 18.1	30.15	.23E-02	566.88	0.35964E-08	0.35964E-02	0.38788E-11	0.27940E-05	0.90911E-06	0.58758E+00
1.0- 21.4	30.15	.23E-02	681.04	0.35964E-08	0.35964E-02	0.38788E-11	0.27940E-05	0.90911E-06	0.58758E+00
1.0- 24.8	30.15	.23E-02	559.88	0.24805E-08	0.24805E-02	0.26391E-11	0.25648E-05	0.45164E-07	0.69725E+01
1.0- 28.1	30.15	.23E-02	559.88	0.24805E-08	0.24805E-02	0.26391E-11	0.25648E-05	0.45164E-07	0.69725E+01
1.0- 31.5	30.15	.23E-02	559.88	0.24805E-08	0.24805E-02	0.26391E-11	0.25648E-05	0.45164E-07	0.69725E+01

AIR INJECTION TESTING RESULTS FOR BOREHOLE NO RDD-4

INTERVAL FEET	ZONE PRESS PSIA	APER- TURE CM.	VOLUME FLOW. ML/M	EQUIVALENT POROUS MEDIA PERMEABILITY					
				INTRINSIC			HYDRAULIC CONDUCTIVITY		
				SQUAR CM.	DARCY	SQUAR FT.	CM/SEC	FT/SEC	GAL/D FT**2
0.7- 3.2	27.90	.39E-02	2651.56	0.65361E-10	0.66227E-02	0.70354E-13	0.63854E-05	0.20949E-06	0.13540E+00
1.0- 3.5	28.65	.38E-02	2554.86	0.59149E-10	0.59933E-02	0.63668E-13	0.57786E-05	0.18959E-06	0.12253E+00
11.0- 13.5	30.90	.24E-02	769.84	0.15090E-10	0.15290E-02	0.16243E-13	0.14743E-05	0.48368E-07	0.31261E-01

AIR INJECTION TESTING RESULTS FOR BOREHOLE NO RDD-5

INTERVAL FEET	ZONE PRESS PSIA	APER- TURE CM.	VOLUME FLOW. ML/M	EQUIVALENT POROUS MEDIA PERMEABILITY					
				INTRINSIC			HYDRAULIC CONDUCTIVITY		
				SQUAR CM.	DARCY	SQUAR FT.	CM/SEC	FT/SEC	GAL/D FT**2
2.0- 4.5	30.35	.22E-02	576.11	0.11897E-10	0.12055E-02	0.12806E-13	0.11623E-05	0.38133E-07	0.24646E-01
5.0- 7.5	30.65	.27E-02	1057.04	0.21515E-10	0.21800E-02	0.23159E-13	0.21019E-05	0.68960E-07	0.44570E-01

AIR INJECTION TESTING RESULTS FOR BOREHOLE NO RDD-6

INTERVAL FEET	ZONE PRESS PSIA	APER- TURE CM.	VOLUME FLOW. ML/M	EQUIVALENT POROUS MEDIA PERMEABILITY					
				INTRINSIC			HYDRAULIC CONDUCTIVITY		
				SQUAR CM.	DARCY	SQUAR FT.	CM/SEC	FT/SEC	GAL/D FT**2
0.5- 3.0	25.00	.52E-02	4668.83	0.14943E-09	0.15141E-01	0.16088E-12	0.14598E-04	0.47894E-06	0.30955E+00
1.0- 3.5	24.80	.52E-02	4797.11	0.15655E-09	0.15866E-01	0.16855E-12	0.15290E-04	0.50190E-06	0.32440E+00
2.0- 4.0	11.60	.20E-01	8723.25	0.89033E-08	0.90216E+00	0.95831E-11	0.86977E-03	0.28519E-05	0.18743E+00
3.0- 5.0	10.70	.26E+00	9689.82	0.18210E-04	0.18445E+00	0.19688E-07	0.17790E+01	0.58033E-06	0.37723E+00
4.0- 6.0	27.85	.61E-02	5660.99	0.25366E-09	0.25693E-01	0.27290E-12	0.24776E-04	0.81300E-06	0.52535E+00
5.0- 7.0	17.05	.84E-02	7059.20	0.64479E-09	0.65333E-01	0.69448E-12	0.62299E-04	0.20663E-06	0.13353E+00
6.0- 8.0	13.40	.12E-01	7736.39	0.18763E-08	0.19011E+00	0.20199E-11	0.18330E-03	0.60138E-05	0.38806E+00
7.0- 9.0	17.05	.83E-02	7042.07	0.63499E-09	0.64333E+00	0.68344E-12	0.62828E-04	0.20338E-06	0.13173E+00
8.0- 10.0	14.95	.10E-01	7492.75	0.10844E-08	0.10999E+00	0.11675E-11	0.10597E-03	0.34766E-05	0.22440E+00
9.0- 11.0	12.75	.13E-01	7828.66	0.15661E-08	0.15955E+00	0.17570E-11	0.15823E-03	0.08228E-05	0.05388E+00
10.0- 12.0	19.45	.71E-02	6445.91	0.38040E-09	0.39446E-01	0.44192E-11	0.38085E-04	0.12484E-05	0.08066E+00
11.0- 13.0	19.55	.70E-02	6392.81	0.38006E-09	0.38566E-01	0.40971E-11	0.37718E-04	0.12281E-05	0.07885E+00
12.0- 14.5	30.40	.26E-02	922.89	0.19011E-10	0.19266E-02	0.20470E-13	0.18579E-05	0.60955E-07	0.39336E-01

AIR INJECTION TESTING RESULTS FOR BOREHOLE NO RUE-1

INTERVAL	ZONE	APER- PRESS	VOLUME FLOW.	EQUIVALENT POROUS MEDIA PERMEABILITY						
				INTRINSIC		HYDRAULIC CONDUCTIVITY				
				SQUAR CM.	DARCY	SQUAR FT.	CM/SEC	FT/SEC	GAL/D FT**2	
FEET	PSIA	CM.	ML/M							
0.5-1.0	13.70	.11	7929.89	0.165	0.167	0.177	0.161	0.529	0.529	0.529
1.0-1.5	4.18	.11	7917.71	1.433	1.455	1.778	1.130	1.994	1.994	1.994
1.5-2.0	3.38	.11	557.18	9.145	9.277	9.999	6.090	4.262	4.262	4.262
2.0-2.5	4.55	.11	455.66	7.339	7.449	7.999	5.555	3.900	3.900	3.900
2.5-3.0	3.33	.11	456.81	7.599	7.688	8.000	5.666	4.000	4.000	4.000
3.0-3.5	3.33	.11	456.81	7.599	7.688	8.000	5.666	4.000	4.000	4.000
3.5-4.0	3.33	.11	333.33	6.666	6.777	7.000	4.666	3.333	3.333	3.333
4.0-4.5	3.33	.11	333.33	6.666	6.777	7.000	4.666	3.333	3.333	3.333
4.5-5.0	3.33	.11	333.33	6.666	6.777	7.000	4.666	3.333	3.333	3.333
5.0-5.5	3.33	.11	333.33	6.666	6.777	7.000	4.666	3.333	3.333	3.333
5.5-6.0	3.33	.11	333.33	6.666	6.777	7.000	4.666	3.333	3.333	3.333
6.0-6.5	3.33	.11	333.33	6.666	6.777	7.000	4.666	3.333	3.333	3.333
6.5-7.0	3.33	.11	333.33	6.666	6.777	7.000	4.666	3.333	3.333	3.333
7.0-7.5	3.33	.11	333.33	6.666	6.777	7.000	4.666	3.333	3.333	3.333
7.5-8.0	3.33	.11	333.33	6.666	6.777	7.000	4.666	3.333	3.333	3.333
8.0-8.5	3.33	.11	333.33	6.666	6.777	7.000	4.666	3.333	3.333	3.333
8.5-9.0	3.33	.11	333.33	6.666	6.777	7.000	4.666	3.333	3.333	3.333
9.0-9.5	3.33	.11	333.33	6.666	6.777	7.000	4.666	3.333	3.333	3.333
9.5-10.0	3.33	.11	333.33	6.666	6.777	7.000	4.666	3.333	3.333	3.333

AIR INJECTION TESTING RESULTS FOR BOREHOLE NO RUE-2

INTERVAL	ZONE	APER- PRESS	VOLUME FLOW.	EQUIVALENT POROUS MEDIA PERMEABILITY						
				INTRINSIC		HYDRAULIC CONDUCTIVITY				
				SQUAR CM.	DARCY	SQUAR FT.	CM/SEC	FT/SEC	GAL/D FT**2	
FEET	PSIA	CM.	ML/M							
0.5-1.0	13.70	.11	7929.89	0.165	0.167	0.177	0.161	0.529	0.529	0.529
1.0-1.5	4.18	.11	7917.71	1.433	1.455	1.778	1.130	1.994	1.994	1.994
1.5-2.0	3.38	.11	557.18	9.145	9.277	9.999	6.090	4.262	4.262	4.262
2.0-2.5	4.55	.11	455.66	7.339	7.449	7.999	5.555	3.900	3.900	3.900
2.5-3.0	3.33	.11	456.81	7.599	7.688	8.000	5.666	4.000	4.000	4.000
3.0-3.5	3.33	.11	456.81	7.599	7.688	8.000	5.666	4.000	4.000	4.000
3.5-4.0	3.33	.11	333.33	6.666	6.777	7.000	4.666	3.333	3.333	3.333
4.0-4.5	3.33	.11	333.33	6.666	6.777	7.000	4.666	3.333	3.333	3.333
4.5-5.0	3.33	.11	333.33	6.666	6.777	7.000	4.666	3.333	3.333	3.333
5.0-5.5	3.33	.11	333.33	6.666	6.777	7.000	4.666	3.333	3.333	3.333
5.5-6.0	3.33	.11	333.33	6.666	6.777	7.000	4.666	3.333	3.333	3.333
6.0-6.5	3.33	.11	333.33	6.666	6.777	7.000	4.666	3.333	3.333	3.333
6.5-7.0	3.33	.11	333.33	6.666	6.777	7.000	4.666	3.333	3.333	3.333
7.0-7.5	3.33	.11	333.33	6.666	6.777	7.000	4.666	3.333	3.333	3.333
7.5-8.0	3.33	.11	333.33	6.666	6.777	7.000	4.666	3.333	3.333	3.333
8.0-8.5	3.33	.11	333.33	6.666	6.777	7.000	4.666	3.333	3.333	3.333
8.5-9.0	3.33	.11	333.33	6.666	6.777	7.000	4.666	3.333	3.333	3.333
9.0-9.5	3.33	.11	333.33	6.666	6.777	7.000	4.666	3.333	3.333	3.333
9.5-10.0	3.33	.11	333.33	6.666	6.777	7.000	4.666	3.333	3.333	3.333

AIR INJECTION TESTING RESULTS FOR BOREHOLE NO RUE-3

INTERVAL	ZONE	APER- PRESS	TURE CM.	VOLUME FLOW.	EQUIVALENT POROUS MEDIA PERMEABILITY							
					FEET	PSIA	ML/M	INTRINSIC		HYDRAULIC CONDUCTIVITY		
								SQUAR CM.	DARCY	SQUAR FT.	CM/SEC	FT/SEC
0.5-1.0	3.0	26.50	.48E-02	4292.26	0.12068E-09	0.12228E-01	0.12990E-12	0.11790E-04	0.38680E-06	0.24999E+00		
1.0-1.5	3.0	24.60	.54E-02	5161.32	0.17047E-09	0.17273E-01	0.18349E-12	0.16654E-04	0.54640E-06	0.35315E+00		
1.5-2.0	4.0	18.90	.74E-02	6609.67	0.43987E-09	0.44570E-01	0.47340E-12	0.42973E-04	0.14899E-06	0.91135E+00		
2.0-2.5	5.0	14.80	.10E-01	7546.83	0.11391E-08	0.11542E+00	0.12262E-11	0.11129E-03	0.36511E-05	0.23590E+01		
2.5-3.0	6.0	14.80	.10E-01	7546.83	0.11391E-08	0.11542E+00	0.12262E-11	0.11129E-03	0.36511E-05	0.23590E+01		
3.0-3.5	7.0	14.65	.10E-01	7619.76	0.11989E-08	0.12148E+00	0.12905E-11	0.11712E-03	0.38422E-05	0.24833E+01		
3.5-4.0	8.0	15.15	.98E-02	7546.83	0.10353E-08	0.10491E+00	0.11144E-11	0.11115E-03	0.33180E-05	0.21444E+01		
4.0-4.5	9.0	16.65	.86E-02	7266.77	0.70707E-09	0.71644E-01	0.76109E-12	0.69077E-04	0.22666E-06	0.14644E+01		
4.5-5.0	10.0	13.95	.11E-01	7619.76	0.14985E-08	0.15183E+00	0.16129E-11	0.14639E-03	0.46022E-05	0.31404E+01		
5.0-5.5	11.0	13.65	.11E-01	7692.87	0.15646E-08	0.15853E+00	0.16841E-11	0.15528E-03	0.50148E-05	0.32411E+01		
5.5-6.0	12.0	14.40	.11E-01	7557.31	0.17999E-08	0.17968E+00	0.19776E-11	0.17258E-03	0.41022E-05	0.26651E+01		
6.0-6.5	13.0	14.80	.11E-01	7588.14	0.17400E-08	0.17491E+00	0.18507E-11	0.17368E-03	0.44000E-05	0.28000E+01		
6.5-7.0	14.0	15.75	.30E-02	2611.07	0.59426E-10	0.62133E-02	0.63965E-13	0.58056E-05	0.19047E-06	0.12311E+01		
7.0-7.5	15.0	13.30	.24E-02	838.44	0.15929E-10	0.16140E-02	0.17146E-13	0.15556E-05	0.51004E-07	0.32999E+01		
7.5-8.0	16.0	11.40	.20E-02	434.75	0.83763E-11	0.84873E-03	0.91162E-14	0.81832E-06	0.26848E-08	0.17335E+01		
8.0-8.5	17.0	12.20	.44E-02	3524.42	0.90438E-10	0.91637E-02	0.97347E-13	0.88335E-05	0.28908E-06	0.18735E+01		
8.5-9.0	18.0	22.60	.57E-02	5388.93	0.20698E-09	0.20972E-01	0.22279E-12	0.20222E-04	0.66340E-06	0.42877E+01		
9.0-9.5	19.0	12.60	.13E-01	7802.60	0.24027E-08	0.24345E+00	0.25862E-11	0.23473E-03	0.77011E-05	0.49774E+01		

AIR INJECTION TESTING RESULTS FOR BOREHOLE NO RUE-4

INTERVAL	ZONE	APER- PRESS	TURE CM.	VOLUME FLOW.	EQUIVALENT POROUS MEDIA PERMEABILITY							
					FEET	PSIA	ML/M	INTRINSIC		HYDRAULIC CONDUCTIVITY		
								SQUAR CM.	DARCY	SQUAR FT.	CM/SEC	FT/SEC
0.5-1.0	3.0	12.75	.13E-01	7828.66	0.25613E-08	0.25953E+00	0.27570E-11	0.25023E-03	0.82095E-05	0.53060E+01		
1.0-1.5	3.0	11.85	.00E+00	0.00	0.00000E+00	0.00000E+00	0.00000E+00	0.00000E+00	0.00000E+00	0.00000E+00		
1.5-2.0	4.0	31.80	.00E+00	0.00	0.00000E+00	0.00000E+00	0.00000E+00	0.00000E+00	0.00000E+00	0.00000E+00		
2.0-2.5	5.0	25.15	.00E+00	0.00	0.00000E+00	0.00000E+00	0.00000E+00	0.00000E+00	0.00000E+00	0.00000E+00		
2.5-3.0	6.0	19.95	.00E+00	44.63	0.13873E-09	0.14057E-01	0.14933E-12	0.13554E-04	0.44467E-06	0.28740E+00		
3.0-3.5	7.0	18.50	.76E-02	6553.94	0.41823E-09	0.42377E-01	0.45010E-12	0.40859E-04	0.13405E-06	0.86640E+00		
3.5-4.0	8.0	18.50	.76E-02	6702.00	0.47069E-09	0.47692E-01	0.50664E-12	0.45983E-04	0.15006E-06	0.97506E+00		
4.0-4.5	9.0	24.50	.55E-02	5076.95	0.18000E-09	0.18242E-01	0.19379E-12	0.17588E-04	0.57704E-06	0.37295E+00		
4.5-5.0	10.0	29.30	.38E-02	2605.69	0.57875E-10	0.58642E-02	0.62296E-13	0.56541E-05	0.18550E-06	0.11989E+00		

AIR INJECTION TESTING RESULTS FOR BOREHOLE NO RUE-5

INTERVAL	ZONE	APER- PRESS	VOLUME FLOW.	EQUIVALENT POROUS MEDIA PERMEABILITY						
				PSIA	CM.	INTRINSIC		HYDRAULIC CONDUCTIVITY		
						ML/M	SQUAR CM.	DARCY	SQUAR FT.	CM/SEC
1.0-1.5	98	44	8671.84	0.4170	0.1701	0.4225	0.4488	0.1333	0.8633	
1.5-2.0	98	44	8710.46	0.4170	0.1701	0.4225	0.4488	0.1333	0.8633	
2.0-2.5	98	44	8710.46	0.4170	0.1701	0.4225	0.4488	0.1333	0.8633	
2.5-3.0	98	44	8710.46	0.4170	0.1701	0.4225	0.4488	0.1333	0.8633	
3.0-3.5	98	44	8710.46	0.4170	0.1701	0.4225	0.4488	0.1333	0.8633	
3.5-4.0	98	44	8710.46	0.4170	0.1701	0.4225	0.4488	0.1333	0.8633	
4.0-4.5	98	44	8710.46	0.4170	0.1701	0.4225	0.4488	0.1333	0.8633	
4.5-5.0	98	44	8710.46	0.4170	0.1701	0.4225	0.4488	0.1333	0.8633	
5.0-5.5	98	44	8710.46	0.4170	0.1701	0.4225	0.4488	0.1333	0.8633	
5.5-6.0	98	44	8710.46	0.4170	0.1701	0.4225	0.4488	0.1333	0.8633	
6.0-6.5	98	44	8710.46	0.4170	0.1701	0.4225	0.4488	0.1333	0.8633	
6.5-7.0	98	44	8710.46	0.4170	0.1701	0.4225	0.4488	0.1333	0.8633	
7.0-7.5	98	44	8710.46	0.4170	0.1701	0.4225	0.4488	0.1333	0.8633	
7.5-8.0	98	44	8710.46	0.4170	0.1701	0.4225	0.4488	0.1333	0.8633	
8.0-8.5	98	44	8710.46	0.4170	0.1701	0.4225	0.4488	0.1333	0.8633	
8.5-9.0	98	44	8710.46	0.4170	0.1701	0.4225	0.4488	0.1333	0.8633	
9.0-9.5	98	44	8710.46	0.4170	0.1701	0.4225	0.4488	0.1333	0.8633	
9.5-10.0	98	44	8710.46	0.4170	0.1701	0.4225	0.4488	0.1333	0.8633	

AIR INJECTION TESTING RESULTS FOR BOREHOLE NO RUE-6

INTERVAL	ZONE	APER- PRESS	VOLUME FLOW.	EQUIVALENT POROUS MEDIA PERMEABILITY						
				PSIA	CM.	INTRINSIC		HYDRAULIC CONDUCTIVITY		
						ML/M	SQUAR CM.	DARCY	SQUAR FT.	CM/SEC
1.0-1.5	98	54	5681.05	0.1679	0.1701	0.1807	0.1640	0.5383	0.3479	
1.5-2.0	98	54	746.24	0.1125	0.1140	0.1188	0.1099	0.3607	0.2331	
2.0-2.5	98	54	515.90	0.1104	0.1104	0.1104	0.1104	0.3539	0.2287	
2.5-3.0	98	54	415.96	0.0778	0.0895	0.0944	0.0857	0.2813	0.1806	
3.0-3.5	98	54	396.79	0.0831	0.0826	0.0842	0.0811	0.2663	0.1721	
3.5-4.0	98	54	4131.95	0.1351	0.1459	0.1369	0.1454	0.4331	0.2799	
4.0-4.5	98	54	4343.12	0.1439	0.1459	0.1459	0.1406	0.4615	0.2982	
4.5-5.0	98	54	4797.98	0.1760	0.1783	0.1783	0.1719	0.5641	0.3646	
5.0-5.5	98	54	1419.53	0.3022	0.3062	0.3253	0.2952	0.9686	0.6260	
5.5-6.0	98	54	3220.37	0.8384	0.8495	0.8801	0.8198	2.2687	1.7368	
6.0-6.5	98	54	3225.07	0.1439	0.1439	0.1439	0.1439	0.7988	0.2629	
6.5-7.0	98	54	4228.04	0.1069	0.1088	0.1155	0.1045	0.3422	0.2216	
7.0-7.5	98	54	5124.03	0.1983	0.1983	0.1983	0.1983	0.6358	0.4194	
7.5-8.0	98	54	3680.04	0.2373	0.2405	0.2558	0.2311	0.7688	0.4917	
8.0-8.5	98	54	7392.37	0.1063	0.1144	0.1144	0.1033	0.3407	0.2202	
8.5-9.0	98	54	7118.48	0.7375	0.7473	0.7939	0.7205	2.2364	1.5279	
9.0-9.5	98	54	6938.54	0.6706	0.6795	0.7211	0.6552	2.1496	1.3893	
9.5-10.0	98	54	4732.41	0.2978	0.3011	0.3199	0.2904	0.9527	0.6158	
10.0-10.5	98	54	5759.99	0.4333	0.4333	0.4333	0.4126	1.2289	0.7942	
10.5-11.0	98	54	6169.25	0.3834	0.3884	0.4126	0.3745	1.1390	0.8989	
11.0-11.5	98	54	6356.69	0.4333	0.4333	0.4333	0.4239	1.2289	0.8989	
11.5-12.0	98	54	6811.98	0.3381	0.3426	0.3633	0.3303	1.0838	0.7804	

AIR INJECTION TESTING RESULTS FOR BOREHOLE NO RW-5

INTERVAL FEET	ZONE PRESS PSIA	APER- TURE CM.	VOLUME FLOW. ML/M	EQUIVALENT POROUS MEDIA PERMEABILITY					
				INTRINSIC		HYDRAULIC CONDUCTIVITY			
				SQUAR CM.	DARCY	SQUAR FT.	CM/SEC	FT/SEC	GAL/D FT**2
2.0-4.5	30.75	.27E-02	1128.38	0.22581E-10	0.22880E-02	0.24306E-13	0.22060E-05	0.72376E-07	0.46778E-01
3.0-5.5	30.75	.30E-02	1453.47	0.29180E-10	0.29566E-02	0.31409E-13	0.28507E-05	0.93526E-07	0.68448E-01
4.0-6.5	30.95	.26E-02	966.08	0.19263E-10	0.19510E-02	0.20735E-13	0.18819E-05	0.61742E-07	0.39905E-01
1.0-13.0	13.40	.12E-01	7769.07	0.18969E-08	0.19220E+00	0.20418E-11	0.18532E-03	0.60799E-05	0.39295E+01
1.2-14.0	13.45	.12E-01	7769.07	0.18585E-08	0.18832E+00	0.20005E-11	0.18157E-03	0.59570E-05	0.38501E+01
1.3-15.0	13.50	.12E-01	7769.07	0.18216E-08	0.18457E+00	0.19607E-11	0.17796E-03	0.58385E-05	0.37735E+01
1.4-16.0	29.90	.34E-02	2054.33	0.43690E-10	0.44269E-02	0.47027E-13	0.42682E-05	0.14003E-06	0.90507E-01
1.5-17.0	24.75	.52E-02	4748.79	0.15553E-09	0.15759E-01	0.16741E-12	0.15194E-05	0.49850E-06	0.32219E+00
1.6-18.0	27.05	.45E-02	3695.62	0.98309E-10	0.99611E-02	0.10582E-12	0.96042E-05	0.31510E-06	0.20365E+00
1.6.3-18.8	20.45	.67E-02	6208.74	0.32913E-09	0.33349E-01	0.35427E-12	0.32154E-04	0.10549E-05	0.68161E+00

AIR INJECTION TESTING RESULTS FOR BOREHOLE NO RW-6

INTERVAL FEET	ZONE PRESS PSIA	APER- TURE CM.	VOLUME FLOW. ML/M	EQUIVALENT POROUS MEDIA PERMEABILITY					
				INTRINSIC		HYDRAULIC CONDUCTIVITY			
				SQUAR CM.	DARCY	SQUAR FT.	CM/SEC	FT/SEC	GAL/D FT**2
1.0-3.5	31.05	.26E-02	990.52	0.19451E-10	0.19709E-02	0.20937E-13	0.19003E-05	0.62346E-07	0.40295E-01
2.0-4.0	30.80	.29E-02	1337.36	0.26664E-10	0.27018E-02	0.28701E-13	0.26050E-05	0.85464E-07	0.55533E-01
3.0-5.0	31.15	.25E-02	899.84	0.17598E-10	0.17831E-02	0.18942E-13	0.17192E-05	0.56480E-07	0.35450E-01
4.0-6.0	30.85	.25E-02	855.32	0.17099E-10	0.17326E-02	0.18405E-13	0.16705E-05	0.54800E-07	0.34484E-01
6.0-8.0	31.05	.25E-02	855.92	0.16808E-10	0.17031E-02	0.18092E-13	0.16421E-05	0.53874E-07	0.34404E-01
7.0-9.0	30.75	.25E-02	878.17	0.17630E-10	0.17863E-02	0.18977E-13	0.17223E-05	0.56507E-07	0.36522E-01
8.0-10.5	30.75	.25E-02	877.54	0.17673E-10	0.17908E-02	0.19023E-13	0.17266E-05	0.56647E-07	0.36612E-01

AIR INJECTION TESTING RESULTS FOR BOREHOLE NO RDW-1

INTERVAL FEET	ZONE PRESS PSIA	APER- TURE CM.	VOLUME FLOW. ML/M	EQUIVALENT POROUS MEDIA PERMEABILITY					
				INTRINSIC			HYDRAULIC CONDUCTIVITY		
				SQUAR CM.	DARCY	SQUAR FT.	CM/SEC	FT/SEC	GAL/D FT**2
0.5- 3.0	10.90	.30E-01	8100.92	0.29493E-07	0.29884E+01	0.31746E-10	0.28813E-02	0.94532E-04	0.61898E+02
1.0- 3.5	10.90	.30E-01	7906.40	0.28104E-07	0.28477E+01	0.30251E-10	0.27456E-02	0.90080E-04	0.58220E+02

AIR INJECTION TESTING RESULTS FOR BOREHOLE NO RDW-2

INTERVAL FEET	ZONE PRESS PSIA	APER- TURE CM.	VOLUME FLOW. ML/M	EQUIVALENT POROUS MEDIA PERMEABILITY					
				INTRINSIC			HYDRAULIC CONDUCTIVITY		
				SQUAR CM.	DARCY	SQUAR FT.	CM/SEC	FT/SEC	GAL/D FT**2
0.5- 3.0	19.85	.67E-02	5981.08	0.33198E-09	0.33638E-01	0.35734E-12	0.32433E-04	0.10641E-05	0.68772E+00
1.0- 3.5	24.60	.53E-02	4856.98	0.15884E-09	0.16095E-01	0.17098E-12	0.15518E-04	0.50917E-05	0.32985E+00
2.0- 4.5	25.80	.49E-02	4446.97	0.13119E-09	0.13293E-01	0.14121E-12	0.12816E-04	0.42849E-05	0.27177E+00
3.0- 5.5	29.10	.66E-02	5972.89	0.32118E-09	0.32544E-01	0.34572E-12	0.31378E-04	0.10245E-05	0.66513E+00
4.0- 6.5	31.00	.34E-02	2152.74	0.43511E-10	0.44087E-02	0.46835E-13	0.42508E-05	0.13946E-06	0.90136E+01
5.0- 7.5	33.35	.19E-02	451.54	0.79836E-11	0.80894E-03	0.85935E-14	0.77996E-06	0.25589E-07	0.16539E-01

AIR INJECTION TESTING RESULTS FOR BOREHOLE NO RDW-3

INTERVAL FEET	ZONE PRESS PSIA	APER- TURE CM.	VOLUME FLOW. ML/M	EQUIVALENT POROUS MEDIA PERMEABILITY					
				INTRINSIC			HYDRAULIC CONDUCTIVITY		
				SQUAR CM.	DARCY	SQUAR FT.	CM/SEC	FT/SEC	GAL/D FT**2
0.7- 3.2	19.20	.73E-02	6587.78	0.42421E-09	0.42983E-01	0.45662E-12	0.41443E-04	0.13597E-05	0.87878E+00

AIR INJECTION TESTING RESULTS FOR BOREHOLE NO RDW-4

INTERVAL FEET	ZONE PRESS PSIA	APER- TURE CM.	VOLUME FLOW. ML/M	EQUIVALENT POROUS MEDIA PERMEABILITY					
				INTRINSIC			HYDRAULIC CONDUCTIVITY		
				SQUAR CM.	DARCY	SQUAR FT.	CM/SEC	FT/SEC	GAL/D FT**2
0.7-3.2	12.40	.17E-01	9735.92	0.53616E-08	0.54326E+00	0.57711E-11	0.52380E-03	0.17185E-04	0.11107E+02
1.0-3.5	12.35	.18E-01	9735.92	0.60555E-08	0.69463E+00	0.73792E-11	0.66974E-03	0.21973E-04	0.14202E+02
1.0-3.5	14.35	.08E-02	6980.81	0.59099E-09	0.59842E-01	0.63571E-12	0.57698E-04	0.18930E-05	0.12235E+01
1.0-3.5	14.30	.10E-01	7432.30	0.11143E-08	0.11291E+00	0.11994E-11	0.10886E-03	0.35716E-05	0.23084E+01
1.0-3.5	28.00	.41E-02	3176.93	0.77405E-10	0.78431E-02	0.83318E-13	0.5621E-05	0.24810E-06	0.16035E+00
1.0-3.5	27.45	.43E-02	3431.72	0.87318E-10	0.88475E-02	0.93989E-13	0.85305E-05	0.27987E-06	0.18889E+00
1.0-3.5	30.55	.32E-02	1717.56	0.34775E-10	0.35235E-02	0.37431E-13	0.33973E-05	0.11146E-06	0.72038E-01
1.0-3.5	31.75	.20E-02	434.75	0.81691E-11	0.82774E-03	0.87932E-14	0.79808E-06	0.26184E-07	0.16923E-01

AIR INJECTION TESTING RESULTS FOR BOREHOLE NO RDW-5

INTERVAL FEET	ZONE PRESS PSIA	APER- TURE CM.	VOLUME FLOW. ML/M	EQUIVALENT POROUS MEDIA PERMEABILITY					
				INTRINSIC			HYDRAULIC CONDUCTIVITY		
				SQUAR CM.	DARCY	SQUAR FT.	CM/SEC	FT/SEC	GAL/D FT**2
0.7-3.2	17.60	.79E-02	6784.88	0.54464E-09	0.55186E-01	0.58625E-12	0.53208E-04	0.17457E-05	0.11283E+01
1.0-3.5	21.15	.63E-02	5879.62	0.27972E-09	0.28342E-01	0.30169E-12	0.27327E-04	0.89655E-06	0.57946E+00
1.0-3.5	31.35	.23E-02	660.37	0.12640E-10	0.12816E-02	0.13614E-13	0.12357E-05	0.40540E-07	0.26247E-01
1.0-3.5	31.00	.26E-02	992.05	0.19420E-10	0.19686E-02	0.20913E-13	0.18998E-05	0.62272E-07	0.40247E-01
1.0-3.5	31.15	.25E-02	857.13	0.16603E-10	0.16823E-02	0.17872E-13	0.16221E-05	0.53217E-07	0.34395E-01
1.0-3.5	31.30	.23E-02	660.37	0.12694E-10	0.12862E-02	0.13664E-13	0.12401E-05	0.40687E-07	0.26297E-01

AIR INJECTION TESTING RESULTS FOR BOREHOLE NO RDW-6

INTERVAL FEET	ZONE PRESS PSIA	APER- TURE CM.	VOLUME FLOW. ML/M	EQUIVALENT POROUS MEDIA PERMEABILITY					
				INTRINSIC			HYDRAULIC CONDUCTIVITY		
				SQUAR CM.	DARCY	SQUAR FT.	CM/SEC	FT/SEC	GAL/D FT**2
5.0-7.5	29.95	.33E-02	1937.60	0.40786E-10	0.41327E-02	0.43902E-13	0.39846E-05	0.13073E-06	0.84492E-01
6.0-8.5	26.55	.46E-02	3819.82	0.10451E-09	0.10589E-01	0.11249E-12	0.10210E-04	0.33496E-06	0.21643E+00
7.0-9.5	26.95	.45E-02	3785.07	0.10059E-09	0.10192E-01	0.10827E-12	0.98272E-05	0.32741E-06	0.20638E+00
8.0-10.5	23.65	.55E-02	5019.09	0.10046E-09	0.10285E-01	0.10424E-12	0.17630E-04	0.57840E-06	0.37383E+00
9.0-11.5	27.40	.43E-02	3435.88	0.87514E-10	0.88673E-02	0.94199E-13	0.85496E-05	0.28050E-06	0.18129E+00

AIR INJECTION TESTING RESULTS FOR BOREHOLE NO RDE-1

INTERVAL FEET	ZONE PRESS PSIA	APER- TURE CM.	VOLUME FLOW. ML/M	EQUIVALENT POROUS MEDIA PERMEABILITY					
				INTRINSIC			HYDRAULIC CONDUCTIVITY		
				SQUAR CM.	DARCY	SQUAR FT.	CM/SEC	FT/SEC	GAL/D FT**2
6.0- 8.5	30.00	.25E-02	885.86	0.18097E-10	0.18337E-02	0.19479E-13	0.17680E-05	0.58004E-07	0.37489E-01
7.0- 9.5	30.40	.25E-02	884.23	0.17670E-10	0.17904E-02	0.19019E-13	0.17262E-05	0.56635E-07	0.36604E-01

AIR INJECTION TESTING RESULTS FOR BOREHOLE NO RDE-2

INTERVAL FEET	ZONE PRESS PSIA	APER- TURE CM.	VOLUME FLOW. ML/M	EQUIVALENT POROUS MEDIA PERMEABILITY					
				INTRINSIC			HYDRAULIC CONDUCTIVITY		
				SQUAR CM.	DARCY	SQUAR FT.	CM/SEC	FT/SEC	GAL/D FT**2
4.0- 6.5	27.85	.31E-02	1422.77	0.32475E-10	0.32905E-02	0.34955E-13	0.31726E-05	0.10409E-06	0.67274E-01
5.0- 7.5	19.15	.68E-02	5861.20	0.33831E-09	0.34279E-01	0.36416E-13	0.33051E-05	0.10844E-06	0.70004E+00
6.0- 8.5	26.05	.41E-02	2840.71	0.35188E-10	0.36184E-02	0.38932E-13	0.33455E-05	0.44099E-06	0.15516E+00
7.0- 9.5	25.60	.42E-02	3021.40	0.33407E-10	0.34512E-02	0.39779E-13	0.31488E-05	0.26734E-06	0.17270E+00
8.0- 10.5	18.80	.69E-02	6034.37	0.36633E-09	0.37118E-01	0.39431E-12	0.35780E-04	0.11742E-05	0.15807E+00

AIR INJECTION TESTING RESULTS FOR BOREHOLE NO RDE-3

INTERVAL FEET	ZONE PRESS PSIA	APER- TURE CM.	VOLUME FLOW. ML/M	EQUIVALENT POROUS MEDIA PERMEABILITY					
				INTRINSIC			HYDRAULIC CONDUCTIVITY		
				SQUAR CM.	DARCY	SQUAR FT.	CM/SEC	FT/SEC	GAL/D FT**2
0.7- 3.2	30.70	.20E-02	455.92	0.89675E-11	0.90863E-03	0.96526E-14	0.87600E-06	0.28743E-07	0.18577E-01
1.0- 3.5	30.70	.20E-02	455.92	0.89675E-11	0.90863E-03	0.96526E-14	0.87600E-06	0.28743E-07	0.18577E-01
7.0- 9.5	28.75	.33E-02	1830.72	0.40956E-10	0.41499E-02	0.44085E-13	0.40012E-05	0.13127E-06	0.84844E-01
8.0- 10.5	28.80	.30E-02	1345.85	0.30607E-10	0.31013E-02	0.32945E-13	0.29902E-05	0.98103E-07	0.63405E-01
9.0- 11.5	28.75	.30E-02	1345.85	0.30731E-10	0.31138E-02	0.33079E-13	0.30022E-05	0.98499E-07	0.63662E-01

AIR INJECTION TESTING RESULTS FOR BOREHOLE NO RDE-4

INTERVAL FEET	ZONE PSIA	APER- TURE CM.	VOLUME FLOW. ML/M	EQUIVALENT POROUS MEDIA PERMEABILITY						
				INTRINSIC		HYDRAULIC CONDUCTIVITY				
				SQUAR CM.	DARCY	SQUAR FT.	CM/SEC	FT/SEC	GAL/D FT**2	
0.7-1.4	3.2-3.5	17.45-18.60	80E-02 74E-02	6848.89 6614.77	0.56301E-09 0.44946E-09	0.57047E-01 0.45542E-01	0.60602E-12 0.48300E-12	0.55003E-04 0.43910E-04	0.10046E-05 0.14406E-05	0.11663E+01 0.93109E+00

AIR INJECTION TESTING RESULTS FOR BOREHOLE NO RDE-5

INTERVAL FEET	ZONE PSIA	APER- TURE CM.	VOLUME FLOW. ML/M	EQUIVALENT POROUS MEDIA PERMEABILITY						
				INTRINSIC		HYDRAULIC CONDUCTIVITY				
				SQUAR CM.	DARCY	SQUAR FT.	CM/SEC	FT/SEC	GAL/D FT**2	
0.8-1.0	3.3-3.4	18.65-18.80	76E-02 71E-02	6780.68 8144.33	0.47867E-09 0.87837E-08	0.48502E-01 0.89000E+00	0.51524E-12 0.94546E-11	0.46764E-04 0.85812E-04	0.15342E-05 0.28153E-04	0.99161E+00 0.18196E+02
1.1-1.3	3.4-3.5	18.80-19.00	71E-02 66E-02	8128.40 7931.58	0.83386E-07 0.29064E-08	0.88544E+00 0.94449E+00	0.80620E-11 0.31280E-11	0.85372E-04 0.28394E-04	0.93155E-04 0.93155E-05	0.18196E+02 0.60807E+01
1.4-1.5	3.5-3.6	19.00-19.10	66E-02 61E-02	8144.33 8144.33	0.15583E-07 0.76511E-08	0.75789E+01 0.75225E+00	0.16773E-10 0.82355E-11	0.15224E-04 0.74747E-04	0.49946E-04 0.24523E-04	0.32281E+02 0.15500E+02
1.6-1.7	3.6-3.7	19.10-19.20	61E-02 56E-02	8144.33 8144.33	0.77772E-08 0.47192E-10	0.76200E+00 0.47817E-02	0.18718E-11 0.50797E-13	0.16909E-04 0.46104E-04	0.55737E-04 0.15126E-04	0.36024E+01 0.97761E+01
1.8-1.9	3.7-3.8	19.20-19.30	56E-02 51E-02	1276.08 1146.65	0.22639E-10 0.47192E-10	0.22939E-02 0.24463E-02	0.24368E-13 0.25988E-13	0.22211E-04 0.23507E-04	0.72561E-07 0.77304E-07	0.46898E+01 0.58015E+01
2.0-2.1	3.8-3.9	19.30-19.40	51E-02 46E-02	1519.05 1800.61	0.34069E-10 0.37036E-10	0.31099E-02 0.37527E-02	0.33003E-13 0.39865E-13	0.20984E-04 0.36182E-04	0.98374E-07 0.11071E-06	0.63308E+01 0.70372E+01
2.2-2.3	3.9-4.0	19.40-19.50	46E-02 41E-02	3465.33 3465.33	0.80564E-10 0.80564E-10	0.89737E-02 0.89737E-02	0.95329E-13 0.95329E-13	0.86522E-05 0.86522E-05	0.28386E-06 0.28386E-06	0.18347E+00 0.18347E+00

AIR INJECTION TESTING RESULTS FOR BOREHOLE NO RDE-6

INTERVAL FEET	ZONE PSIA	APER- TURE CM.	VOLUME FLOW. ML/M	EQUIVALENT POROUS MEDIA PERMEABILITY						
				INTRINSIC		HYDRAULIC CONDUCTIVITY				
				SQUAR CM.	DARCY	SQUAR FT.	CM/SEC	FT/SEC	GAL/D FT**2	
0.7-1.1	3.3-3.5	23.33-23.50	33E-02 33E-02	1675.60 1550.50	0.33299E-09 0.33299E-09	0.32299E-01 0.32299E-01	0.34836E-13 0.34836E-13	0.30891E-05 0.30891E-05	0.18135E-06 0.18135E-06	0.65504E-01 0.65504E-01
1.2-1.3	3.5-3.6	23.50-23.60	33E-02 33E-02	1550.50 1550.50	0.33299E-09 0.33299E-09	0.32299E-01 0.32299E-01	0.34836E-13 0.34836E-13	0.30891E-05 0.30891E-05	0.18135E-06 0.18135E-06	0.65504E-01 0.65504E-01
1.4-1.5	3.6-3.7	23.60-23.70	33E-02 33E-02	1550.50 1550.50	0.33299E-09 0.33299E-09	0.32299E-01 0.32299E-01	0.34836E-13 0.34836E-13	0.30891E-05 0.30891E-05	0.18135E-06 0.18135E-06	0.65504E-01 0.65504E-01
1.6-1.7	3.7-3.8	23.70-23.80	33E-02 33E-02	1550.50 1550.50	0.33299E-09 0.33299E-09	0.32299E-01 0.32299E-01	0.34836E-13 0.34836E-13	0.30891E-05 0.30891E-05	0.18135E-06 0.18135E-06	0.65504E-01 0.65504E-01
1.8-1.9	3.8-3.9	23.80-23.90	33E-02 33E-02	1550.50 1550.50	0.33299E-09 0.33299E-09	0.32299E-01 0.32299E-01	0.34836E-13 0.34836E-13	0.30891E-05 0.30891E-05	0.18135E-06 0.18135E-06	0.65504E-01 0.65504E-01
2.0-2.1	3.9-4.0	23.90-24.00	33E-02 33E-02	1550.50 1550.50	0.33299E-09 0.33299E-09	0.32299E-01 0.32299E-01	0.34836E-13 0.34836E-13	0.30891E-05 0.30891E-05	0.18135E-06 0.18135E-06	0.65504E-01 0.65504E-01
2.2-2.3	4.0-4.1	24.00-24.10	33E-02 33E-02	1550.50 1550.50	0.33299E-09 0.33299E-09	0.32299E-01 0.32299E-01	0.34836E-13 0.34836E-13	0.30891E-05 0.30891E-05	0.18135E-06 0.18135E-06	0.65504E-01 0.65504E-01
2.4-2.5	4.1-4.2	24.10-24.20	33E-02 33E-02	1550.50 1550.50	0.33299E-09 0.33299E-09	0.32299E-01 0.32299E-01	0.34836E-13 0.34836E-13	0.30891E-05 0.30891E-05	0.18135E-06 0.18135E-06	0.65504E-01 0.65504E-01
2.6-2.7	4.2-4.3	24.20-24.30	33E-02 33E-02	1550.50 1550.50	0.33299E-09 0.33299E-09	0.32299E-01 0.32299E-01	0.34836E-13 0.34836E-13	0.30891E-05 0.30891E-05	0.18135E-06 0.18135E-06	0.65504E-01 0.65504E-01
2.8-2.9	4.3-4.4	24.30-24.40	33E-02 33E-02	1550.50 1550.50	0.33299E-09 0.33299E-09	0.32299E-01 0.32299E-01	0.34836E-13 0.34836E-13	0.30891E-05 0.30891E-05	0.18135E-06 0.18135E-06	0.65504E-01 0.65504E-01
3.0-3.1	4.4-4.5	24.40-24.50	33E-02 33E-02	1550.50 1550.50	0.33299E-09 0.33299E-09	0.32299E-01 0.32299E-01	0.34836E-13 0.34836E-13	0.30891E-05 0.30891E-05	0.18135E-06 0.18135E-06	0.65504E-01 0.65504E-01
3.2-3.3	4.5-4.6	24.50-24.60	33E-02 33E-02	1550.50 1550.50	0.33299E-09 0.33299E-09	0.32299E-01 0.32299E-01	0.34836E-13 0.34836E-13	0.30891E-05 0.30891E-05	0.18135E-06 0.18135E-06	0.65504E-01 0.65504E-01
3.4-3.5	4.6-4.7	24.60-24.70	33E-02 33E-02	1550.50 1550.50	0.33299E-09 0.33299E-09	0.32299E-01 0.32299E-01	0.34836E-13 0.34836E-13	0.30891E-05 0.30891E-05	0.18135E-06 0.18135E-06	0.65504E-01 0.65504E-01
3.6-3.7	4.7-4.8	24.70-24.80	33E-02 33E-02	1550.50 1550.50	0.33299E-09 0.33299E-09	0.32299E-01 0.32299E-01	0.34836E-13 0.34836E-13	0.30891E-05 0.30891E-05	0.18135E-06 0.18135E-06	0.65504E-01 0.65504E-01
3.8-3.9	4.8-4.9	24.80-24.90	33E-02 33E-02	1550.50 1550.50	0.33299E-09 0.33299E-09	0.32299E-01 0.32299E-01	0.34836E-13 0.34836E-13	0.30891E-05 0.30891E-05	0.18135E-06 0.18135E-06	0.65504E-01 0.65504E-01
4.0-4.1	4.9-5.0	24.90-25.00	33E-02 33E-02	1550.50 1550.50	0.33299E-09 0.33299E-09	0.32299E-01 0.32299E-01	0.34836E-13 0.34836E-13	0.30891E-05 0.30891E-05	0.18135E-06 0.18135E-06	0.65504E-01 0.65504E-01
4.2-4.3	5.0-5.1	25.00-25.10	33E-02 33E-02	1550.50 1550.50	0.33299E-09 0.33299E-09	0.32299E-01 0.32299E-01	0.34836E-13 0.34836E-13	0.30891E-05 0.30891E-05	0.18135E-06 0.18135E-06	0.65504E-01 0.65504E-01
4.4-4.5	5.1-5.2	25.10-25.20	33E-02 33E-02	1550.50 1550.50	0.33299E-09 0.33299E-09	0.32299E-01 0.32299E-01	0.34836E-13 0.34836E-13	0.30891E-05 0.30891E-05	0.18135E-06 0.18135E-06	0.65504E-01 0.65504E-01
4.6-4.7	5.2-5.3	25.20-25.30	33E-02 33E-02	1550.50 1550.50	0.33299E-09 0.33299E-09	0.32299E-01 0.32299E-01	0.34836E-13 0.34836E-13	0.30891E-05 0.30891E-05	0.18135E-06 0.18135E-06	0.65504E-01 0.65504E-01
4.8-4.9	5.3-5.4	25.30-25.40	33E-02 33E-02	1550.50 1550.50	0.33299E-09 0.33299E-09	0.32299E-01 0.32299E-01	0.34836E-13 0.34836E-13	0.30891E-05 0.30891E-05	0.18135E-06 0.18135E-06	0.65504E-01 0.65504E-01
5.0-5.1	5.4-5.5	25.40-25.50	33E-02 33E-02	1550.50 1550.50	0.33299E-09 0.33299E-09	0.32299E-01 0.32299E-01	0.34836E-13 0.34836E-13	0.30891E-05 0.30891E-05	0.18135E-06 0.18135E-06	0.65504E-01 0.65504E-01

AIR INJECTION TESTING RESULTS FOR BOREHOLE NO RHE-1

INTERVAL FEET	ZONE PSIA	APER- TURE CM.	VOLUME FLOW. ML/M	EQUIVALENT POROUS MEDIA PERMEABILITY					
				INTRINSIC			HYDRAULIC CONDUCTIVITY		
				SQUAR CM.	DARCY	SQUAR FT.	CM/SEC	FT/SEC	GAL/D FT**2
2.0-3.0	13.15	.112E-01	7626.35	0.19730E-08	0.19991E+00	0.21237E-11	0.19275E-03	0.63238E-05	0.40872E+01
3.0-4.0	13.33	.111E-01	7610.47	0.20139E-08	0.20406E+00	0.21677E-11	0.19674E-03	0.64454E-05	0.41719E+01
4.0-5.0	13.51	.110E-01	7610.47	0.20139E-08	0.20406E+00	0.21677E-11	0.19674E-03	0.64454E-05	0.41719E+01
5.0-6.0	13.69	.109E-01	7610.47	0.20139E-08	0.20406E+00	0.21677E-11	0.19674E-03	0.64454E-05	0.41719E+01
6.0-7.0	13.87	.108E-02	4678.91	0.16820E-09	0.17043E-01	0.18105E-12	0.16433E-04	0.53391E-05	0.34845E+00
7.0-8.0	14.05	.107E-02	4694.12	0.17036E-09	0.17262E-01	0.18338E-12	0.16643E-04	0.54688E-05	0.35292E+00
8.0-9.0	14.23	.106E-02	4746.03	0.17317E-09	0.17547E-01	0.18640E-12	0.16918E-04	0.55586E-05	0.35874E+00

AIR INJECTION TESTING RESULTS FOR BOREHOLE NO RHE-2

INTERVAL FEET	ZONE PSIA	APER- TURE CM.	VOLUME FLOW. ML/M	EQUIVALENT POROUS MEDIA PERMEABILITY					
				INTRINSIC			HYDRAULIC CONDUCTIVITY		
				SQUAR CM.	DARCY	SQUAR FT.	CM/SEC	FT/SEC	GAL/D FT**2
0.5-1.0	10.70	.20E+00	8045.42	0.81290E-05	0.82367E+03	0.87500E-08	0.79416E+00	0.26855E-01	0.16840E+05
1.0-2.0	28.60	.38E-02	2685.47	0.61866E-10	0.62680E-02	0.66592E-13	0.60440E-05	0.19829E-06	0.12816E+00
2.0-3.0	28.60	.38E-02	2635.55	0.59928E-10	0.60714E-02	0.64449E-13	0.58505E-05	0.19246E-06	0.12231E+00
3.0-4.0	28.60	.38E-02	2635.55	0.59928E-10	0.60714E-02	0.64449E-13	0.58505E-05	0.19246E-06	0.12231E+00
4.0-5.0	28.60	.38E-02	2635.55	0.59928E-10	0.60714E-02	0.64449E-13	0.58505E-05	0.19246E-06	0.12231E+00
5.0-6.0	28.60	.38E-02	2635.55	0.59928E-10	0.60714E-02	0.64449E-13	0.58505E-05	0.19246E-06	0.12231E+00
6.0-7.0	28.60	.38E-02	2635.55	0.59928E-10	0.60714E-02	0.64449E-13	0.58505E-05	0.19246E-06	0.12231E+00
7.0-8.0	28.60	.38E-02	2635.55	0.59928E-10	0.60714E-02	0.64449E-13	0.58505E-05	0.19246E-06	0.12231E+00
8.0-9.0	28.60	.38E-02	2635.55	0.59928E-10	0.60714E-02	0.64449E-13	0.58505E-05	0.19246E-06	0.12231E+00
9.0-10.0	28.60	.38E-02	2635.55	0.59928E-10	0.60714E-02	0.64449E-13	0.58505E-05	0.19246E-06	0.12231E+00
10.0-11.0	28.60	.38E-02	2635.55	0.59928E-10	0.60714E-02	0.64449E-13	0.58505E-05	0.19246E-06	0.12231E+00
11.0-12.0	28.60	.38E-02	2635.55	0.59928E-10	0.60714E-02	0.64449E-13	0.58505E-05	0.19246E-06	0.12231E+00

AIR INJECTION TESTING RESULTS FOR BOREHOLE NO RHE-3

INTERVAL FEET	ZONE PSIA	APER- TURE CM.	VOLUME FLOW. ML/M	EQUIVALENT POROUS MEDIA PERMEABILITY					
				INTRINSIC			HYDRAULIC CONDUCTIVITY		
				SQUAR CM.	DARCY	SQUAR FT.	CM/SEC	FT/SEC	GAL/D FT**2
0.5-1.0	32.40	.31E-02	1879.19	0.32989E-10	0.33426E-02	0.35509E-13	0.32229E-05	0.10574E-06	0.60344E-01
1.0-2.0	32.40	.31E-02	1585.30	0.26908E-10	0.27264E-02	0.28906E-13	0.26250E-05	0.86624E-07	0.50514E-01
2.0-3.0	32.40	.31E-02	2446.23	0.44086E-10	0.44670E-02	0.47493E-13	0.43080E-05	0.14210E-06	0.80327E-01
3.0-4.0	32.40	.31E-02	2322.52	0.41566E-10	0.42111E-02	0.44735E-13	0.40602E-05	0.13430E-06	0.75327E-01
4.0-5.0	32.40	.31E-02	2319.93	0.41357E-10	0.41908E-02	0.44571E-13	0.40404E-05	0.13321E-06	0.75095E-01
5.0-6.0	32.40	.31E-02	2443.47	0.43069E-10	0.44450E-02	0.47220E-13	0.42080E-05	0.13856E-06	0.78778E-01
6.0-7.0	32.40	.31E-02	3848.61	0.85927E-10	0.87066E-02	0.92420E-13	0.83947E-05	0.27261E-06	0.16881E+00
7.0-8.0	32.40	.31E-02	3314.03	0.66615E-10	0.67499E-02	0.71704E-13	0.65587E-05	0.21342E-06	0.13880E+00
8.0-9.0	32.40	.31E-02	4592.60	0.11621E-09	0.11775E-01	0.12549E-12	0.65587E-05	0.21342E-06	0.13880E+00
9.0-10.0	32.40	.31E-02	3815.10	0.81809E-10	0.82893E-02	0.88885E-13	0.79093E-05	0.25742E-06	0.16074E+00
10.0-11.0	32.40	.31E-02	4074.40	0.91317E-10	0.92527E-02	0.98050E-13	0.89973E-05	0.29226E-06	0.18094E+00
11.0-12.0	32.40	.31E-02	2060.84	0.34950E-10	0.35421E-02	0.37620E-13	0.34415E-05	0.11205E-06	0.72418E-01

AIR INJECTION TESTING RESULTS FOR BOREHOLE NO RHE-4

INTERVAL FEET	ZONE PRESS PSIA	APER- TURE CM.	VOLUME FLOW. ML/M	EQUIVALENT POROUS MEDIA PERMEABILITY					
				INTRINSIC		HYDRAULIC CONDUCTIVITY			
				SQUAR CM.	DARCY	SQUAR FT.	CM/SEC	FT/SEC	GAL/D FT**2
0.5- 3.0	21.00	.65E-02	6066.06	0.30207E-09	0.30608E-01	0.32515E-12	0.29511E-04	0.96821E-06	0.62577E+00
1.0- 3.0	20.95	.65E-02	6133.71	0.30671E-09	0.31070E-01	0.33050E-12	0.29964E-04	0.98308E-06	0.63538E+00
2.0- 3.0	20.65	.65E-02	1332.60	0.27210E-09	0.27570E-01	0.29268E-12	0.26582E-04	0.87212E-06	0.56367E+00
10.0- 13.0	26.00	.48E-02	4183.70	0.12174E-09	0.12335E-01	0.13104E-12	0.11893E-04	0.39020E-06	0.23219E+00
11.0- 13.0	25.90	.48E-02	4183.70	0.12207E-09	0.12450E-01	0.13220E-12	0.12004E-04	0.39304E-06	0.25454E+00

AIR INJECTION TESTING RESULTS FOR BOREHOLE NO RHE-6

INTERVAL FEET	ZONE PRESS PSIA	APER- TURE CM.	VOLUME FLOW. ML/M	EQUIVALENT POROUS MEDIA PERMEABILITY					
				INTRINSIC		HYDRAULIC CONDUCTIVITY			
				SQUAR CM.	DARCY	SQUAR FT.	CM/SEC	FT/SEC	GAL/D FT**2
7.0- 9.5	28.00	.45E-02	4255.30	0.96774E-10	0.98056E-02	0.10417E-12	0.94543E-05	0.31018E-06	0.20047E+00
8.0- 10.5	28.00	.45E-02	4300.31	0.98619E-10	0.99926E-02	0.10615E-12	0.96346E-05	0.31610E-06	0.20430E+00
9.0- 11.5	28.60	.45E-02	4302.94	0.10043E-09	0.10176E-01	0.10810E-12	0.98114E-05	0.32190E-06	0.20805E+00

AIR INJECTION TESTING RESULTS FOR BOREHOLE NO RHE-1

INTERVAL FEET	ZONE PRESS PSIA	APER- TURE CM.	VOLUME FLOW. ML/M	EQUIVALENT POROUS MEDIA PERMEABILITY					
				INTRINSIC			HYDRAULIC CONDUCTIVITY		
				SQUAR CM.	DARCY	SQUAR FT.	CM/SEC	FT/SEC	GAL/D FT**2
0.5-3.0	0.00	.15E-02	0.00	0.35952E-11	0.36428E-03	0.38698E-14	0.35123E-06	0.11523E-07	0.74477E-02
1.0-3.5	0.00	.15E-02	0.00	0.74357E-11	0.75356E-03	0.85268E-14	0.72853E-06	0.23982E-07	0.15444E-01
1.5-4.0	0.00	.15E-02	0.00	0.33377E-11	0.33718E-03	0.35819E-14	0.32451E-06	0.10666E-07	0.68936E-01
2.0-4.5	0.00	.15E-02	0.00	0.27746E-11	0.28136E-03	0.29889E-14	0.27128E-06	0.89222E-08	0.57523E-02
2.5-5.0	0.00	.15E-02	0.00	0.23353E-11	0.23771E-03	0.25183E-14	0.23448E-06	0.76775E-08	0.49622E-02
3.0-5.5	0.00	.15E-02	0.00	0.26735E-11	0.27148E-03	0.28332E-14	0.26333E-06	0.83769E-08	0.54142E-02
1.0-12.0	0.00	.20E-02	0.00	0.28755E-11	0.21038E-03	0.22348E-14	0.20533E-06	0.66523E-08	0.42995E-02

AIR INJECTION TESTING RESULTS FOR BOREHOLE NO RHE-4

INTERVAL FEET	ZONE PRESS PSIA	APER- TURE CM.	VOLUME FLOW. ML/M	EQUIVALENT POROUS MEDIA PERMEABILITY					
				INTRINSIC			HYDRAULIC CONDUCTIVITY		
				SQUAR CM.	DARCY	SQUAR FT.	CM/SEC	FT/SEC	GAL/D FT**2
3.0-5.5	0.00	.16E-02	0.00	0.43949E-11	0.44531E-03	0.47306E-14	0.42936E-06	0.14087E-07	0.91044E-02
4.0-6.0	0.00	.16E-02	0.00	0.42691E-11	0.43257E-03	0.45953E-14	0.41707E-06	0.13683E-07	0.88443E-02
5.0-6.5	0.00	.15E-02	0.00	0.37788E-11	0.38228E-03	0.40666E-14	0.36989E-06	0.12109E-07	0.80265E-02
6.0-7.0	0.00	.15E-02	0.00	0.38748E-11	0.39262E-03	0.41708E-14	0.37855E-06	0.12428E-07	0.82788E-02
7.0-8.0	0.00	.15E-02	0.00	0.38957E-11	0.39473E-03	0.41933E-14	0.38059E-06	0.12486E-07	0.83702E-02
8.0-9.0	0.00	.15E-02	0.00	0.39247E-11	0.39767E-03	0.42245E-14	0.38342E-06	0.12579E-07	0.84383E-02
9.0-11.5	0.00	.15E-02	0.00	0.38787E-11	0.39301E-03	0.41750E-14	0.37893E-06	0.12432E-07	0.83351E-02

AIR INJECTION TESTING RESULTS FOR BOREHOLE NO RHE-5

INTERVAL FEET	ZONE PRESS PSIA	APER- TURE CM.	VOLUME FLOW. ML/M	EQUIVALENT POROUS MEDIA PERMEABILITY					
				INTRINSIC			HYDRAULIC CONDUCTIVITY		
				SQUAR CM.	DARCY	SQUAR FT.	CM/SEC	FT/SEC	GAL/D FT**2
0.5-3.0	0.00	.12E-02	0.00	0.16894E-11	0.17118E-03	0.18185E-14	0.16505E-06	0.54149E-08	0.34998E-02
1.0-3.5	0.00	.12E-02	0.00	0.20555E-11	0.20828E-03	0.22126E-14	0.20088E-06	0.65884E-08	0.42582E-02
2.0-4.5	0.00	.11E-02	0.00	0.15805E-11	0.16095E-03	0.17088E-14	0.15519E-06	0.50914E-08	0.33087E-02
3.0-5.5	0.00	.11E-02	0.00	0.18733E-11	0.18961E-03	0.20443E-14	0.18282E-06	0.59981E-08	0.38976E-02
4.0-6.5	0.00	.11E-02	0.00	0.19456E-11	0.19714E-03	0.20942E-14	0.19007E-06	0.62368E-08	0.40804E-02
5.0-7.5	0.00	.11E-02	0.00	0.18146E-11	0.18338E-03	0.19533E-14	0.17728E-06	0.58163E-08	0.37551E-02
6.0-8.0	0.00	.11E-02	0.00	0.18114E-11	0.18354E-03	0.19497E-14	0.17696E-06	0.58058E-08	0.37524E-02
7.0-9.0	0.00	.11E-02	0.00	0.18033E-11	0.18267E-03	0.19399E-14	0.17687E-06	0.57766E-08	0.37335E-02
8.0-11.0	0.00	.11E-02	0.00	0.18749E-11	0.18992E-03	0.19947E-14	0.18311E-06	0.60976E-08	0.38928E-02
9.0-11.5	0.00	.11E-02	0.00	0.22969E-11	0.23082E-03	0.24182E-14	0.22034E-06	0.94935E-08	0.61358E-02
10.0-12.5	0.00	.11E-02	0.00	0.04511E-11	0.05638E-03	0.06097E-14	0.02562E-06	0.27887E-07	0.17888E-01
11.0-13.5	0.00	.11E-02	0.00	0.19351E-11	0.19607E-03	0.20829E-14	0.18905E-06	0.62024E-08	0.40887E-02

AIR INJECTION TESTING RESULTS FOR BOREHOLE NO RUE-1

INTERVAL FEET	ZONE PRESS PSIA	APER- TURE CM.	VOLUME FLOW. ML/M	EQUIVALENT POROUS MEDIA PERMEABILITY					
				INTRINSIC			HYDRAULIC CONDUCTIVITY		
				SQUAR CM.	DARCY	SQUAR FT.	CM/SEC	FT/SEC	GAL/D FT**2
2.0-4.5	0.00	.17E-02	0.00	0.58208E-11	0.58998E-03	0.62655E-14	0.56866E-06	0.18657E-07	0.12058E-01
3.0-5.5	0.00	.16E-02	0.00	0.44638E-11	0.45223E-03	0.48083E-14	0.43801E-06	0.14385E-07	0.92454E-02
4.0-6.5	0.00	.16E-02	0.00	0.41288E-11	0.41725E-03	0.44083E-14	0.40801E-06	0.13388E-07	0.85357E-02
5.0-7.5	0.00	.14E-02	0.00	0.27699E-11	0.28080E-03	0.29750E-14	0.27509E-06	0.88875E-08	0.55777E-02
13.0-15.5	0.00	.15E-02	0.00	0.38489E-11	0.38932E-03	0.41400E-14	0.37507E-06	0.12233E-07	0.79724E-02
14.0-16.5	0.00	.15E-02	0.00	0.37767E-11	0.38267E-03	0.40522E-14	0.36899E-06	0.12285E-07	0.78236E-02

AIR INJECTION TESTING RESULTS FOR BOREHOLE NO RUE-2

INTERVAL FEET	ZONE PRESS PSIA	APER- TURE CM.	VOLUME FLOW. ML/M	EQUIVALENT POROUS MEDIA PERMEABILITY					
				INTRINSIC			HYDRAULIC CONDUCTIVITY		
				SQUAR CM.	DARCY	SQUAR FT.	CM/SEC	FT/SEC	GAL/D FT**2
4.0-6.5	0.00	.15E-02	0.00	0.34225E-11	0.34678E-03	0.36830E-14	0.33436E-06	0.10978E-07	0.78899E-02
5.0-7.5	0.00	.15E-02	0.00	0.33372E-11	0.33825E-03	0.35987E-14	0.32585E-06	0.10892E-07	0.77157E-02
6.0-8.5	0.00	.15E-02	0.00	0.47251E-11	0.47745E-03	0.48097E-14	0.36393E-06	0.11948E-07	0.71648E-02
7.0-9.5	0.00	.15E-02	0.00	0.41807E-11	0.42280E-03	0.44213E-14	0.40128E-06	0.13165E-07	0.65099E-02
8.0-11.5	0.00	.16E-02	0.00	0.41208E-11	0.41749E-03	0.44351E-14	0.40503E-06	0.13280E-07	0.65355E-02
9.0-11.5	0.00	.16E-02	0.00	0.36338E-11	0.36837E-03	0.39332E-14	0.35517E-06	0.11653E-07	0.55311E-02
16.0-12.5	0.00	.16E-02	0.00	0.43833E-11	0.43553E-03	0.46318E-14	0.42832E-06	0.13798E-07	0.69126E-02

AIR INJECTION TESTING RESULTS FOR BOREHOLE NO RUE-4

INTERVAL FEET	ZONE PRESS PSIA	APER- TURE CM.	VOLUME FLOW. ML/M	EQUIVALENT POROUS MEDIA PERMEABILITY					
				INTRINSIC			HYDRAULIC CONDUCTIVITY		
				SQUAR CM.	DARCY	SQUAR FT.	CM/SEC	FT/SEC	GAL/D FT**2
3.0-5.5	0.00	.18E-02	0.00	0.65588E-11	0.66376E-03	0.78513E-14	0.63998E-06	0.20997E-07	0.13571E-01
4.0-6.5	0.00	.18E-02	0.00	0.41322E-11	0.41774E-03	0.44333E-14	0.40271E-06	0.13234E-07	0.85924E-02
5.0-7.5	0.00	.18E-02	0.00	0.41453E-11	0.41905E-03	0.44471E-14	0.40398E-06	0.13290E-07	0.86208E-02
6.0-8.5	0.00	.18E-02	0.00	0.68330E-11	0.68833E-03	0.73650E-14	0.60808E-06	0.20109E-07	0.14441E-01
7.0-9.5	0.00	.18E-02	0.00	0.48830E-11	0.49333E-03	0.52650E-14	0.47308E-06	0.15398E-07	0.98341E-02
8.0-11.5	0.00	.18E-02	0.00	0.37890E-11	0.38393E-03	0.40750E-14	0.36308E-06	0.12334E-07	0.78544E-02
9.0-11.5	0.00	.18E-02	0.00	0.37890E-11	0.38393E-03	0.40750E-14	0.36308E-06	0.12334E-07	0.78544E-02
11.0-13.5	0.00	.18E-02	0.00	0.42980E-11	0.43476E-03	0.46185E-14	0.41911E-06	0.13733E-07	0.88886E-02

AIR INJECTION TESTING RESULTS FOR BOREHOLE NO RUE-5

INTERVAL FEET	ZONE PSIA	APER- TURE CM.	VOLUME FLOW. ML/M	EQUIVALENT POROUS MEDIA PERMEABILITY					
				INTRINSIC		HYDRAULIC CONDUCTIVITY			
				SQUAR CM.	DARCY	SQUAR FT.	CM/SEC	FT/SEC	GAL/D FT**2
9.0- 11.5	0.00	.16E-02	0.00	0.47726E-11	0.48358E-03	0.51372E-14	0.46626E-06	0.15297E-07	0.98868E-02

AIR INJECTION TESTING RESULTS FOR BOREHOLE NO RUE-6

INTERVAL FEET	ZONE PSIA	APER- TURE CM.	VOLUME FLOW. ML/M	EQUIVALENT POROUS MEDIA PERMEABILITY					
				INTRINSIC		HYDRAULIC CONDUCTIVITY			
				SQUAR CM.	DARCY	SQUAR FT.	CM/SEC	FT/SEC	GAL/D FT**2
5.0- 7.5	0.00	.15E-02	0.00	0.34923E-11	0.35386E-03	0.37591E-14	0.34118E-06	0.11194E-07	0.72346E-02
6.0- 8.0	0.00	.14E-02	0.00	0.31400E-11	0.31816E-03	0.33799E-14	0.30076E-06	0.10064E-07	0.65048E-02
7.0- 9.0	0.00	.10E-02	0.00	0.27072E-11	0.29037E-03	0.24585E-14	0.25846E-06	0.28165E-07	0.10203E-01
8.0- 10.0	0.00	.17E-02	0.00	0.21176E-10	0.21456E-02	0.22793E-13	0.20688E-05	0.67873E-07	0.43867E-01
20.0- 28.5	0.00	.26E-02	0.00	0.19591E-10	0.19851E-02	0.21088E-13	0.19140E-05	0.62795E-07	0.40585E-01

AIR INJECTION TESTING RESULTS FOR BOREHOLE NO RDU-5

INTERVAL FEET	ZONE PRESS PSIA	APER- TURE CM.	VOLUME FLOW. ML/M	EQUIVALENT POROUS MEDIA PERMEABILITY					
				INTRINSIC			HYDRAULIC CONDUCTIVITY		
				SQUAR CM.	DARCY	SQUAR FT.	CM/SEC	FT/SEC	GAL/D FT**2
2.0-4.5	0.00	.15E-02	0.00	0.36880E-11	0.37368E-03	0.39697E-14	0.36029E-06	0.11021E-07	0.76399E-02
3.0-5.5	0.00	.14E-02	0.00	0.38987E-11	0.39503E-03	0.41965E-14	0.38080E-06	0.12496E-07	0.80764E-02
4.0-6.5	0.00	.14E-02	0.00	0.31099E-11	0.31511E-03	0.33474E-14	0.30382E-06	0.99677E-08	0.64423E-02
5.0-7.5	0.00	.14E-02	0.00	0.33256E-11	0.33697E-03	0.35797E-14	0.32490E-06	0.10659E-07	0.68893E-02
6.0-8.5	0.00	.14E-02	0.00	0.32505E-11	0.32987E-03	0.35042E-14	0.31805E-06	0.10435E-07	0.67441E-02
7.0-9.5	0.00	.17E-02	0.00	0.21894E-10	0.22184E-02	0.23566E-13	0.21389E-05	0.70174E-07	0.45355E-01
8.0-10.5	0.00	.20E-02	0.00	0.90288E-11	0.91484E-03	0.97185E-14	0.88206E-06	0.28939E-07	0.18704E-01

AIR INJECTION TESTING RESULTS FOR BOREHOLE NO RDU-6

INTERVAL FEET	ZONE PRESS PSIA	APER- TURE CM.	VOLUME FLOW. ML/M	EQUIVALENT POROUS MEDIA PERMEABILITY					
				INTRINSIC			HYDRAULIC CONDUCTIVITY		
				SQUAR CM.	DARCY	SQUAR FT.	CM/SEC	FT/SEC	GAL/D FT**2
4.0-6.5	0.00	.27E-02	0.00	0.22228E-10	0.22522E-02	0.23926E-13	0.21715E-05	0.71245E-07	0.46047E-01
5.0-7.5	0.00	.13E-02	0.00	0.22685E-11	0.22986E-03	0.24418E-14	0.22162E-06	0.72711E-08	0.46995E-02

AIR INJECTION TESTING RESULTS FOR BOREHOLE NO RDD-4

INTERVAL FEET	ZONE PRESS PSIA	APER- TURE CM.	VOLUME FLOW. ML/M	EQUIVALENT POROUS MEDIA PERMEABILITY					
				INTRINSIC		HYDRAULIC CONDUCTIVITY			
				SQUAR CM.	DARCY	SQUAR FT.	CM/SEC	FT/SEC	GAL/D FT**2
2.0-4.0	0.00	.13	0.00	0.21998E-11	0.22289E-03	0.23678E-14	0.21490E-06	0.78507E-08	0.45173E-02
3.0-5.0	0.00	.11	0.00	0.13481E-11	0.13860E-03	0.14511E-14	0.13171E-06	0.43211E-08	0.27928E-02
4.0-6.0	0.00	.11	0.00	0.20779E-11	0.21071E-03	0.22384E-14	0.20316E-06	0.66655E-08	0.43080E-02
5.0-7.0	0.00	.11	0.00	0.15716E-11	0.15925E-03	0.16917E-14	0.15544E-06	0.50374E-08	0.33255E-02
6.0-8.0	0.00	.11	0.00	0.26288E-11	0.26637E-03	0.28297E-14	0.25582E-06	0.84260E-08	0.55880E-02
7.0-9.0	0.00	.11	0.00	0.38688E-11	0.39201E-03	0.41643E-14	0.37796E-06	0.12480E-07	0.81455E-02
8.0-10.0	0.00	.11	0.00	0.41894E-11	0.41638E-03	0.44233E-14	0.40146E-06	0.13171E-07	0.85129E-02
9.0-11.0	0.00	.11	0.00	0.10018E-10	0.10151E-02	0.10783E-13	0.97869E-06	0.32109E-07	0.20753E-01
10.0-12.0	DECAY TOO SLOW DUE TO EXTREMELY LOW PERMEABILITY								

AIR INJECTION TESTING RESULTS FOR BOREHOLE NO RDD-5

INTERVAL FEET	ZONE PRESS PSIA	APER- TURE CM.	VOLUME FLOW. ML/M	EQUIVALENT POROUS MEDIA PERMEABILITY					
				INTRINSIC		HYDRAULIC CONDUCTIVITY			
				SQUAR CM.	DARCY	SQUAR FT.	CM/SEC	FT/SEC	GAL/D FT**2
0.0-1.0	0.00	.13	0.00	0.21800E-11	0.22200E-03	0.23472E-14	0.21303E-06	0.69093E-08	0.45173E-02
1.0-2.0	0.00	.11	0.00	0.15744E-11	0.15955E-03	0.16949E-14	0.15383E-06	0.50478E-08	0.32628E-02
2.0-3.0	0.00	.11	0.00	0.55444E-11	0.55555E-03	0.58210E-14	0.53240E-06	0.17467E-07	0.11289E-01
3.0-4.0	0.00	.11	0.00	0.55286E-11	0.55397E-03	0.58121E-14	0.53151E-06	0.17467E-07	0.11289E-01
4.0-5.0	0.00	.11	0.00	0.55286E-11	0.55397E-03	0.58121E-14	0.53151E-06	0.17467E-07	0.11289E-01
5.0-6.0	0.00	.11	0.00	0.25999E-11	0.26110E-03	0.27477E-14	0.25399E-06	0.81628E-08	0.53366E-02
6.0-7.0	0.00	.11	0.00	0.31355E-11	0.31466E-03	0.33033E-14	0.30822E-06	0.99168E-08	0.64894E-02
7.0-8.0	0.00	.11	0.00	0.29975E-11	0.30086E-03	0.31633E-14	0.29597E-06	0.95385E-08	0.61649E-02
8.0-9.0	0.00	.11	0.00	0.23178E-11	0.23289E-03	0.24448E-14	0.22422E-06	0.74299E-08	0.48815E-02
9.0-10.0	0.00	.11	0.00	0.22456E-11	0.22488E-03	0.23437E-14	0.23399E-06	0.78721E-08	0.50879E-02
10.0-11.0	DECAY TOO SLOW DUE TO EXTREMELY LOW PERMEABILITY								
11.0-12.0	DECAY TOO SLOW DUE TO EXTREMELY LOW PERMEABILITY								

AIR INJECTION TESTING RESULTS FOR BOREHOLE NO RDD-1

INTERVAL	ZONE	APER- PRESS	VOLUME FLOW.	EQUIVALENT POROUS MEDIA PERMEABILITY					
				INTRINSIC	HYDRAULIC CONDUCTIVITY				
FEET	PSIA	CM.	ML/M	SQUAR CM.	DARCY	SQUAR FT.	CM/SEC	FT/SEC	GAL/D FT**2
1.0-3.5	0.00	.14E-02	0.00	0.31794E-11	0.32216E-03	0.34223E-14	0.31061E-06	0.10191E-07	0.65864E-02
2.0-4.5	0.00	.30E-02	0.00	0.29037E-10	0.29421E-02	0.31255E-13	0.28367E-05	0.93068E-07	0.60152E-01
3.0-5.5	0.00	.17E-02	0.00	0.50671E-11	0.51342E-03	0.54542E-14	0.49503E-06	0.16241E-07	0.10497E-01
4.0-6.5	0.00	.17E-02	0.00	0.58054E-11	0.58824E-03	0.62409E-14	0.56716E-06	0.18608E-07	0.12026E-01
5.0-7.5	0.00	.26E-02	0.00	0.19305E-10	0.19560E-02	0.20779E-13	0.18859E-05	0.61875E-07	0.39991E-01
6.0-8.5	0.00	.13E-02	0.00	0.23298E-11	0.23607E-03	0.25078E-14	0.22761E-06	0.74676E-08	0.48265E-02
7.0-9.5	0.00	.30E-02	0.00	0.29741E-10	0.30135E-02	0.32013E-13	0.29055E-05	0.95326E-07	0.61611E-01
8.0-10.5	0.00	.31E-02	0.00	0.31074E-10	0.32296E-02	0.34308E-13	0.31139E-05	0.10216E-06	0.66028E-01
9.0-11.5	0.00	.35E-02	0.00	0.46857E-10	0.47478E-02	0.50430E-13	0.45777E-05	0.15019E-06	0.97067E-01
10.0-11.5	0.00	.12E-02	0.00	0.19885E-11	0.20149E-03	0.21404E-14	0.19427E-06	0.63736E-08	0.41194E-02
11.0-11.4	0.00	.11E-02	0.00	0.14542E-11	0.14735E-03	0.15653E-14	0.14207E-06	0.46610E-08	0.30125E-02
11.4-13.5	0.00	.11E-02	0.00	0.15660E-11	0.15868E-03	0.16857E-14	0.15299E-06	0.50195E-08	0.32442E-02

AIR INJECTION TESTING RESULTS FOR BOREHOLE NO RDD-2

INTERVAL	ZONE	APER- PRESS	VOLUME FLOW.	EQUIVALENT POROUS MEDIA PERMEABILITY					
				INTRINSIC	HYDRAULIC CONDUCTIVITY				
FEET	PSIA	CM.	ML/M	SQUAR CM.	DARCY	SQUAR FT.	CM/SEC	FT/SEC	GAL/D FT**2
0.5-3.0	0.00	.33E-02	0.00	0.40392E-10	0.40927E-02	0.43477E-13	0.39461E-05	0.12946E-06	0.83675E-01
4.0-5.5	0.00	.29E-02	0.00	0.25598E-10	0.25937E-02	0.27553E-13	0.25008E-05	0.82047E-07	0.53028E-01
5.0-6.5	0.00	.14E-02	0.00	0.32010E-11	0.32434E-03	0.34455E-14	0.31272E-06	0.10260E-07	0.66311E-02
6.0-7.5	0.00	.15E-02	0.00	0.37053E-11	0.37544E-03	0.39884E-14	0.36199E-06	0.11876E-07	0.76758E-02
7.0-8.5	DECAY TOO SLOW DUE TO EXTREMELY LOW PERMEABILITY		0.00						
8.0-10.5	0.00	.14E-02	0.00	0.31357E-11	0.31772E-03	0.33752E-14	0.30634E-06	0.10051E-07	0.64958E-02

AIR INJECTION TESTING RESULTS FOR BOREHOLE NO RW-1

INTERVAL FEET	ZONE PRESS PSIA	APER- TURE CM.	VOLUME FLOW. ML/M	EQUIVALENT POROUS MEDIA PERMEABILITY					
				INTRINSIC		HYDRAULIC CONDUCTIVITY			
				SQUAR CM.	DARCY	SQUAR FT.	CM/SEC	FT/SEC	GAL/D FT**2
6-8	0.00	.29	0.00	0.27593E-10	0.27959E-02	0.29701E-13	0.26957E-05	0.88441E-07	0.57161E-01
7-8	0.00	.11	0.00	0.16450E-11	0.16668E-03	0.17706E-14	0.16071E-06	0.57225E-08	0.34077E-03
8-9	0.00	.11	0.00	0.17421E-11	0.17421E-03	0.18587E-14	0.16097E-06	0.55188E-08	0.35617E-03
9-10	0.00	.11	0.00	0.33983E-11	0.33983E-03	0.42382E-14	0.38375E-06	0.12590E-07	0.81373E-03
10-11	0.00	.11	0.00	0.33983E-11	0.33983E-03	0.37479E-14	0.33401E-06	0.11160E-07	0.72131E-03
11-12	0.00	.11	0.00	0.33983E-11	0.33983E-03	0.36511E-14	0.33138E-06	0.10872E-07	0.70268E-03
12-13	0.00	.21	0.00	0.18884E-10	0.18217E-02	0.18854E-13	0.98511E-06	0.32328E-07	0.28889E-01

AIR INJECTION TESTING RESULTS FOR BOREHOLE NO RW-2

INTERVAL FEET	ZONE PRESS PSIA	APER- TURE CM.	VOLUME FLOW. ML/M	EQUIVALENT POROUS MEDIA PERMEABILITY					
				INTRINSIC		HYDRAULIC CONDUCTIVITY			
				SQUAR CM.	DARCY	SQUAR FT.	CM/SEC	FT/SEC	GAL/D FT**2
0.7-3.2	0.00	.22	0.00	0.11133E-10	0.11287E-02	0.11990E-13	0.10883E-05	0.35704E-07	0.23076E-01
1.0-1.1	0.00	.11	0.00	0.11133E-10	0.11287E-02	0.11972E-13	0.10866E-05	0.35650E-07	0.23041E-01
1.6-1.7	0.00	.11	0.00	0.54452E-11	0.55242E-03	0.58684E-14	0.53263E-06	0.17475E-07	0.11294E-01
8-9	0.00	.11	0.00	0.18049E-10	0.18791E-03	0.11463E-13	0.10404E-05	0.34134E-07	0.22061E-01
9-11	0.00	.15	0.00	0.95140E-11	0.96400E-03	0.10241E-13	0.92946E-06	0.30494E-07	0.27099E-01
11-15	0.00	.15	0.00	0.33807E-11	0.34255E-03	0.36390E-14	0.33028E-06	0.10836E-07	0.70034E-02

AIR INJECTION TESTING RESULTS FOR BOREHOLE NO RW-4

INTERVAL FEET	ZONE PRESS PSIA	APER- TURE CM.	VOLUME FLOW. ML/M	EQUIVALENT POROUS MEDIA PERMEABILITY					
				INTRINSIC		HYDRAULIC CONDUCTIVITY			
				SQUAR CM.	DARCY	SQUAR FT.	CM/SEC	FT/SEC	GAL/D FT**2
15.0-17.5	0.00	.28E-02	0.00	0.23147E-10	0.23453E-02	0.24915E-13	0.22613E-05	0.74190E-07	0.47950E-01

AIR INJECTION TESTING RESULTS FOR BOREHOLE NO RW-5

INTERVAL FEET	ZONE PSIA	APER- TURE CM.	VOLUME FLOW. ML/M	EQUIVALENT POROUS MEDIA PERMEABILITY					
				INTRINSIC			HYDRAULIC CONDUCTIVITY		
				SQUAR CM.	DARCY	SQUAR FT.	CM/SEC	FT/SEC	GAL/D FT**2
1.0-3.5	0.00	.18E-02	0.00	0.66198E-11	0.67075E-03	0.71255E-14	0.64672E-06	0.21218E-07	0.13713E-01
5.0-8.0	0.00	.26E-02	0.00	0.18362E-10	0.18596E-03	0.19754E-14	0.17950E-06	0.55524E-07	0.30327E-01
6.0-9.0	0.00	.11E-02	0.00	0.15880E-11	0.16809E-03	0.17847E-14	0.15436E-06	0.55524E-07	0.30327E-01
7.0-10.0	0.00	.11E-02	0.00	0.16395E-11	0.16612E-03	0.17477E-14	0.16817E-06	0.55524E-07	0.30327E-01
8.0-11.0	0.00	.19E-02	0.00	0.77766E-11	0.78797E-03	0.83787E-14	0.75944E-06	0.27024E-07	0.15479E-01
9.0-12.0	0.00	.22E-02	0.00	0.20449E-10	0.20761E-03	0.22554E-14	0.28817E-06	0.75555E-07	0.42839E-01
10.0-15.0	0.00	.28E-02	0.00	0.23479E-10	0.23790E-03	0.25273E-14	0.22938E-06	0.75555E-07	0.42839E-01

AIR INJECTION TESTING RESULTS FOR BOREHOLE NO RW-6

INTERVAL FEET	ZONE PSIA	APER- TURE CM.	VOLUME FLOW. ML/M	EQUIVALENT POROUS MEDIA PERMEABILITY					
				INTRINSIC			HYDRAULIC CONDUCTIVITY		
				SQUAR CM.	DARCY	SQUAR FT.	CM/SEC	FT/SEC	GAL/D FT**2
5.0-7.0	0.00	.33E-02	0.00	0.46933E-10	0.47660E-03	0.50572E-13	0.45900E-05	0.15850E-06	0.97329E-01
5.0-8.0	0.00	.33E-02	0.00	0.18293E-11	0.18550E-03	0.19699E-14	0.17871E-06	0.55524E-07	0.30327E-01
6.0-8.0	0.00	.33E-02	0.00	0.16828E-11	0.17586E-03	0.18449E-14	0.16444E-06	0.55524E-07	0.30327E-01
7.0-9.0	0.00	.33E-02	0.00	0.37809E-11	0.37588E-03	0.39989E-14	0.36233E-06	0.79399E-07	0.44480E-01
8.0-10.0	0.00	.33E-02	0.00	0.24669E-11	0.25490E-03	0.26760E-14	0.24133E-06	0.79399E-07	0.44480E-01
9.0-11.0	0.00	.33E-02	0.00	0.16668E-11	0.17843E-03	0.18555E-14	0.16444E-06	0.55524E-07	0.30327E-01
10.0-12.0	0.00	.33E-02	0.00	0.26914E-11	0.26591E-03	0.28188E-14	0.25433E-06	0.55524E-07	0.30327E-01
11.0-13.0	0.00	.33E-02	0.00	0.37511E-11	0.38466E-03	0.41785E-14	0.36688E-06	0.55524E-07	0.30327E-01
12.0-14.0	0.00	.33E-02	0.00	0.36859E-11	0.37381E-03	0.39333E-14	0.35964E-06	0.55524E-07	0.30327E-01
13.0-15.0	0.00	.33E-02	0.00	0.17218E-11	0.17446E-03	0.18333E-14	0.16821E-06	0.55524E-07	0.30327E-01

AIR INJECTION TESTING RESULTS FOR BOREHOLE NO RDE-1

INTERVAL FEET	ZONE PRESS PSIA	APER- TURE CM.	VOLUME FLOW. ML/M	EQUIVALENT POROUS MEDIA PERMEABILITY					
				INTRINSIC		HYDRAULIC CONDUCTIVITY			
				SQUAR CM.	DARCY	SQUAR FT.	CM/SEC	FT/SEC	GAL/D FT**2
0.7-3.2	0.00	.16E-02	0.00	0.40965E-11	0.41508E-03	0.44095E-14	0.40021E-06	0.13138E-07	0.84863E-02
1.0-3.2	0.00	.12E-02	0.00	0.20272E-11	0.20541E-03	0.21821E-14	0.19805E-06	0.64977E-08	0.41996E-02
2.0-4.0	0.00	.4E-02	0.00	0.00	0.00	0.00	0.00	0.00	0.00
3.0-5.0	0.00	.5E-02	0.00	0.00	0.00	0.00	0.00	0.00	0.00
4.0-7.0	0.00	.18E-02	0.00	0.59555E-11	0.60348E-03	0.64109E-14	0.58186E-06	0.19090E-07	0.12338E-01
5.0-8.0	0.00	.17E-02	0.00	0.57393E-11	0.58153E-03	0.61777E-14	0.56070E-06	0.18396E-07	0.11809E-01
8.0-10.0	0.00	.11E-02	0.00	0.13153E-11	0.13323E-03	0.14155E-14	0.12849E-06	0.42156E-08	0.27246E-01
9.0-11.0	0.00	.11E-02	0.00	0.13153E-11	0.14447E-03	0.15345E-14	0.13922E-06	0.45695E-08	0.29543E-01
10.0-13.0	0.00	.11E-02	0.00	0.14585E-11	0.14778E-03	0.15694E-14	0.14224E-06	0.45695E-08	0.30238E-01
11.0-14.0	0.00	.11E-02	0.00	0.15302E-11	0.15504E-03	0.16471E-14	0.14949E-06	0.49045E-08	0.31699E-01

AIR INJECTION TESTING RESULTS FOR BOREHOLE NO RDE-2

INTERVAL FEET	ZONE PRESS PSIA	APER- TURE CM.	VOLUME FLOW. ML/M	EQUIVALENT POROUS MEDIA PERMEABILITY					
				INTRINSIC		HYDRAULIC CONDUCTIVITY			
				SQUAR CM.	DARCY	SQUAR FT.	CM/SEC	FT/SEC	GAL/D FT**2
0.7-3.2	0.00	.25E-02	0.00	0.16380E-10	0.16597E-02	0.17631E-13	0.16002E-05	0.52500E-07	0.33932E-01
1.0-3.0	0.00	.25E-02	0.00	0.16333E-10	0.16549E-02	0.17581E-13	0.15956E-05	0.52351E-07	0.33835E-01
2.0-4.0	0.00	.25E-02	0.00	0.17266E-10	0.17495E-02	0.18585E-13	0.16868E-05	0.55342E-07	0.35768E-01
3.0-5.0	0.00	.28E-02	0.00	0.23289E-10	0.23597E-02	0.25068E-13	0.22752E-05	0.74644E-07	0.48244E-01
9.0-11.0	0.00	.97E-03	0.00	0.10023E-11	0.10156E-03	0.10789E-14	0.97923E-07	0.32127E-08	0.20764E-02
10.0-13.0	0.00	.12E-02	0.00	0.18097E-11	0.18337E-03	0.19480E-14	0.17680E-06	0.58005E-08	0.37490E-02

AIR INJECTION TESTING RESULTS FOR BOREHOLE NO RDE-3

INTERVAL FEET	ZONE PSIA	APER- TURE CM.	VOLUME FLOW. ML/M	EQUIVALENT POROUS MEDIA PERMEABILITY					
				INTRINSIC			HYDRAULIC CONDUCTIVITY		
				SQUAR CM.	DARCY	SQUAR FT.	CM/SEC	FT/SEC	GAL/D FT**2
2.0-4.5	0.00	.13E-02	0.00	0.26740E-11	0.27094E-03	0.28783E-14	0.26124E-06	0.85707E-08	0.55394E-02
4.5-5.5	0.00	.11E-02	0.00	0.13720E-11	0.13910E-03	0.14777E-14	0.13412E-06	0.44001E-08	0.28439E-02
5.5-6.5	0.00	.16E-02	0.00	0.38990E-11	0.39516E-03	0.41979E-14	0.38100E-06	0.12500E-07	0.80730E-02
6.5-7.5	0.00	.16E-02	0.00	0.43511E-11	0.44007E-03	0.46835E-14	0.42508E-06	0.13946E-07	0.90136E-02
7.5-8.5	0.00	.13E-02	0.00	0.21710E-11	0.21998E-03	0.23369E-14	0.21210E-06	0.69586E-08	0.44974E-02
8.5-11.5	0.00	.12E-02	0.00	0.20367E-11	0.20637E-03	0.21923E-14	0.19898E-06	0.65281E-08	0.42192E-02

AIR INJECTION TESTING RESULTS FOR BOREHOLE NO RDE-4

INTERVAL FEET	ZONE PSIA	APER- TURE CM.	VOLUME FLOW. ML/M	EQUIVALENT POROUS MEDIA PERMEABILITY					
				INTRINSIC			HYDRAULIC CONDUCTIVITY		
				SQUAR CM.	DARCY	SQUAR FT.	CM/SEC	FT/SEC	GAL/D FT**2
2.0-4.5	0.00	.35E-02	0.00	0.46224E-10	0.46837E-02	0.49755E-13	0.45158E-05	0.14016E-06	0.95757E-01
4.5-6.5	0.00	.10E-02	0.00	0.11394E-11	0.11545E-03	0.12265E-14	0.11132E-06	0.36521E-08	0.23604E-02
6.5-7.5	0.00	.10E-02	0.00	0.11503E-11	0.11656E-03	0.12382E-14	0.11238E-06	0.36871E-08	0.23830E-02
7.5-9.5	0.00	.10E-02	0.00	0.10922E-11	0.11067E-03	0.11757E-14	0.10671E-06	0.35009E-08	0.22627E-02
9.5-10.5	0.00	.10E-02	0.00	0.11684E-11	0.11839E-03	0.12576E-14	0.11414E-06	0.37449E-08	0.24204E-02
10.5-11.5	0.00	.10E-02	0.00	0.11896E-11	0.12054E-03	0.12805E-14	0.11622E-06	0.38130E-08	0.24644E-02

AIR INJECTION TESTING RESULTS FOR BOREHOLE NO RDE-6

INTERVAL FEET	ZONE PSIA	APER- TURE CM.	VOLUME FLOW. ML/M	EQUIVALENT POROUS MEDIA PERMEABILITY					
				INTRINSIC			HYDRAULIC CONDUCTIVITY		
				SQUAR CM.	DARCY	SQUAR FT.	CM/SEC	FT/SEC	GAL/D FT**2
2.0-4.5	0.00	.33E-02	0.00	0.39425E-10	0.39948E-02	0.42437E-13	0.38517E-05	0.12637E-06	0.81673E-01
10.5-13.0	0.00	.11E-02	0.00	0.13302E-11	0.13479E-03	0.14319E-14	0.12996E-06	0.42637E-08	0.27557E-02

AIR INJECTION TESTING RESULTS FOR BOREHOLE NO RDW-4

INTERVAL FEET	ZONE PRESS	APER- TURE CM.	VOLUME FLOW. ML/M	EQUIVALENT POROUS MEDIA PERMEABILITY					
				INTRINSIC		HYDRAULIC CONDUCTIVITY			
				SQUAR CM.	DARCY	SQUAR FT.	CM/SEC	FT/SEC	GAL/D FT**2
8.0- 10.5	0.00	.34E-02	0.00	0.42342E-10	0.42903E-02	0.45576E-13	0.41366E-05	0.13571E-06	0.87714E-01
9.0- 11.5	DECAY TOO SLOW DUE TO EXTREMELY LOW PERMEABILITY								
10.0- 12.5	DECAY TOO SLOW DUE TO EXTREMELY LOW PERMEABILITY								
11.0- 13.5	DECAY TOO SLOW DUE TO EXTREMELY LOW PERMEABILITY								
11.3- 13.8	DECAY TOO SLOW DUE TO EXTREMELY LOW PERMEABILITY								

AIR INJECTION TESTING RESULTS FOR BOREHOLE NO RDW-5

INTERVAL FEET	ZONE PRESS	APER- TURE CM.	VOLUME FLOW. ML/M	EQUIVALENT POROUS MEDIA PERMEABILITY					
				INTRINSIC		HYDRAULIC CONDUCTIVITY			
				SQUAR CM.	DARCY	SQUAR FT.	CM/SEC	FT/SEC	GAL/D FT**2
2.0- 4.5	DECAY TOO SLOW DUE TO EXTREMELY LOW PERMEABILITY								
3.0- 5.5	0.00	.13E-02	0.00	0.24176E-11	0.24497E-03	0.26023E-14	0.23619E-06	0.77490E-08	0.50003E-02
4.0- 6.5	0.00	.34E-02	0.00	0.41567E-10	0.42118E-02	0.44744E-13	0.40609E-05	0.13323E-06	0.86110E-01
5.0- 7.5	0.00	.35E-02	0.00	0.48484E-10	0.49126E-02	0.52187E-13	0.47366E-05	0.15540E-06	0.10044E+00
10.0- 12.5	DECAY TOO SLOW DUE TO EXTREMELY LOW PERMEABILITY								
11.0- 13.5	DECAY TOO SLOW DUE TO EXTREMELY LOW PERMEABILITY								
12.0- 14.5	DECAY TOO SLOW DUE TO EXTREMELY LOW PERMEABILITY								

AIR INJECTION TESTING RESULTS FOR BOREHOLE NO RDW-6

INTERVAL FEET	ZONE PRESS	APER- TURE CM.	VOLUME FLOW. ML/M	EQUIVALENT POROUS MEDIA PERMEABILITY					
				INTRINSIC		HYDRAULIC CONDUCTIVITY			
				SQUAR CM.	DARCY	SQUAR FT.	CM/SEC	FT/SEC	GAL/D FT**2
0.5- 3.0	0.00	.14E-02	0.00	0.20136E-11	0.28509E-03	0.30285E-14	0.27407E-06	0.90181E-08	0.50286E-02
1.0- 3.5	0.00	.13E-02	0.00	0.24150E-11	0.24470E-03	0.25995E-14	0.23593E-06	0.77405E-08	0.50020E-02
2.0- 4.5	DECAY TOO SLOW DUE TO EXTREMELY LOW PERMEABILITY								
3.0- 5.5	DECAY TOO SLOW DUE TO EXTREMELY LOW PERMEABILITY								
4.0- 6.5	0.00	.12E-02	0.00	0.20712E-11	0.20986E-03	0.22294E-14	0.20234E-06	0.66386E-08	0.42906E-02
10.0- 12.5	0.00	.11E-02	0.00	0.14864E-11	0.15060E-03	0.15999E-14	0.14521E-06	0.47641E-08	0.30791E-02
11.0- 13.5	0.00	.13E-02	0.00	0.24803E-11	0.25131E-03	0.26690E-14	0.24231E-06	0.79490E-08	0.51381E-02
11.5- 14.0	DECAY TOO SLOW DUE TO EXTREMELY LOW PERMEABILITY								

AIR INJECTION TESTING RESULTS FOR BOREHOLE NO RDW-1

INTERVAL FEET	ZONE PRESS PSIA	APER- TURE CM.	VOLUME FLOW. ML/M	EQUIVALENT POROUS MEDIA PERMEABILITY					
				INTRINSIC		HYDRAULIC CONDUCTIVITY			
				SQUAR CM.	DARCY	SQUAR FT.	CM/SEC	FT/SEC	GAL/D FT**2
2.0- 4.5	0.00	.19E-02	0.00	0.71045E-11	0.71986E-03	0.76472E-14	0.69407E-06	0.22771E-07	0.14718E-01
3.0- 5.5	0.00	.12E-02	0.00	0.17971E-11	0.18209E-03	0.19344E-14	0.17557E-06	0.57601E-08	0.37229E-02
4.0- 6.5	DECAY TOO SLOW DUE TO EXTREMELY LOW PERMEABILITY								
5.0- 7.5	DECAY TOO SLOW DUE TO EXTREMELY LOW PERMEABILITY								
6.0- 8.5	DECAY TOO SLOW DUE TO EXTREMELY LOW PERMEABILITY								
7.0- 9.5	DECAY TOO SLOW DUE TO EXTREMELY LOW PERMEABILITY								
8.0- 10.5	0.00	.10E-02	0.00	0.11954E-11	0.12113E-03	0.12868E-14	0.11679E-06	0.38316E-08	0.24765E-02
9.0- 11.5	0.00	.10E-02	0.00	0.11320E-11	0.11470E-03	0.12195E-14	0.11059E-06	0.36284E-08	0.23451E-02
10.0- 12.5	0.00	.12E-02	0.00	0.20665E-11	0.20939E-03	0.22243E-14	0.20180E-06	0.66235E-08	0.42809E-02
10.5- 13.0	DECAY TOO SLOW DUE TO EXTREMELY LOW PERMEABILITY								

AIR INJECTION TESTING RESULTS FOR BOREHOLE NO RDW-2

INTERVAL FEET	ZONE PRESS PSIA	APER- TURE CM.	VOLUME FLOW. ML/M	EQUIVALENT POROUS MEDIA PERMEABILITY					
				INTRINSIC		HYDRAULIC CONDUCTIVITY			
				SQUAR CM.	DARCY	SQUAR FT.	CM/SEC	FT/SEC	GAL/D FT**2
6.0- 8.5	0.00	.11E-02	0.00	0.13762E-11	0.13944E-03	0.14813E-14	0.13444E-06	0.44109E-08	0.28500E-02
7.0- 9.5	0.00	.14E-02	0.00	0.27672E-11	0.28039E-03	0.29780E-14	0.27034E-06	0.88695E-08	0.57325E-02
8.0- 10.5	0.00	.16E-02	0.00	0.43461E-11	0.44037E-03	0.46781E-14	0.42459E-06	0.13930E-07	0.90033E-02
9.0- 11.5	0.00	.19E-02	0.00	0.70618E-11	0.71546E-03	0.76004E-14	0.68908E-06	0.22632E-07	0.14620E-01
10.0- 12.5	0.00	.19E-02	0.00	0.13186E-11	0.13360E-03	0.14193E-14	0.12882E-06	0.42263E-08	0.27315E-02
11.0- 13.5	DECAY TOO SLOW DUE TO EXTREMELY LOW PERMEABILITY								

AIR INJECTION TESTING RESULTS FOR BOREHOLE NO RDW-3

INTERVAL FEET	ZONE PRESS PSIA	APER- TURE CM.	VOLUME FLOW. ML/M	EQUIVALENT POROUS MEDIA PERMEABILITY					
				INTRINSIC		HYDRAULIC CONDUCTIVITY			
				SQUAR CM.	DARCY	SQUAR FT.	CM/SEC	FT/SEC	GAL/D FT**2
1.0- 3.5	0.00	.24E-02	0.00	0.15568E-10	0.15775E-02	0.16758E-13	0.15210E-05	0.49900E-07	0.32251E-01
2.0- 4.5	0.00	.22E-02	0.00	0.12354E-10	0.12510E-02	0.13298E-13	0.12069E-05	0.39597E-07	0.25592E-01
3.0- 5.5	DECAY TOO SLOW DUE TO EXTREMELY LOW PERMEABILITY								
4.0- 6.5	DECAY TOO SLOW DUE TO EXTREMELY LOW PERMEABILITY								
5.0- 7.5	DECAY TOO SLOW DUE TO EXTREMELY LOW PERMEABILITY								
6.0- 8.5	0.00	.17E-02	0.00	0.54952E-11	0.55680E-03	0.59150E-14	0.53685E-06	0.17613E-07	0.11384E-01
7.0- 9.5	0.00	.20E-02	0.00	0.20051E-10	0.20422E-02	0.20193E-13	0.21404E-05	0.89900E-07	0.58189E-01
8.0- 10.5	0.00	.26E-02	0.00	0.19283E-10	0.19538E-02	0.20756E-13	0.18038E-05	0.61800E-07	0.39945E-01
9.0- 11.5	0.00	.13E-02	0.00	0.24617E-11	0.24943E-03	0.26498E-14	0.24050E-06	0.78900E-08	0.50990E-02
10.0- 12.5	0.00	.13E-02	0.00	0.10627E-11	0.10873E-03	0.20049E-14	0.18197E-06	0.50700E-08	0.30580E-02
11.0- 13.5	0.00	.20E-02	0.00	0.10448E-10	0.10621E-02	0.11283E-13	0.10724E-05	0.33597E-07	0.21715E-01
12.0- 14.5	0.00	.20E-02	0.00	0.27396E-10	0.27759E-02	0.25489E-13	0.26765E-05	0.78100E-07	0.56750E-01
11.5- 14.0	0.00	.41E-02	0.00	0.77842E-10	0.78873E-02	0.83788E-13	0.76047E-05	0.24950E-06	0.16120E+00

AIR INJECTION TESTING RESULTS FOR BOREHOLE NO PA-3

INTERVAL FEET	ZONE PRESS PSIA	APER- TURE CM.	VOLUME FLOW. ML/M	EQUIVALENT POROUS MEDIA PERMEABILITY					
				INTRINSIC		HYDRAULIC CONDUCTIVITY			
				SQUAR CM.	DARCY	SQUAR FT.	CM/SEC	FT/SEC	GAL/D FT**2
91.0-96.3	26.18	.39E-02	1876.12	0.30537E-10	0.30941E-02	0.32869E-13	0.29833E-05	0.97877E-07	0.63259E-01
94.0-99.3	24.95	.42E-02	2148.27	0.38295E-10	0.38802E-02	0.41220E-13	0.37412E-05	0.12274E-06	0.79331E-01

AIR INJECTION TESTING RESULTS FOR BOREHOLE NO PA-3

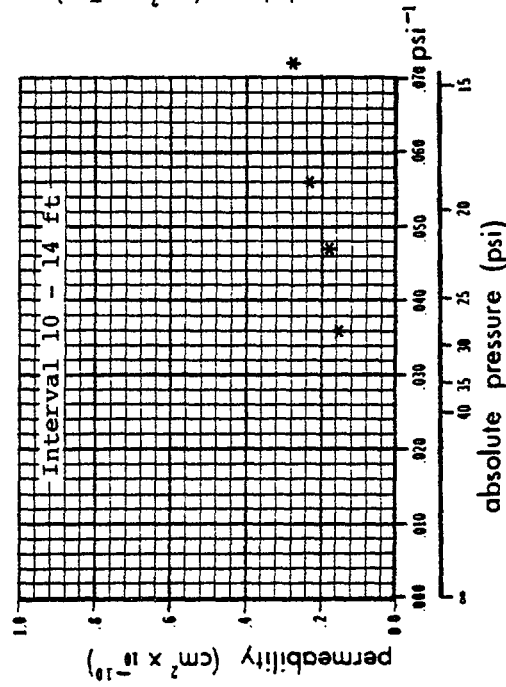
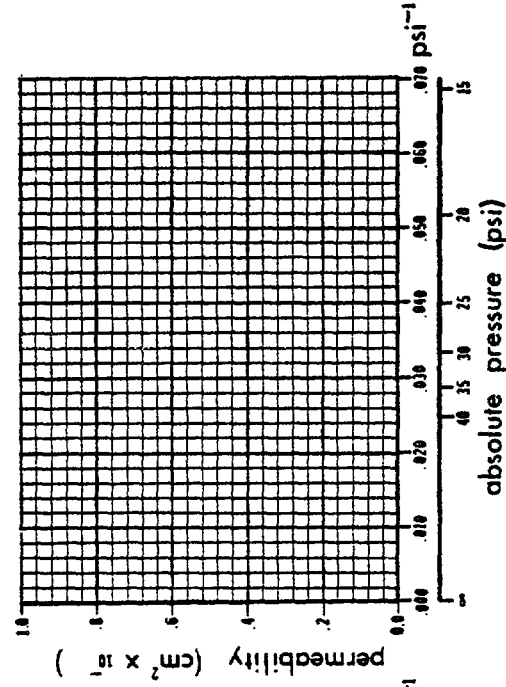
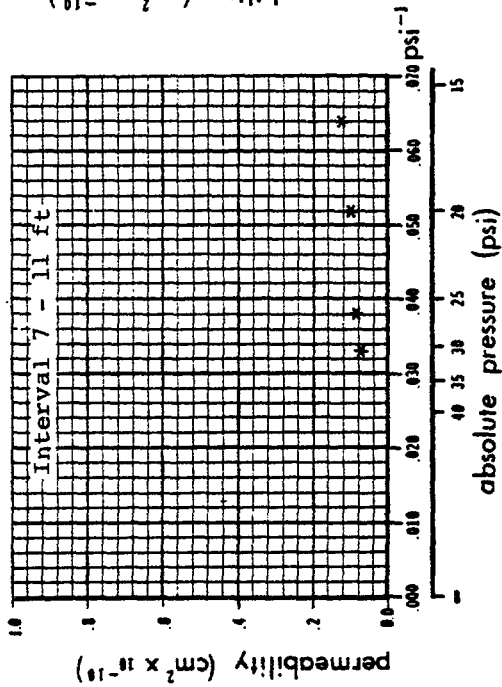
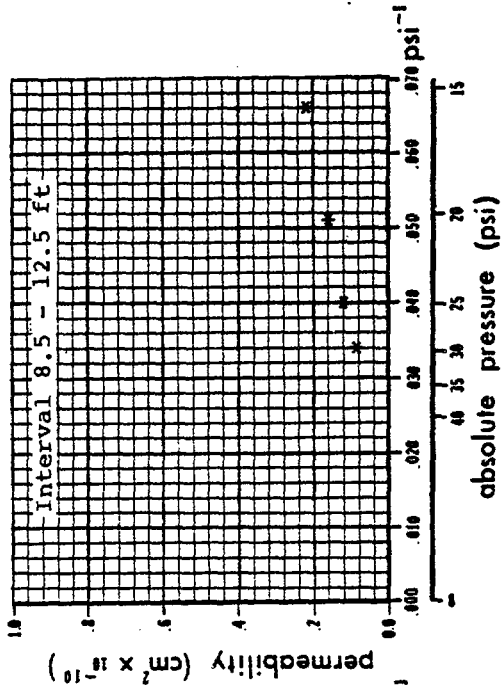
INTERVAL FEET	ZONE PRESS PSIA	APER- TURE CM.	VOLUME FLOW. ML/M	EQUIVALENT POROUS MEDIA PERMEABILITY					
				INTRINSIC		HYDRAULIC CONDUCTIVITY			
				SQUAR CM.	DARCY	SQUAR FT.	CM/SEC	FT/SEC	GAL/D FT**2
3.0-7.0	27.07	.38E-02	1986.60	0.35987E-10	0.36463E-02	0.38736E-13	0.35157E-05	0.11534E-06	0.74549E-01
7.0-11.0	34.98	.42E-02	598.52	0.73783E-11	0.74761E-02	0.79410E-14	0.72808E-06	0.43647E-06	0.15220E-01
11.0-15.0	32.80	.42E-02	123.17	0.31883E-11	0.32835E-02	0.37373E-14	0.30727E-06	0.13048E-06	0.14800E-01
15.0-19.0	32.70	.42E-02	143.45	0.31444E-11	0.31855E-02	0.33844E-14	0.30711E-06	0.10070E-06	0.65135E-01
19.0-23.0	32.27	.42E-02	173.70	0.37887E-11	0.38389E-02	0.40784E-14	0.37011E-06	0.12144E-06	0.78430E-01
23.0-27.0	32.01	.42E-02	160.00	0.30518E-11	0.30923E-02	0.32850E-14	0.30983E-06	0.97817E-06	0.63222E-01
27.0-31.0	32.01	.42E-02	160.00	0.30518E-11	0.30923E-02	0.32850E-14	0.30983E-06	0.97817E-06	0.63222E-01
31.0-35.0	29.87	.17E-02	289.20	0.31216E-11	0.31630E-02	0.33601E-14	0.30497E-06	0.10005E-06	0.64606E-01

APPENDIX VI

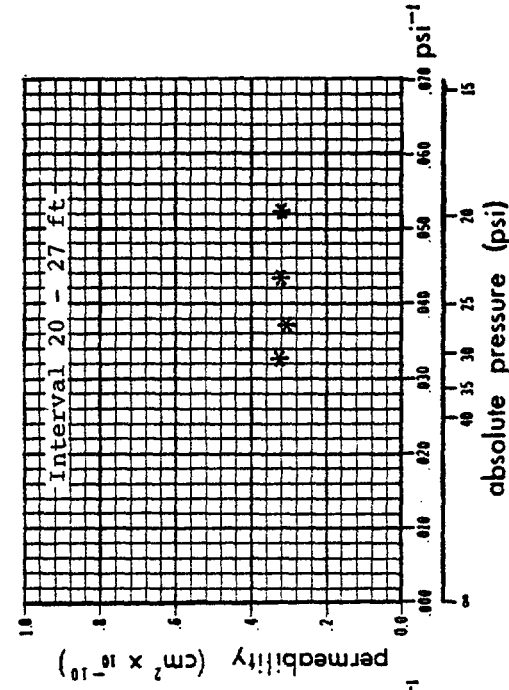
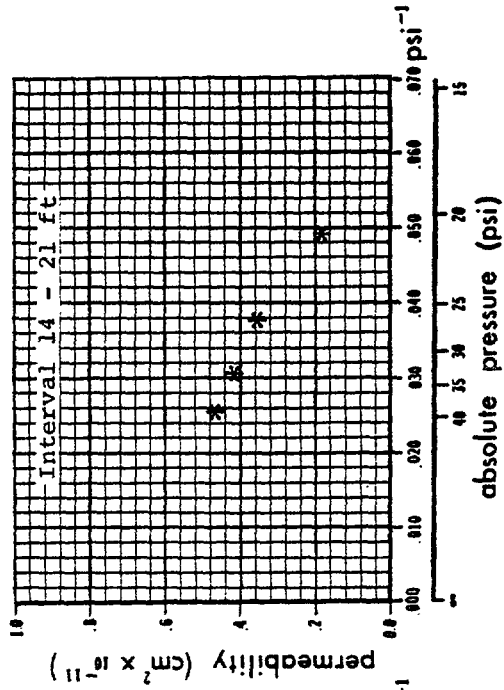
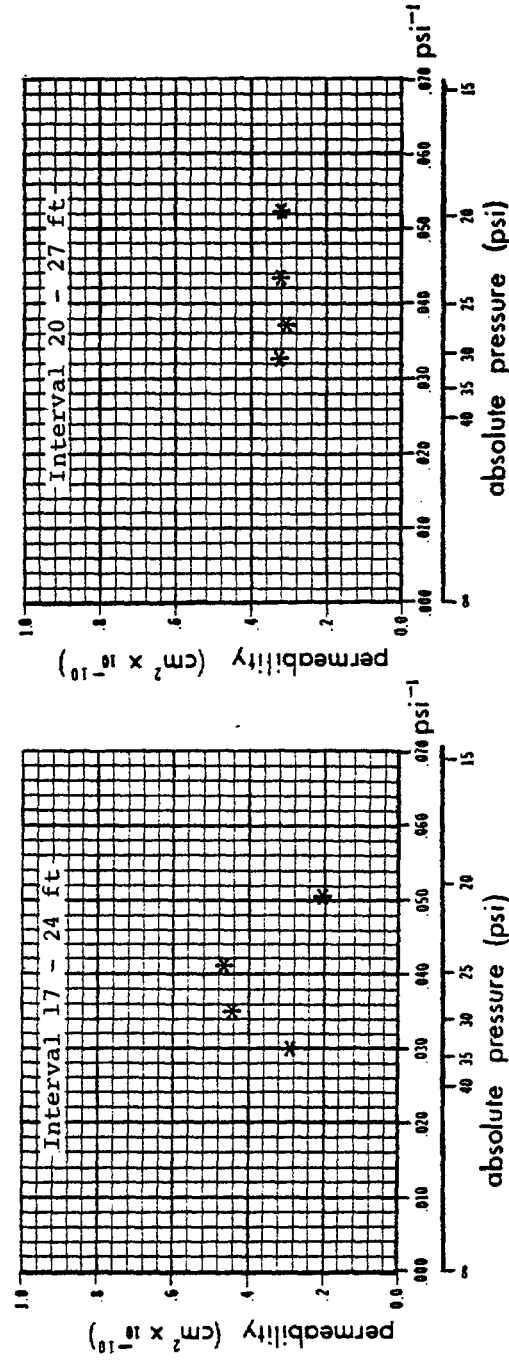
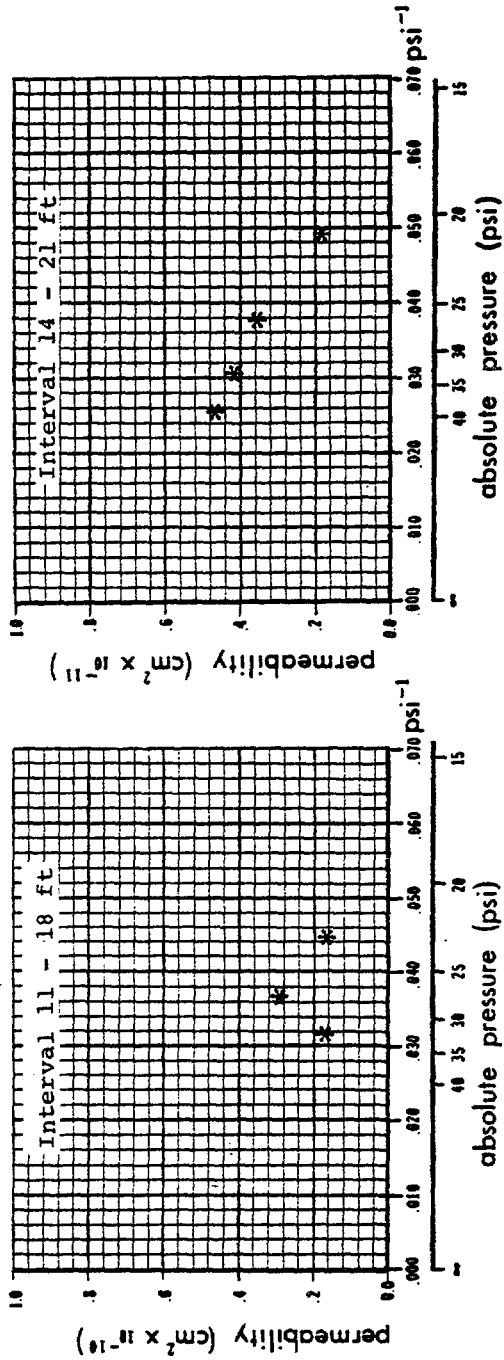
PERMEABILITY-PRESSURE PLOTS
FOR LONGITUDINAL BOREHOLES

APPENDIX VIPERMEABILITY-PRESSURE PLOTS
FOR LONGITUDINAL BOREHOLES

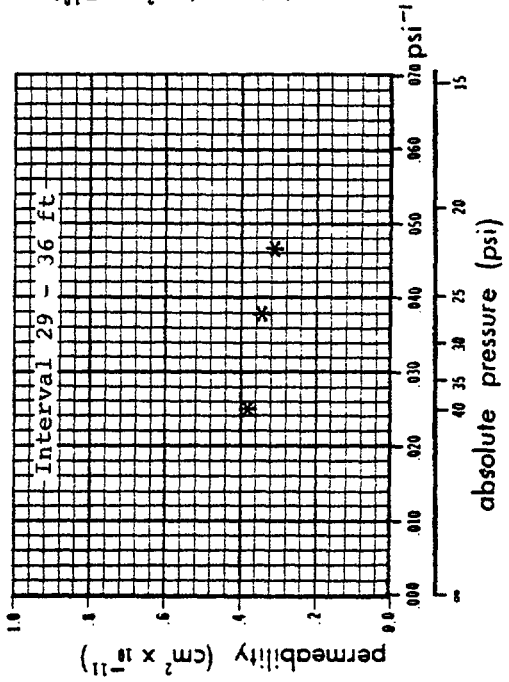
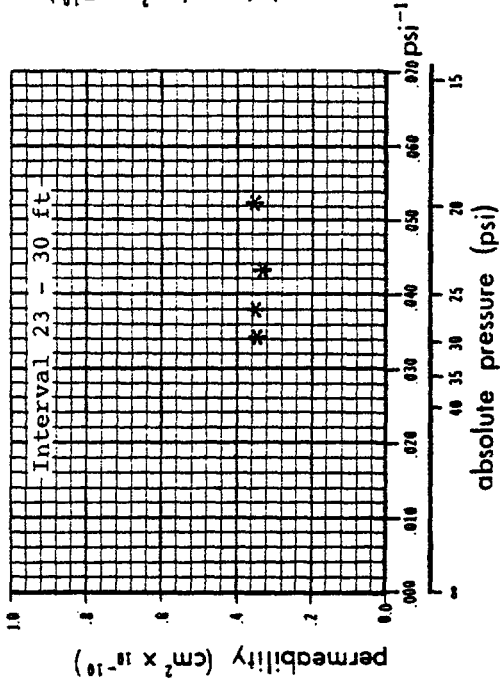
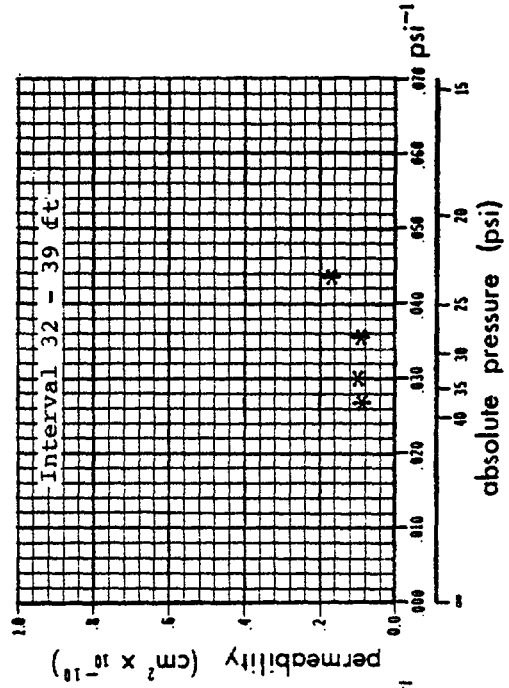
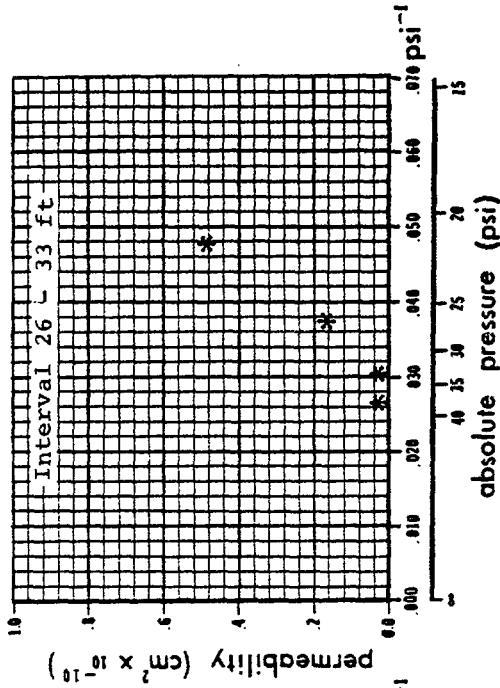
The permeabilities measured along the longitudinal boreholes by systematic nitrogen injection testing are plotted versus the steady state test pressures in this appendix. The significance of these figures is in the variation of the pressure-permeability trends (see sections 8.3.4.1, 9.1.1 and 9.1.2). Note that there are two major types. In the first type permeability decreases with pressure and in the second permeability increases with pressure. A few have a different kind of pattern. In these, the slope of the curve through the points changes sign.



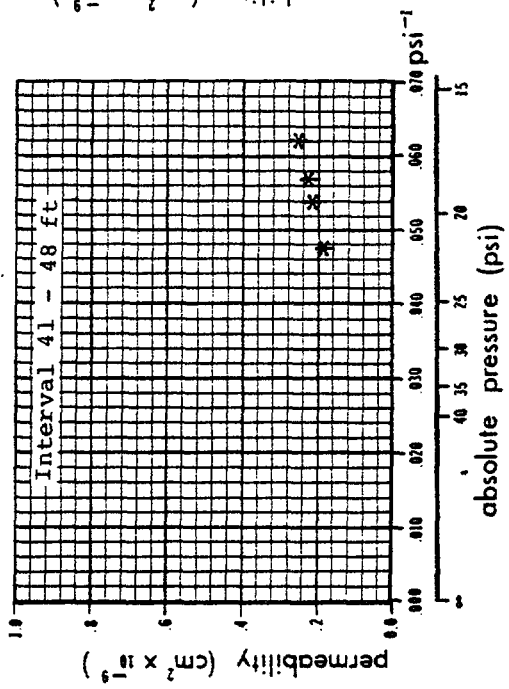
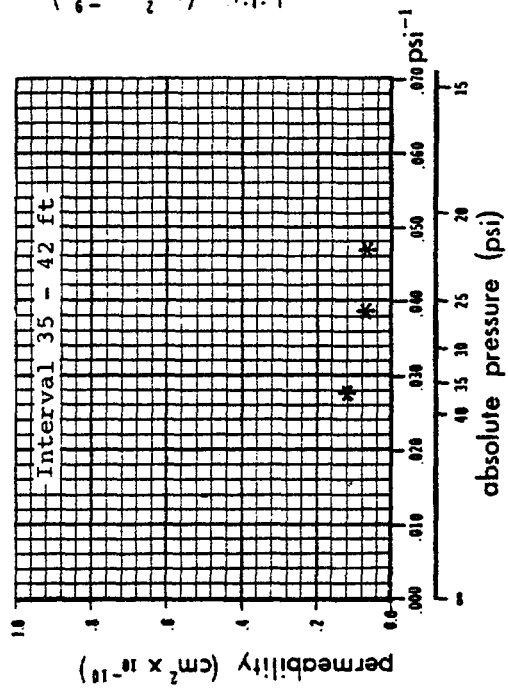
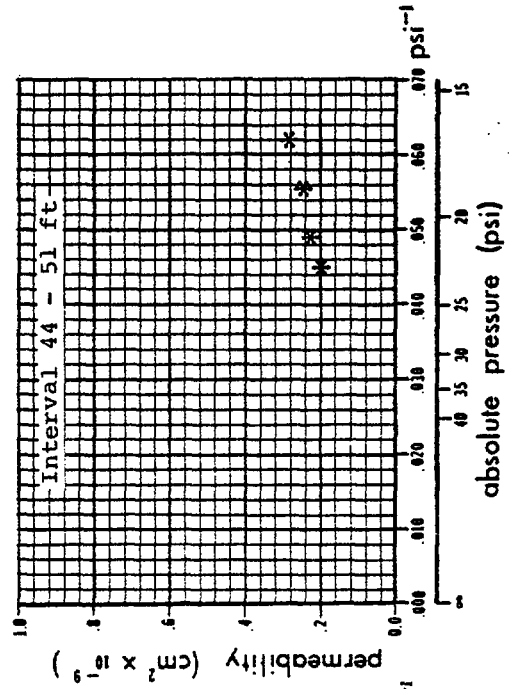
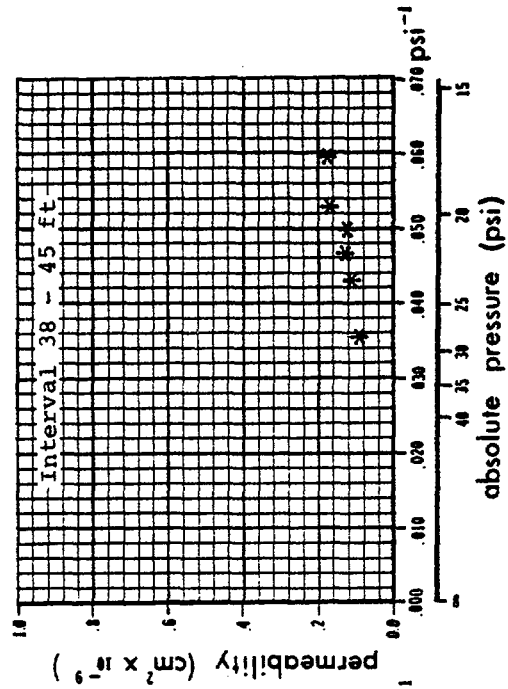
Variation of permeability with pressure. Borehole PA-1



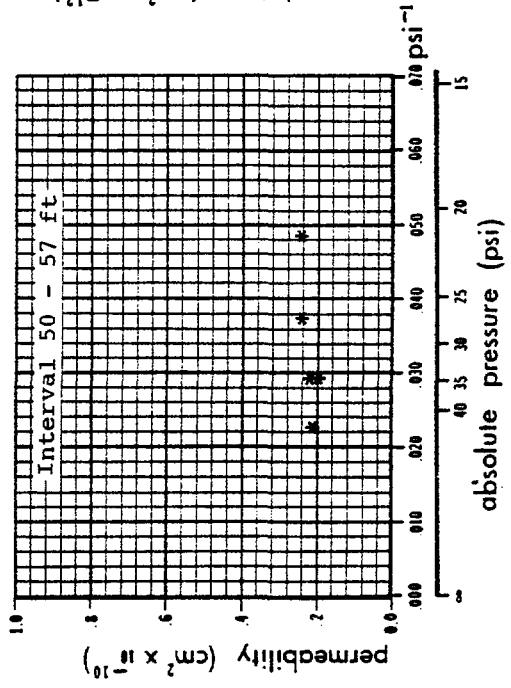
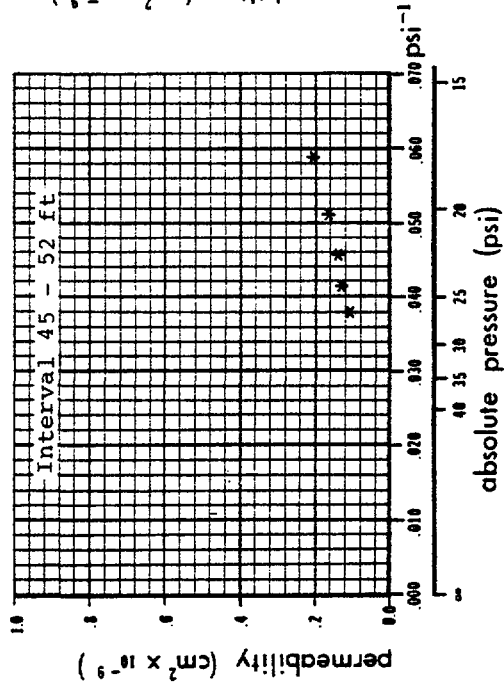
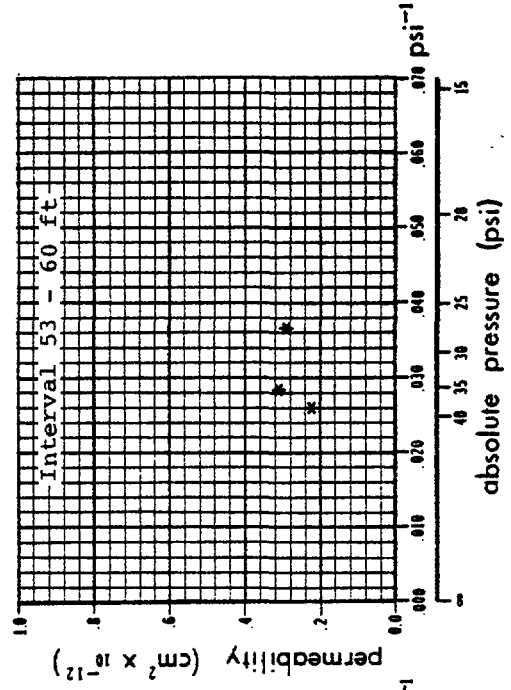
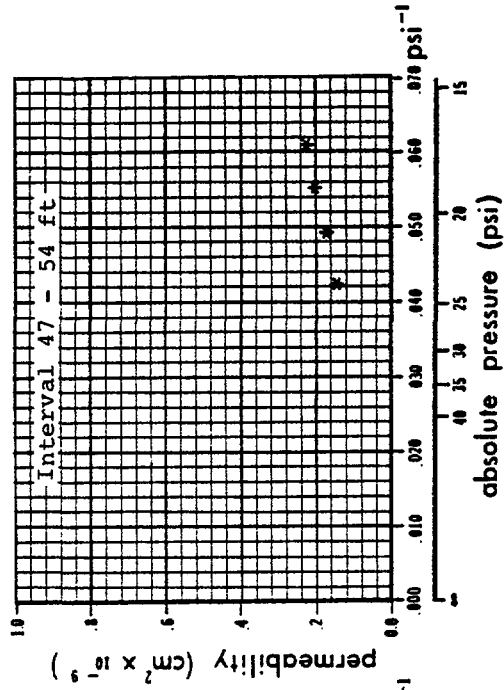
Variation of permeability with pressure, Borehole PA-1



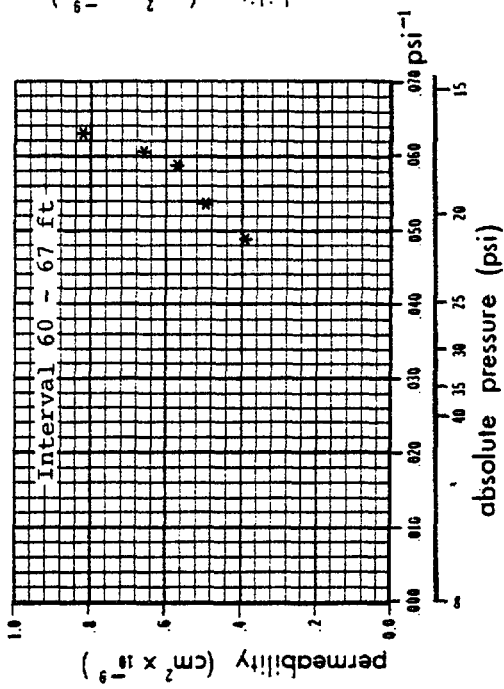
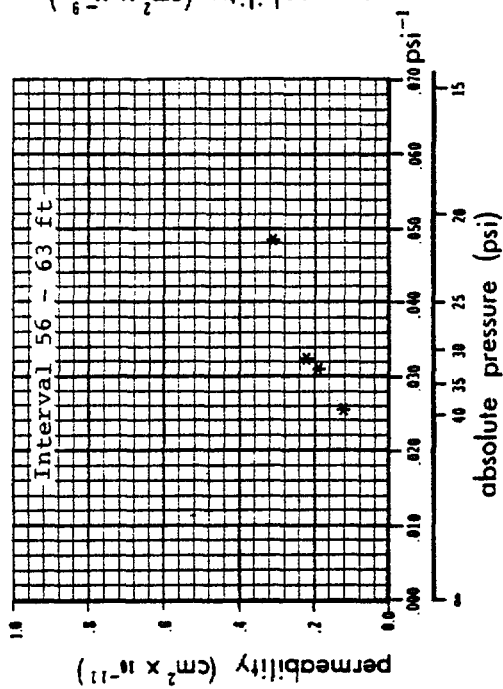
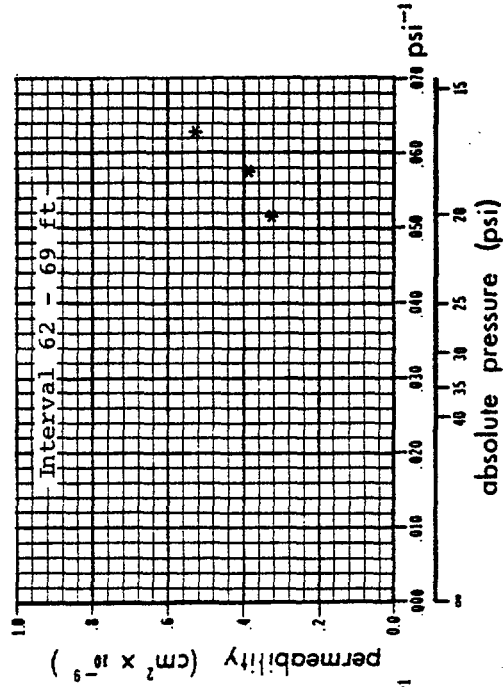
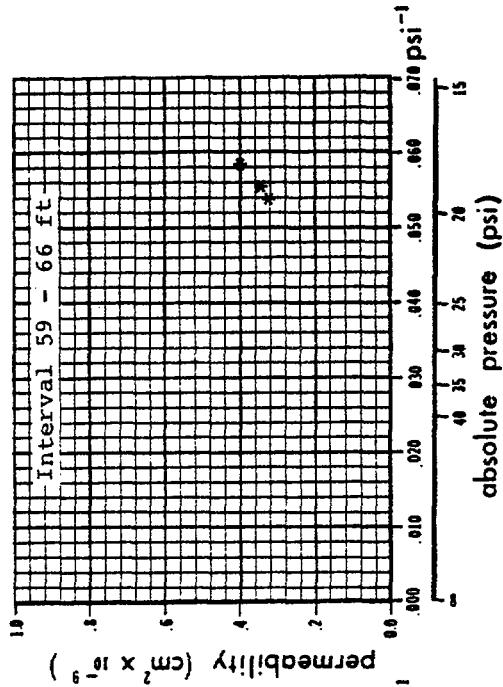
Variation of permeability with pressure. Borehole PA-1



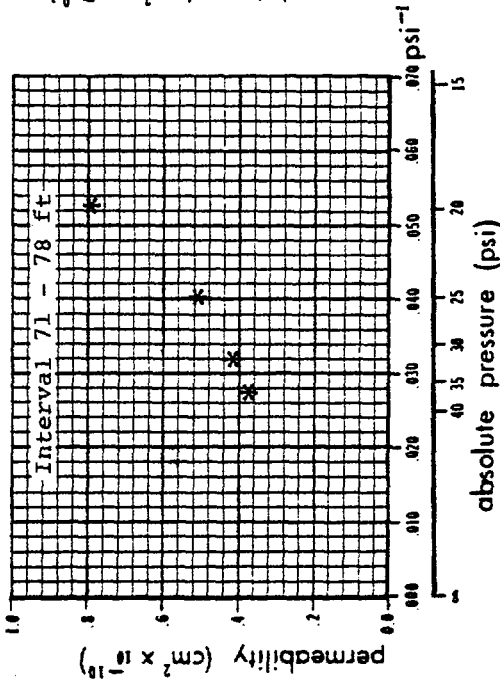
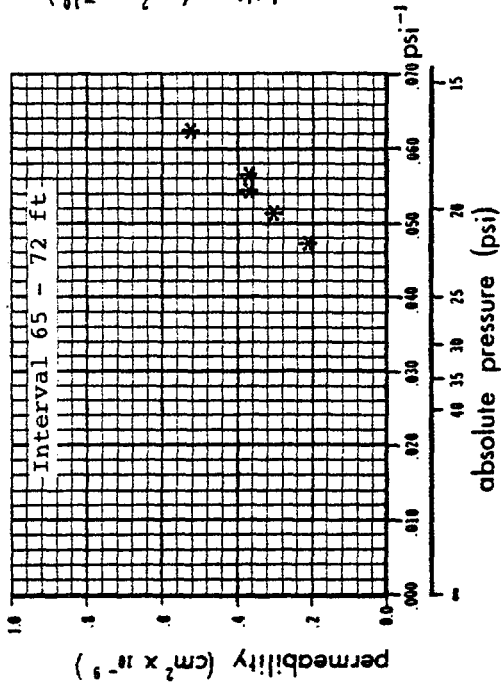
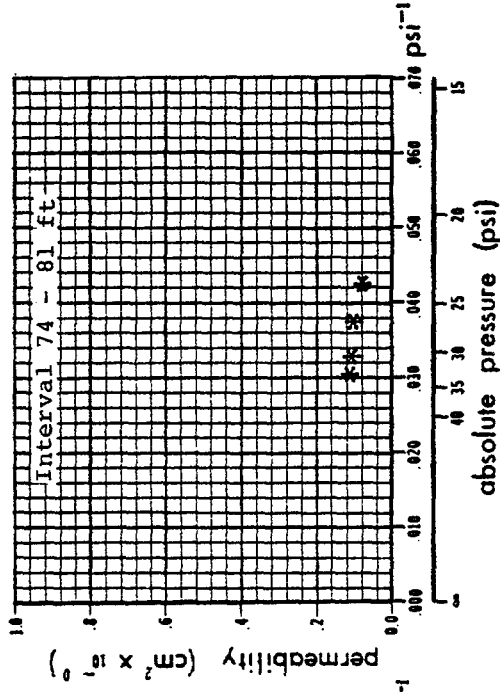
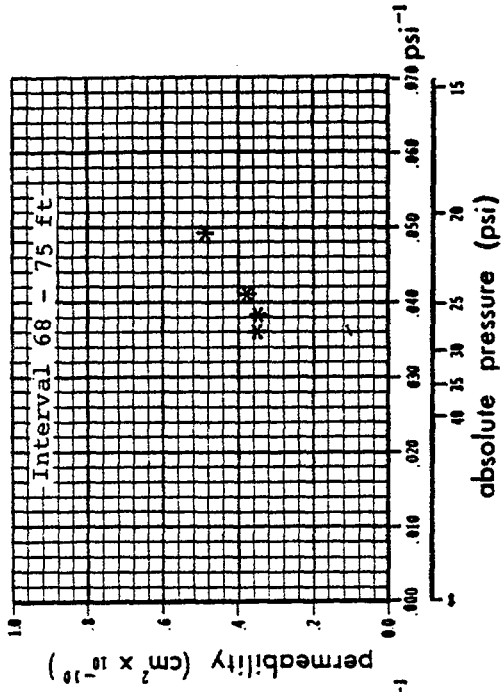
Variation of permeability with pressure, Borehole PA-1



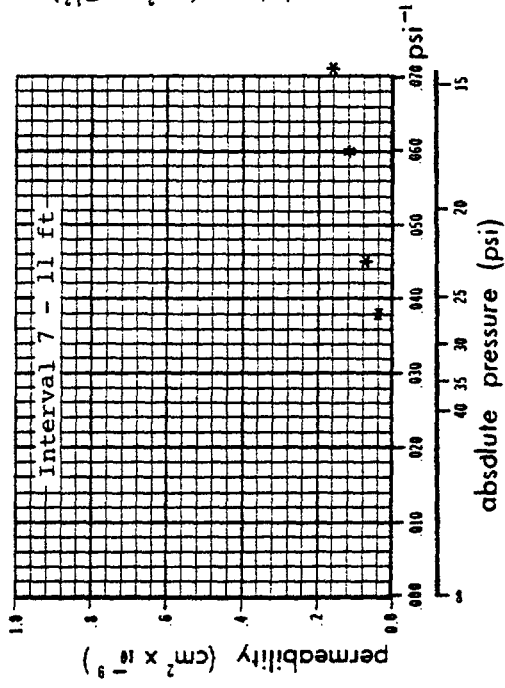
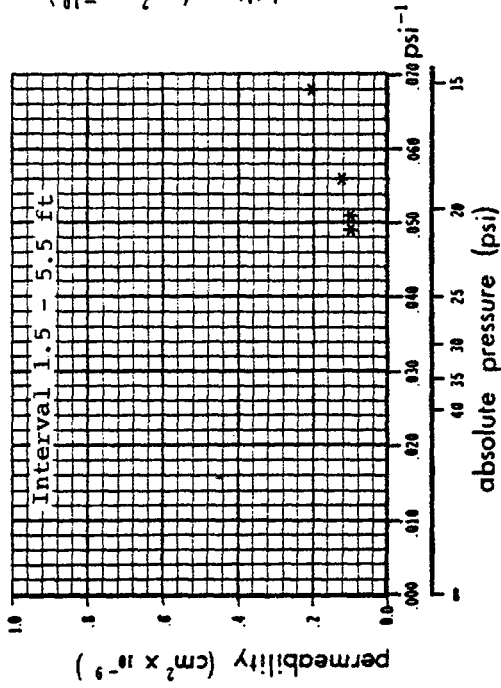
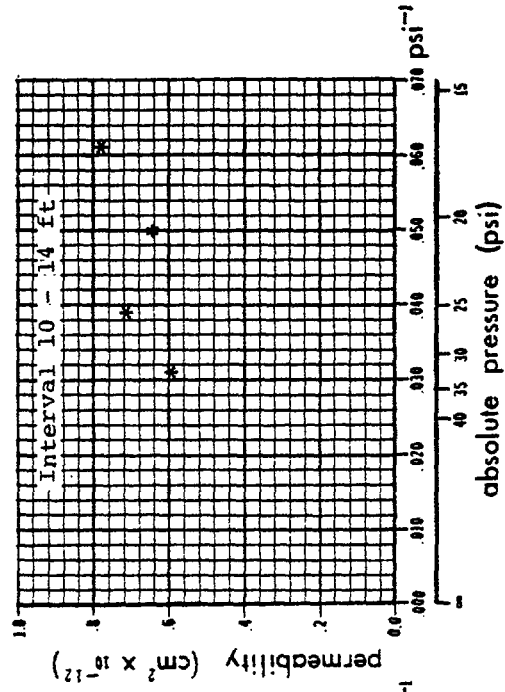
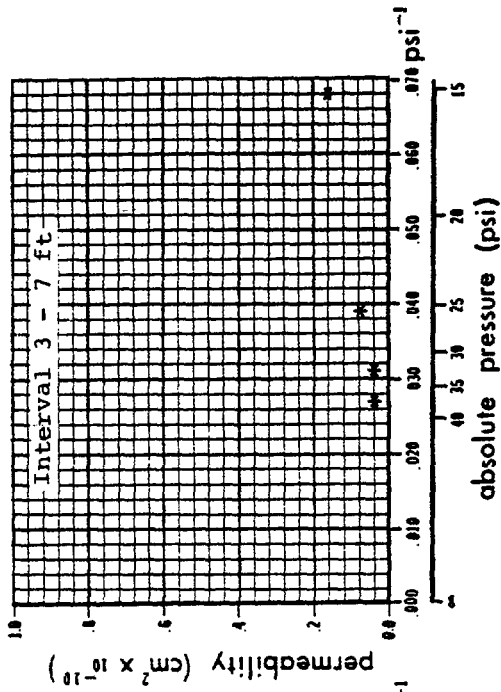
Variation of permeability with pressure. Borehole PA-1



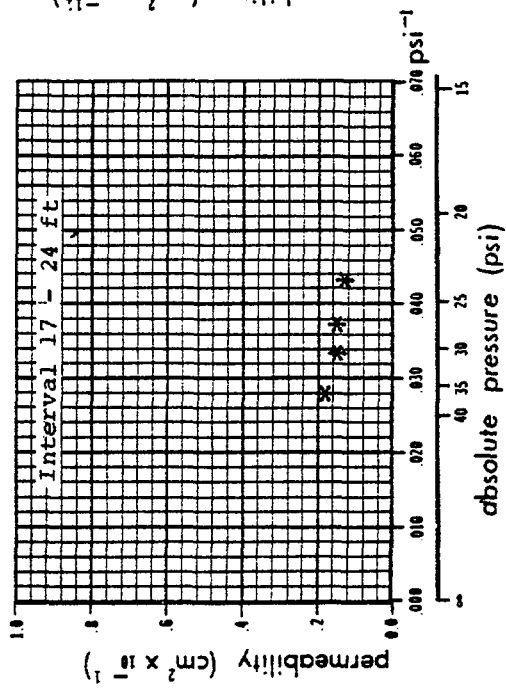
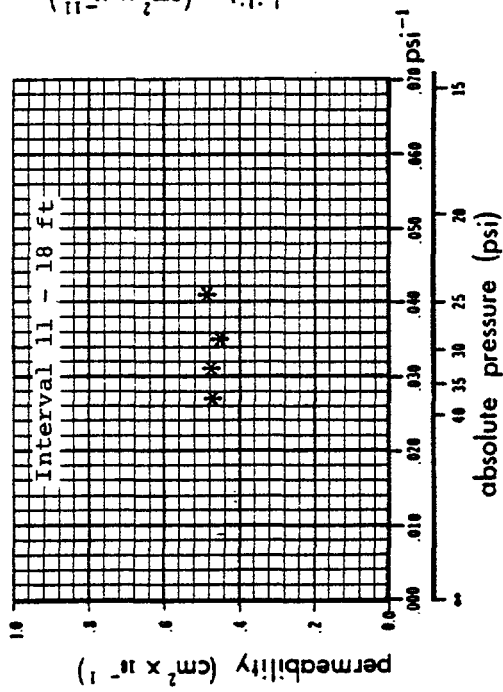
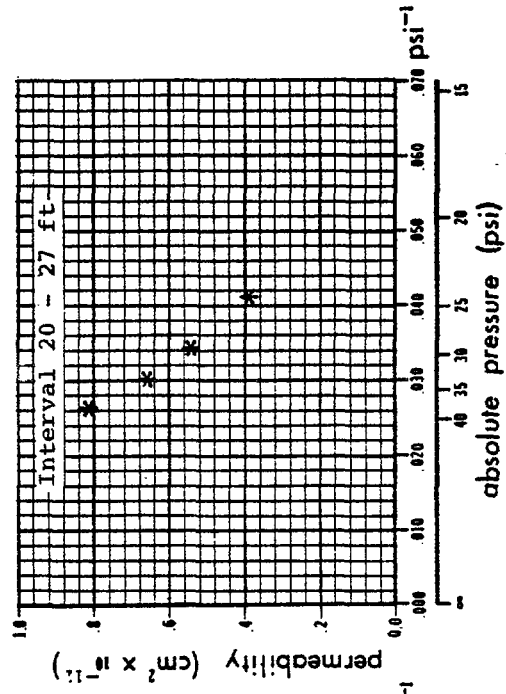
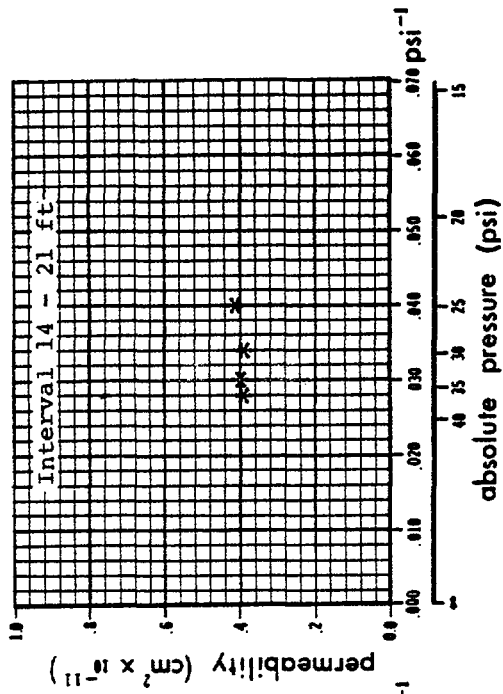
Variation of permeability with pressure, Borehole PA-1



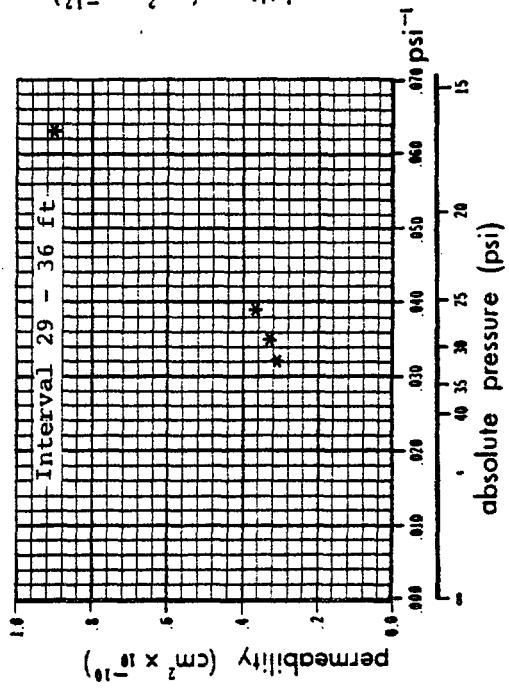
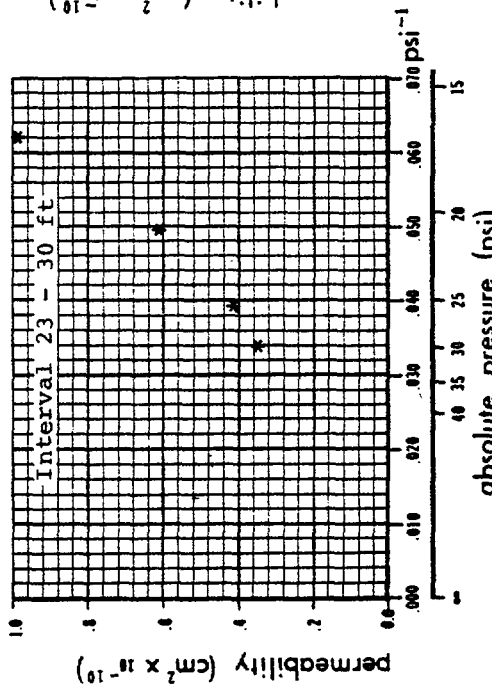
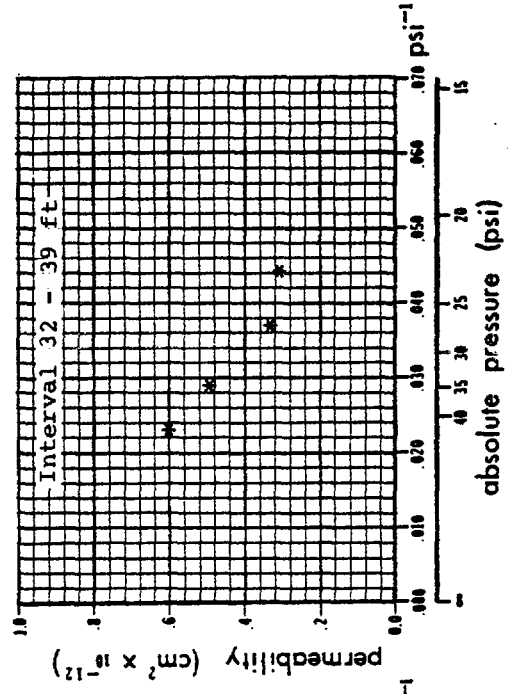
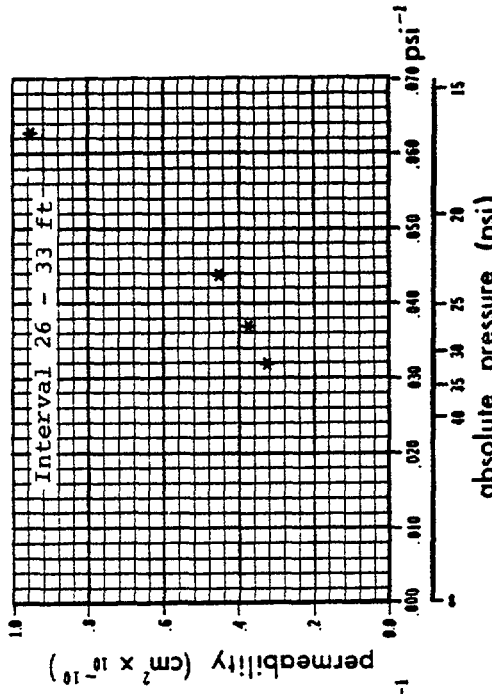
Variation of permeability with pressure. Borehole PA-1



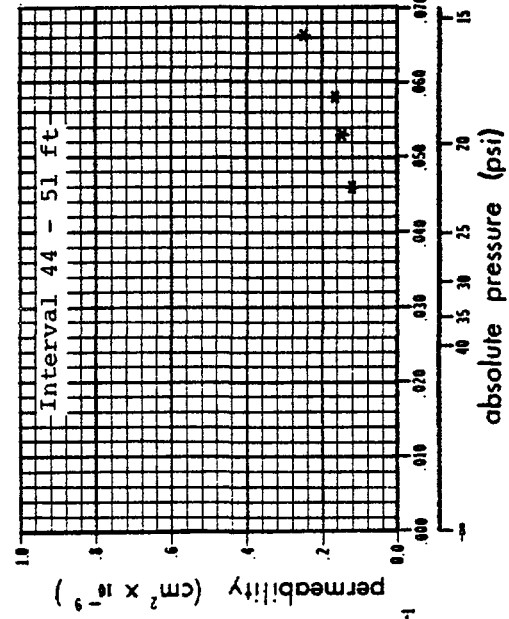
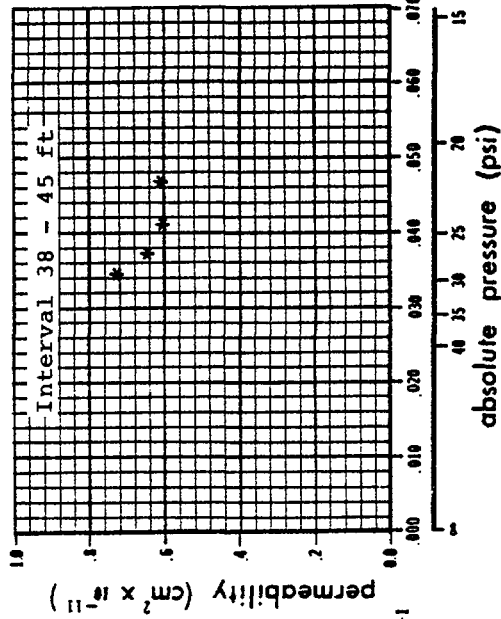
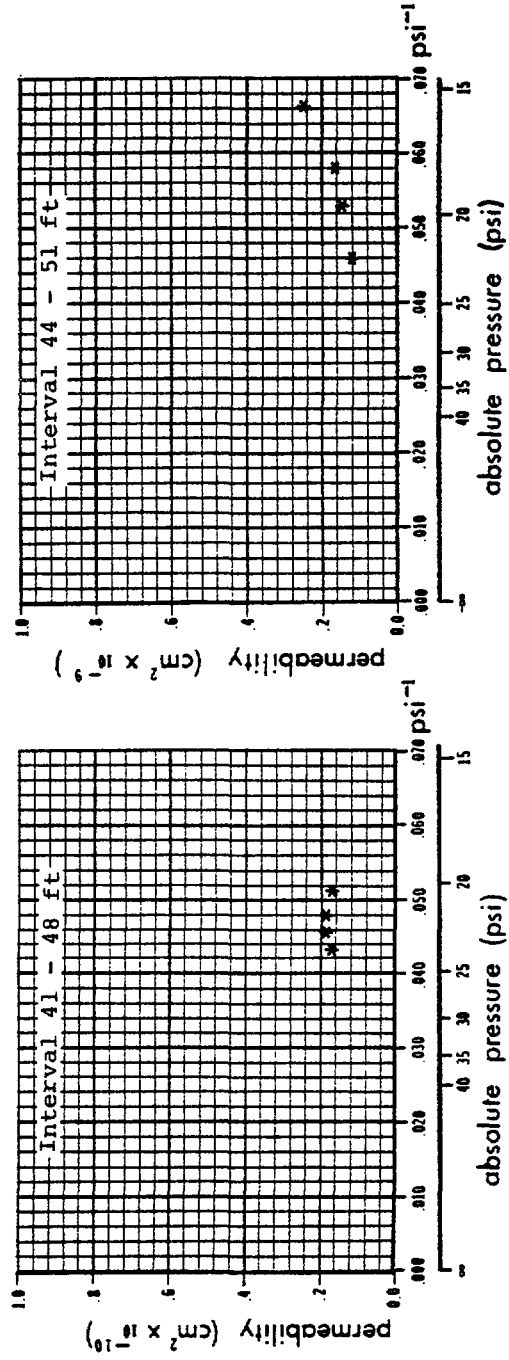
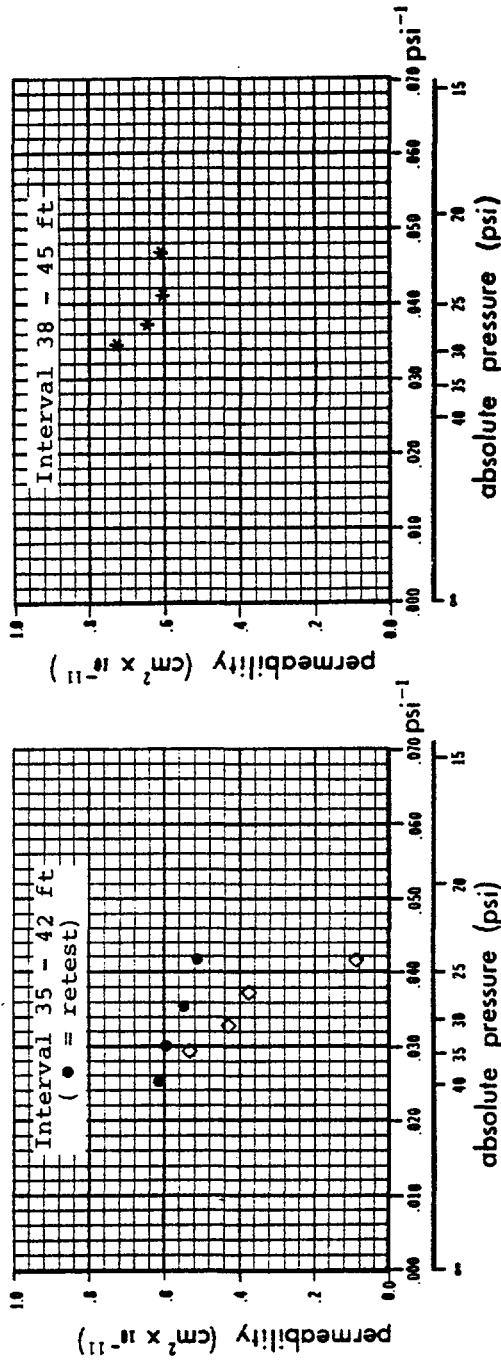
Variation of permeability with pressure. Borehole PA-2



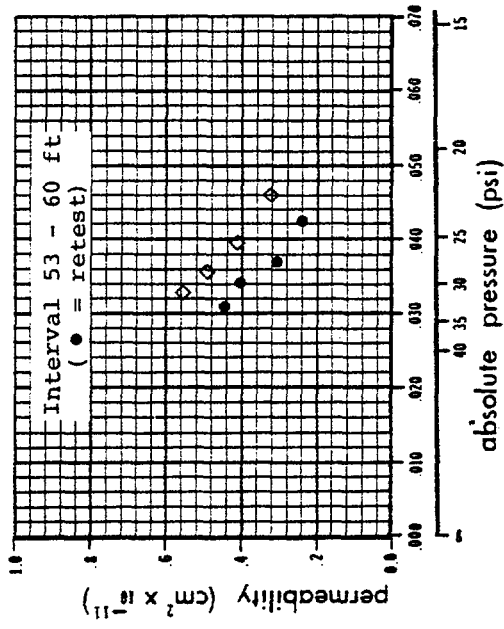
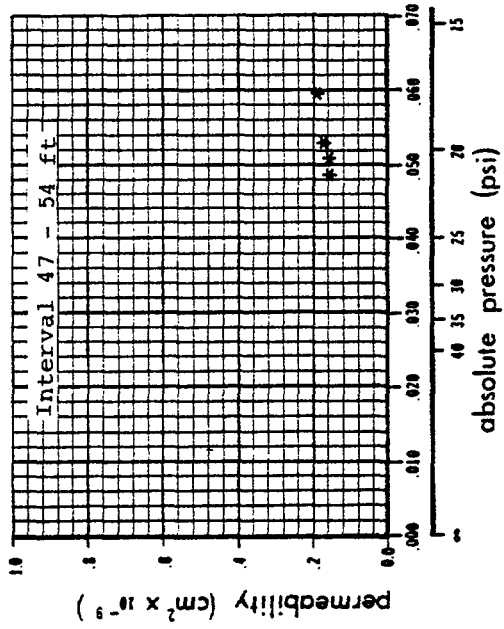
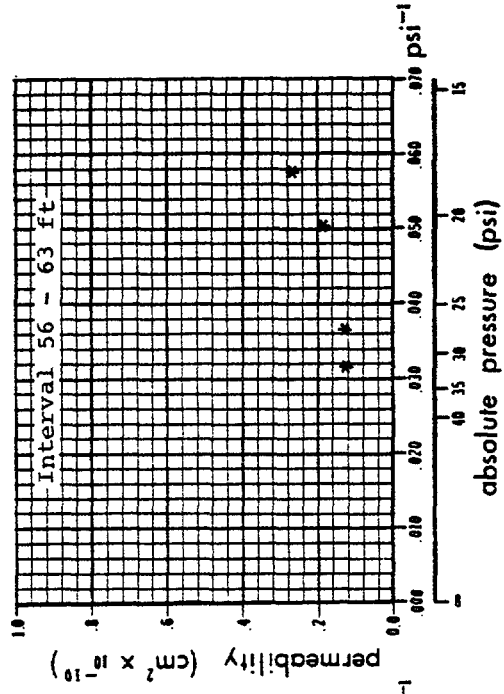
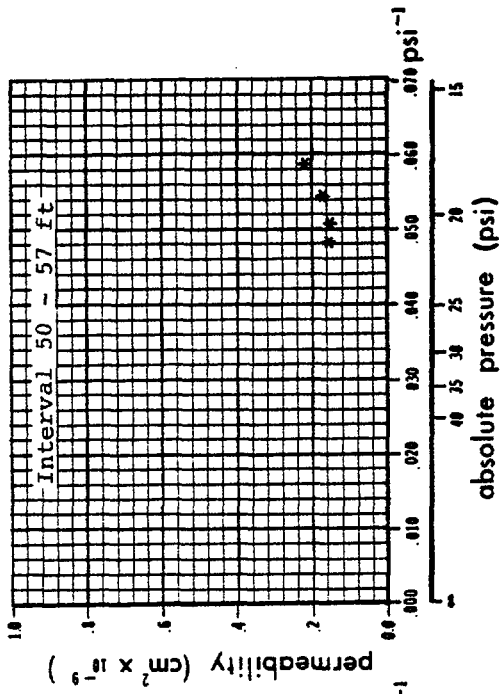
Variation of permeability with pressure. Borehole PA-2



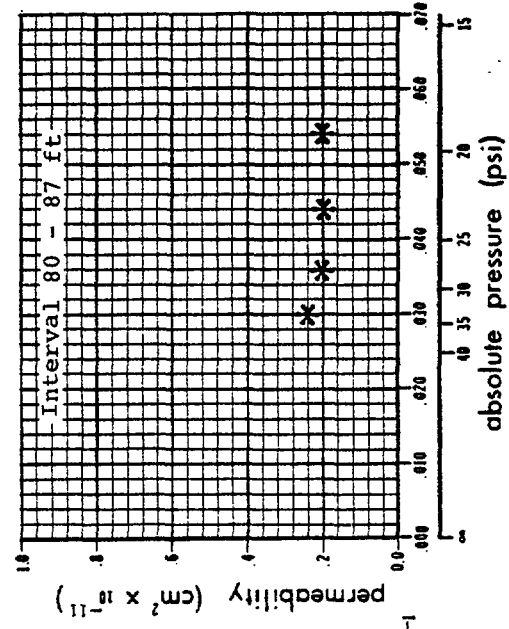
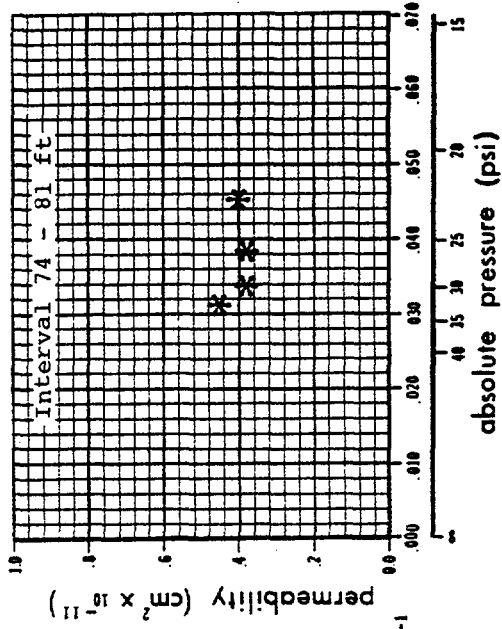
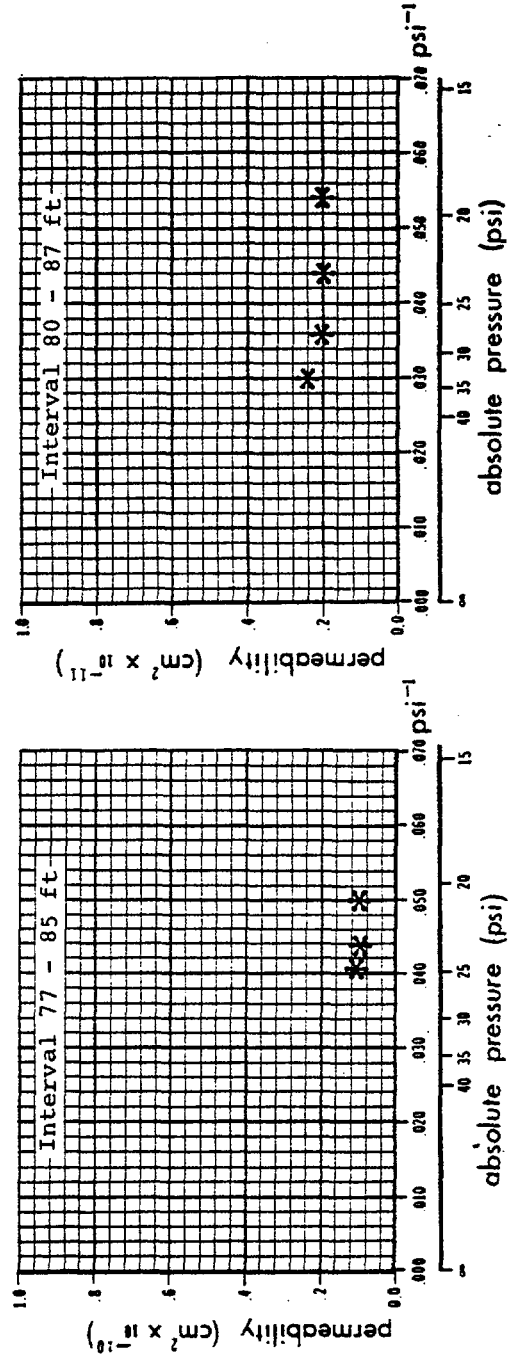
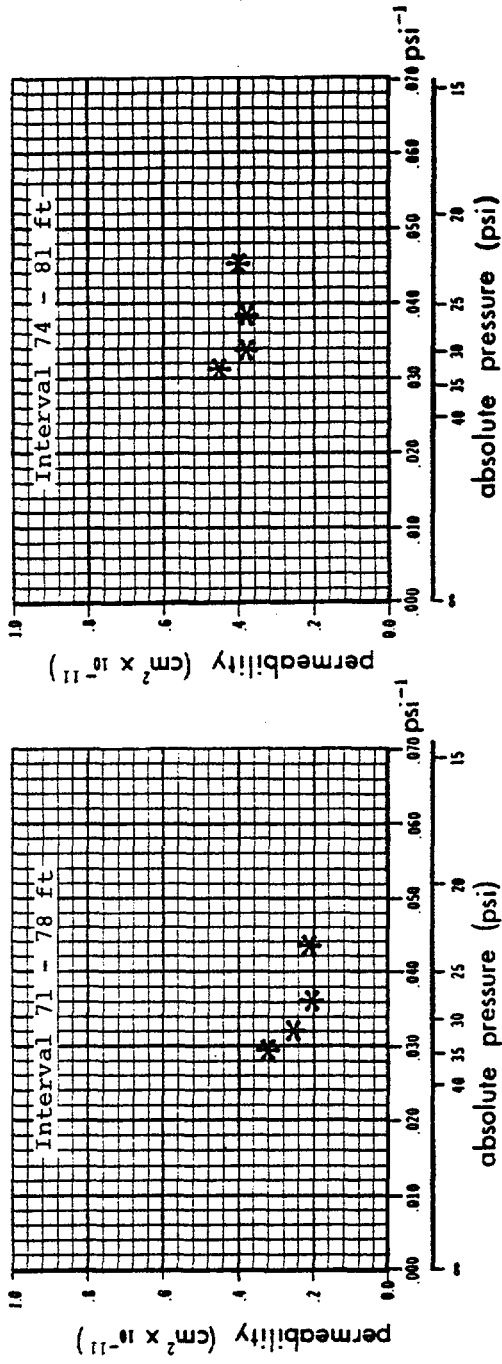
Variation of permeability with pressure. Borehole PA-2



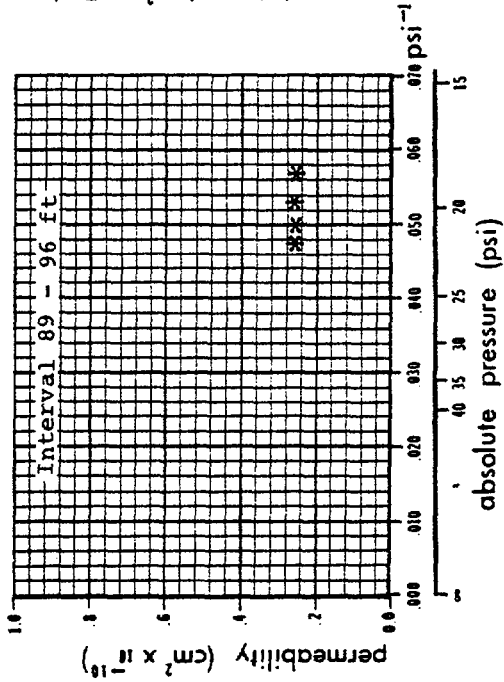
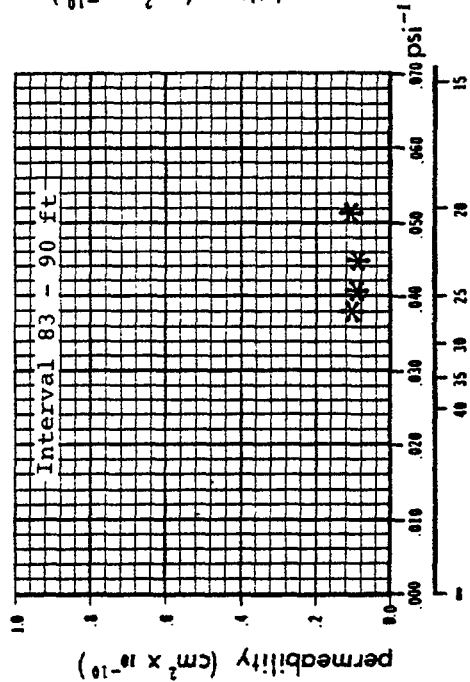
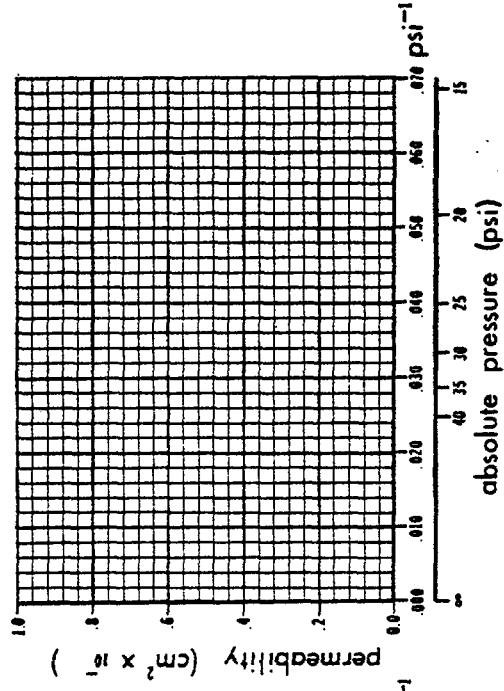
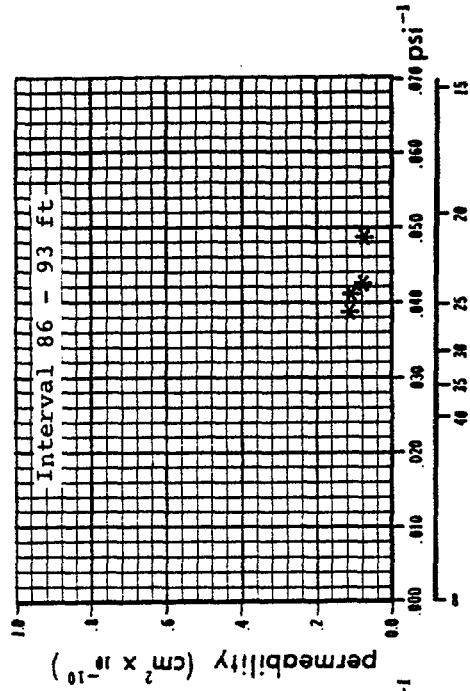
Variation of permeability with pressure. Borehole PA-2



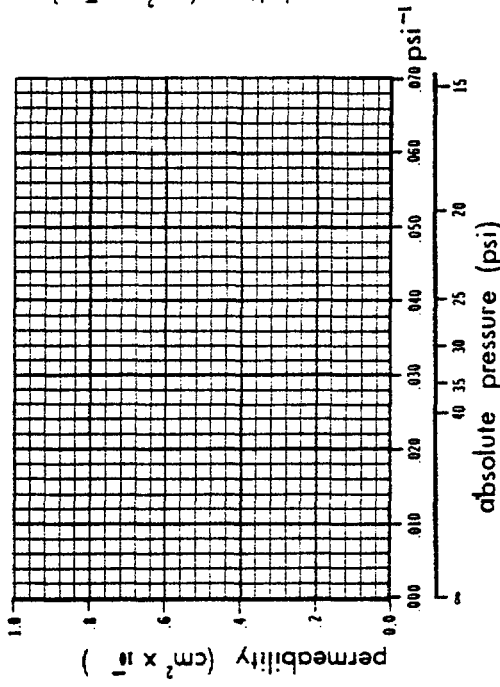
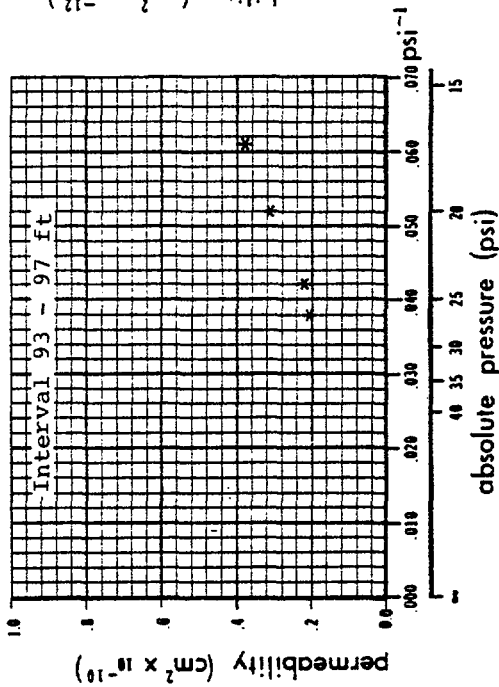
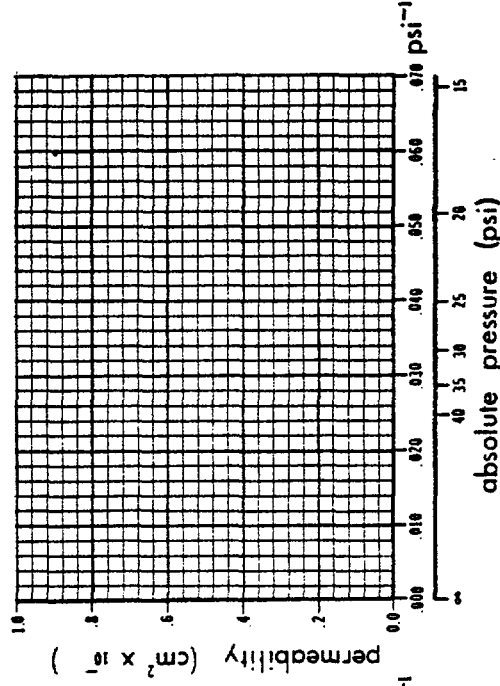
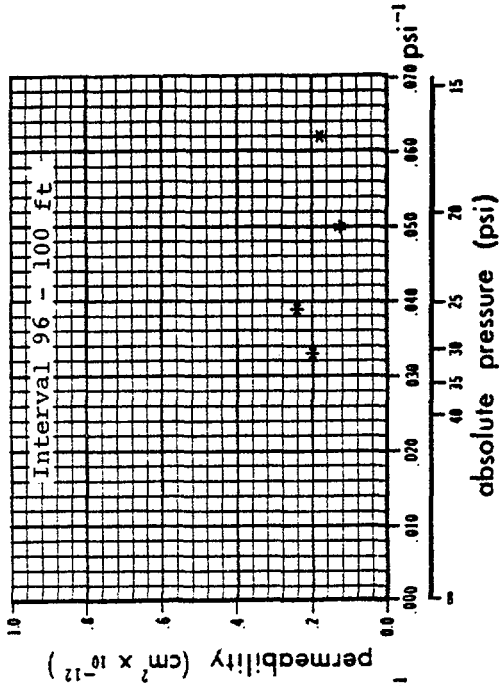
Variation of permeability with pressure. Borehole PA-2



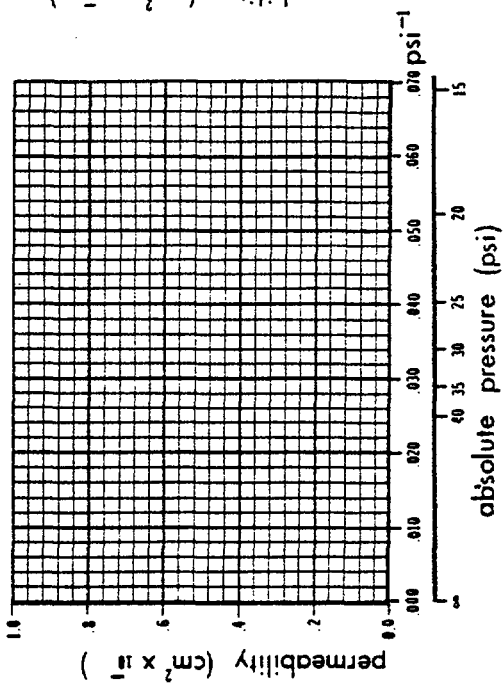
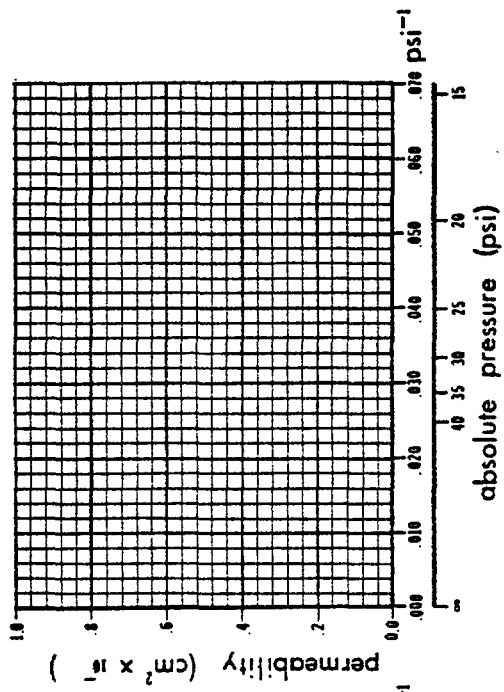
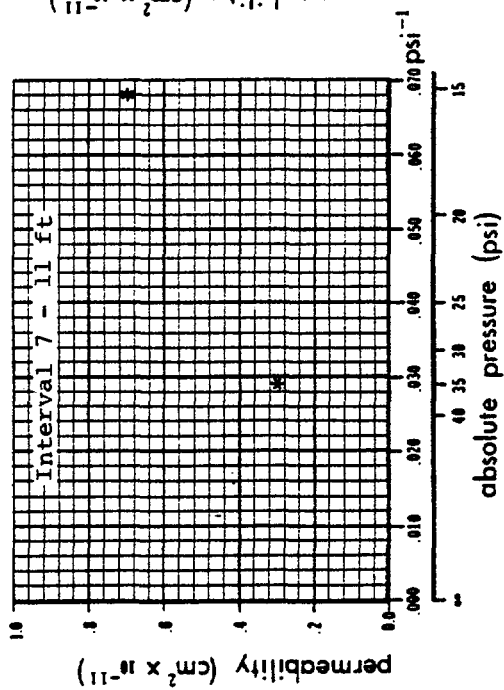
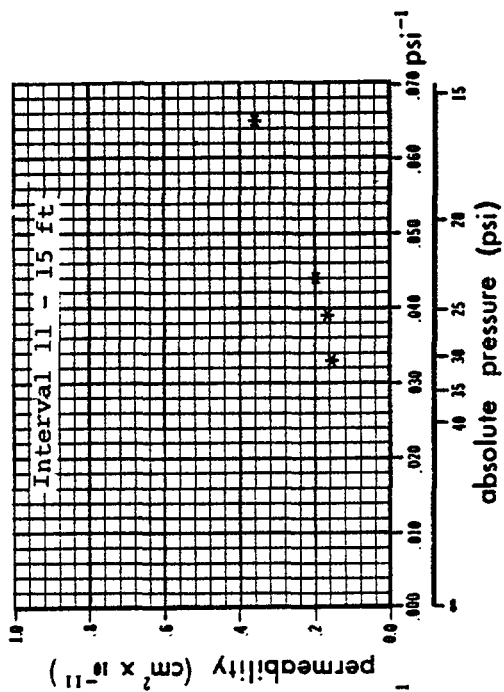
Variation of permeability with pressure. Borehole PA-2



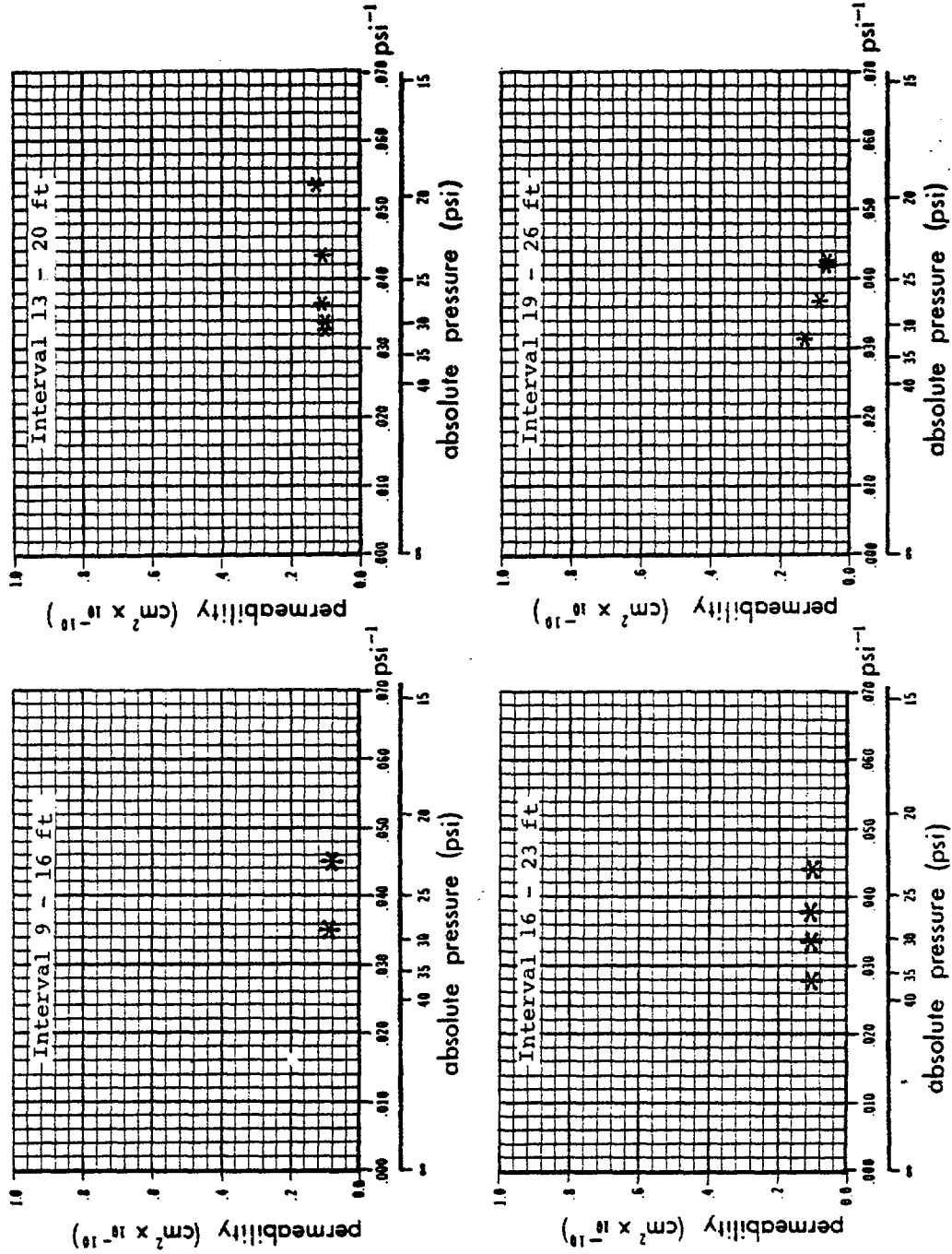
Variation of permeability with pressure. Borehole PA-2



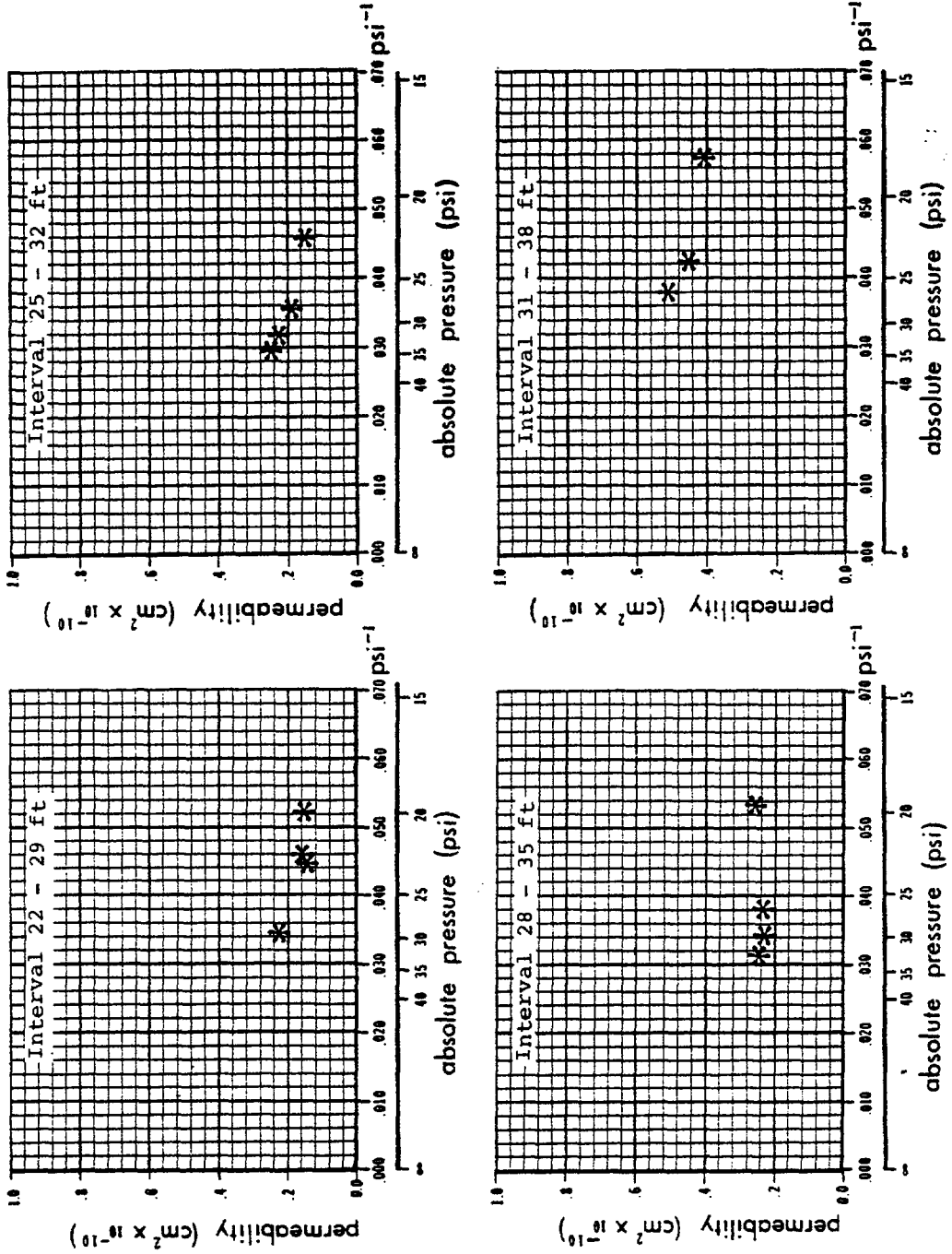
Variation of permeability with pressure. Borehole PA-2



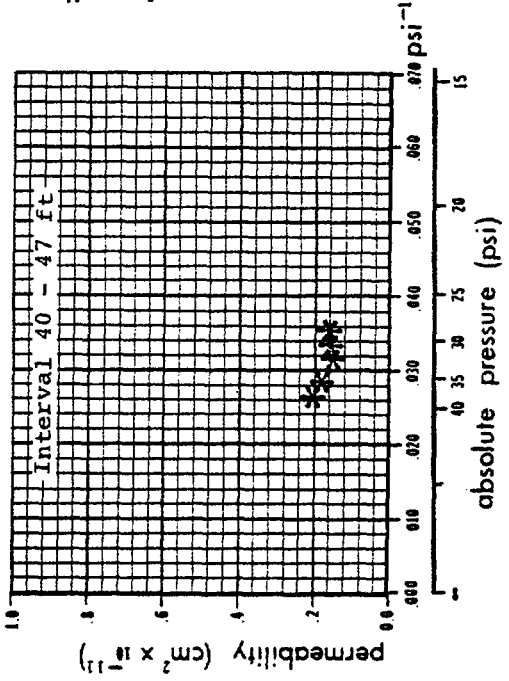
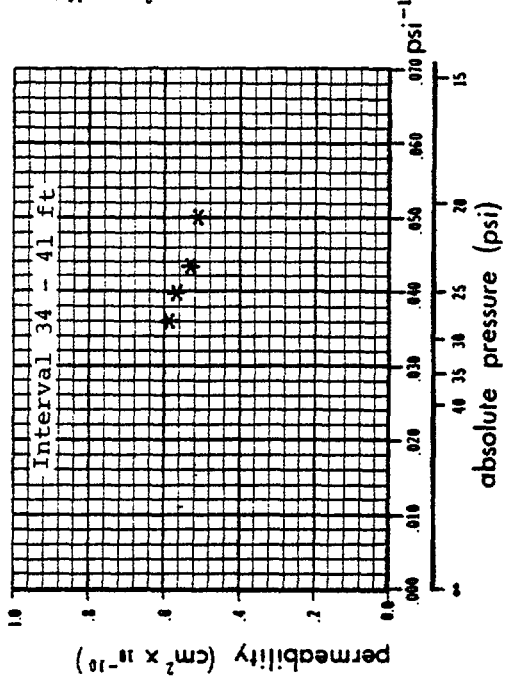
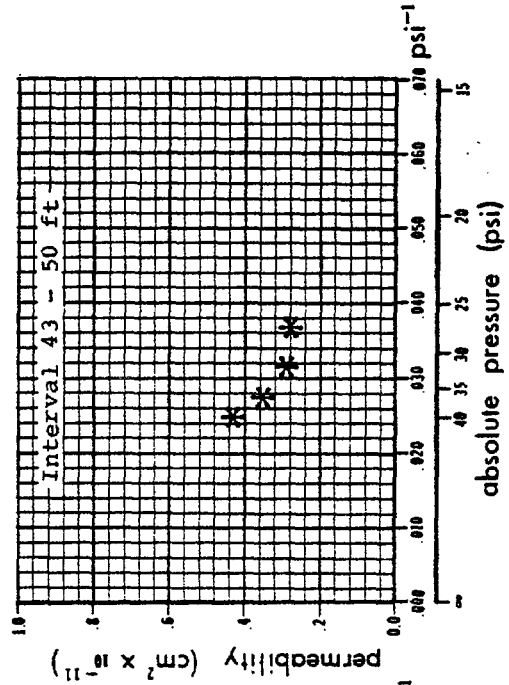
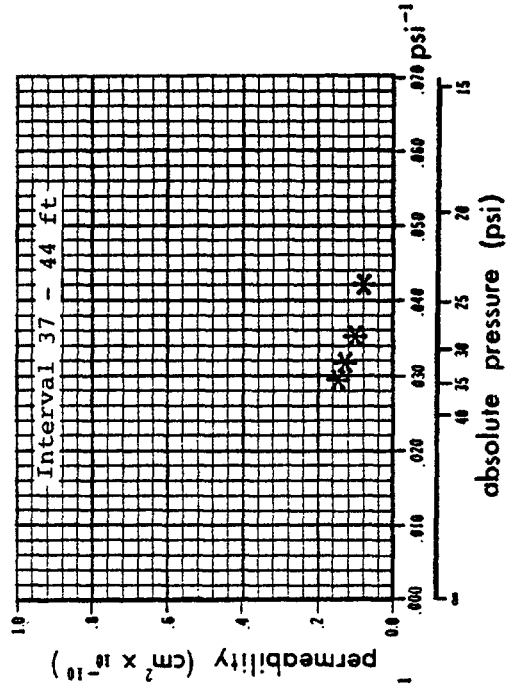
Variation of permeability with pressure. Borehole PA-3



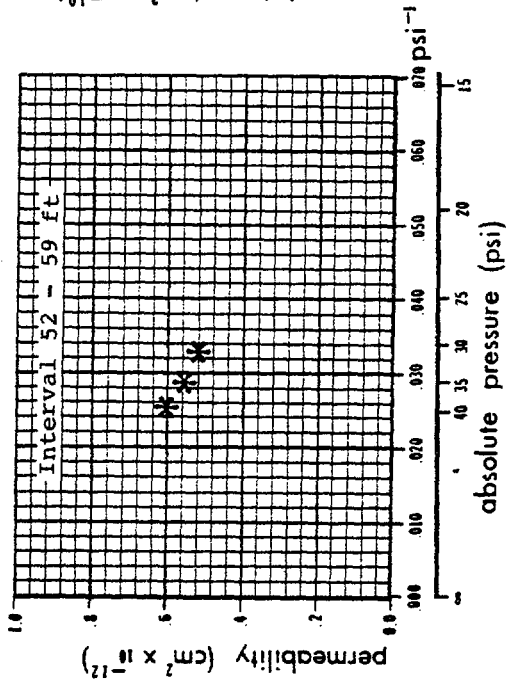
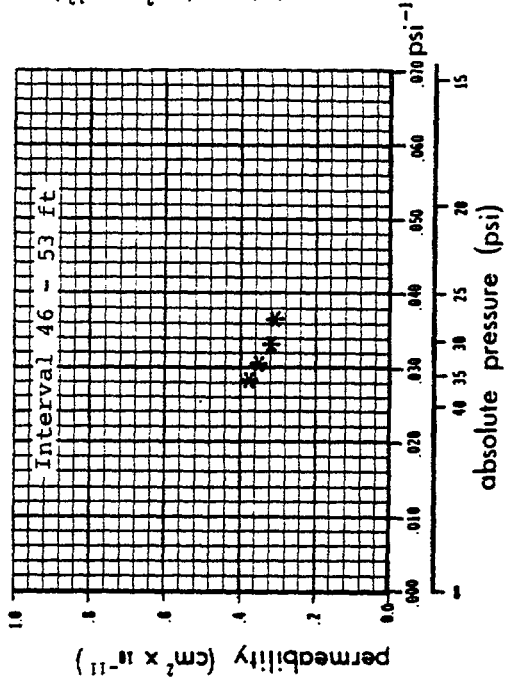
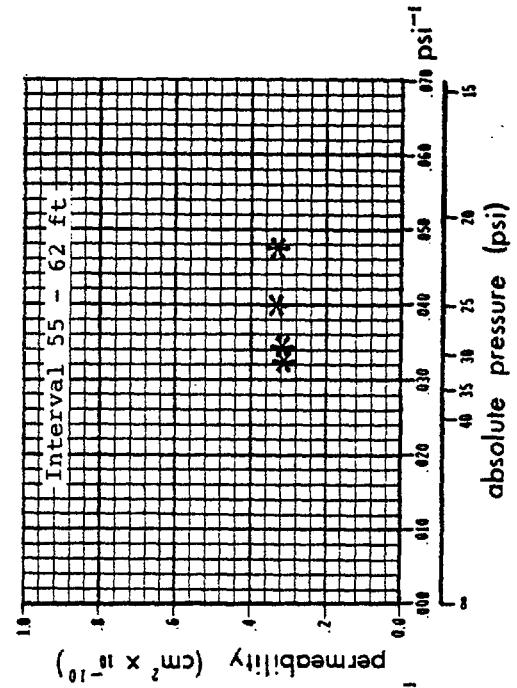
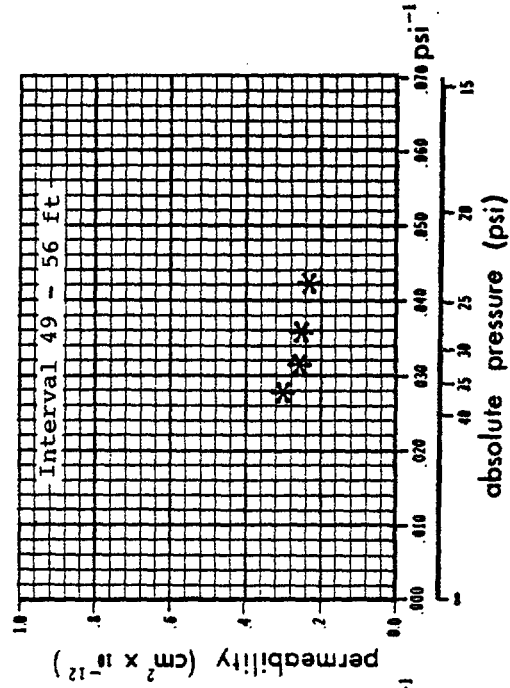
Variation of permeability with pressure. Borehole PA-3



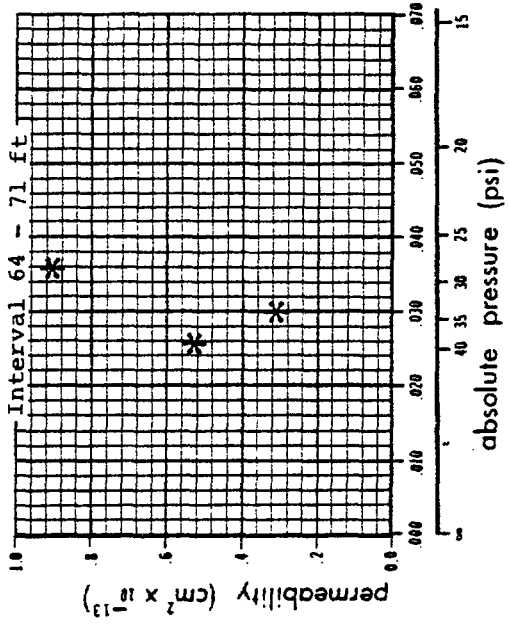
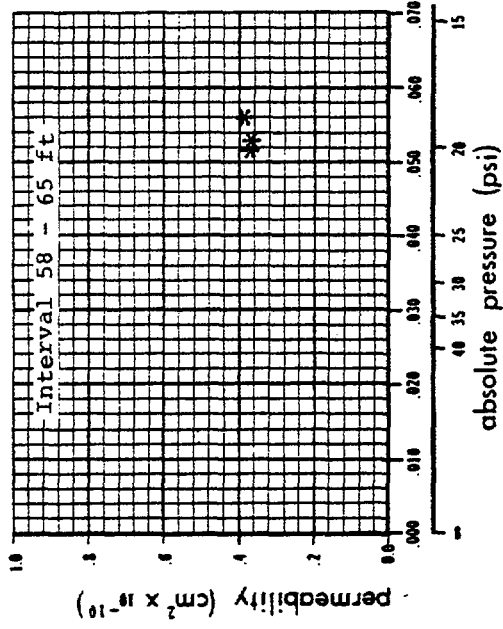
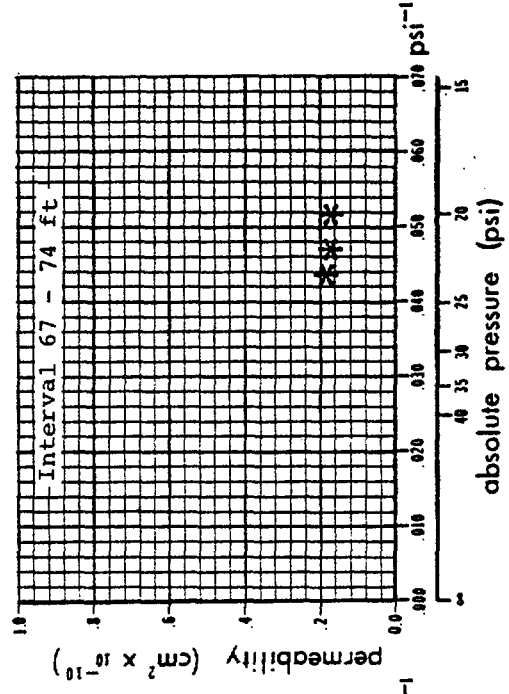
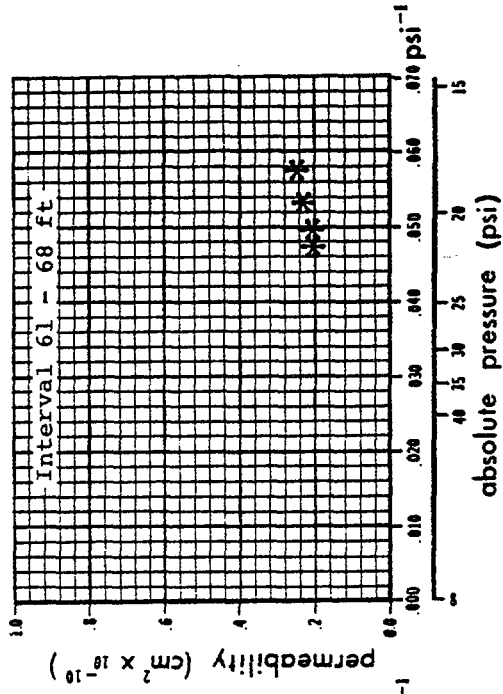
Variation of permeability with pressure, Borehole PA-3



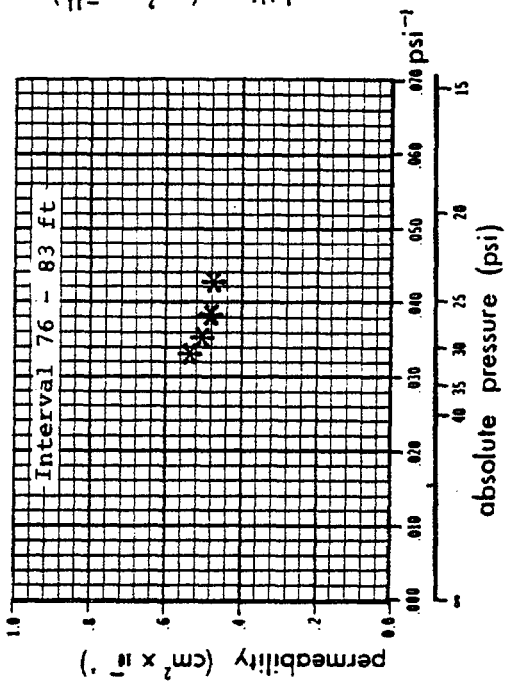
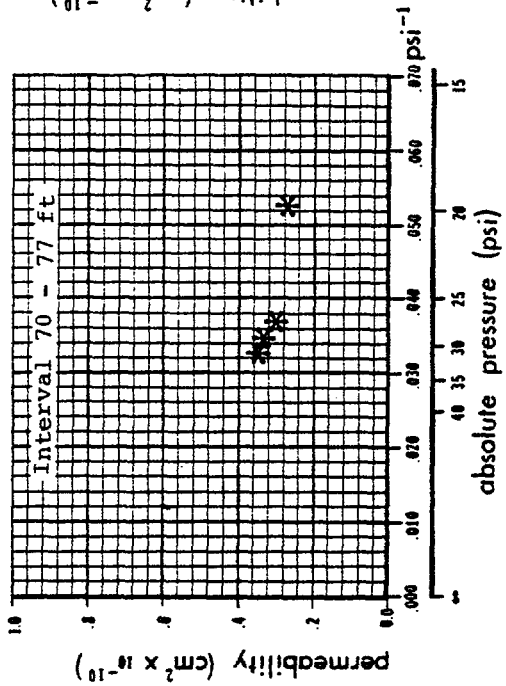
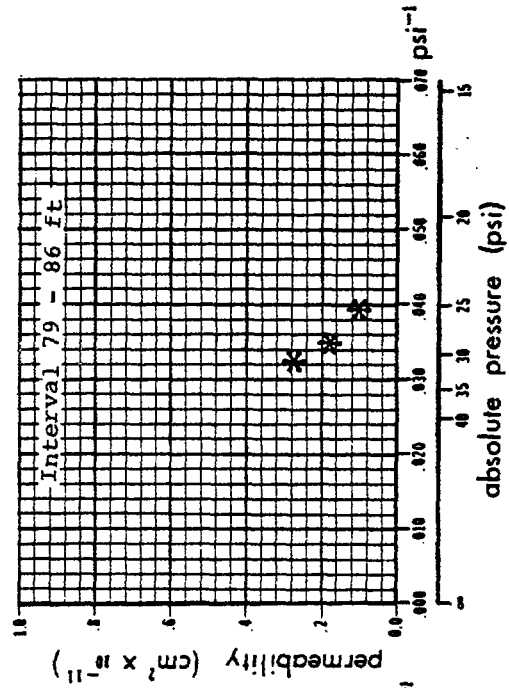
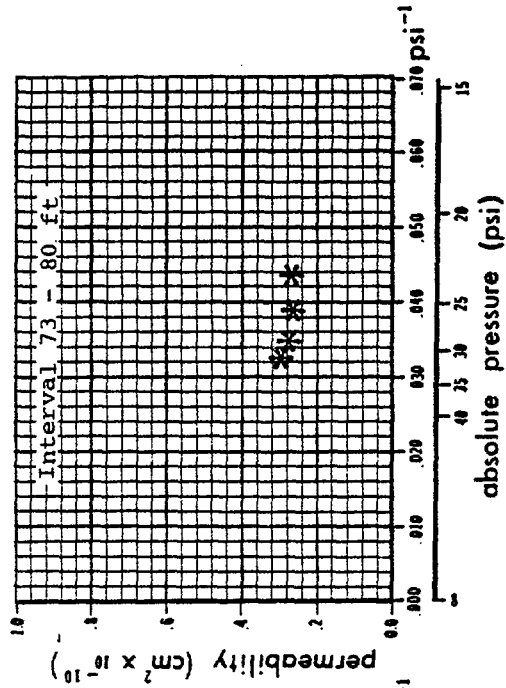
Variation of permeability with pressure. Borehole PA-3



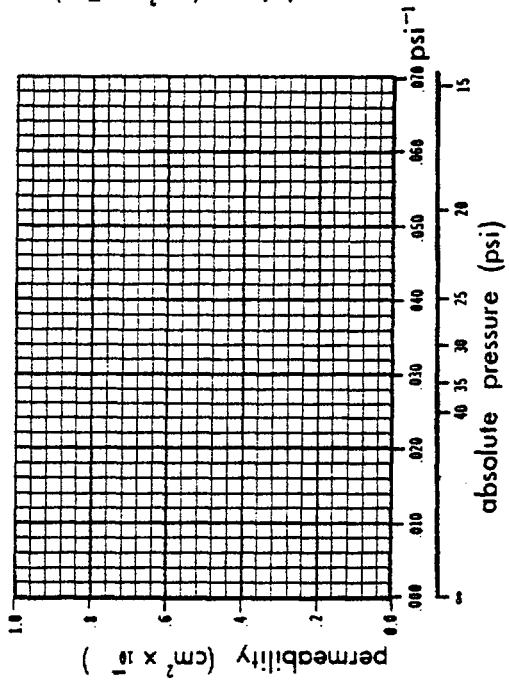
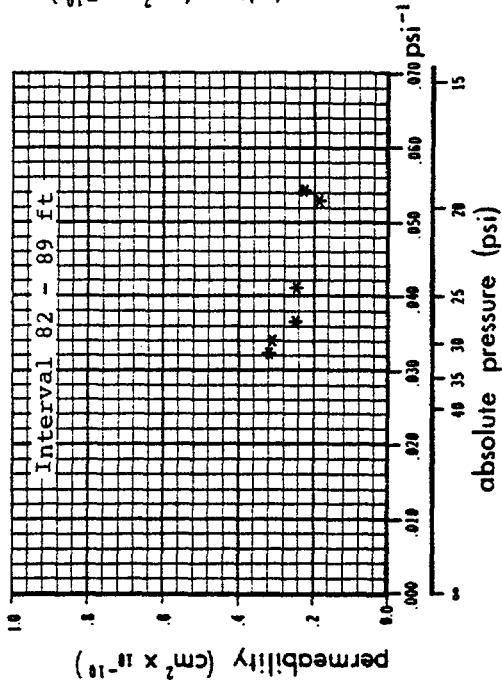
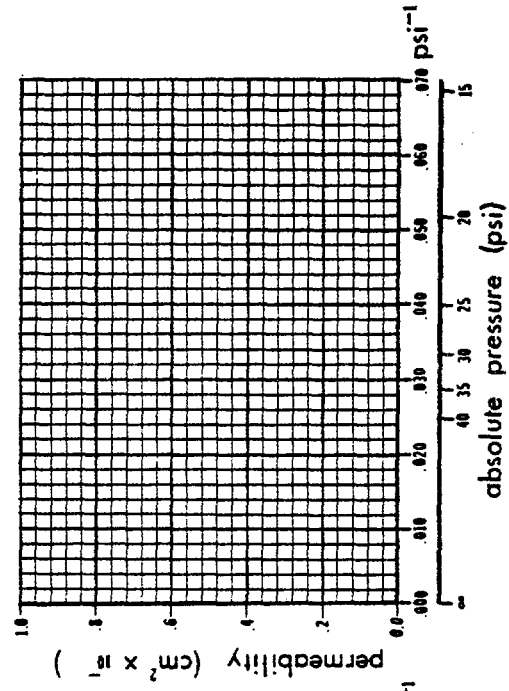
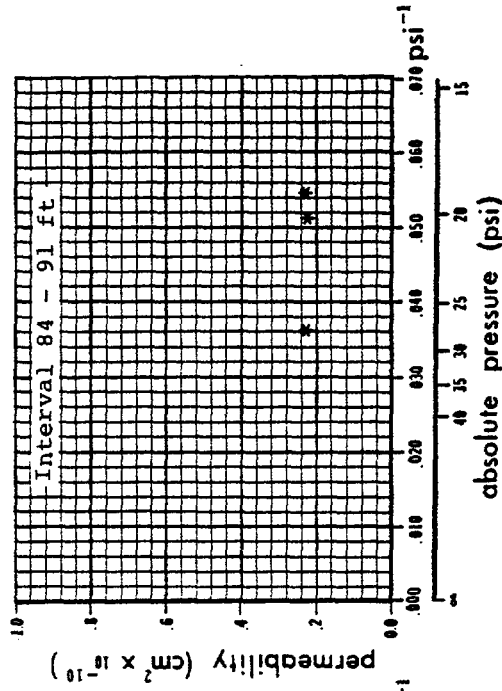
Variation of permeability with pressure. Borehole PA-3



Variation of permeability with pressure. Borehole PA-3



Variation of permeability with pressure. Borehole PA-3



Variation of permeability with pressure. Borehole PA-3

APPENDIX VII

PERMEABILITY PLOTS ALONG
THE RADIAL BOREHOLES

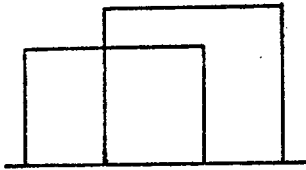
APPENDIX VIIPERMEABILITY PLOTS ALONG THE
RADIAL BOREHOLES

The results of the systematic nitrogen injection testing along the radial boreholes are presented in this Appendix. The core integrity here is referred to the core breakage, that is the frequency of the occurrence of the mechanical or natural breaks in the core. In order to be able to compare the results of the permeabilities along the radial boreholes with the permeabilities along the longitudinal boreholes (section 8.3.4.1) they are plotted on similar scale (the permeability axis in the plots is chosen so that zones with permeabilities of about 10^{-10} cm² be more visible). For this reason in many cases the permeabilities along the radial boreholes plot off the scale and they are shown by broken lines with the actual number appearing on the bar (see explanation in the following page).

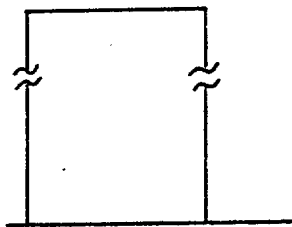
EXPLANATION - RADIAL BOREHOLES



Borehole With Core Integrity



Permeability Of The Interval



Permeability Of The Interval,
not to scale

Figure 17 . Radial Borehole Permeability: 1st Ring.

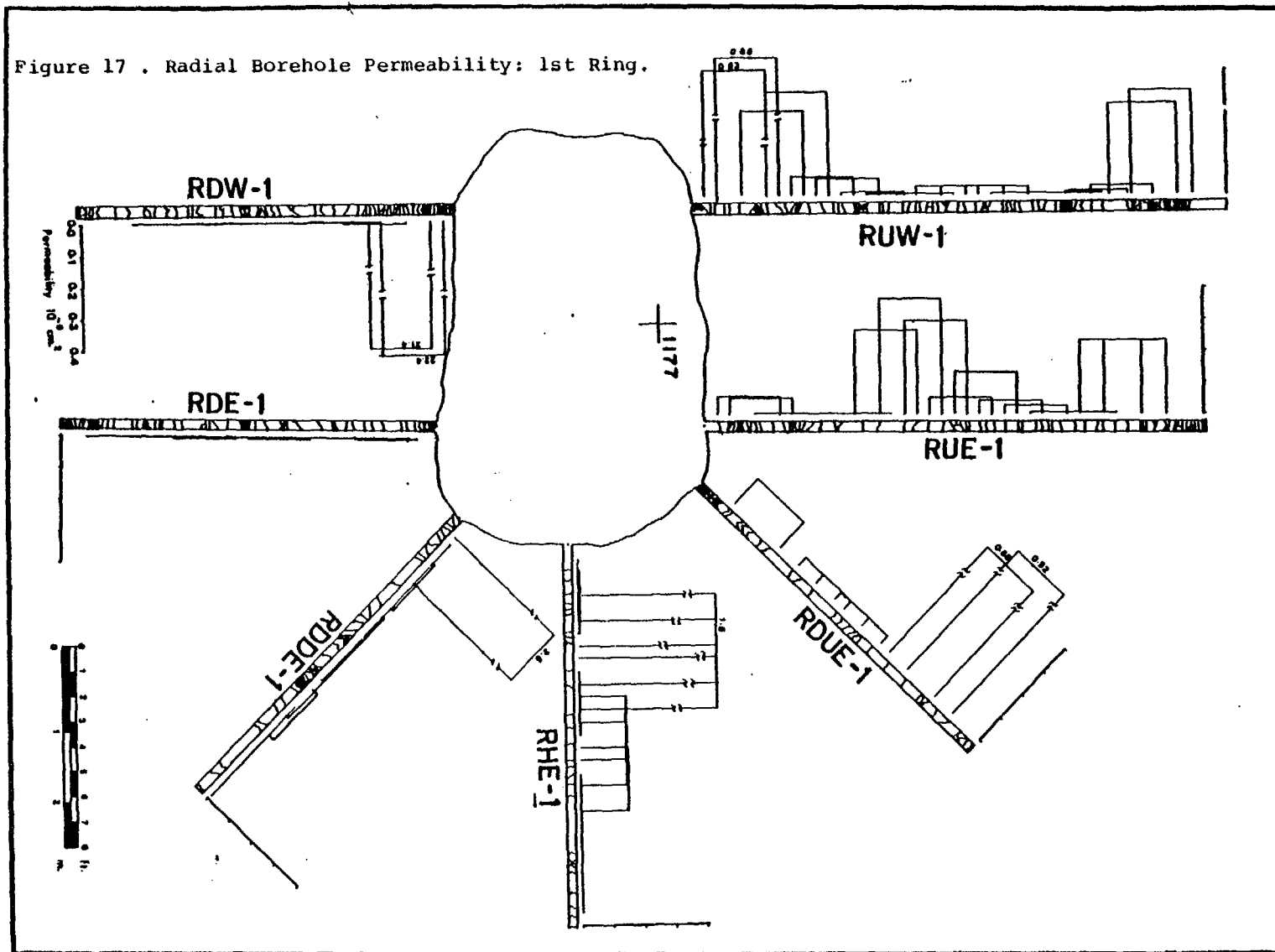


Figure 18. Radial Borehole Permeability: 2nd Ring.

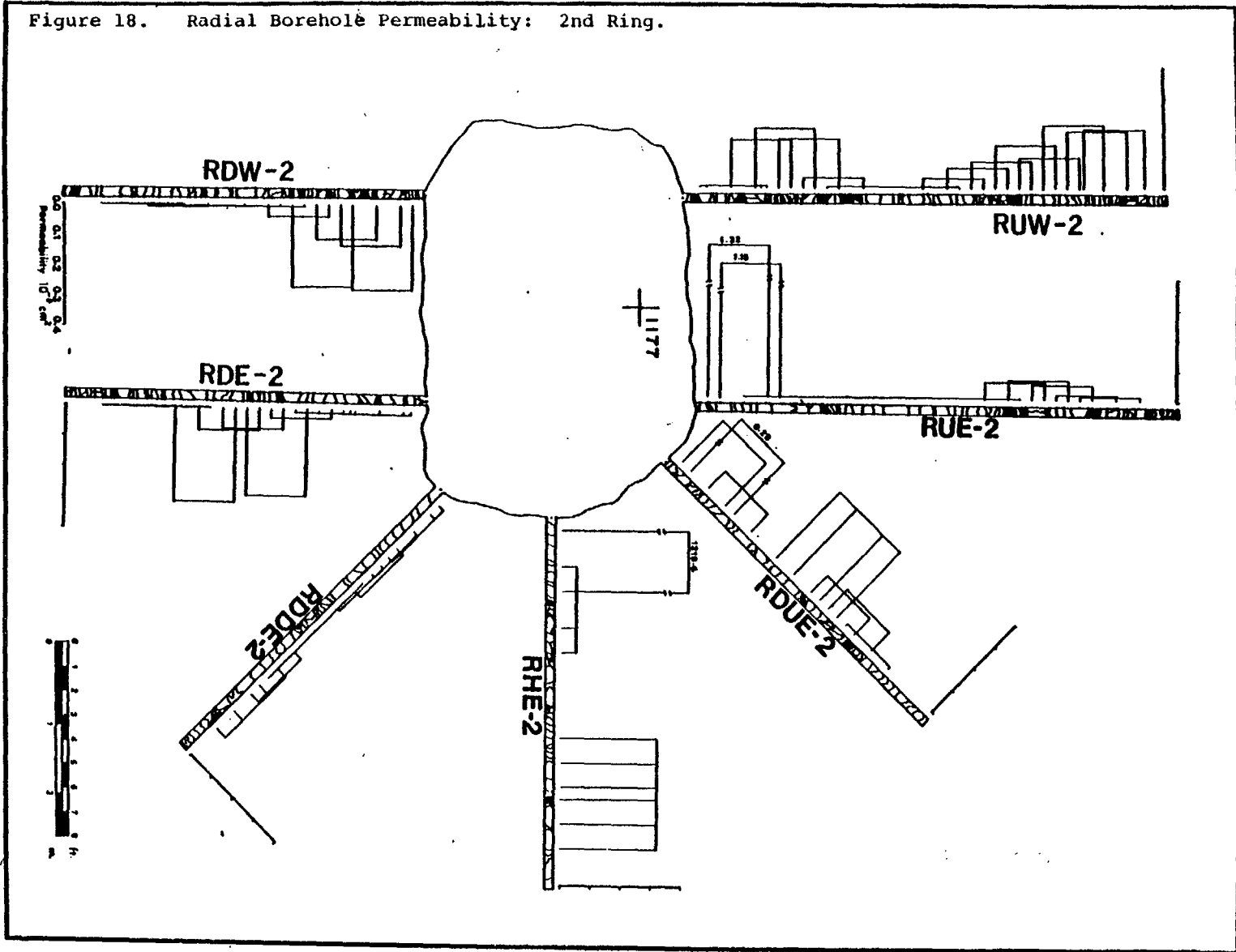
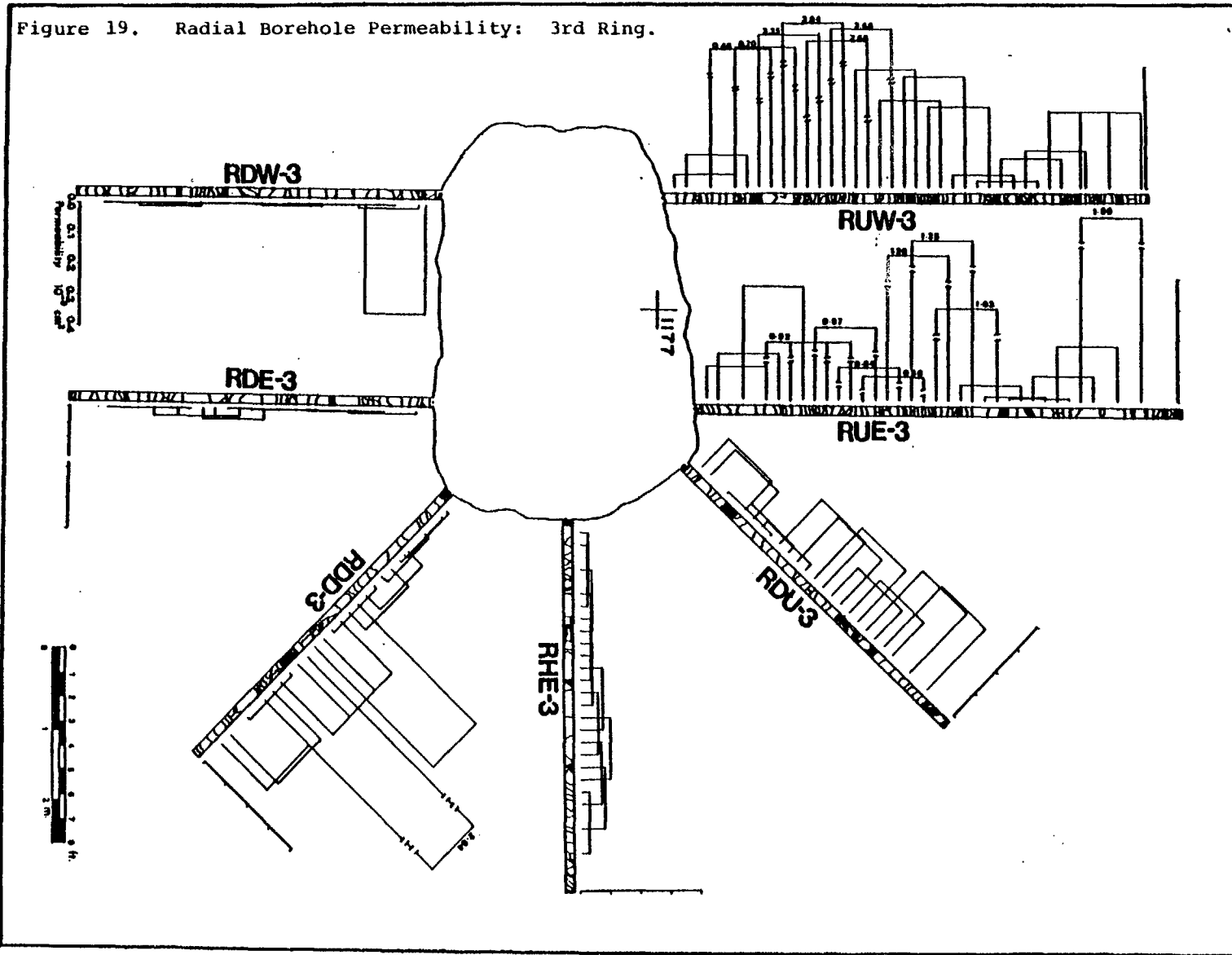
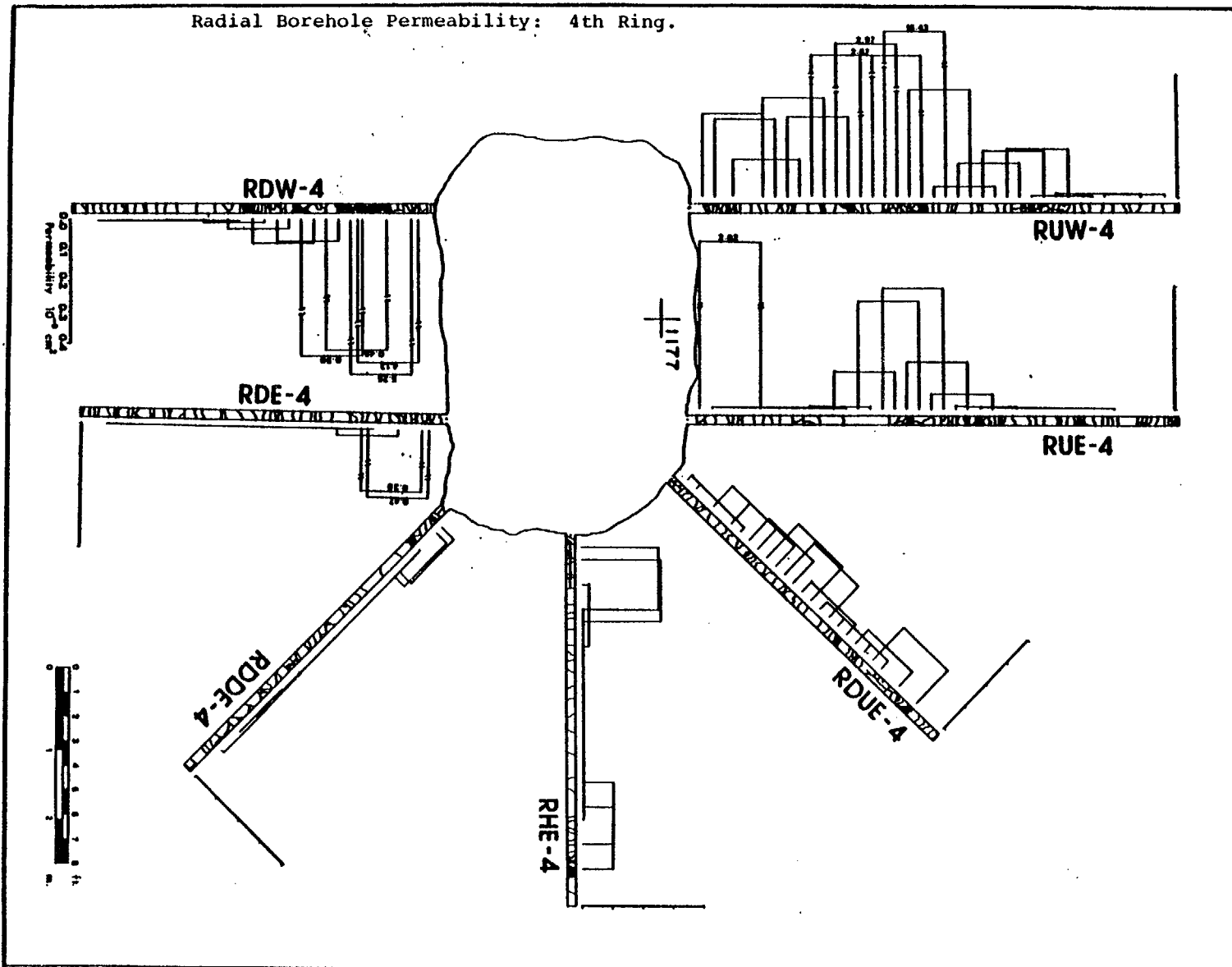


Figure 19. Radial Borehole Permeability: 3rd Ring.



Radial Borehole Permeability: 4th Ring.



Radial Borehole Permeability: 5th Ring.

